

УНИВЕРЗИТЕТ У БЕОГРАДУ ФИЗИЧКИ ФАКУЛТЕТ
UNIVERSITY OF BELGRADE FACULTY OF PHYSICS

Студентски трг 12, 11000 Београд, П.П. 44, Тел: 011-7158-151, Факс: 011-3282-619
Studentski trg 12, 11000 Belgrade, Serbia, POB 44, Tel: +381-11-7158-152, Fax: +381-11-3282-619
www.ff.bg.ac.rs e-mail: dekanat@ff.bg.ac.rs

ВЕЋУ НАУЧНИХ ОБЛАСТИ ПРИРОДНО-МАТЕМАТИЧКИХ НАУКА
УНИВЕРЗИТЕТА У БЕОГРАДУ

Научно-наставно веће Физичког факултета Универзитета у Београду, на својој седници одржаној дана 26. фебруара 2014. године, закључило је да тема: „ПРИМЕНА МУЛТИВАРИЈАНТНЕ АНАЛИЗЕ И МОДЕЛИРАЊЕ ВАРИЈАБИЛНОСТИ РАДОНА У ЛАБОРАТОРИЈСКИМ И РЕАЛНИМ УСЛОВИМА“, кандидата ЈЕЛЕНЕ ФИЛИПОВИЋ, која би била рађена под менторством др Владимир Удовичић, вишег научног сарадника Института за физику, задовољава све услове који се захтевају од теме за израду докторске дисертације и да је за област Нуклеарна физика, којој тема припада, Физички факултет Универзитета у Београду матична организација.

На основу тога предлажем да Веће научних области природно-математичких наука Универзитета у Београду одобри рад на предложеној теми за израду докторске дисертације.

ДЕКАН ФИЗИЧКОГ ФАКУЛТЕТА

Проф. др Јаблан Дојчиловић



УНИВЕРЗИТЕТ У БЕОГРАДУ

Адреса: Студентски трг 1, 11000 Београд, Република Србија
Тел.: 011 3207400; Факс: 011 2638818; Е-mail: officebu@rect.bg.ac.rs

ВЕЋЕ НАУЧНИХ ОБЛАСТИ
ПРИРОДНО-МАТЕМАТИЧКИХ
НАУКА

Београд, 14.04.2014.
02 Број: 61206-1021/2-14
МЦ

На основу члана члана 47. став 5. тачка. 3. Статута Универзитета у Београду ("Гласник Универзитета у Београду", број 162/11-пречишћени текст, 167/12 и 172/13) и чл. 14. – 21. Правилника о већима научних области на Универзитету у Београду ("Гласник Универзитета у Београду", број 134/07, 150/09, 158/11, 164/11 и 165/11), а на захтев Физичког факултета, број: 518/5 од 26.02.2014. године, Веће научних области природно-математичких наука, на седници одржаној 14.04.2014. године, донело је

О Д Л У К У

ДАЈЕ СЕ САГЛАСНОСТ на предлог теме докторске дисертације ЈЕЛЕНЕ ФИЛИПОВИЋ, под називом: „Примена мултиваријантне анализе и моделирање варијабилности радона у лабораторијским и реалним условима“.

ПРЕДСЕДНИК ВЕЋА

Проф. др Павле Младеновић

Доставити:

- Факултету
- архиви Универзитета



The PM_{2.5}-bound polycyclic aromatic hydrocarbon behavior in indoor and outdoor environments, part I: Emission sources

Svetlana Stanišić^{a,*}, Mirjana Perišić^{a,b}, Gordana Jovanović^{a,b}, Tijana Milićević^b, Snježana Herceg Romanić^c, Aleksandar Jovanović^b, Andrej Šoštarić^d, Vladimir Udovičić^b, Andreja Stojić^{a,b}

^a Singidunum University, 32 Danijelova Street, Belgrade, 11000, Serbia

^b Institute of Physics Belgrade, National Institute of the Republic of Serbia, University of Belgrade, 118 Pregrevica Street, 11000, Belgrade, Serbia

^c Institute for Medical Research and Occupational Health, 2 Ksaverska Cesta Street, PO Box 291, 10001, Zagreb, Croatia

^d Institute of Public Health Belgrade, 54 Despota Stefana Street, 11000, Belgrade, Serbia

ARTICLE INFO

Keywords:

Indoor/outdoor air quality
Polycyclic aromatic hydrocarbons
Source apportionment
XGBoost method
Explainable artificial intelligence

ABSTRACT

The previous research, aimed at exploring the relationships between the indoor and outdoor air quality, has evidenced that outdoor PM_{2.5}-bound polycyclic aromatic hydrocarbons (PAH) levels exhibit significant daily and seasonal variations which does not necessary corresponds with PAH indoor dynamics. For the purpose of this study, a three-month measurement campaign was performed simultaneously at indoor and outdoor sampling sites of a university building in an urban area of Belgrade (Serbia), during which the concentrations of O₃, CO, SO₂, NO_x, radon, PM_{2.5} and particle constituents including trace metals (As, Cd, Cr, Mn, Ni and Pb), ions (Cl⁻, Na⁺, Mg²⁺, Ca²⁺, K⁺, NO₃⁻, SO₄²⁻ and NH₄⁺) and 16 US EPA priority PAHs were determined. Additionally, the analysis included 31 meteorological parameters, out of which 24 were obtained from Global Data Assimilation System (GDAS1) database. The Unmix and PAH diagnostic ratios analysis resolved the source profiles for both indoor and outdoor environment, which are comparable in terms of their apportionments and pollutant shares, although it should be emphasized that ratio-implied solutions should be taken with caution since these values do not reflect emission sources only. The highest contributions to air quality were attributed to sources identified as coal combustion and related pyrogenic processes. Noticeable correlations were observed between 5- and 6-ring high molecular weight PAHs, but, except for CO, no significant linear dependencies with other investigated variables were identified. The PAH level predictions in the indoor and outdoor environment was performed by using machine learning XGBoost method.

1. Introduction

Polycyclic aromatic hydrocarbons (PAHs) are a complex group of pollutants generated during incomplete combustion of organic material. Only a small quantity of PAHs in the atmosphere originates from natural sources such as volcanic emissions, forest, and grassland fires. Their origin in ambient air of urban areas is associated with many emission sources, including fossil-fuel burning for power generation, transportation and heating, while in indoor environment, elevated concentrations of PAHs are related to tobacco smoke, the use of gas, coal or electric stoves, and candle burning (Gao et al., 2019). PAHs have

received most attention as a major public health concern globally because a vast number of studies has confirmed that the increased exposure to high-molecular weight (5-ring and more) PAHs is associated with altered mitochondrial dynamics and cumulative oxidative cellular damage (Brehmer et al., 2020). Eight PAHs have been classified by USEPA (1997) as carcinogenic or potentially carcinogenic, including benz[a]anthracene, chrysene, benzo[a]pyrene, benzo[b]fluoranthene, benzo[k]fluoranthene, dibenz[a,h]anthracene, indeno[1,2,3-cd]pyrene, and benzo[g,h,i]perylene. Among them, benzo[a]pyrene belongs to Group 1 of hazardous species – carcinogenic to humans (International Agency for Research on Cancer, 2012), and its emissions are regulated

* Corresponding author.

E-mail addresses: sstanic@singidunum.ac.rs (S. Stanišić), mirjana.perisic@ipb.ac.rs (M. Perišić), gordana.vukovic@ipb.ac.rs (G. Jovanović), tijana.milicevic@ipb.ac.rs (T. Milićević), sherceg@imi.hr (S.H. Romanić), aleksandar.jovanovic@ipb.ac.rs (A. Jovanović), andrej.sostaric@zdravlje.org.rs (A. Šoštarić), vladimir.udovicic@ipb.ac.rs (V. Udovičić), andreja.stojic@ipb.ac.rs (A. Stojić).

<https://doi.org/10.1016/j.envres.2020.110520>

Received 12 July 2020; Received in revised form 17 November 2020; Accepted 20 November 2020

Available online 28 November 2020

0013-9351/© 2020 Elsevier Inc. All rights reserved.

by the Directive 2004/107/Elie et al. (2015). Additionally, benzo[a]anthracene is assigned as probable carcinogenic to humans (Group 2A), and chrysene, benzo[b]fluoranthene, benzo[k]fluoranthene, dibenz[a,h]anthracene, and indeno[1,2,3-cd]pyrene as possibly carcinogenic to humans (Group 2B) (International Agency for Research on Cancer, 2012). The reactive PAH metabolites, emitted from combustion processes or formed in the heterogeneous reactions with atmospheric oxidants are also evidenced to have mutagenic and genotoxic potential (Elie et al., 2015).

Due to their sources and physico-chemical characteristics, PAHs are ubiquitous, found in all environmental compartments. Partitioning of PAHs between the gas and particulate phase has an important impact on their atmospheric fate, transport and chemical transformations of these compounds. It determines the extent of photo-degradation and photo-oxidation, and relative amounts of deposition that can occur by wet scavenging, dry deposition of particles, and by gas exchange between the air and water interface (Tasdemir and Esen, 2007). Generally, low-molecular weight PAHs are presented in a gas phase, while high-molecular weight PAHs are either sorbed to airborne coarse PM fraction and deposited close to the emission sources, or more often bound to fine suspended particles, $PM_{2.5}$ (Alves et al., 2014), which persist for a longer time in the atmosphere and penetrate deeper in the respiratory system. Beside the chemical complexity of PAHs, the gas/particle partitioning of these species also depends on their vapor pressure and concentrations, ambient temperature and type of particles present in the atmosphere (Keyte et al., 2013).

The previous studies have shown that the concentrations of PAHs can be found within the relatively wide range of values and show large variations on a daily and seasonal basis, depending on the vicinity and strength of sources and sinks (Pehneć et al., 2020). Since the major emission source of PAHs is fossil fuel burning, the reports mostly confirm that PAH concentrations reach their maximum during cold season, both indoors and outdoors (Majd et al., 2019; Sarigiannis et al., 2015). Besides increased emissions associated with residential heating, PAH levels in winter season are expected to be high due to reduced vertical air mixing caused by inversion, less intensive atmospheric reactions and enhanced sorption to particles at lower temperature, as a result of reduced vapor pressure and/or shifting in the gas/particle distribution induced by ambient temperature variations (Ravindra et al., 2006).

A number of studies have also reported a strong correlation between indoor and outdoor concentrations of PAHs, as well as their indoor-to-outdoor (I/O) ratio <1 , which indicates that indoor PAHs mostly originate from the outdoor environment (Krugly et al., 2014; Uchiyama et al., 2015). In these cases, the contributions of outdoor sources to indoor air concentrations were expected to follow seasonal variations, as shown in the study of Shi (2018), who estimated that indoor benzo(a)pyrene concentration in typical Beijing residence were outdoor source-affected by 72.3%, 60.3%, 65.2% and 82.9% in spring, summer, autumn and winter, respectively. However, there is also a number of studies which reported the I/O ratios of PAHs exceeding 1. For instance, the combustion of bituminous coal and unprocessed biomass in households in China, India, and other rural regions of Asia, remains the major source of indoor air pollution and PAHs, being present both in particle and gas phase (Wang et al., 2015b; Yao et al., 2019).

In this study, we have identified potential emission sources and investigated the relationships between meteorological parameters and indoor and outdoor O_3 , CO, SO_2 , NO_x , radon, $PM_{2.5}$ and particle constituents including trace metals (As, Cd, Cr, Mn, Ni and Pb), ions (Cl^- , Na^+ , Mg^{2+} , Ca^{2+} , K^+ , NO_3^- , SO_4^{2-} and NH_4^+) and 16 US EPA priority PAHs were determined, simultaneously collected at indoor and outdoor sites of a university building, located in the urban area of Belgrade (Serbia). At this location, lectures are visited by approximately 4000 students in total, and the indoor air sampling was conducted in an amphitheater having the capacity of 350 people. For this purpose, we used Unmix and eXtreme Gradient Boosting, the method that is highly adaptive to non-

parametric data distributions, less sensitive to error term assumptions, and tolerable to noise, chaotic components and heavy tails (Soštarić et al., 2017; Stojić et al., 2019). As shown, the PAH level predictions in the indoor and outdoor environment were successfully performed by using machine learning XGBoost method and the obtained results will be considered by using explainable artificial intelligence methods in the succeeding parts of this paper.

2. Materials and methods

2.1. Study variables

For the purpose of this study, a three-month (March 1st – May 31st) measurement campaign was performed simultaneously at indoor and outdoor sampling sites, during which the concentrations of inorganic gaseous pollutants, radon, $PM_{2.5}$ and particle constituents including trace metals (As, Cd, Cr, Mn, Ni, and Pb), ions (Cl^- , Na^+ , Mg^{2+} , Ca^{2+} , K^+ , NO_3^- , SO_4^{2-} , and NH_4^+) and 16 US EPA PAHs were regularly analyzed. For the analysis, several meteorological parameters were registered, including outdoor ambient air temperature, outdoor relative humidity, outdoor air pressure, wind and rain characteristics, indoor ambient air temperature, indoor relative humidity and indoor air pressure, while 24-parameter data were additionally obtained from Global Data Assimilation System (GDAS1). Additionally, the number of people in an amphitheater and the time they spent indoor was registered hourly.

2.2. Study area

Air sampling was performed at the rooftop and inside of the Singidunum University building ($44^\circ 45' 33.8''N$, $20^\circ 29' 47.6''E$). At this location, lectures are visited by approximately 4000 students in total. The indoor air sampling was conducted in an amphitheater having the capacity of 350 people, and the number of students in the amphitheater during the study period most often ranged from 50 to 80. The University building is surrounded by large residential areas from W, SW and NE side, some of which encompass households with individual fireboxes, while small scale industry referring to the Road Institute of Belgrade, a building company and beverage factory stockroom are located in the nearest vicinity. Additionally, confectionery factory, footwear factory, and several small-scale chemical plants are located 600 m in the NW and S direction, respectively. Around 800 m to the W and SW from the measurement site a large district heating plant and fuel oil heating plant of urban forestry organization, used for the purposes of planting material production, are situated. A boulevard with public transport and moderate vehicle flow passes by approximately 250 m in the SW direction, while a road with intense traffic is about 500 m away in the W–NW direction. The old city center and river confluence are located at the distance exceeding 2 km in the NW direction, while the air quality at the sampling site was occasionally affected by the emissions from two large city municipalities situated just across the river.

2.3. Experimental settings

The outdoor $PM_{2.5}$ and air sampling, as well as meteorological measurements were performed at the rooftop of the building, around 10 m above the ground. The indoor air sampling inlet and $PM_{2.5}$ sampling device were placed at a height of 6 m and 2 m from the floor, respectively.

Air sampling system comprised diaphragm vacuum pump Pfeiffer MVP and manifolds with openings for measuring inorganic gaseous pollutants (O_3 , CO, SO_2 , and NO_x) by using Horiba APOA, APMA, APSA, and APNA, 370 series, and electronically controlled valves, which operated in alternating indoor/outdoor air sampling mode in the 10-min cycles.

The $PM_{2.5}$ sampling was performed by using Svan Leckel LVS6-RV devices operating at a nominal flow rate of $2.3 \text{ m}^3 \text{ h}^{-1}$, over 24 h-

sampling period. The concentrations of PM_{2.5} and their constituents, including trace metals, ions and PAHs were determined at the reference laboratory of the Institute of Public Health of Belgrade. The limit of detection was 1 µg m⁻³.

The outdoor meteorological data were obtained by using Vaisala WXT530 monitoring station set at the building rooftop, while the indoor radon concentrations, ambient air temperature, relative humidity and air pressure were detected by SN1029 radon monitor (Sun Nuclear Corporation, NRSB approval code 31822) and corresponding integrated sensor devices, placed in the center of the amphitheater, at a height of 1 m from the floor.

2.4. Chemical analysis

PM_{2.5} was collected on quartz filters (Whatman QMA, 47 mm) daily, each morning before the start of daily indoor activities and weighted, as described in the Standard SRPS EN 12341:2015 (*Ambient air* - Standard gravimetric measurement method for the determination of the PM₁₀ or PM_{2.5} mass concentration of suspended particulate matter, 2015). The filters were pre-fired to remove organic impurities, and the pre-conditioning of both non-exposed and loaded filters was performed prior to gravimetric measurements. After gravimetric measurements, the surface of each filter, amounting to 13.85 cm², was cut in two pieces – approximately 1.76 cm² each, which were used for the analysis of anions and cations, while the remaining 12.09 cm² were divided and used for the analysis of trace elements and 16 US EPA PAHs.

For ion concentration measurements, the sample pieces underwent an ultra-pure water extraction for 24 h and the aqueous extracts were further analyzed by standard ion chromatography using a Dionex DX-500 IC system according to the MDL 064 Standard operating procedure. The method detection limits are presented in Table 2.

The concentrations of As, Cd, Cr, Ni, and Pb as PM_{2.5} constituents were determined as described in the SRPS EN 14902:2008/AC:2013 Standard (*Ambient air quality* - Standard method for the measurement of Pb, Cd, As and Ni in the PM fraction of suspended particulate matter, 2008). Firstly, CEN/TC 264 N779 procedure was applied for the extraction of the trace elements. In brief, the pieces of exposed quartz filters were treated with an acidic mixture of HNO₃(c)/30% H₂O₂/H₂O (3/2/5) using analytical grade reagents (Merck) and distilled/deionized water (MiliQ, 18.2 MΩ). The filters were digested in closed 100 ml Teflon vessels in the Anton Paar 3000 microwave accelerated reaction system and the concentrations of trace elements were determined by inductively coupled plasma–mass spectrometry (ICP-MS) (device Agilent 7500ce with Octopole Reaction System). Quality control and verification of the applied procedures for microwave digestion and multi-elemental trace analysis using ICP-MS was conducted by 2783 NIST (National Institute of Standard and Technology, MD, USA) standard reference material analysis containing a PM_{2.5} fraction of urban dust from a mixed industrial urban area of Vienna, collected on a polycarbonate membrane filter. The recovery values were within satisfactory range of ±20% from the reference value. The method detection limits are presented in Table 2.

Sixteen US EPA priority PAHs including naphthalene (Nap), acenaphthylene (Ace), acenaphthene (Ane), fluorene (Flu), phenanthrene (Phe), anthracene (Ant), fluoranthene (Fla), pyrene (Pyr), benz[a]anthracene (B[a]A), chrysene (Chy), benzo[b]fluoranthene (B[b]f), benzo[k]fluoranthene (B[k]F), benzo[a]pyrene (B[a]P), dibenz[a,h]anthracene (Db[ah]A), benzo[g,h,i]perylene (B[ghi]P), and indeno [1,2,3-cd]pyrene (In[cd]P) were determined by the procedure described in the SRPS ISO 12884:2010 Standard (*Ambient air* — Determination of total (gas and particle-phase) polycyclic aromatic hydrocarbons — Collection on sorbent-backed filters with gas chromatographic/mass spectrometric analyses, 2010).

Parts of the exposed filters underwent microwave extraction procedure with a solvent mixture of n-hexane and acetone (12.5 ml n-hexane:12.5 ml acetone) according to EPA method 3546. After

extraction, solution volume was reduced by rotary evaporation under reduced pressure (55.6 kPa and with 0.2 ml isoctane) to 1 ml. Afterwards, the n-hexane solution was reduced to 0.25 ml under a nitrogen stream. Known quantities of internal standards were added to estimate the method recovery. PAHs were analyzed using gas chromatography coupled with mass selective detector (Agilent GC 6890/5973 MSD) according to EPA compendium method TO-13A with a DB-5 MS capillary column (30 m × 0.25 mm × 25 µm). The oven temperature program started at 70 °C (duration 4 min), ramp 8 °C min⁻¹ to the end temperature of 310 °C (duration 5 min). The solvent delay was 5 min and the time of run was 46 min. The calibration curves for all 16 PAHs were obtained by spiking seven different quantities of each PAH, all with an R² of the calibration curve above 0.995. Recovery values ranged from 85% to 110% for all the PAHs contained in the internal standard. The method detection limits are presented in Table 2.

Inorganic gaseous pollutant indoor and outdoor measurements were conducted by using Horiba 370 series devices which enabled continual pollutant concentration monitoring with a 2 min-resolution data and detection limit of 1 µg m⁻³ for all species except of CO with detection limit of 0.1 mg m⁻³. More specifically, the CO concentrations were determined by non-dispersion cross modulation infrared spectroscopy method using APMA-370 device, as described in the SRPS EN 14626:2013 Standard. The concentrations of SO₂ were measured by UV fluorescence method using APSA-370 device, as described in the SRPS EN 14212:2013/AC:2015 Standard. The APMA-370 device was used for NO, NO₂, and NO_x concentration measurements by a combination of dual cross-flow modulation type chemiluminescence principle and the referential calculation method according to the SRPS EN 14211:2013

Table 1
Outdoor meteorological data used in analyses.

Outdoor meteorological data abbreviation	Origin	Meaning
WD	Vaisala	Wind direction
WS	Vaisala	Wind speed
Temp	Vaisala	Temperature
Rh	Vaisala	Relative humidity
Pressure	Vaisala	Pressure
Rain duration	Vaisala	Rain duration
Rain total	Vaisala	Rain intensity
Prss	GDAS1	Pressure at surface
Mslp	GDAS1	Pressure reduced to mean sea level
Tpp6	GDAS1	Accumulated precipitation (6 h accumulation)
Mofi	GDAS1	momentum flux intensity (3- or 6-h average)
Mofd	GDAS1	momentum flux direction (3- or 6-h average)
Shif	GDAS1	Sensible heat net flux at surface (3- or 6-h average)
Dswf	GDAS1	Downward short-wave radiation flux (3- or 6-h average)
Rh 2 m	GDAS1	Relative Humidity at 2m AGL
WD 10 m	GDAS1	wind direction at 10 m AGL
WS 10 m	GDAS1	wind speed at 10 m AGL
T0 2 m	GDAS1	Temperature at 2m AGL
Tcld	GDAS1	Total cloud cover (3- or 6-h average)
Cape	GDAS1	Convective available potential energy
Cinh	GDAS1	Convective inhibition
Lisd	GDAS1	Standard lifted index
Lib4	GDAS1	Best 4-layer lifted index
Pblh	GDAS1	Planetary boundary layer height
Tmps	GDAS1	Temperature at surface
Solm	GDAS1	Volumetric soil moisture content
Crai	GDAS1	Categorical rain (yes = 1, no = 0) (3- or 6-h average)
Lcld	GDAS1	Low cloud cover (3- or 6-h average)
Lhtf	GDAS1	Latent heat net flux at surface (3- or 6-h average)
Mcld	GDAS1	Middle cloud cover (3- or 6-h average)
Hcld	GDAS1	High cloud cover (3- or 6-h average)

Table 2
Descriptive statistics.

Variable	Mean	SD	Median	TM	MAD	Min	Max	Range	Skew	Kurtosis	SE	IQR	5th quantile	25th quantile	75th quantile	95th quantile	LOD
ⁱ Acenaphthylene [ng m ⁻³]	0.015	0.022	0.005	0.010	0	0.005	0.120	0.115	2.642	7.368	0.003	0.010	0.005	0.005	0.015	0.061	0.01
^o Acenaphthylene [ng m ⁻³]	0.020	0.038	0.005	0.011	0	0.005	0.262	0.257	4.063	20.989	0.004	0.006	0.005	0.005	0.011	0.087	0.01
ⁱ Acenaphthene [ng m ⁻³]	0.025	0.039	0.005	0.017	0	0.005	0.232	0.227	2.727	9.474	0.005	0.034	0.005	0.005	0.039	0.094	0.01
^o Acenaphthene [ng m ⁻³]	0.015	0.020	0.005	0.010	0	0.005	0.086	0.081	2.141	3.509	0.002	0.006	0.005	0.005	0.011	0.065	0.01
ⁱ Anthracene [ng m ⁻³]	0.029	0.043	0.010	0.020	0.008	0.005	0.286	0.281	3.500	16.369	0.005	0.034	0.005	0.005	0.039	0.089	0.01
^o Anthracene [ng m ⁻³]	0.033	0.034	0.023	0.027	0.026	0.005	0.141	0.136	1.383	1.354	0.004	0.040	0.005	0.005	0.045	0.106	0.01
ⁱ As [ng m ⁻³]	0.705	0.396	0.659	0.666	0.336	0.200	1.865	1.665	0.787	0.222	0.046	0.463	0.200	0.442	0.905	1.492	0.4
^o As [ng m ⁻³]	0.863	0.527	0.696	0.792	0.303	0.200	3.187	2.987	1.789	4.289	0.061	0.534	0.200	0.545	1.078	1.786	0.4
ⁱ Benzo(a)anthracene [ng m ⁻³]	0.326	0.901	0.093	0.157	0.061	0.020	7.249	7.229	6.349	44.574	0.105	0.128	0.028	0.060	0.189	0.786	0.01
^o Benzo(a)anthracene [ng m ⁻³]	0.359	0.534	0.164	0.230	0.148	0.028	2.419	2.391	2.558	6.205	0.062	0.205	0.035	0.085	0.290	1.491	0.01
ⁱ Benzo(a)pyrene [ng m ⁻³]	0.504	0.918	0.220	0.309	0.195	0.033	6.844	6.811	4.771	28.370	0.107	0.349	0.050	0.113	0.461	1.915	0.01
^o Benzo(a)pyrene [ng m ⁻³]	0.484	0.606	0.302	0.343	0.249	0.040	2.869	2.829	2.208	4.272	0.070	0.330	0.050	0.131	0.462	2.047	0.01
ⁱ Benzo(b)fluoranthene [ng m ⁻³]	0.699	1.040	0.331	0.475	0.271	0.084	7.106	7.022	3.821	18.276	0.121	0.435	0.106	0.208	0.643	2.173	0.01
^o Benzo(b)fluoranthene [ng m ⁻³]	0.888	0.892	0.592	0.706	0.444	0.104	3.842	3.738	1.790	2.381	0.104	0.588	0.150	0.290	0.878	3.215	0.01
ⁱ Benzo(ghi)perylene [ng m ⁻³]	0.571	0.727	0.347	0.418	0.241	0.005	4.896	4.891	3.464	15.448	0.085	0.333	0.103	0.198	0.530	1.864	0.01
^o Benzo(ghi)perylene [ng m ⁻³]	0.680	0.639	0.471	0.554	0.324	0.025	2.702	2.677	1.706	2.048	0.074	0.393	0.128	0.298	0.691	2.236	0.01
ⁱ Benzo(k)fluoranthene [ng m ⁻³]	0.595	0.927	0.293	0.395	0.252	0.061	6.472	6.411	4.067	20.567	0.108	0.402	0.080	0.141	0.543	1.866	0.01
^o Benzo(k)fluoranthene [ng m ⁻³]	0.737	0.759	0.479	0.583	0.402	0.074	3.395	3.321	1.753	2.313	0.088	0.526	0.105	0.237	0.763	2.608	0.01
ⁱ Ca ²⁺ [μg m ⁻³]	14.073	19.278	4.000	9.812	0	4.000	71.580	67.580	1.664	1.279	2.241	8.131	4.000	4.000	12.131	57.155	8
^o Ca ²⁺ [μg m ⁻³]	13.773	17.502	4.000	9.665	0	4.000	82.931	78.931	2.090	4.045	2.035	13.634	4.000	4.000	17.634	48.774	8
^o Cape [J kg ⁻¹]	51.783	82.647	12.956	32.783	19.209	0	376.429	376.429	2.187	4.580	9.607	76.688	0	0	76.688	228.632	/
ⁱ Cd [ng m ⁻³]	0.206	0.094	0.223	0.212	0.088	0.025	0.370	0.345	-0.524	-0.674	0.011	0.121	0.025	0.155	0.276	0.332	0.05
^o Cd [ng m ⁻³]	0.236	0.118	0.236	0.232	0.088	0.025	0.610	0.585	0.518	1.129	0.014	0.118	0.042	0.173	0.291	0.425	0.05
ⁱ Chrysene [ng m ⁻³]	0.527	1.214	0.214	0.292	0.161	0.021	9.406	9.385	5.739	36.940	0.141	0.254	0.050	0.129	0.383	1.157	0.01
^o Chrysene [ng m ⁻³]	0.645	0.806	0.357	0.464	0.281	0.025	3.781	3.756	2.271	4.777	0.094	0.432	0.087	0.178	0.609	2.602	0.01
^o Cinh [J kg ⁻¹]	-11.663	17.941	-4.383	-7.922	6.498	-103.941	0	103.941	-2.668	8.900	2.086	14.751	-43.827	-15.385	-0.634	0	/
ⁱ Cl ⁻ [μg m ⁻³]	1.716	3.191	1.000	1.000	0	1.000	23.696	22.696	5.361	30.549	0.371	0	1.000	1.000	3.385	3.385	2
^o Cl ⁻ [μg m ⁻³]	1.312	1.048	1.000	1.017	0	1.000	7.484	6.484	3.862	16.270	0.122	0	1.000	1.000	1.000	3.796	2
ⁱ CO [mg m ⁻³]	0.300	0.089	0.277	0.292	0.066	0.163	0.552	0.389	0.854	0.087	0.010	0.086	0.187	0.244	0.329	0.490	0.1
^o CO [mg m ⁻³]	0.287	0.093	0.259	0.278	0.067	0.154	0.549	0.395	0.879	-0.027	0.011	0.099	0.171	0.224	0.323	0.477	0.1
^o Crai	0.318	0.342	0.250	0.283	0.371	0	1.000	1.000	0.594	-1.113	0.040	0.625	0	0	0.625	0.875	/
ⁱ Cr [ng m ⁻³]	11.878	5.985	11.564	11.264	4.470	3.298	42.497	39.199	1.958	7.436	0.696	5.745	4.350	8.221	13.966	21.841	2

(continued on next page)

Table 2 (continued)

Variable	Mean	SD	Median	TM	MAD	Min	Max	Range	Skew	Kurtosis	SE	IQR	5th quantile	25th quantile	75th quantile	95th quantile	LOD
^o Cr [ng m ⁻³]	11.518	6.309	10.554	10.647	3.096	3.148	43.886	40.738	2.331	8.325	0.733	4.008	4.245	8.770	12.778	22.843	2
ⁱ Dibenz(a,h) anthracene [ng m ⁻³]	0.083	0.092	0.049	0.063	0.041	0.010	0.459	0.449	2.343	5.520	0.011	0.055	0.013	0.030	0.085	0.294	0.01
^o Dibenz(a,h) anthracene [ng m ⁻³]	0.097	0.095	0.076	0.080	0.057	0.010	0.526	0.516	2.401	7.004	0.011	0.076	0.014	0.036	0.112	0.256	0.01
^o Dswf [W m ⁻²]	213.026	83.677	233.059	218.129	76.098	31.203	340.581	309.379	-0.596	-0.624	9.727	107.664	59.545	162.581	270.246	331.919	/
ⁱ Fluoranthene [ng m ⁻³]	0.278	0.318	0.186	0.219	0.159	0.005	1.590	1.585	2.363	6.296	0.037	0.234	0.005	0.089	0.323	0.928	0.01
^o Fluoranthene [ng m ⁻³]	0.303	0.289	0.200	0.256	0.187	0.005	1.339	1.334	1.618	2.381	0.034	0.249	0.005	0.129	0.378	0.934	0.01
ⁱ Fluorene [ng m ⁻³]	0.047	0.087	0.005	0.026	0	0.005	0.483	0.478	2.811	8.697	0.010	0.035	0.005	0.005	0.040	0.246	0.01
^o Fluorene [ng m ⁻³]	0.044	0.090	0.005	0.022	0	0.005	0.565	0.560	3.445	14.293	0.010	0.030	0.005	0.005	0.035	0.214	0.01
^o Hcd [%]	44.152	30.992	44.324	43.252	36.578	0	97.779	97.779	0.082	-1.261	3.603	52.120	0.910	14.834	66.953	96.015	/
ⁱ Hours [h]	4.050	3.328	5.075	3.958	4.571	0	9.917	9.917	-0.044	-1.571	0.387	6.779	0	0.050	6.829	8.571	0.02
ⁱ Indeno(1,2,3-cd) pyrene [ng m ⁻³]	0.468	0.579	0.266	0.345	0.201	0.030	3.600	3.570	2.892	10.465	0.067	0.297	0.079	0.156	0.452	1.559	0.01
^o Indeno(1,2,3-cd) pyrene [ng m ⁻³]	0.544	0.533	0.378	0.436	0.287	0.011	2.287	2.276	1.779	2.434	0.062	0.352	0.087	0.220	0.572	1.899	0.01
^o Lcd [%]	29.195	29.453	20.919	25.591	29.538	0	95.328	95.328	0.833	-0.546	3.424	45.488	0	3.450	48.938	88.440	/
^o Lhft [W m ⁻²]	78.533	37.242	76.203	76.206	41.577	13.514	165.274	151.760	0.452	-0.445	4.329	54.832	26.739	47.589	102.421	150.402	/
^o Lib4 [K]	3.491	3.261	2.958	3.290	3.425	-2.279	10.531	12.810	0.489	-0.731	0.379	4.803	-0.629	0.776	5.579	9.467	/
^o Lisd K]	278.311	3.819	278.185	278.186	4.804	271.856	286.141	14.285	0.252	-1.029	0.444	6.296	272.866	274.967	281.263	284.601	/
^o Mcid [%]	30.270	28.819	21.181	27.393	31.332	0	92.883	92.883	0.605	-0.943	3.350	48.475	0	3.841	52.316	82.871	/
ⁱ Mn [ng m ⁻³]	3.415	2.021	3.043	3.111	1.148	1.000	11.816	10.816	1.831	4.271	0.235	1.556	1.000	2.393	3.949	8.076	2
^o Mn [ng m ⁻³]	3.525	1.479	3.102	3.318	0.845	1.000	9.188	8.188	1.458	2.332	0.172	1.478	2.106	2.580	4.058	6.322	2
^o Mofd [°]	159.516	102.558	146.173	155.967	99.381	1.458	360.091	358.634	0.367	-0.821	11.922	131.346	5.670	90.766	222.112	336.635	/
^o Mofi [N m ⁻²]	0.100	0.081	0.080	0.088	0.068	0.007	0.392	0.385	1.492	2.402	0.009	0.096	0.016	0.040	0.136	0.260	/
^o Mslp [hPa]	1012.724	5.565	1013.741	1013.006	5.473	1000.900	1023.753	22.853	-0.418	-0.610	0.647	8.269	1002.450	1008.730	1016.999	1019.859	/
ⁱ Naphthalene [ng m ⁻³]	0.028	0.043	0.005	0.019	0	0.005	0.224	0.219	2.123	4.940	0.005	0.026	0.005	0.005	0.031	0.106	0.01
^o Naphthalene [ng m ⁻³]	0.041	0.090	0.005	0.022	0	0.005	0.644	0.639	4.558	25.673	0.010	0.037	0.005	0.005	0.042	0.167	0.01
ⁱ NH ₄ [µg m ⁻³]	1.513	1.319	1.213	1.350	1.278	0.100	7.277	7.177	1.476	3.455	0.153	1.686	0.100	0.553	2.239	3.574	0.2
^o NH ₄ [µg m ⁻³]	2.486	2.311	1.955	2.132	2.074	0.100	12.042	11.942	1.516	2.831	0.269	2.707	0.100	0.840	3.548	7.441	0.2
ⁱ Ni [ng m ⁻³]	7.926	8.198	5.118	5.999	2.363	1.000	45.963	44.963	2.833	8.139	0.953	3.851	2.555	4.019	7.869	26.248	2
^o Ni [ng m ⁻³]	7.951	5.867	6.455	6.952	4.144	1.000	31.617	30.617	2.270	6.118	0.682	6.238	2.789	4.042	10.280	16.738	2
ⁱ NO ₃ [µg m ⁻³]	1.279	1.198	1.000	1.000	0	1.000	10.142	9.142	5.889	38.534	0.139	0	1.000	1.000	1.000	2.441	2
^o NO ₃ [µg m ⁻³]	4.423	3.898	3.325	3.776	3.447	1.000	16.987	15.987	1.422	1.892	0.453	5.524	1.000	1.000	6.524	11.475	2
ⁱ Pb [ng m ⁻³]	4.079	2.924	3.621	3.743	1.309	1.000	23.951	22.951	4.305	26.298	0.340	1.706	1.000	2.886	4.592	7.425	2
^o Pblh [m]	512.239	152.702	517.356	509.879	152.207	194.949	1070.878	875.929	0.439	0.935	17.751	202.364	279.869	407.687	610.051	733.540	/
^o Pb [ng m ⁻³]	4.605	2.796	4.145	4.261	1.645	1.000	22.494	21.494	3.646	20.341	0.325	1.902	1.713	3.399	5.302	8.758	2
ⁱ People	185.973	208.428	167.500	154.183	244.629	0	1226.000	1226.000	2.066	6.876	24.229	275.500	0	0.500	276.000	504.950	1
ⁱ Phenanthrene [ng m ⁻³]	0.166	0.266	0.083	0.110	0.116	0.005	1.478	1.473	3.284	12.544	0.031	0.207	0.005	0.005	0.212	0.559	0.01
^o Phenanthrene [ng m ⁻³]	0.170	0.226	0.116	0.124	0.165	0.005	1.215	1.210	2.302	6.289	0.026	0.222	0.005	0.005	0.227	0.595	0.01
ⁱ Pressure [mbar]	992.676	5.536	993.555	992.979	5.421	980.996	1003.425	22.429	-0.441	-0.604	0.643	8.281	982.196	988.749	997.030	999.778	1
ⁱ PM _{2.5} [µg m ⁻³]	16.196	7.340	14.729	15.540	6.859	4.182	45.266	41.083	1.155	2.192	0.853	8.534	6.920	11.550	20.084	28.374	1
^o PM _{2.5} [µg m ⁻³]	17.469	8.003	15.862	16.527	5.411	5.785	50.718	44.933	1.509	3.193	0.930	8.335	7.728	12.493	20.828	31.164	1
^o Pressure [mbar]	992.732	5.548	993.813	993.049	5.336	981.037	1003.086	22.049	-0.471	-0.611	0.645	7.895	982.043	989.185	997.080	999.670	1
^o Prss [hPa]	988.226	5.417	989.418	988.564	5.342	976.491	998.371	21.880	-0.500	-0.585	0.630	8.186	977.957	984.653	992.839	994.732	/
ⁱ Pyrene [ng m ⁻³]	0.320	0.396	0.193	0.237	0.162	0.010	2.451	2.441	2.917	10.602	0.046	0.252	0.032	0.107	0.359	1.146	0.01

(continued on next page)

Table 2 (continued)

Variable	Mean	SD	Median	TM	MAD	Min	Max	Range	Skew	Kurtosis	SE	IQR	5th quantile	25th quantile	75th quantile	95th quantile	LOD
^o Pyrene [ng m ⁻³]	0.338	0.313	0.216	0.282	0.190	0.011	1.426	1.415	1.580	1.835	0.036	0.269	0.053	0.129	0.397	1.046	0.01
^o Rain duration [h]	1.536	2.707	0.025	0.908	0.037	0	12.233	12.233	2.031	3.698	0.315	2.094	0	0	2.094	8.071	0.02
^o Rain total [h]	181.989	394.929	0.200	79.413	0.297	0	1897.600	1897.600	2.689	7.019	45.910	131.025	0	0	131.025	1082.645	0.02
^o Rh 2 m [%]	67.950	13.061	70.443	68.355	17.070	42.081	89.196	47.115	-0.202	-1.155	1.518	21.989	45.916	56.685	78.674	86.306	/
ⁱ Rh [%]	36.783	7.795	36.081	36.741	7.334	20.200	56.985	36.785	0.110	-0.233	0.906	9.109	23.257	32.017	41.126	50.248	0.1
^o Rh [%]	61.534	15.717	59.228	61.545	19.299	31.208	89.668	58.460	0.050	-1.102	1.827	25.973	37.166	49.299	75.272	86.138	0.1
ⁱ Rn Bq m ⁻³	74.525	24.616	67.884	71.065	16.289	40.802	141.425	100.623	1.204	0.746	2.862	23.144	46.196	58.665	81.809	130.946	0.1
^o Shif [W m ⁻²]	25.551	19.374	26.026	25.027	20.546	-23.071	80.690	103.761	0.289	0.197	2.252	27.280	-0.973	11.112	38.392	52.471	/
ⁱ SO ₂ [µg m ⁻³]	1.849	1.453	1.204	1.588	0.683	0.573	6.913	6.340	1.572	1.605	0.169	1.324	0.632	0.924	2.248	4.867	1
^o SO ₂ [µg m ⁻³]	3.155	2.638	2.269	2.671	1.601	0.590	12.225	11.635	1.769	2.851	0.307	2.710	0.886	1.336	4.046	8.596	1
ⁱ SO ₄ ²⁻ [µg m ⁻³]	5.319	3.961	4.466	4.819	3.106	0.500	19.170	18.670	1.223	1.752	0.460	4.221	0.500	2.906	7.127	12.942	1
^o SO ₄ ²⁻ [µg m ⁻³]	7.051	4.498	6.594	6.682	3.612	0.500	23.972	23.472	1.102	1.915	0.523	4.752	0.500	4.207	8.959	15.007	1
^o Solm [frac.]	0.299	0.017	0.299	0.299	0.018	0.260	0.330	0.070	-0.066	-0.635	0.002	0.021	0.276	0.290	0.311	0.328	/
^o T 2 m [°C]	12.766	4.421	13.353	12.725	4.534	4.220	20.853	16.633	0.000	-1.030	0.514	6.747	5.920	8.922	15.668	20.107	/
^o Tcld [%]	58.645	31.046	67.126	60.005	42.229	1.370	99.905	98.535	-0.298	-1.258	3.609	55.332	8.101	28.569	83.901	99.435	/
ⁱ Temp [°C]	23.407	1.525	23.371	23.376	1.635	20.290	27.921	7.631	0.230	-0.095	0.177	2.224	21.076	22.235	24.459	25.821	0.1
^o Tmps [°C]	13.020	4.231	13.439	13.006	4.591	5.015	20.795	15.780	-0.035	-1.020	0.492	6.691	6.356	9.146	15.837	19.966	/
^o Temp [°C]	13.843	4.953	14.148	13.833	5.703	4.785	22.977	18.192	-0.012	-1.005	0.576	7.127	5.587	10.193	17.321	21.746	0.1
^o Tpp6 [m]	0	0.001	0	0.000	0	0	0.003	0.003	1.922	2.835	0.000	0	0	0	0	0.001	/
^o WD 10 m [°]	210.976	60.974	208.671	211.261	70.035	88.849	325.800	236.951	-0.021	-0.892	7.088	94.971	110.998	163.167	258.138	310.858	/
^o WD [°]	220.327	74.935	225.833	222.170	87.768	23.289	359.233	335.944	-0.220	-0.638	8.711	116.300	112.880	166.137	282.437	326.362	1
^o WS 10 m [m s ⁻¹]	3.136	1.103	2.963	3.038	1.239	1.550	6.111	4.561	0.662	-0.178	0.128	1.693	1.736	2.143	3.835	5.318	/
^o WS [m s ⁻¹]	1.467	0.478	1.328	1.427	0.433	0.730	2.759	2.029	0.730	-0.284	0.056	0.589	0.905	1.115	1.704	2.299	0.1

*Abbreviations: standard deviation (SD), truncated mean (TM), median absolute deviation (MAD), standard error (SE), interquartile range (IQR), limit of detection (LOD).

**prefix: i – indoor, o – outdoor.

Standard. Continuous monitoring of O₃ concentrations was performed by the cross-flow modulated ultraviolet absorption method using APOA-370 device according to the SRPS EN 14625:2013 Standard.

The indoor concentrations of radon (Bq m⁻³) were measured by using SN1029 radon monitor (Sun Nuclear Corporation, NRSB approval-code 31822). The device consists of two diffused junction photodiodes which serve as a radon detector and is equipped with sensors for temperature, barometric pressure and relative humidity. The device was set to simultaneously record radon concentration, temperature, atmospheric pressure, and relative humidity with a time resolution of 30 min.

2.5. Meteorological data

The outdoor meteorological data (air pressure, temperature, humidity, rainfall, and wind speed and direction) were obtained by using Vaisala weather station (Weather Transmitter WXT530 Series). Additionally, 24-parameter meteorological data for the sampling site location were obtained with a time resolution of 3 h from Global Data Assimilation System (GDAS1) database, by using MeteInfo software for meteorological data visualization and analysis (Wang, 2014), Table 1.

2.6. Data analysis

After the exclusion of outliers and incomplete cases, a total of 74 samples were used for data analysis. Descriptive statistics (including box plots), probability density functions, correlation analysis (including hierarchical clustering) and time series analysis were obtained and presented by using R packages 'ggdendro' (de Vries and Ripley, 2016), 'Hmisc' (Harrell, 2019), 'ggplot2' (Wickham, 2016), and 'plotly' (Sievert, 2020).

For the purpose of source apportionment, the Unmix receptor model was applied (US EPA Unmix 6). The species were selected for the analysis by using an initial species function. Other pollutants were subsequently added to test stability of the minimal solution and explore whether any of them can lead to a better solution. Finally, a total of 14 and 11 pollutants were chosen as Unmix input variables resulting in a four-factor solution for both indoor and outdoor environments. The concepts underlying Unmix have been described in a geometrical and intuitive manner, and the mathematical details are presented elsewhere (Henry 2003).

Regression analysis by means of XGBoost was implemented for estimating the relationships between each PAH concentrations and all other PAHs, inorganic gaseous pollutants, radon, PM_{2.5} and particle constituents (trace metals and ions), meteorological parameters (measured and GDAS1-modeled), the number of people in the amphitheater and the time they spent indoors, trend, weekday and weekend (39 and 64 parameters in total for indoor and outdoor environment, respectively).

XGBoost refers to a highly effective ML technique of building a complex prediction model by iterative combining ensembles of weak prediction models into a single strong learner. In the tree growing algorithm used by XGBoost each decision tree serves to complement all others and correct for the residuals in the predictions made by the previous ones (Sheridan et al., 2016). The XGBoost was successfully applied in a number of studies due to its core advantages being related to handling sparse data, excellent predictive performance, highly optimized multicore and the complexity penalization of the trees that was not commonly used for previous additive tree models (Mitchell and Frank, 2017; Nielsen, 2016). In this study, we used Python (Python Software Foundation) XGBoost implementation (XGBoost Python Package). The dataset was split into training (80%) and validation (20%) set. Hyperparameter tuning was implemented using a brute-force grid search and stratified 10-fold cross-validation that was replicated ten times. The best performing hyperparameter values were used for the final model. The obtained results will be considered in details by the application of explainable artificial intelligence methods in the

succeeding parts of this paper.

Beside conventional images, we present all the relevant findings as interactive plots produced by using R package 'plotly' hosted at the web page designed to support this paper at www.envpl.ipb.ac.rs/papers/20/PAHs/.

3. Results

As can be seen in Table 2 and Fig. 1, mean indoor PM_{2.5}-related PAH concentrations (4.68 ng m⁻³) were lower than the corresponding outdoor values (5.40 ng m⁻³), although occasional extreme PAH concentration events were shown to reach almost two times higher values in the indoor compared to the outdoor environment (45.79 and 27.49 ng m⁻³, respectively). Concentration distribution of all investigated PAHs, inorganic ions and trace elements in the indoor and outdoor environment, except CO, Cr and radon, appeared to be unimodal and positively skewed with a noticeable long right-sided tail (Fig. 2), which indicates that the majority of the measured pollutant concentrations are distributed within the first quartile of the registered range (Table 2). A sharp symmetrical bell-shaped curve of Rn can be inferred as a result of natural emissions, while the Cr concentration distribution suggests its levels are less affected by human activities (Pongpiachan and Iijima, 2016). Unsurprisingly, in both the indoor and outdoor environment, the concentrations of higher molecular weight (5-ring and more) PAHs in PM fine fraction exceeded the levels of volatile and semi-volatile low weight 2- and 3-ring aromatics, which are under normal ambient conditions almost entirely distributed in a gas phase (Table 2, Fig. 1).

Considering the meteorological factors, the same applies to the rain/precipitation parameters, convective potential energy, and low cloud coverage, whereas convective inhibition data exhibited the opposite, negatively skewed distribution with a long left-sided tail. The uniform to normal distribution of the relative humidity, temperature and PBL height data is evidenced, while wind direction, soil humidity, as well as relative humidity and temperature at 2 m data followed bimodal value distribution patterns implying two distinct ambiances which took turns over the study period. The beginning of the sampling campaign was marked by frequent cyclonic activity, mean daily temperatures below 12 °C, strong wind episodes and frequent precipitation events. A high-pressure system was established over the Balkans in mid-March (17th to 21st), bringing calm weather without precipitations and more sunshine hours, although mean daily temperature did not exceed 12 °C. The last days of March were marked by variable weather conditions, occasional precipitations and strong wind. An upper-level ridge in pressure prevailed in the first days of April causing the arrival of warmer and drier air masses. From April 8th recurrent changes in weather were caused by penetration of cold air fronts and frequent lowering of mean daily temperature. Changeable weather and temperatures below 12 °C, caused by the upper-level trough in the pressure field continued over the first few days of May. Calm and dry weather in the middle of May was followed by a sudden change, when a passage of a cold front led to intense rainfall, significant wind gusts and sharp decrease in temperature. The end of the study campaign was marked by the penetration of warmer and drier air masses from S direction. Details on meteorological conditions are presented in the Supplementary Fig. 1.

According to our results, total PAH concentrations exhibit sharp decrease from the start of the study campaign (March 1st) till April 1st, followed by a slower decline till the end of May. The total PAH concentrations exhibited weekly dynamics with the lowest values in the outdoor environment on Wednesday, which increased to their maximum levels on Friday and subsequently declined on Saturday and Sunday (Supplementary Fig. 2). It should also be noted that outdoor PAH weekly behavior pattern corresponded to indoor air quality variations, with an exception of weekend period, when the increase in outdoor concentrations preceded the rise in indoor PAH levels. The weekly dynamics of PAH levels suggest that the anthropogenic activities were intensified over the working days, particularly on Monday and Friday, while on

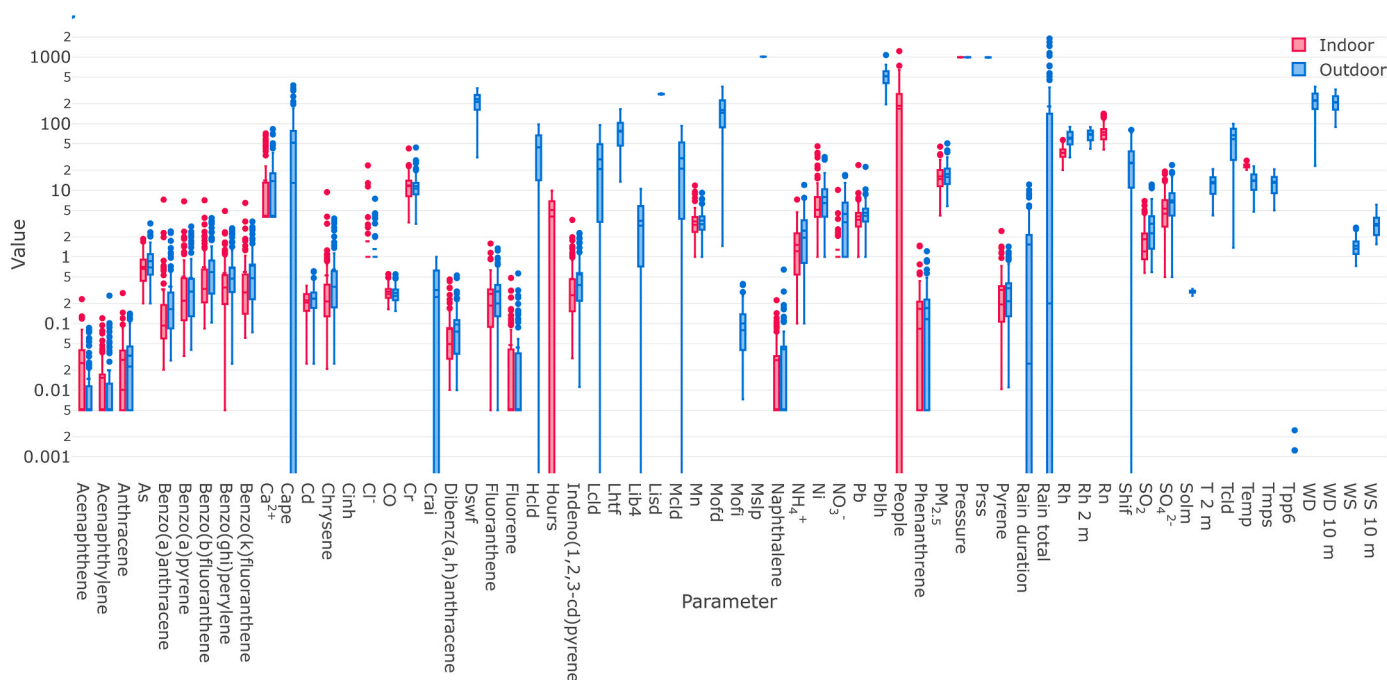


Fig. 1. The box plot of all indoor and outdoor measured parameters.

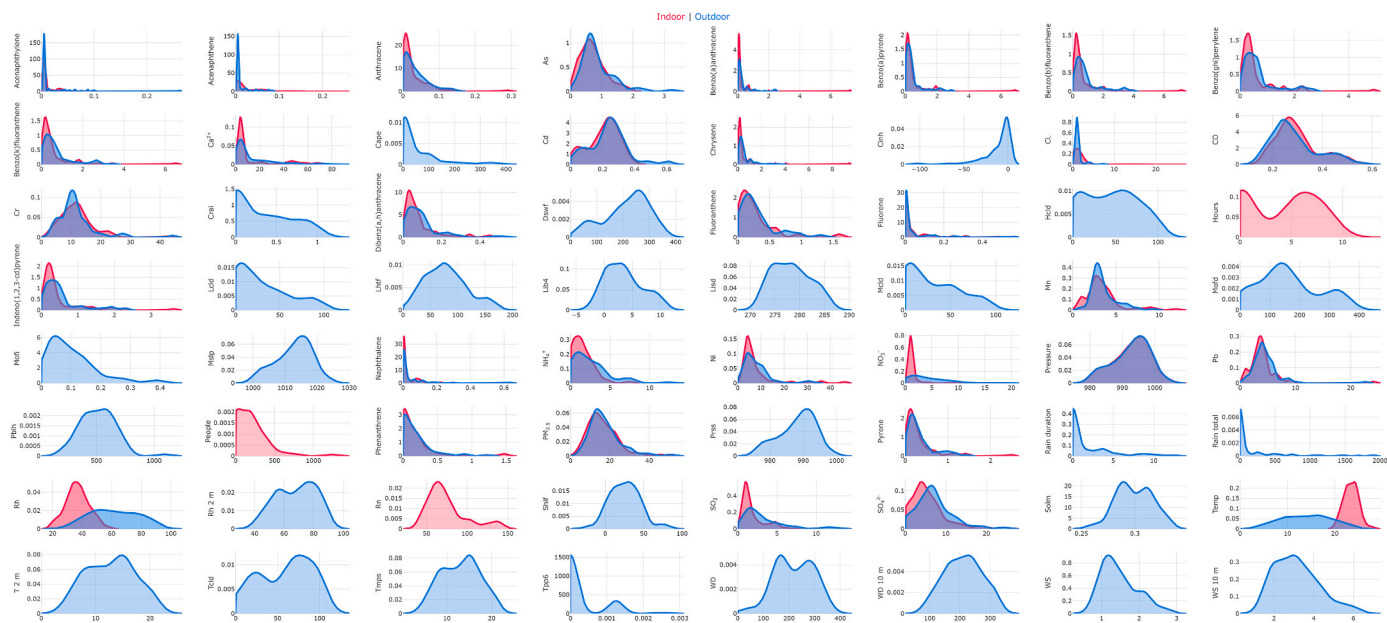


Fig. 2. The probability density function for indoor and outdoor measured parameters.

weekend, pollutant levels declined due to the decrease in industrial and traffic emissions, and the outdoor emission sources took on the role of major pollutant contributors.

As represented by correlation matrix (Fig. 3), significant linear correlation coefficients ($r > 0.90$) were found between the indoor concentrations of B[a]A, Chy, I[cd]P, B[ghi]P, B[k]F, B[b]F, B[a]P, and Fla, and the same applies to the outdoor environment. The correlations between the indoor and outdoor levels of the listed PAHs was in the range from 0.50 to 0.70. These results suggest similar behavior and common sources of the listed contaminants, being discussed in details below. Considering other investigated variables, the correlations were only registered between the indoor and outdoor levels of PAHs and CO ($r = 0.60\text{--}0.80$). We assumed that other functional dependencies apart from

linear could be further investigated to describe associations between PAHs and inorganic pollutants or meteorological variables, which will be considered in details in the succeeding parts of this paper.

The Unmix resolved profiles are presented together with their contributions to the total observed pollutant concentrations in Table 3. A detailed description of profile identification-relevant factors is provided in the following text.

Also, several PAH diagnostic ratios are calculated and considered in the following text.

The XGBoost provided successful and reliable predictions of Pyr, I [cd]P, B[ghi]P, B[k]F, B[b]F, B[a]P, and Chy in indoor and outdoor ambient with relative errors (normalized mean gross error, NMGE) in the range from approx. 10%–20% and correlation coefficients higher

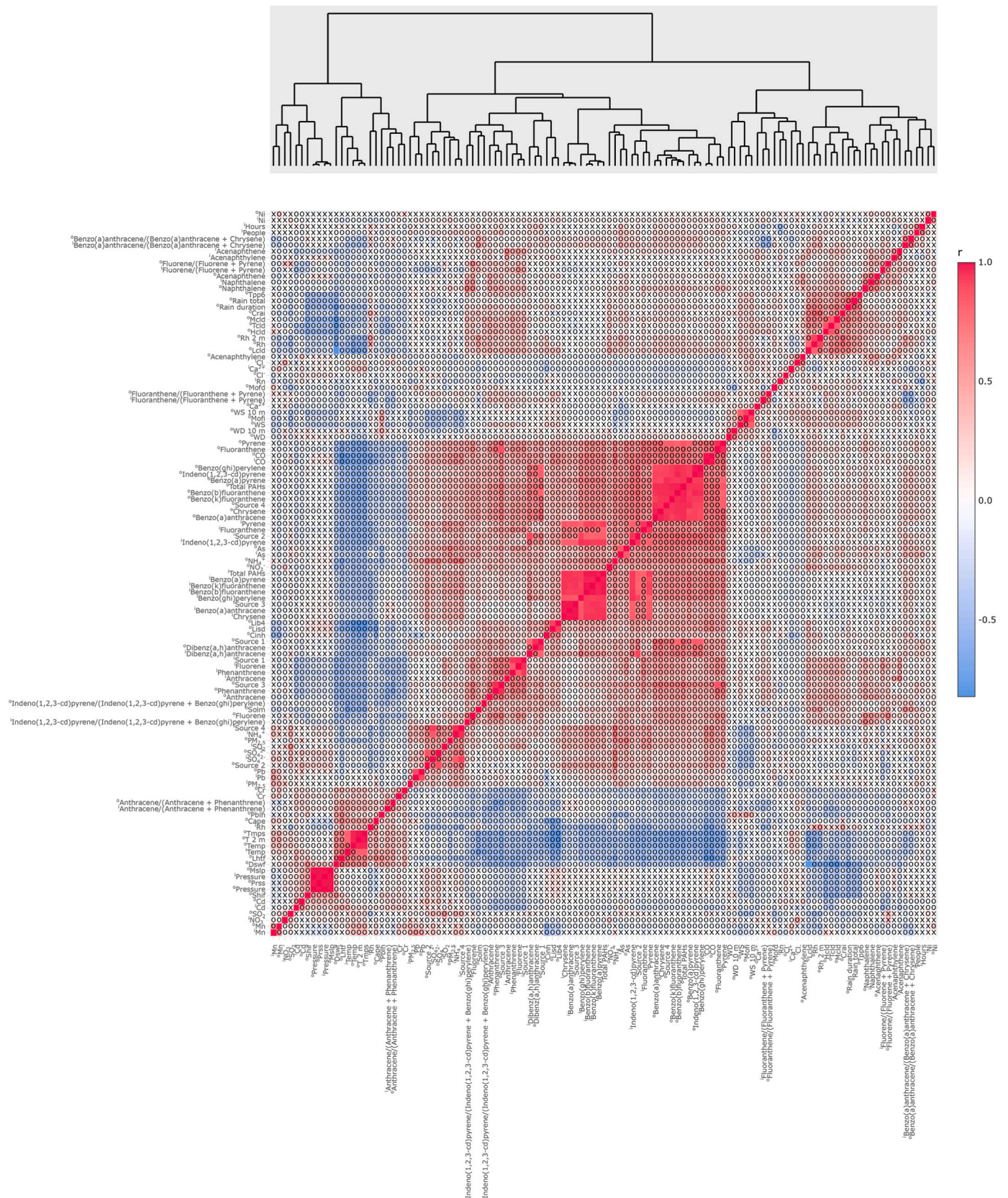


Fig. 3. The correlation matrix for indoor and outdoor measured parameter values.

Table 3
Unmix-resolved source profiles [%].

Species	Indoor				Outdoor			
	Source 1 ⁱ PE	Source 2 ⁱ CPC	Source 3 ⁱ PP	Source 4 ⁱ I/TE	Source 1 ^o CC	Source 2 ^o TE/PE	Source 3 ^o PE	Source 4 ^o PP
SO ₄	0	0	0	100	7.6	74.1	18.3	0
NH ₄	1.7	0	0	98.3	–	–	–	–
Flu	90.4	8.1	1.5	0	–	–	–	–
Phe	74.6	25.4	0	0	0	0	100	0
Fla	38.6	20.2	21.6	19.6	0	28.0	56.9	15.0
Pyr	28.5	15.5	31.8	24.2	–	–	–	–
B[a]A	3.1	8.2	88.7	0	27.7	0	1.2	71.1
Chy	3.8	5.3	80.1	10.9	27.5	0	11.8	60.8
B[b]F	3.9	44.6	34.9	16.6	29.1	16.9	5.6	48.3
B[k]F	5.5	39.8	39.0	15.8	19.2	23.0	7.3	50.5
B[a]P	6.9	49.0	44.1	0	8.7	18.7	0	72.6
I[cd]P	0	79.5	15.5	5.0	40.1	18.1	0	41.8
D[ah]A	0	100	0	0	84.6	13.7	1.7	0
B[ghi]P	0	79.6	18.8	1.6	38.0	21.8	0	40.2
Average contribution	18.4	33.9	26.8	20.9	25.7	19.5	18.4	36.4

ⁱ – indoor, ^o – outdoor.

**PE – petrogenic emissions, CPC – coal and petroleum combustion, PP – pyrogenic processes, I/TE – industrial and traffic emissions, CC – coal combustion, TE/PE – traffic and petrogenic emissions.

than 0.95 (Table 4). Satisfactory predictions were also evidenced for Fla, D[ah]A, and B[a]A, as described by model parameters (NMGE \approx 30%, $r \geq 0.95$). An effective model performance for the listed PAHs is indicated by the high values of coefficient of efficiency (COA = 0.83–0.88; a perfect model has a COA = 1) and index of agreement (IOA > 0.90; the values approaching 1 represent good model performances), as well as low values of mean bias and mean gross error. The prediction of 2- and 3-ring low molecular weight PAHs (Ane, Nap, Phe, Ace, Ant, and Flu) was less accurate (relative error = 35%–70%; and $r = 0.80$ –0.90), which is expected since those compounds are highly volatile and more gas-phase distributed.

4. Discussion

As regards PM_{2.5}-related organic content, the study of Jedynska et al. (2014), aimed to investigate the levels of PAHs in fine particle fraction at street, urban and regional background, has shown that total PAH concentrations did not exceed 2.1 ng m⁻³ for all ten investigated sites in Europe. On the other hand, the studies performed in Asia have shown that the total PM_{2.5}-bound PAH concentrations were up to 50 ng m⁻³ (Wang et al., 2017), and even 70 ng m⁻³ (Xu et al., 2015). While the majority of studies have shown the outdoor PM_{2.5}-bound PAH levels to be higher than the corresponding values in the indoor environment in the same season, some studies have shown the opposite (Wang et al., 2020). In comparison with the previous reports, it becomes evident that PAH concentrations in Serbia are significantly higher than it would be expected, considering the air quality in neighbouring countries and air pollution in Serbia can be attributed to a rise in the number of vehicles over the last two decades, the use of outdated technologies in all production sectors, high number of local fireboxes and long-range transport of pollutants from surrounding industrial countries (Stojić et al., 2015, 2016; Perišić et al., 2017). The study of Cvetković et al. (2015) has investigated source contributions to the registered high concentrations of PAHs in Belgrade area, and shown that all sites were heavily influenced by diesel and gasoline emissions, as well as by stationary sources (combustion of oil, industry, residential heating).

The dominant shares of Flu (90%) and Phe (75%) considered to be associated with petrogenic emissions (ⁱPE) were apportioned to indoor Source 1, together with 2–3 times lower contributions of Fla and Pyr and negligible shares of other pollutants. Petrogenic PAHs mostly originate from the low temperature-combustion of crude oil and its products, including kerosene, gasoline, diesel fuel and lubricating oil, and their contributions was estimated to account for 18.4% of the total indoor

pollutant concentrations. The highest contribution to the observed indoor pollutant concentrations, amounting to 33.9%, was associated with the indoor Source 2 dominated by D[ah]A (100%). The significant shares of other PAHs in the following order I[cd]P=B[ghi]P > B[a]P > B[b]F > B[k]F \gg Phe > Fla > Pyr suggest that the source can be attributed to the coal and petroleum combustion (ⁱCPC). Apart from the dominant portions of Chy (88%) and B[a]A (80%), a smaller share of less alkylated and more stable PAHs including B[a]P, B[k]F, B[b]F, Pyr, Fla, B[ghi]P, and I[cd]P was apportioned to indoor Source 3. Considering the profile composition, this source with the estimated contribution of 26.8% was attributed to high temperature (350–1200 °C) pyrogenic processes (ⁱPP), which can be related to incomplete combustion of fossil fuels and biomass in power plants and local fireboxes, industrial coal and petroleum burning and traffic emissions. At high combustion temperatures organic compounds are cracked to reactive radicals that form stable gaseous high-weight PAHs during pyrosynthesis, which subsequently cool and condense on particles. The contribution of the indoor Source 4 attributed to a mix of industrial and traffic emissions (ⁱI/TE) accounted for 20.9% of total registered indoor pollutant concentrations. The species assigned to this source comprise dominant portions of inorganic ions SO₄²⁻ and NH₄⁺, assigned together with several times lower shares of Fla, Pyr, B[b]F, and B[k]F, suggesting dual emission origin.

The dominant portion of D[ah]A (84.6%) and significant shares of other PAHs in the following order I[cd]P=B[ghi]P > B[b]F = B[a]A = Chy > B[k]F suggest that the outdoor Source 1 with the estimated contribution of 25.7% can be attributed to the coal combustion (^oCC). Apart from the dominant portion of SO₄²⁻ (74.1%), followed by Fla (28%), a smaller shares of B[k]F, B[ghi]P, B[a]P, I[cd]P, B[b]F, and D[ah]A was apportioned to the outdoor Source 2. Considering the profile composition, this source with the estimated contribution of 19.5% was attributed to a mix of traffic and petrogenic emissions (^oTE/PE). The contribution of the outdoor profile 3 attributed to petrogenic emissions (^oPE) was estimated to 18.4% of the registered pollutant concentrations, with the assigned species contributing in the following order Phe (100%) > Fla \gg SO₄²⁻ and the absence of B[a]P. The outdoor Source 4 attributed to pyrogenic processes (^oPP) had the highest contribution of 36.4% to the total outdoor pollutant concentrations, and was distinguished by significant portions of B[a]P (72.6%) = B[a]A > Chy > B[k]F = B[b]F > I[cd]P = B[ghi]P, and the absence of D[ah]A. The origin of outdoor PAHs is mostly dependent on sampling location and surrounding emission sources. In industrial areas, such as the ones explored in the study of Kermani et al. (2019), industrial activities were identified as the main contributor to air quality deterioration. On the other hand,

Table 4
XGBoost model evaluation statistics.

PAH	Indoor						Outdoor									
	FAC2	MB	MGE	NMGE	RMSE	r	COE	IOA	FAC2	MB	MGE	NMGE	RMSE	r	COE	IOA
Ace	0.780	0.002	0.004	0.399	0.006	0.874	0.503	0.751	0.593	-0.004	0.010	0.511	0.016	0.817	0.525	0.763
Ane	0.591	-0.006	0.016	0.610	0.038	0.807	0.491	0.746	0.711	0.002	0.007	0.541	0.011	0.747	0.405	0.703
Ant	0.785	0.004	0.008	0.387	0.012	0.926	0.566	0.783	0.727	0.003	0.010	0.451	0.015	0.798	0.501	0.750
B[a]A	0.846	0.035	0.042	0.311	0.081	0.967	0.681	0.840	0.798	-0.019	0.058	0.192	0.131	0.985	0.833	0.917
B[a]P	0.851	0.019	0.044	0.154	0.071	0.985	0.844	0.922	0.757	0.011	0.048	0.158	0.098	0.983	0.874	0.937
B[b]F	0.915	0.013	0.058	0.127	0.108	0.987	0.881	0.941	0.838	-0.014	0.089	0.109	0.148	0.992	0.897	0.949
B[ghi]P	0.919	0.016	0.035	0.102	0.055	0.995	0.887	0.943	0.850	-0.049	0.062	0.149	0.113	0.989	0.836	0.918
B[k]F	0.915	0.016	0.044	0.126	0.074	0.990	0.877	0.939	0.850	-0.064	0.097	0.158	0.196	0.987	0.844	0.922
Chy	0.854	0.012	0.042	0.186	0.065	0.979	0.810	0.905	0.838	-0.060	0.120	0.212	0.243	0.985	0.827	0.913
D[ah]A	0.818	-0.007	0.019	0.286	0.035	0.969	0.713	0.857	0.753	-0.006	0.025	0.293	0.039	0.945	0.647	0.824
Fla	0.798	-0.029	0.057	0.307	0.153	0.970	0.716	0.858	0.794	0.002	0.021	0.125	0.029	0.987	0.851	0.926
Flu	0.667	0.003	0.010	0.398	0.019	0.942	0.686	0.843	0.487	-0.022	0.035	0.695	0.086	0.939	0.495	0.748
I[cd]P	0.919	-0.002	0.032	0.105	0.058	0.995	0.899	0.949	0.834	-0.016	0.046	0.115	0.082	0.995	0.881	0.940
Nap	0.582	-0.003	0.014	0.568	0.024	0.853	0.502	0.751	0.625	-0.005	0.015	0.451	0.026	0.902	0.628	0.814
Phe	0.665	-0.035	0.056	0.429	0.157	0.971	0.668	0.834	0.612	-0.008	0.036	0.359	0.068	0.953	0.662	0.831
Pyr	0.870	0.019	0.029	0.131	0.050	0.991	0.871	0.935	0.850	-0.010	0.041	0.152	0.080	0.971	0.833	0.916

the study of Liu et al. (2018) has shown that traffic emissions can be considered the most important PAH source, irrespectively of the sampling season, while some researchers (Zhang et al., 2020; Wang et al., 2015a) reported the dominance of coal combustion in colder part of the year.

As can be seen in Fig. 3, the linear correlations exceeding $r = 0.70$ were obtained for the following profile pairs: source profiles with smallest contributions to total indoor and outdoor PAH concentrations assigned to petrogenic emissions (^1PE and ^0PE); indoor and outdoor source profiles related to traffic emissions ($^1\text{I/TE}$ and $^0\text{TE/PE}$); and outdoor source profiles attributed to coal combustion and other pyrogenic processes (^0CC and ^0PP). Our results suggest that coal combustion and related pyrogenic processes are the dominant sources of PAHs in the study area, while the impact of traffic, industrial and gasoline emissions appear to be less significant. All Unmix resolved profiles with the exception of those associated with traffic exhaust, exhibited a sharp decrease in contributions in the range from 55 to 90%, from the start of the study campaign till the first days of April. In the period that followed, the source shares declined more slowly, while the contributions of profiles attributed to traffic emissions exhibited a continual decline over the entire study period reaching 40% and 70% of their initial shares for $^1\text{I/TE}$ and $^0\text{TE/PE}$ respectively, Supplementary Fig. 3.

As shown in the Supplementary Fig. 2, the contributions of almost all sources to the registered PAH concentrations decreased from the March to May. Thereby, the sharpest decline in emissions in the first weeks of the study period exhibited the indoor and outdoor sources related to coal combustion and other pyrogenic processes. The impact of traffic and industrial emissions remained relatively stable till the very end of measurement campaign.

The PAH isomeric pairs, *i.e.* the species with the same atomic structure such as Ant and Phe, are expected to behave similarly in the environment and thus, their concentration ratios are a commonly used tool for emission source identification and distinguishing of PAH pollution originating from pyrogenic and petrogenic processes, *i.e.* diesel and gasoline combustion emission, crude oil processing products and biomass or coal burning (Davis et al., 2019). For instance, the study of Yin and Xu (2018) has applied a diagnostic ratio to the particle-bound PAH source apportionment results, and identified diesel, gasoline, and coal combustion as the main emission sources affecting air quality, and the study of Khan et al. (2015) reported similar findings that were confirmed by the source apportionment analysis. Nevertheless, previous research, based on theoretical considerations and laboratory experiments, have suggested that, although different PAH ratios can be considered as valuable source apportionment indicators, the ratio-based conclusions should be drawn with caution since these values are often noticed to exhibit seasonal variations and can be affected by a number of environmental factors, such as the presence of free radicals, meteorological conditions which favor photoreactions, and particle size and characteristics (Tobiszewski and Namieśnik, 2012). Limited information in the literature regarding the specific conditions of partial or entire removal of PAHs from the environment can be found. However, it has been evidenced that their persistence increases with the molecular weight, which can be explained by the fact that higher molecular weight PAHs are mostly particle-bonded, predominantly (83–88%) found in fine fraction (Hassanvand et al., 2015) and more resistant to solar radiation and free radicals under natural conditions (Oliveira et al., 2019).

The Ant/(Ant + Phe) mean ratio higher than 0.1 with steady increase towards the end of the study period and occasional peaks reaching 0.5 indicated the dominance of pyrogenic sources over the three-month campaign, except the first days of April during which the warmer and drier air masses arrived and the corresponding ratio values were significantly below 0.1, suggesting the contribution of petrogenic emissions (Supplementary Fig. 2). However, the study of Kim et al. (2009) has shown that the Ant/(Ant + Phe) ratio could range from 0 to 1, depending on the extent of Ant photodegradation caused by the irradiation of different thickness layer-soot samples.

The B[a]A/(B[a]A + Chr) mean ratio just below the value of 0.35 for the major part of the study period indicated the impact of coal combustion with occasional contributions of vehicular emissions. In compliance with the aforementioned, in the warmer period around April 1st, the ratio values were lower which could be attributed to the impact of traffic emissions, but also to the fact that B[a]A decays faster when adsorbed on particles, which can add to B[a]A/(B[a]A + Chr) ratio decrease. From April 8th recurrent changes in weather were caused by penetration of cold air fronts and frequent lowering of mean daily temperature. It should be noted that indoor-outdoor B[a]A/(B[a]A + Chr) ratios exhibit stronger correlation (0.71) than other indoor-outdoor ratio values (Fig. 3), which suggests that, over the major part of study period, air quality in the indoor environment was strongly affected by the outdoor emissions related to coal combustion and traffic emissions.

The Fla/(Fla + Pyr) mean ratio in the range from 0.3 to 0.5 suggests the impact of petrogenic sources and combustion of fossil fuels other than coal. The significant decrease in the outdoor Fla/(Fla + Pyr) ratio values over the second part of the study period can be attributed to the changeable weather and temperatures below 12 °C, which caused less intense photoreactions that could otherwise lead to faster decay of particle-adsorbed Pyr (Kim et al., 2009).

The Fl/(Fl + Pyr) mean ratio below 0.5 can be attributed to gasoline emissions. In March, the Fl/(Fl + Pyr) mean ratio had the highest decrease in value of all ratios, which can be associated with calmer weather without precipitations and more sunshine hours, yet mean daily temperature did not exceed 12 °C, which resulted in shorter atmospheric life time of Fl.

The I[cd]P/(I[cd]P + B[ghi]P) mean ratio of 0.43, suggesting the impact of petroleum combustion and pyrogenic sources, was more or less steady throughout the entire study period, although some studies have shown that atmospheric lifetimes of these species and their ratio can be affected by UV radiation and ageing of particle fraction they are sorbed to.

As can be concluded, functional prediction of PM_{2.5}-bound PAHs in the indoor and outdoor environment can be achieved by using ML methods and further research of the pollutant dynamics and its dependency on meteorological factors or particle chemical composition would significantly benefit from the application of ML algorithms. The explained predictions of the obtained regression models by means of explainable artificial intelligence methods will be provided in the succeeding parts of this paper.

5. Conclusions

In this study, 16 US EPA priority PAHs were investigated in indoor and outdoor environment based on a three-month measurement campaign which included the concentrations of inorganic gaseous pollutants, radon, PM_{2.5} and particle-bound trace metals, ions, and PAHs, along with 31 meteorological parameters. The correlation analysis showed noticeable relationships between 5- and 6-ring high molecular weight PAHs, but, except for CO, no significant linear dependencies with other investigated variables were identified. The Unmix source apportionment analysis resolved four source profiles for both indoor and outdoor environment, which are comparable in terms of their apportionments and pollutant shares. The highest contributions to air quality were attributed to sources identified as coal combustion and related pyrogenic processes. Except the impact of traffic and industrial emissions, which remained relatively stable over the study period, the contributions of other sources to the registered PAH concentrations decreased towards the end of the measurement campaign. The analysis of PAH diagnostic ratios revealed the emission sources similar to those identified by source apportionment, although it should be emphasized that ratio-implied solutions should be taken with caution since these values are not a reflection of pollutant sources only, but also point to the impact of environmental factors on air quality. As shown by the evaluation parameters of the XGBoost-obtained models, the prediction of PAH

levels in the indoor and outdoor environment appears to be promising and their levels are partly determined by their molecular structure and physico-chemical properties including volatility and gas-particle phase partitioning. Although the presented methods are relevant for discriminating the origin of PAH emissions, supplementary approaches, such as machine learning and explainable artificial intelligence, are required to enhance the understanding of PAH dynamics and their functional relationships with influential factors in complex indoor and outdoor environments. The major contribution to air quality deterioration and high PAH concentrations in the study area was shown to be associated with coal combustion for heating purposes and other pyrogenic processes. It would be advisable to make a shift towards alternative heating sources which would be eco-friendlier.

CRediT authorship contribution statement

Svetlana Stanišić: Writing - original draft, Writing - review & editing. **Mirjana Perišić:** Data curation. **Gordana Jovanović:** Supervision. **Tijana Milićević:** Writing - original draft, Writing - review & editing. **Snježana Herceg Romanić:** Writing - original draft, Writing - review & editing. **Aleksandar Jovanović:** Conceptualization, Methodology, Software. **Andrej Šošarić:** Visualization, Investigation. **Vladimir Udovičić:** Visualization, Investigation. **Andreja Stojić:** Conceptualization, Methodology, Software.

Declaration of competing interest

The authors declare that they have no known competing financial interests or personal relationships that could have appeared to influence the work reported in this paper.

Acknowledgments

Funding: The authors acknowledge funding provided by the Institute of Physics Belgrade, through the grant by the Ministry of Education, Science and Technological Development of the Republic of Serbia, the Science Fund of the Republic of Serbia #GRANT No. 6524105, AI – ATLAS, as well as the Croatian Science Foundation – Project OPENTOX No. 8366.

Appendix A. Supplementary data

Supplementary data to this article can be found online at <https://doi.org/10.1016/j.envres.2020.110520>.

References

- Alves, C.A., Urban, R.C., Pegas, P.N., Nunes, T., 2014. Indoor/outdoor relationships between PM₁₀ and associated organic compounds in a primary school. *Aerosol Air Qual. Res* 14 (1), 86–98. <https://doi.org/10.4209/aaqr.2013.04.0114>.
- Ambient Air — Determination of Total (Gas and Particle-phase) Polycyclic Aromatic Hydrocarbons — Collection on Sorbent-Backed Filters with Gas Chromatographic/mass Spectrometric Analyses, 2010 available at: <https://iss.rs/en/project/show/iss:proj:24983>.
- Ambient Air - Standard Gravimetric Measurement Method for the Determination of the PM Mass Concentration of Suspended Particulate Matter, 2015 available at: <https://iss.rs/en/project/show/iss:proj:49389>.
- Ambient Air Quality - Standard Method for the Measurement of Pb, Cd, and Ni in the PM Fraction of Suspended Particulate Matter, 2008 available at: <https://iss.rs/en/project/show/iss:proj:18667>.
- Brehmer, C., Norris, C., Barkjohn, K.K., Bergin, M.H., Zhang, J., Cui, X., Teng, Y., Zhang, Y., Black, M., Li, Z., Shafer, M.M., 2020. The impact of household air cleaners on the oxidative potential of PM_{2.5} and the role of metals and sources associated with indoor and outdoor exposure. *Environ. Res.* 181, 108919. <https://doi.org/10.1016/j.envres.2019.108919>.
- Cvetković, A., Jovašević-Stojanović, M., Marković, D., Ristovski, Z., 2015. Concentration and source identification of polycyclic aromatic hydrocarbons in the metropolitan area of Belgrade, Serbia. *Atmos. Environ.* 112, 335–345. <https://doi.org/10.1016/j.atmosenv.2015.04.034>.
- Davis, E., Walker, T., Adams, M., Willis, R., Norris, G., Henry, R., 2019. Source apportionment of polycyclic aromatic hydrocarbons (PAHs) in small craft harbor

- (SCH) surficial sediments in Nova Scotia, Canada. *Sci. Total Environ.* 691, 528–537. <https://doi.org/10.1016/j.scitotenv.2019.07.114>.
- de Vries, A., Ripley, B., 2016. Ggndendro: Create Dendrograms and Tree Diagrams Using 'ggplot2'. R Package Version 0.1-20. <https://CRAN.R-project.org/package=ggndendro>.
- Directive 2004/107/EC of the European parliament and of the council of 15 December 2004 relating to arsenic, cadmium, mercury, nickel and polycyclic aromatic hydrocarbons in ambient air. *Official Journal of the European Union* 23 (1–16), 26/01/2005.
- Elie, M.R., Choi, J., Nkrumah-Elie, Y.M., Gonnerman, G.D., Stevens, J.F., Tanguay, R.L., 2015. Metabolomic analysis to define and compare the effects of PAHs and oxygenated PAHs in developing zebrafish. *Environ. Res.* 140, 502–510. <https://doi.org/10.1016/j.envres.2015.05.009>.
- Gao, X., Xu, Y., Cai, Y., Shi, J., Chen, F., Lin, Z., Chen, T., Xia, Y., Shi, W., Zhao, Z., 2019. Effects of filtered fresh air ventilation on classroom indoor air and biomarkers in saliva and nasal samples: a randomized crossover intervention study in preschool children. *Environ. Res.* 179, 108749. <https://doi.org/10.1016/j.envres.2019.108749>.
- Harrell, F., with contributions from Charles Dupont and many others, 2019. Hmisc: Harrell miscellaneous. R package version 4.3-0. <https://CRAN.R-project.org/package=Hmisc>.
- Hassanvand, M.S., Naddafi, K., Faridi, S., Nabizadeh, R., Sowlat, M.H., Momeniha, F., Gholampour, A., Arhami, M., Kashani, H., Zare, A., Niazi, S., 2015. Characterization of PAHs and metals in indoor/outdoor PM₁₀/PM_{2.5}/PM₁ in a retirement home and a school dormitory. *Sci. Total Environ.* 527, 100–110. <https://doi.org/10.1016/j.scitotenv.2015.05.001>.
- Henry, R.C., 2003. Multivariate receptor modeling by N-dimensional edge detection. *Chemometr. Intell. Lab. Syst. 65* (2), 179–189. [https://doi.org/10.1016/S0169-7439\(02\)00108-9](https://doi.org/10.1016/S0169-7439(02)00108-9).
- International Agency for Research on Cancer, 2012. *A Review of Human Carcinogens. Part F: Chemical Agents and Related Occupations. IARC Monographs on the Evaluation of Carcinogenic Risks to Humans.*
- Jedynska, A., Hoek, G., Eeftens, M., Cyrys, J., Keuken, M., Ampe, C., Beelen, R., Cesaroni, G., Forastiere, F., Cirach, M., de Hoogh, K., 2014. Spatial variations of PAH, hopanes/steranes and EC/OC concentrations within and between European study areas. *Atmos. Environ.* 87, 239–248. <https://doi.org/10.1016/j.atmosenv.2014.01.026>.
- Kermani, M., Jonidi Jafari, A., Gholami, M., Shahsavani, A., Taghizadeh, F., Arfaeina, H., 2019. Ambient air PM_{2.5}-bound PAHs in low traffic, high traffic, and industrial areas along Tehran, Iran. *Human and Ecological Risk Assessment*. Int. J. 1–18. <https://doi.org/10.1080/10807039.2019.1695194>.
- Keyte, I., Harrison, R., Lammel, G., 2013. Chemical reactivity and long-range transport potential of polycyclic aromatic hydrocarbons – a review. *Chem. Soc. Rev.* 42, 9333–9391. <https://doi.org/10.1039/c3cs60147a>.
- Khan, M.F., Latif, M.T., Lim, C.H., Amil, N., Jaafar, S.A., Dominick, D., Nadzir, M.S.M., Sahani, M., Tahir, N.M., 2015. Seasonal effect and source apportionment of polycyclic aromatic hydrocarbons in PM_{2.5}. *Atmos. Environ.* 106, 178–190. <https://doi.org/10.1016/j.atmosenv.2015.01.077>.
- Kim, D., Kumfer, B.M., Anastasio, C., Kennedy, I.M., Young, T.M., 2009. Environmental ageing of polycyclic aromatic hydrocarbons on soot and its effect on source identification. *Chemosphere* 76, 1075–1081. <https://doi.org/10.1016/j.chemosphere.2009.04.031>.
- Krugly, E., Martuzevicius, D., Sidaraviciute, R., Ciuzas, D., Prasauskas, T., Kauneliene, V., Stasiulaitiene, I., Klucinkas, L., 2014. Characterization of particulate and vapor phase polycyclic aromatic hydrocarbons in indoor and outdoor air of primary schools. *Atmos. Environ.* 82, 298–306. <https://doi.org/10.1016/j.atmosenv.2013.10.042>.
- Liu, Y., Yu, Y., Liu, M., Lu, M., Ge, R., Li, S., Liu, X., Dong, W., Qadeer, A., 2018. Characterization and source identification of PM_{2.5}-bound polycyclic aromatic hydrocarbons (PAHs) in different seasons from Shanghai, China. *Sci. Total Environ.* 644, 725–735. <https://doi.org/10.1016/j.scitotenv.2018.07.049>.
- Majd, E., McCormack, M., Davis, M., Curriero, F., Berman, J., Connolly, F., Leaf, P., Rule, A., Green, T., Clemons-Erby, D., Gummerson, C., 2019. Indoor air quality in inner-city schools and its associations with building characteristics and environmental factors. *Environ. Res.* 170, 83–91. <https://doi.org/10.1016/j.envres.2018.12.012>.
- Mitchell, R., Frank, E., 2017. Accelerating the XGBoost algorithm using GPU computing. *PeerJ Computer Science* 3, e127. <https://doi.org/10.7717/peerj-cs.127>.
- Nielsen, D., 2016. *Tree Boosting with XGBoost*. NTNU Norwegian University of Science and Technology.
- Oliveira, M., Slezakova, K., Delerue-Matos, C., Pereira, M.C., Morais, S., 2019. Children environmental exposure to particulate matter and polycyclic aromatic hydrocarbons and biomonitoring in school environments: a review on indoor and outdoor exposure levels, major sources and health impacts. *Environ. Int.* 124, 180–204. <https://doi.org/10.1016/j.envint.2018.12.052>.
- Pehnek, G., Jakovljević, I., Godec, R., Štrukil, Z.S., Žero, S., Huremović, J., Džepina, K., 2020. Carcinogenic organic content of particulate matter at urban locations with different pollution sources. *Science of The Total Environment*, p. 139414. <https://doi.org/10.1016/j.scitotenv.2020.139414>.
- Perišić, M., Rajšić, S., Šoštarić, A., Mijić, Z., Stojić, A., 2017. Levels of PM₁₀-bound species in Belgrade, Serbia: spatio-temporal distributions and related human health risk estimation. *Air Quality, Atmosphere & Health* 10 (1), 93–103. <https://doi.org/10.1007/s11869-016-0411-6>.
- Pongpiachan, S., Iijima, A., 2016. Assessment of selected metals in the ambient air PM₁₀ in urban sites of Bangkok (Thailand). *Environ. Sci. Pollut. Control Ser.* 23 (3), 2948–2961. <https://doi.org/10.1007/s11356-015-5877-5>.
- Ravindra, K., Bencs, L., Wauters, E., De Hoog, J., Roekens, E., Bleux, N., Bergmans, P., Van Grieken, R., 2006. Seasonal and site specific variation in vapor and aerosol phase PAHs over Flanders (Belgium) and their relation with anthropogenic activities. *Atmos. Environ.* 40, 771–785. <https://doi.org/10.1016/j.atmosenv.2005.10.011>.
- Sarigiannis, D.A., Karakitsios, S.P., Zikopoulos, D., Nikolaki, S., Kermenidou, M., 2015. Lung cancer risk from PAHs emitted from biomass combustion. *Environ. Res.* 137, 147–156. <https://doi.org/10.1016/j.envres.2014.12.009>.
- Sheridan, R.P., Wang, W.M., Liaw, A., Ma, J., Gifford, E.M., 2016. Extreme gradient boosting as a method for quantitative structure–activity relationships. *J. Chem. Inf. Model.* 56 (12), 2353–2360. <https://doi.org/10.1021/acs.jcim.6b00591>.
- Shi, S., 2018. Contributions of indoor and outdoor sources to airborne polycyclic aromatic hydrocarbons indoors. *Build. Environ.* 131, 154–162. <https://doi.org/10.1016/j.buildenv.2018.01.001>.
- Sievert, C., 2020. *Interactive Web-Based Data Visualization with R, Plotly, and Shiny*. CRC Press.
- Šoštarić, A., Stojić, S.S., Vuković, G., Mijić, Z., Stojić, A., Gržetić, I., 2017. Rainwater capacities for BTEX scavenging from ambient air. *Atmos. Environ.* 168, 46–54. <https://doi.org/10.1016/j.atmosenv.2017.08.045>.
- Stojić, A., Stanić, N., Vuković, G., Stanišić, S., Perišić, M., Šoštarić, A., Lazić, L., 2019. Explainable extreme gradient boosting tree-based prediction of toluene, ethylbenzene and xylene wet deposition. *Sci. Total Environ.* 653, 140–147. <https://doi.org/10.1016/j.scitotenv.2018.10.368>.
- Stojić, A., Stojić, S.S., Reljin, I., Čabarkapa, M., Šoštarić, A., Perišić, M., Mijić, Z., 2016. Comprehensive analysis of PM₁₀ in Belgrade urban area on the basis of long-term measurements. *Environ. Sci. Pollut. Control Ser.* 23 (11), 10722–10732. <https://doi.org/10.1007/s11356-016-6266-4>.
- Stojić, A., Stojić, S.S., Šoštarić, A., Ilić, L., Mijić, Z., Rajšić, S., 2015. Characterization of VOC sources in an urban area based on PTR-MS measurements and receptor modelling. *Environ. Sci. Pollut. Control Ser.* 22 (17), 13137–13152. <https://doi.org/10.1007/s11356-015-4540-5>.
- Tasdemir, Y., Esen, F., 2007. Urban air PAHs: concentrations, temporal changes and gas/particle partitioning at a traffic site in Turkey. *Atmos. Res.* 84 (1), 1–12. <https://doi.org/10.1016/j.atmosres.2006.04.003>.
- Tobiszewski, M., Namieśnik, J., 2012. PAH diagnostic ratios for the identification of pollution emission sources. *Environ. Pollut.* 162, 110–119. <https://doi.org/10.1016/j.envpol.2011.10.025>.
- Uchiyama, S., Tomizawa, T., Tokoro, A., Aoki, M., Hishiki, M., Yamada, T., Tanaka, R., Sakamoto, H., Yoshida, T., Bekki, K., Inaba, Y., 2015. Gaseous chemical compounds in indoor and outdoor air of 602 houses throughout Japan in winter and summer. *Environ. Res.* 137, 364–372. <https://doi.org/10.1016/j.envres.2014.12.005>.
- United States Environmental Protection Agency (USEPA), 1997. *Office of Pesticide Programs: List of Chemicals Evaluated for Carcinogenic Potential* (Washington, DC, USA).
- Wang, F., Lin, T., Feng, J., Fu, H., Guo, Z., 2015a. Source apportionment of polycyclic aromatic hydrocarbons in PM_{2.5} using positive matrix factorization modeling in Shanghai, China. *Environ. Sci. J. Integr. Environ. Res.: Processes & Impacts* 17 (1), 197–205. <https://doi.org/10.1039/C4EM00570H>.
- Wang, G., Wang, Y., Yin, W., Xu, T., Hu, C., Cheng, J., Hou, J., He, Z., Yuan, J., 2020. Seasonal exposure to PM_{2.5}-bound polycyclic aromatic hydrocarbons and estimated lifetime risk of cancer: a pilot study, 702. *Science of The Total Environment*, p. 135056. <https://doi.org/10.1016/j.scitotenv.2019.135056>.
- Wang, J., Guinot, B., Dong, Z., Li, X., Xu, H., Xiao, S., Ho, S.S.H., Liu, S., Cao, J., 2017. PM_{2.5}-bound polycyclic aromatic hydrocarbons (PAHs), oxygenated-PAHs and phthalate esters (PAEs) inside and outside middle school classrooms in Xi'an, China: concentration, characteristics and health risk assessment. *Aerosol and Air Quality Research* 17 (7), 1811–1824. <https://doi.org/10.4209/aaqr.2017.03.0109>.
- Wang, T., Feng, W., Kuang, D., Deng, Q., Zhang, W., Wang, S., He, M., Zhang, X., Wu, T., Guo, H., 2015b. The effects of heavy metals and their interactions with polycyclic aromatic hydrocarbons on the oxidative stress among coke-oven workers. *Environ. Res.* 140, 405–413. <https://doi.org/10.1016/j.envres.2015.04.013>.
- Wang, Y.Q., 2014. MeteorInfo: GIS software for meteorological data visualization and analysis. *Meteorol. Appl.* 21 (2), 360–368. <https://doi.org/10.1002/met.1345>.
- Wickham, H., 2016. *ggplot2: Elegant Graphics for Data Analysis*. Springer-Verlag, New York. <https://doi.org/10.1007/978-3-319-24277-4>, 2009.
- Xu, H., Guinot, B., Niu, X., Cao, J., Ho, K.F., Zhao, Z., Ho, S.S.H., Liu, S., 2015. Concentrations, particle-size distributions, and indoor/outdoor differences of polycyclic aromatic hydrocarbons (PAHs) in a middle school classroom in Xi'an, China. *Environ. Geochem. Health* 37 (5), 861–873. <https://doi.org/10.1007/s10653-014-9662-z>.
- Yao, Y., Wang, D., Ma, H., Li, C., Chang, X., Low, P., Hammond, S.K., Turyk, M.E., Wang, J., Liu, S., 2019. The impact on T-regulatory cell related immune responses in rural women exposed to polycyclic aromatic hydrocarbons (PAHs) in household air pollution in Gansu, China: a pilot investigation. *Environ. Res.* 173, 306–317. <https://doi.org/10.1016/j.envres.2019.03.053>.
- Yin, H., Xu, L., 2018. Comparative study of PM₁₀/PM_{2.5}-bound PAHs in downtown Beijing, China: concentrations, sources, and health risks. *J. Clean. Prod.* 177, 674–683. <https://doi.org/10.1016/j.jclepro.2017.12.263>.
- Zhang, G., Ma, K., Sun, L., Liu, P., Yue, Y., 2020. Seasonal pollution characteristics, source apportionment and health risks of PM_{2.5}-bound polycyclic aromatic hydrocarbons in an industrial city in northwestern China. *Hum. Ecol. Risk Assess.* 1–18. <https://doi.org/10.1080/10807039.2020.1799186>.



The PM_{2.5}-bound polycyclic aromatic hydrocarbon behavior in indoor and outdoor environments, part II: Explainable prediction of benzo[a]pyrene levels

Andreja Stojić^{a,b}, Gordana Jovanović^{a,b}, Svetlana Stanišić^{b,*}, Snježana Herceg Romanić^c, Andrej Šoštarčić^d, Vladimir Udovičić^a, Mirjana Perišić^{a,b}, Tijana Milićević^a

^a Institute of Physics Belgrade, National Institute of the Republic of Serbia, University of Belgrade, 118 Pregrevica Street, 11000, Belgrade, Serbia

^b Singidunum University, 32 Danijelova Street, 11000, Belgrade, Serbia

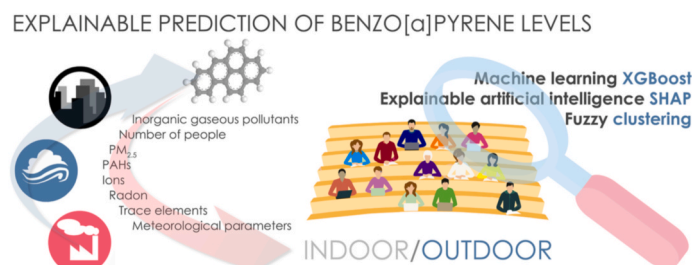
^c Institute for Medical Research and Occupational Health, 2 Ksaverska Cesta Street, PO Box 291, 10001, Zagreb, Croatia

^d Institute of Public Health Belgrade, 54 Despota Stefana Street, 11000, Belgrade, Serbia

HIGHLIGHTS

- Relative errors of the applied machine learning methods were below 15.1%.
- Explainable methodology characterized conditions which govern B[a]P fate.
- Key predictors of B[a]P dynamics were high-ring PAHs, Chy, CO, As, Cr, and PM_{2.5}.
- Out of 31 meteorological parameters, only one significantly affected outdoor B[a]P.
- 4 and 8 environmental condition types shape B[a]P behavior indoors and outdoors.

GRAPHICAL ABSTRACT



ARTICLE INFO

Handling Editor: Volker Matthias

Keywords:

Indoor air pollution
Outdoor air pollution
benzo[a]pyrene
Machine learning
Explainable artificial intelligence

ABSTRACT

Among the polycyclic aromatic hydrocarbons (PAH), benzo[a]pyrene (B[a]P) has been considered more relevant than other species when estimating the potential exposure-related health effects and has been recognized as a marker of carcinogenic potency of air pollutant mixture. The current understanding of the factors which govern non-linear behavior of B[a]P and associated pollutants and environmental processes is insufficient and further research has to rely on the advanced analytical approach which averts the assumptions and avoids simplifications required by linear modeling methods. For the purpose of this study, we employed eXtreme Gradient Boosting (XGBoost), SHapley Additive exPlanations (SHAP) attribution method, and SHAP value fuzzy clustering to investigate the concentrations of inorganic gaseous pollutants, radon, PM_{2.5} and particle constituents including trace metals, ions, 16 US EPA priority PM_{2.5}-bound PAHs and 31 meteorological variables, as key factors which shape indoor and outdoor PM_{2.5}-bound B[a]P distribution in a university building located in the urban area of Belgrade (Serbia). According to the results, the indoor and outdoor B[a]P levels were shown to be highly correlated and mostly influenced by the concentrations of Chry, B[b]F, CO, B[a]A, I[cd]P, B[k]F, Flt, D[ah]A, Pyr, B[ghi]P, Cr, As, and PM_{2.5} in both indoor and outdoor environments. Besides, high B[a]P concentration events were recorded during the periods of low ambient temperature (<12 °C), unstable weather conditions with precipitation and increased soil humidity.

* Corresponding author.

E-mail address: sstanišic@singidunum.ac.rs (S. Stanišić).

1. Introduction

Polycyclic aromatic hydrocarbons (PAHs) are a complex mixture of congeners originating from pyrogenic and petrogenic, as well as anthropogenic and natural sources (Velázquez-Gómez and Lacorte, 2020). Among PAHs, benzo[a]pyrene (B[a]P) has been recognized as a marker of carcinogenic potency of the air pollutant mixture (Liu et al., 2020). According to the IARC (2012), it has been assigned to a group 1 of hazardous species – mutagenic and carcinogenic to humans irrespective of the environment, and its emissions are regulated by the Directive, 2004/107/EC. While two-three ring low molecular weight PAHs mostly occur in the gas phase, the compounds with four aromatic rings and more, including B[a]P, are semi-volatile and 70–90% of their emitted content is adsorbed on particulate matter, overall on the fine inhalable particles with aerodynamic diameter less than $2.5\ \mu\text{m}$ – $\text{PM}_{2.5}$ (Liu et al., 2014; Azari et al., 2020). Previous studies have been focused on levels, spatial and seasonal distribution, sources, local and regional source contributions, personal exposure, B[a]P equivalent toxicity and cancer risks of $\text{PM}_{2.5}$ -bound PAHs (Liu et al., 2017; Han et al., 2019; Yan et al., 2019; Zhang et al., 2019a, 2019b, 2019c; Du et al., 2020; Lao et al., 2020; Ali-Taleshi et al., 2020; Gope et al., 2020). Some of the studies have also reported contrasting findings about carcinogenic potential of PAH mixture depending on the B[a]P content (Brehmer et al., 2020). A study aimed at characterizing indoor air quality in kindergartens located in urban and rural area of Poland has shown that no statistically significant differences exist in the concentrations of total PAHs in indoor versus outdoor air, although the mutagenic effect of outdoor $\text{PM}_{2.5}$ samples was twice as high as the effect of indoor samples (Błaszczuk et al., 2017). The review of Ma and Harrad (2015) has shown that even though the concentrations of both PAHs and B[a]P were higher in the indoor environment, indoor sources emitted proportionally less carcinogenic species than outdoor sources, which was implied by the comparison of I/O ratios for ΣPAH and B[a]P toxicity equivalents. Nevertheless, some studies proved the opposite (Oliveira et al., 2016; Sangiorgi et al., 2013). The previous studies also showed that, depending on a sampling location and environmental factors, B[a]P concentrations can be found within the relatively wide range of values (Rönkkö et al., 2020).

B[a]P atmospheric transformations and persistence are strongly affected by meteorological conditions, including temperature, precipitation, moisture, and solar radiation, as well as the presence of particles and oxidant species, e.g., ozone, nitrate, and hydroxyl radicals (Liu et al., 2017). In addition to this, the particles' chemical content and structure have significant impact on the B[a]P chemodynamics. Considering PAHs' heterogeneous reactions with oxidizing agents such NO_2 and O_3 , B[a]P has been reported to be among the most reactive PAH congener when bound to soot, silica, diesel, or graphite particles together with pyrene (Pyr), anthracene (Ant), benz[a]anthracene (B[a]A), and dibenz[a,h]pyrene (DB[a,h]P) (Keyte et al., 2013 and the references therein). Conversely, on the soot and ammonium sulfate particles a formation of monolayer coverage makes B[a]P less exposed to surface reactions and thus, more persistent.

The study of Lodovici et al. (2003) showed that the level of total particle-bound B[a]P was as low as $0.02\ \text{ng m}^{-3}$ at the regional background site locations, while the study of Hassanvand et al. (2015) registered B[a]P concentrations of 5 or more ng m^{-3} , depending on the season, traffic impact, type of sampling location, and particle fraction. As regards $\text{PM}_{2.5}$ -related organic content, the study of Jedynska et al. (2014), aimed at investigating the levels of PAHs in fine particle fraction at street, urban and regional background, showed that mean B[a]P levels were below $0.2\ \text{ng m}^{-3}$ for all ten investigated sites in Europe. On the other hand, the studies performed in Asia showed that the total $\text{PM}_{2.5}$ -bound B[a]P concentrations considerably exceeded the maximum permissible risk level of $1\ \text{ng m}^{-3}$ (Yury et al., 2018).

In this study, we present promising advanced machine learning (ML) and explainable artificial intelligence (XAI) methodologies (eXtreme

Gradient Boosting – XGBoost and SHapley Additive exPlanations – SHAP) for studying complex, heterogeneous, and non-linear interactions between indoor and outdoor B[a]P levels and $\text{PM}_{2.5}$, PAHs, inorganic gaseous pollutants, trace elements, ions, radon, 31 meteorological parameters, the number of people in the amphitheater, and the time they spent indoor that could not be addressed by traditional approaches. The methods have become increasingly recognized and successfully applied when predicting environmental phenomena (Blair et al., 2019; Gibert et al., 2018; Stojić et al., 2019; Stanišić et al., 2021; Ye et al., 2020). The study aims to provide an insight into the B[a]P behavior by attributing environmental factor importance (SHAP values), impacts (SHAP dependency), mutual relations (relative SHAP values), and interactions (SHAP interactions). Moreover, we aim to identify and characterize governing environmental conditions responsible for shaping the levels of B[a]P concentrations in both environments (SHAP force).

2. Materials and methods

2.1. Measurement campaign

The measurements of inorganic gaseous pollutants, radon, $\text{PM}_{2.5}$ and particle constituents including trace metals, ions, and PAHs were performed from March 1st – May 31st in a building of Singidunum University ($44^\circ 45' 33.8''\text{N}$, $20^\circ 29' 47.6''\text{E}$), situated in the urban area of Belgrade, Serbia. In the residential area surrounding the measurement site, there is a large number of households with individual fireboxes using coal and wood, while approx. 1 km in the W/SW direction and W/NW direction, there are two heating plants operating with the total production capacity of 230 MW and 50 MW, respectively, mainly fueled with natural gas and crude oil. During the three-month study campaign, the outdoor pollutants were sampled at the rooftop of the University building, at the open space 10 m above ground. For the indoor sampling, sampling inlets and $\text{PM}_{2.5}$ sampling device were placed at a height of 6 m and 2 m off the floor in an amphitheater with a capacity of 350 seats where lectures for often 50 to 80 students were given. During the study campaign, the number of people and the time they spent in the amphitheater was registered hourly.

$\text{PM}_{2.5}$ was collected daily on quartz filters (Whatman QMA, 47 mm) by Svan Leckel LVS6-RV devices with a flow rate of $2.3\ \text{m}^3\ \text{h}^{-1}$, over 24 h sampling period. Inorganic gases (O_3 , CO, SO_2 , and NO_x) were measured by Horiba devices APOA, APMA, APSA, and APNA, 370 series, for the continuous monitoring of pollutants with 2-min resolution using ultraviolet absorption, infrared spectroscopy, ultraviolet fluorescence, and chemiluminescence methods, respectively. The measurements were performed according to the following European Standards EN 14211:2012, EN 14212:2012, EN 14625:2012 and EN 14626:2012. The limit of detection (LOD) for O_3 , SO_2 , and NO_x was $1\ \mu\text{g m}^{-3}$ while for CO it was $0.1\ \text{mg m}^{-3}$.

The outdoor meteorological data were obtained by using Vaisala WXT530 monitoring station, while the indoor radon concentrations, ambient air temperature, relative humidity and air pressure were detected by SN1029 radon monitor (Sun Nuclear Corporation, NRSB approval-code 31822). The LOD for radon was $0.1\ \text{Bq m}^{-3}$. More details on the study area, sampling campaign and chemical analyses are described in the Part 1 of this paper (Stanišić et al., 2021).

2.2. Chemical analyses of $\text{PM}_{2.5}$ constituents, quality assurance and quality control

In brief, gravimetric measurements of $\text{PM}_{2.5}$ were conducted according to the European Standard EN 12341:2014. Prior to gravimetric determination, the pre-fired and preconditioned non-exposed filters were measured representing control blanks. After preconditioning for 48 h in a Class 100 clean room with automatic temperature and pressure regulation, the filters were weighed twice using a micro-balance (Precisa XR 125 SB). Mass concentrations of $\text{PM}_{2.5}$ were calculated as average

values. Loaded filters were stored in a cool room at 4 °C prior to chemical analysis. After gravimetric measurements, the surface of each filter amounting to 13.85 cm² was cut in two pieces - approximately 1.76 cm² each, which were used for the analysis of anions and cations (Cl⁻, Ca²⁺, K⁺, NO₃⁻, SO₄²⁻, and NH₄⁺), while the remaining 12.09 cm² were divided and used for the analysis of trace elements (As, Cd, Cr, Mn, Ni, and Pb) and 16 US EPA PAHs.

The inorganic PM constituents were determined by the standard methods for elements (European Standards (EN) 14902:2005). The extraction of the trace elements was performed by a mixture of HNO₃ (30%):H₂O₂:H₂O (3:2:5) using analytical grade reagents (Merck) and distilled/deionized water (MiliQ, 18.2 MΩ) (CEN/TC 264 N779). After microwave accelerated digestion (Anton Paar 3000), the concentrations of trace elements were determined by inductively coupled plasma-mass spectrometry (ICP-MS) (Agilent 7500ce with Octopole Reaction System). Quality control was conducted by 2783 NIST standard reference material (National Institute of Standard and Technology, MD, USA). The recovery values were within satisfactory range of ±20% in relation to the reference value while method LOD was: 0.4 ng m⁻³ for As, 0.05 ng m⁻³ for Cd, and 2 ng m⁻³ for Cr, Mn, Ni, and Pb.

For the determination of ion concentrations, the filter pieces were extracted by ultra-pure water for 24 h. The aqueous extracts were further analyzed by standard ion chromatography (Dionex DX500 IC system, MDL 064 Standard operating procedure). The LOD was: 2 μg m⁻³ for Cl⁻ and NO₃⁻, 1 μg m⁻³ for SO₄²⁻, 0.2 μg m⁻³ for NH₄⁺, 2 μg m⁻³ for K⁺ and 8 μg m⁻³ for Ca²⁺.

The concentrations of priority PAHs including naphthalene (Nap), acenaphthylene (Acy), acenaphthene (Ace), fluorene (Flu), phenanthrene (Phe), anthracene (Ant), fluoranthene (Flt), pyrene (Pyr), benz[a]anthracene (B[a]A), chrysene (Chry), benzo[b]fluoranthene (B[b]F), benzo[k]fluoranthene (B[k]F), benzo[a]pyrene (B[a]P), dibenz[a,h]anthracene (DB[ah]A), benzo[g,h,i]perylene (B[ghi]P), and indeno[1,2,3-cd]pyrene (I[cd]P) were determined following the Standard ISO 12884:2010. Further details have previously been illustrated in the studies preceding this one (Stanišić et al., 2021; Cvetković et al., 2015). The filters were microwave-extracted by a solvent mixture of n-hexane and acetone, 12.5 mL:12.5 mL (US EPA, 2007). Solution was rotary evaporated to 1 mL under reduced pressure (55.6 kPa and with 0.2 mL isooctane) and to 0.25 mL under a nitrogen stream. The PAHs were analyzed using gas chromatography coupled with mass selective detector (Agilent GC 6890/5973 MSD) with a DB-5 MS capillary column (30 m × 0.25 mm × 25 μm) according to EPA Compendium Method TO-13 A. The oven temperature was attained by applying the following steps: (1) isothermal heating for 4 min at 70 °C, (2) heating from 70 °C to 310 °C at 8 °C min⁻¹, and (3) 5 min of isothermal heating at 310 °C. Solvent delay was 5 min and the time of run was 46 min. Helium was used as the carrier gas. The injector was set to 300 °C. Prior to the analysis, calibration curves (R² > 0.995) were obtained using Ultra Scientific PAH Mixture PM-831, which contains 16 priority PAHs. The concentration of calibration solutions was between 5 and 200 ng mL⁻¹.

We used Ultra Scientific PAH Mixture PM-831, which consists of 16 compounds, each of 500.8 ± 2.5 μg/mL concentration as external standard for calibration curve. We determined concentrations of 16 priority USEPA PAHs: Nap, Acy, Ace, Flu, Phe, Ant, Flt, Pyr, B[a]A, Chry, B[b]F, B[k]F, B[a]P, I[cd]P, DB[ah]A, and B[ghi]P.

To estimate method recovery, Ultra Scientific Semi-Volatiles Internal Standard Mixture ISM-560 containing: Ace-d₁₀, Chry-d₁₀, 1,4-dichlorobenzene, Nap-d₈, Perylen-d₁₂, and Phe-d₁₀ was used as internal standard. Recovery values ranged from 85% to 110% for all the PAHs in the internal standard. The LOD was calculated as three times signal/noise and it was 0.01 ng m⁻³ for all PAH species. The limit of quantification was determined as 3.3 times of LOD. Field and laboratory blank were also prepared and analyzed, and all data were corrected with reference to the blanks.

2.3. Data analysis

2.3.1. Machine learning

The relationships between indoor and outdoor levels of B[a]P (74 samples) and other investigated parameters (other PAHs, inorganic gaseous pollutants, radon, PM_{2.5} and particle constituents including trace metals and ions, meteorological parameters including measured and GDAS1-modeled, the number of people and the time they spent indoor, trend, weekday and weekend – 39 and 64 parameters in total for indoor and outdoor environment, respectively) were explored by the regression analysis, implemented by eXtreme Gradient Boosting. Briefly, XGBoost is a highly effective ensemble method of supervised machine learning based on a sequential tree-growing algorithm. Iteratively reweighing the training data to improve regression performance, each decision tree aims to complement all the others and correct for residuals in the predictions made by the previous trees. XGBoost is based on a gradient descent algorithm, used to minimize loss when adding new models. The method includes system optimization and algorithmic enhancements through parallelized sequential tree building, tree pruning, regularization, weighted quantile sketch algorithm implementation, cross-validation, etc. Outperforming standard deep neural network models on tabular-style datasets, XGBoost was successfully applied across various domains especially due to its core advantages referring to computational efficiency and competitive accuracy, even when data is sparse and unstructured (Hartmann, 2019; Lundberg et al., 2020). In this study, we used Python (Python Software Foundation) XGBoost implementation (XGBoost Python Package). The data were split into training (80%) and validation (20%) sets. The criterion for splitting the data set into training and test set was that both data subsets should follow the same probability distribution. In this study, we have identified the PAH outliers according to the tradeoff between the split criteria and the necessity to maximize the total size of the data. The same indoor and outdoor events were used for training/testing. Hyperparameter tuning was implemented by using a brute-force grid search and 10-fold stratified cross-validation which was replicated 10 times. The best performing hyperparameter values were used for the final model.

2.3.2. Explainable artificial intelligence

The explainability of ML model behavior which operates with high-dimensional input data in a non-linear and nested fashion is crucial for understanding the process being modeled. Until recently, the inability to explain the predictions from accurate, but complex models, posed a serious limitation in understanding the governing factors that shape a prediction. For this purpose, we employed the advanced explainable artificial intelligence method, which is capable to avoid the trade-off between accuracy and interpretability and provide the straightforward and meaningful interpretation of the ML model-derived decisions, now being shifted towards user-readable logic rules to match human intuition.

2.3.2.1. Shapley additive exPlanations. SHapley Additive exPlanations (SHAP) is a method based on Shapley values, calculated as a measure of feature importance using a game-theory approach, that provide an impact of features on individual predictions (Lundberg and Lee, 2017). The Shapley value method provides fairly distributed payouts among the cooperating players (features) depending on their contribution to the joint payout (prediction). It perfectly apportions the difference between the prediction and the average prediction among the features (Molnar, 2019). Thus, SHAP assigns each feature the importance as a measure of its contribution to a particular prediction and interpret the impact of having a certain value for a given feature in comparison to the prediction of a model if that feature took some baseline value. The SHAP explanations represent the only possible locally accurate and globally consistent feature contribution values (Chen et al., 2019; Stojić et al., 2019). The method provides valuable insights into a model's behavior

by overcoming the main drawback of inconsistency and minimizes the possibility of underestimating the importance of a feature with a certain attribution value, capturing feature interaction effects based on generalization of Shapley values, and interpreting the model's global behavior while retaining local faithfulness (Lundberg et al., 2020).

In this study we used Python SHAP implementation (SHAP Python package) and the TreeExplainer which reduces the complexity of exact Shapley value computation from exponential to low-order polynomial time by leveraging the internal structure of tree-based models (Lundberg et al., 2020). The captured attributed importance of a feature, the change of a feature importance over its value range, as well as its interaction effects with other features are visually presented as SHAP summary plots, SHAP dependency plots, and SHAP interaction plots, respectively.

A change in the absolute SHAP value of a feature does not clearly indicate its relationships with other features. To gain an insight into relative relationships among feature attributions for each individual prediction, we introduced the relative SHAP values. They show the relative influence of a feature to the prediction and are defined as a share of absolute SHAP in total attributed importance of all features for the particular case.

The stabilities of the obtained absolute and relative SHAP values were evaluated by 50 times-replicated bootstrap method. The stabilities are presented in figures as error bars.

2.3.2.2. Fuzzy clustering. The fuzzy clustering of absolute SHAP attributions was performed to identify and characterize indoor and outdoor ambient conditions responsible for B[a]P behavior. It was chosen because each B[a]P concentration will not necessarily belong to a single class of environmental conditions which shapes it. Fuzzy clustering was performed by using R (R: A language and environment for statistical computing) 'cluster' package (Maechler et al., 2019). The obtained results were presented as force plots. A detailed analysis of each cluster was performed based on the statistical character of its absolute and relative SHAP values, as well as the measured parameter values.

Beside conventional images, we present all relevant findings as interactive plots by using R package 'plotly' (Sievert, 2020) hosted at the web page designed to support this paper at www.envpl.ipb.ac.rs/papers/20/PAHs/.

3. Results and discussion

The mean PM_{2.5} and B[a]P levels in the indoor and outdoor environments were 16.2 vs. 17.5 $\mu\text{g m}^{-3}$ and 0.50 vs. 0.48 ng m^{-3} , respectively, while both indoor and outdoor B[a]P mean concentrations were below the recommended level of 1 ng m^{-3} (Directive, 2004/107/EC).

As it can be seen in Fig. 1, extreme concentration events (ranging from 2.0 to 6.8 ng m^{-3}) were mostly registered over a few days in March and May, when mean daily temperature did not exceed 12 °C. As a higher molecular weight PAH, B[a]P is almost completely particle-bonded which makes it less reactive vs. solar radiation and free

radicals, and its affinity towards particle phase increases with ambient air temperature lowering and decrease of vapor pressure. Beside the intense fossil fuel combustion for heating purposes, the described gas-particle phase distribution additionally contributes to higher B[a]P concentrations in cold season and significant seasonal differences in mean pollutant levels. For instance, the study of Jedrychowski et al. (2007) showed that winter B[a]P concentrations were 4.3 ng m^{-3} and 6.1 ng m^{-3} , while summer levels were 0.8 ng m^{-3} and 0.9 ng m^{-3} for indoor and outdoor environment, respectively.

Similarly to the study of Jedrychowski et al. (2007), our results showed that indoor/outdoor (I/O) B[a]P ratio was mainly below 1, with a few exceptions when the calculated values were in the range from 2 to 10 (Fig. 1). Conversely, some studies (Romagnoli et al., 2014) reported the outdoor B[a]P concentrations to be significantly lower throughout the year than the corresponding indoor levels. For instance, the study aimed at characterizing levels of PAHs at preschool environment in Portugal and assessing the exposure-related health risk, showed that carcinogenic risk due to indoor PAH-related exposure was 4–18 times higher than for outdoors (Oliveira et al., 2016). In compliance with this, the research focused on the impact of outdoor environment on indoor air quality in office buildings in Milano (Italy) throughout the year confirmed a strict correlation between indoor and outdoor PM concentrations. However, the reported B[a]P concentrations were higher indoor (I/O = 2.3) suggesting that indoor sources did not contribute to higher PM mass emissions but significantly affected human health through the apportionment of the particles enriched by carcinogenic species (Sangiorgi et al., 2013).

According to our results, the extreme B[a]P I/O ratio values (Fig. 1) were detected in the days when the indoor B[a]P remained concentrated while the frequent changes in the weather conditions, followed by significant wind gusts, precipitation events and sunshine hours considerably affected the outdoor air quality (Part 1 of this paper, Stanišić et al., 2021). The differences between reported B[a]P I/O ratio values can be explained by the fact that variable meteorological conditions govern more rapid outdoor concentration variations, while indoor air quality remains less affected. This further suggests that the long-term I/O ratio calculations excluding the extremely low or high pollutant values could better reflect an environment in which B[a]P pollution occurs.

In this study, XGBoost was successfully employed for exploring complex, heterogeneous, and non-linear relationships between B[a]P concentrations and key factors which shape their indoor and outdoor distribution including inorganic gaseous pollutants, radon, PM_{2.5} and their constituents including trace metals, ions, all other US EPA priority PM_{2.5}-bound PAHs, 31 meteorological variables, the number of people and the time they spent indoor, trend, weekday, and weekend. The predicted/observed calculated relative errors were 15.1% and 14.5%, while the r^2 were 0.96 and 0.95 for indoor and outdoor, respectively (Fig. 2).

The data analysis revealed a correlation of 0.67 ($p < 0.05$) between indoor and outdoor B[a]P levels (Figure S1). Further, both the indoor and outdoor B[a]P concentrations exhibited correlations above 0.9 with

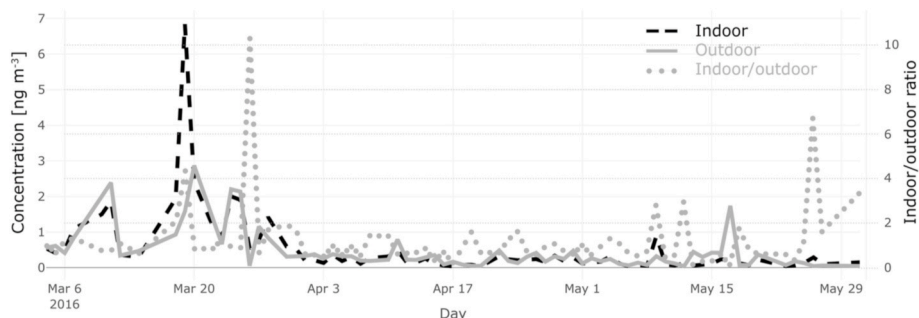


Fig. 1. Benzo(a)pyrene concentrations and indoor/outdoor ratio.

B[a]A, Chry, I[cd]P, B[ghi]P, B[b]F, and B[k]F levels from the corresponding environment, while also significant correlations of 0.89 and 0.82, respectively, were found with indoor and outdoor Pyr. The persistent influence of the listed pollutants on B[a]P behavior was also confirmed by the correlation of SHAP values higher than 0.8 (Figure S2a). However, relative SHAP value correlations, slightly above 0.8, reveal a more variable impact of B[a]A, B[b]F, B[k]F, and Chry (Figure S2b), and even more for indoor and outdoor Pyr (<0.7). It is known that Chy and Pyr can be distributed between gas and particle phase upon emission, which distinguishes them slightly from B[a]P, B[a]A, B[k]F, I[cd]F, B[ghi]P, and B[b]F, which exhibit high mutual correlations because they are found to be mostly PM-bonded (Oliveira et al., 2016).

Yet, according to absolute and relative SHAP values (Fig. 3), Chy appears to be the most important B[a]P predictor in the indoor environment (absolute SHAP: 0.11 ng m⁻³; relative SHAP: 18.23%), followed by B[b]F, CO, B[a]A, I[cd]P, B[k]F, Flt, D[ah]A, Pyr, B[ghi]P, Cr, and PM_{2.5}, while in the outdoor environment B[a]P levels could be more accurately predicted by B[b]F concentrations, although the significance of B[a]A, B[k]F, B[ghi]P, I[cd]P, Pyr, CO, As, and Flt, as well as the significance of Chry (absolute SHAP: 0.01 ng m⁻³; relative SHAP: 3.61%) were also evidenced. It can be assumed that in the indoor environment, semivolatile Chry is more particle-bonded and has similar fate to B[a]P, while outdoor Chry has been shown to be less important for B[a]P level prediction probably since it is, unlike B[a]P, more distributed in the gas phase, as well as more resistant to atmospheric reactions with oxidative species (Estève et al., 2004; Perraudin et al., 2007). On the other hand, Pyr has a comparable influence on B[a]P levels in both indoor and outdoor environment, which is supported by the fact that these species have very similar molecular structure and environmental behavior, and thus, they exhibit equal reactivity with hydroxyl and nitrate radical species. Also, the increased levels of Chry, Pyr, and B[a]P suggest that these species share the same source in both indoor and outdoor environment, which can probably be attributed to fuel-burning for heating purposes as identified by Unmix source apportionment and PAH diagnostic ratios (Part 1 of this paper, Stanišić et al., 2021), or more specifically to coal combustion, when considering the association between outdoor As and B[a]P levels. In the indoor environment, the evidenced relationship between B[a]P and Cr levels indicates the contribution of diesel and gasoline emissions, which are the major source of PAHs in the warm season. Namely, the study area was located 80 m from the main road, and thus, the impact of motor vehicle emission on indoor air quality could be registered. Unsurprisingly, SHAP values suggested no associations between indoor and outdoor B[a]P levels and highly volatile PAHs including Nap, Acy, and Ace,

which are normally distributed in a gas phase.

The results of SHAP analysis revealed that the impact of PM_{2.5} on B[a]P levels is less evident in the outdoor than indoor environment which can be explained by the inconsistent matrix-specific interactions of PAHs and particles at the molecular level. Namely, B[a]P is mostly entirely found within the fine particle fraction, but the chemical nature and the amount of bonding varies with particle composition and environmental factors (Lammel et al., 2010). To particles with higher organic content, B[a]P is most often bonded by solvation, and this process is enhanced in the presence of moisture and usually less temperature dependent compared to the weaker bond of adsorption type that occurs on particles with higher inorganic content. It appears that adsorption was the dominant mechanism involved in pollutant particle distribution in the outdoor environment, which made B[a]P more prone to transformations and oxidation with free OH radicals and less resistant to UV decomposition that also takes part in the outdoor environment.

The low SHAP values (Fig. 3) and dependence plots (Figures S3) showed that neither indoor nor outdoor B[a]P behavior exhibit significant weekend dynamic pattern or meteorologically-driven trend. While previous studies (Jung et al., 2014) mostly reported that B[a]P atmospheric persistence and levels were affected by the seasonal variations of temperature, relative humidity, and pressure, our results (the SHAP values from 0.2 to 0.4, Fig. 3, and SHAP dependencies, Figures S3) showed that only the increase in soil moisture (Solm>0.3) was positively associated with the increased outdoor B[a]P levels (1–3 ng m⁻³). Beside temperatures below 12 °C, changeable weather conditions with precipitations, and consequently increased soil moisture, characterized the episodes of high B[a]P levels in the beginning and the end of March along with mid-April and May (Fig. 1). As already mentioned, B[a]P and other high-weight PAHs are hydrophobic and almost entirely found within the fine particle fraction, which implies that their atmospheric removal is regularly affected by dry deposition (Keyte et al., 2013). After being deposited in the soil, B[a]P decay on particles via heterogenous reactions is reduced with the increase of soil moisture, which leads to higher B[a]P levels in the soil and thus, larger pollutant pool for volatilization. Although the volatility of B[a]P is generally low (vapor pressure, $p = 7.9 \cdot 10^{-6}$ Pa at 298 K) and its tendency to volatilize upon being bond to solid surfaces is limited, volatilization from the particles' surfaces still occurs and appears to contribute up to 9% to total B[a]P emissions as shown by the study conducted in the European region (Keyte et al., 2013), which can explain the positive association between soil moisture and outdoor B[a]P levels. In addition, soil moisture is recognized as one of the most important factors for controlling particulate/dust resuspension because it enhances the strength of inter-particle bonds by promoting the development of a humid film between soil grains that makes soil an important secondary emission source of particles depending on the texture and mechanical composition (Niederer et al., 2018). We note that the SHAP analysis indicated that the indoor levels of B[a]P were independent of the number of attendants and employees, as well as the time they spend indoors.

As shown by the dependence plot (Figures S3), the non-proportional relationships are evident: the elevated outdoor and indoor B[a]P concentrations are followed by increased levels of the main predicting species (B[a]A, B[b]F, I[cd]P, Chy, B[ghi]P, B[k]F, and Pyr). According to the relative SHAP values (Fig. 3), B[a]A (21%), B[b]F (21%), and B[k]F (15%) isomers are recognized as the main compounds which explain the outdoor B[a]P dynamics, i.e., contribute to the environment which is associated with B[a]P specific behavior and fate. The relationships between B[a]P and other PAH species are less evident, as shown by relative SHAP values below 10%. The non-proportional relationships are also confirmed between B[a]P and other considered parameters in the following order: CO, As, Cr, PM_{2.5}, and Rn (Fig. 3). Considering the relative SHAP values, their significance appears to be more evident in the indoor than outdoor environment. The main compounds which explain the indoor B[a]P dynamics were Chry (18%), B[k]F (17%), and CO (10%).

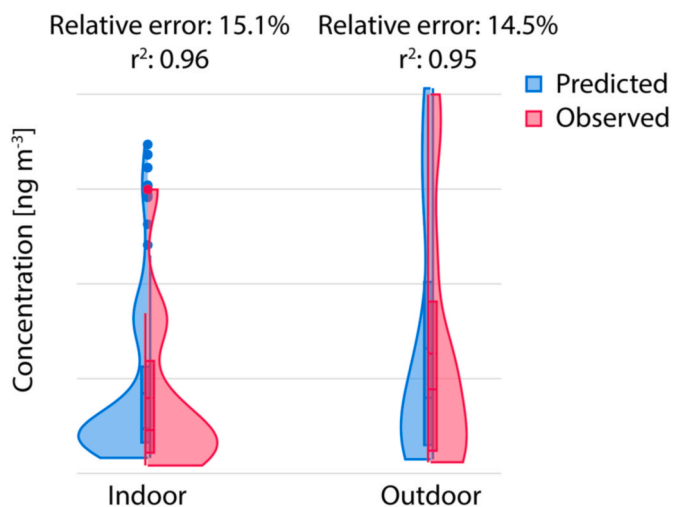


Fig. 2. XGBoost model evaluation.

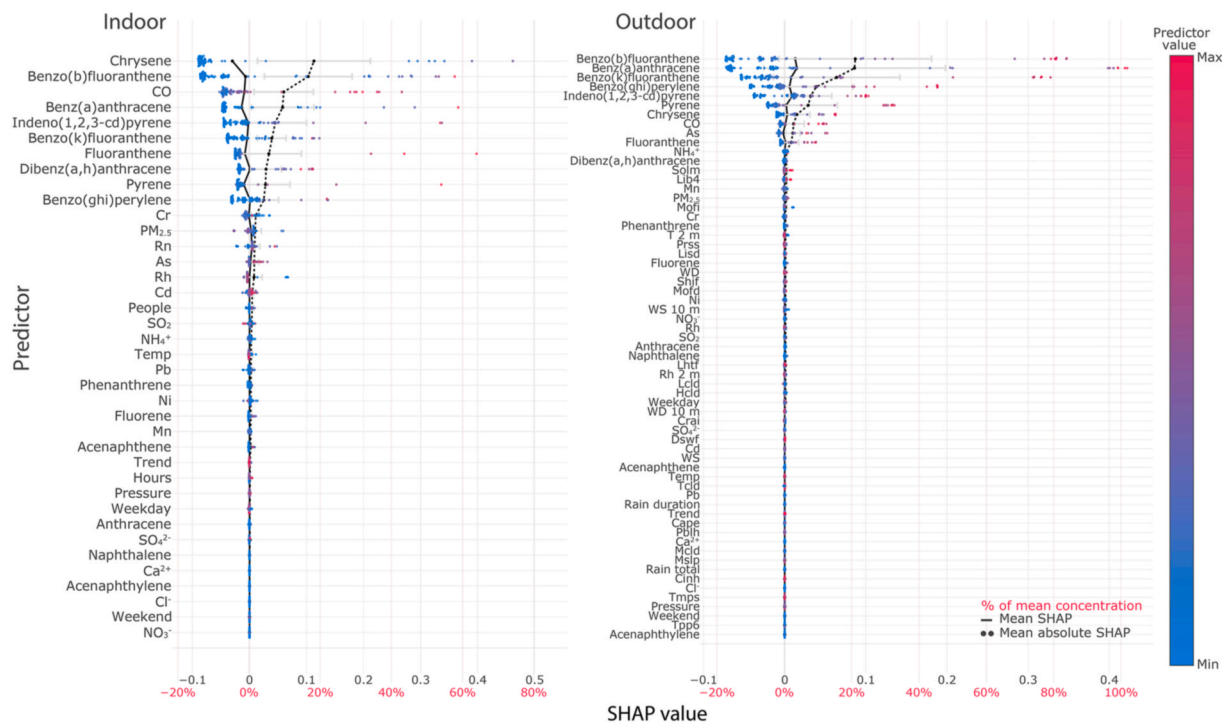


Fig. 3. Indoor (left) and outdoor (right) benzo(a)pyrene SHAP summary plots.

The impact of B[b]F on B[a]P levels is very similar in both environments and increases with B[b]F concentrations (Figure S3.3). Its share to the other governing factors decreases above B[b]F concentration of 2 ng m^{-3} which means that other factors overtake the leading role in shaping B[a]P levels above 0.8 ng m^{-3} . The influence of B[k]F on B[a]P environmental fate is more pronounced for low levels indoors and

high levels outdoors, but we have not found the explanation for this observation.

The impacts of Chry and B[a]A on B[a]P levels are very similar in shape (Figures S3.6 and S3.2), with relative SHAP 18% and 21% in the indoor and outdoor environments, respectively. This implies that, although semi-volatile, Chry is more prone to be particle-bound in the

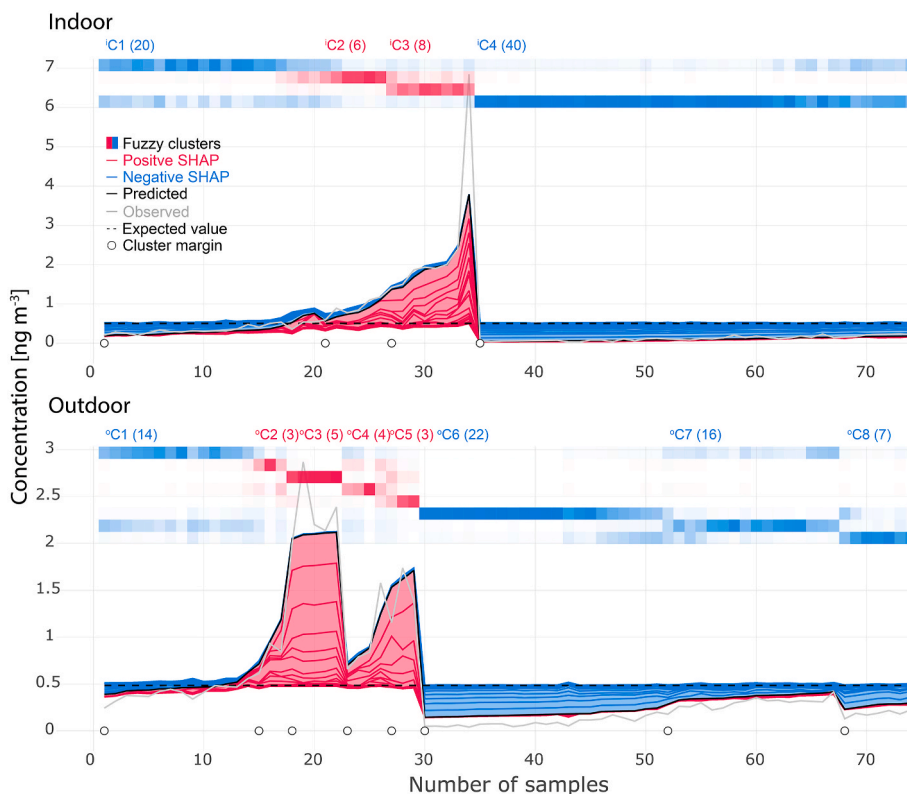


Fig. 4. Indoor (above) and outdoor (below) benzo(a)pyrene SHAP force plots.

conditions of limited photo oxidative reactions. This is confirmed by SHAP dependency analysis which reveals two types of environmental conditions interrelating these compounds characterized by Chry levels below/above 0.9 ng m^{-3} corresponding to the occurrence of this compound predominantly in a gaseous/particulate phase.

${}^i\text{C1-}{}^i\text{C4}$ refers to four clusters being identified for indoor environment by the SHAP value fuzzy clustering, while ${}^o\text{C1-}{}^o\text{C8}$ refers to eight clusters that were identified for outdoor environment. Most of the investigated days were assigned to ${}^o\text{C6}$ (Figs. 4 and 5). The predictors used for cluster differentiation in this study (13 for indoor and 9 for outdoor environment) explain the approximately 90% of B[a]P level dynamics in total. The number of clusters indicate the complexity of the ambient, diversity of emission sources, and abundance of environmental influences. As can be seen in all clusters, mostly particle-bound 4-, 5- and 6-ring PAHs (B[a]A, B[b]F, B[k]F, D[ah]A, and I[cd]P) characterized the environment in which both low and high concentrations of B[a]P were registered, but non-negligible is the impact of 4-ring semi-volatile PAH congeners Chry and Pyr, which show ambivalent chemodynamics depending on the molecular structure, and CO (absolute value of relative SHAP ranging from 6.3 to 9.3%). The pollutants D[ah]A, Cr, As, Rn, and $\text{PM}_{2.5}$, for which low SHAP values (<0.1) were observed, had minor potential for explaining the indoor and/or outdoor environment that shaped B[a]P level dynamics.

During the 60 days in total, being attributed to ${}^i\text{C4}$ (3rd April - 31st May) and ${}^i\text{C1}$ (4th March - 26th May), the investigated parameters defined the indoor environment in which low concentrations of PAHs and particularly B[a]P were registered (mean B[a]P concentrations 0.07 and 0.36 ng m^{-3} for clusters ${}^i\text{C4}$ and ${}^i\text{C1}$, respectively). The range of the

lowest concentrations (${}^i\text{C4}$: $0.03\text{--}0.24 \text{ ng m}^{-3}$) is well-separated from the others (fuzzy cluster membership 88%), indicating that the specific environmental conditions governing their occurrence were associated with the dominant influence of $\text{Chy} > \text{B[b]F} > \text{CO} > \text{B[a]A} > \text{I[cd]P} > \text{B[k]F}$ (relative SHAP ranging from -7.4 to -18%). Indoor low levels clustered in ${}^i\text{C4}$ were observed during the warmer part of the measurement campaign and thus can be predominantly attributed to the reduction of the intensity of the outdoor emission sources related to heating and enhanced photodegradation of PAHs. The range of slightly higher concentrations (${}^i\text{C1}$: $0.2\text{--}0.54 \text{ ng m}^{-3}$) is not well-differentiated (fuzzy cluster membership 69%), which can be probably attributed to the influences that do not originate from the features used in this study. The decrease of B[a]P concentrations was mostly affected by $\text{Chry} > \text{B[a]A} > \text{B[b]F}$ (in average 18.9, 10.3, and 8.5%, respectively).

Conversely, during the period attributed to ${}^i\text{C2}$ (7th March - 9th May) and ${}^i\text{C3}$ (10th March - 28th March), the investigated parameters dominantly defined the indoor environment in which high concentrations of B[a]P, B[a]A, B[b]F, B[k]F, Chry, D[ah]A, and I[cd]P ($0.5\text{--}3 \text{ ng m}^{-3}$), as well as CO were registered ($>0.35 \text{ mg m}^{-3}$), whereas the concentrations of Cr were noticeably lower ($<6.5 \text{ ng m}^{-3}$) than during the events assigned to ${}^i\text{C4}$ and ${}^i\text{C1}$. The ${}^i\text{C2}$ and ${}^i\text{C3}$ periods were associated with changeable weather, low temperature, occasional precipitations, and pronounced cold front breakthroughs that led to the intensified PAH emissions from heating sources and reduced B[a]P ambient decomposition by photolytic reactions. The observed B[a]P mean concentrations and ranges were ${}^i\text{C2}$: 0.90 ; $0.6\text{--}1.2 \text{ ng m}^{-3}$ and ${}^i\text{C3}$: 2.48 ; $1.4\text{--}2.4 \text{ ng m}^{-3}$. Both clusters were characterized by the dominant impact of B[b]F (relative SHAP 18.9 and 25.3%) and differentiated by the impact of Chry

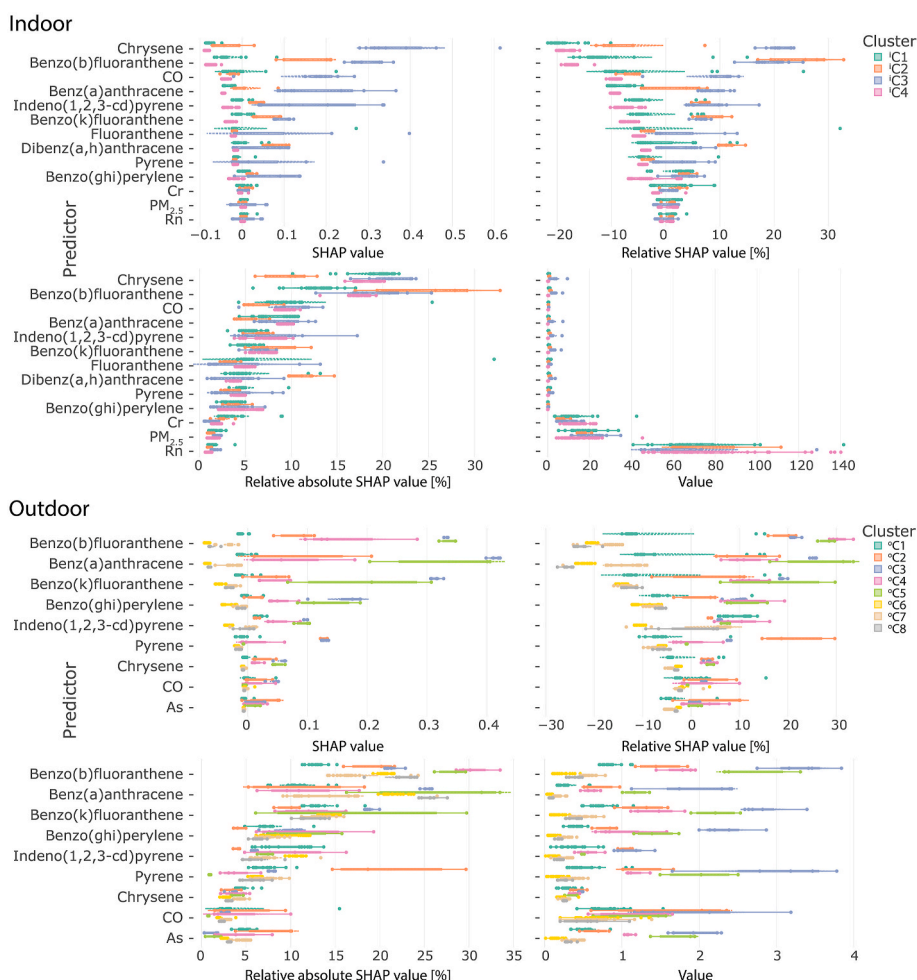


Fig. 5. Indoor (above) and outdoor (below) benzo(a)pyrene SHAP force plot cluster statistics.

and CO which is negative for $^{13}\text{C}_2$ negative, and positive for $^{13}\text{C}_3$. We did not observe the cause of differentiation within the features used in this study.

During the days attributed to clusters $^{\circ}\text{C}_2$, $^{\circ}\text{C}_3$, $^{\circ}\text{C}_4$, and $^{\circ}\text{C}_5$, the elevated concentrations of predictors including I[cd]P, Chry, B[ghi]P, and B[k]F ($>1 \text{ ng m}^{-3}$), B[a]A, B[b]F, and particularly Pyr ($>0.5 \text{ ng m}^{-3}$), As ($>1.2 \text{ ng m}^{-3}$), and CO ($>0.35 \text{ mg m}^{-3}$) shaped the outdoor environment (Figs. 4 and 5) in which high B[a]P concentrations were registered (0.8, 2.3, 1.0, and 1.4 ng m^{-3} , respectively). Over the 14 days assigned to $^{\circ}\text{C}_1$ (4th March - 20th May), the increase of B[a]P levels was mostly affected by I[cd]P concentrations, although its impact was not dominating. Over the days assigned to $^{\circ}\text{C}_6$ (22 days in total in the period 26th March - 31st May), $^{\circ}\text{C}_7$ (16 days in the period 30th March - 24th May) and $^{\circ}\text{C}_8$ (7 days in the period 8th April - 3rd May), the concentrations of investigated parameters including As ($<0.7 \text{ ng m}^{-3}$), B[a]A, B[b]F, B[ghi]P, Pyr, B[k]F, Chry, and I[cd]P ($<1 \text{ ng m}^{-3}$) defined the environment in which low B[a]P levels were registered (0.1, 0.3, and 0.2 ng m^{-3} , respectively). Additionally, the attributions of all predictors to the observed B[a]P concentrations were low, as implied by negative SHAP values and high errors calculated for $^{\circ}\text{C}_6$ (absolute error 0.09 and relative error 97.8%) and $^{\circ}\text{C}_8$ (absolute error 0.09 and relative error 46.6%). This further indicates that other environmental factors (e.g., UV PAH degradation or photochemical formation of PAH derivatives initiated by the presence of peroxides, O_3 , and nitrate and hydroxyl radicals) played an important role in B[a]P environmental fate over the corresponding days.

Based on the absolute SHAP interaction values (Figure S4), the interactions between the following pairs of pollutants: $\text{PM}_{2.5}$ -Chry, CO-DB[ah]A, CO-Rn, CO-B[b]F, Chry-B[k]F and As-Chry appeared to be the most prominent features that shape the indoor environment while B[a]A-B[ghi]P and B[a]A-B[b]F were extracted as the most significant interactions in the outdoor ambience. Additionally, the SHAP relative values point to CO-D[ah]A indoor as the most influential interaction, and the potential explanation has been already discussed in the previous text.

4. Conclusions

The indoor air quality has attracted growing attention since the research has shown that it does not represent a simple reflection of the outdoor pollutant concentrations. Additionally, the findings that some pollutants, including carcinogenic B[a]P, can be more concentrated indoors emphasizes the significance of the internal air quality for human health and well-being. In this study, the machine learning and explainable artificial intelligence methods were successfully employed (relative errors $\leq 15.1\%$) for exploring the sources of indoor and outdoor B[a]P in a university building, and examine its relationships with other air pollutants and meteorological factors. According to the results, Chry and B[b]F concentrations were found to be the main factors which explain the environment, associated with B[a]P specific behavior and fate, followed by other long-lived particle-bound PAHs, including B[a]A, I[cd]P, B[k]F, Flt, D[ah]A, Pyr, and B[ghi]P. Less important associations were recorded between B[a]P concentrations and the levels of inorganic contaminants (CO, As, and Cr), $\text{PM}_{2.5}$, as well as soil moisture, whereas the impacts of other investigated parameters appeared to be negligible. As can be concluded, the ongoing developments and advances in machine learning and artificial intelligence in general, have resulted in complex modeling which have the potential to enhance our understanding of air pollution and related environmental processes.

Author contribution

Andreja Stojić; ; Tijana Miličević: Conceptualization, Methodology, Software. Mirjana Perišić; : Data curation. Andrej Šošarić; ; Vladimir Udovičić; : Visualization, Investigation. Gordana Jovanović; : Supervision. Svetlana Stanišić; ; Snježana Herceg Romanić; : Writing – original

draft, Writing- Reviewing and Editing.

Declaration of competing interest

The authors declare that they have no known competing financial interests or personal relationships that could have appeared to influence the work reported in this paper.

Acknowledgments

The authors acknowledge funding provided by the Institute of Physics Belgrade, through the grant by the Ministry of Education, Science and Technological Development of the Republic of Serbia, the Science Fund of the Republic of Serbia #GRANT No. 6524105, AI – ATLAS, as well as “Analysis of organic pollutants in biological systems and the environment”, institutional financing of scientific activity, Croatia.

Appendix A. Supplementary data

Supplementary data to this article can be found online at <https://doi.org/10.1016/j.chemosphere.2021.133154>.




References

- Ali-Taleshi, M.S., Moeinaddini, M., Bakhtiari, A.R., Feiznia, S., Squizzato, S., Bourliva, A., 2020. A one-year monitoring of spatiotemporal variations of $\text{PM}_{2.5}$ -bound PAHs in Tehran, Iran: source apportionment, local and regional sources origins and source-specific cancer risk assessment. *Environ. Pollut.* 274, 115883. <https://doi.org/10.1016/j.envpol.2020.115883>.
- Azari, M.R., Mohammadian, Y., Pourahmad, J., Khodagholi, F., Mehrabi, Y., 2020. Additive toxicity of Co-exposure to pristine multi-walled carbon nanotubes and benzo α pyrene in lung cells. *Environ. Res.* 183, 109219. <https://doi.org/10.1016/j.envres.2020.109219>.
- Blair, G.S., Henrys, P., Leeson, A., Watkins, J., Eastoe, E., Jarvis, S., Young, P.J., 2019. Young data science of the natural environment: a research roadmap. *Front. Environ. Sci.* 121, 1–14. <https://doi.org/10.3389/fenvs.2019.00121>.
- Błaszczak, E., Rogula-Kozłowska, W., Klejnowski, K., Kubiesa, P., Fulara, I., Mielżyńska-Svach, D., 2017. Indoor air quality in urban and rural kindergartens: short-term studies in Silesia, Poland. *Air Qual. Atmos. Health* 10, 1207–1220. <https://doi.org/10.1007/s11869-017-0505-9>.
- Brehmer, C., Norris, C., Barkjohn, K.K., Bergin, M.H., Zhang, J., Cui, X., Teng, Y., Zhang, Y., Black, M., Li, Z., Shafer, M.M., 2020. The impact of household air cleaners on the oxidative potential of $\text{PM}_{2.5}$ and the role of metals and sources associated with indoor and outdoor exposure. *Environ. Res.* 181, 108919. <https://doi.org/10.1016/j.envres.2019.108919>.
- Chen, H., Lundberg, S., Lee, S.I., 2019. Explaining Models by Propagating Shapley Values of Local Components arXiv preprint arXiv:1911.11888.
- Cvetković, A., Jovašević-Stojanović, M., Marković, D., Ristovski, Z., 2015. Concentration and source identification of polycyclic aromatic hydrocarbons in the metropolitan area of Belgrade, Serbia. *Atmos. Environ.* 112, 335–345. <https://doi.org/10.1016/j.atmosenv.2015.04.034>.
- Directive, 2004. 107/EC of the European parliament and of the council of 15 December 2004 relating to arsenic, cadmium, mercury, nickel and polycyclic aromatic hydrocarbons in ambient air. *Off. J. European Union* 23 (1–16), 26/01/2005.
- Du, W., Yun, X., Chen, Y., Zhong, Q., Wang, W., Wang, L., Qi, M., Shen, G., Tao, S., 2020. PAHs emissions from residential biomass burning in real-world cooking stoves in rural China. *Environ. Pollut.* 267, 115592. <https://doi.org/10.1016/j.envpol.2020.115592>.
- Estève, W., Budzinski, H., Villenave, E., 2004. Relative rate constants for the heterogeneous reactions of OH, NO_2 and NO radicals with polycyclic aromatic hydrocarbons adsorbed on carbonaceous particles. Part 1: PAHs adsorbed on 1–2 μm calibrated graphite particles. *Atmos. Environ.* 38, 6063–6072. <https://doi.org/10.1016/j.atmosenv.2004.05.059>.
- European Standards (EN) 12341, 2014. 2014. Ambient Air. Standard Gravimetric Measurement Method for the Determination of the PM_{10} or $\text{PM}_{2.5}$ Mass Concentration of Suspended Particulate Matter. <https://cds.cern.ch/record/2624772>. (Accessed 27 January 2021).
- European Standards (EN) 14211, 2012a. 2012. Ambient Air. Standard Method for the Measurement of the Concentration of Nitrogen Dioxide and Nitrogen Monoxide by Chemiluminescence. <https://www.en-standard.eu/bs-en-14211-2012-ambient-air-standard-method-for-the-measurement-of-the-concentration-of-nitrogen-dioxide-and-nitrogen-monoxide-by-chemiluminescence/>. (Accessed 27 January 2021).
- European Standards (EN) 14212, 2012b. 2012. Ambient Air. Standard Method for the Measurement of the Concentration of Sulphur Dioxide by Ultraviolet Fluorescence. <https://www.sis.se/en/produkter/environment-health-protection-safety/air-quality/ambient-atmospheres/ssen142122012/>. (Accessed 27 January 2021).

- European Standards (EN) 14625, 2012c. 2012. Ambient Air. Standard Method for the Measurement of the Concentration of Ozone by Ultraviolet Photometry. <https://sh.op.bsigroup.com/ProductDetail?pid=00000000030210754>. (Accessed 27 January 2021).
- European Standards (EN) 14626, 2012d. 2012. Ambient Air. Standard Method for the Measurement of the Concentration of Carbon Monoxide by Non-dispersive Infrared Spectroscopy. <https://www.en-standard.eu/bs-en-14626-2012-ambient-air-standard-method-for-the-measurement-of-the-concentration-of-carbon-monoxide-by-non-dispersive-infrared-spectroscopy/>. (Accessed 27 January 2021).
- European Standards (EN) 14902, 2005. 2005. Ambient Air Quality. Standard Method for the Measurement of Pb, Cd, AS, and Ni in the PM₁₀ Fraction of Suspended Particulate Matter. <https://www.antpedia.com/standard/pdf/13.040.20/1703/EN%2014902-20056234.pdf>. (Accessed 27 January 2021).
- Gibert, K., Horsburgh, S.J., Athanasiadis, N.I., Holmes, G., 2018. Environmental data science. *Environ. Model. Software* 106, 4–12. <https://doi.org/10.1016/j.envsoft.2018.04.005>.
- Gope, M., Masto, R.E., Basu, A., Bhattacharyya, D., Saha, R., Hoque, R.R., Khillare, P.S., Balachandran, S., 2020. Elucidating the distribution and sources of street dust bound PAHs in Durgapur, India: a probabilistic health risk assessment study by Monte-Carlo simulation. *Environ. Pollut.* 267, 115669. <https://doi.org/10.1016/j.envpol.2020.115669>.
- Han, J., Liang, Y., Zhao, B., Wang, Y., Xing, F., Qin, L., 2019. Polycyclic aromatic hydrocarbon (PAHs) geographical distribution in China and their source, risk assessment analysis. *Environ. Pollut.* 251, 312–327. <https://doi.org/10.1016/j.envpol.2019.05.022>.
- Hartmann, J., 2019. Classification Using Decision Tree Ensembles. <https://doi.org/10.2139/ssrn.3484009>, 27 January 2021.
- Hassanvand, M.S., Naddafi, K., Faridi, S., Nabizadeh, R., Sowlat, M.H., Momeni, F., Gholampour, A., Arhami, M., Kashani, H., Zare, A., Niazi, S., 2015. Characterization of PAHs and metals in indoor/outdoor PM₁₀/PM_{2.5}/PM₁ in a retirement home and a school dormitory. *Sci. Total Environ.* 527, 100–110. <https://doi.org/10.1016/j.scitotenv.2015.05.001>.
- International Agency for Research on Cancer, 2012. A Review of Human Carcinogens. Part F: Chemical Agents and Related Occupations. IARC Monographs on the Evaluation of Carcinogenic Risks to Humans. [https://www.thelancet.com/journals/lanonc/article/PIIS1470-2045\(09\)70358-4/fulltext](https://www.thelancet.com/journals/lanonc/article/PIIS1470-2045(09)70358-4/fulltext). (Accessed 27 January 2021).
- International Standardization Organization (ISO) 12884, 2000. 2020. Ambient Air — Determination of Total (Gas and Particle-phase) Polycyclic Aromatic Hydrocarbons — Collection on Sorbent-Backed Filters with Gas Chromatographic/mass Spectrometric Analyses. <https://www.iso.org/standard/1343.html>. (Accessed 27 January 2021).
- Jedrychowski, W., Pac, A., Choi, H., Jacek, R., Sochacka-Tatara, E., Dumyahn, T.S., Spengler, J.D., Camann, D.E., Perera, F.P., 2007. Personal exposure to fine particles and benzo [a] pyrene. Relation with indoor and outdoor concentrations of these pollutants in Krakow. *IJOMEH* 20, 339–348. <https://doi.org/10.2478/v10001-007-0035-z>.
- Jedynska, A., Hoek, G., Eeftens, M., Cyrys, J., Keuken, M., Ampe, C., Beelen, R., Cesaroni, G., Forastiere, F., Cirach, M., De Hoogh, K., 2014. Spatial variations of PAH, hopanes/steranes and EC/OC concentrations within and between European study areas. *Atmos. Environ.* 87, 239–248. <https://doi.org/10.1016/j.atmosenv.2014.01.026>.
- Jung, K.H., Liu, B., Lovinsky-Desir, S., Yan, B., Camann, D., Sjodin, A., Li, Z., Perera, F., Kinney, P., Chillrud, S., Miller, R.L., 2014. Time trends of polycyclic aromatic hydrocarbon exposure in New York City from 2001 to 2012: assessed by repeat air and urine samples. *Environ. Res.* 131, 95–103. <https://doi.org/10.1016/j.envres.2014.02.017>.
- Keyte, I.J., Harrison, R.M., Lammel, G., 2013. Chemical reactivity and long-range transport potential of polycyclic aromatic hydrocarbons—a review. *Chem. Soc. Rev.* 42, 9333–9391. <https://doi.org/10.1039/C3CS60147A>.
- Lammel, G., Klánová, J., Ilić, P., Kohoutek, J., Gasić, B., Kovačić, I., Skrdlíková, L., 2010. Polycyclic aromatic hydrocarbons in air on small spatial and temporal scales e II. Mass size distributions and gas-particle partitioning. *Atmos. Environ.* 44, 5022–5027. <https://doi.org/10.1016/j.atmosenv.2010.07.034>.
- Lao, J.Y., Wang, S.Q., Chen, Y.Q., Bao, L.J., Lam, P.K., Zeng, E.Y., 2020. Dermal exposure to particle-bound polycyclic aromatic hydrocarbons from barbecue fume as impacted by physicochemical conditions. *Environ. Pollut.* 260, 114080. <https://doi.org/10.1016/j.envpol.2020.114080>.
- Liu, B., Xue, Z., Zhu, X., Jia, C., 2017. Long-term trends (1990–2014), health risks, and sources of atmospheric polycyclic aromatic hydrocarbons (PAHs) in the US. *Environ. Pollut.* 220, 1171–1179. <https://doi.org/10.1016/j.envpol.2016.11.018>.
- Liu, D., Xu, Y., Chaemfa, C., Tian, C., Li, J., Luo, C., Zhang, G., 2014. Concentrations, seasonal variations, and outflow of atmospheric polycyclic aromatic hydrocarbons (PAHs) at Ningbo site, Eastern China. *Atmos. Pollut. Res.* 5, 203–209. <https://doi.org/10.5094/APR.2014.025>.
- Liu, W., Wang, D., Wang, Y., Zeng, X., Ni, L., Tao, Y., Wu, J., Liu, J., Zou, Y., He, R., Zhang, J., 2020. Improved comprehensive ecological risk assessment method and sensitivity analysis of polycyclic aromatic hydrocarbons (PAHs). *Environ. Res.* 109500. <https://doi.org/10.1016/j.envres.2020.109500>.
- Lodovici, M., Venturini, M., Marini, E., Grechi, D., Dolara, P., 2003. Polycyclic aromatic hydrocarbons air levels in Florence, Italy, and their correlation with other air pollutants. *Chemosphere* 50, 377–382. [https://doi.org/10.1016/S0045-6535\(02\)00404-6](https://doi.org/10.1016/S0045-6535(02)00404-6).
- Lundberg, S.M., Erion, G., Chen, H., DeGrave, A., Prutkin, J.M., Nair, B., Katz, R., Himmelfarb, J., Bansal, N., Lee, S.I., 2020. From local explanations to global understanding with explainable AI for trees. *Nat. Mach. Intell.* 2, 2522–2539. <https://doi.org/10.1038/s42256-019-0138-9>.
- Lundberg, S.M., Lee, S.I., 2017. A unified approach to interpreting model predictions. In: Guyon, I., Luxburg, U.V., Bengio, S., Wallach, H., Fergus, R., Vishwanathan, S., Garnett, R. (Eds.), *Advances in Neural Information Processing Systems*, vol. 30. NIPS 2017, pp. 4765–4774. In: <https://proceedings.neurips.cc/paper/2017/hash/8a20a8621978632d76c43dfd28b67767-Abstract.html>. (Accessed 27 January 2021).
- Ma, Y., Harrad, S., 2015. Spatiotemporal analysis and human exposure assessment on polycyclic aromatic hydrocarbons in indoor air, settled house dust, and diet: a review. *Environ. Int.* 84, 7–16. <https://doi.org/10.1016/j.envint.2015.07.006>.
- Maechler, M., Rousseeuw, P., Struyf, A., Hubert, M., Hornik, K., 2019. Cluster: Cluster Analysis Basics and Extensions. R package version 2.1.0. <https://cran.r-project.org/web/packages/cluster/cluster.pdf>. (Accessed 27 January 2021).
- Molnar, C., 2019. *Interpretable Machine Learning: A Guide for Making Black Box Models Explainable*. URL <https://christophm.github.io/interpretable-ml-book>. (Accessed 27 January 2021).
- Nieder, R., Benbi, D.K., Reichl, F.X., 2018. Soil-borne particles and their impact on environment and human health. In: Nieder, R., Benbi, D.K., Reichl, F.-X. (Eds.), *Soil Components and Human Health*. Springer, Dordrecht, pp. 99–177. <https://doi.org/10.1007/978-94-024-1222-2>.
- Oliveira, M., Slezakova, K., Delerue-Matos, C., Do Carmo Pereira, M., Morais, S., 2016. Assessment of polycyclic aromatic hydrocarbons in indoor and outdoor air of preschool environments (3–5 years old children). *Environ. Pollut.* 208, 382–394. <https://doi.org/10.1016/j.envpol.2015.10.004>.
- Perraudin, E., Budzinski, H., Villenave, E., 2007. Kinetic study of the reactions of ozone with polycyclic aromatic hydrocarbons adsorbed on atmospheric model particles. *J. Atmos. Chem.* 56, 57–82. <https://doi.org/10.1007/s10874-006-9042-x>.
- Romagnoli, P., Balducci, C., Perilli, M., Gherardi, M., Gordiani, A., Giarazzo, C., Gatto, M.P., Cecinato, A., 2014. Indoor PAHs at schools, homes and offices in Rome, Italy. *Atmos. Environ.* 92, 51–59. <https://doi.org/10.1016/j.atmosenv.2014.03.063>.
- Rönkkö, T.J., Hirvonen, M.R., Happonen, M.S., Leskinen, A., Koponen, H., Mikkonen, S., Bauer, S., Ihtantola, T., Hakkarainen, H., Miettinen, M., Orasche, J., 2020. Air quality intervention during the Nanjing youth olympic games altered PM sources, chemical composition, and toxicological responses. *Environ. Res.* 109360. <https://doi.org/10.1016/j.envres.2020.109360>.
- Sangiorgi, G., Ferrero, L., Ferrini, B.S., Porto, C.L., Perrone, M.G., Zangrando, R., Gambaro, A., Lazzati, Z., Bolzacchini, E., 2013. Indoor airborne particle sources and semi-volatile partitioning effect of outdoor fine PM in offices. *Atmos. Environ.* 65, 205–214. <https://doi.org/10.1016/j.atmosenv.2012.10.050>.
- Sievert, C., 2020. *Interactive Web-Based Data Visualization with R, Plotly, and Shiny*. CRC Press.
- Stanišić, S., Perišić, M., Jovanović, G., Miličević, T., Romanić, S.H., Jovanović, A., Šostarić, A., Udovičić, V., Stojić, A., 2021. The PM_{2.5}-bound polycyclic aromatic hydrocarbon behavior in indoor and outdoor environments, part I: emission sources. *Environ. Res.* 193, 110520. <https://doi.org/10.1016/j.envres.2020.110520>.
- Stojić, A., Stanić, N., Vuković, G., Stanišić, S., Perišić, M., Šostarić, A., Lazić, L., 2019. Explainable extreme gradient boosting tree-based prediction of toluene, ethylbenzene and xylene wet deposition. *Sci. Total Environ.* 653, 140–147. <https://doi.org/10.1016/j.scitotenv.2018.10.368>.
- United States Environmental Protection Agency (US EPA), 2007. Test Method 3546: Microwave Extraction, pp. 1–13. <https://www.epa.gov/sites/production/files/2015-12/documents/3546.pdf>. (Accessed 27 January 2021).
- Velázquez-Gómez, M., Lacorte, S., 2020. Organic pollutants in indoor dust from Ecuadorian Amazonia areas affected by oil extractivism. *Environ. Res.* 109499. <https://doi.org/10.1016/j.envres.2020.109499>.
- Yan, D., Wu, S., Zhou, S., Tong, G., Li, F., Wang, Y., Li, B., 2019. Characteristics, sources and health risk assessment of airborne particulate PAHs in Chinese cities: a review. *Environ. Pollut.* 248, 804–814. <https://doi.org/10.1016/j.envpol.2019.02.068>.
- Ye, Z., Yang, J., Zhong, N., Tu, X., Jia, J., Wang, J., 2020. Tackling environmental challenges in pollution controls using artificial intelligence: a review. *Sci. Total Environ.* 699, 134279. <https://doi.org/10.1016/j.scitotenv.2019.134279>.
- Yury, B., Zhang, Z., Ding, Y., Zheng, Z., Wu, B., Gao, P., Jia, J., Lin, N., Feng, Y., 2018. Distribution, inhalation and health risk of PM_{2.5} related PAHs in indoor environments. *Ecotoxicol. Environ. Saf.* 164, 409–415. <https://doi.org/10.1016/j.ecoenv.2018.08.044>.
- Zhang, J., Liu, W., Xu, Y., Cai, C., Liu, Y., Tao, S., Liu, W., 2019b. Distribution characteristics of and personal exposure with polycyclic aromatic hydrocarbons and particulate matter in indoor and outdoor air of rural households in Northern China. *Environ. Pollut.* 255, 113176. <https://doi.org/10.1016/j.envpol.2019.113176>.
- Zhang, J., Yang, L., Ledoux, F., Courcot, D., Mellouki, A., Gao, Y., Jiang, P., Li, Y., Wang, W., 2019a. PM_{2.5}-bound polycyclic aromatic hydrocarbons (PAHs) and nitrated PAHs (NPAHs) in rural and suburban areas in Shandong and Henan Provinces during the 2016 Chinese New Year's holiday. *Environ. Pollut.* 250, 782–791. <https://doi.org/10.1016/j.envpol.2019.04.040>.
- Zhang, Y., Zheng, H., Zhang, L., Zhang, Z., Xing, X., Qi, S., 2019c. Fine particle-bound polycyclic aromatic hydrocarbons (PAHs) at an urban site of Wuhan, central China: characteristics, potential sources and cancer risks apportionment. *Environ. Pollut.* 246, 319–327. <https://doi.org/10.1016/j.envpol.2018.11.111>.

Note

Results of the first national indoor radon survey performed in Serbia

Maja Eremić Savković¹, Vladimir Udovičić^{2,8} ,
Dimitrije Maletić², Gordana Pantelić³, Predrag Ujić³,
Igor Čeliković³ , Sofija Forkapić⁴, Vladimir Marković⁵ ,
Vesna Arsić⁶, Jovana Ilić⁶ and Branko Markoski⁷

¹ Serbian Radiation and Nuclear Safety and Security Directorate, Belgrade, Serbia

² Institute of Physics Belgrade, University of Belgrade, Serbia

³ Vinča Institute of Nuclear Sciences, University of Belgrade, Serbia

⁴ Department of Physics, Faculty of Science, University of Novi Sad, Serbia

⁵ Faculty of Science, University of Kragujevac, Serbia

⁶ Serbian Institute of Occupational Health 'Dr Dragomir Karajovic', Serbia

⁷ Technical Faculty 'Mihajlo Pupin', University of Novi Sad, Serbia

E-mail: udovicic@ipb.ac.rs

Received 31 July 2019, revised 24 December 2019

Accepted for publication 10 February 2020

Published 27 May 2020



CrossMark

Abstract

The first step in every systematic approach to investigating population exposure to radon on a national level is to perform a comprehensive indoor radon survey. Based on general knowledge of the radon levels in Serbia and corresponding doses, the results obtained from a national indoor radon survey would allow policymakers to decide whether it is necessary to establish a national radon programme. For this reason, Serbia initiated work on a national radon action plan (RAP) in 2014 when it was decided to carry out the first national indoor radon survey. The responsibility for establishing the RAP in Serbia is that of the national regulatory body in the field of radiation protection—the Serbian Radiation and Nuclear Safety and Security Directorate (SRBATOM), formerly known as the Serbian Radiation Protection and Nuclear Safety Agency. The first national indoor radon survey was supported by the International Atomic Energy Agency (IAEA) through a Technical Cooperation Programme. Thanks to the IAEA, we received 6000 passive radon devices based on track-etched detectors. In addition, in order to ensure technical support for the project, SRBATOM formed a task force made up of expert radon representatives from national research institutions. This paper presents a thorough description of the sampling design of the first Serbian indoor radon survey. It also presents the results of the national indoor radon

⁸ Author to whom any correspondence should be addressed.

survey, including descriptive statistics and testing of the distribution of the obtained results for log-normality. Based on GPS coordinates, indoor radon data were projected onto a map of 10 km × 10 km grid cells. Two values were calculated for each cell to create two distinct maps. One map shows the arithmetic mean value of indoor radon concentration per grid cell, and the other map shows the number of radon detectors per grid cell used for the calculation of mean values.

Keywords: radon survey, radon action plan, radon map

1. Introduction

According to recent epidemiological studies, an increase in the risk of lung cancer is positively related to an increase in indoor ^{222}Rn concentration (Darby *et al* 2005). As a result, international regulations and recommendations (WHO 2009, EURATOM 2013, IAEA 2014), as well as comprehensive national radon programmes, have been set up in many countries with the aim of reducing population exposure to indoor radon and the corresponding risks. The representative national indoor radon survey is one of the first steps in a national radon programme aimed at identifying existing exposure situations in the country and radon priority areas (RPA), with a focus on reducing individual risks in these areas.

Radon levels in dwellings have been extensively investigated and monitored worldwide over the last 30 years. On the basis of experiences from abroad, guidelines for performing indoor radon surveys have recently been published (United Nations Scientific Committee on the Effects of Atomic Radiation (UNSCEAR) Report 2008, Font 2009, IAEA 2013, Da Silva and Bossew 2014). In the last decade, national and regional indoor radon surveys were carried out in almost all countries of southeast Europe (Radolić *et al* 2006, Stojanovska *et al* 2012, Cosma *et al* 2013, Kunovska *et al* 2018, Vukotić *et al* 2019).

At the European level, the Radiation Environmental Monitoring (REM) group of the Joint Research Centre (JRC) of the European Commission initiated a project in 2006 to develop a European Atlas of Natural Radiation. One of the maps in this Atlas is the European Indoor Radon Map (EIRM). The aim of the project, among other activities, was to provide information about the levels of environmental radiation by collecting and evaluating the data and harmonising procedures (Dubois *et al* 2010, Bossew *et al* 2015). A digital version of the European Atlas of Natural Radiation was completed and published (Cinelli *et al* 2019). Additionally, a qualitative overview of the indoor radon surveys in Europe was presented in a review article (Pantelić *et al* 2019).

Based on the acquired knowledge from research on radon, a group of radon professionals in Serbia organised a Radon Forum in 2014 and decided to start work on a national radon action plan (RAP). One of the conclusions of the meeting was that the focal point in Serbia for all national radon activities is the regulatory body in the field of radiation protection, the Serbian Radiation and Nuclear Safety and Security Directorate (SRBATOM), formerly known as the Serbian Radiation Protection and Nuclear Safety Agency (SRPNA). SRBATOM formed a 'radon working group' composed of representatives from institutes and universities with radon-related research experience. The short- and long-term plans of the RAP were described in a paper by Udovičić *et al* 2016. The first national indoor radon survey was conducted in 2015–2016 as the first step in establishing a RAP in Serbia. The project was

supported by the IAEA through the national project: SRB9003—Enhancing the Regulatory Infrastructure and Legislative System, with two components:

- An expert mission on ‘National Radon Trial Survey and Raising Awareness of Key Stakeholders’ held on 2 February 2015 in SRBATOM, Belgrade. The objective of the IAEA expert mission was to find the best and most appropriate sampling design of the first national indoor radon survey in Serbia. We targeted two key stakeholders in the project: the Ministry of Environmental Protection and the Ministry of Education, Science and Technological Development;
- Equipment: provision of 6000 track-etched radon detectors; distribution of the detectors across Serbian territory was the responsibility of SRBATOM.

The paper details the sampling design of the first national indoor radon survey. The results of the first national indoor radon survey, together with descriptive statistics are given as well. For the purpose of presenting the data, a map of 10 km × 10 km grid cells, was created. The result was the creation of two distinct maps: one showing the annual average indoor radon concentration per grid cell, and the other showing the number of radon detectors per cell used to calculate mean values.

2. Materials and methods

It is well known that there are two types of indoor radon surveys:

- population-weighted surveys where indoor radon levels are measured in randomly selected dwellings (to estimate the distribution of public exposure to radon), and
- geographically based surveys where dwellings are randomly selected to obtain a minimum number of measurements per chosen area unit, e.g. a grid square or an administrative unit (to identify radon priority areas or to create a radon map).

In the case of Serbia, some of the relevant data from the last census held in 2011 include: a total population of around 7 200 000 (ca. 4 270 000 living in urban and ca. 2 910 000 living in rural areas) with a mean population density of 95 km⁻², total area of ca. 88 000 km², and a total of ca. 3 200 000 housing units. When carefully designed, surveys can in principle meet the requirements and objectives of both types of survey. We opted for a stratified sampling design (a sampling design in which the target is partitioned into separate groups—STRATA). We defined STRATA according to the administrative division of Serbia into districts; the number of districts is 25.

A good communication strategy during the realisation of the national programme for indoor radon measurement was applied. The radon-risk communication plan consisted of several elements: general information about radon and a leaflet with detailed guidelines regarding the placing of the detector that was given to each volunteer; the internet sites for radon professionals (radon forum) and the public; public relations and education (presentations in schools); and communication with key stakeholders and public media (newspapers, TV, radio stations, etc).

Each institution within the radon working group was responsible for a given set of administrative regions (districts). The number of detectors intended to be deployed per district was set according to the size of the population in each district. The majority of detectors were given to physics teachers in high schools and the rest to environmental protection officers in municipalities of these districts. After we gave a lecture on radon and the national campaign in each selected school, we asked pupils to participate in the campaign by placing detectors in

Table 1. Descriptive statistics of the dataset used to estimate the seasonal correction factor. Rn(12) and Rn(6) denote the radon concentrations measured by detectors exposed for 12 and 6 months, respectively. AM(SD)—arithmetic mean and standard deviation.

	AM(SD)	Minimum	Maximum	Median
Rn(12)/Rn(6)	0.79(0.17)	0.52	1.39	0.76

their homes. Physics teachers were responsible for collecting the detectors and sending them back to SRBATOM. Environmental protection officers distributed the rest of the detectors to volunteers who received information regarding the survey over public media. There was no preselection of volunteers, but everybody who expressed their wish to participate was able to. The only limitation was the number of available detectors.

Each participant completed a predefined questionnaire, which, in terms of building characteristics, included information about the type of building (whether a dwelling was a family house or a flat in an apartment building), on which floor the dwelling was, the year of construction, existence of a cellar, wall material, type of heating, existence of hydro-isolation and window design. In total, 6000 passive radon devices based on a CR-39 detector (Radtrak², Radonova) were distributed during October 2015 and left in houses and apartments for 6 months (until April 2016). One detector was deployed in each dwelling, except for 100 randomly selected dwellings (covering typical dwellings across Serbia according to the monography by Jovanović Popović *et al* 2013), where an additional detector was deployed for 12 months in order to gain a proper estimation of the annual indoor radon concentration. Afterwards, the detectors were collected and sent to the authorised laboratory (Radonova) to be processed, and we subsequently received data from the first national indoor radon survey in Serbia. Finally, each participant in the project received a report with the result of the radon measurement and recommendations for further action.

3. Results and discussion

The first important fact about the national indoor radon survey performed in Serbia was the relatively high return rate of detectors (88%), i.e. that the number of collected detectors was 5300. Since distribution of detectors was on a voluntary basis, this could create bias in the survey as it was reported in some other national surveys (Burke and Murphy 2011). Since participants in the projects were mainly high-school students and volunteers, there could be a tendency for participation in such studies to be biased towards people who are more highly educated, which can further be correlated with their level of wealth and consequently their housing. In addition, the survey could be biased toward more urban rather than rural areas and younger rather than older households. A potential social bias can be expected and this is going to be the subject of significant analysis.

During the project preparation phase, we obtained 63 of the 100 deployed pairs of detectors with results aimed at estimating a seasonal correction factor, which is determined as the arithmetic mean (AM) of the ratio of radon concentrations obtained from detectors exposed in certain dwellings for 12 months—R(12) and 6 months—R(6). Descriptive statistics that include the arithmetic mean (AM), standard deviation (SD), minimum, maximum and median used to deduce the seasonal correction factor are presented in table 1. The obtained seasonal correction factor of 0.79 is almost the same as the previously reported value

Table 2. Descriptive statistics of the dataset from the national indoor radon survey in Serbia with applied seasonal correction factors.

AM(SD) Bq m ⁻³	Minimum Bq m ⁻³	Maximum Bq m ⁻³	Median Bq m ⁻³	GM(GSD) Bq m ⁻³
105(150)	3	4335	60	60(3)

Table 3. Distribution of the data on national radon legislation.

0–200 Bq m ⁻³	200–400 Bq m ⁻³	>400 Bq m ⁻³	>1000 Bq m ⁻³
4137 (87%)	479 (10%)	158 (3%)	14 (0.3%)

(Daraktchieva *et al* 2018) of 0.82 applied for the same exposure time of six months starting from October.

The descriptive statistics of the dataset from the national indoor radon survey in Serbia, with applied seasonal correction factors, are presented in table 2. GM—geometric mean; GSD—geometric standard deviation.

The frequency table and exceedance probabilities with respect to national radon action levels are presented in table 3. The current legislation in Serbia regarding radon prescribes action levels for chronic exposure to radon in homes of 200 Bq m⁻³ for newly built structures, and 400 Bq m⁻³ for existing buildings.

As a part of the standard analysis of the data obtained from the indoor radon surveys, empirical distribution was tested for log-normality (IAEA 2013). The log-normal distribution of the seasonally corrected annual average indoor radon concentrations obtained from the national indoor radon survey in Serbia is shown in figure 1, while a quantile–quantile plot of the log-transformed data for indoor radon concentrations is given in figure 2.

Since we chose a stratified sampling design, we have presented the results per district. The distribution of the number of returned detectors with results, the average radon concentration, and the number and percentage of houses with radon levels exceeding 400 Bq m⁻³ by district are shown in table 4. Based on the numbers of collected as well as distributed detectors, the national indoor radon survey is population-weighted. The number of collected detectors from the Belgrade district was five times greater than the average number of collected detectors from other districts. This ratio is in good agreement with data from the last census regarding the size of the populations in districts in Serbia.

According to Article 103 of the European Union Basic Safety Standards (EU-BSS), member states are obliged to identify areas where the annual average radon concentration in a significant number of buildings is expected to exceed the respective national reference level. The question of delineation of radon priority areas (RPA) is very sensitive and left to each country to decide on its own operable definition. Consequently, there are numerous definitions of RPA across the EU (Bossew 2018). The obtained distribution of radon concentration per district and the percentage of houses with an annual average radon concentration exceeding a certain level will serve as a guideline for the Serbian authority first to define RPA and then to delineate RPA.

The results presented in table 4 also show the limitations of the survey in the low number of results obtained from some districts (Pčinja, Mačva, Toplica and central Banat). Improving this will be the task of future national indoor radon measurement campaigns.

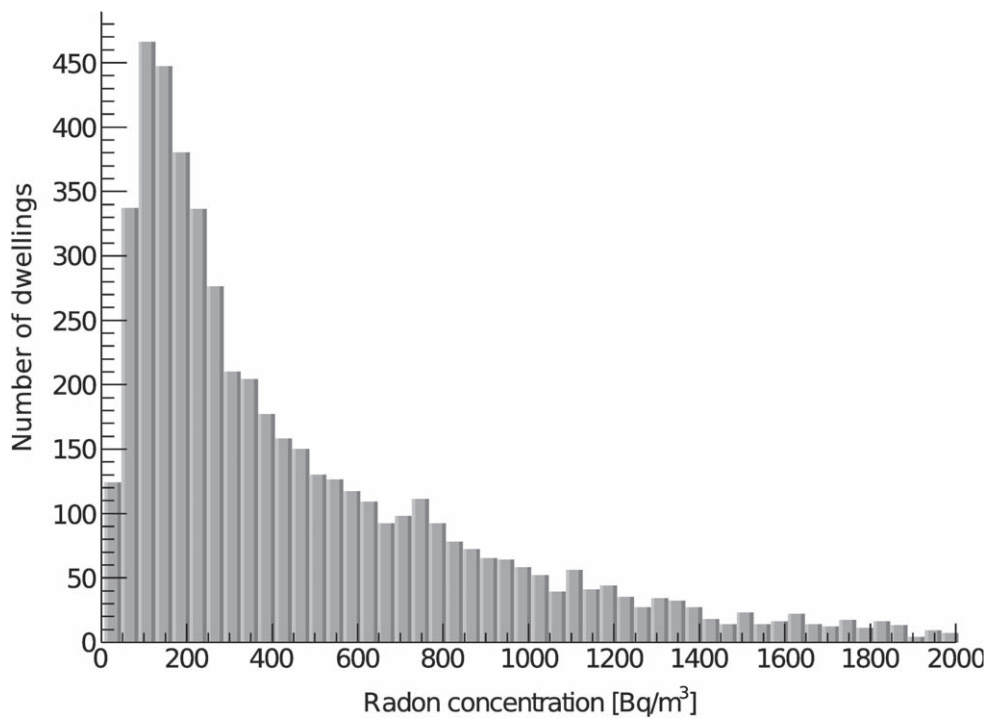


Figure 1. Log-normal distribution of the seasonally corrected annual average indoor radon concentrations measured during the national indoor radon survey in Serbia.

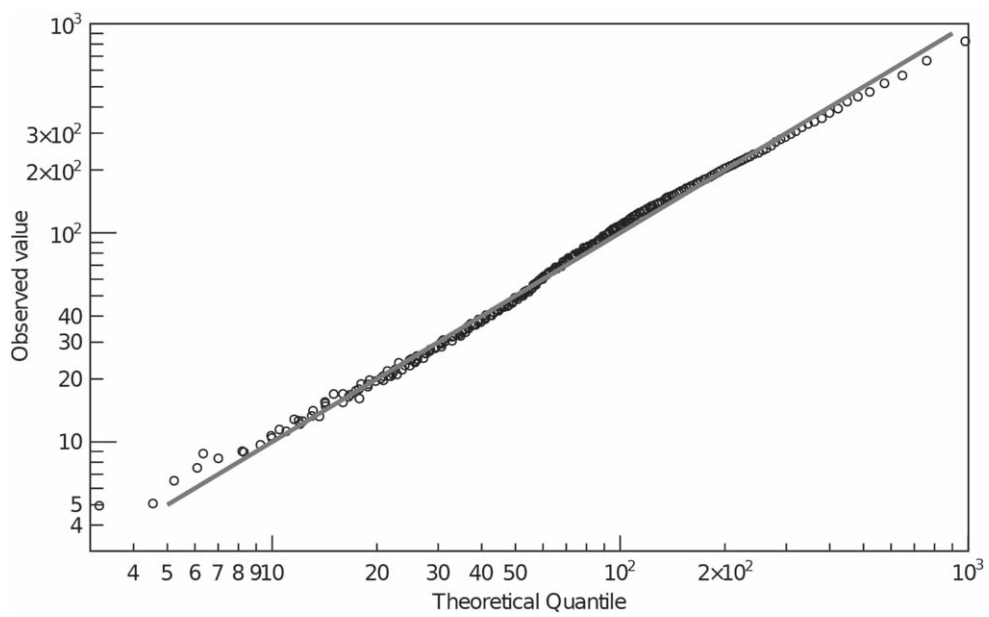


Figure 2. Quantile-quantile plot of the log-transformed data for indoor radon concentrations.

Table 4. Distribution of the population (based on data from the last census in 2011), number of returned detectors, arithmetic mean (AM) with standard deviation (SD) and geometric mean (GM) with geometric standard deviation (GSD) of the indoor radon concentration, number and percentage of dwellings with radon levels exceeding 400 Bq m⁻³ by district.

District	Population (Census 2011)	N	AM(SD) (Bq m ⁻³)	GM (GSD) (Bq m ⁻³)	Number of dwellings with radon levels exceeding 400 Bq m ⁻³	Percentage of dwellings with radon levels exceeding 400 Bq m ⁻³
Central Banat	186,851	37	159(96)	135(2)	1	2.7
Podunavlje	198,184	245	155(206)	92(3)	22	9
Braničevo	180,480	269	144(198)	93(3)	20	7.4
Srem	311,053	199	136(148)	85(3)	11	5.5
West Bačka	187,581	125	135(119)	91(3)	4	3.2
Mačva	297,778	20	129(110)	84(3)	0	0
Nišava	373,404	332	125(332)	68(3)	12	3.6
Pčinja	158,717	10	124(120)	77(3)	1	10
Zlatibor	284,929	330	119(159)	65(3)	20	6.1
North Banat	146,690	54	119(64)	99(2)	0	0
Pomoravlje	212,839	108	114(134)	73(2)	5	4.6
Zaječar	118,295	174	107(105)	71(3)	3	1.7
North Bačka	185,552	88	104(89)	72(3)	1	1.1
Moravica	212,149	173	103(149)	60(3)	9	5.2
South Banat	291,327	126	93(96)	55(3)	1	0.8
Toplica	90,600	31	91(87)	70(3)	1	3.2
Bor	123,848	128	90(114)	47(3)	4	3.1
South Bačka	607,835	523	87(92)	50(3)	7	1.3
Jablanica	215,463	62	86(77)	70(2)	1	1.6
Rasina	240,463	125	84(85)	56(3)	1	0.8
Belgrade	1,639,121	1040	79(115)	41(3)	28	2.7
Raška	300,102	226	78(89)	54(2)	2	0.9
Kolubara	174,228	158	77(99)	47(3)	3	1.9
Pirot	92,277	109	70(73)	60(2)	0	0
Šumadija	290,900	258	70(74)	46(3)	3	1.2

Indoor radon data based on GPS coordinates were projected onto a map of 10 km × 10 km grid cells and are shown in figure 3.

The second map shows the distribution of the number of measurements of annual indoor radon concentrations in 10 km × 10 km grid cells (figure 3). The total number of non-empty cells is 429, with a minimum 1 to a maximum 146 detectors per cell. Since the total area of the Republic of Serbia is ca. 88 000 km² and the number of empty cells is 450, this means that within this survey we covered 50% of the territory.

4. Conclusions

The first national indoor radon survey in Serbia was performed between October 2015 and April 2016. The survey was population-weighted. From the obtained results, the estimated annual arithmetic mean radon level is 105 Bq m⁻³. Based on our results and the fact that 3%

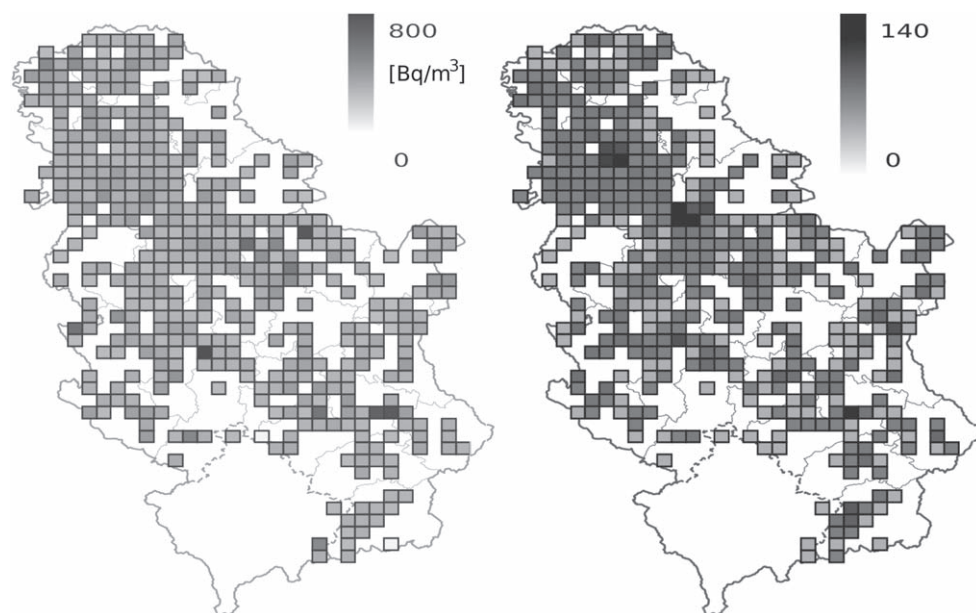


Figure 3. Indoor radon map of the Republic of Serbia (left) and the distribution of the number of measurements over $10 \text{ km} \times 10 \text{ km}$ grid cells of seasonally corrected annual average indoor radon concentrations (right).


of all measurements exceeded the currently defined action level of 400 Bq m^{-3} , we conclude that Serbia has a radon problem. The results of the national radon survey serve to evaluate the existing exposure situation and give a good basis for the next steps in establishing and developing a RAP in Serbia with the main goal of reducing population exposure to indoor radon and the corresponding risks to public health. The indoor radon data based on GPS coordinates were projected onto a map with $10 \text{ km} \times 10 \text{ km}$ grid cells. The obtained distribution of radon concentration per district and the percentage of dwellings with an annual average radon concentration exceeding a certain level will serve as a guideline for the Serbian authority to establish a definition of RPA, to provide additional measurements in districts where necessary, and, finally, to use all these data to delineate RPA.

Acknowledgments

The authors acknowledge the financial support of the International Atomic Energy Agency through the national project: SRB9003—Enhancing the Regulatory Infrastructure and Legislative System and Serbian Radiation Protection and Nuclear Safety Agency.

ORCID iDs

Vladimir Udovičić  <https://orcid.org/0000-0002-7839-1537>

Igor Čeliković  <https://orcid.org/0000-0002-5642-4393>

Vladimir Marković  <https://orcid.org/0000-0002-5566-8169>

References

- Bossew P, Tollefsen T, Cinelli G, Gruber V and De Cort M 2015 Status of the European Atlas of Natural Radiation *Radiat. Prot. Dosim.* **167** 29–36
- Burke Ó and Murphy P 2011 The use of volunteer radon measurements for radon mapping purposes: an examination of sampling bias issues *J. Radiol. Prot.* **31** 319–28
- Bossew P 2018 Radon priority areas - definition, estimation and uncertainty *Nucl. Tech. Radiat. Prot.* **33** 286–92
- Cinelli G, Tollefsen T, Bossew P, Gruber V, Bogucarskis K, De Felice L and De Cort M 2019 Digital version of the European Atlas of Natural Radiation *J. Environ. Radioact.* **196** 240–52
- Cosma C, Cucos A and Dicu T 2013 Preliminary results regarding the first map of residential radon in some regions in Romania *Radiat. Prot. Dosim.* **155** 343–50
- Daraktchieva Z, Howarth C B, Gooding T D, Bradley E J and Hutt N 2018 *Validation Scheme for Organisations Making Measurements of Radon in UK Buildings* PHE-CRCE-040 Centre for Radiation, Chemical and Environmental Hazards Public Health England
- Darby S *et al* 2005 Radon in homes and risk of lung cancer: collaborative analysis of individual data from 13 European case-control studies *Brit. Med. J.* **330** 223–7
- Da Silva N C and Bossew P 2014 The planned Brazilian indoor radon survey—concepts and particular challenges *Radiat. Prot. Dosim.* **162** 105–9
- Dubois G, Bossew P, Tollefsen T and De Cort M 2010 First steps towards a European Atlas of Natural Radiation: status of the European indoor radon map *J. Environ. Radioact.* **101** 786–98
- EUR-Lex 2013 *Council Directive 2013/59/Euratom 02013L0059* <http://data.europa.eu/eli/dir/2013/59/2014-01-17>
- Font L L 2009 On radon surveys: design and data interpretation *Radiat. Meas.* **44** 964–8
- IAEA 2013 National and regional surveys of radon concentration in dwellings; review of methodology and measurement techniques *IAEA Analytical Quality in Nuclear Application Series No. 33, Report IAEA/AQ/33*
- IAEA 2014 *Radiation Protection and Safety of Radiation Sources: International Basic Safety Standards* (IAEA Safety Standards Series) No. GSR Part 3 (Vienna: IAEA)
- Jovanović Popović M, Ignjatović D, Radivojević A, Rajčić A, Čuković Ignjatović N, Đukanović L J and Nedić M 2013 *National Typology of Residential Buildings in Serbia* (Belgrade: Faculty of Architecture University of Belgrade)
- Kunovska B, Ivanova K, Badulin V, Cenova M and Angelova A 2018 Assessment of residential radon exposure in Bulgaria *Radiat. Prot. Dosim.* **181** 34–7
- Pantelić G, Čeliković I, Živanović M, Vukanac I, Krneta Nikolić J, Cinelli G and Gruber V 2019 Qualitative overview of indoor radon surveys in Europe *J. Environ. Radioact.* **204** 163–74
- Radolić V, Vuković B, Stanić D, Katić M, Faj Z, Šuveljak B, Lukačević I, Faj D, Lukić M and Planinić J 2006 National survey of indoor radon levels in Croatia *J. Radioanal. Nucl. Chem.* **269** 87–90
- Stojanovska Z, Januseki J, Boev B and Ristova M 2012 Indoor exposure of population to radon in the FYR of Macedonia *Radiat. Prot. Dosim.* **148** 162–7
- Udovičić V *et al* 2016 First steps towards national radon action plan in Serbia *Nukleonika* **61** 361–5
- UNSCEAR (United Nation Scientific Committee on the Effects of Atomic Radiation Report) 2008 *Sources and Effects of Ionizing Radiation, Report to the General Assembly* (New York: United Nations)
- Vukotić P *et al* 2019 Radon survey in Montenegro—a base to set national radon reference and ‘urgent action’ level *J. Environ. Radioact.* **196** 232–9
- Zeeb H, Shannoun F and WHO 2009 *WHO Handbook on Indoor Radon: A Public Health Perspective* (IRIS: World Health Organization) <https://apps.who.int/iris/handle/10665/44149>

INDOOR RADON, THORON AND THEIR PROGENY CONCENTRATIONS IN HIGH THORON RURAL SERBIA ENVIRONMENTS

Zora S. Zunic¹, Z. Stojanovska², N. Veselinovic¹, R. Mishra³, I. V. Yarmoshenko^{4,*}, B. K. Sapra³, T. Ishikawa⁵, Y. Omori⁵, Z. Curguz⁶, P. Bossew⁷, V. Udovicic⁸ and R. C. Ramola⁹

¹Institute for Nuclear Sciences ‘Vinca’, University of Belgrade, PO Box 522, Belgrade, Serbia

²Faculty of Medical Sciences, Goce Delcev University, Stip, Republic of Macedonia

³Radiological Physics and Advisory Division, Bhabha Atomic Research Centre, Anushakti Nagar, Mumbai, India

⁴Institute of Industrial Ecology, Ural Branch of Russian Academy of Science, Ekaterinburg, Russia

⁵Department of Radiation Physics and Chemistry, Fukushima Medical University, Fukushima, Japan

⁶Faculty of Transport, University of East Sarajevo, Doboje, Republic of Srpska

⁷German Federal Radioprotection Authority, div. SW 1.1, Köpenicker Allee 120-130, D-10318 Berlin, Germany

⁸Institute of Physics, University of Belgrade, Pregrevica 118, Belgrade Serbia

⁹Department of Physics, H.N.B Garhwal University, Tehri Garhwal, India

*Corresponding author: ivy@ecko.uran.ru

This article deals with the variation of radon (Rn), thoron (Tn) and their progeny concentrations expressed in terms of equilibrium equivalent concentrations (EERC and EETC), in 40 houses, in four villages of Sokobanja municipality, Southern Serbia. Two types of passive detectors were used: (1) discriminative radon–thoron detector for simultaneous Rn and Tn gases measurements and (2) direct Tn and Rn progeny sensors (DRPS/DTPS) for measuring Rn and Tn progeny concentrations. Detectors were exposed simultaneously for a single period of 12 months. Variations of Tn and EETC appear higher than those of Rn and EERC. Analysis of the spatial variation of the measured concentrations is also reported. This work is part of a wider survey of Rn, Tn and their progeny concentrations in indoor environments throughout the Balkan region started in 2011 year.

INTRODUCTION

Considering the importance of Rn and Tn decay products contribution in the overall exposure of the population, this paper deals with the results of the survey of Tn and Rn long-term equilibrium factor measurements in 40 dwellings in Sokobanja municipality (Southern Serbia). Although primarily, the research started as a small project designed in 2008 on investigating indoor Rn in the schools^(1–4), lately, in 2011–12, it was expanded on the houses surroundings schools aimed to investigate through a specifically developed model, i.e. selecting the houses as uniformly as possible in concentric shells around schools within a village, to be able to detect an effect of distance between schools and dwellings, to achieve a possible local relation between schools and residential Rn concentrations, to find out whether an estimate of Rn concentrations in dwellings given Rn in schools, is possible. Thus, this research is a continuation of the previous one in the houses of the villages in the same district⁽⁵⁾.

THE STUDY REGION

Sokobanja municipality is an administrative unit belonging to Zajecarski okrug which is one of 29 ones in Serbia, and was selected because the initial negotiations (2008) and further collaboration with regional authorities, with schools and generally with the population was acceptable. Demographic data about the towns and villages which were included in this study refers to the census of 2002. Population in the villages seems to be decreasing, as people move to large towns for work but in the villages seem to build weekend houses and houses for eventual retirement. In Sokobanja municipality there are around 19 000 inhabitants on an area of 525 km². The range of Rn concentrations in schools, as found in the surveys during 2008–10⁽²⁾, was between a few 10 s and over 200 Bq/m³. In Sokobanja municipality, schools tend to have lower Rn levels in the West and higher ones in the East and in the South⁽⁴⁾. The Sokobanja basin is essentially of Tertiary geology with bordering mountains Mesozoic. The basin is crossed by a

tectonic line which runs right through Sokobanja town and Jezero village.

This article deals with the results from survey included 40 houses over the four villages, i.e. Blendija Josanica, Jezero and Sokobanja little towns. The main objective was to examine variations and correlations between concentrations in these villages and compare them to the already published results⁽⁵⁾ related to this region.

At the same time this survey, initiated, started and performed in Serbia⁽¹⁻⁵⁾ triggered indirectly a more extensive program considering the relation schools-dwellings throughout additional countries of the Balkan region with the same pattern of measurements and with the same detectors.

MEASUREMENTS

Rn, Tn and their progeny concentrations measurements

Two different types of passive detectors were used (Figure 1): (1) discriminative Rn/Tn detectors for simultaneous Rn and Tn gases measurements (RADUET) for a large scale survey, provided and analyzed by National Institute for Radiological Sciences (NIRS), Chiba (Japan) and (2) direct Tn and Rn progeny sensors (DRPS/DTPS) for measuring Rn and Tn progeny concentrations, expressed in terms of equilibrium equivalent concentrations (EERC and EETC). DTPSs/DRPSs detectors were supplied and then analyzed by collaborators from Bhabha Atomic Research Centre, BARC, Mumbai (India).

Radon-thoron discriminative dosimeters for large scale survey⁽⁶⁾ with nuclear track detectors (RADUET) consist of two CR-39 detector chips fixed in the lower sections of two diffusion chambers (diameters 60 and 30 mm): the primary chamber of

the detector is sensitive to Rn activity, whereas the secondary chamber is sensitive to both Rn and Tn. Thus, these detectors allow the simultaneous measurements of Rn and Tn gases. The Rn/Tn detectors were calibrated using radon and thoron chambers in NIRS which has organized international intercomparison experiments on radon and thoron measurements⁽⁷⁾.

DRPS/DTPSs detectors consist of two absorber-mounted LR 115-type track detectors for measuring time-averaged Rn and Tn progeny concentrations⁽⁸⁾. They are absorber-mounted (aluminized mylar of 50-mm thickness) LR-115-type nuclear track detectors, which selectively detect only the 8.78-MeV alpha particles emitted from ²¹²Po atoms formed from the radioactive decay of ²¹²Pb and ²¹²Bi atoms deposited on the absorber surface. Similarly, DRPS has an absorber thickness of 37 mm to detect mainly the alpha particles emitted from ²¹⁴Po (7.69 MeV) formed from the eventual decay of ²¹⁸Po, ²¹⁴Pb and ²¹⁴Bi atoms deposited on it.

Detectors have been calibrated under laboratory controlled conditions as well as in real indoor environments⁽⁸⁻¹¹⁾. It has been observed that in general indoor environments (such as the ones considered in this work), when the ventilation rate is between 0.5 and 1.2 h⁻¹, the calibration factor remains constant. This has also been proved by model calculations using Jacobi and Nazaroff particle deposition model⁽⁹⁾. Further, it may be added that, for a broad variability of ventilation rates of uncharacterized environments, an overall uncertainty of 40% can be assigned to its central value. Parallel passive long-term measurements of Rn, Tn and EERC and EETC allow the determination of long-term mean equilibrium factors F for both Rn and Tn. The LLD of DTPS is 0.1 Bq/m³ and that for DRPS is 1 Bq/m³.

As it was in the previous research⁽⁵⁾ the highlight of this work was the simultaneous measurement of Tn and Rn gases and their progeny in the same position inside each room, i.e. a position close to the wall, chosen mainly to reduce the Tn measurement uncertainty.

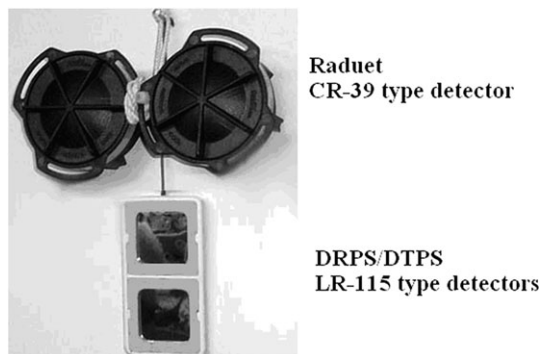


Figure 1. Two passive types detectors RADUET and DRPS/DTPS deployed in the rural houses of Sokobanja municipality.

House types and location of detectors

Discriminative passive Rn/Tn monitors and DTPS/DRPS detectors were deployed in the selected houses and exposed simultaneously for a single period of 12 months. The monitors were placed on the wall in living rooms on ground floors or 'elevated ground floors', which means typically ~1–1.5 m above ground, accessible over a few stairs, but still lower than what would usually be called 'mezzanine'. Given the hilly to mountainous topography houses are often located along a slope, which sometimes makes classification ambiguous; a nominal ground floor room may be in contact with ground at one

side or even extend below surface, while its other side is above ground. Usually houses have no or only partial basement. The most of the houses include older, traditionally built brick and stone houses some were as modern ones which include concrete elements. 'Living rooms' means, in our context, living rooms proper, sleeping rooms, dining rooms and sometimes kitchens which serve as living and dining rooms. In the most cases the measurement devices were fixed on walls, because it was thought that this would best guarantee that they remain undisturbed during the sampling period.

RESULTS AND DISCUSSION

Descriptive statistic of Rn and Tn gas concentrations and EERC and EETC in indoor air of 40 houses located in four villages of Serbia is presented in Table 1. The Tn were generally higher than the Rn (32 out of 40 measurements). The values of the GM for Rn (43 Bq m^{-3}), EERC (10 Bq m^{-3}) and EETC (0.86 Bq m^{-3}) obtained in this study are practically the same to those measured in previous study (49, 11 and 0.8 Bq m^{-3} , respectively). In comparison with same study the value for Tn (89 Bq m^{-3}) is lower than the previously obtained results: Tn (135 Bq m^{-3})⁽⁵⁾.

The correlation between concentrations measured was investigated applying log-transformed values for loss function. The obtained linear regression models are given on Figures 2 and 3. There is no significant correlation between Rn and EERC. Significant positive correlation was found between EETC and Tn.

It is well known that Rn, Tn and their progeny concentrations in indoor environment are subject of high variation caused by many factors, such as meteorological conditions, geology, building characteristic, life style of habitants, etc. Considering CV and GSD values in the Table 1, it is obvious that all measured concentrations have been varied similarly except the EERC which has lower variation. The smaller variations of the EERC over Rn concentrations were obtained in the previous surveys^(5, 12–14). On the other hand, the correlation between Rn and

EERC was significant only in Kosovo⁽¹²⁾ and Macedonia⁽¹³⁾ surveys. Such results can be associated with limitations of the method applied to measurements of Rn EEC which is caused by using mean characteristics of indoor aerosols and ventilation without more careful individual room assessment.

Further analysis concerned the examination of variations depending on the type of room and the village. It was found that the type of room in the investigated region, did not affect significantly measured concentrations. The difference between log-transformed concentration measured in different villages and type of rooms were tested by the non-parametric Kruskal–Wallis test. The only effect of village was significant at the 95% level of significance for Rn, EERC and EETC.

The statistics of each of the village is shown in Table 2. In Sokobanja the mean Rn concentration is higher than in the other three villages. The difference between Tn gas concentrations in the municipalities was not significant. EERC in Jezero, Josanica, Sokobanja are similar, but in Blendija EERC is higher. EETC in Blendija, Jezero, Josanica are similar, but in Sokobanja is lower. Relatively high EETC

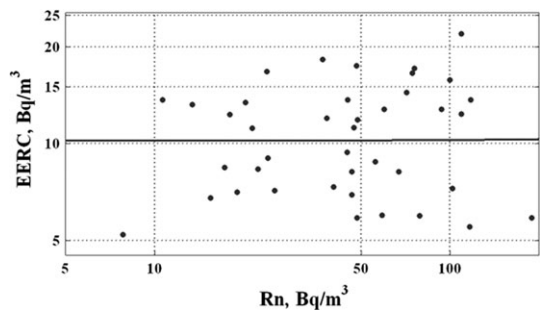


Figure 2. Linear regression model $EERC = 0.0006 \cdot Rn + 10$ (slope factor is insignificant, $p > 0.1$; Spearman $R = 0.08$, $p > 0.14$; loss function: $(\ln(OBS) - \ln(PRED))^2$).

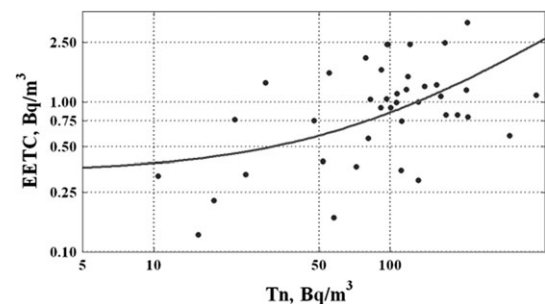


Figure 3. Linear regression model $EETC = 0.005 (\pm 0.03) \cdot Tn + 0.34 (\pm 0.06)$ (with 95% CI; Spearman $R = 0.37$, $p < 0.05$; loss function: $(\ln(OBS) - \ln(PRED))^2$).

Table 1. Descriptive statistics of indoor Rn, Tn and their progeny concentrations in 40 houses of Sokobanja municipality.

Statistic	Rn	Tn	EERC	EETC
Minimum (Bq m^{-3})	8	10	5	0.1
Maximum (Bq m^{-3})	189	412	22	3.4
Median (Bq m^{-3})	47	103	11	1.0
AM (Bq m^{-3})	55	116	11	1.1
CV (%)	69	69	38	66
GM (Bq m^{-3})	43	89	10	0.86
GSD	2.1	2.2	1.5	2.1

Table 2. The results of the measured Rn, Tn, EERC EETC in each village of Sokobanja municipality, Bq m⁻³.

Statistics	Rn	Tn	EERC	EETC
Blendija				
Mean	46	89	16	1.2
SD	37	43	2.7	0.5
GM	36	76	15	1.2
GSD	2.2	2.1	1.2	1.4
Jezero				
Mean	40	144	9.5	1.5
SD	21	99	3.8	0.6
GM	34	119	8.9	1.4
GSD	1.9	1.9	1.5	1.5
Josanica				
Mean	41	96	10	1.0
SD	31	59	2.8	1.1
GM	32	81	9.8	0.8
GSD	2.2	2.0	1.3	2.1
Sokobanja				
Mean	84	104	11	0.6
SD	46	74	4.8	0.4
GM	71	72	11	0.5
GSD	1.9	2.8	1.5	2.1

indicates that most probably the thorium content in the soil and building materials is relatively high in whole region.

CONCLUSION

This work presents simultaneous long-term measurements of Rn, Tn, EER and EET concentrations in rural houses with nuclear track detectors. Rn concentration in the region is compatible with the worldwide value. At the same time, relatively high EETC was found (higher than worldwide average value). The EERC concentrations showed lower variations than the other measured concentrations and absence of correlation with parent Rn. This requires further investigation of the factors influencing on disequilibrium between Rn and progeny including real variability of such characteristic as aerosols concentrations, aerosols attachment and ventilation rates.

ACKNOWLEDGMENTS

The authors gratefully acknowledge the cooperation with the Ministry of Education, Science and Technological Development of the Republic of Serbia and the financial support through its funding under project P41028, and the excellent collaboration with the owners of the houses in the villages of Sokobanja community, Serbia. The special thanks goes to Mr Nebojsa Matejic who guided the research team.

REFERENCES

1. Carpentieri, C. *et al.* Assessment of long-term radon concentration measurement precision in field conditions (Serbian schools) for a survey carried out by an international collaboration. *Radiat. Prot. Dosim.* **145**(2–3), 305–311 (2011).
2. Zunić, Z. S. *et al.* Some results of a radon survey in 207 Serbian schools. *Rom. J. Phys.* **8**(Suppl.), S320–S327 (2010).
3. Bochicchio, F. *et al.* Radon in indoor air of primary schools: a systematic survey to evaluate factors affecting radon concentration levels and their variability. *Indoor Air.* **24**(3), 315–326 (2014).
4. Bossew, P. *et al.* Geographical distribution of the annual mean radon concentrations in primary schools of Southern Serbia—application of geostatistical methods. *J. Environ. Radioact.* **127**, 141–148 (2014).
5. Mishra, R. *et al.* An evaluation of thoron (and radon) equilibrium factor close to walls based on long-term measurements in dwellings. *Radiat. Prot. Dosim.* **160**(1–3), 164–168 (2014).
6. Tokonami, S., Takahashi, H., Kobayashi, Y., Zhuo, W. and Hulber, E. Up-to date radon-thoron discriminative detector for a large scale survey. *Rev. Sci. Instrum.* **76**, 113505 (2005).
7. Janik, M., Ishikawa, T., Omori, Y. and Kavasi, N. Radon and thoron intercomparison experiments for integrated monitors at NIRS, Japan. *Rev. Sci. Instrum.* **85**, 022001 (2014).
8. Mishra, R. and Mayya, Y. S. Study of a deposition based direct thoron progeny sensor (DTPS) technique for estimating equilibrium equivalent thoron concentration (EETC) in indoor environment. *Radiat. Meas.* **43**, 1408–1416 (2008).
9. Mishra, R., Mayya, Y. S. and Kushwaha, H. S. Measurement of ²²⁰Rn/²²²Rn progeny deposition velocities on surfaces and their comparison with theoretical models. *J. Aerosol Sci.* **40**, 1–15 (2009).
10. Mishra, R., Prajith, R., Sapra, B. K. and Mayya, Y. S. An Integrated approach for the assessment of the thoron progeny exposures using direct thoron progeny sensors. *Radiat. Prot. Dosim.* **141**(4), 363–366 (2010).
11. Mishra, R., Rout, R., Prajith, R., Jalaluddin, S., Sapra, B. K. and Mayya, Y. S. Innovative easy-to-use passive technique for ²²²Rn and ²²⁰Rn decay product detection. *Radiat. Prot. Dosim.* **171**(2), 181–186 (2016).
12. Gulan, L. *et al.* Field experience on indoor radon, thoron and their progenies with solid state detectors in a survey of Kosovo and Metohija. *Radiat. Prot. Dosim.* **152**(1–3), 189–197 (2012).
13. Stojanovska, Z. *et al.* Results from time integrated measurements of indoor radon, thoron and their decay product concentrations in schools in the Republic of Macedonia. *Radiat. Prot. Dosim.* **162**(1–2), 152–156 (2014).
14. Curguz, Z. *et al.* Long-term measurements of radon, thoron and their airborne progeny in 25 schools in Republic of Srpska. *J. Environ. Radioact.* **148**, 163–169 (2015).



An underground laboratory as a facility for studies of cosmic-ray solar modulation



N. Veselinović, A. Dragić*, M. Savić, D. Maletić, D. Joković, R. Banjanac, V. Udovičić

Institute of Physics, University of Belgrade, Pregrevica 118, 11080 Zemun, Serbia

ARTICLE INFO

Keywords:

Cosmic ray muons
Forbush decrease
Response function

ABSTRACT

The possibility of utilizing a shallow underground laboratory for the study of energy dependent solar modulation process is investigated. The laboratory is equipped with muon detectors at ground level and underground (25mwe), and with an underground asymmetric muon telescope to have a single site detection system sensitive to different median energies of primary cosmic-ray particles. The detector response functions to galactic cosmic rays are determined from Monte Carlo simulation of muon generation and propagation through the atmosphere and soil, based on CORSIKA and GEANT4 simulation packages. The present setup is suitable for studies of energy dependence of Forbush decreases and other transient or quasi-periodic cosmic-ray variations.

© 2017 Elsevier B.V. All rights reserved.

1. Introduction

Galactic cosmic rays (GCR) arriving at Earth after propagating through the heliosphere interact with nuclei in the atmosphere. These interactions of primary CRs lead to production of a cascade (shower) of secondary particles: hadrons, electrons, photons, muons, neutrinos. Ground based CR detectors are designed to detect some species of secondary cosmic radiation. Widely in use are neutron monitors [1,2], muon telescopes [3,4], various types of air shower arrays [5], γ -ray air Cherenkov detectors [6], air fluorescence detectors [7] etc.

The flux and energy spectra of GCR are modulated by the solar magnetic field, convected by the solar wind. Particularly affected are GCR at the low energy side of the spectrum (up to ~ 100 GeV). Therefore, secondary CRs generated in the atmosphere can be used for studying solar and heliospheric processes. Among the best known effects of the solar modulation are CR flux variations with 11 year period of the solar cycle, 22 year magnetic cycle, diurnal variation and Forbush decrease. The so called corotation with the solar magnetic field results in the flux variation with the 27-day period of solar rotation.

Modulation effects have been studied extensively by neutron monitors (NM) [8,9], sensitive up to several tens of GeV, depending on their geomagnetic location and atmospheric depth. Muon detectors at ground level are sensitive to primary particles of higher energies than NMs. Underground muon detectors correspond to even higher energy primaries. For this reason muon observations complement NM observations in studies of long-term CR variations, CR anisotropy and gradients

or rigidity spectrum of Forbush decreases. However, muon observations suffer from difficulties to disentangle variations of atmospheric origin. While the effect of atmospheric pressure is similar to NMs and easy to account for, the temperature effect is more complicated. The entire temperature profile of the atmosphere is contributing, with different net temperature effect on muon flux at different atmospheric layers, as a result of interplay of positive and negative temperature effects. The positive temperature effect is a consequence of reduced atmospheric density with the temperature increase, resulting in less pion interactions and more decays into muons [10]. The negative temperature effect comes from the increased altitude of muon production at the periods of high temperature, with the longer muon path length and the higher decay probability before reaching the ground level [11]. Both effects are accounted for by the integral method of Dorman [12]. The negative temperature effect is dominant for low energy muons (detected at ground level) and the positive for high energy muons (detected deep underground). At shallow depth of several tens of meters of water equivalent both temperature effects contribute to the overall temperature effect. Several detector systems with different sensitivity to primaries at the same location have the advantage of sharing common atmospheric and geomagnetic conditions.

Belgrade CR station is equipped with muon detectors at ground level and at the depth of 25 m.w.e. Underground laboratory is reached only by muons exceeding energy threshold of 12 GeV. The existing detectors are recently amended by additional setup in an attempt to fully exploit laboratory's possibilities to study solar modulation at different

* Corresponding author.

E-mail address: dragic@ipb.ac.rs (A. Dragić).

median rigidities. In the present paper the detector systems at the Belgrade CR station are described. Response functions of muon detectors to galactic cosmic rays are calculated. The detector system represents useful extension of modulation studies with neutron monitors to higher energies, as it is demonstrated in the case of a recent Forbush event.

2. Description of Belgrade CR station

The Belgrade cosmic-ray station, situated at the Low Background Laboratory for Nuclear Physics at Institute of Physics, is located at near-sea level at the altitude of 78 m a.s.l. Its geographic position is: latitude 44°51'N and longitude 20°23'E, with vertical cut-off rigidity 5.3 GV. It consists of the ground level lab (GLL) and the underground lab (UL) which has useful area of 45 m², dug at a depth of 12 m. The soil overburden consists of loess with an average density 2.0 ± 0.1 g/cm³. Together with the 30 cm layer of reinforced concrete the laboratory depth is equivalent to 25 m.w.e. At this depth, practically only the muonic component of the atmospheric shower is present [13].

2.1. Old setup

The experimental setup [14] consists of two identical sets of detectors and read out electronics, one situated in the GLL and the other in the UL. Each setup utilizes a plastic scintillation detector with dimensions 100 cm × 100 cm × 5 cm equipped with 4 PMTs optically attached to beveled corners of a detector. Preamplifier output of two diagonally opposing PMTs are summed and fed to a digitizer input (CAEN FADC, type N1728B). FADC operates at 100 MHz frequency with 14 bit resolution. The events generating enough scintillation light to produce simultaneous signals in both inputs exceeding the given threshold are identified as muon events. The simulated total energy deposit spectrum is presented on the left panel of Fig. 1. After the appropriate threshold conditions are imposed on the signals from two diagonals, the spectrum is reduced to the one represented on the right panel of the same figure. Contribution from different CR components are indicated on both graphs and experimentally recorded spectrum is plotted as well.

Particle identification is verified by a two-step Monte Carlo simulation. In the first step development of CR showers in the atmosphere is traced, starting from the primary particles at the top of the atmosphere by CORSIKA simulation package. CORSIKA output contains information on generated particles (muons, electrons, photons, etc.) and their momenta at given observation level. More details on CORSIKA simulation will be given in Section 3. This output serves as an input for the second step in simulation, based on GEANT4. In the later step energy deposit by CR particles in the plastic scintillator detector are determined, together with the light collection at PMTs. Contributions from different CR components to recorded spectrum are also shown in Fig. 1.

According to the simulation, 87.5% of events in the coincident spectrum originate from muons. To account for the contribution from other particles to the experimental spectrum not all the events in the spectrum are counted when muon time series are constructed. Muon events are defined by setting the threshold corresponding to muon fraction of recorded spectrum. Threshold is set in terms of “constant fraction” of the spectrum maximum, which also reduces count rate fluctuations due to inevitable shifts of the spectrum during long-term measurements.

2.2. Upgrade of the detector system

Existing detectors enable monitoring of CR variations at two different median energies. An update is contemplated that would provide more differentiated response. Two ideas are considered. First one was to extend the sensitivity to higher energies with detection of multi-muon events underground. An array of horizontally oriented muon detectors ought to be placed in the UL. Simultaneous triggering of more than

one detector is an indication of a multi-muon event. The idea was exploited in the EMMA underground array [15], located at the deeper underground laboratory in Pyhasalmi mine, Finland, with the intention to reach energies in the so called knee region. For a shallow underground laboratory, exceeding the energy region of solar modulation would open the possibility to study CR flux variations originating outside the heliosphere. Second idea is an asymmetric muon telescope separating muons with respect to zenith angle. Later idea is much less expensive to be put into practice.

Both ideas will be explained in detail and response function to GCR for existing and contemplated detectors calculated in the next section.

3. Calculation of response functions

Nature of variations of primary cosmic radiation can be deduced from the record of ground based cosmic ray detectors provided relation between the spectra of primary and secondary particles at surface level are known with sufficient accuracy. Relation can be expressed in terms of rigidity or kinetic energy.

Total detector count rate can be expressed as:

$$N(E_{th}, h, t) = \sum_i \int_{E_{th}}^{\infty} Y_i(E, h) \cdot J_i(E, t) dE \quad (1)$$

where E is primary particle energy, i is type of primary particle (we take into account protons and α particles), $J_i(E, t)$ is energy spectrum of primary particles, h is atmospheric depth and $Y_i(E, h)$ is the so called yield function. E_{th} is the threshold energy of primary particles. It depends on location (geomagnetic latitude and atmospheric altitude) and detector construction details. At a given location on Earth, only particles with rigidity above vertical rigidity cut-off contribute to the count rate. Also, detector construction often prevents detection of low energy particles. For instance, muon detectors are sometimes covered with a layer of lead. In present configuration our detectors are lead free.

Historically, yield functions were calculated empirically, often exploiting the latitude variations of neutron and muonic CR component [16–18]. With the advancement of computing power and modern transport simulation codes it became possible to calculate yield functions from the interaction processes in the atmosphere [19,20]. The yield function for muons is calculated as:

$$Y_i(E, h) = \int_{E_{th}}^{\infty} \int S(\theta, \phi) \cdot \Phi_{i,\mu}(E_i, h, E, \theta, \phi) dE d\Omega \quad (2)$$

where $S(\theta, \phi)$ is the effective detector area and integration is performed over upper hemisphere. $\Phi_{i,\mu}(E_i, h, E, \theta, \phi)$ is the differential muon flux per primary particle of the type i with the energy E_i .

Total differential response function:

$$W(E, h, t) = \sum_i Y_i(E, h) \cdot J_i(E, t) \quad (3)$$

when normalized to the total count rate gives the fraction of count rate originating from the primary particles with the energy in the infinitesimal interval around E . Integration of differential response function gives the cumulative response function.

The response functions of our CR detectors are calculated using Monte Carlo simulation of CR transport through the atmosphere with CORSIKA simulation package. Simulation was performed with protons and α -particles as primary particles. They make ~94% (79% + 14.7%) of all primaries [21]. Implemented hadron interaction models were FLUKA for energies below 80 GeV, and QGSJET II-04 for higher energies. If the old version of QGSJET is used, a small discontinuity in response function is noticed at the boundary energy between two models. Geomagnetic field corresponds to the location of Belgrade $B_x = 22.61$ μ T, $B_z = 42.27$ μ T. Power law form of differential energy spectrum of galactic cosmic rays $J_p(E) \sim E^{-2.7}$ is assumed. Energy range of primary particles is between 1 GeV and $2 \cdot 10^7$ GeV. Interval of zenith angles is $0^\circ < \theta < 70^\circ$. Low energy thresholds for secondary particles are: 150 MeV for hadrons and muons and 15 MeV for electrons

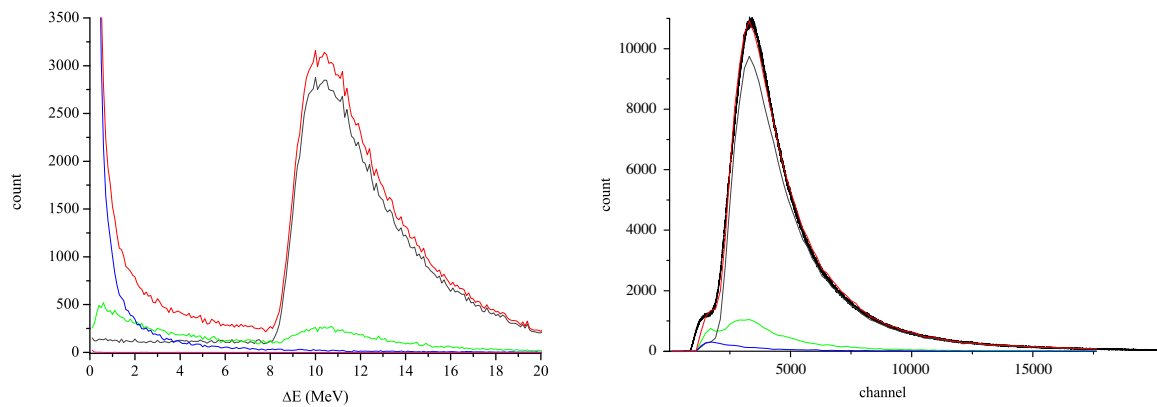


Fig. 1. Left — ΔE spectrum in the plastic scintillator detector, derived from GEANT simulation; right — the same, but for the events exceeding threshold on both diagonals. Contribution of different CR components to the total energy deposit in the detector: muons—gray line, photons—blue line, electrons—green line and sum of all contributions — red line. The black curve on the right panel is the experimental spectrum. (For interpretation of the references to color in this figure legend, the reader is referred to the web version of this article.)

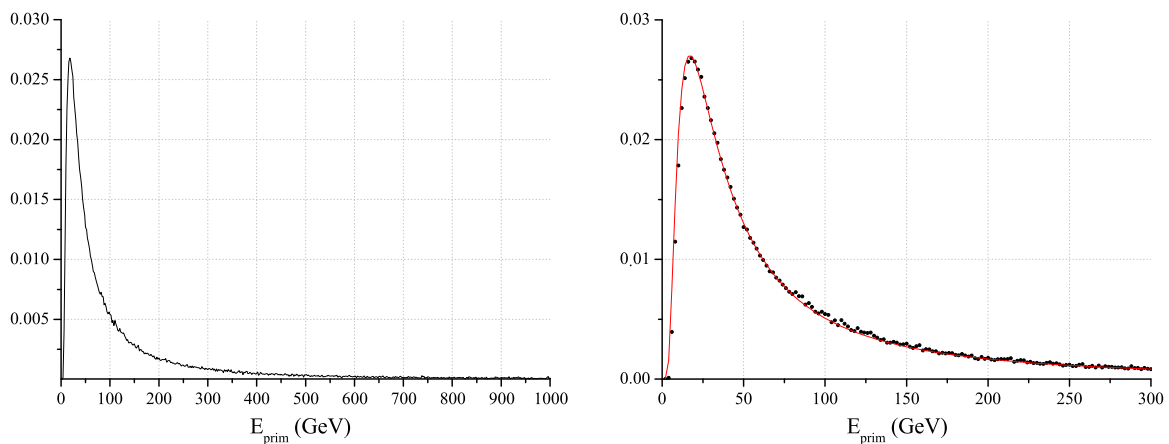


Fig. 2. Left: normalized total response function of ground level muon detector to galactic cosmic rays; right: same as left, fitted with Dorman function (red line). (For interpretation of the references to color in this figure legend, the reader is referred to the web version of this article.)

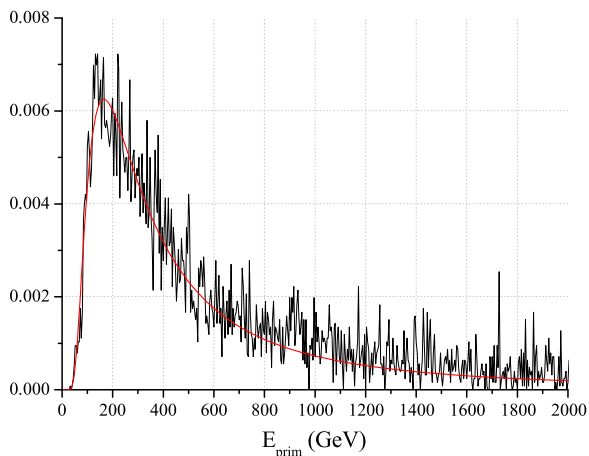


Fig. 3. Response function for multi-muon events in UL to galactic cosmic rays.

and photons. Selected atmospheric model is AT511 (Central European atmosphere for May 11 1993). Observational level is at 78m a.s.l.

For calculation of response functions for underground detectors, simulation of particle propagation through the soil overburden is performed using the code based on GEANT4 package. For precise calculation of energy loss, chemical composition of the soil needs to be known. The

composition used in our work is taken from a geochemical study of neighboring loess sections of Batajnica and Stari Slankamen [22]. Most abundant constituents are quartz (SiO_2) 70%, alumina (Al_2O_3) 15% and quicklime (CaO) 10%, while others include Fe_2O_3 , MgO , TiO_2 , K_2O ,... Inaccuracy of our knowledge of the soil chemical composition should not strongly affect our results since, at relevant energies, dominant energy loss mechanism for muons is ionization which, according to Bethe–Bloch formula depends mostly on $\langle Z \rangle / \langle A \rangle$. Soil density profile is probed during laboratory construction. It varies slowly with depth and average density is found to be $(2.0 \pm 0.1) \text{ g/cm}^3$.

In the simulation, the effective area and angular acceptance of different modes of asymmetric muon telescope (single, coincident and anticoincident) are taken into account.

According to Dorman [12], response function can be parametrized as:

$$W(E) = \begin{cases} 0, & \text{if } E < E_{th}; \\ a \cdot k \cdot \exp(-aE^{-k}), & \text{otherwise;} \\ \frac{a \cdot k \cdot \exp(-aE^{-k})}{E^{(k+1)}(1 - aE_{th}^{-k})}, & \end{cases} \quad (4)$$

with the high energy asymptotics: $W(E) \approx a \cdot k \cdot E^{-(k+1)}$.

3.1. Ground level

Calculated response function for ground level muon detector is presented on Fig. 2, together with fitted Dorman function (4).

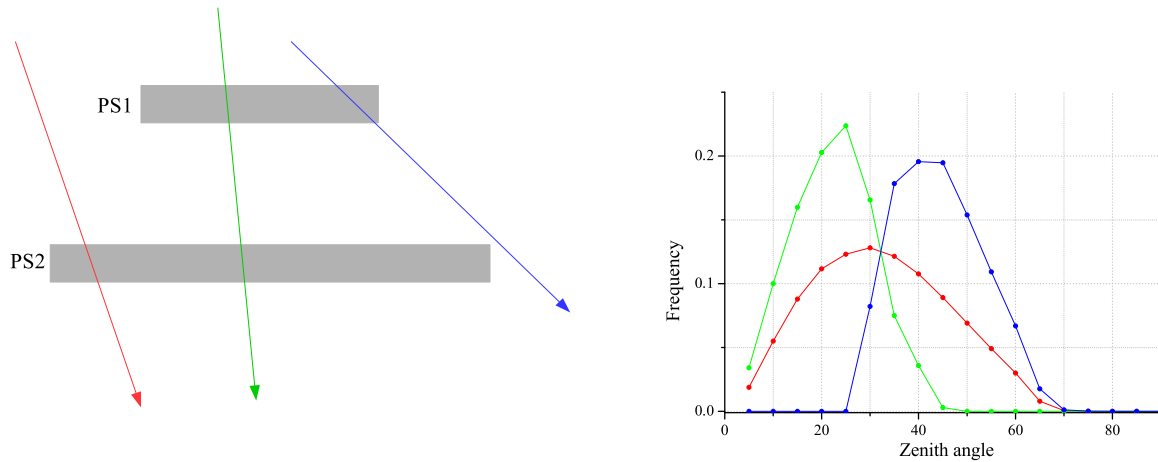


Fig. 4. Left: Schematic view of the asymmetric muon telescope; PS1 — plastic scintillator detector 1, PS2 — plastic scintillator detector 2. Right: angular distribution of detected muons in single mode (red), coincident mode (green) and anticoincident mode (blue), normalized to number of counts in each mode. (For interpretation of the references to color in this figure legend, the reader is referred to the web version of this article.)

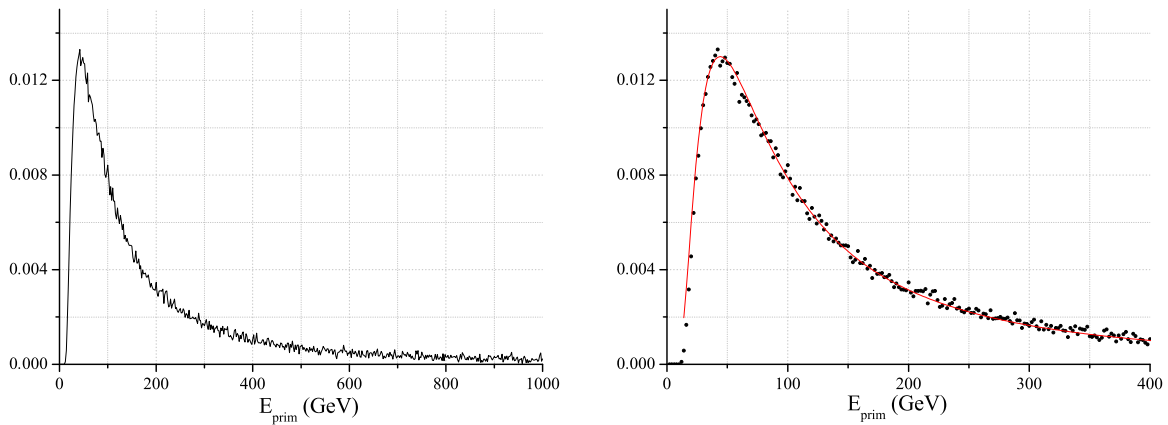


Fig. 5. Response function of single mode of ASYMUT in the UL to galactic cosmic rays. On the right panel the energy interval of interest is enlarged and Dorman function fit is plotted (red line). (For interpretation of the references to color in this figure legend, the reader is referred to the web version of this article.)

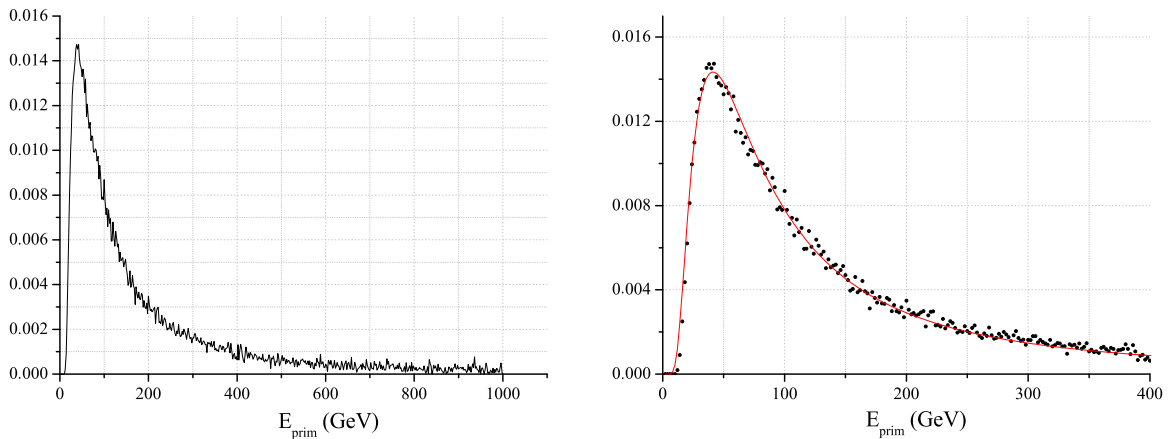


Fig. 6. Response function of coincident mode of asymmetric muon telescope in the UL to galactic cosmic rays. On the right panel the interesting energy interval is enlarged and Dorman function fit is plotted (red line). (For interpretation of the references to color in this figure legend, the reader is referred to the web version of this article.)

3.2. Underground

3.2.1. Multi-muon events

Count rate of multi-muon events underground turned out to be too low for the above mentioned array detector experiment to be feasible in our laboratory. To collect enough events for construction of the response function (Fig. 3), allowed muon separation is 200 m, fairly

exceeding laboratory dimensions. Under these conditions calculated median energy is 270 GeV.

3.2.2. ASYmmetric MUon Telescope (ASYMUT)

Asymmetric muon telescope is an inexpensive detector, constructed from components already available in the laboratory. It consists of two plastic scintillators of unequal dimensions. The lower is identical to the

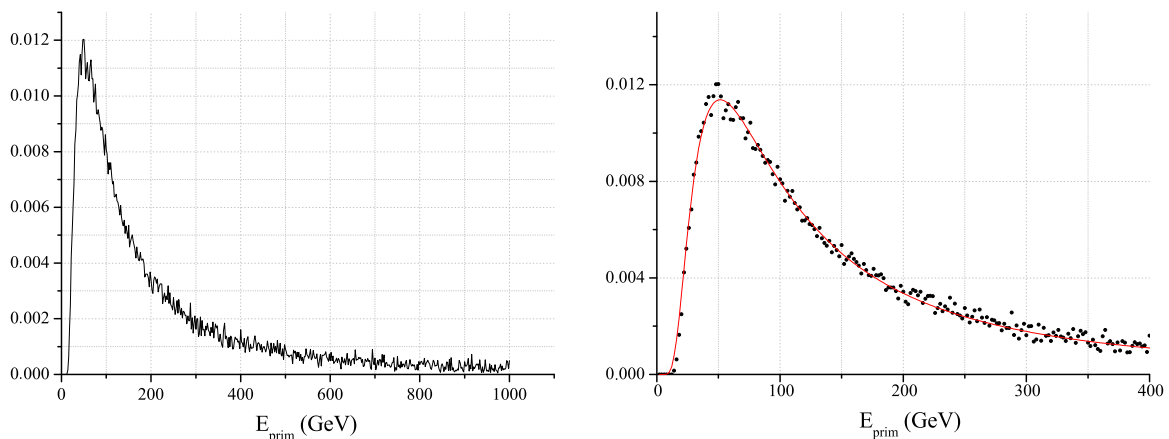


Fig. 7. Response function of anticoincident mode of asymmetric muon telescope in the UL to galactic cosmic rays. On the right panel the interesting energy interval is enlarged and Dorman function fit is plotted (red line). (For interpretation of the references to color in this figure legend, the reader is referred to the web version of this article.)

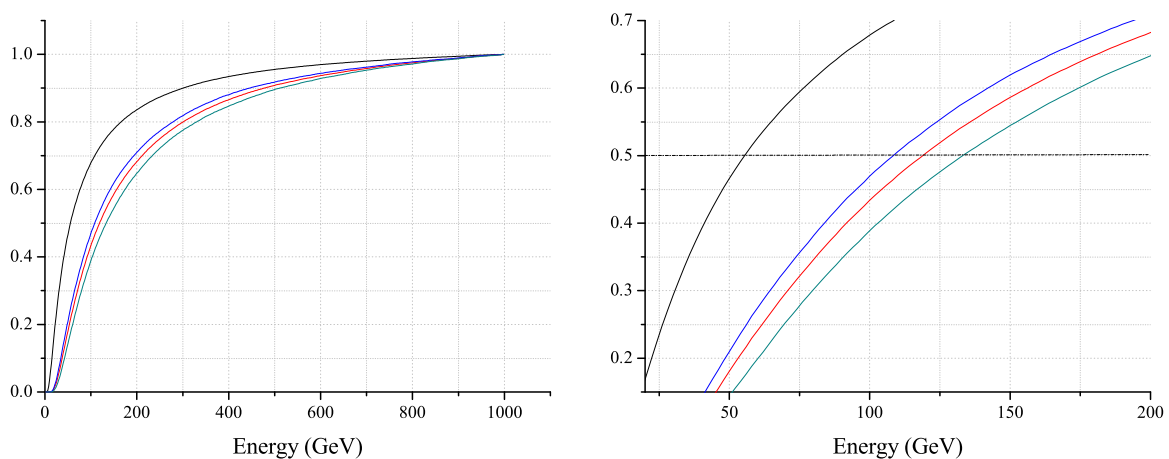


Fig. 8. Cumulative response function to galactic cosmic rays of different muon detectors in the Belgrade CR station: black curve — GLL; red curve — single UL; green curve — CC mode and blue curve — ANTI CC mode of asymmetric muon telescope. The 0.5 level corresponds to median energy. Cumulative response function with enlarged region around this level is shown in the right picture. (For interpretation of the references to color in this figure legend, the reader is referred to the web version of this article.)

one located in the GLL ($100 \times 100 \times 5$ cm) and upper one is $50 \times 46 \times 5$ cm. Detectors are separated vertically by 78 cm, as depicted in Fig. 4, to have roughly the same count rate in the coincident and anticoincident mode. Lower detector in single mode operates in the same manner as the one in the GLL, with wide angular acceptance. The coincident mode is composed of the events registered in both upper and lower detector. In the anticoincident mode, muons passing through the upper but not the lower detector are counted. Therefore, the later mode favors inclined muon paths. Different angular distribution means different path length of muons registered in three modes of ASYMUT (right part of Fig. 4) and also different energy distribution of parental primary particles.

The response functions to GCR of three modes of ASYMUT are shown on Figs. 5–7 and respective cumulative response functions are shown on Fig. 8.

Important parameters describing shapes of response functions are summarized in Table 1. The most often used characteristics of a detector system is its median energy E_{med} . Primary particles with the energy below E_{med} give 50% contribution to detector count rate. The energy interval $(E_{0.05}, E_{0.95})$ is responsible for 90% of registered events. Fitted value of the parameter k from Dorman function (Eq. (4)) is also presented. The parameters $E_{0.05}$ and E_{med} are determined with 1 GeV accuracy, while the uncertainty of $E_{0.95}$ is much higher due to small number of very high energy events and is conservatively estimated as 10%.

Table 1

Sensitivity of Belgrade CR detectors (GLL — ground level; UL — underground based ASYMUT single mode; CC — ASYMUT coincident mode; ANTI — ASYMUT anticoincident mode) to GCR primary particles. Primaries with the energy below $E_{0.05}$ (and above $E_{0.95}$) contribute with 5% to the count rate of a corresponding detector. E_{med} is median energy, E_{th} threshold energy and k is Dorman parameter.

det	E_{th} (GeV)	$E_{0.05}$ (GeV)	E_{med} (GeV)	$E_{0.95}$ (GeV)	k
GLL	5	11	59	915	0.894(1)
UL	12	31	137	1811	0.971(4)
CC	12	27	121	1585	1.015(3)
ANTI	14	35	157	2031	0.992(4)

3.3. Conclusions

Usefulness of our setup for solar modulation studies is tested on the example of investigation of a Forbush decrease of 8 March 2012. In the first half of March 2012 several M and X class solar flares erupted from the active region 1429 on the Sun. The strongest were two X class flares that bursted on March 7. The first one is the X5.4 class flare (peaked at 00:24 UT) and the second one is the X1.3 class flare (peaked at 01:14 UT). The two flares were accompanied by two fast CMEs, one of which was Earth-directed [23]. Several magnetic storms were also registered on Earth, and a series of Forbush decreases is registered. The most pronounced one was registered on March 8. Characteristics of this event as recorded by various neutron monitors and our detectors are compared.

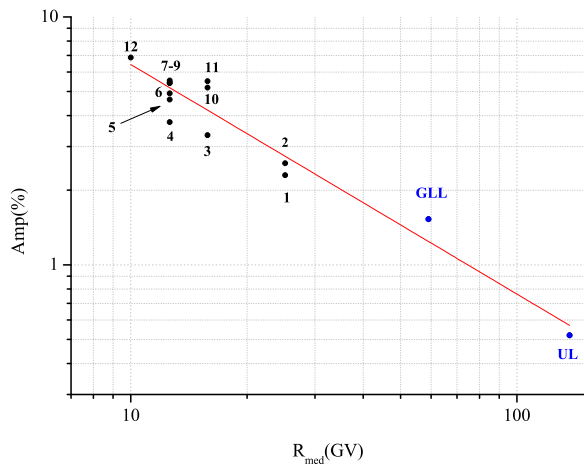


Fig. 9. Rigidity spectrum of FD from 12 March 2012. Black points represent the amplitude of the event as seen by twelve NMs: 1 — Athens, 2 — Mexico City; 3 — Almaty, 4 — Lomnický štít; 5 — Moscow; 6 — Kiel; 7 — Yakutsk; 8 — Apatity; 9 — Inuvik; 10 — McMurdo; 11 — Thule; 12 — South Pole. Blue points are from Belgrade CR station: GLL — ground level and UL — underground. (For interpretation of the references to color in this figure legend, the reader is referred to the web version of this article.)

Amplitude of a Forbush decrease is one of its main characteristics. Dependence of FD amplitude on median rigidity (or energy) is expected to follow the power law: $\Delta N/N \sim R^{-\gamma}$ [12].

For investigation of rigidity spectrum of mentioned FD data from 12 NMs are combined with the data from our two detectors (GLL and UL) that were operational at the time of the event. Neutron monitor data in the period between 1 March 2012 and 1 April 2012 are taken from the NMDB database (www.nmdb.eu) [24]. The exponent of the rigidity spectrum of this FD γ is obtained by the least-square fitting of the data with the power function (Fig. 9) and found to be $\gamma = 0.92 \pm 0.18$. Presented analysis illustrates applicability of our setup for studies of consequences of CR solar modulation process in the energy region exceeding sensitivity of neutron monitors.

Acknowledgments

We are very grateful to late Prof. Ivan Aničin for his enthusiastic contributions, deep insights and valuable advice not just regarding work presented in this paper but also for being a real spiritus agens of our lab. We acknowledge the NMDB database (www.nmdb.eu), founded under the European Union's FP7 programme (contract no. 213007) for providing NM data. The present work was funded by the Ministry of Education, Science and Technological Development of the Republic of Serbia, under the Project No. 171002.

References

- [1] J.A. Simpson, The cosmic ray nucleonic component: The invention and scientific uses of the neutron monitor, *Cosmic Rays Earth* (2000) 11–32.
- [2] J.W. Bieber, Neutron monitoring: Past, present, future, in: Jonathan F.O. (Ed.) AIP Conference Proceedings, vol. 1516, No. 1, 2013.
- [3] M.L. Duldig, Muon observations, in: *Cosmic Rays and Earth*, Springer, Netherlands, 2000, pp. 207–226.
- [4] S. Cecchini, M. Spurio, Atmospheric muons: experimental aspects, *Geosci. Instrum. Methods Data Syst. Discuss.* 2 (2012) 603–641.
- [5] K.-H. Kampert, A.A. Watson, Extensive air showers and ultra high-energy cosmic rays: a historical review, *Eur. Phys. J. H* 37 (3) (2012) 359–412.
- [6] A. de Angelis, O. Mansutti, M. Persic, Very-high energy gamma astrophysics, *Riv. Nuovo Cimento* 31 (4) (2008) 187–246. <http://dx.doi.org/10.1393/ncr/i2008-10032-2>.
- [7] F. Arqueros, J.R. Hörandel, B. Keilhauer, Air fluorescence relevant for cosmic-ray detection — review of pioneering measurements, *Nucl. Instrum. Methods A* 597 (2008) 23–31. <http://dx.doi.org/10.1016/j.nima.2008.08.055>.
- [8] J.A. Lockwood, W.R. Webber, The 11 year solar modulation of cosmic rays as deduced from neutron monitor variations and direct measurements at low energies, *J. Geophys. Res.* 72 (23) (1967) 5977–5989.
- [9] I.G. Usoskin, G.A. Bazilevskaya, G.A. Kovaltsov, Solar modulation parameter for cosmic rays since 1936 reconstructed from ground-based neutron monitors and ionization chambers, *J. Geophys. Res.* 116 (2011) A02104. <http://dx.doi.org/10.1029/2010JA016105>.
- [10] A. Duperier, The meson intensity at the surface of the earth and the temperature at the production level, *Proc. Phys. Soc. A* 62 (11) (1949) 684.
- [11] P.M. Blackett, On the instability of the barytron and the temperature effect of cosmic rays, *Phys. Rev.* 54 (11) (1938) 973.
- [12] L. Dorman, *Cosmic Rays in the Earth's Atmosphere and Underground*, Springer Science + Business Media, LLC., New York, 2004.
- [13] G. Hausser, Cosmic ray-induced background in ge-spectrometry, *Nucl. Instrum. Methods B* 83 (1–2) (1993) 223–228.
- [14] A. Dragić, V. Udovičić, R. Banjanac, D. Joković, D. Maletić, N. Veselinović, M. Savić, J. Puzović, I.V. Aničin, The new setup in the Belgrade low-level and cosmic-ray laboratory, *Nucl. Technol. Radiat. Prot.* 26 (3) (2011) 181–192. <http://dx.doi.org/10.2298/NTRP1101064N>.
- [15] T. Kalliokoski, L. Bezrukov, T. Enqvist, H. Fynbo, L. Inzhechik, P. Jones, J. Joutsenvaara, J. Karjalainen, P. Kuusiniemi, K. Loo, B. Lubsandorzhiev, V. Petkov, T. Rih, J. Sarkamo, M. Slupecki, W. Trzaska, A. Virkajrvi, Can EMMA solve the puzzle of the knee? *Prog. Part. Nucl. Phys.* 66 (2011) 468–472.
- [16] W.H. Fonger, Cosmic radiation intensity-time variations and their origin. II. Energy dependence of 27-day variations, *Phys. Rev.* 91 (2) (1953) 351.
- [17] E.E. Brown, Neutron yield functions for the nucleonic component of cosmic radiation, *Il Nuovo Cimento* (1955–1965) 6 (4) (1957) 956–962.
- [18] L. Dorman, *Cosmic Ray Variations*, State Publishing House for Technical and Theoretical Literature, 1957.
- [19] E.O. Fluckiger, et al., A parameterized neutron monitor yield function for space weather applications, in: *Proceedings of the 30th International Cosmic Ray Conference*, Mexico City, Mexico, vol. 1 (SH), 2008, pp. 289–292.
- [20] M. Zazyan, A. Chilingarian, Calculations of the sensitivity of the particle detectors of ASEC and SEVAN networks to galactic and solar cosmic rays, *Astropart. Phys.* 32 (2009) 185–192.
- [21] K. Nakamura, et al., 24. Cosmic rays, *J. Phys. G* 37 (2010) 075021.
- [22] B. Bugle, B. Glaser, L. Zoller, U. Hambach, S. Markovic, I. Glaser, N. Gerasimenko, Geochemical characterization and origin of Southeastern and Eastern European loesses (Serbia, Romania, Ukraine), *Quat. Sci. Rev.* 27 (2008) 1058–1075.
- [23] NASA Goddard Space Weather Research Center, Summary of the space weather event associated with the X5.4 and X1.3 flare on March 7.
- [24] H. Mavromichalaki, et al., Applications and usage of the real-time Neutron Monitor Database, *Adv. Space Res.* 47 (12) (2011) 2210–2222.

MULTIYEAR INDOOR RADON VARIABILITY IN A FAMILY HOUSE – A CASE STUDY IN SERBIA

by

**Vladimir I. UDOVIČIĆ^{1*}, Dimitrije M. MALETIĆ¹, Radomir M. BANJANAC¹,
Dejan R. JOKOVIĆ¹, Aleksandar L. DRAGIĆ¹, Nikola B. VESELINOVIĆ¹,
Jelena Z. ŽIVANOVIĆ¹, Mihailo R. SAVIĆ¹, and Sofija M. FORKAPIĆ²**

¹Institute of Physics, University of Belgrade, Belgrade, Serbia

²Department of Physics, Faculty of Science, University of Novi Sad, Novi Sad, Serbia

Scientific paper

<http://doi.org/10.2298/NTRP1802174U>

The indoor radon behavior has complex dynamics due to the influence of the large number of different parameters: the state of indoor atmosphere (temperature, pressure, and relative humidity), aerosol concentration, the exchange rate between indoor and outdoor air, construction materials, and living habits. As a result, indoor radon concentration shows variation, with the usual periodicity of one day and one year. It is well-known that seasonal variation of the radon concentration exists. It is particularly interesting to investigate indoor radon variation at the same measuring location and time period, each year, due to estimation of individual annual dose from radon exposure. The long-term indoor radon measurements, in a typical family house in Serbia, were performed. Measurements were taken during 2014, 2015, and 2016, in February and July, each year. The following measuring techniques were used: active and charcoal canisters methods. Analysis of the obtained results, using multivariate analysis methods, is presented.

Key words: radon variability, multivariate regression analysis, multi-seasonal radon measurements, indoor radon

INTRODUCTION

The research of the dynamics of radon in various environments, especially indoors, is of great importance in terms of protection against ionizing radiation and in designing of measures for its reduction. Published results and development of many models to describe the behavior of indoor radon, indicates the complexity of this research, especially with models for prediction of the variability of radon [1-3]. This is because the variability of radon depends on a large number of variables such as local geology, permeability of soil, building materials used for the buildings, the state of the indoor atmosphere (temperature, pressure and relative humidity), aerosol concentration, the exchange rate between indoor and outdoor air, construction materials, as well as the living habits of people. It is known that the indoor radon concentration variation has periodicity of one day and one year. It is also well-known that the seasonal variation of the radon concentration exists. This is why it is particularly interesting to investigate indoor radon variation at the same measuring location and time period, year after

year, in order to estimate the individual annual dose from radon exposure. In that sense, we performed long-term indoor radon measurements in a typical family house in Serbia. Measurements were taken during the 2014, 2015, and 2016, in February and July, each year. We used the following measuring techniques: active and charcoal canisters methods. The detailed analysis of the obtained results using multivariate analysis (MVA) methods is presented in this paper.

First, MVA methods were tested on the radon variability studies in the Underground Low Background Laboratory in the Institute of Physics, Belgrade [4, 5]. Several climate variables: air temperature, pressure, and humidity were considered. Further advance was made by using all the publicly available climate variables monitored by nearby automatic meteorological station. In order to analyze the dependence of radon variation on multiple variables, multivariate analysis needs to be used. The goal was to find an appropriate method, out of the wide spectrum of multivariate analysis methods that are developed for the analysis of data from high-energy physics experiments, to analyze the measurements of variations of radon concentrations in indoor spaces. Previous

* Corresponding author; e-mail: udovicic@ipb.ac.rs

analysis were done using the maximum of 18 climate parameters and use and comparison of 8 different multivariate methods. In this paper the number of variables is reduced to the most important ones and new derived variables, like vapor pressure, simple modeled solar irradiance and simple modeled precipitation, which were introduced in the multivariate analysis.

INDOOR RADON MEASUREMENTS METHODS

Depending on the integrated measurement time, methods of measurement of the indoor radon concentrations may be divided into long-term and short-term ones. The device for the performed short-term radon measurements is SN1029 radon monitor (manufactured by the Sun Nuclear Corporation, NRSB approval-code 31822) with the following characteristics: the measurement range from 1 Bqm^{-3} to 99.99 kBqm^{-3} , accuracy equal to $\pm 25 \%$, sensitivity of $0.16 \text{ counts hour per Bqm}^{-3}$. The device consists of two diffused junction photodiodes as the radon detector which is furnished with sensors for temperature, barometric pressure, and relative humidity. The sampling time was set to 2 h. The method for Charcoal Canister used is: EERF Standard Operating Procedures for Radon-222 Measurement Using Charcoal Canisters [6], also used by major laboratories which conduct radon measurements in Serbia [7]. Exposure time of the charcoal canisters was 48 h. The connection between short term and long term measurements has attracted some interest previously [8].

The family house, selected for the measurements and analysis of variations of radon concentrations, is a typical house in Belgrade residential areas, with requirement of existence of cellar. House is built on limestone soil. Radon measurements were carried out in the living room of the family house, which is built of standard materials (brick, concrete, mortar) and isolated with styrofoam. During the period of measurements (winter-summer 2014, 2015, and 2016), the house was naturally ventilated and air conditioning was used in heating mode at the beginning of the measurement period. During the winter period measurements, the electrical heating was used in addition to air conditioning. Measured radon concentrations, room temperature (T_{id}), atmospheric pressure (P_{id}) and relative humidity (H_{id}) inside the house, were obtained using radon monitor. Values of meteorological variables, in the measurement period, were obtained from an automatic meteorological station, located near the house in which the measurement was performed. We used the following meteorological variables: external air temperature (T), also at height of 5cm, pressure (P) and humidity (H), solar irradiation, wind speed, precipitation, temperature of the soil at depths of 10 cm, 20 cm and 50 cm. The natural ventilation routine was not monitored. Since the ventilation is of

crucial importance for the level of radon indoors [9], Multivariate regression analysis was used mainly for winter periods.

MULTIVARIATE REGRESSION ANALYSIS

In many fields of physics, especially in high-energy physics, there is the demand for detailed analyses of a large amount of data. For this purpose, the data analysis environment ROOT [10], is developed. ROOT is modular scientific software framework, which provides all the functionalities needed to deal with big data processing, statistical analysis, visualization and storage. A specific functionality gives the developed Toolkit for Multivariate Analysis (TMVA) [11]. The TMVA provides an environment for the processing, parallel evaluation and application of multivariate regression techniques.

TMVA is used to create, test and apply all available regression multivariate methods, implemented in ROOT, in order to find methods which are the most appropriate and yield maximum information on the dependence of indoor radon concentrations on the multitude of meteorological variables. Regression methods are used to find out which regression method can, if any, on the basis of input meteorological variables only, give an output that would satisfactorily close match the observed variations of radon concentrations. The output of usage of multivariate regression analysis methods has mapped functional behavior, which can be used to evaluate the measurements of radon concentrations using input meteorological variables only. All the methods make use of training events, for which the desired output is known and is used for training of Multivariate regression methods, and test events, which are used to test the MVA methods outputs.

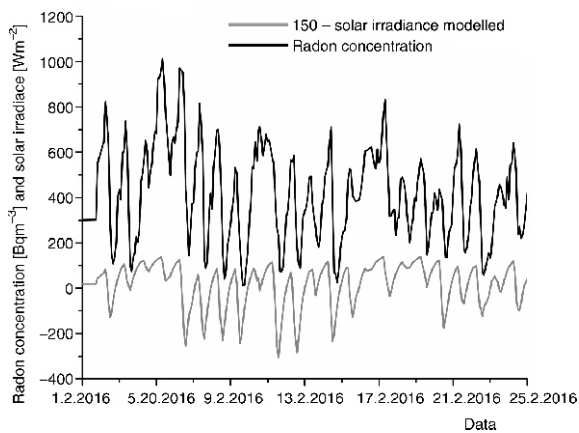
RESULTS

Measurements were performed during February and July in 2014, 2015, and 2016 using radon monitor and charcoal canister measurements. The descriptive results are summarized in tab. 1. The measurements using radon monitor and charcoal canisters are in good agreement.

Previous work done by researchers from the Low Background Laboratory, Institute of Physics, Belgrade, using the MVA analysis in search of connections between radon concentration and meteorological variables, included only one period of measurement, February or July 2014 [4]. Now the MVA analysis is using all the measured data February/July 2014-2016. New variables introduced in MVA analysis are modeled solar irradiance, modeled precipitation and vapor

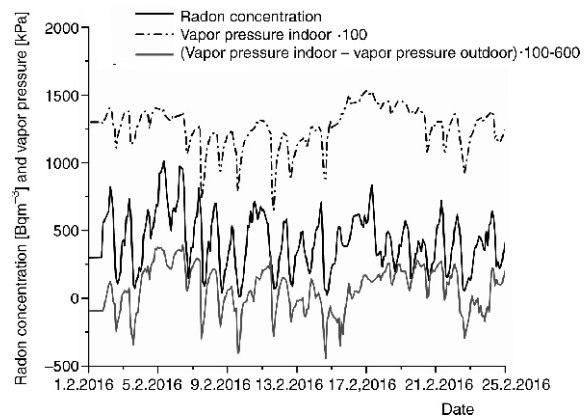
Table 1. Descriptive results of February and July 2014, 2015, and 2016 measurements, using radon monitor and charcoal canisters (only in February)

Results of measurements	2014		2015		2016	
	Feb.	July	Feb.	July	Feb.	July
Minimal radon activity using radon monitor [Bqm^{-3}]	15	0	28	0	12	3
Maximal radon activity using radon monitor [Bqm^{-3}]	1000	286	915	88	1013	262
Median radon activity using radon monitor [Bqm^{-3}]	418	25	524	22	412	28
Arithmetic mean of radon activity using radon monitor (standard deviation) [Bqm^{-3}]	402 (216)	40 (41)	508 (207)	27 (18)	423 (214)	39 (32)
Room temperature using radon monitor (standard deviation) [$^{\circ}\text{C}$]	20.4 (0.8)	24.7 (0.9)	21.2 (0.6)	24.9 (0.8)	22.3 (0.6)	24.6 (0.8)
Relative humidity using radon monitor (standard deviation) [%]	67.4 (5.7)	67.8 (4.8)	68.2 (4.8)	51.5 (4.7)	64.0 (6.4)	58.9 (7.5)
Radon activity using charcoal canister (standard deviation) [Bqm^{-3}]	432 (10)	/	518 (6)	/	407 (5)	/

**Figure 1. Modeled solar irradiance in comparison with measured radon concentration during February 2016**

pressure. In order to make use of intensity of solar irradiance during the whole day and night, the solar irradiance is modeled so that it includes 80 % of solar irradiance value from the previous measurement (previous hour) with addition of solar irradiance value for the actual hour of measurement (fig. 1). The value of 80 % is chosen so that the modeled solar irradiation has the best correlation with the radon measurements. Similar model of precipitation was used in this analysis. The next new variable is vapor pressure. The vapor pressure variable is calculated using the slope $s(T)$, of the relationship between saturation vapor pressure and air temperature and is given by [12, 13], so that the vapor pressure equals relative humidity times saturation vapor pressure, fig. 2.

Before the start of training of Multivariate regression methods using TMVA toolkit in ROOT, the description of input meteorological variables is performed, mainly by looking into inter-correlations of input variables and their connections with the measured radon concentrations. The MVA is using all the measured data. Table 2 presents the meteorological variables and their module value of correlation with the measured radon concentrations (target), which is indicative in finding linear dependence of radon mea-

**Figure 2. Vapor pressure in comparison with measured radon concentration during February 2016**

surements and input variables. The second column in tab. 2 presents us with correlation ratio values which indicate if there are some functional dependence (not only linear) between input variables and radon concentration, and the last column presents the mutual information which indicates if there is a non-functional dependence of input variables and radon measurements [11].

From tab. 2 it can be noticed that linear correlated values are not the only ones which can be used in MVA analysis, for example variable solar irradiance has high mutual information with the radon measurements.

In the data preparation for MVA training the whole dataset is consisting of many events. An event includes time of measurement, radon measurement and meteorological variables. The dataset is randomly split in two halves, one half of the events will be used for training of multivariate regression methods, and the other half of events for testing of methods, mainly to compare the measured and MVA evaluated values for radon concentration.

It turns out that the methods best suited for our purpose is the Boosted Decision Trees (BDT) method. This means that BDT gives the smallest difference be-

Table 2. Input variable rank and values for correlation, correlation ratio and mutual information, all with the measured radon concentrations (target) for February and July 2014-2016 measurements

Variable	Correlation with target		Correlation ratio		Mutual information	
	Rank	Value	Rank	Value	Rank	Value
Soil temperature depth 20 cm [°C]	1	0.87	1	0.60	13	1.48
Soil temperature depth 50 cm [°C]	2	0.86	2	0.57	14	1.31
Soil temperature depth 10 cm [°C]	3	0.82	3	0.54	9	1.84
Temperature outdoor [°C]	4	0.82	5	0.53	8	1.85
Vapor indoor – vapor od [mbar]	5	0.81	9	0.41	11	1.73
Temperature od – temperature id [°C]	6	0.80	4	0.53	6	1.92
Temperature height 5 cm [°C]	7	0.77	8	0.48	7	1.91
Vapor od [mbar]	8	0.76	10	0.41	5	1.92
Temperature id [°C]	9	0.75	7	0.49	17	1.16
Solar irradiance [Wm ⁻²]	10	0.61	6	0.50	2	2.23
Humidity indoor [%]	11	0.45	11	0.26	1	2.26
Humidity outdoor [%]	12	0.31	13	0.20	10	1.76
Air pressure outdoor [mbar]	13	0.27	17	0.07	12	1.55
Wind speed [ms ⁻¹]	14	0.22	16	0.01	16	1.28
Air pressure indoor [mbar]	15	0.17	18	0.04	15	1.31
Humidity od – Humidity id [%]	16	0.10	14	0.19	4	2.11
Precipitation [Lm ⁻²]	17	0.01	15	0.19	18	1.13
Vapor indoor [mbar]	18	0.002	12	0.02	3	2.17

tween the measured radon concentration from test sample and the evaluation of value of radon concentration using input variables only. This can be seen in fig. 3, which shows the distribution of BDT and BDTG regression method outputs (evaluated values) in comparison with the measured radon concentration during February 2016.

Since TMVA has 12 different regression methods implemented, only some of those will give useful results when evaluating the radon concentration measurements. Table 4 summaries the results of MVA analysis. It shows the MVA methods RMS of difference of evaluated and measured radon concentration. Also, tab. 4 shows the mutual information of measured and MVA evaluated radon concentration. Besides

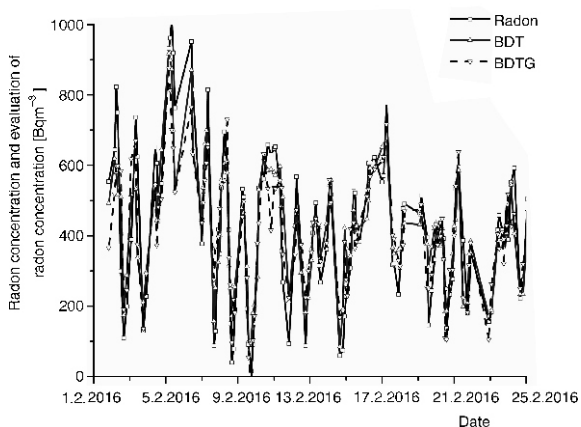


Figure 3. Comparison of MVA evaluated radon concentration and measured one from the test sample of events during February 2016

BDT, the Multi-Layer Perceptron (MLP) [10], an implementation of Artificial Neural Network multivariate method, also gives good results.

The MVA regression analysis results in mapped functional behavior and, as opposed to possible existence of theoretical modeling, which is independent of the number of measurements, MVA depends on the number of events. More events, the better mapped function we get as a result. In this sense, if the number of measurements is not great, multivariate analysis can be used only as help, to indicate which variables are more important to be used in theoretical modeling, for comparison of mapped and modeled functions, and modeled function test.

CONCLUSION

Indoor radon variation at one location in the same periods (February and July), was investigated for three years. Long-term indoor radon measurements show intense seasonal variation. The results obtained with different measuring methods are in good agreement. The radon behavior in the house is almost the same and shows good reproducibility year by year. The small variations in the year by year dynamics are originated mostly from the variations in meteorological variables during winter seasons and mostly due to ventilation habits during summer season. Ventilation habits were not monitored nor taken into account in MVA regression analysis. The preliminary results using multivariate analysis methods in TMVA are shown. Main output of Multivariate regression analy-

Table 3. Input variable correlation with the measured radon concentrations for February and July 2016

Correlation with target			
February 2016		July 2016	
Variable	Value	Variable	Value
Vapor id-vapor od [mbar]	0.58	Soil temperature depth 20 cm [°C]	0.46
Humidity id [%]	0.54	Soil temperature depth 50 cm [°C]	0.42
Vapor id [mbar]	0.52	Solar irradiance	0.32
Solar irradiance [Wm ⁻²]	0.48	Temperature id [°C]	0.30
Temperature od – temperature id [°C]	0.46	Soil temperature depth 10 cm [°C]	0.24
Temperature [°C]	0.44	Temperature od [°C]	0.21
Soil temperature depth 10 cm [°C]	0.43	Humidity od [%]	0.20
Soil temperature depth 20 cm [°C]	0.42	Humidity id [%]	0.19
Humidity [%]	0.38	Air pressure [mbar]	0.17
Temperature height 5 cm [°C]	0.32	Precipitation [Lm ⁻²]	0.17
Temperature id [°C]	0.29	Temperature od – temperature id [°C]	0.16
Air pressure od [mbar]	0.23	Air pressure id [mbar]	0.16
Air pressure id [mbar]	0.21	Humidity od – humidity id [%]	0.14
Soil temperature depth 50 cm [°C]	0.20	Wind speed [ms ⁻²]	0.13
Precipitation [Lm ⁻²]	0.19	Temperature height 5 cm [°C]	0.12
Humidity od – humidity id [%]	0.15	Vapor id [mbar]	0.06
Vapor od [mbar]	0.08	Vapor od [mbar]	0.03
Wind speed [ms ⁻¹]	0.05	Vapor id – vapor od [mbar]	0.02

Table 4. RMS of MVA method's evaluation error and mutual information; February/July 2014-2016

MVA method	RMS [Bqm ⁻³]	Mutual information
BDT	85.5	1.477
BDTG	92.1	1.614
MLP	101	1.401

sis is the initial version of *mapped* function of radon concentration dependence on multitude of meteorological variables. Simplification of MVA methods can be made by choosing only the most important input variables and exclude the other variables.

ACKNOWLEDGEMENTS

The authors acknowledge the financial support of the Ministry of Science, Technology and Development of Serbia within the projects: Nuclear Methods Investigations of Rare Processes and Cosmic Rays (grant number 171002) and Biosensing Technologies and Global System for Continuous Research and Integrated Management (grant number 43002).

AUTHORS' CONTRIBUTIONS

The idea for this paper came as a result of discussions of V. I. Udovičić, R. M. Banjanac, D. R. Joković, A. L. Dragić, and D. M. Maletić. Gathering climate data and MVA analysis was done by D. M. Maletić and V. I. Udovičić. Performed indoor radon measurements were done by V. I. Udovičić and S. M. Forkapić. Writing of the paper was done by D. M. Maletić and V. I. Udovičić. A. L. Dragić gave idea about using MVA

methods in cosmic and radon measurements. N. B. Veselinović and M. R. Savić analyzed and validated climate data. J. Z. Živanović helped with MVA analysis. D. R. Joković helped with data analysis and paper technical preparation.

REFERENCES

- [1] Collignan, B., *et al.*, Development of a Methodology to Characterize Radon Entry in Dwellings, *Building and Environment*, 57 (2012), Nov., pp. 176-183
- [2] Li, F., Baixeras, C., The RAGENA Dynamic Model of Radon Generation, Entry and Accumulation Indoors, *Science of the Total Environment*, 307 (2003), 1-3, pp. 55-69
- [3] Jelle, B. P., *et al.*, Development of a Model for Radon Concentration in Indoor Air, *Science of the Total Environment*, 416 (2012), Jan., pp. 343-350
- [4] Maletić, D., *et al.*, Comparison of Multivariate Classification and Regression Methods for Indoor Radon Measurements, *Nucl Technol Radiat*, 29 (2014), 1, pp. 17-23
- [5] Udovičić, V., *et al.*, Radon Problem in an Underground Low-Level Laboratory, *Radiation Measurements*, 44 (2009), 9-10, pp. 1009-1012
- [6] ***, EPA 520/5-87-005, Gray D.J, Windham S.T, United States Environmental Protection Agency, Montgomery, 1987
- [7] Živanović, M. Z., *et al.*, Radon Measurements with Charcoal Canisters, *Nucl Technol Radiat*, 31 (2016), 1, pp. 65-72
- [8] Stojanovska, Z., *et al.*, Prediction of Long-Term Indoor Radon Concentrations Based on Short-Term Measurements, *Nucl Technol Radiat*, 32 (2017), 1, pp. 77-84
- [9] Nikolić, M. D., *et al.*, Modelling Radiation Exposure in Homes from Siporex Blocks by Using Exhalation Rates of Radon, *Nucl Technol Radiat*, 30 (2015), 4, pp. 301-305
- [10] Brun, R., Rademakers, F., ROOT – An Object Oriented Data Analysis Framework, *Nucl. Inst. Meth. in Phys. Res., A* 389 (1997), 1-2, pp. 81-86

- [11] Hoescker, A., et al., TMVA – Toolkit for Multivariate Data Analysis, PoS ACAT 040, arXiv:physics/070303, 2007
- [12] Murray, F. W., On the Computation of Saturation Vapor Pressure, *J. Applied Meteorology*, 6 (1967), 1, pp. 203-204

- [13] Tetens, O., About Some Meteorological Aspects (in German), *Z. Geophys*, 6 (1930), pp. 207-309

Received on October 6, 2018

Accepted on June 8, 2018

**Владимир И. УДОВИЧИЋ, Димитрије М. МАЛЕТИЋ, Радомир М. БАЊАНАЦ,
Дејан Р. ЈОКОВИЋ, Александар Л. ДРАГИЋ, Никола Б. ВЕСЕЛИНОВИЋ,
Јелена З. ЖИВАНОВИЋ, Михаило Р. САВИЋ, Софија М. ФОРКАПИЋ**

**СТУДИЈА СЛУЧАЈА ВИШЕГОДИШЊЕ ВАРИЈАБИЛНОСТИ РАДОНА
У ПОРОДИЧНОЈ КУЋИ У СРБИЈИ**

Понашање радона у затвореном простору има сложену динамику због утицаја великог броја различитих параметара који утичу на његову варијабилност: метеоролошких (температура, притисак и релативна влажност), концентрације аеросола, брзине размене између унутрашњег и спољашњег ваздуха, грађевинских материјала и животних навика. Као резултат, концентрација радона у затвореним просторијама показује варијацију, уз стандардну периодичност од једног дана и једне године. Годишња варијабилност је добро позната сезонска варијација концентрације радона. Посебно је интересантно пратити вишегодишње варијације концентрације радона на истој мерној локацији и временском периоду, пре свега због процене индивидуалних годишњих доза од изложености радону. У типичној породичној кући у Србији извршена су дуготрајна мерења радона у дневном боравку. Мерења су рађена током 2014, 2015, и 2016. године, у фебруару и јулу, сваке године. Коришћене су следеће мерне технике: активна и метода коришћења угљених канистера. Добијени резултати анализирани су коришћењем мултиваријантне регресионе анализе.

Кључне речи: варијабилност радона, мултиваријантна регресиона анализа, радон у затвореним просторијама, вишегодишње мерење радона



Rigidity dependence of Forbush decreases in the energy region exceeding the sensitivity of neutron monitors

M. Savić, N. Veselinović*, A. Dragić, D. Maletić, D. Joković, R. Banjanac, V. Udovičić

Institute of Physics, University of Belgrade, Pregrevica 118, 11080 Zemun, Serbia

Received 2 May 2018; received in revised form 14 September 2018; accepted 24 September 2018

Available online 28 September 2018

Abstract

Applicability of our present setup for solar modulation studies in a shallow underground laboratory is tested on four prominent examples of Forbush decrease during solar cycle 24. Forbush decreases are of interest in space weather application and study of energy-dependent solar modulation, and they have been studied extensively. The characteristics of these events, as recorded by various neutron monitors and our detectors, were compared, and rigidity spectrum was found. Linear regression was performed to find power indices that correspond to each event. As expected, a steeper spectrum during more intense extreme solar events with strong X-flares shows a greater modulation of galactic cosmic rays. Presented comparative analysis illustrates the applicability of our setup for studies of solar modulation in the energy region exceeding the sensitivity of neutron monitors.

© 2018 COSPAR. Published by Elsevier Ltd. All rights reserved.

Keywords: Forbush decrease; Muon CR station; Median rigidity

1. Introduction

Galactic cosmic rays (GCRs) traverse the heliosphere; this leads to variation in the cosmic ray (CR) flux due to solar activity. The influence of solar and heliospheric modulation is pronounced for primary CR particles with low rigidity or momentum over unit charge. CRs interact, upon arrival, with Earth's atmosphere causing electromagnetic and hadronic showers. A network of ground-based CR detectors, neutron monitors (NMs), and muon detectors, located at various locations around the globe, as well as airborne balloons and satellites, provide valuable data to study the effect of these modulations on the integrated CR flux with time. Energies of the primary particles in NMs are sensitive to the state of solar activity and reach up to 40 GeV. Muon detectors have a significant response from 10 GeV up to several hundred GeV for surface, and

one order of magnitude greater for underground detectors, depending on the depth (Duldig, 2000). This energy interval allows muon detectors to monitor not only modulation effects on lower-energy CRs but also galactic effects on primary CRs with high energies where solar modulation is negligible. Because of the sensitivity to different energies of the primary particle flux, observations of muon detectors complement those of NMs in studies of long-term CR variations, CR anisotropy, and gradients or rigidity spectrum of Forbush decreases (FDs).

FDs (Forbush, 1954) represent decreases of the observed GCR intensity under the influence of coronal mass ejections (CMEs) and interplanetary counterparts of coronal mass ejections (ICMEs) and/or high-speed streams of solar wind (HSS) from the coronal holes (Belov, 2008). FDs belong to two types depending on the drivers: non-recurrent and recurrent decreases. This work addresses several non-recurrent FDs.

These sporadic FDs are caused by ICMEs. As the matter with its magnetic field moves through the solar system,

* Corresponding author.

E-mail address: veselinovic@ipb.ac.rs (N. Veselinović).

it suppresses the CR intensity. FDs of this kind have an asymmetric profile, and the intensity of GCRs has a sudden onset and recovers gradually. Sometimes an early phase of FD prior to the dip (precursor of FD) shows an increase in CR intensity. These precursors of FDs are caused by GCR acceleration at the front of the advancing disturbance on the outer boundary of the ICME, as the primary CR particles are being reflected from the approaching shock (Papailiou et al., 2013). The FD profile depends on the area, velocity, and intensity of CME magnetic field produced in extreme events that originate at the Sun (Chauhan et al., 2008).

Data from observed modulation of GCR intensity contain information regarding the transport of GCRs through the interplanetary environment. GCR transport parameters are connected with the interplanetary magnetic field (IMF) in the heliosphere. It is empirically established that the radial diffusion coefficient is proportional to the rigidity of CR (Ahluwalia, 2005). In this article, we present an analysis of the amplitude of FD during four events, which were recorded by plastic scintillator muon detectors, located at the Belgrade muon station, as well as by a network of NMs.

2. Belgrade CR station

The Low-Background Laboratory for Nuclear Physics (LBNP) is a part of the Institute of Physics, University of Belgrade. It is composed of two separate laboratory facilities, ground-level laboratory (GLL) and underground laboratory (UL), dug into a cliff. The overburden of the UL is approximately 12 m of loess soil, which is equivalent to 25 m of water (m.w.e). Laboratory is dedicated to measurements of low radiation activities and studies of muon and electromagnetic components of CRs at ground and shallow underground levels. The geographic position of the laboratory is at 75 m a.s.l., at 44°51'N latitude and 20°23'E longitude; geomagnetic vertical rigidity cutoff is 5.3 GV at the surface. The equipment was upgraded in 2008, and now, it consists of two identical sets of detectors and accompanying data processing electronics: one is situated in GLL and the other in UL. Detectors are a pair of plastic scintillator detectors, with dimensions of 100 cm × 100 cm × 5 cm and four PMTs that are directly coupled to the corners. Signals from two opposite PMTs on a single detector are summed, and the coincidence of the two diagonals is found. Fig. 1 presents the coincident sum spectra of two diagonals of large scintillator detectors.

Summing over diagonals suppresses the acquisition of electromagnetic component of the secondary CR shower and collects mainly the muon component of secondary CRs. A well-defined peak in the energy spectra corresponds to a muon energy loss of ~11 MeV. The average muon flux measured in the laboratory is 137(6) muons/m²s for GLL and 45(2) muons/m²s for UL. For more detailed description, see Dragić et al. (2011). Integral of this distribution, without low energy part, is used to form time series of this

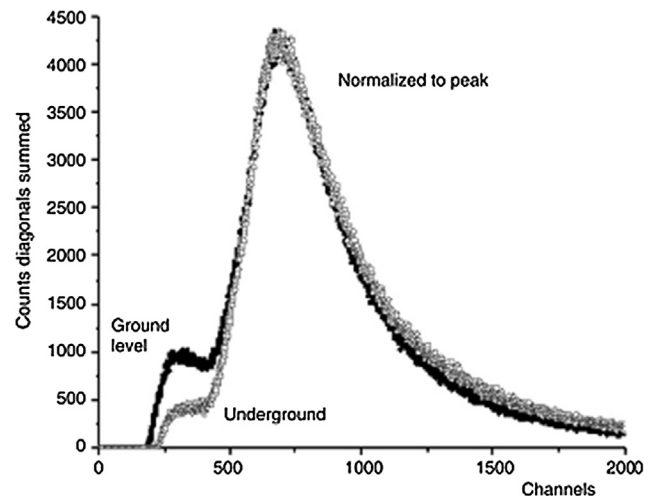


Fig. 1. The coincident spectra of two diagonals of large plastic detectors in UL and GLL normalized for comparison.

CR muons spectrum integrated over different time intervals. This time series is then corrected for efficiency, atmospheric pressure, and temperature (Savić et al., 2015).

The CR flux measured at the ground level varies because of changes in atmospheric conditions. Effects of the atmospheric pressure can be easily accounted for, similar like for NMs, but the temperature effect is somewhat more difficult to treat. The difficulties arise from the interplay of positive and negative temperature effects. With temperature increase, the atmospheric density decreases; hence, less pions interact and more muons are created from decay. The result is a positive effect of more muons at the ground level. On the other hand, the altitude of muon production level is high due to the expansion of the atmosphere when the temperature is high, muon path length is long, and decay probability of muons is high before they reach the ground level. Negative effect is dominant for low-energy muons (mostly detected in GLL) and positive for high-energy muons. A proper treatment of the temperature effect requires knowledge of the entire temperature profile of the atmosphere. This meteorological variation must be corrected to study CR variations originating outside the atmosphere.

For ground (and underground)-based CR detectors, the response function, i.e., the relation between particles of GCR spectra at the top of the atmosphere and recorded secondary particles at the surface level, should be accurately known. The total detector count rate can be expressed as follows (Caballero-Lopez and Moraal, 2012):

$$\begin{aligned} N(R_0, h, t) &= \sum_i \int_{R_0}^{\infty} (S_i(R, h) j_i(R, t)) dR \\ &= \int_{R_0}^{\infty} W(R, h, t) dR \end{aligned} \quad (1)$$

where $N(R_0, h, t)$ is the detector counting rate, R_0 is the geomagnetic cutoff rigidity, h is the atmospheric depth, and t represents time. $S_i(R, h)$ represents the detector yield

function for primary particles of type i and $j_i(R, t)$ represents the primary particle rigidity spectrum of type i at time t . The total response function $W(R, h, t)$ is the sum of $S_i(R, h)$ and $j_i(R, t)$. The maximum value of this function is in the range of 4–7 GV at sea level, depending on the solar modulation epoch at time t (Clem and Dorman, 2000). One of the methods to find this response function is to use the numerical simulation of propagation of CRs through the atmosphere. CORSIKA simulation package (Heck et al., 1998) was to simulate CR transport through the atmosphere and GEANT4 (Agostinelli et al., 2003) to simulate the propagation of secondary CRs through overburden and response of the detectors to find the relationship between the count rate at our site and the flux of primary particles on top of the atmosphere.

The excellent agreement of the simulated and measured flux (Fig. 2) allows us to establish that the cutoff energy for primary CR protons for showers detected in GLL is caused by its geomagnetic rigidity, and the median energy is ~ 60 GeV. For UL, the cutoff energy due to earth overburden is 12 GeV, and the median energy is ~ 120 GeV. These values give us opportunity to study solar modulation at energies exceeding energies detected with a NM. Observation of the solar activity and related magnetic disturbances in the heliosphere that create transient CR intensity variation at several different energies can provide an energy-dependent description of these phenomena.

3. Data analysis

The new setup in the LBLNP, presented by Dragić et al. (2011) coincides with the start of the 24th solar cycle, thus allowing us to observe the increase and decrease in solar activity and the effect of solar modulation at energies higher than ones studied using NMs.

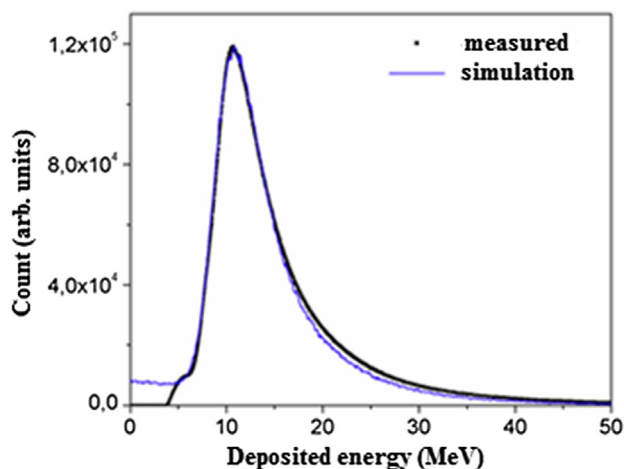


Fig. 2. Simulated (blue line) and measured spectra (black line) for muon detectors in UL. (For interpretation of the references to colour in this figure legend, the reader is referred to the web version of this article.)

Muon time series was searched for days where the average muon flux was significantly lower than the background level. The background level is determined from the moving averages of hourly count rates 10 days before the event. These decreases in the count rate, in GLL and UL, are then compared with space weather events of solar cycle 24. Data collected in UG and GLL are compared with four NM stations from the neutron monitor database [<http://www.nmdb.eu/>]. Three of these NMs (Athens, Rome, and Jungfraujoch) have cutoff rigidity and geographic proximity similar to the Belgrade CR station.

A high correlation is found between the count rates measured by the NMs in the LBLNP in March 2012 (Table 1), but for GLL and UL, as the cutoff energy of the primary flux increases, the correlation slightly decreases.

3.1. Selected Forbush decreases

The Belgrade CR station has detected, both in GLL and UL, several significant structures connected to some extreme solar effects. Several, more prominent, Forbush decreases occurred in March 2012, September 2014, June 2015, and most recently in September 2017.

The FD that occurred on March 8, 2012 was recorded at the Belgrade CR station as well as at other stations (Fig. 3). This FD was separated into two following two CMEs. These CMEs produced an intense disturbance in the interplanetary space and caused a severe geomagnetic storm when the shockwave reached Earth on March 8, 2012. During this event, a very complex combination of modulation occurs (Lingri et al., 2016). Two CMEs from the same active region as the September 10 (X1.6) flare produced FD on September 12, 2014. There was a relatively fast partial halo CME and a larger and rapidly moving halo CME trailing behind the first one on September 10. These two gave rise to the FD that was first detected by NMs on September 12, 2014. This FD was not a classical two-step FD as expected, probably due to the interaction of slower and faster CMEs. The FD profile (Fig. 3) showed a small second step several hours after the first, similar to the FD that occurred in February 2011 (Papaioannou et al., 2013). In June 2015, a large activity occurred in the Sun from powerful AR 2371 that produced several CMEs from the Sun. These CMEs induced a complex modulation of GCRs that led to an FD occurrence on June 22, 2015 with an unusual structure (Samara et al., 2018).

A sudden burst of activity from the Sun early in September 2017, after a prolonged period of low solar activity, produced several flares, including the largest solar flare seen from Earth since 2006, an X9.3 flare. This activity produced several Earth-directed CMEs. Throughout this time, Earth experienced a series of geomagnetic storms, which started promptly after the first CME. This unusual activity produced an FD, which was recorded with detectors in terms of ground level enhancement (GLE) on Earth and Mars (Guo et al., 2018).

Table 1

Correlation matrix of the linear correlation coefficient (in%) for recorded hourly flux at the Belgrade CR station with its temperature- and pressure-corrected underground and ground-level detectors (UL_tpc and GLL_tpc), only pressure-corrected detectors (UL_pc, GLL_pc), and raw data detectors (UL_raw and GLL_raw) and recordings at Rome, Oulu, Jungfraujoch (Jung.) and Athens NMs for March 2012.

UL_tpc	75	81	80	81	76	73	78	86	97	100
UL_pc	77	83	83	83	73	78	72	84	100	97
UL_raw	57	71	70	74	94	49	51	100	84	86
GLL_tpc	86	86	84	83	59	90	100	51	72	78
GLL_pc	90	92	90	89	56	100	90	49	78	73
GLL_raw	63	79	78	81	100	56	59	94	73	76
Oulu	90	98	98	100	81	89	83	74	83	81
Jung.	91	98	100	98	78	92	84	70	83	80
Rome	91	100	98	98	79	92	86	71	83	81
Athens	100	91	91	90	63	90	86	57	77	75
	Athens	Rome	Jung.	Oulu	GLL_raw	GLL_pc	GLL_tpc	UL_raw	UL_pc	UL_tpc

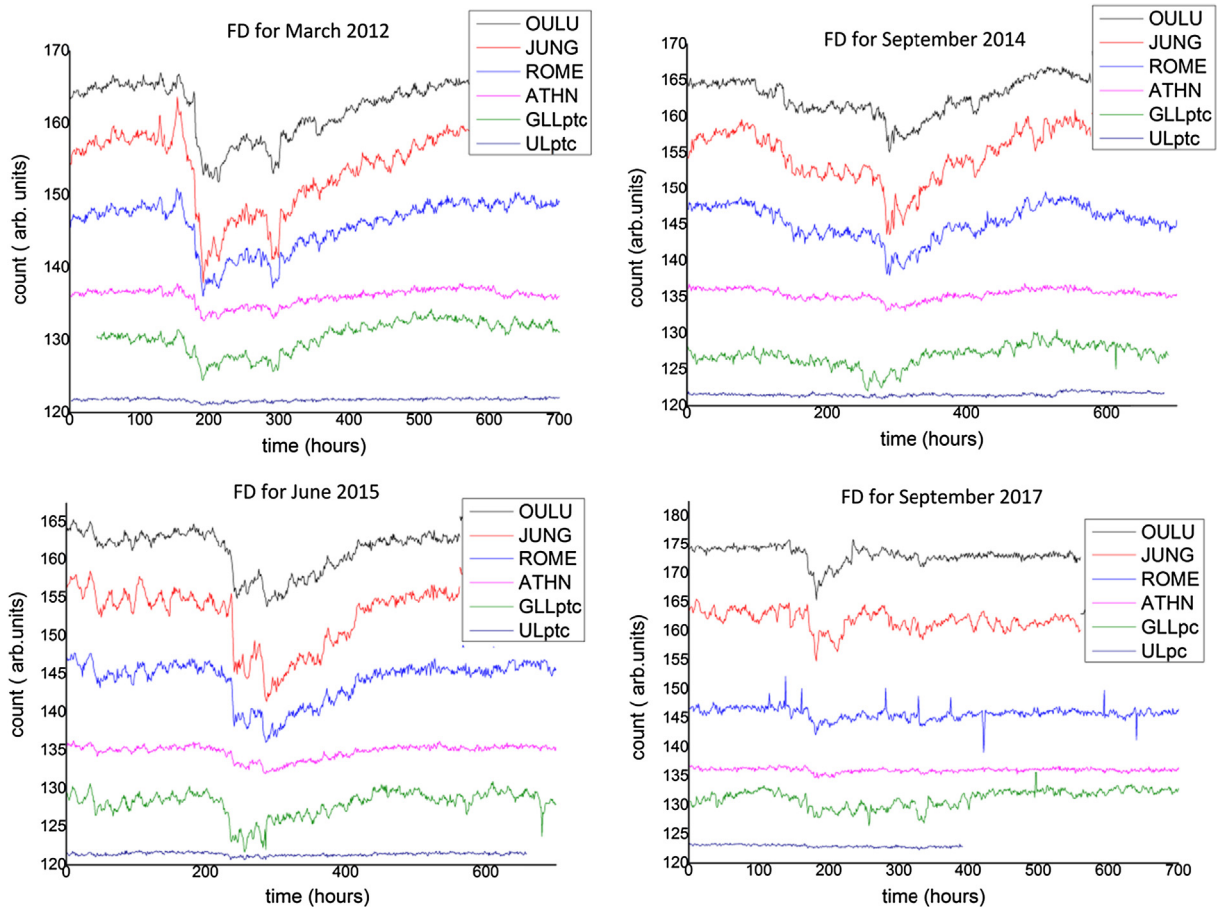


Fig. 3. Comparison of hourly time series over a one month period for pressure- and temperature-corrected count rates of the Belgrade muon monitor station (GLL_{ptc} and UL_{ptc}) and NMs at Athens (ATHN), Rome (ROME), Jungfraujoch (JUNG), and Oulu (OULU) for extreme solar events in March 2012, September 2014, and June 2015. Count rates are shifted for comparison. For extreme solar event in September 2017, for GLL and UL, the count rate is pressure-corrected only.

4. FD and median rigidity

For each event, we study the energy dependence of FD amplitude. The energy dependence of FD amplitude is

expected to follow the power law: $\Delta N/N \sim R^{-\gamma}$ (Cane, 2000). To obtain reliable values of amplitudes, we defined amplitude as a relative decrease in the hourly count rate of the minimum compared with the average of seven days'

Table 2
Median and cutoff rigidity for several stations.

Stations	Median rigidity R_m (GV)	Min. rigidity R_0 (GV)
Athens	25.1	8.53
Mexico	25.1	8.28
Almaty	15.8	6.69
Lomnický štít	12.6	3.84
Moscow	15.8	2.43
Kiel	15.8	2.36
Yakutsk	12.6	1.65
Apatity	12.6	0.65
Inuvik	12.6	0.3
Mc Murdo	12.6	0.3
Thule	12.6	0.3
South Pole	10	0.1
UL	122	12.3
GLL	63	5.3

count rate before FDs (not including possible precursory increases). Such a long base period was used because of the higher activity of the Sun prior to registered FDs and sensitivity of the muon detectors.

Amplitudes are determined for two of our detectors and for 12 NMs. To investigate the rigidity spectrum of

Table 3

Power indices of the median rigidity dependence of the dip of the FD. Power indices are obtained for NMs only, NMs and the Belgrade muon station, and Belgrade station only.

γ	NM only	NM + Belgrade	Belgrade station only
March 2012	0.82 ± 0.08	0.78 ± 0.03	0.715
Sept. 2014	0.79 ± 0.16	0.67 ± 0.06	0.744
June 2015	0.57 ± 0.05	0.58 ± 0.02	0.764
Sept. 2017	1.27 ± 0.16	0.86 ± 0.07	0.739

mentioned FDs, the median rigidity R_m is defined. R_m is the rigidity of the response of the detector to GCR spectrum where 50% of the detector counting rate lies below R_m (Ahluwalia and Fikani, 2007). For this study, we used a list of R_m for 12 NM stations given by Minamino et al. (2014). For an NM, the median rigidity can be computed from the detector response function derived from surveys for particulate station, usually around the minima of solar activity; this is because the intensity of lowest rigidity GCRs is maximum at that time.

For the Belgrade muon station, R_m was found using the response function acquired by the Monte Carlo method of

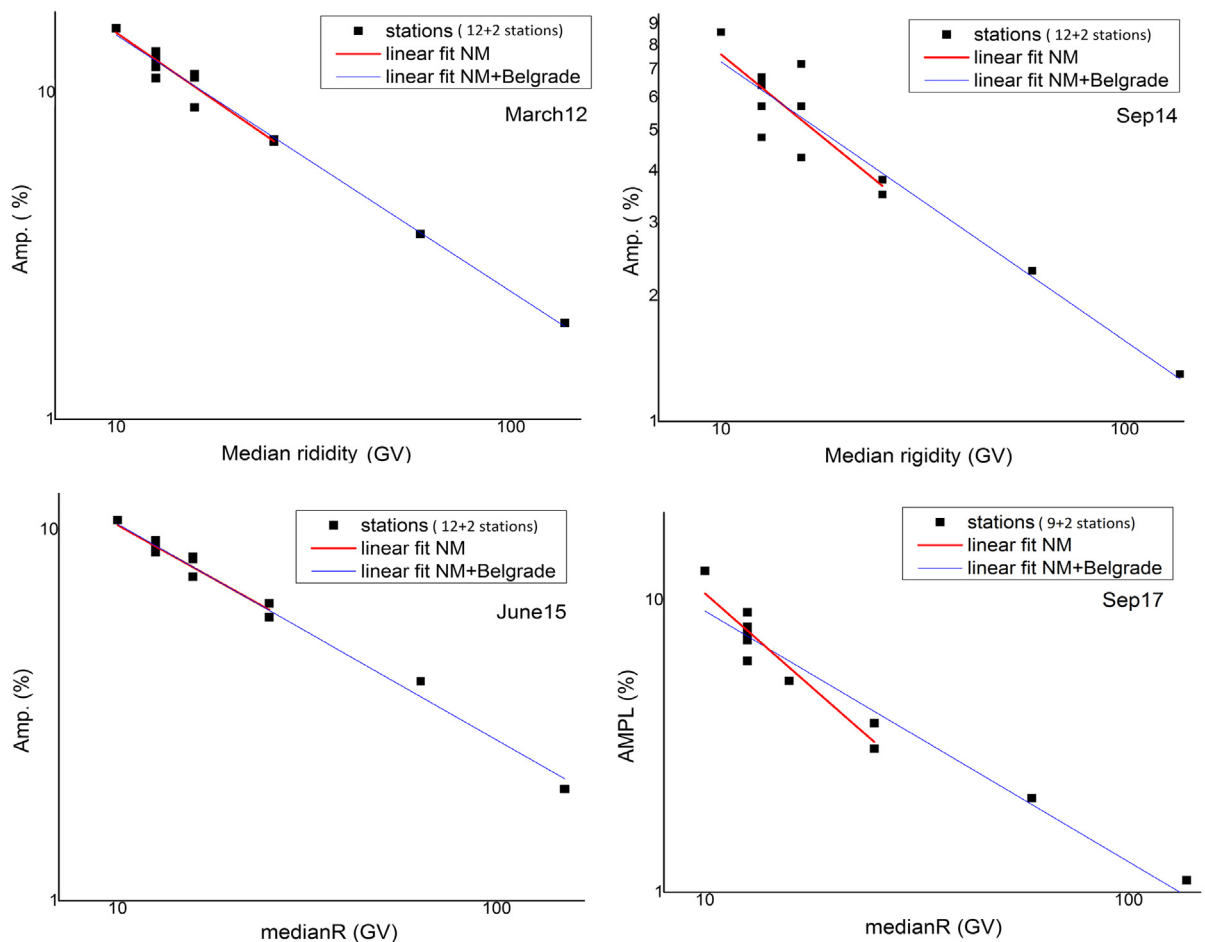


Fig. 4. Rigidity spectrum of FD from March 8, 2012, September 12, 2014, June 22, 2015, and September 8, 2017. Points represent the amplitude of the event as seen by NMs and the Belgrade CR station.

CR transport. Approximate values of R_m for the detectors used in this study are provided in Table 2.

For every selected event, a scatter plot is drawn (Fig. 4). All plots show, plotted in log-log scale, a clear median rigidity dependence of the amplitude of FD decrease.

Linear regression was performed to find power indices corresponding to each event. Power indices are given in Table 3.

Higher power indices can be due to more complex variations in GCRs. This more complex variation is a result of a series of CMEs during this event that leads to large compound ICME structure with multiple shocks and transient flow (Zhao and Zhang, 2016). Results obtained from the power law are generally consistent with those obtained in previous studies (Ahluwalia and Fikani, 2007, Lingri et al., 2016, Klyueva et al., 2017) conducted for NMs only.

A more significant difference observed for indices during the 2017 event was because we used only pressure-corrected data for the muon flux recorded at the Belgrade station. For all other events and data, we performed both pressure and temperature correction. Without temperature corrections, variation in the count rate in muon detectors is higher and it can affect the results.

We expect that when the newly improved, internally developed technique for temperature correction of the CR flux is implemented, the amplitude of the FD measured at the Belgrade muon station will be more consistent with other events and measurements. More data points on the graphs are needed to understand indices better, particularly in an energy region between NM and our laboratory. Similar work (Braun et al., 2009) discussed the extension up to 15 and 33 GeV, but there are no data available for FDs during cycle 24 and cannot be incorporated into this work. As for other operating muon telescopes, there is an agreement between the data obtained at our stations data and the URAGAN data for FD in June 2015 (Barbashina et al., 2016), but we have no data on other FDs and/or median energies of other stations. Our new experimental setup described elsewhere (Veselinović et al. 2017) will provide two additional median energies (121 and 157 GeV) to monitor variations in the CR flux.

5. Conclusion

The Belgrade CR station, with both ground level and underground setups, monitors the effect of solar modulation on the CR flux since 2008. Extreme solar events, like Forbush decreases, were detected during solar cycle 24 at the site, suggesting that these phenomena can be studied at energies higher than typical ones detected with NMs. GLL and UL data, as well as data from several NM stations, were used to analyze four intense FDs. The magnitude of FDs is energy (rigidity) dependent and follows the power law. Data used to find the rigidity dependence of these transient solar modulation of GCR were obtained over much higher range of rigidities than region NMs are

sensitive in, thus allowing more extensive studies of CR solar modulation processes.

Acknowledgements

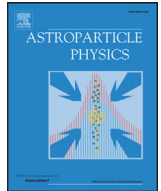
We acknowledge the NMDB (www.nmdb.eu), founded under the European Union's FP7 programme (contract no. 213007), for providing data. We acknowledge individual monitors for following the information given on the respective station information page. *Athens NM data were kindly provided by the Physics Department of the National and Kapodistrian University of Athens. Jungfrauoch NM data were kindly provided by the Physikalisches Institut, University of Bern, Switzerland. Oulu NM data were kindly provided by <http://cosmicrays oulu.fi> and Sodankylä Geophysical Observatory. Rome NM data were kindly provided by SVIRCO NM, supported by INAF/IAPS-UNIRoma3 COLLABORATION.* We thank the anonymous referees for useful advices.

The present work was funded by the Ministry of Education, Science and Technological Development of the Republic of Serbia, under Project No. 171002.

References

- Agostinelli, S., et al., GEANT4—A Simulation Toolkit, 2003. Nuclear Instruments and Methods in Physics Research Section A 506, pp. 250–303. [https://doi.org/10.1016/S0168-9002\(03\)01368-8](https://doi.org/10.1016/S0168-9002(03)01368-8).
- Ahluwalia, H.S., 2005. Cycle 20 solar wind modulation of galactic cosmic rays: understanding the challenge. *J. Geophys. Res.* 110, A10106. <https://doi.org/10.1029/2005JA011106>.
- Ahluwalia, H.S., Fikani, M.M., 2007. Cosmic ray detector response to transient solar modulation: Forbush decreases. *J. Geophys. Res.* 112 (A8), A08105. <https://doi.org/10.1029/2006JA011958>.
- Barbashina, N.S., Ampilogov, N.V., Astapov, I.I., Borog, V.V., Dmitrieva, A.N., Petrukhin, A.A., Sitko, O.A., Shutenko, V.V., Yakovleva, E.I., 2016. Characteristics of the Forbush decrease of 22 June 2015 measured by means of the muon hodoscope URAGAN. *J. Phys.: Conf. Ser.* 675 (3). <https://doi.org/10.1088/1742-6596/675/3/032038>, article id. 032038.
- Belov, A.V., 2008. Forbush effects and their connection with solar, interplanetary and geomagnetic phenomena. In: Proceedings of the International Astronomical Union 4.S257, pp. 439–450. <https://doi.org/10.1017/S1743921309029676>.
- Braun, I., Engler, J., Hörandela, J.R., Milke, J., 2009. Forbush decreases and solar events seen in the 10–20 GeV energy range by the Karlsruhe Muon Telescope. *Adv. Space Res.* 43 (4), 480–488. <https://doi.org/10.1016/j.asr.2008.07.012>.
- Caballero-Lopez, R.A., Moraal, H., 2012. Cosmic-ray yield and response functions in the atmosphere. *J. Geophys. Res. Space Phys.* 117 (A12), 7461–7469. <https://doi.org/10.1029/2012JA017794>.
- Cane, H.V., 2000. Coronal mass ejections and Forbush decreases. *Space Sci. Rev.* 93 (1–2), 55–77. <https://doi.org/10.1023/1026532125747>.
- Chauhan, M.L., Jain Manjula, S.K., Shrivastava, S.K., 2008. Study of two major Forbush decrease events of 2005. In: Proceedings of the 30th International Cosmic Ray Conference, Mexico City, vol. 1 (SH), pp. 307–310. <https://doi.org/10.7529/ICRC2011/V10/0097>.
- Clem, J.M., Dorman, L.I., 2000. Neutron monitor response functions, cosmic rays and earth. *Space Sci. Rev.* 93 (1/2), 335–359. <https://doi.org/10.1023/A:1026515722112>.
- Dragić, A., Udovičić, V., Banjanac, R., Joković, D., Maletić, D., Veselinović, N., Savić, M., Puzović, J., Aničin, I.V., 2011. The new setup in the Belgrade low-level and cosmic-ray laboratory. *Nucl.*

- Technol. Radiat. Protect. 26 (3), 181–192. <https://doi.org/10.2298/NTRP1101064N>.
- Duldig, M.L., 2000. Muon observations. In: Bieber, J.W., Eroshenko, E., Evenson, P., Flückiger, E.O., Kallenbach, R. (Eds.), *Cosmic Rays and Earth*. Space Sciences Series of ISSI. Springer, Dordrecht, pp. 207–226. https://doi.org/10.1007/978-94-017-1187-6_1.
- Forbush, S.E., 1954. World-wide cosmic ray variations, 1937–1952. *J. Geophys. Res.* 59 (4), 525–542. <https://doi.org/10.1029/JZ059i004p00525>.
- Guo, J., Dumbović, M., Wimmer-Schweingruber, R.F., Temmer, M., Lohf, H., Wang, Y., Veronig, A., Hassler, D.M., Leila, M., Mays, L. M., Zeitlin, C., Ehresmann, B., Witasse, O., Freiherr von Forstner, J. L., Heber, B., Holmström, M., Posner, A., 2018. Modeling the evolution and propagation of the 2017 September 9th and 10th CMEs and SEPs arriving at Mars constrained by remote-sensing and in-situ measurement. Also Available at: arXiv preprint arXiv:1803.00461.
- Heck, D., Knapp, J., Capdevielle, J.N., Schatz, G., Thouw, T., 1998. *CORSIKA: a Monte Carlo code to simulate extensive air showers*. Forschungszentrum Karlsruhe GmbH, p. V +90, TIB Hannover, D-30167 Hannover.
- Klyueva, A.I., Belov, A.V., Eroshenko, E.A., 2017. Specific features of the rigidity spectrum of Forbush effects. *Geomag. Aeron.* 57 (2), 177–189. <https://doi.org/10.1134/S0016793217020050>.
- Lingri, D., Mavromichalaki, H., Belov, A., Eroshenko, E., Yanke, V., Abunin, A., Abunina, M., 2016. Solar activity parameters and associated Forbush decreases during the minimum between cycles 23 and 24 and the ascending phase of cycle 24. *Sol. Phys.* 291 (3), 1025–1041. <https://doi.org/10.1007/s11207-016-0863-8>.
- Minamino, Mohanty, Morishita, et al. for the GRAPES-3 Collaboration, 2014. Rigidity Dependence of Forbush Decreases, Poster #654. In: *Proceedings of the 33rd International Cosmic Ray Conference*, Rio de Janeiro, Brazil, pp. 3612–3615.
- Papailiou, M., Mavromichalaki, H., Abunina, M., Belov, A., Eroshenko, E., Yanke, V., Kryakunova, O., 2013. Forbush decreases associated with western solar sources and geomagnetic storms: a study on precursors. *Sol. Phys.* 283 (2), 557–563. <https://doi.org/10.1007/s11207-013-0231-x>.
- Papaioannou, A., Belov, A.A., Mavromichalaki, H., Eroshenko, E., Yanke, V., Asvestari, E., Abunin, A., Abunina, M., 2013. The first Forbush decrease of solar cycle 24. *J. Phys. Conf. Ser.* 409 (1). <https://doi.org/10.1088/1742-6596/409/1/012202>.
- Samara, E., Smpontias, I.A., Lytrosyngounis, I., Lingri, D., Mavromichalaki, H., Sgouropoulos, C., 2018. Unusual cosmic ray variations during the Forbush decreases of June 2015. *Sol. Phys.* 293 (67). <https://doi.org/10.1007/S11207-018-1290-9>.
- Savić, M., Maletić, D., Joković, D., Veselinović, N., Banjanac, R., Udovičić, V., Dragić, V., 2015. Pressure and temperature effect corrections of atmospheric muon data in the Belgrade cosmic-ray station. *J. Phys. Conf. Ser.* 632 (1). <https://doi.org/10.1088/1742-6596/632/1/012059>, article id. 012059.
- Veselinović, N., Dragić, A., Savić, M., Maletić, D., Joković, D., Banjanac, R., Udovičić, V., 2017. An underground laboratory as a facility for studies of cosmic-ray solar modulation. *Nucl. Instrum. Meth.* A875, 10–15. <https://doi.org/10.1016/j.nima.2017.09.008>.
- Zhao, L.-L., Zhang, H., 2016. Transient galactic cosmic-ray modulation during solar cycle 24: a comparative study of two prominent forbush decrease events. *Astrophys. J.* 827 (1). <https://doi.org/10.3847/0004-637X>.



A novel method for atmospheric correction of cosmic-ray data based on principal component analysis



M. Savić, A. Dragić*, D. Maletić, N. Veselinović, R. Banjanac, D. Joković, V. Udovičić

Institute of Physics, University of Belgrade, Pregrevica 118, Zemun 11080, Serbia

ARTICLE INFO

Article history:

Received 23 August 2018
Revised 8 December 2018
Accepted 29 January 2019
Available online 29 January 2019

Keywords:

Cosmic rays
Muons
Atmospheric corrections
Principal component analysis

ABSTRACT

A new method for atmospheric correction of cosmic ray data is designed. It's fully empirical, based on the principal component analysis. The method requires knowledge of the pressure and the temperature profile of the atmosphere. It's applicable to all muon detectors. The method is tested on muon data from two detectors in Belgrade cosmic ray station, one located on the ground level and the other at the depth of 25 mwe. Correction reduces variance by 64.5% in ground level detector data and 38.1% in underground data. At the same time, the amplitude of the annual variation is reduced by 86.0% at ground level and 54.9% underground. With the same data sets the presented method performs better than the integral correction method.

© 2019 Elsevier B.V. All rights reserved.

1. Introduction

Count rates of ground based or underground cosmic-ray (CR) muon detectors are affected by atmospheric parameters (air pressure and temperature at different heights). The proper description of atmospheric effects is necessary for understanding primary CR variations, originating outside of the atmosphere.

Early studies in CR temporal variations [1,2] revealed the existence of a variation caused by the change of air pressure, the so called "barometric effect". With the increase in pressure the atmosphere represents thicker absorber, resulting in reduced number of muons reaching the ground level. Therefore, muon flux is expected to be anti-correlated with atmospheric pressure.

Observed negative correlation between muon flux and atmospheric temperature, the so called "negative temperature effect", has been explained by Blackett [3] to be a consequence of muon decay. During warm periods the atmosphere is expanded and the main layer of muon production (~100 mb) is higher, resulting in longer muon path and lower surviving probability to the ground level. Low energy muons are more affected, while the flux of high energy muons, capable of penetrating great depth, does not suffer. At deep underground experiments another type of temperature effect, "positive temperature effect" is pronounced [4]. Development of nuclear emulsions capable of detecting energetic charged particles lead to discovery of charged pions in CRs and $\pi - \mu$ decay [5–7]. The positive temperature effect is interpreted as a conse-

quence of latter process [8,9]. Pions created in the interactions of primary CR particles with the atmospheric nuclei can decay into muons or interact with air nuclei. Higher temperature in the production layer means lower air density and consequently, lower interaction probability and higher muon production.

In most cases linear regression is sufficient to account for the barometric effect. The temperature effects are treated by empirical and theoretical methods. In addition to the barometric coefficient β , **the method of effective level of generation** [8] introduces two empirical parameters: α_H to encounter for muon intensity variations δI_μ correlated with the change of the height of generation level δH (negative effect) and α_T for the changes of the temperature of this level (positive temperature effect).

$$\delta I_\mu = \beta \delta p + \alpha_H \delta H + \alpha_T \delta T \quad (1)$$

Duperier method has been successfully used in many studies for the atmospheric corrections of muon data ([10–15] etc.).

It's been argued [16,17] that for correct temperature correction of muon detectors count rate the vertical temperature profile of the entire atmosphere needs to be known. In the so called **integral method** the muon intensity variations caused by the temperature are described by the equation:

$$\frac{\delta I_\mu}{I_\mu} = \int_0^{h_0} W_T(h) \delta T(h) dh \quad (2)$$

where $\delta T(h)$ is the variation of temperature at isobaric level h with respect to the referent value and $W_T(h)$ is the temperature coefficient density. The coefficients are calculated theoretically and the best known calculations are given in references [18,19].

* Corresponding author.

E-mail address: dragic@ipb.ac.rs (A. Dragić).

The **mass-average temperature method** [20] is a variant of the integral method, based on the assumption of small changes of the temperature coefficient density $W_T(h)$ with the atmospheric depth h allowing its average value \overline{W}_T to be put in front of the integral in the Eq. (2) and on determination of the mass-averaged temperature T_m :

$$\frac{\delta I_\mu}{I_\mu} = \overline{W}_T(h) \int_0^{h_0} \delta T(h) dh = \overline{W}_T(h) \cdot \delta T_m \quad (3)$$

The method was used in numerous studies ([21–23] to name a few).

Another form of the integral method is **the effective temperature method** [24]. By introducing the temperature coefficient α_T :

$$\alpha_T = \int_0^{h_0} W_T(h) dh$$

the Eq. (2) can be normalized as:

$$\frac{\delta I_\mu}{I_\mu} = \int_0^{h_0} W_T(h) dh \cdot \frac{\int_0^{h_0} W_T(h) \delta T(h) dh}{\int_0^{h_0} W_T(h) dh} = \alpha_T \cdot \delta T_{eff} \quad (4)$$

where the effective temperature T_{eff} is defined as:

$$T_{eff} = \frac{\int_0^{h_0} W_T(h) T(h) dh}{\int_0^{h_0} W_T(h) dh}$$

The latter method is popular with the underground muon telescopes [25,26].

Different methods of atmospheric correction might be compared on the basis of several criteria. One is requirement of the lowest variance of corrected data. Since the most prominent temperature effect on CR time series is seasonal variation, another criterion is the smallest residual amplitude of seasonal variation after correction is applied. The latter does not take into account possible genuine seasonal variation of non-atmospheric origin.

Early studies comparing Duprier's empirical and Dorman's theoretical methods ([27] and references therein) found similar accuracy of two methods, with essentially the same corrections at sea level, but with the integral method overestimating the temperature effect.

A more recent study [28] compared different methods of atmospheric correction for data from Nagoya and Tibet supertelescopes, as well as Yakutsk, Moscow and Novosibirsk telescopes. They found the mass-averaged temperature method to practically coincide with the integral method. On the other hand, the effective level of generation method for Nagoya shows discrepancy from the integral method in winter time, being able to eliminate only 50% of the temperature effect. Even with the integral method in the case of Tibet muon telescope the removal of temperature effect is achieved with the density of temperature coefficients 3 times higher than calculated ones. The precise origin of disagreement is unknown.

The method of the effective level of generation takes care of key physical causes of the temperature effect. However, it does not make optimal use of the temperature data. Also, the assumption of a single level of main muon production is a simplification. Detailed CORSIKA simulation of the shower development in the atmosphere reveals the actual distribution of the muon generation heights (see Fig. 1).

Different implementations of the integral method exist, employing different approximations, choice of parameters, models of the atmosphere, whether kaon contribution is taken into account, leading to differences in calculated density temperature coefficients (see for instance discussion in [29]). As already mentioned, on the case of Tibet telescope [28] theoretical calculations do not fully correspond to the local experimental conditions and the origin of disagreement is difficult to trace.

The effective temperature method lacks universality, since it works best with the data from deep underground detectors.

Here we propose a new method for atmospheric corrections. It's fully empirical, makes use of the available temperature data through entire atmosphere and it's applicable to arbitrary detector irrespective to energy sensitivity and is simple to implement. The method is based on the principal component analysis, thus reducing dimensionality of the problem, exploiting correlations between atmospheric variables and ensuring mutual independence of correction parameters. The price is loss of clear physical interpretation of these parameters, since the pressure and the temperature at different levels are treated on equal footing.

2. Method description

2.1. Meteorological data

Set of variables that enter principal component decomposition consists of atmospheric temperature profile for the given location as well as locally measured atmospheric pressure. Meteorological balloon soundings for Belgrade are not done frequently enough to be used for suggested analysis. As a consequence, modeled temperatures were used instead. However, there were enough balloon sounding data for testing consistency of the modeled temperatures.

There are several weather and global climate numerical models available today. Here, Global Forecast System [30] data was used. GFS is a weather forecast model, developed by National Centers for Environmental Prediction [31], which is able to predict large number of atmospheric and land-soil parameters. Apart from forecast data, GFS also provides retrospective data produced taking into account most recent measurements by a world wide array of meteorological stations. Retrospective data are produced four times a day at 00:00, 06:00, 12:00 and 18:00 UTC. Data with finer temporal resolution are obtained by cubic spline interpolation. Temperatures for the following 25 isobaric levels (in mb) were used for initial analysis: 10, 20, 30, 50, 70, 100, 150, 200, 250, 300, 350, 400, 450, 500, 550, 600, 650, 700, 750, 800, 850, 900, 925, 975, 1000. Horizontal spatial resolution for modeled data is 0.5 degrees, so coordinates closest to the experiment location (latitude 44.86, longitude 20.39), were selected with this precision. Before any further analysis was done, GFS modeled temperature profiles were compared to local meteorological balloon soundings for Belgrade, where balloon data was available. Fig. 2 shows profile of differences between modeled and measured values for different isobaric levels. Disagreement was found between measured and modeled temperature at the lowest level. As a result, it was decided not to use temperature data for isobaric level of 1000 mb in further analysis. Ground temperature data measured by local meteorological stations was used for lowest layer instead. Similar problem with the GFS data was reported before by [28] who found 5°C deviation in the summer time near ground level at Yakutsk location.

Atmospheric pressure and ground level temperature from the Republic Hydro-meteorological Service of Serbia was used to compose unique local pressure and temperature time series.

2.2. Cosmic-ray data

The analysis is performed on data from Belgrade muon detectors. The Belgrade cosmic-ray station, together with the present detector arrangement is described in details elsewhere [32]. Two muon detectors are located in the laboratory, one at the ground level and the other at the depth of 25 mwe. Data are recorded on the event-by event basis and can be integrated into the time series with the arbitrary time resolution. For most purposes hourly data are used. Muon detectors are sensitive to primary cosmic rays

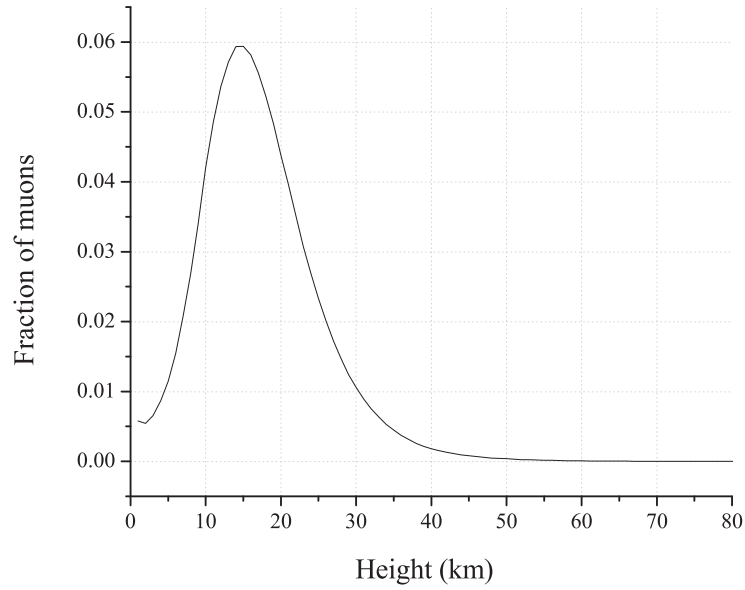


Fig. 1. Distribution of muon generation at different heights in the atmosphere, according to CORSIKA simulation.

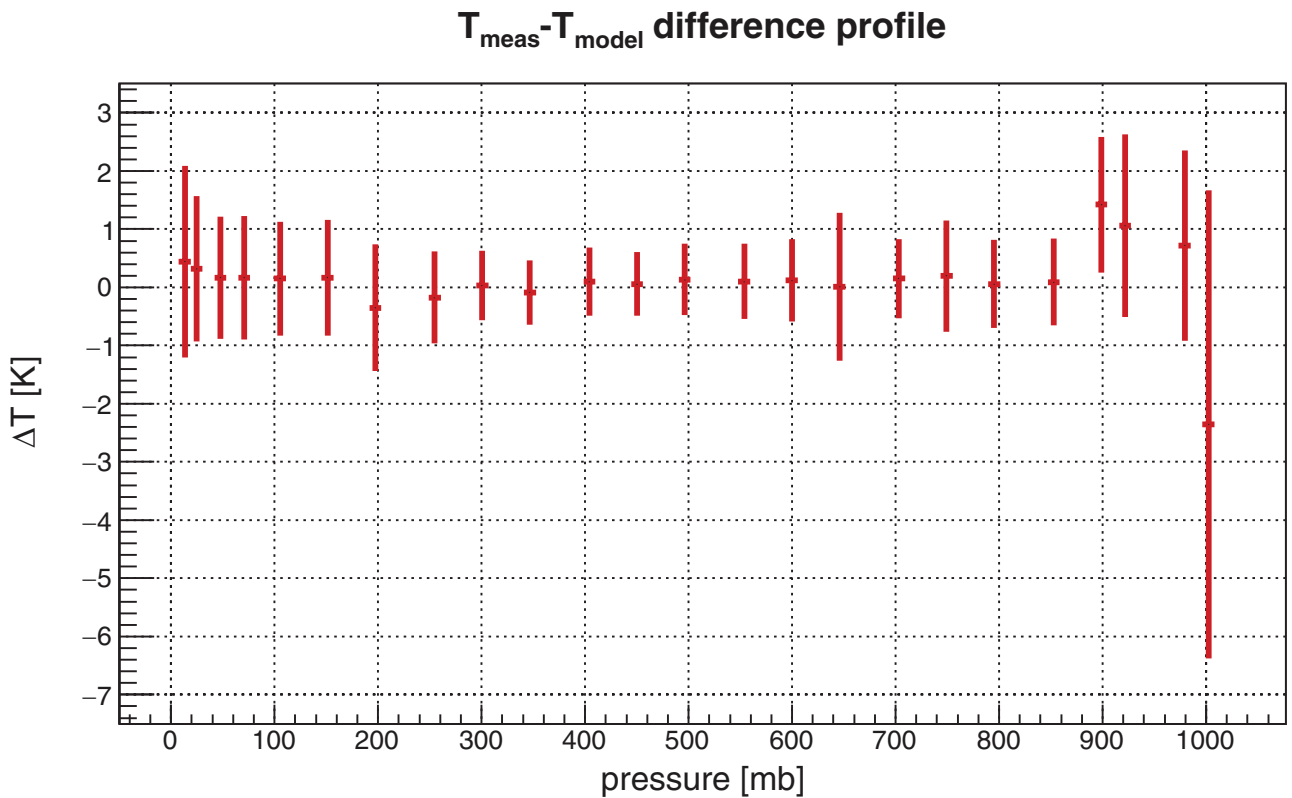


Fig. 2. Distribution of differences between measured temperatures and modeled by GFS.

of 59 GeV median energy in the case of ground level detector and 137 GeV for underground detector.

2.3. Principal component decomposition

Principal component analysis is a convenient and widely used data reduction method when dealing with strongly correlated

data. It transforms the original set of variables into a set of uncorrelated variables (called principal components (PC)). The principal components are ordered according to decreasing variance. In our case, there are 26 input variables: 24 modeled temperatures (isobaric level 1000 mb temperature excluded), locally measured ground level temperature and local atmospheric pressure. Initial variables were centered and normalized before

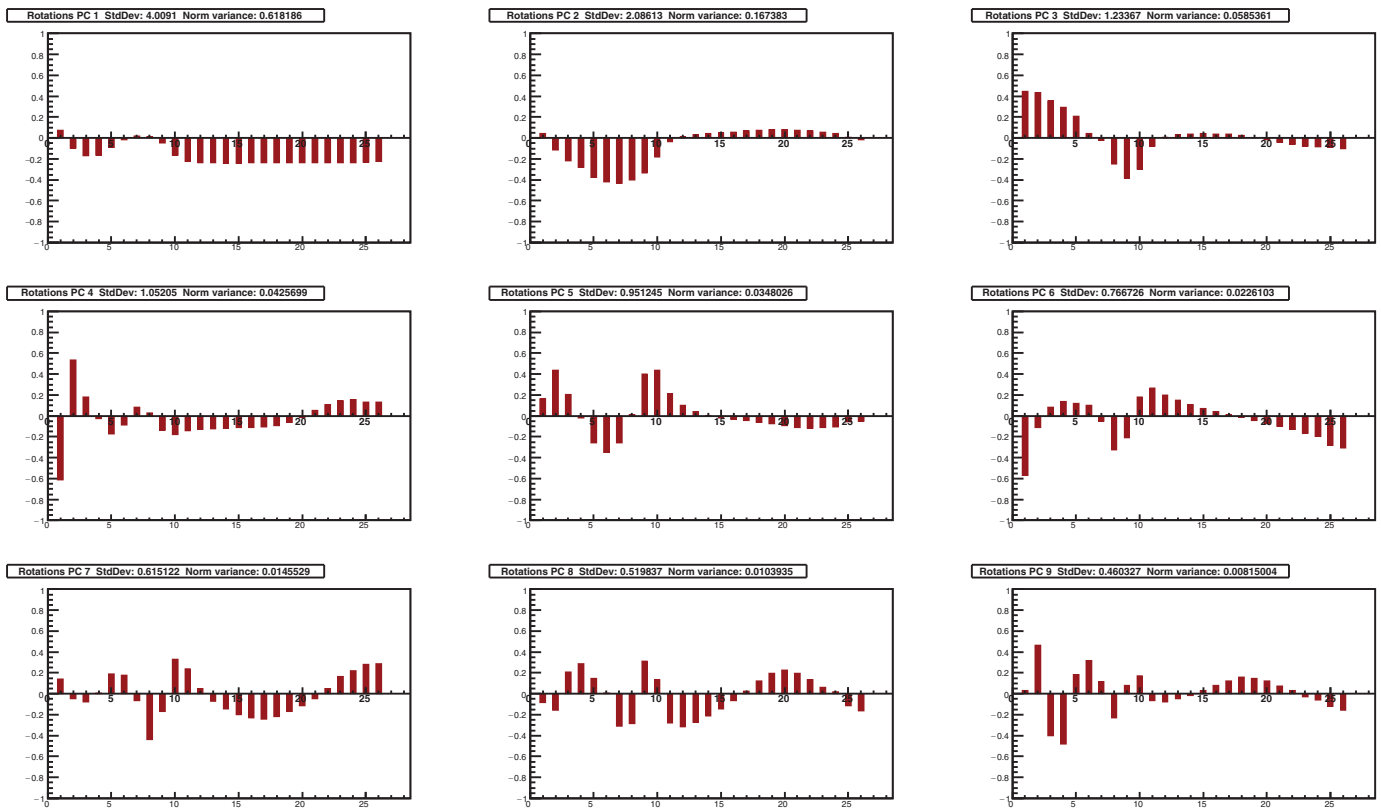


Fig. 3. Composition of nine principal components with largest variance (in decreasing order). Input variables are displayed on X-axis: 1 being pressure, 2 temperature of 10 mb isobaric level, 26 being local ground level temperature. Y-axis represents rotations.

decomposition. After decomposition, a new set of 26 principal components was obtained. Decomposition should not be regarded as universal, but it should be redone for every location and period under study.

One year was selected as a suitable time period for the analysis, in order to reduce possible seasonal bias, due to atmospheric temperature annual variation. Additional criteria were quality and consistency of muon data. Taking this into account, final time interval selected for analysis was from 01.06.2010 to 31.05.2011.

Fig. 3 shows composition plots for the first nine principal components, that account for 98% of total variance. X-axis represents input atmospheric variables, first being atmospheric pressure, followed by 10 mb layer temperature, last being ground level local temperature. Y-axis represents decomposition rotations for a given principal component. Interesting features observed on these plots are that first two principal components depend almost exclusively on temperature. The first one is mostly combination of temperatures in the troposphere (isobaric levels 250–1000 mb) with almost equal weights. The second eigenvector accounts for significant variance of temperatures in higher atmospheric levels (10–250 mb), with the strongest contribution centered in the tropopause. Components 3 to 6 have mixed p-T composition. The correlation of atmospheric pressure and temperature at different heights is not surprising. The diurnal and semi-diurnal oscillations of pressure are attributed to the warming of the upper atmosphere by the Sun [33]. This correlation makes it impossible to define a single barometric parameter in PCA based method of atmospheric corrections. It's worth mentioning that Dorman [34] recognizes three different barometric effects: absorption, decay and genera-

tion effect. It also indicates that empirical methods with separated pressure and temperature corrections might lead to overcorrection.

The values of the eigenvectors for these first nine components are also given in [Table 1](#).

Fig. 4 shows plot of proportion of variance as well as plot of cumulative variance for obtained principal components. Corresponding numerical values are given in [Table 2](#).

Usually, only a first few principal components (containing high fraction of total variance) are of practical interest. There are various different methods and rules for choosing how many PCs to retain in the analysis, none completely free of subjectivity (see for example a thorough discussion in [35]). A rule based on cumulative percentage of total variation usually recommends to retain PCs responsible for 70–90% of total variation. When one or two components are dominant, higher value (95%) is appropriate. In our case it would mean keeping first 6 PCs. According to Kaiser's rule only PCs with the eigenvalue $\lambda > 1$ should be retained. Jolliffe [35] suggested 0.7 as correct level, exceeded by six of our PCs. Another rule proposes to retain components with the eigenvalue above mean, a condition satisfied by first seven of our PCs. Another popular model is broken stick, but in application to our problem is too restrictive, leading to only two relevant PCs. The scree graph or log-eigenvalue diagram don't provide clean cut with our set of PCs.

To test the meaningfulness of potentially relevant PCs, the time series from PC data are constructed and tested whether they are distinguishable from white noise. The procedure is often done when principal component analysis is applied to atmospheric physics problems [36]. The time series with hourly resolution for the first three PCs are plotted on [Fig. 5](#).

Table 1
Definition of first nine principal components.

Variables	Principal components								
	PC1	PC2	PC3	PC4	PC5	PC6	PC7	PC8	PC9
<i>p</i>	0.07699	0.04117	0.44694	-0.61285	0.16301	-0.57121	0.14028	-0.08106	0.03443
<i>T</i> (10)	-0.0947	-0.11603	0.43488	0.5344	0.43741	-0.11036	-0.04499	-0.15825	0.46469
<i>T</i> (20)	-0.16947	-0.21766	0.35754	0.18029	0.20527	0.08546	-0.07719	0.20635	-0.40309
<i>T</i> (30)	-0.16476	-0.27825	0.29593	-0.02505	-0.02204	0.14134	0.00634	0.28574	-0.47812
<i>T</i> (50)	-0.09124	-0.37682	0.20969	-0.17322	-0.25798	0.12084	0.19349	0.14645	0.18493
<i>T</i> (70)	-0.01483	-0.42304	0.04507	-0.08651	-0.3472	0.09965	0.18155	0.01024	0.31886
<i>T</i> (100)	0.02192	-0.43132	-0.02451	0.08228	-0.25692	-0.04937	-0.06464	-0.3103	0.1183
<i>T</i> (150)	0.01487	-0.40127	-0.24673	0.03037	0.012	-0.32566	-0.43658	-0.28393	-0.23316
<i>T</i> (200)	-0.04737	-0.33404	-0.38636	-0.13563	0.40141	-0.2069	-0.16852	0.31181	0.07995
<i>T</i> (250)	-0.16218	-0.17984	-0.29739	-0.18123	0.43708	0.18013	0.32866	0.13662	0.17389
<i>T</i> (300)	-0.22473	-0.03266	-0.07561	-0.14073	0.21179	0.26504	0.23807	-0.27931	-0.06785
<i>T</i> (350)	-0.2369	0.01439	0.00488	-0.12991	0.0998	0.1988	0.05306	-0.31612	-0.0771
<i>T</i> (400)	-0.23956	0.03362	0.02958	-0.12159	0.04075	0.14932	-0.06959	-0.27189	-0.04852
<i>T</i> (450)	-0.24028	0.04271	0.0402	-0.11503	0.00384	0.10744	-0.14772	-0.21165	-0.01823
<i>T</i> (500)	-0.24005	0.04935	0.0428	-0.11304	-0.02187	0.07218	-0.19893	-0.14512	0.03068
<i>T</i> (550)	-0.23958	0.05695	0.03965	-0.11295	-0.03254	0.0388	-0.23263	-0.06843	0.08056
<i>T</i> (600)	-0.23881	0.06549	0.03681	-0.10649	-0.04369	0.01102	-0.24562	0.02401	0.12499
<i>T</i> (650)	-0.23854	0.07279	0.0236	-0.09184	-0.06132	-0.01542	-0.21788	0.12597	0.15977
<i>T</i> (700)	-0.23835	0.0801	0.00429	-0.06052	-0.07601	-0.04668	-0.16785	0.19559	0.14932
<i>T</i> (750)	-0.23842	0.08071	-0.01837	-0.01332	-0.09245	-0.07308	-0.11295	0.22563	0.12401
<i>T</i> (800)	-0.23814	0.07557	-0.03907	0.05036	-0.10989	-0.09943	-0.04696	0.19596	0.07735
<i>T</i> (850)	-0.23701	0.0675	-0.06202	0.1081	-0.11988	-0.12745	0.04989	0.13672	0.0304
<i>T</i> (900)	-0.23535	0.05462	-0.07977	0.14776	-0.11454	-0.16955	0.16551	0.06204	-0.02952
<i>T</i> (925)	-0.23414	0.04606	-0.08313	0.15641	-0.10257	-0.19925	0.21877	0.01715	-0.05804
<i>T</i> (975)	-0.23108	0.00789	-0.08827	0.13022	-0.05888	-0.28046	0.284	-0.11523	-0.12249
<i>T</i> (1000)	-0.22494	-0.01582	-0.10092	0.13401	-0.04977	-0.30749	0.28553	-0.16516	-0.15908

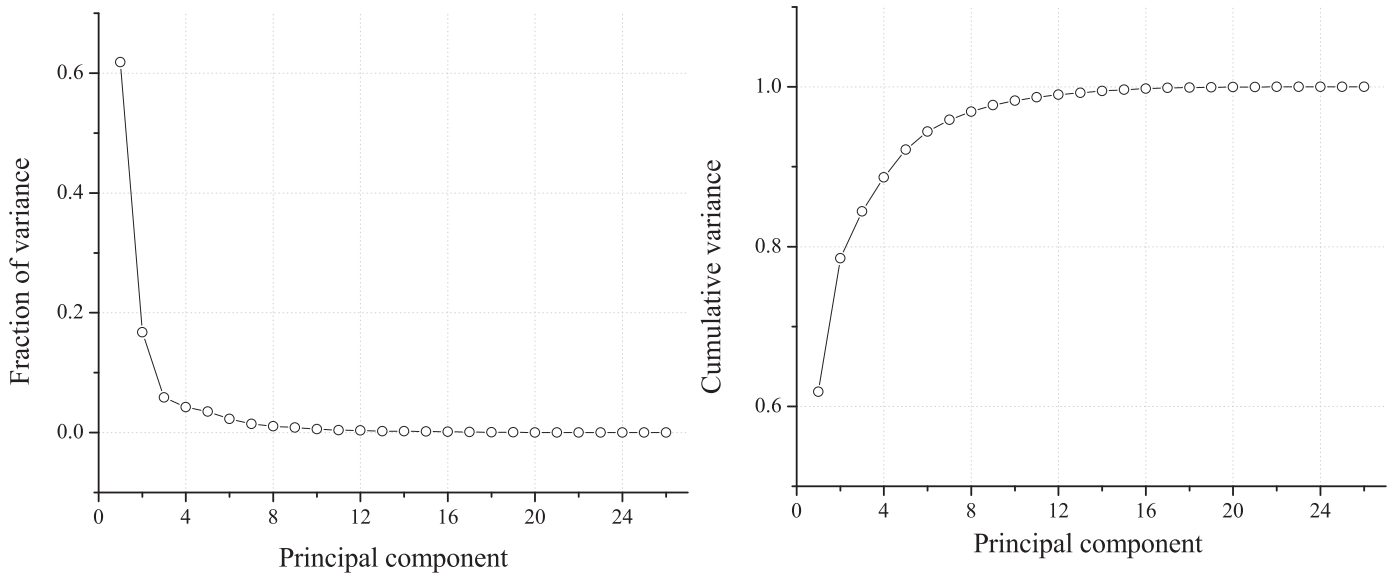


Fig. 4. Proportion of variance (left) and cumulative proportion of variance (right) for all 26 principal components.

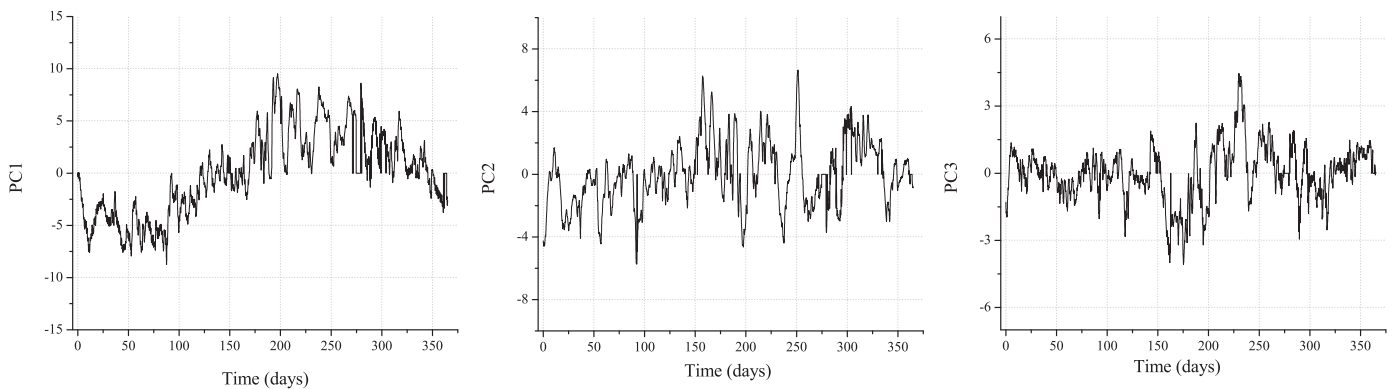


Fig. 5. Time series of the first 3 PCs.

Table 2
Variance (individual and cumulative) for all 26 PCs.

Principal component	Eigenvalue	Percentage of variance	Cumulative variance (%)
1	4.0091	0.618186	0.618186
2	2.08613	0.167383	0.785569
3	1.23367	0.0585361	0.844105
4	1.05205	0.0425699	0.886675
5	0.951245	0.0348026	0.921478
6	0.766726	0.0226103	0.944088
7	0.615122	0.0145529	0.958641
8	0.519837	0.0103935	0.969034
9	0.460327	0.00815004	0.977184
10	0.382006	0.00561263	0.982797
11	0.32832	0.00414592	0.986943
12	0.294489	0.00333553	0.990278
13	0.247876	0.00236317	0.992642
14	0.239462	0.00220546	0.994847
15	0.206157	0.00163465	0.996482
16	0.184453	0.00130857	0.99779
17	0.144657	8.04834E-4	0.998595
18	0.119676	5.5086E-4	0.999146
19	0.0938189	3.38538E-4	0.999485
20	0.0739496	2.10328E-4	0.999695
21	0.0586253	1.32189E-4	0.999827
22	0.0414996	6.62391E-5	0.999893
23	0.0338811	4.41511E-5	0.999937
24	0.0281359	3.04472E-5	0.999968
25	0.0219102	1.84637E-5	0.999986
26	0.0188263	1.36319E-5	1

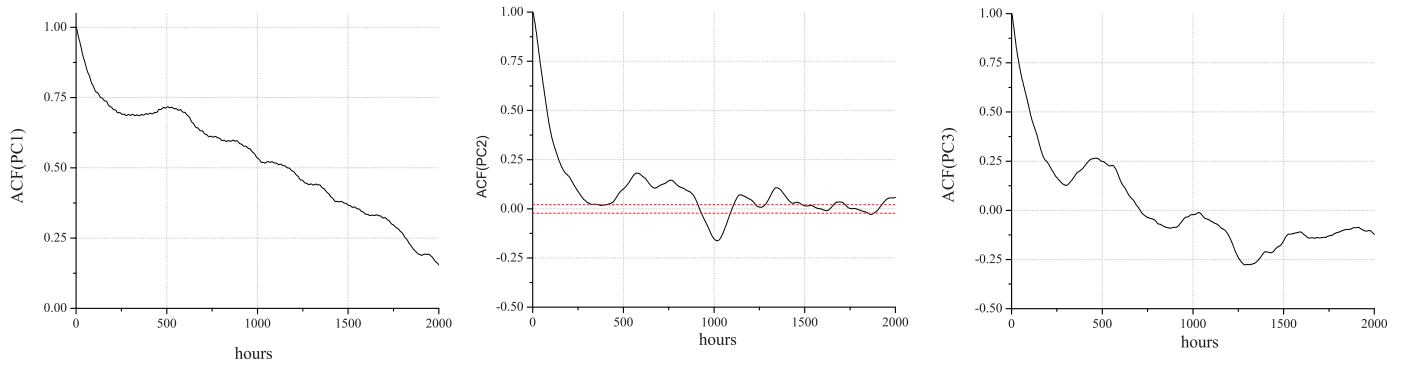


Fig. 6. Autocorrelation function of the first 3 PCs. Time lag is given in hours. In the case of PC2, 95% significance level is indicated by dashed red line. (For interpretation of the references to color in this figure legend, the reader is referred to the web version of this article.)

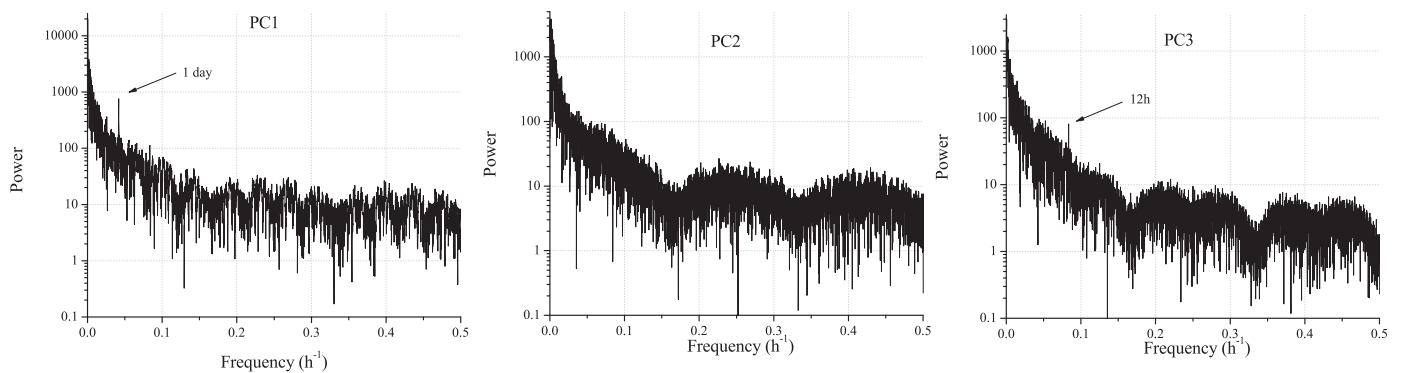


Fig. 7. Spectral analysis of time series of the first 3 PCs.

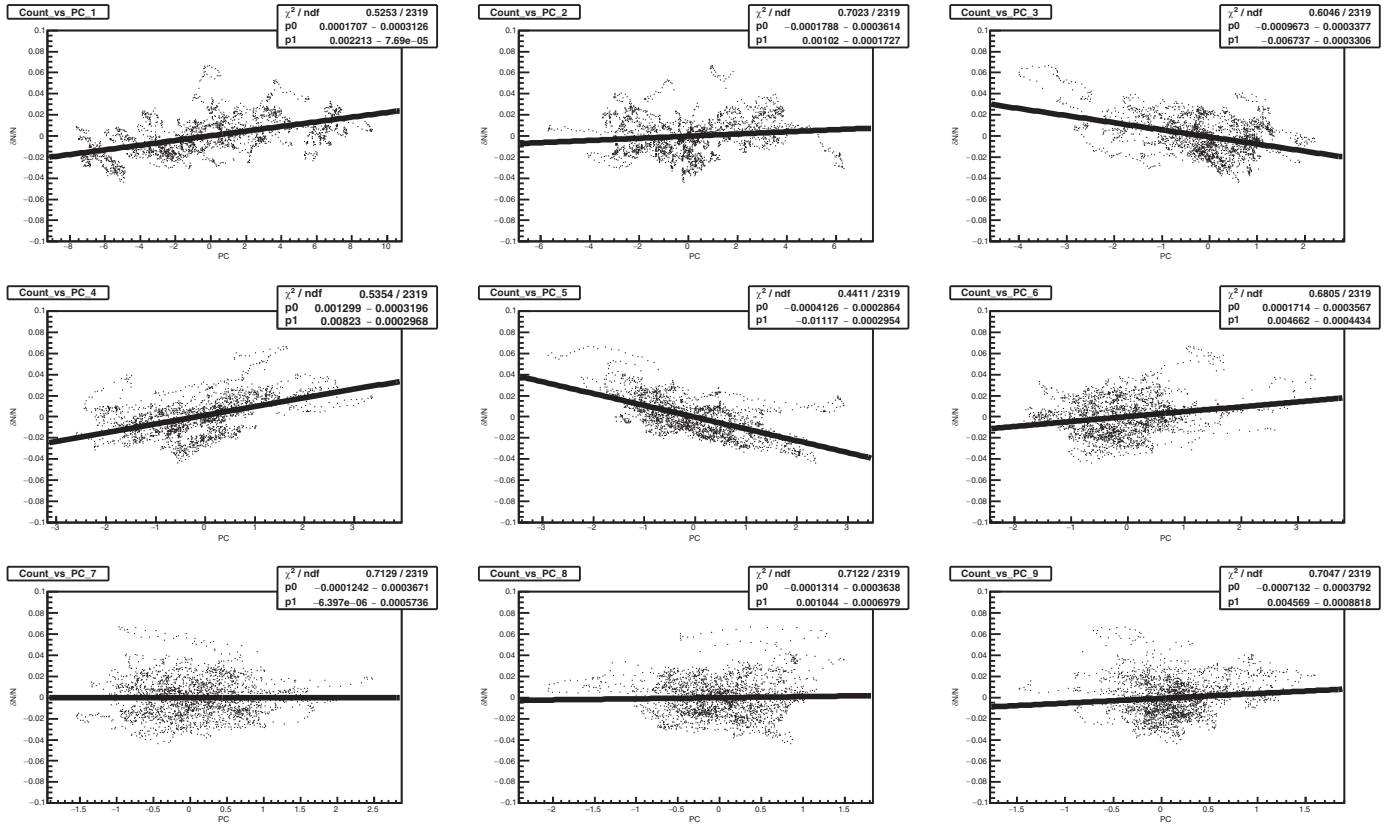


Fig. 8. Muon count dependence on principal components for the first nine principal components (GLL).

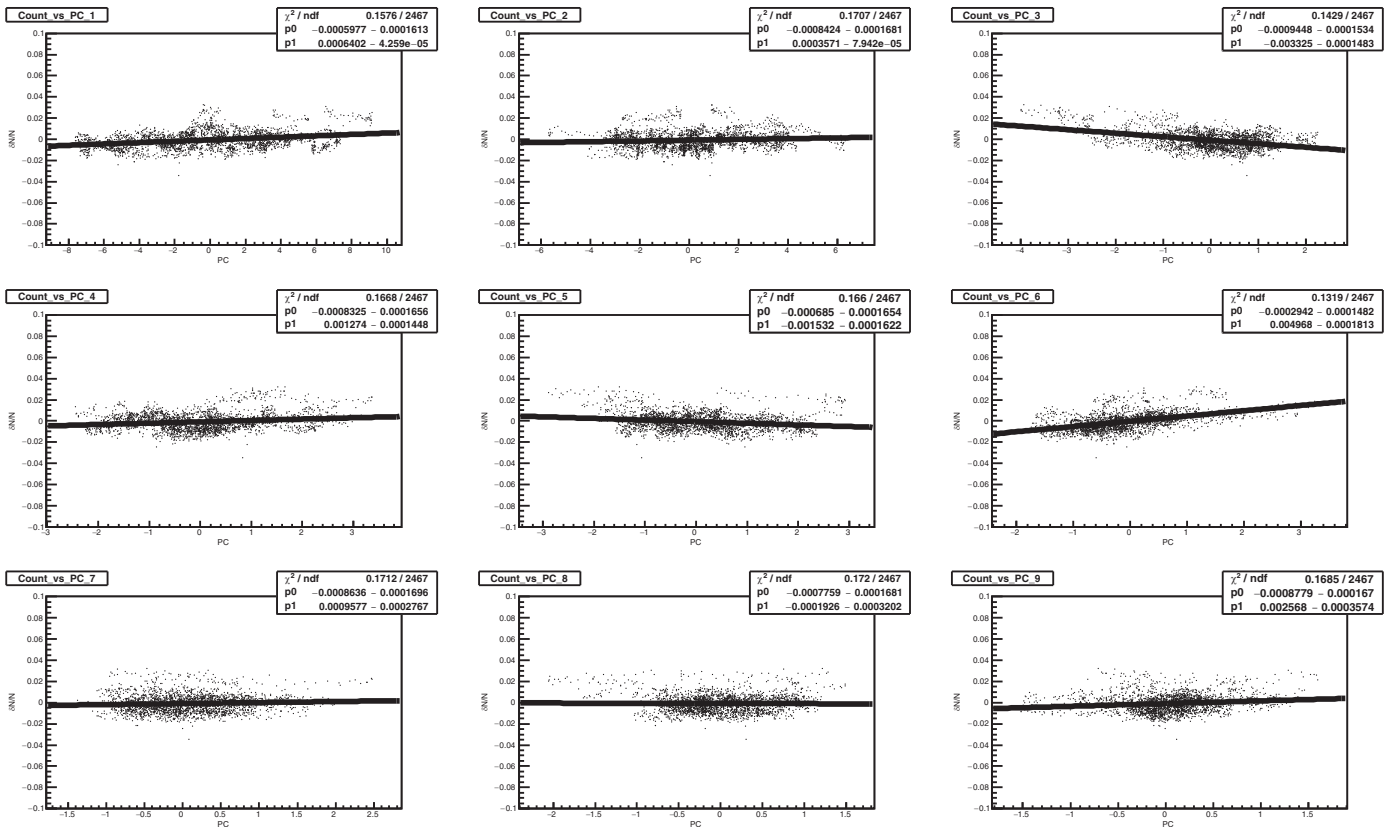


Fig. 9. Muon count dependence on principal components for the first nine principal components (UL).

The subsequent temperature and pressure measurements are highly correlated, as evident from autocorrelation function plot for selected PCs (Fig. 6).

The spectral analysis of the PC time series reveals, for PCs with the strong pressure component, semi-diurnal periodicity in addition to diurnal (Fig. 7).

Since our purpose is the regression of muon data with principal components, selecting the components with significantly high variance is not the main issue. It is more important to identify PCs with high correlation with CR data. Components with relatively low variance, can have high predictive power.

2.4. Correlation of principal components with CR muon count rate and correction of muon data

Scatter plot of muon count rate vs. PCs, together with the linear fit for the first nine principal components are shown on Fig. 8 (GLL) and Fig. 9 (UL). In the analysis hourly summed muon counts and principal component values for the respective hour were used. To minimize the effect of geomagnetic disturbances, only data for International Quiet Days were taken into account. The International Quiet Days are the days with minimum geomagnetic activity for each month. The selection of quiet days is deduced from K_p index. In our analysis 5 quietest days for each month are considered. The values of correlation coefficients are listed in Table 3.

Principal components PC1, PC3, PC4, PC5 and PC6 have been identified as ones with significant contribution to the muon flux variation. Interestingly enough, the PC2, responsible for 16.7% variance of the meteorological data has very little effect on muon flux, at neither ground nor underground level. Ground level muon flux variation is more affected by the first principal component, depending chiefly on the temperature in the troposphere. The finding agrees with usual negative temperature effect. The other PCs are difficult to compare with traditional correction parameters. Yet, the effect of PC3, that is composed more from upper atmosphere temperatures and hence could be loosely associated with positive temperature effect, is more pronounced for the underground muon flux. Fourth and fifth principal components with strong pressure contribution affect more ground level muon flux. On the other hand, PC6, also the one with high pressure component, has more pronounced influence on underground muon flux.

Gradients obtained from the fits for the significant principal components 1, 3, 4, 5 and 6 were then used to calculate the PCA corrected muon count according to the formula:

$$N_{\mu}^{(corr)} = N_{\mu} - \langle N_{\mu} \rangle \sum_i k_i PC_i, \quad i = 1, 3, 4, 5, 6 \quad (5)$$

where $N_{\mu}^{(corr)}$ corr is the corrected muon count, N_{μ} is the raw muon count, $\langle N_{\mu} \rangle$ is the mean count for the whole period, k_i are the gradients and PC_i are the corresponding principal components. Resulting corrected muon count time series are plotted on Figs. 10 (GLL) and 11 (UL) along with raw and pressure only corrected time series. Pressure corrected time series are produced for reference. Barometric coefficient was determined by applying linear regression to the same data set used for PCA. Data was previously corrected for temperature effect using integral method, as in Ref. [37]. Pressure corrected and PCA corrected time series are fitted with sine function with annual period in order to illustrate how PCA correction affects yearly variation induced by temperature effect.

PCA based atmospheric corrections remove 64.5% of total variance in GLL time series and 38.1% in UL time series. Pressure corrected CR time series exhibit annual variation, a consequence of

Table 3
Correlation coefficients between principal components and muon count rate in the ground level laboratory (GLL) and underground laboratory (UL).

PC	1	2	3	4	5	6	7	8	9	10	11	12	13	14	15	16	17	18	19	20	21	22	23	24	25	26
GLL	0.43	0.01	-0.37	0.48	-0.55	0.30	-0.01	0.03	-0.01	0.06	0.00	-0.04	0.00	0.01	0.02	-0.01	0.00	-0.01	-0.01	0.03	-0.03	0.00	0.02	-0.01	0.04	0.02
UL	0.26	0.02	-0.48	0.21	-0.19	0.52	0.02	0.04	0.07	0.04	0.01	-0.04	-0.07	0.06	-0.02	-0.05	0.04	0.04	-0.02	-0.02	0.00	0.01	0.00	-0.03	0.01	0.01

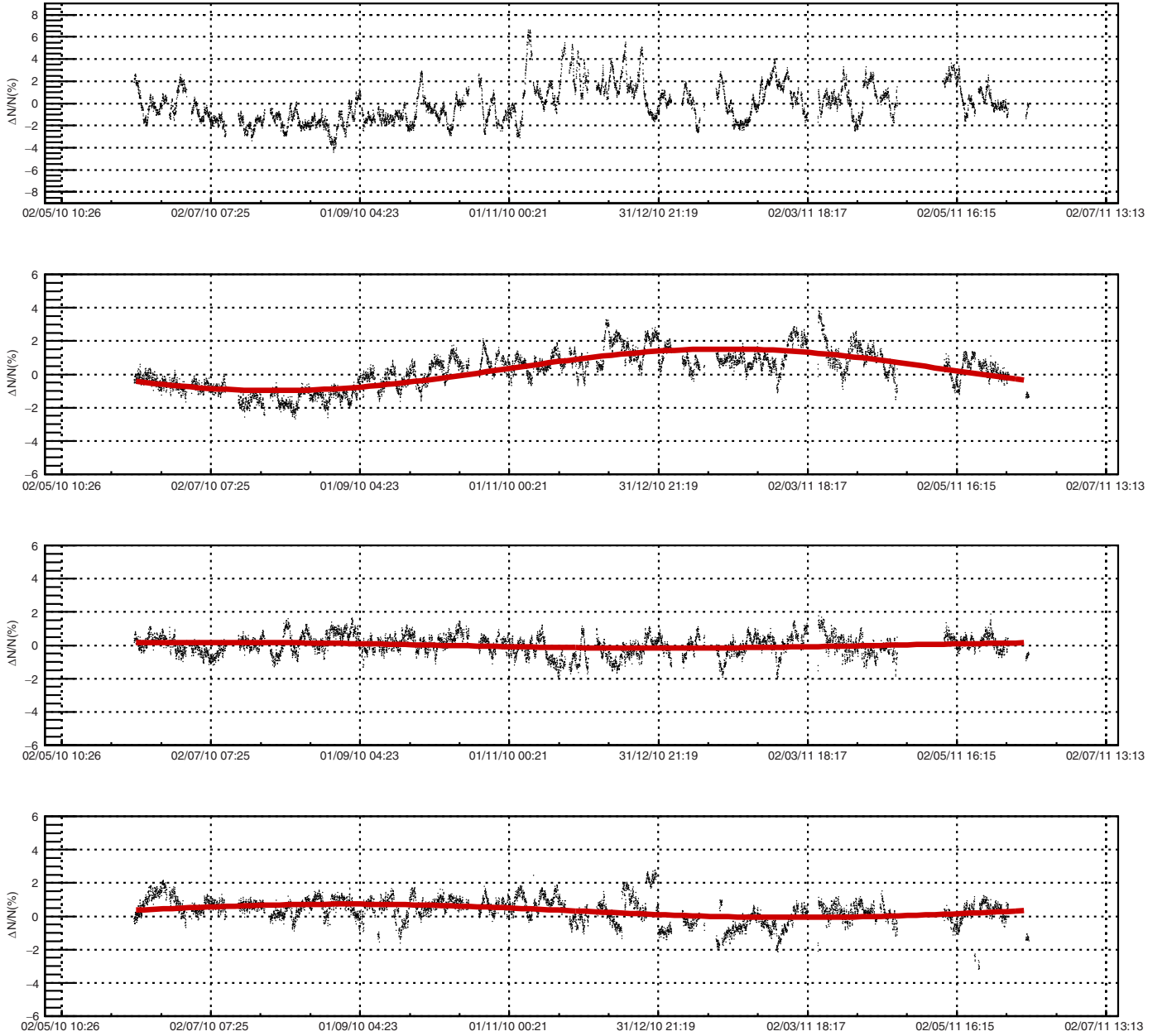


Fig. 10. Raw (upper panel), pressure corrected (middle panel), pressure+temperature corrected with PCA method (3rd panel from the top) and pressure+temperature corrected with integral method (lower panel) normalized muon count rate for GLL. The sine function with one year period is fitted to the data.

the temperature effect. The performance of the temperature correction may be tested by comparing the amplitude of the annual variation before and after correction. With presented method the amplitude of the annual variation is reduced by 86% (54.9%) in the case of GLL (UL) with respect to the pressure only corrected time series.

To further test the new method, the atmospheric correction of GLL data are performed by the integral method. The correction resulted in 56.25% of variance reduction and 68.1% of reduction of the amplitude of the annual wave. At least in the case of our CR data set the new method performs somewhat better than the integral method.

3. Conclusion

The principal component analysis is successfully used to construct a new empirical method for the atmospheric corrections of CR muon data. The method is equally applicable to all muon detectors, irrespective to location: ground level, shallow or deep underground. It requires knowledge of the atmospheric pressure and temperatures along the entire atmosphere, which is nowadays available in databases such as GFS. The method is suitable for the near real-time correction, with the delay defined by the availability of the atmospheric data (one day in the case of present GFS data). When applied to Belgrade muon data from two detectors

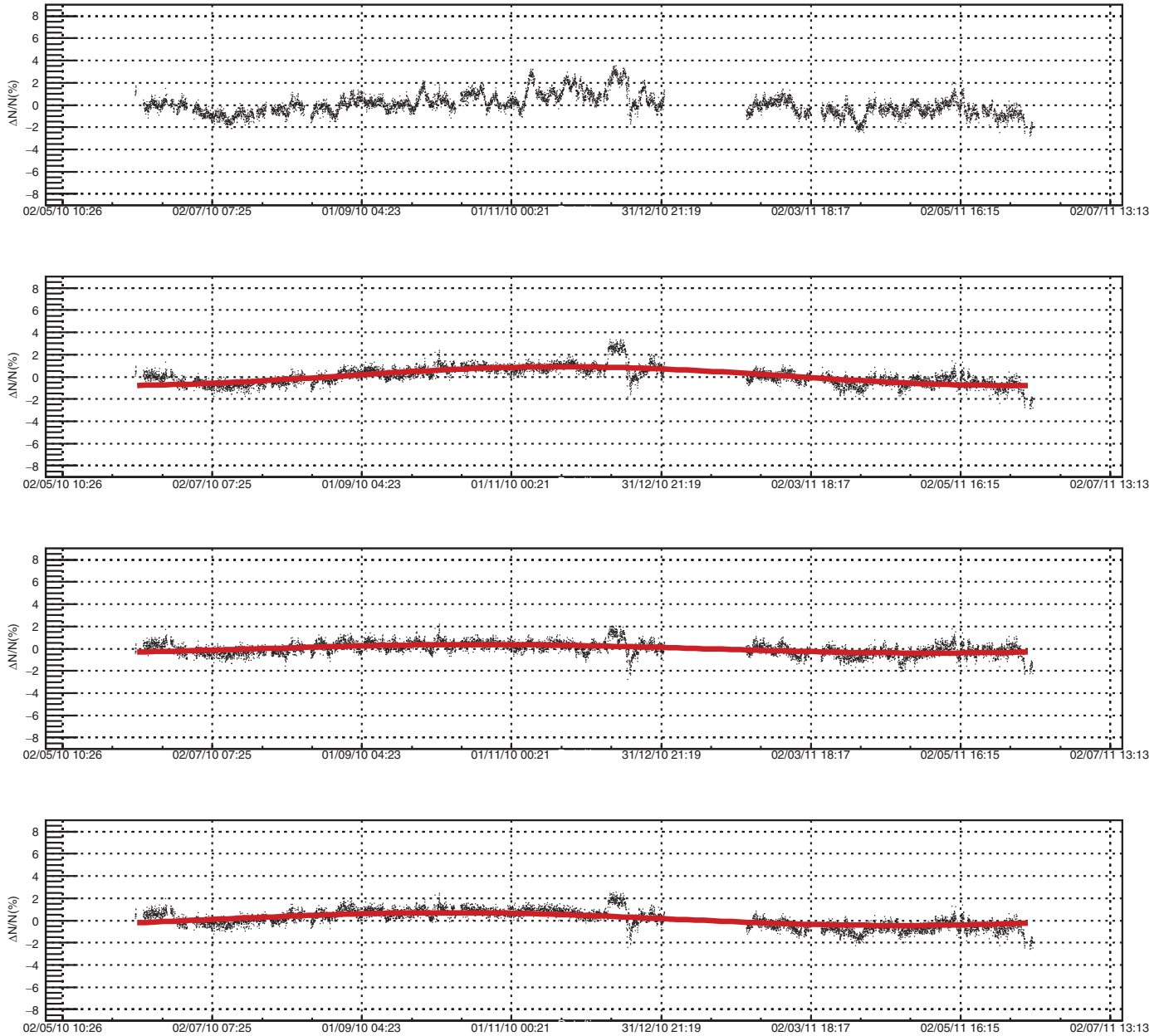


Fig. 11. Raw (upper panel), pressure corrected (middle panel), pressure+temperature corrected with PCA method (3rd panel from the top) and pressure+temperature corrected with integral method (lower panel) normalized muon count rate for UL. The sine function with one year period is fitted to the data.

(ground level and at 25 mwe), the method requires correction to five parameters, determined from linear regression. With the same CR dataset, the present method yields results superior to the integral method in terms of variance reduction and reduction of the annual variation. The new method is also suitable for temperature corrections of the neutron monitor data, which is seldom done in practice.

Acknowledgments

The authors are deeply grateful to Dr. Viktor Yanke for the encouragement and useful advice. The present work was funded by the Ministry of Education, Science and Technological Development of the Republic of Serbia, under the Project no. 171002.

References

- [1] L. Myssowsky, L. Tuwim, Unregelmäßige intensitätsschwankungen der höhenstrahlung in geringer seehöhe, *Zeitsch. Phys.* 39 (2–3) (1926) 146–150.
- [2] E. Steinke, Über schwankungen und barometereffekt der kosmischen ultrastrahlung im meeresniveau, *Zeitsch. Phys.* 64 (1–2) (1930) 48–63.
- [3] P.M. Blackett, On the instability of the barytron and the temperature effect of cosmic rays, *Phys. Rev.* 54 (11) (1938) 973.
- [4] M. Forro, Temperature effect of cosmic radiation at 1000-m water equivalent depth, *Phys. Rev.* 72 (9) (1947) 868.
- [5] C.M.G. Lattes, G.P. Occhialini, C.F. Powell, Observations on the tracks of slow mesons in photographic emulsions, *Nature* 160 (4067) (1947) 486.
- [6] C.M.G. Lattes, H. Muirhead, G.P. Occhialini, C.F. Powell, Processes involving charged mesons, *Nature* 159 (4047) (1947) 694.
- [7] G. Occhialini, C. Powell, Nuclear disintegrations produced by slow charged particles of small mass, *Nature* 159 (4032) (1947) 186.
- [8] A. Duperier, The meson intensity at the surface of the earth and the temperature at the production level, *Proc. Phys. Soc. Lond. Sect. A* 62 (11) (1949) 684.
- [9] A. Duperier, Temperature of the upper atmosphere and meson production, *Nature* 167 (4243) (1951) 312.

- [10] C. Baker, D. Hall, J. Humble, M. Duldig, Atmospheric correction analysis for the Mawson muon telescopes, in: International Cosmic Ray Conference, 3, 1993, p. 753.
- [11] A. Maghrabi, M. Almutayri, Atmospheric effect on cosmic ray muons at high cut-off rigidity station, *Adv. Astron.* 2016 (2016).
- [12] C.R. Braga, A. Dal Lago, T. Kuwabara, N.J. Schuch, K. Munakata, Temperature effect correction for the cosmic ray muon data observed at the Brazilian Southern Space Observatory in São Martinho da Serra, *J. Phys.* 409 (2013) 012138 IOP Publishing..
- [13] G.C. Castagnoli, M. Dodero, Temperature effect of the muon component underground and pion attenuation length, *Il Nuovo Cimento B* (1965–1970) 51 (2) (1967) 525–534.
- [14] A. Fenton, R. Jacklyn, R. Taylor, Cosmic ray observations at 42 m we underground at hobart, tasmania, *Il Nuovo Cimento* (1955–1965) 22 (2) (1961) 285–295.
- [15] M. Zazyan, M. Ganeva, M. Berkova, V. Yanke, R. Hippler, Atmospheric effect corrections of mustang data, *J. Space Weather Space Clim.* 5 (2015) A6.
- [16] L. Dorman, The temperature effect of the hard component of cosmic rays, *Doklady Akad. Nauk SSSR* 95 (1954).
- [17] E. Feinberg, On the nature of cosmic ray barometric and temperature effects, *DAN SSSR* 53 (5) (1946) 421–424.
- [18] L.I. Dorman, Cosmic ray variations, Technical Report, Foreign Technology Div Wright-Patterson AFB OHIO, 1957.
- [19] K. Maeda, M. Wada, Atmospheric temperature effect upon the cosmic-ray intensity at sea level, *J. Sci. Res. Inst.* 48 (1954).
- [20] V. Dvornikov, Y.Y. Krest'yannikov, A. Sergeev, Determination of the variation of average-mass temperature of the atmosphere by data of cosmic ray intensity, *Geomag. Aeron.* 16 (1976) 923–925.
- [21] V. Yanchukovsky, G.Y. Filimonov, R. Hisamov, Atmospheric variations in muon intensity for different zenith angles, *Bull. Russ. Acad. Sci.* 71 (7) (2007) 1038–1040.
- [22] R. De Mendonça, C. Braga, E. Echer, A. Dal Lago, K. Munakata, T. Kuwabara, M. Kozai, C. Kato, M. Rockenbach, N. Schuch, et al., The temperature effect in secondary cosmic rays (muons) observed at the ground: analysis of the Global MUON Detector Network data, *Astrophys. J.* 830 (2) (2016) 88.
- [23] A. Dmitrieva, I. Astapov, A. Kovylyaeva, D. Pankova, Temperature effect correction for muon flux at the earth surface: estimation of the accuracy of different methods, *J. Phys.* 409 (2013) 012130. IOP Publishing.
- [24] P.H. Barrett, L.M. Bollinger, G. Cocconi, Y. Eisenberg, K. Greisen, Interpretation of cosmic-ray measurements far underground, *Rev. Mod. Phys.* 24 (3) (1952) 133.
- [25] S. Tilav, P. Desiati, T. Kuwabara, D. Rocco, F. Rothmaier, M. Simmons, H. Wissing, et al., Atmospheric variations as observed by IceCube, arXiv:1001.0776 (2010).
- [26] P. Adamson, C. Andreopoulos, K. Arms, R. Armstrong, D. Auty, D. Ayres, C. Backhouse, J. Barnett, G. Barr, W. Barrett, et al., Observation of muon intensity variations by season with the Minos far detector, *Phys. Rev. D* 81 (1) (2010) 012001.
- [27] H. Carmichael, M. Bercovitch, J.F. Steljes, Introduction of meteorological corrections into meson monitor data, *Tellus* 19 (1) (1967) 143–160, doi:10.1111/j.2153-3490.1967.tb01468.x.
- [28] M.D. Berkova, A.V. Belov, E.A. Eroshenko, V.G. Yanke, Temperature effect of the muon component and practical questions for considering it in real time, *Bull. Russ. Acad. Sci.* 75 (6) (2011) 820–824, doi:10.3103/S1062873811060086.
- [29] A. Dmitrieva, R. Kokoulin, A. Petrukhin, D. Timashkov, Corrections for temperature effect for ground-based muon hodoscopes, *Astropart. Phys.* 34 (6) (2011) 401–411, doi:10.1016/j.astropartphys.2010.10.013.
- [30] Global forecast system (GFS), <https://www.ncdc.noaa.gov/data-access/modeldata/model-datasets/global-forecast-system-gfs>.
- [31] National centers for environmental prediction (NCEP), <http://www.ncep.noaa.gov/>.
- [32] A. Dragić, V. Udovičić, R. Banjanac, D. Joković, D. Maletić, N. Veselinović, M. Savić, J. Puzović, I.V. Aničin, The new setup in the Belgrade low-level and cosmic-ray laboratory, *Nucl. Technol. Radiat. Protect.* 26 (3) (2011) 181–192.
- [33] B. Haurwitz, The diurnal surface-pressure oscillation, *Arch. Meteorol. Geophys. Bioklimatol. Ser. A* 14 (4) (1965) 361–379, doi:10.1007/BF02253483.
- [34] L.I. Dorman, *Cosmic Rays in the Earth's Atmosphere and Underground*, Springer Netherlands, 2004, doi:10.1007/978-1-4020-2113-8.
- [35] I. Jolliffe, *Principal Component Analysis*, Springer-Verlag, 2002, doi:10.1007/b98835.
- [36] R.W. Preisendorfer, D.M. Curtis, *Principal component analysis in meteorology and oceanography*, Elsevier, Amsterdam, 1988.
- [37] M. Savić, D. Maletić, D. Joković, N. Veselinović, R. Banjanac, V. Udovičić, A. Dragić, Pressure and temperature effect corrections of atmospheric muon data in the belgrade cosmic-ray station, *J. Phys. Conf. Ser.* 632 (1) (2015) 012059.



Radon variability due to floor level in two typical residential buildings in Serbia

Vladimir Udovicic ,
Nikola Veselinovic,
Dimitrije Maletic,
Radomir Banjanac,
Aleksandar Dragic,
Dejan Jokovic,
Mihailo Savic,
David Knezevic,
Maja Eremic Savkovic

Abstract. It is well known that one of the factors that influence the indoor radon variability is the floor level of the buildings. Considering the fact that the main source of indoor radon is radon in soil gas, it is expected that the radon concentration decreases at higher floors. Thus at higher floors the dominant source of radon is originating from building materials, and in some cases there may be deviations from the generally established regularity. In such sense, we chose one freestanding single-family house with loft and other 16-floor high-rise residential building for this study. The indoor radon measurements were performed by two methods: passive and active. We used passive devices based on track-etched detectors: Radtrak² Radonova. For the short-term indoor radon measurements, we used two active devices: SN1029 and SN1030 (manufactured by Sun Nuclear Corporation). The first device was fixed in the living room at the ground level and the second was moved through the floors of the residential building. Every measuring cycle at the specified floor lasted seven days with the sampling time of 2 h. The results show two different indoor radon behaviours regarding radon variability due to floor level. In the single-family house with loft we registered intense difference between radon concentration in the ground level and loft, while in the high-rise residential building the radon level was almost the same at all floors, and hence we may conclude that radon originated mainly from building materials.

Keywords: Radon variability • Time series

Introduction

Radon sources in the buildings are primarily from soil, building materials and water. Considering the nature of the occurrence and all the sources, the concentration of radon is higher in the ground-floor rooms compared with that in the higher floors of the dwellings in apartments. In the literature one can find a lot of papers dealing with the influence of various factors, including the floor levels, on the radon concentration and variability. In one group of the articles, investigation of the indoor radon concentration distribution due to floor levels of the buildings is the part of the data analysis which was drawn from the national or regional radon surveys [1–6] and others are dedicated to these specific studies [7–11]. In the case of the big buildings with a several number of floors a deviation from the general regularity can be observed, since the dominant source of indoor radon at higher floors is building materials. On the other hand, the radon variability due to floor level, especially in big cities with a much higher number of high-rise buildings and population density compared with rural environments, may have an impact on the assessments of the effective dose from radon exposure at the national level. Usually, the indoor radon map represents the arithmetic mean value of indoor radon concentration on the ground floor, and thus it is not

V. Udovicic✉, N. Veselinovic, D. Maletic, R. Banjanac,
A. Dragic, D. Jokovic, M. Savic, D. Knezevic
Institute of Physics Belgrade
University of Belgrade
Pregrevica 118 St., 11080 Belgrade, Serbia
E-mail: udovicic@ipb.ac.rs

M. Eremic Savkovic
Serbian Radiation and Nuclear Safety and Security
Directorate
Masarikova 5 St., 11000 Belgrade, Serbia

Received: 30 November 2019
Accepted: 17 January 2020

representative of the radon exposure to all citizens since most people do not live on the ground floor. So, it is necessary to convert indoor radon map to a dose map. One of the examples is presented as a plan to develop models that allow correction from ground-floor dwellings to the real situation, accounting data from the national buildings database [12]. In Serbia, national typology of residential buildings is based on the results from the monography “National typology of residential buildings of Serbia” by a group of authors from the Faculty of Architecture [13]. There are six types of the residential buildings in Serbia: two for family housing – freestanding single-family house and single-family house in a row and four types for multifamily housing – freestanding residential building and residential building (lamella) (apartment block with repeated multiple lamellar cores and separate entrances), residential building in a row, and high-rise residential building. Distribution of buildings by type at the national level shows that 97% of all residential buildings are family housing. Also, for all defined types of buildings, number of floors ranges from one to eight above the ground level. Freestanding family houses are mostly ground floor (37%) or ground floor with loft in use (26%), while there is a very low representation of houses that have more than two floors (5%), with average floor level of family buildings of 1.4 [13]. In such sense, we chose one freestanding single-family house with loft with well-known radon characteristics [14] and one 16-floor high-rise residential building for this study.

Materials and methods

Two housing units were selected, one from the family housing group and one high-rise residential building from the collective housing group. The family house has a characteristic construction style in which the house has been built for several years with constant upgrading, which can potentially be a source of radon entry into such houses. The house has a basement and is made of standard materials (brick block, concrete, plaster). Finally, insulation was made using 5-cm thick styrofoam. Long-term measurements of radon concentrations have been carried out in this house by various methods, and several scientific papers have been published so far [14–16].

From the group of residential buildings for collective housing, we chose high-rise building in New Belgrade. It was built in the 1960s as block type. The soliter has a basement, while on the ground floor there are outlets and business premises. The apartments are located in the first floor upward. The soliter has 16 floors. One of the important parameters in the selection of building in municipality New Belgrade is the fact that this municipality is the most populated in Serbia.

The long-term radon measurements were performed with passive device Radtrak² Radonova based on CR-39 track detector. The detectors were exposed for three months from March to June. In the high-rise building, passive radon detectors were deployed at some of the floors in one or several apartments. Time series of measured radon concentrations in the studied residential buildings were obtained using two active devices: SN1029 with the following characteristics declared by the manufacturer – the measurement ranging from 1 Bq·m⁻³ to 99.99 kBq·m⁻³, accuracy equal to ±25%, sensitivity of 0.16 counts/h/Bq·m⁻³ and SN1030 with the following characteristics – the measurement ranging from 1 Bq·m⁻³ to 99.99 kBq·m⁻³, accuracy equal to ±20%, sensitivity of 0.4 counts/h/Bq·m⁻³. SN1029 device were calibrated at the accredited metrological Lab (SUJCHBO Kamenna, Czech Republic) in 2015 and model SN1030 were calibrated by the manufacturer in 2017. The both instruments participated in 2018 NRPI Intercomparisons of radon gas continuous monitors and also, SN1029 device participated in 2015 NRPI Intercomparisons of radon gas measurement devices at SURO v.v.i. Institute, Prague, Czech Republic within the IAEA Technical Cooperation Projects RER 9153 and RER 9127, with excellent results. These are measuring devices of simple construction and practical application. It is a counter with the addition of a sensor for measuring meteorological parameters. The operator can adjust the time sequences from 0.5 h to 24 h. One measurement cycle can take 1000 h or a total of 720 time sequences (the number of successive measurements, i.e. points in a time series). The devices were set to operate in a 2-h time sequence. One was fixed in the downstairs living room and the other was fixed in repositioning floors in apartment buildings. Each measurement cycle on a given floor lasted seven days.

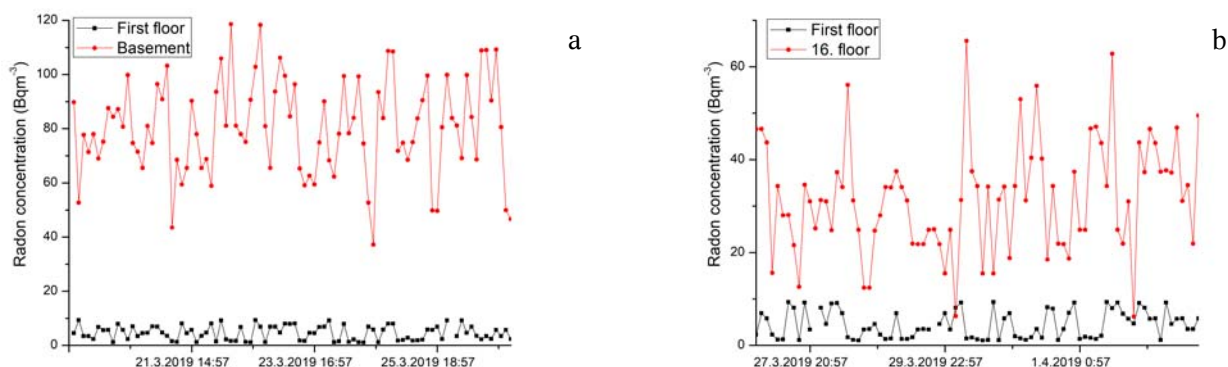


Fig. 1. The time series of the radon concentrations at the first floor vs. basement (a) and 16th floor (b) in the big residential building.

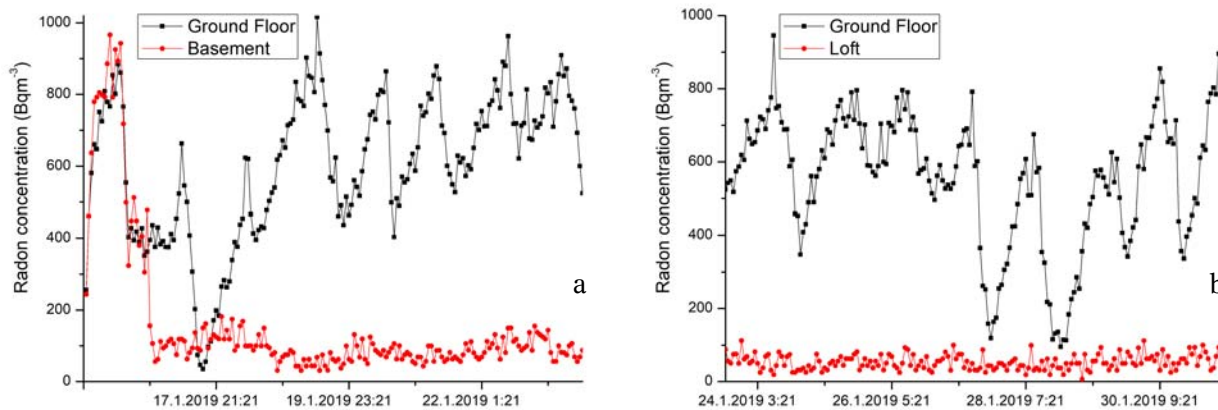


Fig. 2. The time series of the radon concentrations at the first floor vs. basement (a) and loft (b) in the single-family house.

Table 1. Results of indoor radon measurements in the high-rise residential building using passive (Radtrak² Radonova) and active radon devices

Floor level	Radon concentration/ Passive device (Radtrak ²) [Bq·m ⁻³]	Average radon concentration per floor level (Radtrak ²) [Bq·m ⁻³]	Arithmetic mean (standard deviation) radon concentration over measuring cycle [Bq·m ⁻³]
Basement	52 ± 10	53.5	81(17)
	69 ± 12		
	38 ± 10		
	55 ± 10		
1	<10	14	5(3)
	14 ± 8		
2	17 ± 8	17	24(9)
3			25(10)
4	21 ± 8	20.5	26(11)
	20 ± 8		
5	11 ± 8	19	
	27 ± 10		
6	22 ± 8	17	
	12 ± 8		
7	17 ± 8		
	23 ± 8		
8	22 ± 8	22	
9	15 ± 8	17.7	24(10)
	16 ± 8		
10	22 ± 8	17.5	
	12 ± 8		
11	17 ± 8	16	
	16 ± 8		
12	<10	<10	
14	20 ± 8	18.5	29(9)
	17 ± 8		
15	15 ± 8	15.5	
	16 ± 8		
16	31 ± 8	31	32(12)
Overall mean	24	21.6	30

Results and discussions

Figure 1 shows the illustrative examples that show radon time series from high-rise building, and Fig. 2 originates from the observed single-family house.

The arithmetic mean radon concentrations obtained from long- and short-term measurements are shown in Tables 1 and 2 for high-rise building and single-family house with loft, respectively.

In the family house, it is possible to notice marked variations in radon concentration with 1-day periodicity. Also interesting is the ratio of radon concentration on the ground floor to the basement of the house, which is the opposite of the usual situation in houses with a basement. This inverse behaviour can be explained by the fact that the basement does not cover the whole ground floor but a smaller part of it. The rest of the ground floor is covered by a concrete slab as a substrate, but cracks and poor joint with the walls are potential sources of elevated radon. Also, the differences in the results between two methods, passive and active devices, are due to the fact that presented radon values are measured in different seasons. With high-rise residential building, the situation is the opposite and it can be considered from the first floor that the dominant source of radon is the building material. There may even be a slight increase in the mean radon concentration on the higher floors. Also, the results show very low radon level on the first floor (well below the outdoor values) in the apartment. In such sense, we performed test intercomparison radon measurements for two active devices SN1029 and SN1030 in well-defined and controlled radon atmosphere (radon concentration below 30 Bq·m⁻³) in the Underground Low-background Laboratory in the Institute of Physics Belgrade [17, 18]. Additional testing includes the same place and time of the measurements but different sampling time set to 1, 2, 4, 8 and 12 h. The results are shown in Table 3.

In the above performed measurements, both devices show significant differences in the low-level radon range, which may originate from individual instruments characteristics presented in the “Materials and methods” section.

Table 2. Results of indoor radon measurements in the single-family house with loft using passive (Radtrak² Radonova) and active radon devices

Floor level	Radon concentration/Passive device (Radtrak ²) [Bq·m ⁻³]	Arithmetic mean (standard deviation) radon concentration over measuring cycle [Bq·m ⁻³]
Basement		160(202)
Ground level	330 ± 50	579(194)
Loft	18 ± 8	53(21)

Table 3. Test intercomparison indoor radon measurements with active radon devices SN1029 and SN1030

	Arithmetic mean (standard deviation) radon concentration over measuring cycle [Bq·m ⁻³]				
Sampling time [h]	1	2	4	8	12
SN1029	28(12)	28(11)	27(7)	23(6)	32(14)
SN1030	12(6)	14(7)	10(3)	12(5)	14(6)

Conclusions

The results show that the radon behaviour in two different residential buildings is diametrically opposite. In the single-family house with loft we registered intense difference between radon concentration in the ground level and loft, while in the high-rise residential building the radon level was almost the same at all floors and hence we may conclude that radon originated mainly from building materials. However, the results from the high-rise building can be predicted on the basis of work of a group of authors who have determined the internal exposure from construction material used in Serbia which originates from the exhalation of radon and thoron [19] and the study presented in this article [10]. We can expect similar results in any other multistorey buildings in Serbia. In the future work, we will focus on the additional radon measurements in the typical residential buildings from other types of houses.

Acknowledgments. The authors acknowledge funding provided by the Institute of Physics Belgrade through the grant by the Ministry of Education, Science and Technological Development of the Republic of Serbia.

ORCID

V. Udovicic  <http://orcid.org/0000-0002-7839-1537>

References

- Bochicchio, F., Campos-Venuti, G., Piermattei, S., Nucetelli, C., Risica, S., Tommasino, L., Torri, G., Magnoni, M., Agnesod, G., Sgorbati, G., Bonomi, M., Minach, L., Trotti, F., Malisan, M. R., Maggiolo, S., Gaidolfi, L., Giannardi, C., Rongoni, A., Lombardi, M., Cherubini, G., D'Ostilio, S., Cristofaro, C., Pugliese, M., Martucci, V., Crispino, A., Cuzzocrea, P., Sansone Santamaria, A., & Cappai, M. (2005). Annual average and seasonal variations of residential radon concentration for all the Italian Regions. *Radiat. Meas.*, *40*, 686–694.
- Friedmann, H. (2005). Final results of the Austrian Radon Project. *Health Phys.*, *89*(4), 339–348.
- Du, L., Prasauskas, T., Leivo, V., Turunen, M., Pekkonen, M., Kiviste, M., Aaltonen, A., Martuzevicius, D., & Haverinen-Shaughnessy, U. (2015). Assessment of indoor environmental quality in existing multi-family buildings in North-East Europe. *Environ. Int.*, *79*, 74–84.
- Cucoş (Dinu), A., Cosma, C., Dicu, T., Begy, R., Moldovan, M., Papp, B., Niță, D., Burghel, B., & Sainz, C. (2012). Thorough investigations on indoor radon in Băița radon-prone area (Romania). *Sci. Total Environ.*, *431*, 78–83.
- Yarmoshenko, I., Vasilyev, A., Malinovsky, G., Bossew, P., Žunić, Z. S., Onischenko, A., & Zhukovsky, M. (2016). Variance of indoor radon concentration: Major influencing factors. *Sci. Total Environ.*, *541*, 155–160.
- Kropat, G., Bochud, F., Jaboyedoff, M., Laedermann, J. P., Murith, C., Palacios, M., & Baechler, S. (2014). Major influencing factors of indoor radon concentrations in Switzerland. *J. Environ. Radioact.*, *129*, 7–22.
- Borgoni, R., De Francesco, D., De Bartolo, D., & Tzavidis, N. (2014). Hierarchical modeling of indoor radon concentration: how much do geology and building factors matter? *J. Environ. Radioact.*, *138*, 227–237.
- Xie, D., Liao, M., & Kearfott, K. J. (2015). Influence of environmental factors on indoor radon concentration levels in the basement and ground floor of a building – A case study. *Radiat. Meas.*, *82*, 52–58.
- Man, C. K., & Yeung, H. S. (1999). Modeling and measuring the indoor radon concentrations in high-rise buildings in Hong Kong. *Appl. Radiat. Isot.*, *50*, 1131–1135.
- Vukotić, P., Zekić, R., Antović, N. M., & Andjelić, T. (2019). Radon concentrations in multi-story buildings in Montenegro. *Nucl. Technol. Radiat. Prot.*, *34*, 165–174.
- Lorenzo-González, M., Ruano-Ravina, A., Peón, J., Piñeiro, M., & Barros-Dios, J. M. (2017). Residential radon in Galicia: a cross-sectional study in a radon-prone area. *J. Radiol. Prot.*, *37*(3), 728–741.
- Elío, J., Cinelli, G., Bossew, P., Gutiérrez-Villanueva, J. L., Tollefsen, T., De Cort, M., Nogarotto, A., & Braga, R. (2019). The first version of the Pan-European Indoor Radon Map. *Nat. Hazards Earth Syst. Sci.*, *19*, 2451–2464.
- Jovanović Popović, M., Ignjatović, D., Radivojević, A., Rajčić, A., Čuković Ignjatović, N., Đukanović, Lj., & Nedić, M. (2013). *National typology of residential*

- buildings in Serbia*. Belgrade: Faculty of Architecture University of Belgrade.
14. Udovičić, V., Maletić, D., Banjanac, R., Joković, D., Dragić, A., Veselinović, N., Živanović, J., Savić, M., & Forkapić, S. (2018). Multiyear indoor radon variability in a family house—A case study in Serbia. *Nucl. Technol. Radiat. Prot.*, 33(2), 174–179.
 15. Maletić, D., Udovičić, V., Banjanac, R., Joković, D., Dragić, A., Veselinović, N., & Filipović, J. (2014). Comparison of multivariate classification and regression methods for indoor radon measurements. *Nucl. Technol. Radiat. Prot.*, 29, 17–23.
 16. Filipović, J., Maletić, D., Udovičić, V., Banjanac, R., Joković, D., Savić, M., & Veselinović, N. (2016). The use of multivariate analysis of the radon variability in the underground laboratory and indoor environment. *Nukleonika*, 61(3), 357–360. DOI: 10.1515/nuka-2016-0059.
 17. Udovičić, V., Aničin, I., Joković, D., Dragić, A., Banjanac, R., Grabež, B., & Veselinović, N. (2011). Radon time-series analysis in the Underground Low-level Laboratory in Belgrade, Serbia. *Radiat. Prot. Dosim.*, 145(2/3), 155–158.
 18. Udovičić, V., Filipović, J., Dragić, A., Banjanac, R., Joković, D., Maletić, D., Grabež, B., & Veselinović, N. (2014). Daily and seasonal radon variability in the underground low-background laboratory in Belgrade, Serbia. *Radiat. Prot. Dosim.*, 160(1/3), 62–64.
 19. Ujić, P., Čeliković, I., Kandić, A., Vukanac, I., Đurašević, M., Dragosavac, D., & Žunić, Z. S. (2010). Internal exposure from building materials exhaling ^{222}Rn and ^{220}Rn as compared to external exposure due to their natural radioactivity content. *Appl. Radiat. Isot.*, 68, 201–206.



Correlation analysis of solar energetic particles and secondary cosmic ray flux

Nikola Veselinović^a, Mihailo Savić, Aleksandar Dragić, Dimitrije Maletić, Radomir Banjanac, Dejan Joković, David Knežević, and Vladimir Udovičić

Institute of Physics Belgrade, University of Belgrade, Pregrevica 118, Belgrade 11080, Serbia

Received 31 January 2021 / Accepted 5 May 2021 / Published online 8 June 2021
© The Author(s), under exclusive licence to EDP Sciences, SIF and Springer-Verlag GmbH Germany, part of Springer Nature 2021

Abstract. Galactic cosmic rays entering heliosphere are modulated by interplanetary magnetic field which is carried away from the Sun by the solar wind. Cosmic rays are additionally modulated by coronal mass ejections and shock waves, which can produce Forbush decrease, a transient decrease in the observed galactic cosmic ray intensity. Measurements of magnetic field and plasma parameters in near-Earth space detect regularly coronal mass ejections, so it is important to understand the correlation between near-Earth particles fluxes associated with these coronal mass ejections and Forbush decreases. By combining in situ measurements of solar energetic particles with ground-based observations by the Belgrade muon detector, we analysed the dynamics of the variation of galactic cosmic rays. Correlation between variations of the flux of the cosmic rays and average in situ particle fluxes was investigated during Forbush decreases. Correlation exhibited dependence on the energy of solar wind particles, but also on cut-off rigidities of cosmic rays detected on the ground. The goal of cross-correlation analysis is to help in better understanding of how coronal mass ejections affect space weather as well as the effects they have on primary cosmic ray variations as detected by ground-based cosmic ray detectors.

1 Introduction

Space weather has been widely used as a term to define impact of the Sun, heliosphere and geomagnetic field on our biosphere and our technological systems. Understanding space weather is a matter of both scientific interest and practical importance as its impact could potentially be hazardous to our civilisation. Cosmic ray (CR) observations can also be used to study space weather. Primary (or galactic) CRs are high-energy nuclei (mainly protons) that originate from outside of our solar system. Their flux and energy range is covering several tens of orders of magnitude (flux from 10^{-28} up to 10^4 ($\text{m}^2 \text{sr sec eV/nucleon}$)⁻¹ and energy range up to 10^{21} eV [10]). As charged particles, CRs are sensitive to magnetic field, so often it is more convenient to use geomagnetic rigidity instead of energy to characterise primary CRs. Geomagnetic rigidity is defined as $R = B\rho = pq$, where B is the magnetic field, ρ is the gyroradius of the particle due to this field, p is the particle momentum and q is its charge [14]. As they traverse interplanetary space, galactic CRs interact with helio-

spheric magnetic field. The heliosphere is the region of space around the Sun dominated by the solar wind and the interplanetary magnetic field (IMF). The solar wind is a stream of supersonic plasma blowing outward from the Sun. IMF represents solar magnetic field carried by highly conducting solar wind plasma. Interaction of CRs with this large-scale field modulates CRs flux intensity measured on Earth, which is nested deep inside the heliosphere. Interaction with the heliosphere causes gradient and curvature drift motion of CRs and scattering by the magnetic irregularities embedded in the solar wind [19]. Variations in the solar magnetic field directly affect the heliosphere, most prominent being the solar cycle variation with a period of about 11 years. Solar cycle affects activity of the Sun which is visible in varying number of sunspots, solar flares (SFs) and coronal mass ejections (CMEs). Coronal mass ejection is an extreme solar activity event, followed by significant release of charged particles and accompanying magnetic field from solar corona. Intensity of measured CRs flux anticorrelates with the activity of the Sun, with lower intensity during maximum of the solar cycle and higher intensity during minimum of solar activity.

One of the transient phenomena of this interaction is the Forbush decrease (FD), which represents a rapid depression in CR flux. It is usually characterised by a sudden decrease reaching minimum within one day, followed by a subsequent gradual recovery phase, which

Supplementary information The online version of this article (<https://doi.org/10.1140/epjd/s10053-021-00172-x>) contains supplementary information, which is available to authorized users.

^a e-mail: veselinovic@ipb.ac.rs (corresponding author)

can last for several days. Typical causes of FD are transient interplanetary events related to interplanetary coronal mass ejections (ICMEs). If the speed of the ICME is greater than fast magnetosonic wave speed in the solar wind reference frame, ambient solar wind plasma will be compressed. The shock can be formed, which is driven ahead of ICME and can cause enhancement of IMF. FD can also be formed due to corotating interaction regions between different solar wind streams with different speed [2]. In this paper, we will only focus on ICME induced FDs, of which we will study four cases.

Correlation between parameters characterising FDs (like magnitude of the decrease, duration, one-step or two-step FDs, etc.) and solar wind parameters has been studied for some time. There is reasonable evidence for correlation between FD magnitude and amplitude of magnetic field enhancement B , velocity of CME, maximum solar wind velocities and other parameters as shown in [7, 22]. Also, profile of FDs is modelled and compared with CME magnetic structure, starting from the simple force-free flux rope with circular cross section, but it can deviate from this ideal concept. FD magnitude is explained with cumulative effect of diffusion of CRs through the turbulent sheath region [3, 11]. FD is also energy dependent, where amplitude of decrease is typically around several percent. Higher-rigidity CRs only weakly interact with magnetic disturbances, so no significant change of the flux can be expected for CRs with rigidity of several dozen GV [9]. In order to detect FD at any location, larger statistics are needed for CRs of lower energy. CRs also interact with geomagnetic field which imposes the minimal rigidity CRs must have in order to reach Earth's surface. This geomagnetic cut-off rigidity depends on geomagnetic latitude. It is smaller at the poles and increases with latitude, with some exceptions due to deviation of Earth's magnetic field from the magnetic dipole model (i.e., South Atlantic anomaly [4]).

Primary CRs arriving at Earth interact with atoms and molecules in Earth's atmosphere. CRs with energy above 300–400 MeV/nucleon generate showers of secondary particles. These secondary CRs consist of electrons and photons (electromagnetic component) and harder, in terms of energy, nuclear component of the cascade. Nuclear component, at the bottom of the atmosphere, is composed mainly of muons, protons, neutrons and neutrinos. Secondary CRs can be observed with detectors in the atmosphere (balloon probes), on the ground or even underground. High-energy muons can penetrate deep underground and can be an important component of the background in experiments requiring high sensitivity (dark matter search, proton decay, etc.).

There is a well-known correlation between parameters of solar wind plasma and CR flux, and the goal of this paper is to extend the study of FDs, specifically its magnitude and time evolution, to wider range of parameters of the heliosphere measured routinely with satellites. We concentrate our study on previously scarcely used parameters of the solar wind, particularly flux of

charged particles of different energies. These particles are the source of inhomogeneity in the IMF, so the goal is to try and find distinguishing characteristics of FDs, like magnitude of decrease and FD profile that can be related to the satellite proton flux data, and examine their potential correlation with other space weather parameters. This additional information can be useful in finding explicit connection between parameters of solar wind and CR flux and can lead to better understanding of these complex processes.

2 CR data

In order to provide higher count rate, detector on Earth has to be omnidirectional and to detect integral flux over different range of energies. For the last seventy years secondary CRs are measured using standard ground-based neutron monitors (NMs) [6]. There is a worldwide network of NMs (<http://www01.nmdb.eu/>) that measures flux of secondary CRs originated from primary CRs with rigidity range approximately between 1 GV and 20 GV. Every node of the worldwide network of ground stations has its unique cut-off rigidity depending on its geomagnetic coordinates and height. The other type of widely used ground-based CR detectors are muon monitors. Muon monitors are sensitive to primary CRs of higher rigidity and complement NMs measurements [26]. Worldwide network of these muon stations is still rudimentary, but it can provide insight into flux variation of primary CRs with energies higher than CRs detected by NMs. Since both NMs and muon detectors are energy-integrating detectors and use entire atmosphere above it as a moderator, it is not trivial to relate count rate of these detectors to the flux or energy spectrum of primary CRs at the top of the atmosphere. One needs to know the response of a detector to a unit flux of CRs with the given energy, the so-called detector yield function. Yield functions can be calculated either theoretically, using a numerical simulation of the nucleonic cascade caused by energetic cosmic rays in the Earth's atmosphere, e.g., [8], or semi-empirically, for example based on a latitudinal survey [16].

As flux of secondary cosmic rays is also sensitive to varying properties of the atmosphere through which these CRs propagate, it is necessary to conduct flux correction of the measured flux for atmospheric parameters, where atmospheric pressure correction is the most important. In addition to atmospheric pressure, CR muons are sensitive to temperature variations in the atmosphere, starting from the top of the atmosphere all the way to the ground level. There are several procedures for corrections of these effects which are regularly used. Most commonly used are the integral method and the method of effective level of generation, but some novel techniques have also been introduced in recent years [25]. Correction for these atmospheric parameters is necessary in order to increase detector sensitivity to

Table 1 Properties of primary CR flux related to muons detected at Belgrade CR station

Detector	Muon flux 1/(m ² s)	$E_{0.05}$ (GeV)	E_{med} (GeV)	$E_{0.95}$ (GeV)	Cut-off rigidity (GV)
GLL	137(6)	11	59(2)	915	5.3
UL	45(2)	31	137(5)	1811	12

variations of primary CRs flux and more precisely study the influence of solar modulation on galactic CRs.

Belgrade CR station started collecting data with the current experimental set-up in 2009. The station consists of two separate detector units: one placed on ground level (GLL) and the other in shallow underground (UL), both utilising the same experimental set-up. Such configuration provides opportunity to monitor muon fluxes in two different energy ranges with all other external parameters (such as atmospheric parameters, geomagnetic location and experimental set-up) being the same. Underground part of the station detects muons originated from primary CRs with higher energy because of the layer of soil overburden (13 m of loess) which absorbs lower-energy muons. Details of the detector systems at the Belgrade CRs station as well as calculated response functions are presented in [29]. The station is situated at the Laboratory for Nuclear Physics at the Institute of Physics Belgrade, Serbia. The altitude of the station is 78 m above sea level. Its geographic coordinates are: 44°51' N and 20°23' E, with geomagnetic latitude of 39°32' N. Sensitivity of Belgrade CR detectors to galactic CRs is given in Table 1, where primary CRs with the energy below $E_{0.05}$ (and above $E_{0.95}$) contribute with 5% to the count rate of the corresponding detector, and E_{med} is median energy based on simulation. In preparation for the analysis, detected muon count rates are corrected for efficiency, as well as for barometric and atmospheric temperature effects. Temperature effect correction is done using integral method [24].

3 Satellite data

In recent years, satellites provide new direct measurements of primary CRs flux in the heliosphere and the geomagnetic field. Also, detectors mounted on spacecraft allow us to probe even further, as Voyager recently crossed heliospheric boundary and for the first time galactic CRs flux was measured outside the heliosphere. The problem with such measurements is limitation to the size of the detectors, due to constraints of the construction of the satellites. In order to have valid statistics and good resolution, only low-energy particle flux can be measured. These low-energy particles are sensitive to geomagnetic field, which can introduce additional perturbation. Also, measurements of low-energy CRs can be masked by the increased flux of low-energy solar energetic particles (SEPs) in the MeV energy range. FDs detected by ground-based detectors are measured in energy range several orders of

magnitude higher than the energy range available to satellites measurements. (NMs detect flux that originate from ~ 10 GeV, single muon detectors higher than that up to ~ 100 GeV, while solar weather satellite measurements range up to several 100 MeV.) SEP occurrence is sporadic and depends on which part of the solar cycle we are in, so long-term studies with stable data quality are necessary if we are to study solar modulation of CRs. Such long-term measurements have been performed with various spacecrafts during the last four decades. Data measured on different interplanetary locations are then used for modelling of the heliosphere, which is important for understanding and forecasting space weather. This is a relatively new and dynamic field that is still expanding. More in situ measurements that can be catalogued [17] and compared with data from ground based stations will improve our understanding of near space environment.

In this paper, we use proton data from ERNE (Energetic and Relativistic Nuclei and Electron experiment) detector at the SOHO (Solar and Heliospheric Observatory) (https://omniweb.gsfc.nasa.gov/ftpbrowser/flux_spectr_m.html), which has been performing measurements in Lagrangian point L1 for the last quarter of a century described in [13] and references therein. Experiments that collect in situ particles data are ERNE and COSTEP (Comprehensive SupraThermal and Energetic Particle analyser), where data are combined to meet requirements of the mission. ERNE detector provides proton flux data in relatively large energy range (1.6 to 131 MeV) separated in several energy channels (1.3–1.6, 1.6–2.0, 2.0–2.5, 2.5–3.2, 3.2–4.0, 4.0–5.0, 5.0–6.4, 6.4–8.0, 8.0–10, 10–13, 13–16, 16–20, 20–25, 25–32, 32–40, 40–50, 50–64, 64–80, 80–100, 100–130 MeV). Measurements are taken with two different detectors: LED (low-energy detector) covers lower-energy and HED (high-energy detector) which covers higher-energy channels [28]. Satellites, including SOHO, also measure in situ parameters of the space environment and gather data about magnetic field, solar wind and concentration and flux of various types of particles on the location. Satellite data relevant to heliospheric studies are, among other places, available at GSFC/Space Physics Data Facility, in the form of low- and high-resolution OMNI data (https://spdf.gsfc.nasa.gov/pub/data/omni/low_res_omni/). In this study, we used the low-resolution OMNI data that contain hourly data for the solar wind magnetic field and plasma parameters, energetic proton fluxes, and geomagnetic and solar activity indices for different regions in proximity to Earth [12].

4 Four prominent FD events during rising phase of solar cycle 24

Previous (24th) solar cycle started in December 2008 and ended in November 2019 (as available from Sunspot Index and Long-term Solar Observations database <http://www.sidc.be/silso/node/167>). It had an unusually weak maximum, with smoothed maximum international sunspot number of 116. For comparison, in cycles 22 and 23 this number was 214 and 180, respectively (as available from Sunspot Index and Long-term Solar Observations database <http://sidc.be/silso/home>). Same period was also characterised by smaller number of FDs, especially ones with larger amplitudes.

There were fifteen strong FDs (with magnitude of decrease larger than 5% for particles with 10 GV rigidity) recorded in the rising phase of solar cycle 24, however in this study we will limit our analysis to four events detected by the Belgrade Cosmic Ray Station (<http://www.cosmic.ipb.ac.rs/>). Other prominent FDs that occurred in this period have not being detected by either GLL or UL detector due to discontinuity of operation, so they have been omitted from this study. All four events followed ejections from an active region on the Sun, accompanied by a solar flare with interplanetary shock wave and sudden storm commencing (SSC), and disturbance in the geomagnetic field. All of these FDs were seen by the NM detector network as well.

First significant FD of solar cycle 24 was recorded on 18 February 2011 and has been caused by a CME heading directly towards Earth [20]. It has been detected by most ground stations around the world. Its morphology is influenced by the interaction of two CMEs, first slower and the second faster (with respective speeds of 390 km/s and 1020 km/s), that occurred a day apart [27]. Geomagnetic activity has been relatively weak due to orientation of the magnetic field of the ejecta [21].

Second event was observed on 7 March 2012. It included an X-class flare (X5.4), that occurred in NOAA AR 11429 with an intense halo CME, followed by several smaller flares and another partial CME. It caused one of the strongest FDs of the last solar cycle. Observed solar activity was also related to the intense geomagnetic storm that followed [15].

A strong SF (X1.6) was detected by several spacecrafts during 10 September 2014, originating from active region NOAA AR 2158. Based on the SOHO coronagraph images, this flare was associated with a CME that was aimed towards Earth, where it arrived on September 12. This activity resulted in a major geomagnetic storm, one of the strongest in 2014.

In the second half of June 2015, solar activity was very intense, since a number of CMEs and flares were produced from the powerful AR 12371, which dominated solar activity during that period [23]. The impact of these CMEs on the Earth's magnetosphere resulted in a moderate to severe G4-class geomagnetic storm that occurred on the summer solstice. The result was a very interesting and unusual modulation galactic CRs flux, which appeared as a series of FDs.

For the study of FD events and their relationship with IMF and geomagnetic disturbances, researchers from IZMIRAN (Pushkov Institute of Terrestrial Magnetism, Ionosphere and Radio Wave Propagation, Russian Academy of Sciences) created an FD database (<http://spaceweather.izmiran.ru/eng/dbs.html>) which contains various FD parameters, as well as their relationship with heliospheric and geomagnetic parameters covering several solar cycles [1]. Properties of the four selected FDs, taken from the IZMIRAN database, are given in Table 2.

5 Data analysis

In order to establish the usability of SOHO SEP flux data in the study of CR variations, we will first analyse how muon count rate time series compare with some of the IMF parameters more commonly used in the analysis of solar activity-induced CR variations. To this end, we compare hourly muon count rates (measured by Belgrade muon station and corrected for atmospheric effects) with time series for selected parameters from OMNI database. To give more weight to this qualitative analysis, we concentrate only on periods of extreme solar activity, in particular periods of the occurrence of four FD events described in Sect. 4. We then examine the relationship between measured muon count rates and the SOHO/ERNE SEP flux data and analyse any discerning features in comparison with the ones observed in OMNI data time series. The period selected for this analysis is approximately one solar rotation of 27 days. All probes at L1 are about an hour upstream of the magnetosphere so all their data are interspersed with data from spacecraft close to Earth (e.g., IMP 8). In order to compute hourly averages "at Earth" this time shift has to be taken into account (https://omniweb.gsfc.nasa.gov/html/ow_data.html).

Next, we investigate the short-term correlation between SEP flux and muon count rate data during time periods of four selected FDs. Muon time series for this procedure were selected for times where average muon flux was significantly lower than the background level. Background level was determined from moving averages for hourly count rates 10 days before the event. We then perform correlative analysis between SOHO SEP flux data and muon count rates for a period of one year (from 01.06.2010 to 31.05.2011), in order to establish the long-term relationship. For further insight, we also look into the correlation between these variables during the periods of reduced geomagnetic activity (International Quiet Days) and increased geomagnetic activity (International Disturbed Days).

Finally, we look in greater detail into SOHO SEP flux time series. In order to perform more quantitative analysis, time-integrated flux is calculated for SEP data for different SOHO energy bins and for the duration of selected FD events. In order to provide a parameter for characterisation for different FD events, calculated integral flux is plotted as a function of proton energy and

Table 2 Selected FD and interplanetary disturbance parameters (taken from IZMIRAN database)

Parameter	FD 1	FD 2	FD 3	FD 4	Parameter comment
Date of FD	18.2.2011.	8.3.2012.	12.9.2014.	22.6.2015.	
Date of parent solar event	15.2.2011.	7.3.2012.	10.9.2014.	21.6.2015.	
AR number	1158	11429	2158	12371	NOAA active region
V_{meanC}	584	1198	906	1040	The average ICME velocity between the Sun and the Earth, calculated using the time of the beginning of the associated CME observations (in km/s)
V_{max}	691	737	730	742	Maximal hourly solar wind speed in the event (in km/s)
B_{max}	31	23.1	31.7	37.7	Maximal hourly IMF strength in the event (in nT)
B_{zmin}	- 5.5	- 16.1	- 9.5	- 26.3	Minimal hourly Bz component of the IMF in the event (in nT)
R_{bulk}	72.25	146.2	131.35	171.25	An estimate of the maximum proton rigidity (in GV) that can be reflected by the total magnetic field, integrated from the event onset to the FD minimum
Magn	5.2	11.7	8.5	8.4	FD magnitude for particles with 10 GV rigidity, calculated as maximal range CRs density variations in the event, obtained by GSM from NM network data (in %)
MagnM	4.7	13.1	6.9	10.4	FD magnitude for particles with 10 GV rigidity, corrected on magnetospheric effect with Dst-index (in %)
TminM	7	20	9	11	Time from the FD onset to minimum, calculated from the data corrected for magnetospheric effect
Kp_{max}	5	8	6.33	8.33	Maximal Kp-index in the event
Ap_{max}	48	207	94	236	Maximal 3-hour Ap-index in the event
Dst_{min}	- 30	- 143	- 75	- 204	Minimal Dst-index in the event (in nT)
Flare class	X2.2	X5.4	X1.6	M2.6	Associated X-ray flare data
SSN	85	97	126	56	Number of sunspot at the FD onset day

fitted with a power function. Dependence of magnitude for selected FDs on the exponents obtained from fitted distributions is then analysed.

6 Results and discussion

Comparison between time series of selected IMF parameters from OMNI database and muon count rate time

series during the periods of four selected FD events is shown in Fig. 1. Observed anticorrelation between muon count rates and proton flux and temperature, as well as with the overall IMF magnetic field and detected plasma speed, is in agreement with previously stated evidence in the literature [30].

Similar comparison between muon count rate time series and selected channels of SOHO/ERNE proton flux data for the same time intervals is shown in Fig.

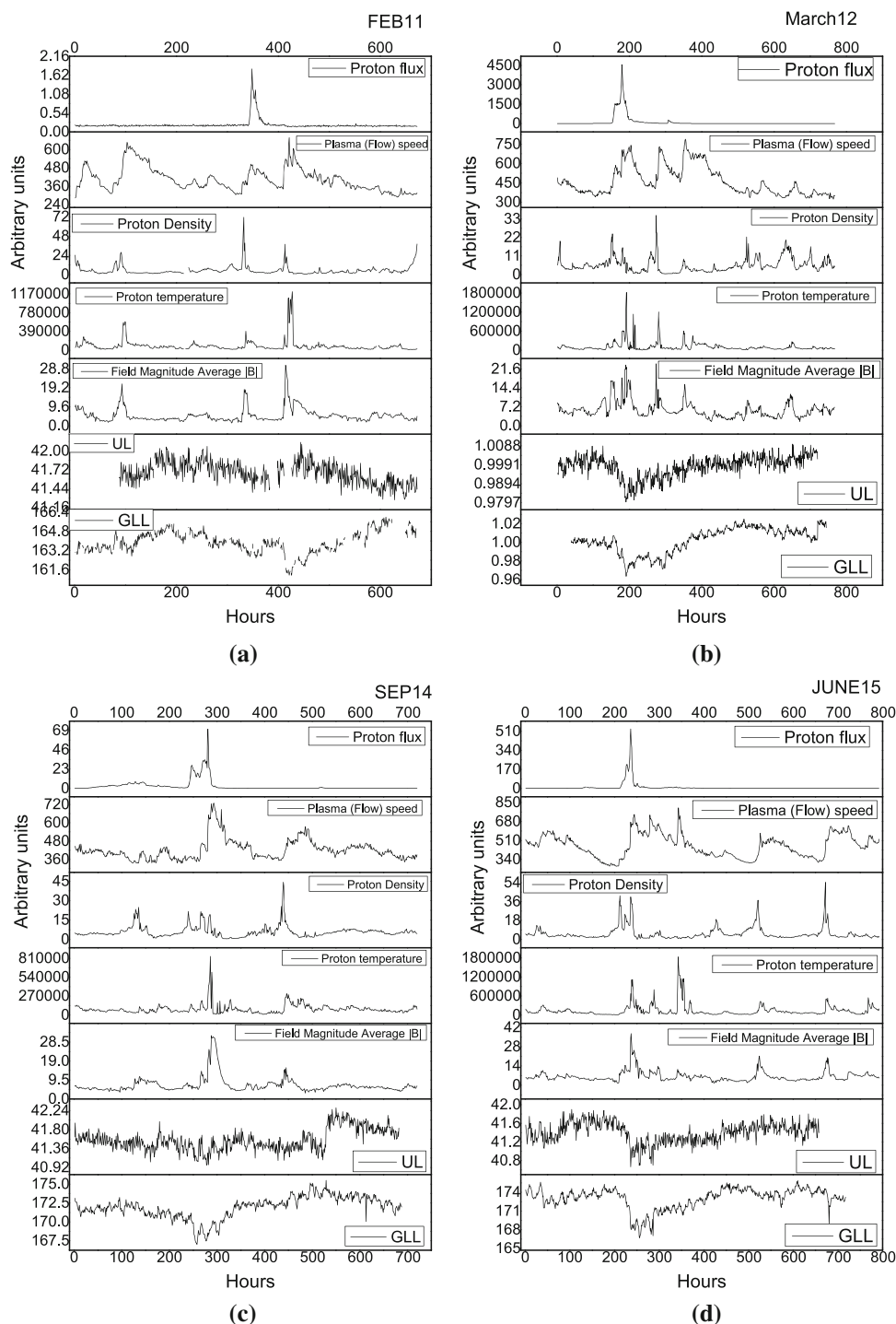


Fig. 1 Time series for particle and plasma parameters (taken from OMNI database) in the time interval of approximately one month around the occurrence of four selected FD events: **a** February 2011 (start of time interval on 1 February), **b** March 2012 (start of time interval on 1 March), **c** September 2014 (start of time interval on 1 September) and **d** June 2015 (start of time interval on 13 June)

2. For the sake of clarity, we chose three energy channels (1.6–2 MeV, 16–20 MeV, 100–130 MeV), approximately one order of magnitude apart, where first channel is measured with LED and the other two with HED detector on SOHO/ERNE instrument. In case of the

February 2011 event, there is an observable time lag (≈ 55 h) between the increase of measured proton flux at low-energy channels (1.6–2 MeV and 16–20 MeV energy channels) and the beginning of FD recorded at ground station. This time lag is also present between

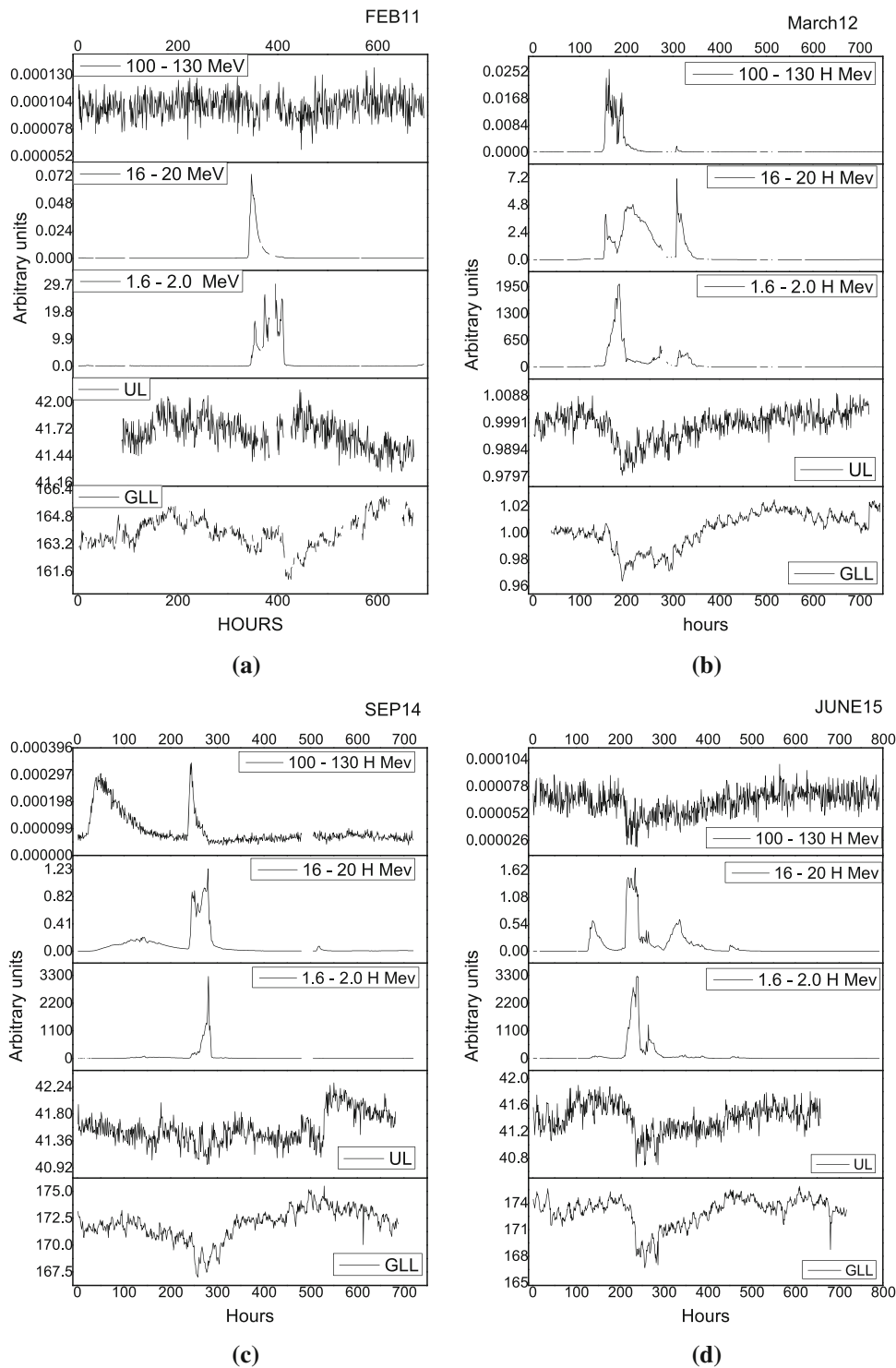


Fig. 2 Hourly time series for different proton channels from SOHO/ERNE and two muon detectors at Belgrade CR station, in the time interval of approximately one month around the occurrence of four selected FD events: **a**) February (start of time interval on 1 February) 2011, **b** March 2012 (start of time interval on 1 March), **c** September 2014 (start of time interval on 1 September) and **d** June 2015 (start of time interval on 13 June)

OMNI proton flux data and ground station measurements for this FD alone. FD is a complex modulation of CR flux that depends on a lot of parameters, like magnitude of magnetic field and its components,

speed of solar wind and CMEs (with CME average speed ≈ 490 km/s), most of which are listed in Table 2. Parameter values for all four ICMEs are mostly comparable, but one difference that stands out is the discrep-

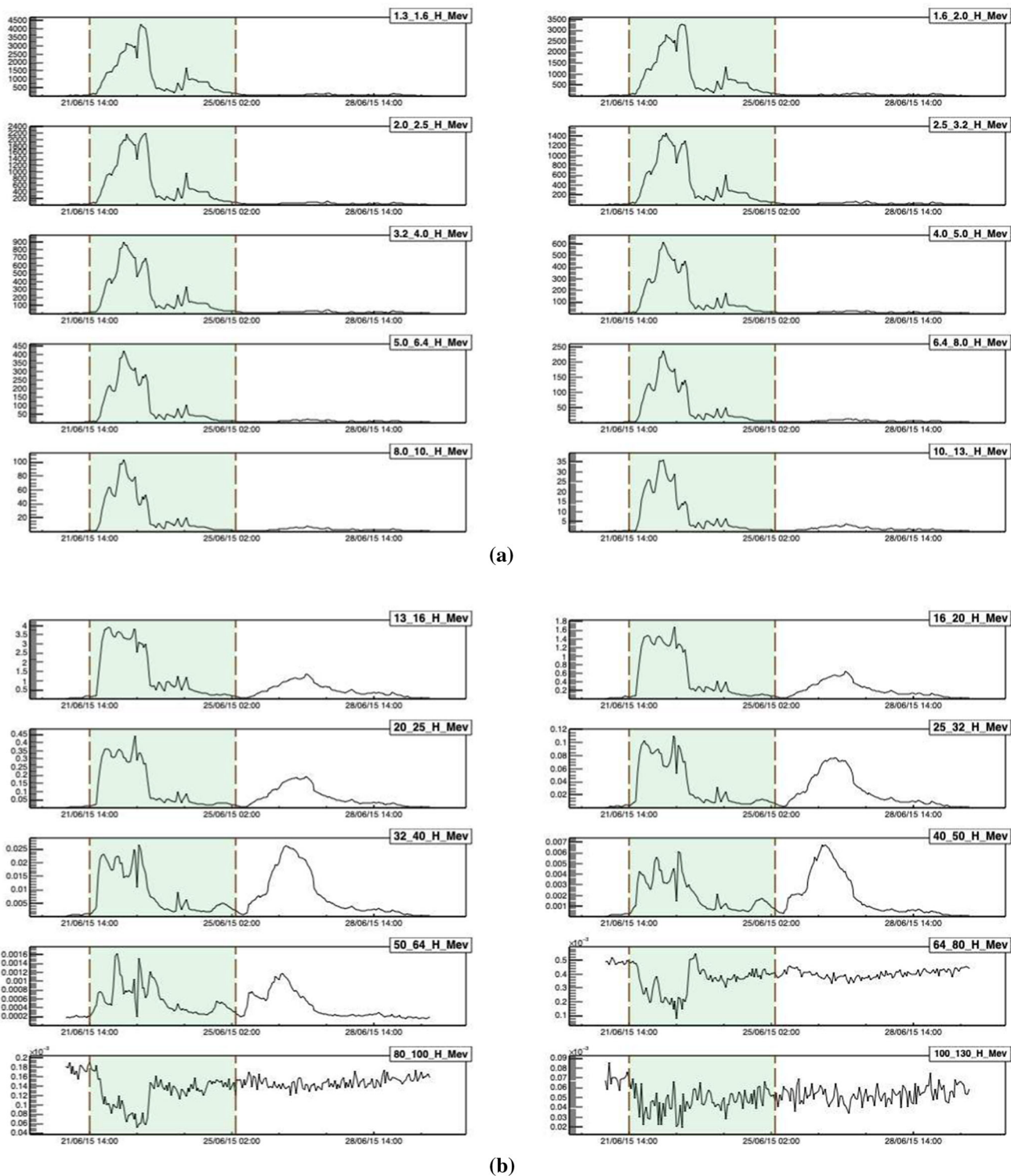


Fig. 3 Differential SEP fluxes during extreme solar event in June 2015, measured by SOHO/ERNE proton channels. Vertical dashed lines indicate the time for the start and the end of interval used to calculate the integral flux

ancy in average CME velocity (584 km/s from Table 2.) for the FD of February 2011, which can possibly explain the observed time lag for this particular FD.

Based on the observed time lag and other coincident features, we can establish good agreement between

SOHO low-energy channel data and OMNI data time series. As for high-energy channels, SEP time series in 100–130 MeV energy range for February 2011 and June 2015 events appear to correlate with muon count rate measurements on the ground. One possible explanation

Table 3 Statistical correlation between Belgrade CR station and SOHO/ERNE measurements during the periods of four selected FD events

FD	Energy range (MeV)	GLL		UL	
		Pearson coefficient	<i>P</i> value	Pearson coefficient	<i>P</i> value
FEB 11	1.6–2.0 H	– 0.10877	0.01	– 0.05285	0.2
	16–20 H	– 0.18384	2×10^{-5}	– 0.10732	0.01
	100–130 H	0.24204	$< 10^{-6}$	– 0.13212	0.02
MAR 12	1.6–2.0 H	– 0.48477	$< 10^{-6}$	– 0.43994	$< 10^{-6}$
	16–20 H	– 0.72033	$< 10^{-6}$	– 0.68221	$< 10^{-6}$
	100–130 H	– 0.29172	$< 10^{-6}$	– 0.27822	$< 10^{-6}$
SEP 14	1.6–2.0 H	– 0.2839	$< 10^{-6}$	– 0.48052	$< 10^{-6}$
	16–20 H	– 0.37814	$< 10^{-6}$	– 0.63735	$< 10^{-6}$
	100–130 H	– 0.04951	0.007	– 0.10466	0.2
JUN 15	1.6–2.0 H	– 0.3921	$< 10^{-6}$	– 0.27531	$< 10^{-6}$
	16–20 H	– 0.31229	$< 10^{-6}$	– 0.17113	$< 10^{-6}$
	100–130 H	0.48588	$< 10^{-6}$	0.39296	$< 10^{-6}$

could be that in addition to SEP these energy channels are also populated by very low-energy CRs.

We can further investigate this assumption by looking more closely into SOHO SEP flux time series for one of the two weaker FD events. We have selected June 2015 event, as time series for higher-energy channels appear to be slightly more informative. Figure 3 shows proton flux series for all energy channels measured by SOHO/ERNE detector. From these plots, it is apparent that proton fluxes for energies larger than 64 MeV exhibit different dynamic relative to fluxes of lower energies, and seem to be in anticorrelation with them. This indeed supports the assumption these channels are populated by low-energy CR.

Another way we can illustrate this observation more quantitatively is by performing relative analysis. Firstly, we will look into short-term correlations between proton flux and muon count rate time series during four selected FD events. Correlation between respective time series was found using Pearson correlation coefficient. For significance two-tailed test is used. Correlation coefficient and its significance level between ground station and in situ measurement from SOHO/ERNE instrument is given in Table 3.

Due to higher energy of the primary CRs detected in UL, the correlation between SEPs and measured flux in UL is smaller than correlation between SEPs and flux measured in GLL. The greatest anticorrelation (i.e., between GLL and UL data and 16–20 MeV protons ≈ -0.7) is observed for the strongest ICME (and corresponding FD) of March 2012, and this anticorrelation is observed in all energy channels. However, for lower-intensity events of June 2015 and February 2011, correlations between detected CR flux in GLL and highest energy channel (100–130 MeV) are mostly positive. These observations further confirm the assumption about high-energy channels being populated by low-energy CR, which is especially evident in case of low-intensity FD events.

Table 4 Pearson correlation coefficient for the correlation between CR flux detected at Belgrade CR station (GLL detector) and flux of protons of different energies detected with SOHO/ERNE detector, for the period of one year (from June 2010 May 2011)

	GLL	
	Pearson coefficient	<i>P</i> value
H 1.3–1.6 MeV	– 0.02	0.13
H 1.6–2.0 MeV	– 0.02	0.16
H 2.0–2.5 MeV	– 0.02	0.20
H 2.5–3.2 MeV	– 0.01	0.27
H 3.2–4.0 MeV	– 0.01	0.36
H 4.0–5.0 MeV	– 0.01	0.57
H 5.0–6.4 MeV	< 0.01	0.75
H 6.4–8.0 MeV	< 0.01	1.00
H 8.0–10 MeV	< 0.01	0.78
H 10–13 MeV	0.01	0.57
H 13–16 MeV	0.01	0.41
H 16–20 MeV	0.01	0.31
H 20–25 MeV	0.01	0.26
H 25–32 MeV	0.01	0.24
H 32–40 MeV	0.01	0.27
H 40–50 MeV	0.01	0.46
H 50–64 MeV	< 0.01	0.80
H 64–80 MeV	0.05	< 0.01
H 80–100 MeV	0.12	< 0.01
H 100–130 MeV	0.07	< 0.01

Similar results, with even greater correlation between the entire time profile for flux measured with NMs and solar wind speed and magnetic field during ICME, are reported for stronger FDs during solar cycle 23 [5].

Next, we will analyse long-term correlations between SOHO proton flux and measured muon count rates. Pearson coefficients for this correlation over a period of one year (from June 2010 May 2011), when activity of the Sun was low at the commencement of the 11-years cycle, are presented in Table 4. Here we see very

Table 5 Pearson correlation coefficient for the correlation between CR flux detected at Belgrade CR station (GLL detector) and flux of protons of different energies detected with SOHO/ERNE detector, during international geomagnetically quiet and disturbed days for the period of one year (from June 2010 May 2011)

	GLL Quiet days		GLL Disturbed days	
	Pearson coefficient	<i>P</i> value	Pearson coefficient	<i>P</i> value
H 1.3–1.6 MeV	0.01	0.61	– 0.05	0.13
H 1.6–2.0 MeV	0.01	0.80	– 0.05	0.14
H 2.0–2.5 MeV	0.02	0.30	– 0.05	0.13
H 2.5–3.2 MeV	0.03	0.11	– 0.05	0.12
H 3.2–4.0 MeV	0.04	0.04	– 0.05	0.10
H 4.0–5.0 MeV	0.05	0.02	– 0.06	0.08
H 5.0–6.4 MeV	0.05	0.01	– 0.06	0.07
H 6.4–8.0 MeV	0.06	0.01	– 0.06	0.06
H 8.0–10 MeV	0.06	0.01	– 0.06	0.06
H 10–13 MeV	0.06	0.01	– 0.06	0.07
H 13–16 MeV	0.06	< 0.01	– 0.06	0.08
H 16–20 MeV	0.06	< 0.01	– 0.05	0.10
H 20–25 MeV	0.06	< 0.01	– 0.05	0.12
H 25–32 MeV	0.06	< 0.01	– 0.05	0.15
H 32–40 MeV	0.06	< 0.01	– 0.04	0.20
H 40–50 MeV	0.06	< 0.01	– 0.02	0.57
H 50–64 MeV	0.07	< 0.01	0.07	0.03
H 64–80 MeV	0.25	< 0.01	0.08	0.02
H 80–100 MeV	0.38	< 0.01	0.11	< 0.01
H 100–130 MeV	0.15	< 0.01	0.09	0.01

little correlation between CR and proton fluxes in all but the highest energy channels (above 64 MeV).

Table 5 shows the same correlation analysis if only data for 10 geomagnetically quietest or 5 geomagnetically most disturbed days of each month (http://isgi.unistra.fr/events_qdays.php) are used. The fact that we observe a significant increase of positive correlation coefficients in the case of geomagnetically quiet days, further corroborates the assumption about the mixed nature of particles that populate higher-energy channels. Consequentially, care should be taken how data from these channels are treated in analysis.

To provide further quantitative support for the use of SOHO SEP flux measurements in the analysis of FD events, we will calculate integral proton flux in all energy channels for the four selected FDs. Integration intervals are selected to include the period of increased proton flux that corresponds to a particular FD, but not to extend the interval to include potential follow-up structures that cannot be associated with the event. One such selection for all energy channels, for June 2015 event, is indicated by dashed lines in Fig. 3. In Fig. 4, we show thusly calculated integral flux as a function of particle energy (where lower boundary values from SOHO SEP energy bins are taken), using both linear and log scale for clarity.

One feature that can be noticed from plots in Fig. 4 is that integral flux drops off is more steeply in February 2011 than for others studied FDs, where a change in the trend between high-energy and low-energy range can be observed. FD that occurred in March 2012 was the longest and the most intensive of the four. Steepness of

the integral flux for this FD shows relatively more populated proton channels with higher energies compared to weaker FD. This is in agreement with strongest modulation of CRs flux during this FD. There is a discontinuity in the integral flux between proton energy channel 13–16 MeV and 16–20 MeV due to different acquisition method from different instruments, and possibly because of degradation of the detectors on board the spacecraft [13] and saturation of the instrument due to high intensity of solar protons [18].

One simple way to characterise relative abundance of SEP particles of different energies for a given event would be to fit described integral flux distribution with a power function, where (in a simple approximation) larger exponent would indicate greater relative abundance of lower-energy particles, while smaller exponent would point to greater relative abundance of higher-energy particles. Distributions were fitted with a power function given by the formula $I(E) = a * E^b$ (where I is the integral flux and E is particle energy), resulting fits represented by red lines in Fig. 4, while values for the exponents of power function fits are represented in Table 6.

If SOHO protons flux measurements are to be proved useful in the analysis of FD events, SEP flux characteristics should correlate with some of the FD and interplanetary disturbance parameters. To test this, we have analysed dependence of different FD parameters on the exponent of the integral proton flux power distribution (labelled b in the formula in previous paragraph). We have found some correlation for most tested parameters, most striking being one between the magnitude

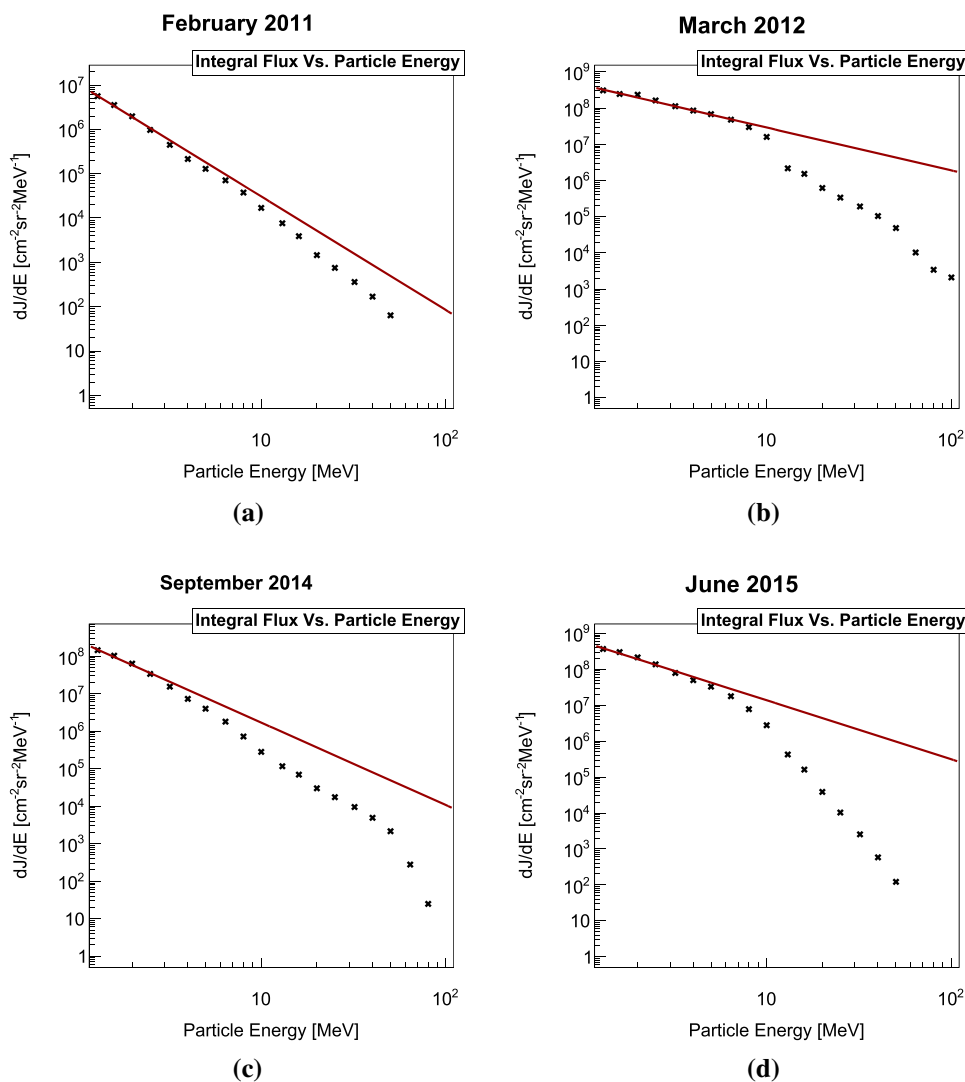


Fig. 4 Time-integrated flux of differential SEP fluxes during the four selected FD events: **a** February 2011, **b** March 2012, **c** September 2014 and **d** June 2015, in linear and logarithmic scale. Power function fits are represented by red lines

Table 6 Exponent values of power function fits of integral proton flux distributions

FD	Power function exponent values
FEB 2011	- 2.56
MAR 2012	- 1.18
SEP 2014	- 2.20
JUN 2015	- 1.64

of FD for particles with 10 GV rigidity (corrected for magnetospheric effect) and the exponent of the integral flux. This dependence (strictly for illustrative purposes fitted with linear fit) is shown in Fig. 5.

Observed strong dependence is potentially a very good indicator that SOHO SEP flux measurements can be a valid source of data to be used in the analysis of

interplanetary disturbances and their interaction with cosmic rays.

7 Conclusions

Analysing strong aperiodic variations of cosmic ray flux, such as Forbush decreases, allows us to study violent processes that occur on the Sun, and corresponding perturbations in the heliosphere, using Earth-based detectors. In addition to cosmic ray flux and magnetic field data commonly used to study such events, we have extended analysis to include proton flux measurements, obtained using spacecraft mounted detectors. Based on the analysis of four selected Forbush decrease events, we have found SOHO/ERNE proton flux measurements to be consistent with solar plasma parameters, as well as with observations by the ground-based muon detectors.

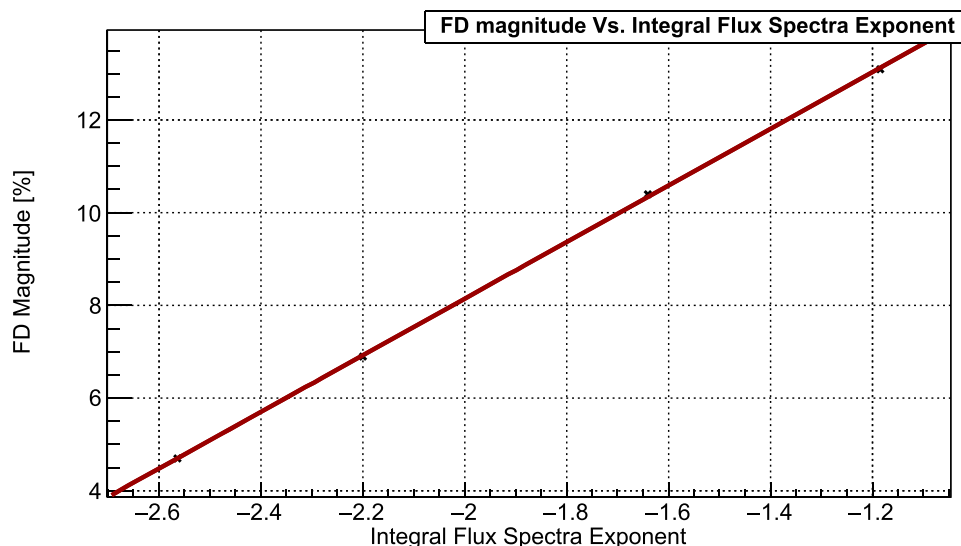


Fig. 5 Dependence of FD magnitude, corrected for magnetospheric effect with Dst-index for particles with 10 GV rigidity, on the power exponent of the integral SEP flux, four selected FD events: **a** February 2011, **b** March 2012, **c** September 2014 and **d** June 2015. Linear fit (for illustrative purposes) is indicated by the red line

We have concluded that during Forbush decrease events lower-proton-energy channels are dominated by SEP particles, while in higher-energy channels there is a contribution of low-energy cosmic rays, especially apparent during less intense events. We have found a clear correlation between Forbush decrease magnitude (corrected for magnetospheric effect with Dst-index for particles with 10 GV rigidity) and power exponent of the integral flux of SOHO/ERNE measurements. This result gives grounds to further pursue the analysis of heliospheric proton flux data, as it may yield additional valuable information. Such information can potentially help us to classify and study in greater detail the dynamics of interaction of cosmic rays in the heliosphere.

Acknowledgements The authors acknowledge funding provided by the Institute of Physics Belgrade, through the grant by the Ministry of Education, Science and Technological Development of the Republic of Serbia. We also acknowledge use of NASA/GSFC's Space Physics Data Facility's OMNIWeb (or CDAWeb or ftp) service and OMNI data as well as team behind SOHO, which is a project of international collaboration between ESA and NASA. We would also like to thank the referees for constructive and useful advice.

Data Availability Statement "This manuscript has data included as electronic supplementary material".

References

1. A.A. Abunin, M.A. Abunina, A.V. Belov, S.P. Gaidash, E.A. Eroshenko, I.I. Pryamushkina, L.A. Trefilova, E.I. Gamza, *J. Phys. Conf. Ser.* **1181**, 012062 (2019). <https://doi.org/10.1088/1742-6596/1181/1/012062>
2. K.P. Arunbabu, H.M. Antia, S.R. Dugad, S.K. Gupta, Y. Hayashi, S. Kawakami, P.K. Mohanty, T. Nonaka, A. Oshima, P. Subramanian, *A and A* **555**, A139 (2013). <https://doi.org/10.1051/0004-6361/201220830>
3. K.P. Arunbabu, H.M. Antia, S.R. Dugad, S.K. Gupta, Y. Hayashi, S. Kawakami, P.K. Mohanty, A. Oshima, P. Subramanian, *A and A* **580**, A41 (2015). <https://doi.org/10.1051/0004-6361/201425115>
4. C.R.A. Augusto, V. Kopenkin, C.E. Navia, K.H. Tsui, H. Shigueoka, A.C. Fauth, E. Kemp, E.J.T. Manganote, M.A. Leigui de Oliveira, P. Miranda, R. Ticona, A. Velarde, *ApJ* **759**, 143 (2012). <https://doi.org/10.1088/0004-637X/759/2/143>
5. A. Bhaskar, G. Vichare, K.P. Arunbabu et al., *Astrophys. Space Sci.* **361**, 242 (2016). <https://doi.org/10.1007/s10509-016-2827-8>
6. V. Belov, *SpaceSci. Rev.* **93**(1), 79–105 (2000). <https://doi.org/10.1023/A:1026584109817>
7. H.V. Cane, *Space Sci. Rev.* **93**, 55–77 (2000). <https://doi.org/10.1023/A:1026532125747>
8. J.M. Clem, L.I. Dorman, *Space Sci. Rev.* **93**, 335–359 (2000). <https://doi.org/10.1023/A:1026508915269>
9. E.S. Comedi, A.S. Elias, B.S. Zossi, S. Bruno, *JASTP* **211**, 105475 (2020). <https://doi.org/10.1016/j.jastp.2020.105475>
10. M. Duldig, *Science* **314**(5798), 429–430 (2006). <https://doi.org/10.1126/science.1134046>
11. M. Dumbović, B. Vršnak, J. Guo et al., *Sol. Phys.* **295**, 104 (2020). <https://doi.org/10.1007/s11207-020-01671-7>
12. J.H. King, N.E. Papitashvili, *J. Geophys. Res.* **110**, A02104 (2005). <https://doi.org/10.1029/2004JA010649>
13. P. Kühl, B. Heber, R. Gómez-Herrero, O. Malandraki, A. Posner, H. Sierks, *J. Space Weather Space Clim.* (2020). <https://doi.org/10.1051/swsc/2020056>
14. S.Y. Lee, *Accelerator Physics*, 2nd edn. (World Scientific, Singapore, 2004)

15. M. Livada, H. Mavromichalaki, C. Plainaki, *Astrophys. Space Sci.* **363**, 8 (2018). <https://doi.org/10.1007/s10509-017-3230-9>
16. R.A. Caballero-Lopez, H. Moraal, *JGR Space Phys.* **117**, A12 (2012). <https://doi.org/10.1029/2012JA017794>
17. R. Miteva, S.W. Samwel, M.V. Costa-Duarte, *JASTP* (2018). <https://doi.org/10.1016/j.jastp.2017.05.003>
18. R. Miteva, D. Danov, in *Proceedings of the tenth Workshop 'Solar Influences on the Magnetosphere, Ionosphere and Atmosphere', Primorsko, Bulgaria*, ed. by K. Georgieva, B. Kirov, D. Danov, 2018. <https://doi.org/10.31401/WS.2018.proc>
19. H. Moraal, *Space Sci. Rev.* **176**, 299–319 (2013). <https://doi.org/10.1007/s11214-011-9819-3>
20. S.Y. Oh, Y. Yi, *A Sol. Phys.* **280**, 197–204 (2012). <https://doi.org/10.1007/s11207-012-0053-2>
21. A. Papaioannou, A. Belov, H. Mavromichalaki et al., *J. Phys. Conf. Ser.* **409**, 012202 (2013). <https://doi.org/10.1088/1742-6596/409/1/012202>
22. A. Papaioannou, M. Belov, E. Abunina, A. Eroshenko, A. Abunin, S. Anastasiadis, Patsourakos, H. Mavromichalaki, *ApJ* **890**, 101 (2020). <https://doi.org/10.3847/1538-4357/ab6bd1>
23. E. Samara, A. Smponias, I. Lytrosyngounis et al., *Sol. Phys.* **293**, 67 (2018). <https://doi.org/10.1007/s11207-018-1290-9>
24. M. Savić, A. Dragić, N. Veselinović et al., *XXV ECRS 2016 Proceedings—eConf C16-09-04.3*, e-Print: 1701.00164 [physics.ins-det], [arXiv:1701.00164v1](https://arxiv.org/abs/1701.00164)
25. M. Savić, A. Dragić, D. Maletić et al., *Astropart. Phys.* (2019). <https://doi.org/10.1016/j.astropartphys.2019.01.006>
26. M. Savić, N. Veselinović, A. Dragić et al., *ASR* **63**, 4 (2019). <https://doi.org/10.1016/j.asr.2018.09.034>. ISSN 0273-1177
27. M. Temmer, A.M. Veronig, V. Peinhart, B. Vršnak, *ApJ* **785**, 85 (2014). <https://doi.org/10.1088/0004-637X/785/2/85>
28. J. Torsti, E. Valtonen, M. Lumme et al., *Sol. Phys.* **162**, 505–531 (1995). <https://doi.org/10.1007/BF00733438>
29. N. Veselinović, A. Dragić, M. Savić, D. Maletić, D. Joković, R. Banjanac, V. Udovičić, *NIM A* **875**, 1 (2017). <https://doi.org/10.1016/j.nima.2017.09.008>. ISSN 0168-9002
30. L.-L. Zhao, H. Zhang, *ApJ* **827**, 13 (2016). <https://doi.org/10.3847/0004-637X>

Space Weather



RESEARCH ARTICLE

10.1029/2020SW002712

Key Points:

- Correction of meteorological effects on muon component of secondary cosmic rays significantly extends the usability of muon monitors
- A new method for modeling of meteorological effects utilizing multivariate analysis and machine learning techniques is presented
- Correction efficiency of the best performing algorithm is greater than for other commonly used methods

Correspondence to:


M. Savić,
msavic@ipb.ac.rs

Citation:

Savić, M., Maletić, D., Dragić, A., Veselinović, N., Joković, D., Banjanac, R., et al. (2021). Modeling meteorological effects on cosmic ray muons utilizing multivariate analysis. *Space Weather*, 19, e2020SW002712. <https://doi.org/10.1029/2020SW002712>

Received 30 DEC 2020
 Accepted 13 JUL 2021

Modeling Meteorological Effects on Cosmic Ray Muons Utilizing Multivariate Analysis

M. Savić¹ , D. Maletić¹, A. Dragić¹, N. Veselinović¹, D. Joković¹, R. Banjanac¹, V. Udovičić¹, and D. Knežević¹

¹Institute of Physics Belgrade, University of Belgrade, Belgrade, Serbia

Abstract Correction of meteorological effects on muon component of secondary cosmic rays significantly extends the usability of muon monitors. We propose a new data driven empirical method for correction of meteorological effects on muon component of secondary cosmic rays, based on multivariate analysis. Several multivariate algorithms implemented in Toolkit for Multivariate Data Analysis with ROOT framework are trained and then applied to correct muon count rate for barometric and temperature effects. The effect of corrections on periodic and aperiodic cosmic ray variations is analyzed and compared with integral correction method, as well as with neutron monitor data. The best results are achieved by the application of linear discriminant method, which increases sensitivity of our muon detector to cosmic ray variations beyond other commonly used methods.

Plain Language Summary Primary cosmic rays are energetic particles that arrive at Earth from space. On their journey toward Earth they are affected by the solar wind (a stream of charged particles emanating from the sun), which has information about various solar processes embedded in it. In top layers of the atmosphere primary cosmic rays interact with nuclei of air molecules and produce large number of secondary particles that propagate toward Earth's surface. These secondary particles preserve information about variations of primary cosmic rays, which allows for the study of solar processes using Earth based detectors. One type of secondary particles that can be detected on the ground are muons. However, muons are affected by the conditions in the atmosphere, which can disturb the information about variations of primary cosmic rays. That is why it is important to model these atmospheric effects on cosmic ray muons as well as possible so they can be corrected for. In this study, we present a new method for modeling and correction of atmospheric effects on cosmic ray muons, that is based on multivariate analysis utilizing machine learning algorithms. This method increases sensitivity of our muon detector to cosmic ray variations beyond other commonly used methods.

1. Introduction

Meteorological effects on muon component of secondary cosmic rays have been known and studied for almost a century. A number of meteorological parameters contribute to variation of muon flux in the atmosphere, but two are the most significant: atmospheric pressure and atmospheric temperature.

Aperiodic fluctuations of intensity, discovered in the very early cosmic ray measurements, were eventually attributed to the variation of atmospheric pressure by Myssowsky & Tuwim (1926) (associated effect dubbed *barometric*), while *temperature effect* has been discovered more than a decade later and has two components: *negative* (first quantitatively described by Blackett, 1938) and *positive* (suggested by Forró, 1947). Barometric effect represents variation of muon flux due to variation of the mass of the absorber (air column) above the detector. Negative temperature effect is a consequence of dependence of effective height of muon generation level on the atmospheric temperature, resulting in longer muon path and increased probability of decay with higher temperature. Positive temperature effect has to do with positive correlation between atmospheric temperature and air density, decreasing the probability of nuclear interactions and increasing the probability of decay of muon-generating pions with the increase of temperature.

In order to study variations of primary cosmic rays (CR) using Earth based muon detectors, it is of the utmost importance to describe these meteorological effects as precisely as possible so they can be corrected for. A precise correction for meteorological effects significantly increases sensitivity of muon detectors to CR variations, making them a more usable counterpart to neutron monitors (the other widely used type of

© 2021. The Authors.

This is an open access article under the terms of the [Creative Commons Attribution-NonCommercial-NoDerivs License](https://creativecommons.org/licenses/by-nc-nd/4.0/), which permits use and distribution in any medium, provided the original work is properly cited, the use is non-commercial and no modifications or adaptations are made.

ground based cosmic ray detectors), as muon detectors are normally responsive to higher energy primary cosmic rays. Additionally, muon monitors have a unique application in diagnostics of the atmosphere, allowing for prediction of atmospheric temperatures provided a good model of meteorological effects is available (Belov et al., 1987; Kohno et al., 1981).

Several empirical and theoretical models of meteorological effects have been proposed over the years, based on which corrections can be performed. Even though full set of meteorological effects is larger, in this analysis we will concentrate on the correction of temperature and barometric effect only, so results can be more easily compared to other methods.

Some of the most commonly used methods for temperature correction are: method of effective level of generation, introduced by Duperier (1949), integral method, developed by Feinberg (1946), Dorman (1954), and others (Maeda & Wada, 1954; Wada, 1962), method of mass-averaged temperature developed by Dvornikov et al. (1976), and method of effective temperature (mostly applicable to underground detectors) (Barrett et al., 1952).

Each of these methods have their own advantages, but in this study, we have decided to use the integral method as a reference against which to compare the results of our analysis. Main reason being is that it is derived from the theory of meteorological effects, which involves the most detailed analysis, as well as it being the least approximative. According to this approach, relative variation of muon count rate due to the temperature effect can be expressed as:

$$\left(\frac{\delta I}{I}\right)_{temp} = \int_0^{h_0} \alpha(h) \cdot \delta T(h) \cdot dh, \quad (1)$$

where α is temperature coefficient density function, δT is temperature variation and h_0 is atmospheric depth of the observation level expressed in g/cm^2 . Temperature coefficient density function is calculated theoretically, while temperature variation is calculated relative to some reference temperature for the period, usually mean temperature. In practical application, integration in Equation 1 is substituted with a sum, taking into account some finite number of isobaric levels.

Analysis of barometric effect is also included in the theory of meteorological effects, but barometric coefficient is rarely calculated theoretically. Most commonly it is determined using linear regression, assuming linear dependence between atmospheric pressure and muon flux:

$$\left(\frac{\delta I}{I}\right)_{pres} = \beta \cdot \delta P, \quad (2)$$

where β is barometric coefficient, and δP represents atmospheric pressure variation.

Each of the mentioned methods is at least in some part approximative, so the idea behind this work is to introduce a new empirical method for correction of meteorological effects that would be data driven, assuming as little as possible upfront. Other advantages of such approach are that it does not depend on the design of the detector, location of the site or topology of the surrounding terrain (as these would ideally be factored in by the model), and that it can be applied in near-real time. Additionally, proposed method can be used in the analysis and potential correction of temperature effect of neutron component of cosmic rays, as part of detected neutrons can originate from cosmic ray muons captured in the nuclei of the shielding of a neutron monitor detector (Dorman, 2004). Finally, in principle it can easily be generalized to take wider set of meteorological parameters into account.

As the presented problem is multidimensional, involving a relatively large number of correlated variables, we have decided to employ multivariate analysis, relying on machine learning techniques. In some recent work (Morozova et al., 2017; Savic et al., 2019) decorrelation of atmospheric variables and numerical modeling has been successfully applied to the study of interaction of cosmic rays with Earth's atmosphere, so utilizing adaptive and flexible machine learning methods could possibly yield further improvement, potentially revealing additional dependencies and taking higher order effects into account. This approach involves application of a number of multivariate algorithms, more or less rooted in statistical machine learning, to our problem and comparing their consistency and effectiveness with selected reference results.

Large part of variations observed in continuous cosmic ray measurements can be attributed to different space weather phenomena, due to modulation of primary cosmic rays in the heliosphere. In terms of temporal properties, they can be classified as periodic or aperiodic. We will test how newly introduced methods for correction of meteorological effects affect the sensitivity for detection of both periodic as well as aperiodic variations of muon flux of nonterrestrial origin, and how it ultimately compares to the sensitivity of neutron monitors.

2. Data

For the analysis of meteorological effects both muon flux and meteorological data are needed. Muon flux was measured experimentally in the Low Background Laboratory at the Institute of Physics Belgrade, while meteorological data is a combination of modeled atmospheric temperature profiles, and atmospheric pressure and ground level temperature measured locally.

2.1. CR Muon Data

Low Background Laboratory (LBL) is located on the grounds of the Institute of Physics Belgrade. Geographical coordinates for the laboratory are $44^{\circ}51'N$ and $20^{\circ}23'E$, with elevation of 75 m and geomagnetic cutoff rigidity of 5.3 GV. Detector system is comprised of a $100 \times 100 \times 5$ cm plastic scintillator with accompanying read-out electronics. Median energy for the detector system is (59 ± 2) GeV (Veselinović et al., 2017), with muon flux of $(1.37 \pm 0.06) \times 10^{-2}$ per cm^2 s. Electron contamination determined for a previously used experimental setup was $\sim 24\%$ (Dragić et al., 2008), and is assumed to be comparable for the current one (Joković, 2011). More detailed description of the laboratory and the experimental setup can be found elsewhere (Dragić et al., 2011). Native muon count rate data has time resolution of 5 min, but hour sums are also frequently used in analysis.

Continuous cosmic ray muon flux measurements have been ongoing in LBL since 2002, current setup being utilized since 2009. Data are available to public via an online interface on the Belgrade Cosmic Ray Station internet site (Low Background Laboratory for Nuclear Physics, 2020).

As with any long-term measurement, some shorter interruptions and inconsistencies are unavoidable, hence when choosing the interval to be used for the analysis we decided to use a one-year period from June 1, 2010 to May 31, 2011, where measurements had the most continuity and consistency. Additionally, using a one-year period should remove any potential bias, primarily due to annual temperature variation.

2.2. Meteorological Data

Meteorological parameters needed for the analysis come from two sources: Atmospheric temperature profile data are produced by an atmospheric numerical model, while atmospheric pressure and ground temperature data come from local measurements.

Meteorological balloon soundings above Belgrade done by Republic Hydro-meteorological Service of Serbia (RHMZ, 2020) are not frequent enough for the purposes of this analysis, so modeled data for atmospheric temperature profile are used instead. Several numerical atmospheric models can provide such data. In this work, we have chosen Global Forecast System (GFS) produced by National Centers for Environmental Prediction (GFS, 2020), which has been found to be in best agreement with balloon soundings done above Belgrade. Comparison was done where soundings data were available, as described in our previous study (Savić et al., 2019). GFS provides a large number of modeled atmospheric parameters among which are atmospheric temperatures for different isobaric levels. Modeled data sets are being produced four times per day (at hours 00:00, 06:00, 12:00, and 18:00). In addition, analysis data are also available, reprocessed *post festum* and taking into account real data measured by world network of meteorological services. In this analysis, we have been using such reprocessed atmospheric temperatures for the following isobaric levels: 10, 20, 30, 50, 70, 100, 150, 200, 250, 300, 350, 400, 450, 500, 550, 600, 650, 700, 750, 800, 850, 900, 925, and 975 mb. Data are available with spatial resolution of 0.5° of geographical longitude/latitude, so coordinates closest to the laboratory coordinates were chosen. Data were then interpolated with cubic spline, similar as in Berkova et al. (2012), and sampled in finer time resolution needed for the analysis.

Atmospheric pressure and ground temperature data are compiled from different meteorological stations in and around Belgrade, and then interpolated as described in more detail elsewhere (Savic et al., 2016). Finally, unique time series of combined modeled and measured meteorological data, with finest time resolution of 5 min, is assembled to be used in the analysis.

3. Methodology

The use of machine learning has seen an unprecedented expansion in the last decade. The main strength of such approach being that it does not assume any a priori model, but is data driven and thus able to potentially discover hidden dependencies. This is especially true when applied to large data sets with many correlated variables. In this study, we want to establish whether such approach would yield any improvements when applied to the problem of meteorological effect on cosmic ray muons.

To test this, we have decided to use toolkit for multivariate analysis (TMVA) package which provides a ROOT-integrated environment for application of multivariate classification and regression techniques (Hoecker et al., 2007). The package has been developed for the use in high-energy physics and contains implementation of a number of supervised learning algorithms, which utilize training and testing procedures on a sample data set to determine the mapping function. Mapping function maps the input parameters to output target value, trying to model the actual functional dependence (“target” function) as accurately as possible. The structure of the mapping function is algorithm specific, and can be a single global function or a set of local models. Trained algorithm is then applied to the full data set and provides either a signal/background separation (in case of classification) or prediction of target value (in case of regression).

For us, the later application is especially interesting. The idea is to train the mapping function, using meteorological parameters as input variables, and muon count rate as the regression target, and use trained function to produce the predicted target output for a larger data set. In principle, implementation of this procedure is specific for different analysis frameworks. TMVA provides template code for the training and application of multivariate methods, where optimal parameters obtained in the training/testing phase are stored in “weight” files to be used in the application phase. Thusly predicted muon count rate would ideally contain only variations related to meteorological effects, while the residual difference between modeled and measured muon count rate would contain variations of non-meteorological origin. We would apply this procedure for a number of algorithms implemented in TMVA, compare their performance and efficiency based on several criteria, and finally suggest the methods best suited for the modeling, and ultimately the correction, of meteorological effects.

Corrected muon count rate would be calculated according to the following equation:

$$N_{\mu}^{(corr)} = \Delta N_{\mu} + \langle N_{\mu} \rangle, \quad (3)$$

where

$$\Delta N_{\mu} = N_{\mu}^{(mod)} - N_{\mu} \quad (4)$$

is the difference between the modeled and measured muon count rate.

Not all machine learning methods are equally suited for all types of problems and selection of the optimal method for a particular application is rarely straightforward. The efficiency of different algorithms depends on a number of factors: Whether they are used for classification or regression, is correlation between parameters linear or nonlinear, what is the general complexity of the problem and required level of optimization, and so on. One can only assume the efficiency of any given algorithm upfront but there is no clear general rule which one will perform best in a particular situation. Often, several algorithms with specific strengths and weaknesses can be applied to the same problem and only through analysis of the final result the optimal one can be determined. For this reason, in our analysis we have decided to indiscriminately include the largest number of algorithm classes available in TMVA, and only after extensive parallel testing narrow the selection down to the optimal one.

We will briefly describe different classes of multivariate methods available in TMVA, as well as list specific algorithms that were chosen as representative for each class. First class are methods based on probability

density estimation (PDE) techniques, where actual probability density function is estimated based on the available data. Here we have selected to test two specific multidimensional implementations, somewhat similar in nature: PDE range-search (PDE-RS) and k-nearest neighbor (KNN) algorithms. Examples of use of this approach for multivariate regression are scarce, but the success with which PDERS was applied in classification problems in high-energy physics (Carli & Koblitz, 2003) motivated its use here. Second class are methods based on function discriminant analysis. These methods are widely used for dimensionality reduction and classification. Here, we selected the linear discriminant (LD) algorithm which shares some similarities in the approach with principal component analysis (PCA), in that it maps a space of potentially correlated input variables onto a smaller space of uncorrelated variables, but in addition to PCA it also maximizes the separation between output classes, making it a natural choice for application to our problem. Algorithms that employ higher order functions were also tested, but as could be expected performed more poorly. Application of artificial neural networks (ANN) to multivariate regression problems has seen expansion in recent years, where ANN methods often perform better than more straightforward regression techniques, especially if some degree of nonlinearity is present. Even though the dependence of cosmic ray muon flux on atmospheric temperatures is linear, we felt it is certainly worth investigating how ANN methods would perform when applied to this problem, and if any additional hidden dependence would be revealed. We have chosen to apply the MLP, as it is the fastest and most flexible available ANN algorithm in TMVA. Finally, method of boosted regression trees (BDT) employs a larger number (*forest*) of binary decision trees, which split the phase space of input variables based on a yes/no decision to a series of sequential cuts applied, so to predict a specific value of the output variable. They have been very successfully applied to classification problems in high-energy physics (Lalchand, 2020), but can also be used for multivariate regression with the similar rationale as for the ANN. We have selected two representative algorithms for testing: boosted decision tree (BDT) and gradient boosted decision tree (BDTG).

In this analysis, the procedure is applied to correction of barometric and temperature effect but it is easy to see how it can be extended to include more atmospheric variables, especially as such data is readily available from atmospheric numerical models.

3.1. Training Procedure

For the training/testing data subset we have selected data for the 10 geomagnetically quietest days of each month (list provided by GFZ German Research Center for Geosciences, GFZ Potsdam, 2020), as we expect variations due to meteorological effects to be more pronounced here. This subset was then further split into training and testing data set, where 70% of randomly selected data was used for training while remaining 30% was used for testing. Data time resolution used was 5 min as it gave us a larger statistics for training.

There is a number of settings that can be manipulated for each of the multivariate algorithms used. They vary from some basic parameters, to selection of different subalgorithms or various options that can be turned on or off. For each algorithm, we have selected the optimal set of parameters. The criterium for optimal performance was minimizing the average quadratic deviation of the modeled output versus the target value. Also, where allowed by the algorithm, input variables were decorrelated prior to further processing.

Table 1 shows the values of average quadratic deviation for the modeled output (modeled muon count rate) versus the target value (measured muon count rate) for different algorithms. First two columns refer to the training data subset while second two columns refer to the testing data subset. First and third column represent average quadratic deviation defined as $(\sum(f_{MVA} - f_{target})^2)^{1/2}$ (where f_{MVA} and f_{target} represent modeled and measured count rates, respectively), while second and fourth columns represent truncated average quadratic deviation which takes into account 90% of data with least deviation. As previously mentioned, the criterium for selection of optimal parameters for every algorithm is the minimal value of average quadratic deviation for the test data subset.

3.2. Algorithm Performance Analysis

All presented multivariate algorithms have no built in knowledge about the studied effect, so in addition to quantitative test mentioned in the section above, we introduce some qualitative analysis designed to estimate the integrity of modeled data. Prime concern here would be to test whether the suggested procedure

Table 1
Average Quadratic Deviation for Selected Multivariate Methods

Method	Training		Testing	
	Average deviation (counts/5 min)	Truncated deviation (counts/5 min)	Average deviation (counts/5 min)	Truncated average (counts/5 min)
PDERS	234	185	258	201
KNN	224	177	233	185
LD	286	225	284	223
MLP	228	180	234	186
BDT	219	182	237	188
BDTG	223	174	236	187

Abbreviations: BDT, boosted decision tree; BDTG, gradient boosted decision tree; KNN, k-nearest neighbor; LD, linear discriminant.

for the correction of barometric and temperature effect (PT correction) removes these meteorological effects only, while leaving all other features nonperturbed. To this end, we will analyze several distributions of modeled data, compare them with raw and reference PT corrected data (obtained using the integral method) and look for possible anomalous features.

First, we will look into structure of distributions of difference between modeled and measured muon count rate as a function of measured count. We want to make comparison between these distributions in the training phase (for the test data subset) and after the trained algorithm was applied to the full data set. We would expect these distributions to be consistent, and appearance of some new structures or strong trends would point to some perturbation in the application phase. We have selected two examples to illustrate the difference in consistency of application of trained algorithms—BDTG and PDERS, their distributions shown in Figure 1.

We can see that distributions for BDTG algorithm for test data subset (Figure 1a) and full data set (Figure 1b) are fairly similar, and any structures and trends in the test distributions are mostly well replicated in the full data set distributions (different statistics taken into account). This is the case for most applied algorithms except for PDERS, where some dependence of the count rate, negligible for the test data distribution (Figure 1c), exists for the full data set distribution (Figure 1d).

Another, more important feature, is that for some algorithms distributions we analyzed in the previous paragraph are not smooth, but rather display some structures. To get further insight into these structures, for all featured methods we plotted distributions of modeled muon count rate along with the distribution of raw count rate on the same graph, as shown in Figure 2.

In order to better understand shapes of distributions and any structures observed in plots in Figure 2, it would be helpful to compare them to equivalent plots for muon count rates corrected for pressure and temperature effects using a well-established reference method. However, before we take a look at these distributions, we will first briefly describe procedures used to obtain reference PT correction.

Temperature and barometric effect are typically corrected for independently, where one of several methods mentioned in Section 1 is used for temperature correction, and barometric coefficient for pressure correction is determined empirically. Integral method for correction of temperature effect is widely accepted as the most accurate one. It is based on the theory of meteorological effects and takes complete atmospheric temperature profile and relevant processes into account. Most thorough description of the theory of meteorological effects is given by Dorman (2004), where temperature coefficient density function $\alpha(h)$ in Equation 1 is given in its integral form. In order to be applied, this function is then calculated through integration, substituting parameters specific to the location of the experiment. Temperature coefficient density functions for the location of Low Background Laboratory for Nuclear Physics were calculated using Monte Carlo integration technique. In order to determine barometric coefficient, temperature corrected muon data were plotted as a function of atmospheric pressure (using entries for 10 geomagnetically quietest days

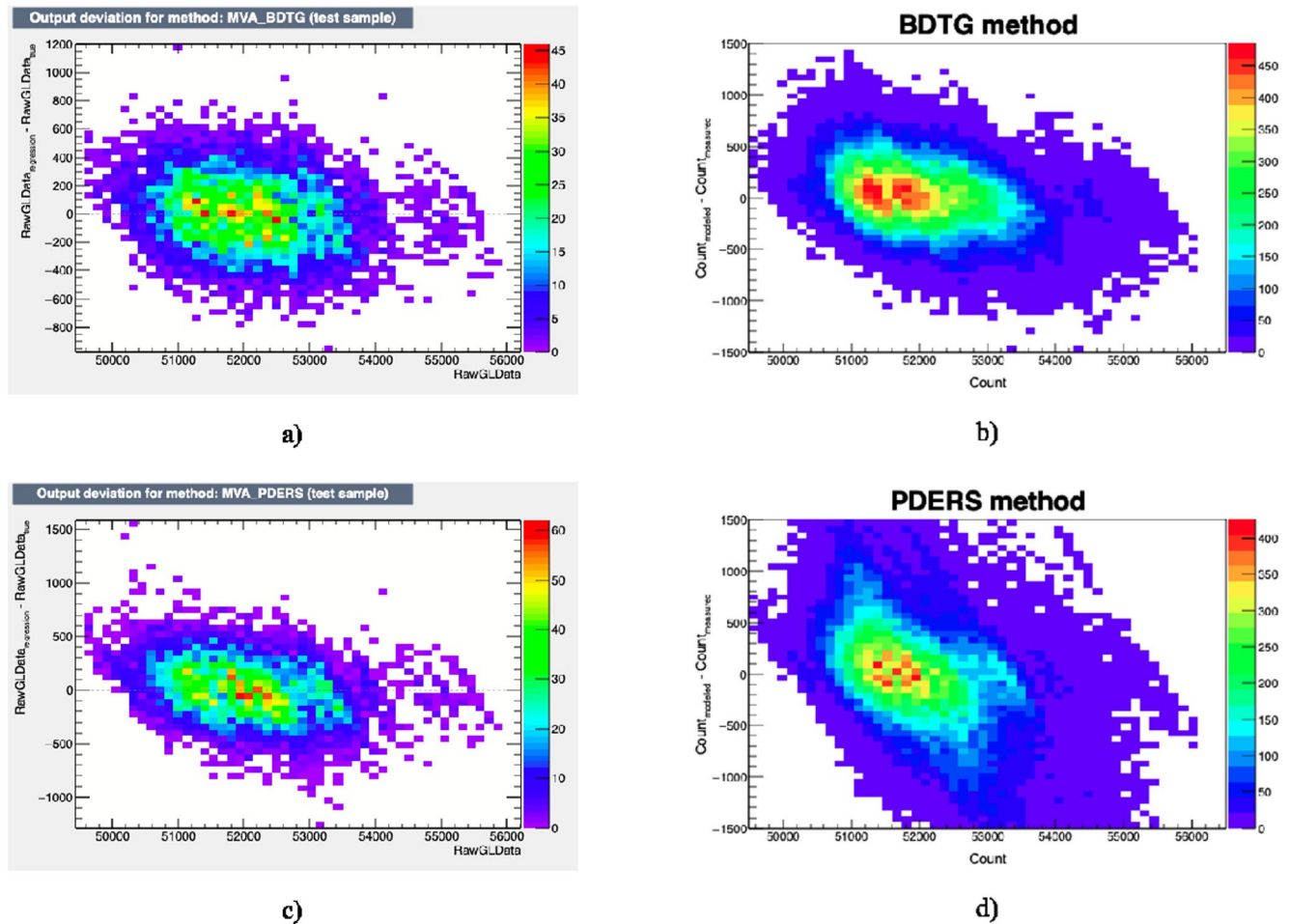


Figure 1. Distribution of difference between modeled (regression) and measured (true) muon count rate as a function of measured muon count rate for: (a) gradient Boosted decision tree (BDTG)—test data set, (b) BDTG—full data set, (c) PDERS—test data set, and (d) PDERS—full data set.

of each month only), coefficient determined via linear regression separately for each calendar year. Both procedures are presented in greater detail in our previous work (Savic et al., 2016).

Distributions equivalent to ones shown in Figures 1 and 2 were plotted for reference pressure and temperature corrected data, as shown in Figure 3. The analog for the modeled muon count rate is calculated from the variation due to pressure and temperature effects calculated based on the integral method. It is worth pointing out that distributions for reference PT corrected data are noticeably less smooth, which can be mostly attributed to lower statistics used as only hour summed data was available for this correction.

Based on these plots, we can conclude that we should not expect a significant deviation between raw and corrected data and that corresponding distributions should not have any characteristic structures. Most plots in Figure 2 are consistent with this expectation, however, some structures can be observed in KNN plots, and to a degree in BDT plots, while distribution plotted for PDERS algorithm does not have these structures but appears to somewhat deviate from raw data distribution.

Another insight into performance and consistency of different multivariate algorithms when applied to the modeling of meteorological parameters can be gathered by the way of spectral analysis of PT corrected data. Pressure and temperature corrected muon count rate was determined for all selected algorithms using modeled data, as described in Section 3. Since some gaps exist in our muon data, Lomb-Scargle algorithm was used to obtain the power spectra, as it is less sensitive to uneven data sampling (Press et al., 2007). Figure 4 shows power spectra for raw and muon count rates corrected for pressure and temperature effects using integral and two illustrative examples of multivariate methods. Full spectrum as well as selected interval

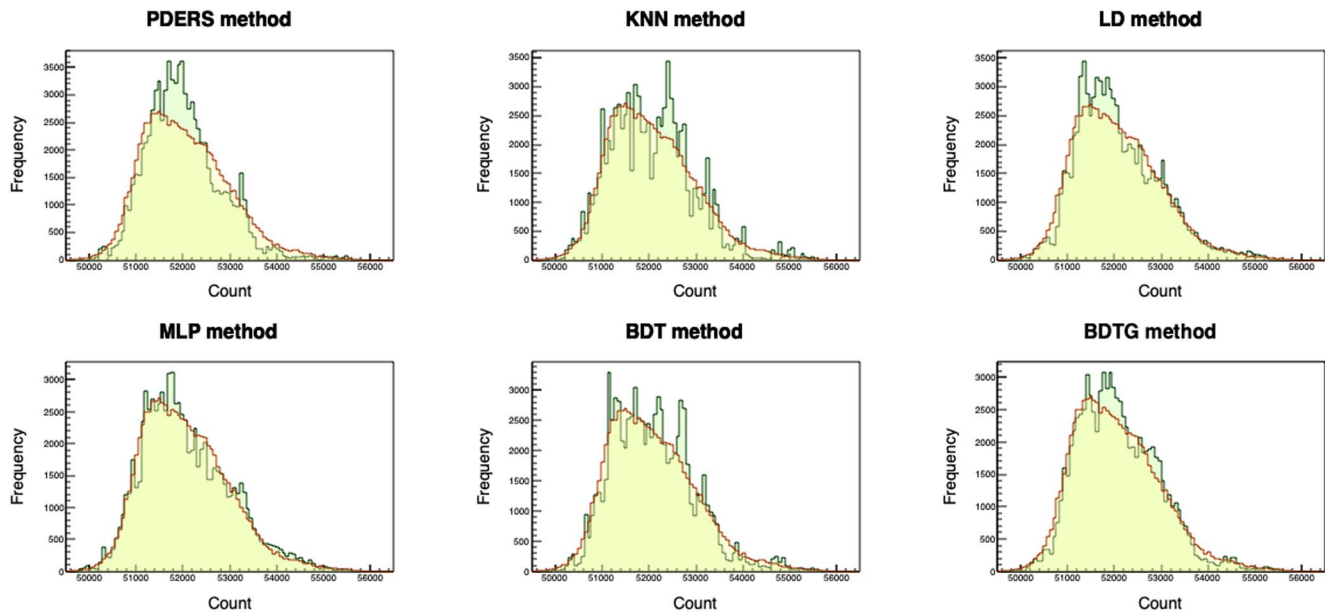


Figure 2. Comparison between distributions of raw (yellow) and muon count rate modeled by selected multivariate methods (green).

of frequencies around the periodicity of one day are shown, red dashed line indicating significance level of 0.01.

If integral method is again used as a reference, we can see that thus obtained PT correction does not remove daily variation, but rather makes it more pronounced. This should not come as a surprise, as only smaller part of the diurnal variation can be attributed to meteorological effects (Quenby & Thambyahpillai, 1960), while larger part is of nonmeteorological origin. Hence, removing variation due to atmospheric pressure would make daily variation more prominent. LD, and to a degree BDT/BDTG methods, have an effect on daily variation similar to the integral method, but for BDT method (bottom right in Figure 4) we observe emergence of some frequencies with significant power that cannot be associated with any known periodicity of cosmic rays, and probably have artificial origin. Such features are even more pronounced for the remaining multivariate algorithms, where in addition an over-reduction of power frequency corresponding to diurnal variation to can be observed. Over-reduction of daily variation coupled with introduction of artificial variations with significant powers points to possible inadequateness or overtraining of some of the multivariate methods.

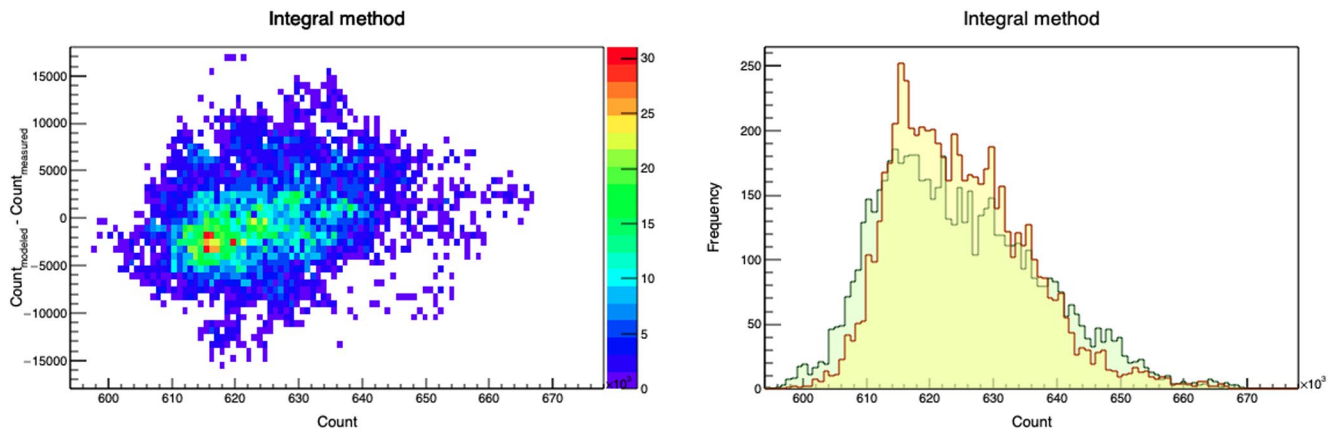


Figure 3. Distribution of difference between muon count rate calculated from the variation due to pressure and temperature effect using integral method and measured muon count rate as a function of measured muon count rate (left), and comparison between distributions of raw (yellow) and calculated muon count rate (green) shown on the right.

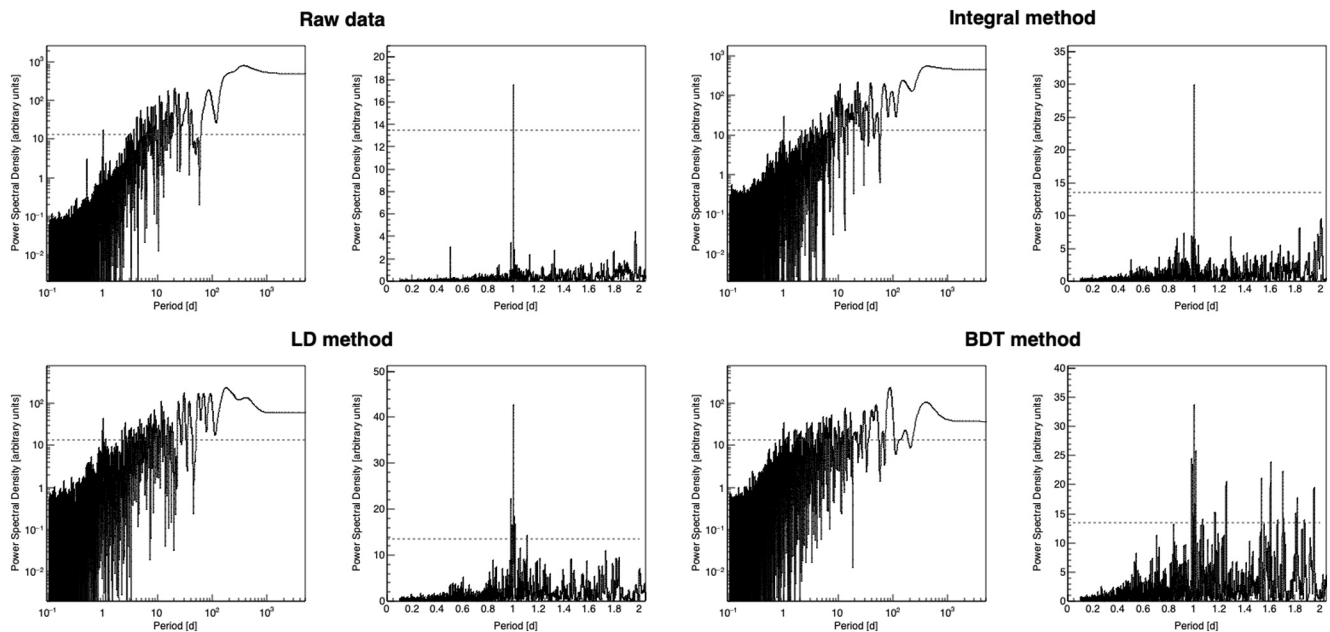


Figure 4. Power spectra for raw data (top left), PT corrected data using integral method (top right), and PT corrected data using selected multivariate methods (second row). For each method, both full spectrum and a range of frequencies around periodicity of one day are shown. Significance level of 0.01 is indicated by the red dashed line.

The effect on annual variation is difficult to determine based on the spectral analysis as period of only one year is analyzed, but we will introduce some quantitative tests in the next section that will help us with this estimate.

4. Results

We will use two criteria to estimate the efficiency of newly introduced methods for PT corrections. One will rely on the effectiveness with which the multivariate algorithms remove the annual variation and reduce variance, while the other will be based on the effect the correction has on detection sensitivity for aperiodic events, such as Forbush decreases (Forbush, 1937). In both cases, we will compare the results with the ones obtained by the integral method.

4.1. Effects of PT Correction on Periodic CR Variations

Significant part of the annual variation of cosmic ray muon flux can be attributed to the variation of atmospheric temperature (Hess, 1940). As mentioned before, the effectiveness with which this effect is corrected for will affect the detector sensitivity to variations of primary cosmic rays of non-atmospheric origin.

We will examine time series for pressure and temperature corrected data and compare them with raw and pressure corrected time series, especially taking note of how PT correction affects the annual variation. In order to estimate this effect, we fit the time series (except for raw data) with sine function with a period of one year. The amplitude of pressure corrected data determined from such fit will be used as an estimate of the annual muon flux variation, and serve as a reference against which to compare the effect of PT correction by different methods. In Figure 5 time series for raw, pressure corrected and pressure and temperature corrected data are shown. For the sake of simplicity, not all time series for data PT corrected using multivariate algorithms are shown, but rather only characteristic ones. Table 2 shows values for the annual variation amplitude for pressure and PT corrected time series, as well as possibly more informative reduction of annual variation calculated relative to the amplitude of the pressure corrected muon flux.

While, time series in Figure 5 for data PT corrected using integral, LD and BDTG methods do not seem to have some unexpected fluctuations, that is not the case for MLP method, where one can observe some

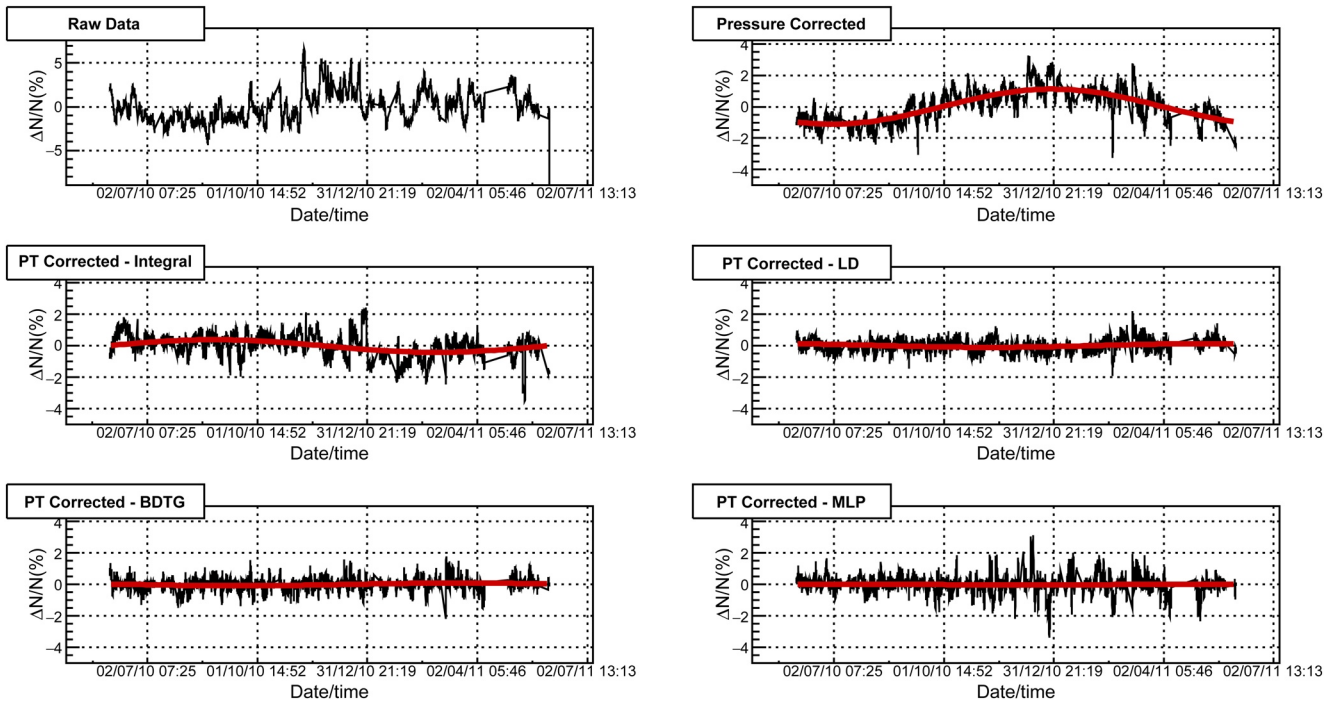


Figure 5. Muon count rate time series for the period from June 1, 2010 to May 31, 2011: raw data (top left), pressure corrected data (top right), PT corrected data using integral method (second row left) and data PT corrected using selected multivariate methods.

data that appears to deviate from the mean more significantly than what would be intuitively expected. For remaining multivariate algorithms this is even more the case. In order to try and quantify this visual comparison, we will analyze the effect corrections have on standard deviation of the data. If calculated relative to the mean muon flux for the whole period, standard deviation would be sensitive to the residual annual variation. To make standard deviation independent of the seasonal variation, we used a moving ten-day window to determine the mean value and then calculated the standard deviation relative to it.

Figure 6 shows distributions of relative variation of muon flux in respect to the moving window mean value for raw data and PT corrected data using integral, LD and MLP methods. It is based on these distributions that standard deviation was determined and results are presented in Table 3. Comparing standard deviations for PT corrected muon flux obtained by multivariate methods with the one obtained by the integral method, we can see that for LD, BDT, and BDTG algorithms they have comparable values. The difference is somewhat larger in the case of MLP, which is in accordance with features observed in Figure 6, while it is significantly larger for the remaining algorithms. This indicates that PT correction performed using KNN and PDERS (and possibly MLP) algorithms probably introduces some artificial features into PT corrected muon flux data.

One way to evaluate the effectiveness of different algorithms in reduction of the seasonal variation even better, would be to compare the PT corrected muon data to pressure corrected time series for selected neutron monitor detectors. The reasoning is based on a well-known fact that meteorological effects on the neutron component of secondary cosmic rays are dominated by the barometric effect. Temperature effect does exist for the secondary cosmic ray neutrons, but whether calculated theoretically (Dorman, 2004) or determined experimentally (Kaminer et al., 1965), it is still an order of magnitude smaller than for the muon component and typically not corrected for in neutron monitor data. Based on this, we

Table 2

Amplitude and Reduction of the Amplitude of Annual Variation Relative to Pressure Corrected Data (P Corrected) for PT Corrected Data (Using Integral and Selected Multivariate Methods)

Method	Amplitude (%)	Relative reduction (% of P corrected)
P corrected	1.11 ± 0.09	/
Integral	0.40 ± 0.03	64 ± 6
PDERS	0.09 ± 0.02	92 ± 3
KNN	0.24 ± 0.04	79 ± 5
LD	0.11 ± 0.03	90 ± 4
MLP	0.03 ± 0.01	98 ± 2
BDT	0.12 ± 0.03	89 ± 4
BDTG	0.086 ± 0.009	92 ± 2

Abbreviations: BDT, boosted decision tree; BDTG, gradient boosted decision tree; KNN, k-nearest neighbor; LD, linear discriminant.

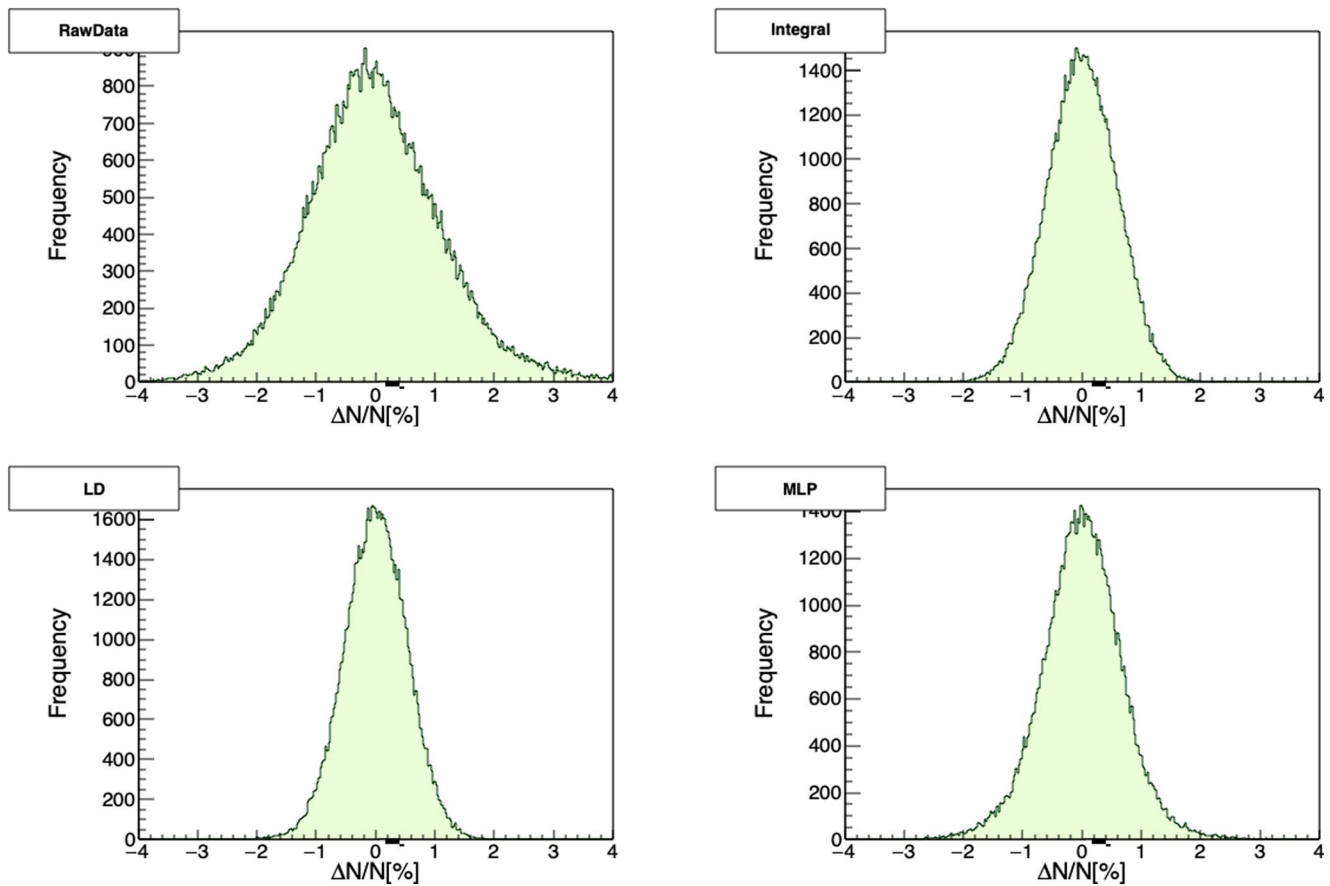


Figure 6. Relative variation of muon count rate calculated in respect to mean count in the ten-day moving window, for raw data (top left), PT corrected using integral method (top right), and data PT corrected using selected multivariate methods (second row).

believe pressure corrected neutron monitor data to be (in the first approximation) independent from meteorological effects, and hence a good reference for the evaluation of effectiveness of different methods for PT corrections of muon flux data.

For this comparison, we have chosen neutron monitors located in Athens and Rome, as they had the most consistent operation in the period we use for the analysis. Respective geomagnetic cutoff rigidities for these neutron monitors are 8.53 and 6.27 GV. Pressure and efficiency corrected relative neutron count rate was acquired via Neutron Monitor Database (NEST, 2020), presented for the said period in Figure 7. As for the muon flux data, relative neutron count rate time series were fitted with sinusoidal function, with a period of one year, to obtain the amplitude used as an estimate of the annual variation. Neutron monitors are more sensitive to lower energy secondaries than muon detectors so their time series can exhibit larger variations, which in turn can affect the fitting algorithm. However, in this case the fits seem to be dominantly affected by the relatively stable period between June and November 2010, hence we believe them to be a reliable estimate of the seasonal variation amplitude. Thus acquired annual variation amplitude for Rome neutron monitor is $(0.29 \pm 0.01)\%$, while for the Athens neutron monitor it is $(0.17 \pm 0.05)\%$.

Table 3
Standard Deviation of Relative Variation of Muon Count Rate for Raw and Data Corrected for Pressure and Temperature Effect (Using Integral and Selected Multivariate Methods)

Method	Raw	Integral	PDERS	KNN	LD	MLP	BDT	BDTG
Relative deviation (%)	1.117	0.592	0.990	0.785	0.533	0.687	0.607	0.551

Abbreviations: BDT, boosted decision tree; BDTG, gradient boosted decision tree; KNN, k-nearest neighbor; LD, linear discriminant.

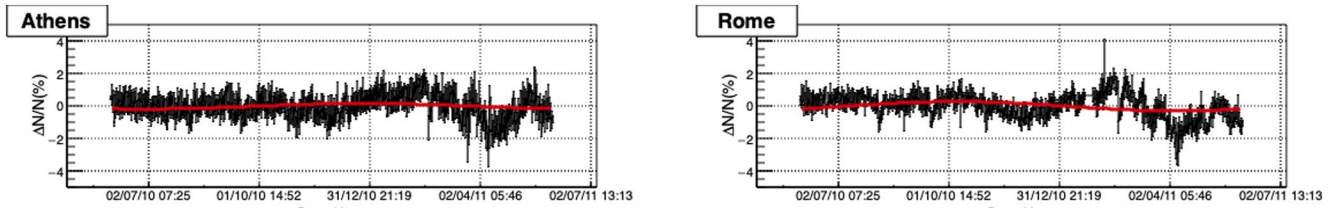


Figure 7. Relative neutron count rate time series for the period from June 1, 2010 to May 31, 2011 for Athens (left) and Rome (right) neutron monitors.

Comparing these values with the ones in Table 2, we see that methods KNN, LD, and BDT yield the most similar results. PDERS and MLP seem to underestimate the annual variation, while the integral method estimates a somewhat larger value.

Observed overall poor performance of KNN and PDERS algorithms could possibly be explained by the fact that these algorithms perform best when applied to problems involving strong nonlinear correlations, and are less efficient when dependencies between variables are dominantly linear (Hoecker et al., 2007). Additionally, these algorithms typically need a large training sample, so possibly statistics in our analysis was inadequate. However, artificial neural networks (such as MLP) should in principle be well suited for multivariate linear regression, and perform better than observed results suggest. Most likely, using minimization of the average quadratic deviation as a sole criterium for the selection of optimal parameters in the training phase may lead to overtraining (Montgomery et al., 2006), and additional qualitative criteria (i.e., ones introduced here) and more careful parameter control should also be used. BDT and BDTG algorithms performed reasonably well even though they are not optimized for treatment of linear multivariate problems, however, spectral analysis indicates a further improvement can be made. Additionally, all algorithms would probably benefit from a longer data interval of several years being used.

4.2. Effects of PT Correction on Aperiodic CR Variations

As mentioned before, apart from increasing sensitivity of muon detectors to periodic variations of primary cosmic rays, correcting raw muon flux data for meteorological parameters also affects detector sensitivity to aperiodic events which occur due to heliospheric modulation of primary cosmic rays. Here, we will analyze the effect PT correction, performed by application of different multivariate algorithms, has on detection of Forbush decrease events. We have chosen to concentrate on Forbush decreases as our muon detector is much less sensitive to other aperiodic events, such as ground level enhancements (GLE).

Forbush decrease (FD) events are typically characterized by their amplitude, so it could be a natural choice for a parameter to be used as a measure of detection sensitivity. However, another requirement for definition of sensitivity could be that detected signal significantly deviates from random fluctuations. That is, why we have decided to use the ratio of the amplitude to the standard deviation of muon flux, or relative amplitude, as an estimate of sensitivity to aperiodic events, rather than the actual amplitude. As we primarily focus on the magnitude of Forbush decreases, when we mention an FD event in the following text it mainly refers to the decrease phase and not the recovery phase.

To determine the amplitude, we have used a method proposed by Barbashina et al. (2009). The idea is to make the result independent from different trends leading up to, and following the actual FD. To do this, two intervals are defined: one i days before the onset of the FD, where i can have value $(1, \dots, n)$ days, and the other p days after the end of the decrease, where p can have value $(1, \dots, m)$ days. These intervals are then detrended using fit parameters obtained from linear regression. Mean count is determined for the detrended time series before the onset of FD for j days (where $j = 1, \dots, i$), and for the detrended time series during recovery stage for q days (where $q = 1, \dots, p$). Thus, in total we obtain $n!$ values for mean detrended count before the onset of FD, and $m!$ values for mean detrended count for the recovery stage. FD amplitude estimate is then calculated for each combination of “before” and “after” values according to the following formula:

$$A_{ij}^{pq} = \frac{\langle I_{before}^{(i,j)} \rangle - \langle I_{after}^{(p,q)} \rangle}{\langle I_{before}^{(i,j)} \rangle} \times 100\%, \quad (5)$$

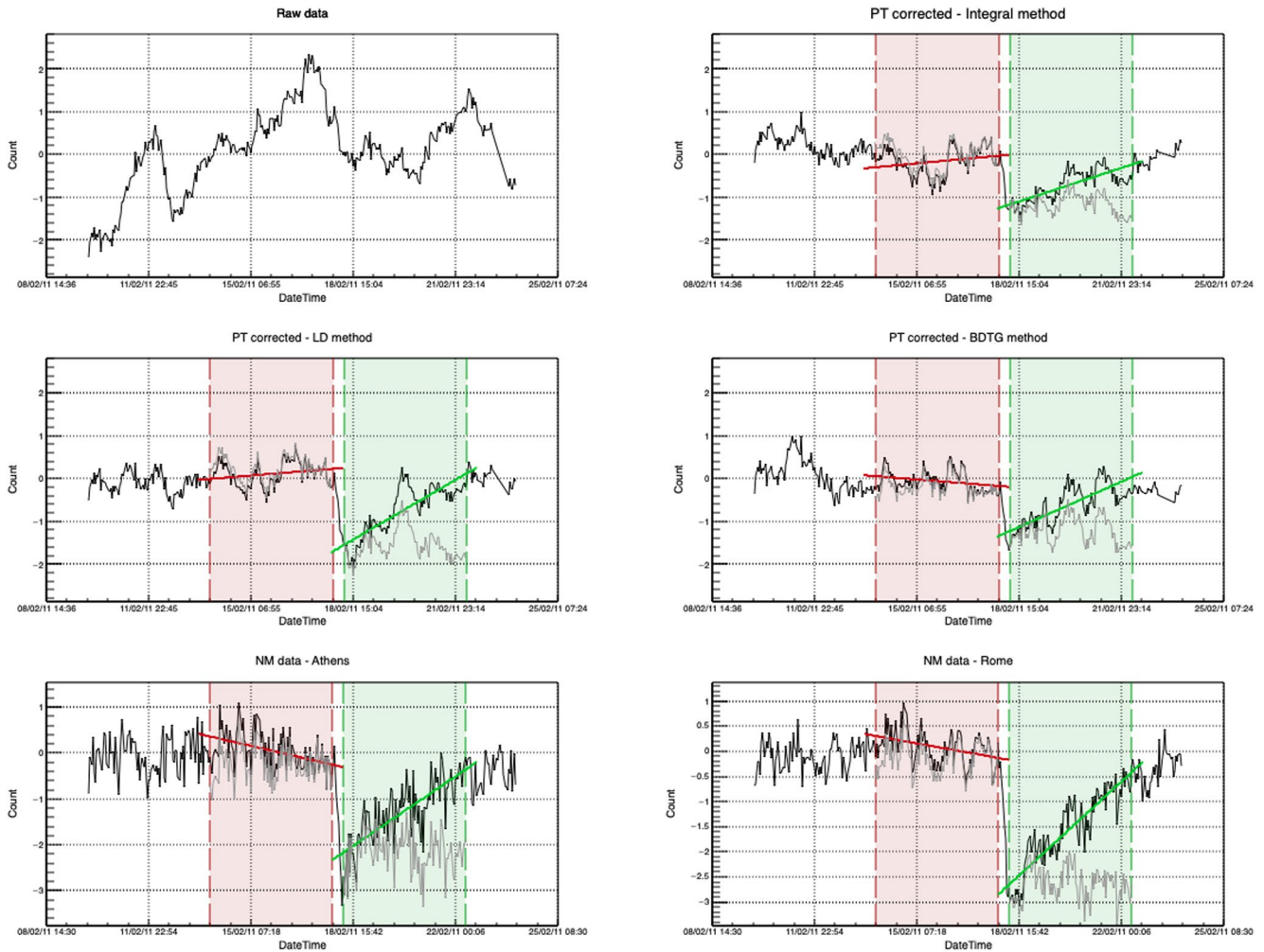


Figure 8. Time series for the interval around Forbush decrease of February 18, 2011: raw muon data (top left), PT corrected muon data using integral (top right), linear discriminant (center left) and gradient boosted decision tree (center right) methods, and neutron monitor data for Athens (bottom left) and Rome (bottom right) neutron monitors. Interval leading into (red) and following the Forbush decrease (FD) (green) are highlighted, as well as detrended intervals used to determine FD amplitude (gray).

where I_{before} and I_{after} are respective values for mean detrended count for intervals before the onset and after the end of the Forbush decrease. Finally, FD amplitude is calculated as the average of individual A_{ij}^{pq} values, rms deviation from the mean of the distribution used as an error estimate.

During the one-year period we used for the analysis there was a large number of Forbush events, but most of them had rather small amplitudes. We have analyzed several, however, here we will focus on the one with the largest magnitude as the results are most easily interpreted. The event is a Forbush decrease that occurred on February 18, 2011 in relation to X2.2 solar flare, and according to IZMIRAN space weather database (IZMIRAN, 2020) had 10 GV rigidity particle variation magnitude of 5.4. In Figure 8, we have shown plots that represent procedure described in the previous paragraph, applied to PT corrected datasets using integral method and selected multivariate algorithms. Procedure is also applied to pressure and efficiency corrected data for Athens and Rome neutron monitors, raw data also presented for reference. On the plots, interval leading into the onset of FD is indicated by red dashed lines, while recovery interval after the decrease is indicated by green dashed lines. We have chosen the lengths of both intervals to be four days ($n = m = 4$). Linear fits are represented by solid red and green lines, respectively, while detrended intervals are plotted using gray lines. Amplitudes and relative amplitudes calculated from the differences of means of detrended intervals are shown in Table 4.

Table 4
Amplitudes and Relative Amplitudes for the Forbush Decrease of February 18, 2011 for PT Corrected Muon Data and Selected Neutron Monitors

Method/NM monitor	Integral	LD	BDTG	Athens	Rome
FD amplitude (%)	1.38 ± 0.14	1.96 ± 0.18	1.10 ± 0.13	1.97 ± 0.15	2.68 ± 0.15
Relative FD amplitude	4.31 ± 0.44	7.09 ± 0.65	4.78 ± 0.56	5.30 ± 0.40	8.65 ± 0.48

Abbreviations: BDTG, gradient boosted decision tree; FD, Forbush decrease; LD, linear discriminant.

We see that relative amplitudes for this Forbush decrease, calculated based on data corrected for pressure and temperature using LD and BDTG algorithms, have sensitivity that is comparable or better than the sensitivity of integral method, even approaching the sensitivity of reference neutron monitors in the case of LD algorithm. However, when LD algorithm is concerned, such result can be at least in part explained by the fact that the calculated absolute FD amplitude is larger than expected for a muon detector. We would expect this value to be comparable to the value calculated based on the integral method. The reason for this discrepancy could be systematic, but also could be somewhat related to features of the studied FD event. Ideally, we should extend this analysis to more events, but selected time period was relatively calm in terms of solar activity, and February 2011 event was the only significant one with magnitude for 10 GV rigidity particles larger than five. Preliminary analysis done on Forbush decrease events of larger magnitude, that are outside the period used for analysis in this work, does show somewhat smaller effect for LD method, so that could be one of the focuses in the continuation of this work. We have excluded plots for the remaining multivariate algorithms as the results were either poorer (in the case of BDT and MLP) or inconsistent (in the case of PDERS and KNN).

5. Conclusions

We have selected a number of multivariate algorithms included in the TMVA package to apply for the correction of barometric and temperature effect on cosmic ray muons. Optimal parameters were determined for each algorithm based on the average quadratic deviation of modeled from measured data. Different distributions of modeled data for training phase and after the application of trained methods were compared to estimate the performance of selected algorithms. Pressure and temperature correction was done and spectral analysis performed to further test the algorithm consistency. The effect of the correction was analyzed for long-term (annual) and short-term (Forbush decrease) cosmic ray variations. In both cases, the efficiency of multivariate algorithms was compared to integral method and pressure corrected neutron monitor data.

Multidimensional probability density estimator algorithms (PDERS and KNN) appear not to be well suited for the modeling of pressure and temperature effect, most likely due to highly linear correlations between variables. MLP seems to have underperformed, while methods based on boosted decision trees (particularly BDTG) proved to be more successful, especially when effect on aperiodic variations was concerned. It should be expected that both MLP and BDT(G) methods can be improved if a longer period is used for analysis and parameters beyond average quadratic deviation of modeled data are used for algorithm optimization during training phase. Out of presented algorithms, LD proved to be the most consistent and effective in removing the pressure and temperature effects. In terms of the effect of PT correction on annual and aperiodic variations, this method matched or outperformed the integral method, while the effect it had on aperiodic effects was somewhat overestimative. This could give us grounds to assume at least part of the temperature effect is not taken into account by the integral method, and that there could be room for further improvement in modeling of meteorological effects beyond what theory currently provides.

Data Availability Statement

Raw muon count rate data set used in this study are publicly available online on the Belgrade Cosmic Ray Station site (<http://www.cosmic.ipb.ac.rs/>). Modeled atmospheric temperature data are available online on the NOAA GFS page (<https://www.ncdc.noaa.gov/data-access/model-data/model-datasets/global-forecast->

system-gfs). Latest atmospheric pressure and ground temperature data are available online on the site of Republic Hydro-meteorological Service of Serbia (<http://www.hidmet.gov.rs/>). List of international geomagnetically quiet days can be downloaded from the GFZ site (<https://www.gfz-potsdam.de/en/kp-index/>). Neutron monitor data can be accessed online via NEST browser interface (<http://www01.nmdb.eu/nest/>).

Acknowledgments

The authors acknowledge funding provided by the Institute of Physics Belgrade, through the grant by the Ministry of Education, Science and Technological Development of the Republic of Serbia.

References

- Barbashina, N., Dmitrieva, A., Kompaniets, K., Petrukhin, A., Timashkov, D., Shutenko, V., et al. (2009). Specific features of studying Forbush decreases in the muon flux. *Bulletin of the Russian Academy of Sciences: Physics*, 73, 343–346. <https://doi.org/10.3103/S1062873809030198>
- Barrett, P. H., Bollinger, L. M., Cocconi, G., Eisenberg, Y., & Greisen, K. (1952). Interpretation of cosmic-ray measurements far underground. *Reviews of Modern Physics*, 24, 133–178. <https://doi.org/10.1103/RevModPhys.24.133>
- Belov, A., Blokh, Y., Dorman, L., & Rogovaya, S. (1987). The temperature diagnostics of the atmosphere allowing for the temperature of the near-surface layer. *International Cosmic Ray Conference*, 4, 263.
- Berkova, M., Belov, A., Eroshenko, E., & Yanke, V. (2012). Temperature effect of muon component and practical questions of how to take into account in real time. *Astrophysics and Space Sciences Transactions*, 8, 41–44. <https://doi.org/10.5194/astra-8-41-2012>
- Blackett, P. M. S. (1938). On the instability of the Barytron and the temperature effect of cosmic rays. *Physical Review*, 54, 973–974. <https://doi.org/10.1103/PhysRev.54.973>
- Carli, T., & Koblitz, B. (2003). A multi-variate discrimination technique based on range-searching. *Nuclear Instruments and Methods in Physics Research Section A: Accelerators, Spectrometers, Detectors and Associated Equipment*, 501, 576–588. [https://doi.org/10.1016/S0168-9002\(03\)00376-0](https://doi.org/10.1016/S0168-9002(03)00376-0)
- Dorman, L. I. (1954). On the temperature effect of the hard component of cosmic rays. *Reports of Academy of Sciences of USSR (DAN SSSR)*, 95, 49–52.
- Dorman, L. I. (2004). *Cosmic rays in the Earth's atmosphere and underground*. Springer. Retrieved from <https://books.google.rs/books?id=mKlv68WBU5kC>
- Dragić, A., Joković, D., Banjanac, R., Udovičić, V., Panić, B., Puzović, J., & Aničin, I. (2008). Measurement of cosmic ray muon flux in the Belgrade ground level and underground laboratories. *Nuclear Instruments and Methods in Physics Research Section A: Accelerators, Spectrometers, Detectors and Associated Equipment*, 591(3), 470–475.
- Dragic, A. L., Udovicic, V. I., Banjanac, R., Jokovic, D. R., Maletic, D. M., Veselinovic, N. B., et al. (2011). The new set-up in the Belgrade low-level and cosmic-ray laboratory. *Nuclear Technology & Radiation Protection*, 26(3), 181–192. <https://doi.org/10.2298/NTRP1103181D>
- Duperier, A. (1949). The meson intensity at the surface of the Earth and the temperature at the production level. *Proceedings of the Physical Society Section A*, 62(11), 684–696. <https://doi.org/10.1088/0370-1298/62/11/302>
- Dvornikov, V. M., Krestyannikov, Y. Y., & Sergeev, A. (1976). Determination of the mass-average temperature on the cosmic ray intensity data. *Geomagnetism and Aeronomy*, 16, 923–925.
- Feinberg, E. L. (1946). On the nature of cosmic ray barometric and temperature effects. *Reports of Academy of Sciences of USSR (DAN SSSR)*, 53, 421–424. <https://doi.org/10.1038/157421a0>
- Forbush, S. E. (1937). On the effects in cosmic-ray intensity observed during the recent magnetic storm. *Physical Review*, 51, 1108–1109. <https://doi.org/10.1103/PhysRev.51.1108.3>
- Forró, M. (1947). Temperature effect of cosmic radiation at 1000-m water equivalent depth. *Physical Review*, 72, 868–869. <https://doi.org/10.1103/PhysRev.72.868>
- GFS. (2020). Retrieved from <https://www.ncdc.noaa.gov/data-access/model-data/model-datasets/global-forecast-system-gfs>
- GFZ Potsdam. (2020). Retrieved from <https://www.gfz-potsdam.de/en/kp-index/>
- Hess, V. F. (1940). On the seasonal and the atmospheric temperature effect in cosmic radiation. *Physical Review*, 57, 781–785. <https://doi.org/10.1103/PhysRev.57.781>
- Hoecker, A., Speckmayer, P., Stelzer, J., Therhaag, J., von Toerne, E., Voss, H., & Zemla, A. (2007). *Tmva—Toolkit for multivariate data analysis*. Ithaca, NY: Cornell University.
- IZMIRAN. (2020). Retrieved from <http://spaceweather.izmiran.ru/eng/dbs.html>
- Joković, D. (2011). *Detekcija i spektroskopija miona iz kosmičkog zračenja plastičnim scintilacionim detektorima (Detection and spectroscopy of cosmic ray muons with plastic scintillation detectors) (Doctoral dissertation)*. Faculty of Physics, University of Belgrade. Retrieved from <http://www.cosmic.ipb.ac.rs/documents/jokovic-thesis.pdf>
- Kaminer, N. S., Ilgatch, S. F., & Khadakhanova, T. S. (1965). Temperature effect of the cosmic ray neutron component. In *Proceedings of the 9th International Cosmic Ray Conference* (Vol. 1, p. 486).
- Kohno, T., Imai, K., Inue, A., Kodama, M., & Wada, M. (1981). Estimation of the vertical profile of atmospheric temperature from cosmic-ray components. In *Proceedings of the 17th International Cosmic Ray Conference* (Vol. 10, p. 289).
- Lalchand, V. (2020). Extracting more from boosted decision trees: A high energy physics case study. In *33rd Annual Conference on Neural Information Processing Systems* (Vol. 1).
- Low Background Laboratory for Nuclear Physics. (2020). Retrieved from <http://www.cosmic.ipb.ac.rs/>
- Maeda, K., & Wada, M. (1954). Atmospheric temperature effect upon the cosmic ray intensity at sea level. *Journal of the Scientific Research Institute*, 48, 71–79.
- Montgomery, D. C., Peck, E. A., & Vining, G. G. (2006). *Introduction to linear regression analysis* (4th ed.). Hoboken, NJ: Wiley & Sons.
- Morozova, A. L., Blanco, J. J., & Ribeiro, P. (2017). Modes of temperature and pressure variability in midlatitude troposphere and lower stratosphere in relation to cosmic ray variations. *Space Weather*, 15(5), 673–690. <https://doi.org/10.1002/2016SW001582>
- Myssowsky, L., & Tuwim, L. (1926). Unregelmäßige intensitätsschwankungen der höhenstrahlung in geringer seehöhe. *Zeitschrift für Physik*, 39, 146–150. <https://doi.org/10.1007/BF01321981>
- NEST. (2020). Retrieved from <http://www01.nmdb.eu/nest/>
- Press, W. H., Teukolsky, S. A., Vetterling, W. T., & Flannery, B. P. (2007). *Numerical recipes 3rd edition: The art of scientific computing* (3rd ed.). New York: Cambridge University Press.
- Quenby, J. J., & Thambyahpillai, T. (1960). Atmospheric temperature effects on the solar daily variation of cosmic ray intensity. *The Philosophical Magazine: A Journal of Theoretical Experimental and Applied Physics*, 5(54), 585–600. <https://doi.org/10.1080/14786436008241210>
- RHMZ. (2020). Retrieved from <http://www.hidmet.gov.rs/index-eng.php>

- Savic, M., Dragic, A., Veselinovic, N., Udovicic, V., Banjanac, R., Jokovic, D., & Maletic, D. (2016). Effect of pressure and temperature corrections on muon flux variability at ground level and underground. In *25th European cosmic ray Symposium*.
- Savic, M. R., Dragic, A. L., Maletic, D. M., Veselinovic, N. B., Banjanac, R. M., Jokovic, D. R., & Udovicic, V. I. (2019). A novel method for atmospheric correction of cosmic-ray data based on principal component analysis. *Astroparticle Physics*, *109*, 1–11. <https://doi.org/10.1016/j.astropartphys.2019.01.006>
- Veselinović, N., Dragić, A., Savić, M., Maletić, D., Joković, D., Banjanac, R., & Udovičić, V. (2017). An underground laboratory as a facility for studies of cosmic-ray solar modulation. *Nuclear Instruments and Methods in Physics Research Section A: Accelerators, Spectrometers, Detectors and Associated Equipment*, *875*, 10–15. <https://doi.org/10.1016/j.nima.2017.09.008>
- Wada, M. (1962). Atmospheric effects on the cosmic-ray meson intensity. *Journal of the Physical Society of Japan Supplement*, *17*, 508. <https://doi.org/10.1143/jpsj.17.1805>



JRC CONFERENCE AND WORKSHOP REPORTS

2nd International Workshop on the European Atlas of Natural Radiation

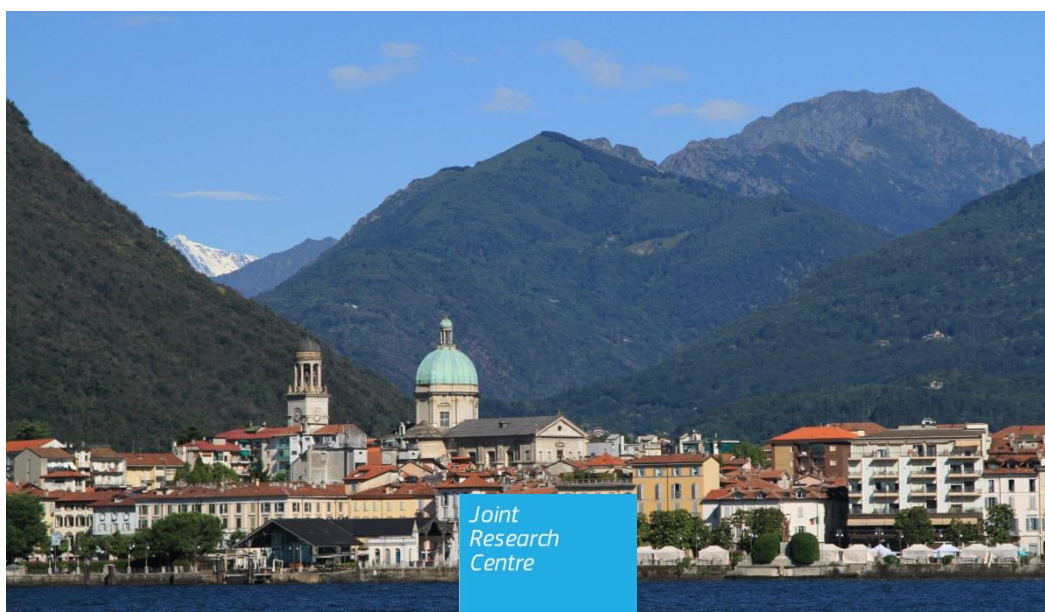
Book of Abstracts

*Verbania, Italy
6-9 November 2017*

Edited by:

Tore Tollefsen, Giorgia Cinelli
and Marc De Cort

2017



EUR 28820 EN

6.3 From motivation through the national radon survey to European indoor radon map

Vladimir Udovičić¹, Dimitrije Maletić¹, Maja Eremić Savković², Sofija Forkapić³

¹ *Institute of Physics Belgrade, University of Belgrade, Belgrade, Serbia*

² *Serbian Radiation Protection and Nuclear Safety Agency, Belgrade, Serbia*

³ *Department of Physics, Faculty of Science, University of Novi Sad, Novi Sad, Serbia*

E-mail: udovicic@ipb.ac.rs

By 2014, radon issues were treated in Serbia through the scientific research projects. Among radon professionals, there was always the desire to create a radon risk map first of all. In 2014, with a certain amount of lucky circumstances, there was a chance that the radon problem would be raised to the national level. In that sense, Serbia has started to work on the national radon action plan (RAP), and in 2014 made its decision to perform the first national indoor radon survey. The responsibility for the establishment RAP and make indoor radon map in Serbia is on national regulatory body in the field of radiation protection: Serbian Radiation Protection and Nuclear Safety Agency (SRPNA). The project was supported by the IAEA through the technical cooperation programme. In this work, the planning and execution of the survey, including sampling design of the first national indoor radon survey are described in detail. Also, the results from national indoor radon survey and indoor radon mapping based on GPS coordinates was transformed to square map by creating a 10 km x 10 km squares where the starting point (0,0) is the center of Belgrade - Slavia Square are presented. To complete our work, we prepare data from the first Serbian indoor radon survey together with the data from indoor radon survey of Vojvodina, north province of Republic of Serbia performed during 2002-2005, and send to European Indoor Radon Map Group in JRC, Ispra, Italy.

Публикације категорије М30

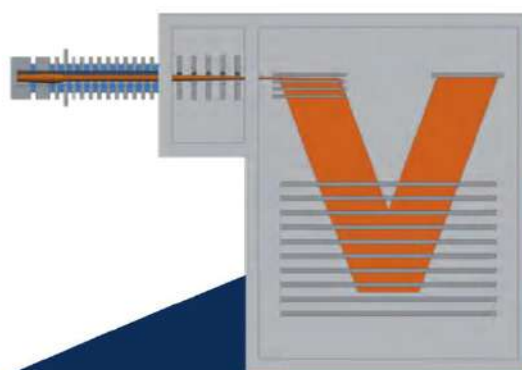
Публикације после избора у претходно звање

CONFERENCE SERIES

Armin Hansel, Jürgen Dunkl

Contributions

8th International Conference on
Proton Transfer Reaction
Mass Spectrometry and its Applications



innsbruck university press

Explainable machine learning prediction of VOC in an university building microenvironment

Andreja Stojić¹, Gordana Vuković¹, Svetlana Stanišić², Vladimir Udovičić¹, Nenad Stanić² and Andrej Šoštarić³

¹ Institute of Physics Belgrade, National Institute of the Republic of Serbia, University of Belgrade, Pregrevica 118, 11000 Belgrade, Serbia, andreja@ipb.ac.rs

² Singidunum University, Danijelova 32, 11000 Belgrade, Serbia

³ Institute of Public Health Belgrade, Despota Stefana 54, 11000 Belgrade, Serbia

Abstract

In this study we applied a novel SHapley Additive exPlanations feature attribution framework to examine the relevance of meteorological parameters and identify key factors that govern indoor and outdoor isoprene concentrations obtained by PTR-MS measurements in an university environment. According to the results, ambient temperature appeared to be far the most important predictor of isoprene levels, followed by relative humidity and air pressure.

Introduction

Spatial evolution of isoprene concentrations in different environments depends on biogenic and anthropogenic emission sources and ambient conditions. Even the past environmental conditions experienced by the leaves, the soil moisture stress, and the age of leaves, have shown to affect isoprene fluxes (Müller et al., 2008). Once emitted in the air, isoprene fate is also dependent on meteorological conditions – it is dispersed under the influence of wind, subjected to photochemical reactions being predominantly enhanced by solar radiation (Cheng et al., 2018), or it acts as a precursor in the reactions of secondary organic aerosol formation under low relative humidity conditions (Zhang et al., 2011). In this study, we used the SHapley Additive exPlanations (SHAP) framework to obtain a more detailed insight into the meteorological factors that govern isoprene concentrations in indoor and outdoor environment.

Experimental Methods

Isoprene concentrations were measured in real time using proton transfer reaction mass spectrometer (Standard PTR-quad-MS, Ionicon Analytik, GmbH, Austria) in the period from March to July 2016. The measurement site was located at Singidunum University, Belgrade, Serbia (44°78' N, 20°48' E). Drift tube parameters included: pressure, ranging from 2.04 to 2.14 mbar; temperature 60°C; E/N parameter, 145 Td providing reaction time of 90 μs. The count rate of H₃O⁺H₂O was 3 to 8% of the 9.2·10⁶ counts s⁻¹ count rate of primary H₃O⁺ ions.

Regression analysis by means of eXtreme Gradient Boosting (XGBoost Python Package) was implemented for estimating the relationships between isoprene indoor/outdoor concentrations and meteorological parameters, including outdoor temperature, pressure, relative humidity and wind speed and direction, as well as the indoor temperature, pressure and relative humidity.

Accurate interpretation a model's prediction supports deeper understanding of the process being modeled. The SHAP method (Lundberg and Lee, 2017), based on unification and additive attribution algorithms, offers uniquely consistent, locally accurate attribution values attributing to each feature the change in the expected model prediction when conditioning on that feature.

Results and Discussion

The SHAP analysis (Stojić et al., 2019) was successfully applied to reveal in which respect the ambient conditions affected indoor and outdoor concentrations of isoprene as confirmed by the XGBoost predicted/observed relative errors of 18% and 25%, and the correlation coefficients of 0.88 and 0.91, respectively. The SHAP summary plot and the magnitude of mean SHAP values, as a measure of feature importance (Figure 1), suggest that ambient temperature appeared to be far the most important predictor of isoprene outdoor levels, followed by relative humidity and pressure, whereas the impact of wind speed and direction could be considered negligible.

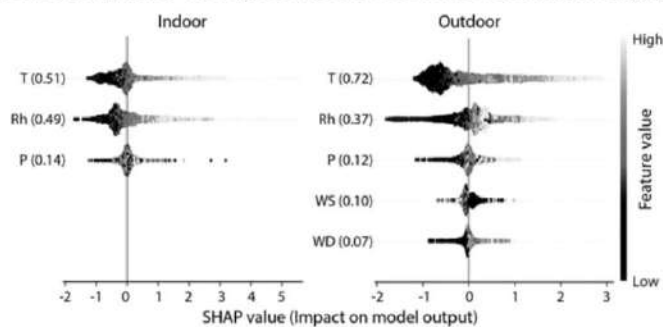


Figure 1: SHAP summary plot and mean SHAP value magnitude (values in brackets).

The dot density, in which each dot represents a particular measurement, show that lower temperatures were the most common in the dataset. However, a smooth increase in the model's output and long-tailed distribution reaching to the right suggest that increased temperature and its extreme values could significantly affect outdoor isoprene distribution. Similar results were registered for indoor isoprene (Figure 1). Furthermore, the SHAP analysis allowed for distinguishing between main (Figure 2) and interaction effects (Figure 3, right) of the most influential predictors of indoor and outdoor isoprene levels.

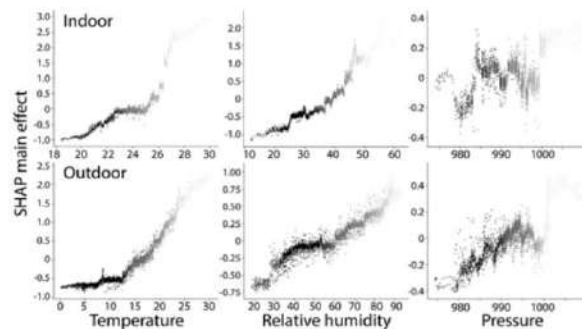


Figure 2: SHAP main effects.

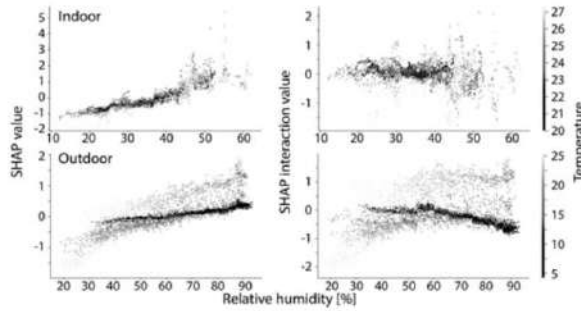


Figure 3: SHAP dependence (left) and interaction plots (right).

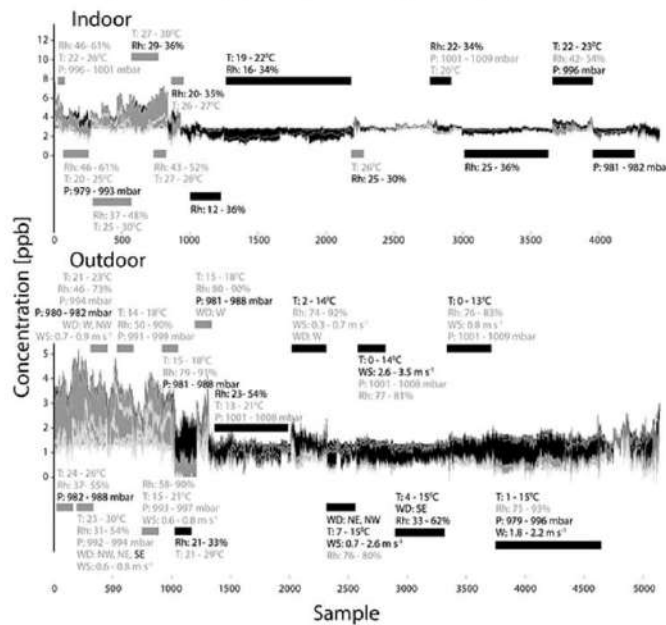


Figure 4: SHAP supervised clustering (contributors which push the model output from the base value higher/lower are presented in grey/black).

As showed by SHAP dependence plot (Figure 3, left), relative humidity has a stronger influence on isoprene concentrations in indoor than outdoor environment. Additionally, the same Figure reveals that higher indoor air temperatures were accompanied by increased relative humidity. For outdoor, the opposite tendency was observed, but with lower SHAP values and related impact on the model's output. Interactions among temperature and relative humidity caused most of the variance in the isoprene concentrations, as can be seen in Figure 3 (right). Supervised SHAP

clustering classified indoor and outdoor isoprene level of pollutants into several subgroups, annotated by features which define them (Figure 4). As can be noted, the relationships between indoor/outdoor isoprene concentrations and ambient conditions were particularly evident for the temperatures above 15°C and relative humidity exceeding 40%.

As can be concluded, our knowledge of isoprene/volatile organic compound behavior and environmental fate could benefit from further investigation of interrelationships between major air pollutants and meteorological features.

Acknowledgments

This paper was realized as part of projects No III43007 and No III41011, which were financed by the Ministry of Education, Science and Technological Development of the Republic of Serbia for the period 2011-19.

References

- [1] J.F., Müller, T., Stavrou, S., Wallens, I.D., Smedt, M.V., Roozendaal, M.J., Potosnak, J., Rinne, B., Mungler, A. Goldstein, and A.B., Guenther, Global isoprene emissions estimated using MEGAN, ECMWF analyses and a detailed canopy environment model, *Atmospheric Chemistry and Physics*, 8(5), 1329-1341, (2008).
- [2] X. Cheng, H. Li, Y. Zhang, Y. Li, W. Zhang, X. Wang, F. Bi, H. Zhang, J. Gao, F. Chai, X. Lun, Y. Chen, J. Gao, J. Lv, Atmospheric isoprene and monoterpenes in a typical urban area of Beijing: Pollution characterization, chemical reactivity and source identification, *Journal of Environmental Sciences*, 71, 150–167, (2018).
- [3] H. Zhang, J.D. Surratt, Y.H. Lin, J. Bapat, R.M. Kamens, Effect of relative humidity on SOA formation from isoprene/NO photooxidation: enhancement of 2-methylglyceric acid and its corresponding oligoesters under dry conditions, *Atmospheric Chemistry and Physics*, 11, 6411–6424, (2011).
- [4] S.M. Lundberg, and S.I. Lee, A unified approach to interpreting model predictions. In *Advances in Neural Information Processing Systems*, pp. 4765-4774, (2017).
- [5] XGBoost Python Package, Available at: <https://github.com/dmlc/xgboost/tree/master/python-package>
- [6] A. Stojić, N. Stanić, G. Vuković, S. Stanišić, M. Perišić, A. Šoštarić, L. Lazić, Explainable extreme gradient boosting tree-based prediction of toluene, ethylbenzene and xylene wet deposition, *Science of The Total Environment*, 653, 140–147, (2019).

Multifractality of isoprene temporal dynamics in outdoor and indoor university environment

Andreja Stojić¹, Gordana Vuković¹, Svetlana Stanišić², Vojin Čučuz³, Dragomir Trifunović³, Vladimir Udovičić¹ and Andrej Šoštarić⁴

¹ Institute of Physics Belgrade, National Institute of the Republic of Serbia, University of Belgrade, Pregrevica 118, 11000 Belgrade, Serbia, andreja@ipb.ac.rs

² Singidunum University, Danijelova 32, 11000 Belgrade, Serbia

³ School of Electrical Engineering, University of Belgrade, 73 Bulevar kralja Aleksandra, 11000 Belgrade, Serbia

⁴ Institute of Public Health Belgrade, Despota Stefana 54, 11000 Belgrade, Serbia

Abstract

In this study the multiscale multifractal method was used with the aim to capture the fractal behaviour of indoor and outdoor isoprene time series obtained by PTR-MS measurements in an university environment (Belgrade, Serbia), as well as to investigate to what extent variations in isoprene levels can be considered random or persistent. As shown, isoprene time series exhibited persistency, slightly affected by the concentrations occurring randomly only at the level of small fluctuations and small scales within the time frame of 20 hours. The results herein presented contribute to better understanding of isoprene temporal evolution and provide theoretical background for enhanced forecasting of volatile organic compound concentrations in general.

Introduction

A number of literature sources have demonstrated that the behavior of heterogeneous and dynamic environmental systems or nonlinear processes, such as temporal and spatial evolution of isoprene, can be described by multifractal formalism. In this study we used multiscale multifractal method (MMA) for capturing the fractal behavior of isoprene outdoor and indoor concentration time series in an university environment and to investigate to what extent variations in isoprene levels can be considered random or persistent.

Experimental Methods

Isoprene concentrations were measured in real time using proton transfer reaction mass spectrometer (Standard PTR-quad-MS, Ionicon Analytik, GmbH, Austria) in the period from March to July 2016. The measurement site was located at Singidunum University, Belgrade, Serbia (44°78' N, 20°48' E). Drift tube parameters included: pressure, ranging from 2.04 to 2.14 mbar; temperature, 60 °C; voltage, 600 V; E/N parameter, 145 Td providing reaction time of 90 μs. The count rate of H₃O+H₂O was 3 to 8% of the 9.2·10⁶ counts s⁻¹ count rate of primary H₃O⁺ ions. The measurements were performed continuously, except for brief interruptions for background level determination (10 min, 4 times per day) and calibration (5 times for the entire period).

Data Analysis

MMA is a generalization of the standard multifractal detrended fluctuation analysis (MF-DFA) (Stojić et al, 2016), which adds the dependence on scale, providing a broader analysis of the fluctuation properties, as well as more general and stable results (Stojić et al, 2017, Gierałtowski et al, 2012). For imputing missing data we employed *missForest*, a random forest based non-parametric algorithm available in R package and capable to deal with high dimensions, complex interactions and nonlinear data structure. The algorithm uses bootstrap aggregation of multiple regression trees and continues repeating the imputation procedure until a pre-defined stopping criterion is met, *i.e.* until the difference between the newly imputed data matrix and the previous one increases for the first time with respect to both variable types.

Results and Discussion

The complete indoor and outdoor isoprene time series obtained by missing value imputations are presented in Figure 1. The correlation between indoor and outdoor pollutant concentrations was 0.74. The *missForest* algorithm performed well, with predicted/observed out-of-bag normalized root mean squared error (NRMSE) of 0.009/0.011, and 0.078/0.083; and imputation out-of-bag NRMSE of 0.009 and 0.075, for indoor and outdoor isoprene concentrations, respectively.

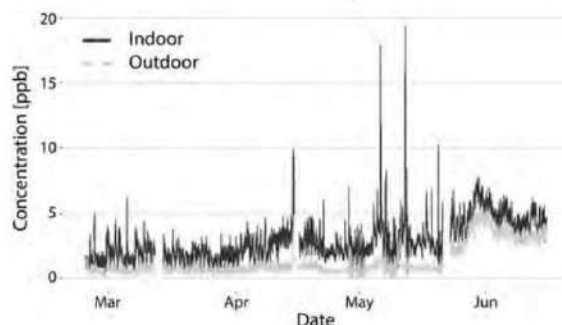


Figure 1: Isoprene indoor/outdoor time series.

The density of Miss Forest predicted and observed isoprene concentrations are in good agreement (Figure 2). Both indoor and outdoor isoprene concentrations fluctuated randomly over time (Hurst exponent, $H=0.7-1.35$), and their variation patterns were characterized by long-range correlated and persistent structure (Figure 3). Furthermore, the investigation of randomized isoprene time-series (Figure 4) revealed that the multifractality of the compound's indoor and outdoor concentration originates from both nonlinear correlations and a fat-tailed probability distribution.

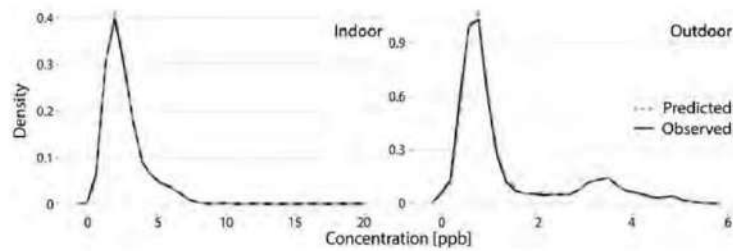


Figure 2: The density of predicted and observed isoprene concentrations.

As indicated by the minima and maxima of Hurst exponent and multifractal parameter (Figure 3), the indoor isoprene time-series were more influenced by small fluctuations compared to outdoor isoprene time-series, which mainly approached the most recognized fractal phenomena with long memory known as “pink noise”. The variations could be explored with respect to different emission sources of isoprene that dominate over indoor and outdoor environment. Current knowledge suggests that three main sources of outdoor isoprene refer to vehicle emissions, evaporative emissions from petroleum products and plant emissions, although at temperatures exceeding 25°C dominant part of outdoor isoprene might be assigned to biogenic sources (Bari et al., 2015). On the other hand, the indoor isoprene levels are mostly affected by adhesives, coatings and the occupant’s breath (Huang et al., 2016). In addition, non negligible factors are distinguishing features of interior spaces and occasional contributions of outdoor air through air-conditioning and building openings.

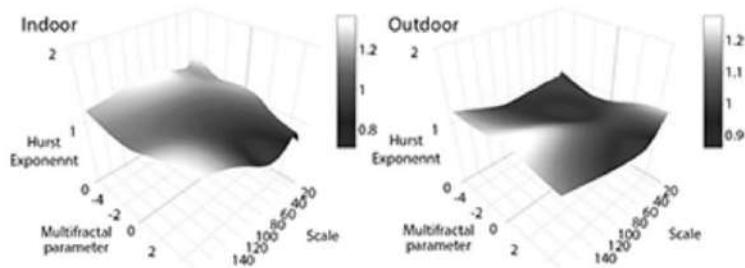


Figure 3: Isoprene indoor/outdoor time series Hurst surfaces.

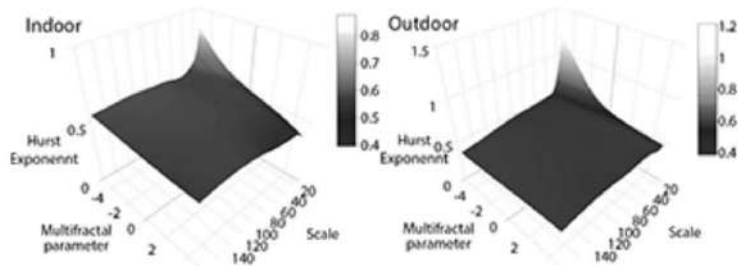


Figure 4: Isoprene randomized indoor/outdoor time series Hurst surfaces.

Indoor and outdoor isoprene time-series could be considered statistically different as indicated by the values of generalized distance Hurst coefficient (Figure 5) which highly exceeded the threshold value (0.065). The differences are primarily caused by strong fluctuations in both domains (negative and positive) of the multifractality parameter's interval at temporal scales between 60 and 160.

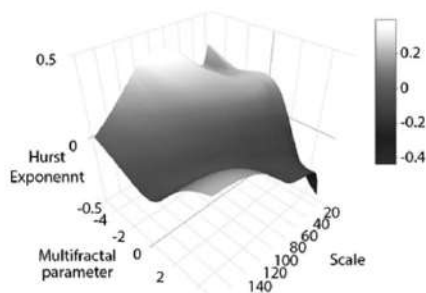


Figure 5: The difference between isoprene indoor and outdoor time series Hurst surfaces

Acknowledgments

This paper was realized as part of projects No III43007 and No III41011, which were financed by the Ministry of Education, Science and Technological Development of the Republic of Serbia for the period 2011-19.

References

- [1] J. Gieraltowski, J. Żebrowski, and R. Baranowski, Multiscale multifractal analysis of heart rate variability recordings with a large number of occurrences of arrhythmia, *Physical Review E* 85(2), 021915, (2012).
- [2] A. Stojić, S.S. Stojić, I. Reljin, M. Čabarkapa, A. Šoštarić, M. Perišić, and Z. Mijić, Comprehensive analysis of PM10 in Belgrade urban area on the basis of long-term measurements. *Environmental Science and Pollution Research*, 23(11), 10722-10732, (2016).
- [3] A. Stojić, S. Stanišić Stojić, M. Perišić, and Z. Mijić, Multiscale multifractal analysis of nonlinearity in particulate matter time series. 6th International WeBIOPATR Workshop & Conference Particulate Matter: Research and Management, September 6-8, Belgrade, Serbia, pp. 1-4, (2017).
- [4] Md. A. Bari, W. B. Kindzierski, A. J. Wheeler, M.-É. Héroux, L. A. Wallace, Source apportionment of indoor and outdoor volatile organic compounds at homes in Edmonton, Canada, *Building and Environment* 90, 114-124, (2015).
- [5] Z. Huang, Y. Zhang, Q. Yan, Z. Zhang, X. Wang, Real-time monitoring of respiratory absorption factors of volatile organic compounds in ambient air by proton transfer reaction time-of-flight mass spectrometry, *Journal of Hazardous Materials* 320, 547-555, (2016).



TEERAS 2017

III EAST EUROPEAN
RADON SYMPOSIUM

15 - 19 MAY
PARK HOTEL MOSKVA
SOFIA

Book of Abstracts



certainty. In reality, design and model based approaches often come together. In this presentation, the subject will be explained in more detail, including statistical discussions. Examples will be given. The considerations presented here apply to all kind of environmental surveys.

OP5

Effectiveness studies of mitigation techniques using theoretical models simulated by finite elements software

Eduardo Muñoz¹, Borja Frutos^{1}, Manuel Olaya¹*

¹Institute for Building Sciences Eduardo Torroja, CSIC

Behavior of generation, transport, immission and accumulation of radon gas in buildings can be studied theoretically through models where physical processes and the boundary conditions, that define the scenarios, are implemented. The numerical calculation for the resolution of the differential equations by finite elements is proving to be a powerful tool for the purpose of predictions of radon behavior in building. This field of work is of great interest for the study of the effectiveness of protection systems in a step prior to its execution, allowing its optimization and better adjustment in order to achieve a guarantee of success. This work aims to show the capabilities of the model generated in the finite element calculation platform, Comsol Multiphysics, once calibrated and validated with measurements experiences. The results show a parametric study of several protection solutions and the effectiveness depending on the different possibilities of execution.

OP6

FIRST SERBIAN INDOOR RADON MAP

Vladimir Udovičić^{1}, Dimitrije Maletić¹, Maja Eremić Savković², Slađan Velinov², Bojana Spasić², Branko Markoski³*

¹Institute of Physics Belgrade, University of Belgrade, Belgrade, Serbia

²Serbian Radiation Protection and Nuclear Safety Agency, Belgrade, Serbia

³Technical Faculty "Mihajlo Pupin", University of Novi Sad, Zrenjanin, Serbia

The first step in every systematic approach to the radon issues on the national level is to make indoor radon map. On the basis of the obtained results from the national indoor radon survey, the policy makers may conclude if it is necessary to establish national radon strategy and action plan. In that sense, Serbia has started work on the national radon action plan (RAP) in 2014 and made decision to perform first national in-

door radon survey. The responsibility for the establishment RAP and make indoor radon map in Serbia is on national regulatory body in the field of radiation protection: Serbian Radiation Protection and Nuclear Safety Agency (SRPNA). The project was supported by the IAEA through the technical cooperation, the national project: Enhancing the Regulatory Infrastructure and Legislative System. From the IAEA we have received 6000 passive radon devices based on track-etched detectors. The distribution of detectors across the Serbian territory was the responsibility of SRPNA. The main partner in the project was Institute of Physics Belgrade as a leading institution in the technical support. In this work, the sampling design of the first national indoor radon survey is described in detail. Also, the results from national indoor radon survey are presented, included descriptive statistics, testing the log-normal distribution of the obtained data and representativeness of the sample design with respect to Serbian National Census Data. Indoor radon mapping based on GPS coordinates was transformed to square map by creating a 10km x 10km squares where the starting point (0,0) is the center of Belgrade - Slavia Square. For each square two values are calculated and used to create two maps. One map shows the median value of radon concentration and the second map shows the number of radon detectors used for calculation of median values.

OP7

Karst as influencing factor of the geogenic radon potential

Peter Bossew, Winfried Meyer, Bernd Hoffmann

German Federal Office for Radiation Protection, Berlin

It has been known for long that in karst regions high indoor radon (Rn) concentrations can be encountered. The geological reason is “macro-permeability” of the rock, i.e. fissures, caves and ducts in calcareous rock, which can transport Rn dissolved in water or by advection with air over long distances from its source. The latter may be located far below the surface in different lithological units, still physically connected to the surface by these ducts. Karst regions with occurrence of elevated indoor Rn have been identified, among other, in the USA and in Europe, e.g. Swiss Jura, Slovenia and Ireland. Studies about Rn transport and temporal dynamics has been performed in karst caves, e.g. in Hungary and Slovenia. Given its radiological significance, the resulting indoor Rn problem in karst regions is often treated under the auspices of mitigation and remediation, e.g. Long et al. (2016) or Tunno et al. (2017). However, the question is also relevant from the point of view of Rn prediction. In Ireland (Hodgson et al. 2013), and Switzerland (Kropat 2015) karst has been recognized as relevant predictor of areas with elevated Rn potential. In this

P2

Correlative, multivariate and periodicity analysis of the variations of low radon concentrations in an shallow underground laboratory

Dimitrije Maletic 1, Vladimir Udovicic 1, Radomir Banjanac 1, Dejan Jokovic 1, Mihailo Savic 1, Nikola Veselinovic 1, Jelena Zivanovic 1, Aleksandar Dragic 1*

Institute of Physics, University of Belgrade

The results of correlative, multivariate and periodicity analysis of the variation of low radon concentrations in shallow underground laboratory, in the Institute of Physics Belgrade, is presented and discussed. Correlative and periodicity analysis results show possible connection of environmental variables with radon concentration. Multivariate classification and regression methods are used to study the connection of climate variables and the variation of radon concentrations. Resulting 'mapped' functional behaviour of radon concentrations on input variables can be used as a good tool for further study of radon concentration connection with independent variables or group of strongly correlated variables. The result presented in this paper suggest the usefulness of multivariate method analysis as a helping tool for prediction of radon concentrations and a tool for checking the model of radon concentration in shallow underground laboratory and underground spaces with ventilation.

P3

Development of protocol for radon measurements in multi-storey buildings in Russia

Aleksey Vasilyev, Georgy Malinovsky, Alexandra Onishchenko*

Institute of Industrial Ecology, Ekaterinburg, Russia

Radon is one of the most important indoor pollutant, which is the second cause of lung cancer next to smoking. To investigate the relationship between radon and lung cancer it is necessary to assess indoor radon concentration. Multi-storey block buildings represent the main type of dwellings in urban cities of Russia. Despite the existing radon measurements protocols being reasonable for single-family houses, short-term measurements in multi-storey buildings are still an open question (number of measurements, number of floors to study, etc.) Radon concentrations on different floors in multi-storey building are unpredictable even if we know the radon entry and dilution rates. Main physical quantities, affecting indoor radon concentrations in multi-storey energy-efficient buildings in Ekaterinburg, Russia, were studied and related multi-cham-

**The Henryk Niewodniczanski
Institute of Nuclear Physics
Polish Academy of Sciences
Radzikowskiego 152, 31-342 Kraków, Poland**

www.ifj.edu.pl/badania/publikacje

Kraków, May 2019

**BOOK of ABSTRACTS
3rd International Conference
“Radon in the Environment 2019”
27-31 May 2019, Kraków, Poland**

RADON VARIABILITY DUE TO FLOOR LEVEL IN THE TWO TYPICAL RESIDENTIAL BUILDINGS IN SERBIA

Vladimir Udovičić¹, Nikola Veselinović¹, Dimitrije Maletić¹, Radomir Banjanac¹, Aleksandar Dragić¹, Dejan Joković¹, Mihailo Savić¹, David Knezević¹, Maja Eremić Savković²

¹Institute of Physics Belgrade, University of Belgrade, Belgrade, Serbia

²Serbian Radiation and Nuclear Safety and Security Directorate, Belgrade, Serbia

E-mail: udovicic@ipb.ac.rs

It is well known that one of the factors that influences the indoor radon variability is the floor level of the buildings. Considering the fact that the main source of indoor radon is radon in soil gas, it is expected that the radon concentration decreases at higher floors. Thus, at higher floors the dominant source of radon is originating from building materials and in some cases there may be deviations from the generally established regularity. On the other hand, the radon variability due to floor level, especially in big cities with a much higher number of high-rise buildings and population density compared with rural environments, may have an impact on the assessments of collective dose from radon.

According to the national typology [1], there are six types of residential buildings in Serbia; two for family housing: Freestanding single-family house and single-family house in a row, and four for multi-family housing: Freestanding residential building, residential building - lamela (apartment block with repeated multiple – lamellar – cores and separate entrances), residential building in a row and high-rise residential building. Distribution of buildings by type at national level shows that 97.23% of all residential buildings are family housing. Also, for all defined types of buildings number of floors ranges from one to eight above the ground level. Freestanding family houses are mostly ground floor (37%) or ground floor with loft in use (26%), while there is a very low representation of houses that have more than two floors (5%), with average height of family buildings of 1.4. In that sense, we chose one freestanding single-family house with loft with well-known radon characteristics [2] and one sixteenth floor high-rise residential building for this study.

The indoor radon measurements are performed with two active devices. One was fixed in the living room at the ground level and the second one was moved through the floors of the residential building. Every measuring cycle at the specified floor lasted seven days with the sampling time of the two hours. In this work, the analysis of the obtained results is shown in details.

Ref.

- [1] Jovanović Popović M., Ignjatović D., Radivojević A., Rajčić A., Čuković Ignjatović N., Đukanović Lj. & Nedić M. (2013), National Typology of Residential Buildings in Serbia, Faculty of Architecture University of Belgrade, Belgrade (2013), ISBN 978-86-7924-102-3.
- [2] Udovičić V., Maletić D., Banjanac R., Joković D., Dragić A., Veselinović N., Živanović J., Savić M., Forkapić S. Multiyear Indoor Radon Variability in a Family House – a Case Study in Serbia, Nuclear Technology and Radiation Protection Vol. XXXIII, No. 2 (2018), pp. 174-179.

A34

PILOT STUDY ON MITIGATION SOLUTIONS FOR BUILDINGS WITH AN ELEVATED RADON LEVELS IN SERBIA

Maja Eremic-Savkovic¹, Vladimir Udovicic², Dimitrije Maletic², Aleksandar Djordjevic³

¹Serbian Radiation and Nuclear Safety and Security Directorate, Belgrade, Serbia

²Institute of Physics Belgrade, University of Belgrade, Belgrade, Serbia

³ASBA TIM d.o.o., Belgrade, Serbia

E-mail: eremic.savkovic@srbatom.gov.rs

Radon contributes to almost 50% of the overall high-effective annual dose to the population received from all sources of natural radioactivity. Harmful effects of radon have been proven in a large number of epidemiological studies. Radon problem has received a special attention in many countries in the world and most of them have established national radon programmes.

Serbian Radiation and Nuclear Safety and Security Directorate (SRBATOM) conducted National Indoor Radon measurement campaign in more than 5 thousands dwellings in the Republic of Serbia. We used CR-39-type detectors, period of exposure was six months, in heating season. The results showed that 3% of all measurements are above the intervention levels for chronic exposure to radon in homes 400 Bq/m³ for existing buildings and 0.3% of all results were above 1000 Bq/m³.

In 2017 SRBATOM established multi-disciplinarian team consisting of experts for indoor radon measurement and building professionals. We chose 20 houses with an elevated radon levels (at voluntary base) and devised the project on two parts: one was consisted of indoor radon diagnostics with active device and the second one was technical analysis of houses which included existing conditions of the house, used technical standards during the building process and building codes. In this work we represent obtained results in details, with outcomes on mitigation solutions for the investigated houses.

**ДРУШТВО ЗА ЗАШТИТУ ОД ЗРАЧЕЊА
СРБИЈЕ И ЦРНЕ ГОРЕ**



**ЗБОРНИК
РАДОВА**

**XXIX СИМПОЗИЈУМ ДЗЗСЦГ
Сребрно језеро
27- 29. септембар 2017. године**

**Београд
2017. године**

**XXIX СИМПОЗИЈУМ ДРУШТВА
ЗА ЗАШТИТУ ОД ЗРАЧЕЊА
СРБИЈЕ И ЦРНЕ ГОРЕ**

Сребрно језеро, од 27.09. до 29.09.2017. године

Организатори:

ДРУШТВО ЗА ЗАШТИТУ ОД ЗРАЧЕЊА СРБИЈЕ И ЦРНЕ ГОРЕ

ИНСТИТУТ ЗА НУКЛЕАРНЕ НАУКЕ „ВИНЧА“

Лабораторија за заштиту од зрачења и заштиту животне средине „Заштита“

Организациони одбор:

Председник: Гордана Пантелић

Чланови:

Маја Еремић Савковић, Агенција за заштиту од јонизујућих зрачења и нуклеарну сигурност, Београд

Вера Спасојевић Тишма, Нуклеарни објекти Србије, Београд

Иван Кнежевић, Нуклеарни објекти Србије, Београд

Данијела Аранђић, Институт за нуклеарне науке „Винча“, Београд

Јелена Станковић Петровић, Институт за нуклеарне науке „Винча“, Београд

Милица Рајачић, Институт за нуклеарне науке „Винча“, Београд

Сандра Ђеклић, Институт за нуклеарне науке „Винча“, Београд

Наташа Сарап, Институт за нуклеарне науке „Винча“, Београд

Предраг Божовић, Институт за нуклеарне науке „Винча“, Београд

Никола Кржановић, Институт за нуклеарне науке „Винча“, Београд

Редакциони одбор:

др Невенка Антовић, Природно математички факултет, Подгорица

др Перко Вукотић, Природно математички факултет, Подгорица

др Софија Форкапић, Природно математички факултет, Нови Сад

др Душан Мрђа, Природно математички факултет, Нови Сад

др Миодраг Крмар, Природно математички факултет, Нови Сад

др Драгослав Никезић, Природно математички факултет, Крагујевац

др Ненад Стевановић, Природно математички факултет, Крагујевац

др Јелена Ајтић, Факултет ветеринарске медицине, Београд

др Владимир Удовичић, Институт за физику, Земун, Београд

др Драгана Тодоровић, Институт за нуклеарне науке „Винча“, Београд

др Ивана Вуканац, Институт за нуклеарне науке „Винча“, Београд

др Јелена Крнета Николић, Институт за нуклеарне науке „Винча“, Београд

др Марија Јанковић, Институт за нуклеарне науке „Винча“, Београд

др Милош Живановић, Институт за нуклеарне науке „Винча“, Београд

др Оливера Цирај-Бјелац, Институт за нуклеарне науке „Винча“, Београд

др Србољуб Станковић, Институт за нуклеарне науке „Винча“, Београд

STUDIJA SLUČAJA SEZONSKE VARIJACIJE KONCENTRACIJE RADONA U PORODIČNOJ KUĆI U SRBIJI

Vladimir UDOVIČIĆ¹, Dimitrije MALETIĆ¹, Aleksandar DRAGIĆ¹, Radomir BANJANAC¹, Dejan JOKOVIĆ¹ i Sofija FORKAPIĆ²

1) *Univerzitet u Beogradu, Institut za fiziku u Beogradu, Beograd, Srbija, udovicic@ipb.ac.rs*

2) *Univerzitet u Novom Sadu, PMF Novi Sad, Novi Sad, Srbija, sofija@df.uns.ac.rs*

SADRŽAJ

Usled uticaja velikog broja parametara, ponašanje radona u zatvorenim prostorijama ima složenu dinamiku. Na osnovu merenja koncentracije radona, izdvajaju se dve periodičnosti, dnevna i sezonska. U ovom radu su prikazani rezultati merenja koncentracije radona u jednoj tipičnoj porodičnoj kući u Srbiji, u toku tri sukcesivne godine u februaru i julu svake godine. Korišćene su sledeće tehnike merenja radona: aktivna i metoda ugljenih kanistara. Takođe su prikazani rezultati ovih interkomparativnih merenja.

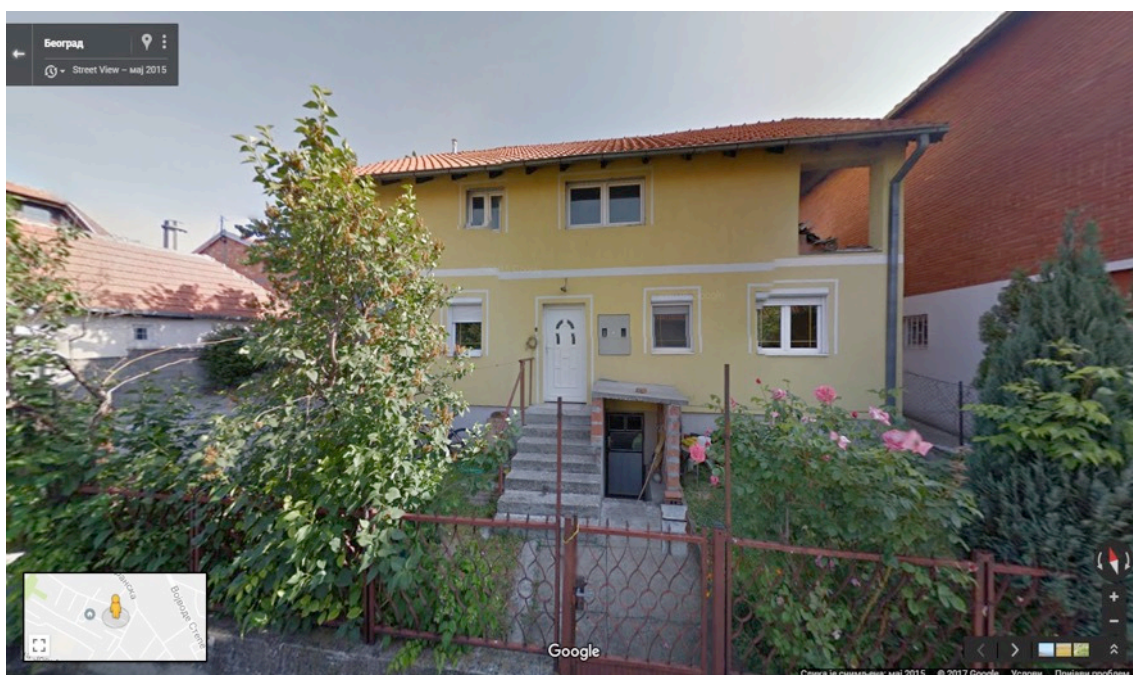
1. UVOD

Istraživanje dinamike radona i primena mera za njegovo smanjenje u različitim sredinama, naročito u zatvorenim prostorijama, ima veliki značaj u smislu zaštite od jonizujućih zračenja. Objavljeni rezultati i razvoj mnogih modela kojima se opisuje ponašanje radona ukazuju na složenost ovog istraživanja, posebno sa modelima za predviđanje varijabilnosti radona [1-3]. To je zato što varijabilnost radona zavisi od velikog broja faktora kao što su geologija, propustljivost zemljišta, građevinski materijali koji se koriste za izgradnju kuća i zgrada, stanje unutrašnje atmosfere (temperatura, pritisak i relativna vlažnost), koncentracija aerosola, brzina razmene između unutrašnjeg i spoljašnjeg vazduha, kao i životnih navika ljudi. Poznato je da varijabilnost koncentracije radona ima dve glavne periodičnosti i to od jednog dana i jedne godine. Takođe je poznato da postoji sezonska varijacija koncentracije radona. To je razlog zašto je posebno zanimljivo istražiti varijaciju radona na istom mernom mestu, iz godine u godinu, zbog procene individualne godišnje doze od izlaganja radonu. U tom smislu, pratili smo dugoročne varijacije koncentracije radona u jednoj tipičnoj porodičnoj kući u Srbiji. Merenja su obavljena tokom 2014., 2015. i 2016. godine, u februaru i julu, svake godine. Koristili smo sledeće merne tehnike: aktivna i metoda korišćenja ugljenih kanistara. Detaljna analiza dobijenih rezultata je prikazana u ovom radu.

2. METODE MERENJA RADONA

Vremenske serije merenih koncentracija radona, temperature i relativne vlažnosti u ispitivanoj kući dobijene su pomoću uređaja SN1029 (proizvođača Sun Nuclear Corporation). To je merni uređaj jednostavne konstrukcije i primene u praksi. U suštini, radi se o brojaču sa dodatkom senzora za merenje meteoroloških parametara. Nedostatak uređaja je nemogućnost merenja koncentracije radona u zemljištu i vodi. Operater može podesiti vremenske sekvence od 0,5 sati do 24 sati. Jedan ciklus merenja može trajati 1000 sati ili ukupno 720 vremenskih sekvenci (broj sukcesivnih merenja, odnosno tačaka u vremenskoj seriji). Uređaj je bio podešen da radi u vremenskoj sekvenci od 2 sata.

Simultano su mereni temperatura, vazdušni pritisak i vlažnost. U saradnji sa kolegama iz Laboratorije za ispitivanje radioaktivnosti uzoraka i doze jonizujućeg i nejonizujućeg zračenja, PMF, Novi Sad urađena su interkomparativna merenja, korišćenjem standardne skrining metode za merenje koncentracije radona pomoću adsorpcije na aktivnom uglju prema US EPA protokolu 520/5-87-005 [4], tokom februara 2014., 2015. i 2016. godine. Porodična kuća izabrana za merenja i analize varijacije radona je tipična kuća u Beogradu (slika 1).



Slika 1. Porodična kuća u kojoj su vršena merenja

Karakterističan je stil gradnje u kome se kuća gradi više godina uz konstantno dograđivanje i nadogradnju, što potencijalno može biti izvor ulaska radona u takve kuće. Kuća ima podrum i izgrađena je od standardnih materijala (cigla-blok, beton, malter). Na kraju je urađena i izolacija korišćenjem stiropora debljine 5 cm. Merenja radona su izvršena u dnevnoj sobi porodične kuće. Tokom perioda merenja (zima-leto 2014, 2015. i 2016), kuća je prirodno ventilirana i korišćen je klima uređaj u oba režima, grejanja i hlađenja. Tokom zimskog perioda merenja pored klima uređaja, korišćena je termoakumulaciona peć i uljani radijatori. Izmerene koncentracije radona, sobna temperatura (T) i relativna vlažnost unutar kuće su dobijeni korišćenjem radon monitora.

3. REZULTATI

Merenja su obavljena tokom februara i jula 2014., 2015. i 2016. koristeći radon monitor i metode pomoću adsorpcije na aktivnom uglju. Rezultati su prikazani u tabeli 1. Uočena je izrazita sezonska varijacija radona, pri čemu je koncentracija radona u zimskom periodu za red veličine veća nego u letnjem periodu. Rezultati merenja radona pomoću dve različite metode su u dobroj saglasnosti.

Tabela 1. Rezultati merenja radona, temperature i vlažnosti vazduha tokom februara i jula 2014., 2015. i 2016.

	2014.		2015.		2016.	
	Februar	Juli	Februar	Juli	Februar	Juli
Minimum [Bqm ⁻³]	15	0	28	0	12	3
Maximum [Bqm ⁻³]	1000	286	915	88	1013	262
Mediana [Bqm ⁻³]	418	25	524	22	412	28
AM(SD) [Bqm ⁻³]	402(216)	40(41)	508(207)	27(18)	423(214)	39(32)
Temperatura [°C]	20,4(0,8)	24,7(0,9)	21,2(0,6)	24,9(0,8)	22,3(0,6)	24,6(0,8)
Vlažnost [%]	67,4(5,7)	67,8(4,8)	68,2(4,8)	51,5(4,7)	64,0(6,4)	58,9(7,5)
Ugljeni kanister [Bqm ⁻³]	432(10)	/	518(6)	/	407(5)	/

4. ZAKLJUČAK

U ovom radu, praćena je varijabilnost radona u dnevnoj sobi jedne porodične kuće u Beogradu tokom dva izabrana meseca u godini (februar i juli), i to tri godine za redom, 2014., 2015. i 2016. Rezultati pokazuju izrazitu sezonsku varijaciju, s tim što nivoi radona za iste mesece u godini pokazuju relativnu reproducibilnost. Male varijacije su uslovljene, pre svega varijacijama meteo parametara. Takođe, interkomparativna merenja radona dvema različitim metodama pokazuju dobru saglasnost.

5. ZAHVALNICA

Ovaj rad je realizovan uz podršku Ministarstva prosvete, nauke i tehnološkog razvoja Republike Srbije u okviru projekta pod brojem III43002.

6. LITERATURA

- [1] D. Maletić, V. Udovičić, R. Banjanac, D. Joković, A. Dragić, N. Veselinović, J. Filipović. Comparison of multivariate classification and regression methods for indoor radon measurements. *Nuclear Technology and Radiation Protection* 29, 2014, 17-23.
- [2] D. Maletić, V. Udovičić, R. Banjanac, D. Joković, A. Dragić, N. Veselinović, J. Filipović. Correlative and multivariate analysis of increased radon concentration in underground laboratory. *Radiation Protection Dosimetry* 162 (1-2), 2014, 148-151.
- [3] J. Filipović, D. Maletić, V. Udovičić, R. Banjanac, D. Joković, M. Savić, N. Veselinović. The use of multivariate analysis of the radon variability in the underground laboratory and indoor environment. *Nukleonika* 61(3), 2016, 357-360.
- [4] EPA 520/5-87-005, Gray D.J, Windham S.T, United States Environmental Protection Agency, Montgomery, 1987.

**CASE STUDY OF THE INDOOR RADON SEASONAL
VARIABILITY IN THE FAMILY HOUSE IN SERBIA**

**Vladimir UDOVIČIĆ¹, Dimitrije MALETIĆ¹, Aleksandar DRAGIĆ¹, Radomir
BANJANAC¹, Dejan JOKOVIĆ¹ i Sofija FORKAPIĆ²**

1) *University of Belgrade, Institute of Physics Belgrade, Belgrade, Serbia,
udovicic@ipb.ac.rs*

2) *University of Novi Sad, PMF Novi Sad, Novi Sad, Serbia, sofija@df.uns.ac.rs*

ABSTRACT

Due to the impact of a large number of parameters, the behavior of radon indoors has complex dynamics. Radon time-series analysis, based on the short-term indoor radon measurements performed worldwide, shows two main periodicity: daily and seasonal. This paper presents the results of the indoor radon measurements in a typical family house in Serbia, during three successive years in February and July each year. The following techniques were used for radon measurements: active and charcoal canister methods. It also presents the results of these intercomparison measurements.

KORIŠĆENJE MULTIVARIJANTNE ANALIZE ZA PREDVIĐANJE GEOGENOG RADONSKOG POTENCIJALA

Sofija FORKAPIĆ¹, Dimitrije MALETIĆ², Jovica VASIN³, Kristina BIKIT¹,
Dušan MRDA¹, Ištvan BIKIT¹, Vladimir UDOVIČIĆ², Radomir BANJANAC²

1) Univerzitet u Novom Sadu, Prirodno-matematički fakultet, Novi Sad, Srbija,

sofija@df.uns.ac.rs

2) Univerzitet u Beograd, Institut za fiziku, Beograd, Srbija, maletic@ipb.ac.rs

3) Univerzitet u Novom Sadu, Institut za ratarstvo i povrtarstvo, Novi Sad, Srbija,
jovica.vasin@ifvcns.ns.ac.rs

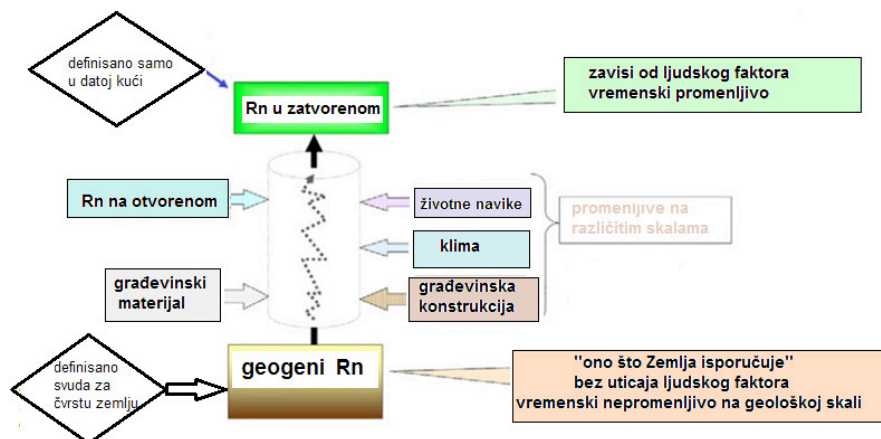
SADRŽAJ

Geogeni radonski potencijal koji izdvaja radon u podzemnim slojevima kao dominantan uzrok akumulacije radona u zatvorenim prostorijama i koji je nezavisan od ljudskog uticaja i vremenski konstantan u geološkim okvirima predstavlja glavni alat za iznalaženje radonom ugroženih područja. U nedostatku podataka za permeabilnost zemljišta za radon i malog broja merenja radona u zemljištu, upotrebljena je multivarijantna analiza velikog broja raspoloživih geohemijskih podataka, merenja radioaktivnosti zemljišta i koncentracija aktivnosti radona u zatvorenim prostorijama datih lokacija na području Vojvodine. Nekoliko uporedivih metoda iz ROOT okvira za analize softverskog paketa TMVA je korišćeno za analizu zavisnosti koncentracije radona u zatvorenom od mnoštva ulaznih varijabli. BDTG kao najpodobnija metoda je pokazala da su varijable sa najvećim uticajem na koncentraciju radona u zatvorenim prostorijama pored sadržaja ukupnog azota, koncentracije aktivnosti radionuklida u zemljištu na profilu dubine od 30 cm i sadržaj humusa i gline. Dobijeni rezultati pokazuju dobro slaganje sa nedavnim ispitivanjem emanacije radona iz zemljišta na području grada Novog Sada.

1. UVOD

Poznato je da radon i njegovi kratkoživeći potomci daju najveći doprinos efektivnoj dozi koju stanovništvo primi od jonizujućih zračenja [1]. Nedavna epidemiološka istraživanja pokazala su da rizik od radona postoji i pri koncentracijama za koje se ranije smatralo da su zanemarive. U svim evropskim zemljama se sprovode mapiranja radona, a rezultati se sumiraju u publikaciji zajedničkog istraživačkog centra Evropske komisije (JRC EC) koji koordinira projekt izrade evropskog atlasa prirodne radioaktivnosti. Naime, sve države članice EU (uključujući i zemlje kandidate za članstvo) prema direktivi EU [2] moraju propisati referentne nivoe radona u boravišnim i radnim prostorijama i identifikovati područja sa visokim radonskim potencijalom. Postoje dva koncepta u definiciji radonskog potencijala: prema broju objekata sa koncentracijama radona iznad referentnog nivoa – indoor radon potential IRP i prema lokalnim geofizičkim parametrima kao što su koncentracija radona u zemljištu i permeabilnost zemljišta (geogeni radonski potencijal GRP). Na koncentraciju radona u boravišnim i radnim prostorijama utiče mnogo faktora koji se mogu podeliti na privremene koji zavise od antropogenog uticaja ili trenutnih uslova (kao što su životne navike, način gradnje, građevinski materijal, meteorološki uslovi) i trajne koje zavise od geofizičkih parametara (kao što su raspored stena u tlu, sadržaj uranijuma i radijuma u zemljištu i stenama, permeabilnost zemljišta za radon, granulacija i hemijske

karakteristike zemljišta). Radon dominantno potiče od povišene koncentracije radijuma i uranijuma u stenama koje se nalaze duboko ispod tla i zbog toga što je radon inertan gas lako napušta mesto formiranja i difunduje kroz debele slojeve zemljišta usled gradijenta u koncentraciji i pritisku.



Slika 1. Kompleksni uticaji na radon u zatvorenim prostorijama i geogeni radonski potencijal [4]

Geogeni radonski potencijal (GRP) određenog područja se može odrediti na osnovu koncentracije radona u zemljištu i permeabilnosti zemljišta na osnovu sledeće empirijske formule [5]:

$$GRP = \frac{C}{-\log_{10} k \cdot 10} \quad (1)$$

gde je C koncentracija radona [Bq/m^3] u zemljištu i k permeabilnost zemljišta [m^2]. Ovako određeni geogeni radonski potencijal se upoređuje sa kartama geomorfoloških jedinica datog područja, kartama koncentracije uranijuma i radijuma u zemljištu i pedološkim kartama u cilju identifikacije radonom ugroženih područja. U nedostatku merenja koncentracije radona u zemljištu, kao i zbog nemogućnosti da se meri permeabilnost zemljišta za radon, naši prvi pokušaji da se proceni GRP na osnovu postojećih baza podataka su bili da se detaljno analiziraju korelacije između dostupnih geohemijskih podataka i merenja koncentracije radona u zatvorenim prostorijama kako bi se predvidela radonom ugrožena područja i validovale geogene prognoze. U tu svrhu primenjeni su multivarijantnimetodi, razvijeni u CERN-u za analizu velikog broja događaja u eksperimentalnoj fizici visokih energija, kako bi se ispitale sve moguće korelacije između velikog broja sistematskih ispitivanja koncentracija radona u zatvorenom na području Vojvodine u periodu od 2002-2005. godine koje je sprovela Laboratorija za ispitivanje radioaktivnosti uzoraka i doze jonizujućeg i nejonizujućeg zračenja, PMF-a u Novom Sadu. [6]. Za vojvođansko zemljište postoji bogata sistematika merenja radioaktivnosti i geohemijskih karakteristika nastala upravo u tom periodu (2001-2010) u saradnji laboratorije u Novom Sadu sa Institutom za ratarstvo i povrtarstvo iz Novog Sada. Izbor lokaliteta za poređenje vrednosti je bio po kriterijumima zastupljenosti površina podpojedininim geomorfološkim celinama [7] i pojedinim tipovima zemljišta [8-9].

Institut za fiziku u Beogradu je primenio sve dostupne regresione metode implementirane u TMVA (Toolkit for Multivariate analysis) [10] da bi odredio i rangirao korelacione koeficijente u cilju iznalaženja najpogodnijeg metoda koji će dati najbolje korelacije

koncentracija radona od mnoštva ulaznih parametara. Da bi ova multivarijantna klasifikacija bila moguća set ulaznih događaja je morao biti podeljen na one koji odgovaraju signalu (povišene koncentracije radona) i one koje odgovaraju fonu (ispod granice od 120 Bq/m^3 koja daje najbolje razdvajanje rezultata) (slika 3). Metoda multivarijantne regresije, međutim, ne zahteva ovakvo preliminarno razdvajanje podataka i zbog toga je opštijeg karaktera.

2. METODOLOGIJA UZORKOVANJA I MERENJA

Merenje koncentracije radona u zatvorenim prostorijama je sprovedeno metodom trag detektora tipa CR39 koji su u zatvorenoj difuzionoj komori bili izlagani na oko 3000 lokacija u Vojvodini u prizemnim prostorijama u trajanju od 90 dana u zimskim mesecima: decembar, januar i februar u periodu od 2002-2005. Nagrizanje i očitavanje tragova je izvršeno kod proizvođača opreme Radosys Company, Mađarska. Za ovu studiju izračunate su srednje vrednosti koncentracija radona za mesta u neposrednoj blizini lokaliteta uzorkovanja zemljišta. Tipovi zemljišta kojim pripadaju ispitivani uzorci su: černozem, humoglej, fluvisol, pseudoglej, solonjec, kambisol, solončak i arenosol, po IUSS klasifikaciji [9]. Sa svake odabrane lokacije uzeto je 10 mikro uzoraka zemljišta sa površine od $10 \times 10 \text{ m}$, a zatim napravljen jedan kompozitni uzorak mešanjem. Za ispitivanje radioaktivnosti uzorci zemljišta su uzeti sa dve dubine: iz površinskog sloja (0–10 cm) i sa dubine do 30 cm agrohemijskom sondom. Hemijske analize zemljišta su izvršene samo na uzorcima sa dubine od 30 cm. Uzorci zemljišta su sušeni na 105°C do konstantne mase, usitnjeni, homogenizovani i mereniu cilindričnim posudama na kapi detektora. Koncentracije aktivnosti radionuklida gama emitera u zemljištu određene su metodom niskofonske gama spektrometrije na dva HPGe detektora visoke rezolucije u pasivnoj zaštiti. Za prikupljane i analizu gama spektara korišćen je softver Genie 2000. pH-vrednost određena je u suspenziji zemljišta sa vodom ($10 \text{ g} : 25 \text{ cm}^3$) i suspenziji zemljišta sa kalijum hloridom, potenciometrijski, pH metar PHM62 standard-Radiometar Copenhagen. Sadržaj humusa određen je metodom Tjurin-a; ukupan sadržaj azota po Kjeldahlu na sistemu za digestiju i titraciju Tacator; lakopristupačni fosfor i lakopristupačni kalijum (ekstrakcijom sa amonijum laktatom) - AL metodom. Za određivanje mehaničkog sastava zemljišta korišćene su metode: frakcionisanje pomoću serije sita i pipet metoda. U cilju ostvarivanja peptizacije mehaničkih elemenata uzorci zemljišta se tretiraju natrijum-pirofosfatom. Na osnovu veličine čestica prema IUSS klasifikaciji mogu se odrediti sledeće frakcije: krupan pesak (0,2–2 mm), sitan pesak (0,02–0,2 mm), fini prah (0,002–0,02 mm) i glina ($<0,002 \text{ mm}$) [9].

3. REZULTATI I DISKUSIJA

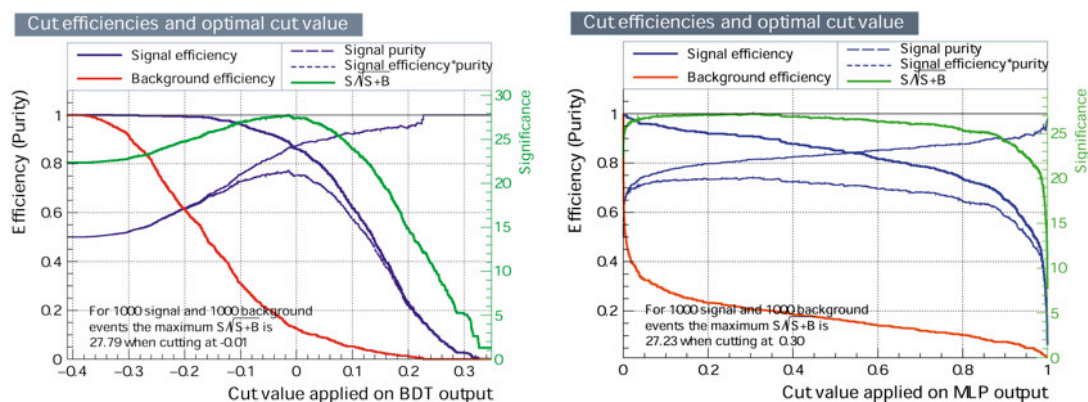
U tabeli 1. prikazani su linearni korelacioni koeficijenti koji nam ukazuju na veličinu korelacije između ulaznih veličina i koncentracije radona. Može se uočiti da radon najbolje korelira sa radionuklidima na dubini od 30 cm.

Za primenu multivarijantnih metoda, ispitivani uzorak mora da ima značajnu statistiku. Pošto to nije bilo zadovoljeno, veštački se povećao uzorak dupliranjem svih vrednosti, ali uz modifikaciju množenjem inicijalnih vrednosti ulaznih parametara i koncentracija radona sa 1+slučajne Gausove vrednosti sa sigma 1/10.

Tabela 1. Korelacioni koeficijenti između radona i ulaznih parametara

Redni br.	Parametar	Korelacioni koeficijent
1	Elevation	+0,11
2	pH	0
3	CaCO ₃	-0,03
4	Humus	+0,15
5	Ukupan N	+0,13
6	P ₂ O ₅	-0,01
7	K ₂ O	+0,01
8	Krupan pesak	-0,08
9	Sitan pesak	-0,19
10	Prah	+0,16
11	Glina	+0,17
12	Ra-226 30cm	+0,27
13	U-238 30cm	+0,17
14	Th-232 30cm	+0,22
15	K-40 30cm	+0,10
16	U-238 površina	-0,17
17	Ra-226 površina	+0,04
18	Th-232 površina	0
19	K-40 površina	+0,02
20	Cs-137 površina	-0,17

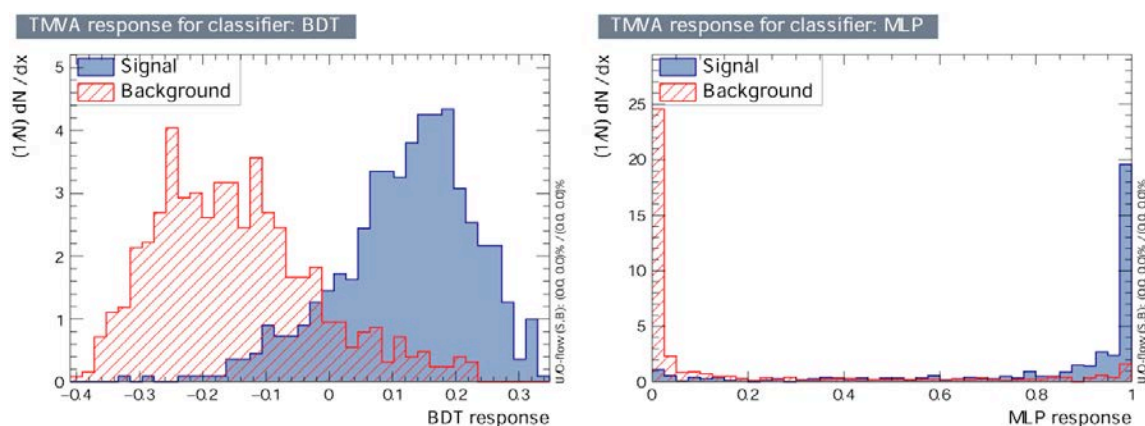
Ulazni parametri (karakteristike zemljišta i sadržaj radionuklida na površini i na dubini od 30 cm) su korišćeni za testiranje i evaluaciju 12 multivarijantnih metoda koje postoje u okviru TMVA. Najbolji metod je onaj koji zadržava maksimalnu vrednost odbacivanja fona pri najvećoj efikasnosti signala (slika 2). Na osnovu takvog kriterijuma kao metoda koja najefikasnije klasifikuje ulazne događaje, odabrana je metoda BDT (Boosted Decision Trees method). Ovo se može ilustrovati na slici 3. koja prikazuje raspodelu izlaznih veličina BDT klasifikacione metode za ulazne signale i fonske događaje. Drugi najbolji izbor je primena ANN Multilayer Perceptrons metode (MLP).



Slika 2. Efikasnost odsecanja i optimalna vrednost odsecanja za BDT (levo) i MLP (desno) multivarijantnih metoda za radonske koncentracije

Tabela 2. Rezultati evaluacije metoda rangirani po najboljoj efikasnosti signali i čistoći površine. @B je deo fonskih događaja koji su klasifikovani kao događaji signala

MVA metoda	Efikasnost signala prema efikasnosti fona (greška):				podela	značaj
	@B=0,01	@B=0,10	@B=0,30	ROC-integ		
BDT	0,212(16)	0,814(16)	0,959(08)	0,932	0,609	1,614
BDTG	0,243(17)	0,767(17)	0,966(07)	0,927	0,611	1,676
MLPBNN	0,224(17)	0,754(17)	0,957(08)	0,922	0,600	1,579
MLP	0,228(17)	0,728(18)	0,955(08)	0,919	0,577	1,540
SVM	0,211(16)	0,797(16)	0,938(09)	0,918	0,587	1,611
RuleFit	0,162(15)	0,671(19)	0,906(12)	0,891	0,482	1,263
LikelihoodPCA	0,000(00)	0,491(20)	0,845(14)	0,843	0,404	1,099
LD	0,047(08)	0,348(19)	0,744(18)	0,789	0,271	0,806
Likelihood	0,031(07)	0,328(19)	0,674(19)	0,764	0,208	0,589
FDA_GA	0,031(07)	0,147(14)	0,363(19)	0,611	0,093	0,353



Slika 3. Raspodela izlaznih vrednosti BDT i ANN MLP klasifikacionih metoda za ulazni signal i fonske događaje

Rangiranje BDTG ulaznih varijabli (tabela 3) je izvedena brojanjem koliko često se varijable koriste pri donošenju odluka u svakom čvorištu stabla, pri čemu je ova vrednost otežana brojem podela i brojem događaja u čvoru. Kao što se vidi iz tabele 3, pored ukupnog azota, najvažnije varijable za koncentracije radona u zatvorenim prostorijama su koncentracije radionuklida na 30cm dubine.

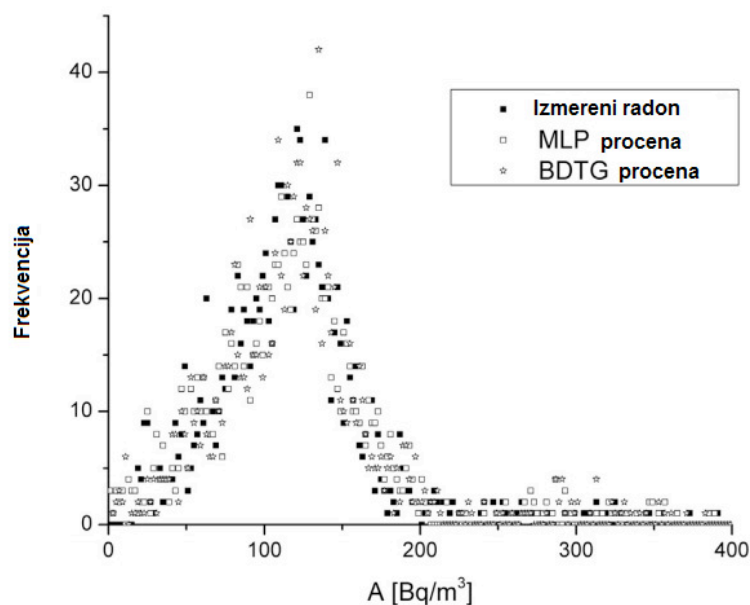
Najbolji regresioni metodi koji daju izlazne veličine najpribližnije stvarnim vrednostima koncentracije radona su ponovo BDT, a kao druga MLP, isto kao i u slučaju multivarijantnog klasifikatora. Slika 4 prikazuje distribuciju koncentracija radona i izlaznih veličina iz MLP evaluacije koncentracija radona na osnovu svih ulaznih parametara.

Da bi procenili kvalitet korišćenog metoda poređene su razlike između izlaznih vrednosti iz MLP multivarijantne regresione metode i vrednosti merenih koncentracija radona (slika 5). Slika ukazuje na dobru moć predviđanja varijacija koncentracija radona na

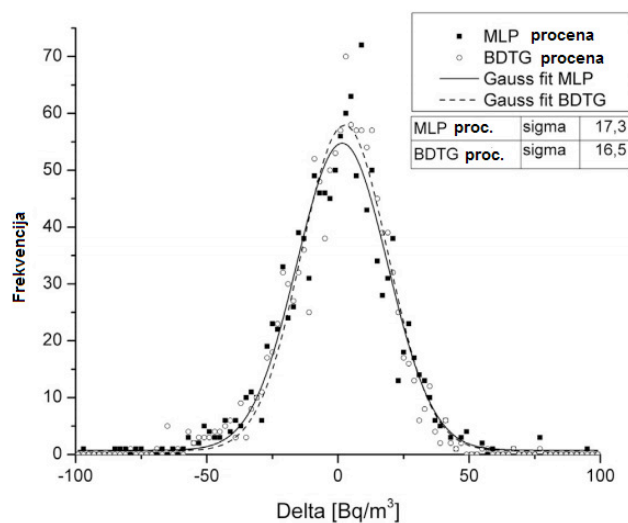
osnovu celokupnog seta ulaznih parametara pomoću multivarijantnih regresionih metoda.

Tabela 3. Ulazni parametri poređani po značaju za BDTG MVA metodu za radon

BDTG rang	Parametar	Značaj varijable $\times 10^{-2}$
1	Ukupan N	6,490
2	U-238 30cm	6,425
3	K-40 30cm	6,040
4	Th-232 30cm	5,495
5	Humus	5,490
6	K ₂ O	5,406
7	glina	5,360
8	U-238 površina	5,218
9	Sitan pesak	5,116
10	CaCO ₃	5,081
11	P ₂ O ₅	5,003
12	Cs-137 površina	4,715
13	Ra-226 30cm	4,656
14	Nadmorska visina	4,595
15	K-40 površina	4,509
16	pH	4,435
17	Ra-226 površina	4,188
18	Prah	4,082
19	Th-232 surface	4,026
20	Krupan pesak	3,671



Slika 4. Raspodela merenih koncentracija radona i izlaznih podataka iz MLP multivarijantnog regresionog metoda za koncentracije radona



Slika 5. Raspodela razlika izlaznih veličina iz MLP metoda i merenih radonskih koncentracija

4. ZAKLJUČAK

U ovom radu detaljno je opisana mogućnost primene multivarijantne analize za procenu radonskog potencijala. Odabrana je najadekvatnija metoda za analizu radonskih merenja među velikim brojem multivarijantnih metoda, koje su razvijene za analizu podataka u fizici visokih energija i implementirane u TMVA softverski paket. Evaluacijom i rangiranjem dobijenih rezultata na osnovu efikasnosti i čistoće signala izdvojene su dve metode koje daju najbolje rezultate u analizama: BDT i MLP koja se bazira na veštačkoj neuralnoj mreži (ANN). Rezultati dalje multivarijantne analize daju uvid u zavisnost koncentracije radona od koncentracija ostalih radionuklida u zemljištu i geohemijskih karakteristika zemljišta. BDTG multivarijantni metod pokazuje da su varijable od najvećeg značaja za koncentracije radona u zatvorenom: koncentracije radionuklida u dubljim slojevima zemljišta, ali takođe sadržaji humusa i gline u zemljištu (tabela 3). Dodatno, multivarijantni regresioni metodi daju dobru aproksimaciju koncentracije radona korišćenjem celokupnog seta ulaznih parametara. Sve to potvrđuje da su radio-geohemijski podaci korisni za generisanje mapa radonom ugroženih područja. Potvrđena je pretpostavka da tip zemljišta koji sadrži najveći procenat gline i humusa u najvećoj meri adsorbuje i zadržava radon u zemljištu i doprinosi povišenim koncentracijama radona u zatvorenom, odnosno radonskom potencijalu. Ovaj zaključak se može primeniti za odabir lokacija za buduća merenja permeabilnosti zemljišta kada se nabavi neophodna oprema. Dobijena najbolja korelacije koncentracija radona sa sadržajem ukupnog azota u zemljištu predstavlja interesantan rezultat koji će biti dalje proučavan u narednim studijama proučavanja emanacije radona iz zemljišta.

5. ZAHVALNICA

Autori se zahvaljuju na finansijskog podršci Pokrajinskom sekretarijatu za zaštitu životne sredine i održivog razvoja i Ministarstvu prosvete, nauke i tehnološkog razvoja u okviru projekata OI171002 i III43002.

6. LITERATURA

- [1] UNSCEAR, 2008, Ionizing Radiation: Sources and Effects, UNSCEAR 2008 REPORT, VOLUME II, United Nations, New York (2008)
- [2] WHO, 2009 Handbook on Indoor Radon – a Public Health Perspective
- [3] Council Directive 2013/59/EURATOM of 5 December 2013 laying down basic safety standards for protection against the dangers arising from exposure to ionising radiation, and repealing Directives 89/618/Euratom, 90/641/Euratom, 96/29/Euratom, 97/43/Euratom and 2003/122/Euratom, Article 74 Indoor exposure to radon
- [4] V. Gruber et al., The European map of geogenic radon potential, *Journal of Radiological Protection* 33 (2013) 51-60
- [5] Neznal M, Neznal M, Matolin M, Barnet i and Miksova J 2004 The New Method for Assessing the Radon Risk of Building Sites (*Czech Geological Survey Special Papers vol 16*) (Prague: Czech Geological Survey)
- [6] Forkapić, S., et al., 2007. Indoor radon in rural dwellings of the south-Pannonian region. *Radiat. Prot. Dosim.*123 , pp. 378-383
- [7] Koščal, M., Menković, Lj., Knežević, M., Mijatović, M., (2005): Geomorfološka karta Vojvodine sa tumačem. Geozavod – Gemini, Beograd
- [8] Nejgebauer, V., et al., 1971. Pedološka karta Vojvodine (R 1 : 50.000). Institut za poljoprivredna istraživanja, Novi Sad
- [9] IUSS Working Group WRB, 2014: World Reference Base for Soil Resources 2014. International soil classification system for naming soils and creating legends for soil maps. World Soil Resources Reports No. 106. FAO, Rome.
- [10] Hoecker, A., et al., 2007. TMVA - Toolkit for Multivariate Data Analysis, PoS ACAT 040, arXiv:physics/070303

НИСКОФОНСКА ЛАБОРАТОРИЈА ИНСТИТУТА ЗА ФИЗИКУ

- ПРВИХ ДВАДЕСЕТ ГОДИНА -

Владимир УДОВИЧИЋ, Александар ДРАГИЋ, Радомир БАЊАНАЦ, Дејан ЈОКОВИЋ, Димитрије МАЛЕТИЋ, Никола ВЕСЕЛИНОВИЋ, Михаило САВИЋ, Давид КНЕЖЕВИЋ,

Институт за физику, Београд, Србија, banjanac@ipb.ac.rs

САДРЖАЈ

Представљена је делатност сарадника Нискофонске лабораторије од њене изградње до данас. Почетна мерења концентрације радона, интензитета космичког зрачења и фона гама зрачења временом су, методолошким приступом, прерасла у континуирани мониторинг. Статистички значајни резултати добијени након дуготрајних мерења, допуњени поузданим симулацијама и анализирани напредним мултиваријантним техникама јасно идентификују Нискофонску лабораторију у свим њеним областима истраживања.

1. УВОД

Природа овог рада је ревијална и представља ретроспективу најважнијих резултата сарадника Лабораторије током последње две деценије.

Почетак научне каријере прва три потписана коаутора практично коинцидира са изградњом подземне лабораторије и конституисањем Нискофонске лабораторије за нуклеарну физику, Института за физику. Иницијална замисао др Радована Антанасијевића и професора др Ивана Аничина о постојању референтне лабораторије за мерење малих активности и проучавање ретких нуклеарних процеса, реализована је 1997. године у оквиру Института за физику. Непроцењиву подршку двојице учитеља додатно је обогатила сарадња колеге Александра Драгића са академиком Звонком Марићем, његовим ментором на теоријским радовима, који је такође веома био заинтересован за Плазма фокус експеримент. У мерењима на тој фузијоној машини, значајна је била техничка подршка Бошка Антанасијевића, Бате Панића и др Драгутина Шевића, као и теоријски прорачуни колеге Јовице Станојевића, па је 2000. године одбрањена прва дисертација на Плазма фокус експерименту, колеге Душана Јоксимовића. После дуже паузе изазване дотрајалошћу опреме, пре неколико година покушана је ревитализација овог експеримента, ентузијазмом колега др Драгана Лукића и Мирослава Максимовића, али је процењено да она захтева значајније инвестирање.

Знања стечена на Плазма фокус експерименту употребом чврстих детектора трагова примењивана су и у првим мерењима концентрације радона у подземној лабораторији. У области детектора трагова, поред великог ауторитета др Радована Антанасијевића, оснивача и првог руководиоца Лабораторије, који је знање преносио на млађе сараднике вредно је поменути и корисне инструкције колегинице др Бојане Грабеж као и искуство професора др Јована Вуковића. То је све заједно допринело да 2006. године у Лабораторији буде одбрањена нова докторска дисертација, колеге Владимира Удовичића поново на тему Плазма фокус експеримента. Убрзо, током 2007. године придружио му се колега

Александар Драгић, одбраном дисертације са теоријским радом о позитронијуму у сарадњи са академиком Звонком Марићем.

Сарадња са професором др Иштваном Бикитом, испред новосадске лабораторије за нуклеарну физику, ПМФ-а у Новом Саду, била је драгоцену већ на почетку током емпиријске селекције радијационо чистих грађевинских материјала за градњу Лабораторије. Први резултати мерења концентрације радона током градње подземне лабораторије публиковани су већ 1999. године [1]. И током наредног периода, проблематика радона била је присутна, периодичном провером у надземној и подземној лабораторији (НЛ/ПЛ), детекторима трагова и канистрима са активним угљем. Упоредо са постепеним опремањем Лабораторије потребном инструментацијом, предност су добијале две примарне области. Најпре је 2001. године иницијативом професора др Ивана Аничина, уз подршку његових асистената др Јована Пузовића и др Горана Шкоре, и виспиреним саветима професора др Ђуре Крмпотића у Институту за физику покренута проблематика физике космичког зрачења. Тих година Лабораторија је остала без неколицине сарадника, а непроцењив је био губитак великог Радета, др Радована Антанасијевића нашег драгог шефа, и Лабораторија од те 2003. године носи његово име. Лабораторију су у кратком периоду напустили Драгутин Шевић, Бошко Антанасијевић, Надежда Антанасијевић, Зорка Продановић и Јовица Станојевић, али је стигло и прво појачање. Колега Дејан Јоковић се од самог почетка укључио у покретање проблематике космичког зрачења на којој је магистрирао, а 2011. године и докторирао.

Основна намена надземних или плитко укопаних нискофонских лабораторија је мерење малих активности, било узорака из природе или вештачки обогаћених (НОРМ и ТЕНОРМ), пошто је низак фон обрнуто пропорционалан осетљивости мерења или минималној детектабилној активности мереног узорка. Фон је најчешће синоним за фон гама зрачења којим се, пошто је моноенергетско, јасно идентификује одређени радио изотоп. За мерење гама зрачења најчешће су у употреби германијумски детектори, са ултимативним захтевима за радијационо чистим криостатом, што веће активне запремине (ефикасности), и смештене у одговарајућој пасивној заштити (најчешће олову). Високо осетљива мерења фона, којима се фундаментално истражују ретки процеси (двоструки бета распада и тамна материја) спроводе се у дубоким подземним лабораторијама у којима је минимизован утицај космичког зрачења. Ипак, и плитко укопане лабораторије могу послужити у анализи оних компоненти фона које генерише космичко зрачење (због боље статистике), а које су релевантне у високо осетљивим мерењима у дубоким лабораторијама, као и у селекцији радијационо чистих материјала који се уграђују у инструментацију тих високо осетљивих истраживања. Главни циљ, анулирање нуклеонске компоненте космичког зрачења, присутне на површини и све до око 15 метара воденог еквивалента (м.в.е), постигнуто је укопавањем земунске лабораторије у десну обалу Дунава. Добијено је 12 метара заштитног слоја земље, леса (еквивалентног са 25 метара воде) па је и најпродорнија компонента космичког зрачења, наелектрисани миони, редукована интегрално скоро 4 пута.

Први резултат релативног смањења флукса миона, подземне у односу на надземни простор (око 4 пута), добијен је двома техникама, пластичним сцинтилатором NE102 и преносним германијумским детектором (рел. ефикасности 20%). На жалост, овај први Ge детектор, позајмљен из Винче, није био од користи за нискофонска мерења због његове радијационе запрљаности услед рада на мониторингу

реакторских неутрона. У прво време, Лабораторија је располагала и планарним Ge(Li) детектором, добијеним од колега из Новог Сада, којим се могао детектовати тек нискоенергетски део фона амбијенталног гама зрачења, до око 200keV. Поред доминантних Pb-X пикова, од оловног оклопа, јасно се издвајала линија од урана 238 (тачније његовог првог потомка Th-234) на 63.3keV, што је послужило за први чланак о анализи узорака са ураном [2]. Током годину дана и непосредно пре набавке првог и још увек јединог германијумског детектора у Лабораторији, у подземној лабораторији је био у употреби још један позајмљени Ge детектор, из Лабораторије за заштиту од зрачења из Винче, а у циљу компаративних мерења истих узорака.

2. ПРОБЛЕМАТИКА КОСМИЧКОГ ЗРАЧЕЊА

Прегледни рад, из 2011. године, [3], садржи и детаље конструкције саме подземне лабораторије и описа њеног радног режима, па ће се надаље прича фокусирати на три доминантне области истраживања у Лабораторији. Хронолошки, прва област којом смо се бавили од 2001. године је космичко зрачење, и још увек је област која је предмет интересовања највећег броја сарадника.

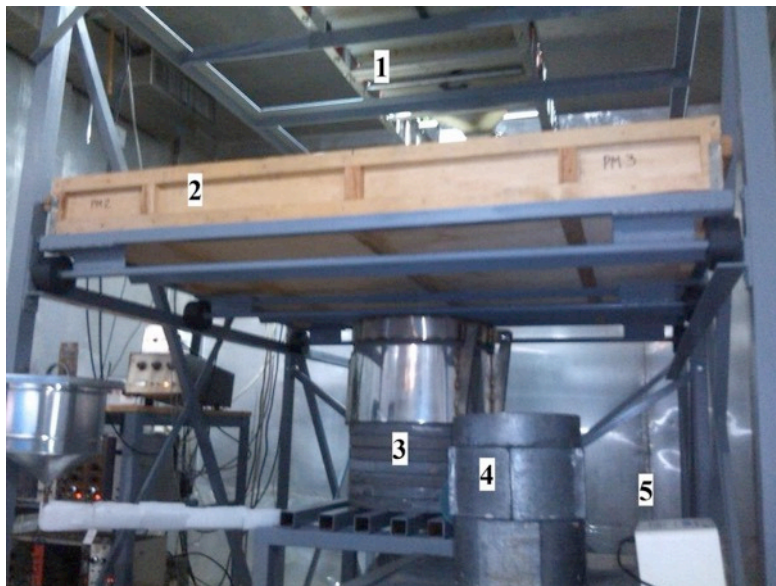
Континуирани мониторинг интензитета космичког зрачења у НЛ/ПЛ, траје непрекидно од 2002. године до данас, у почетку са два једнака пластична сцинтилатора мале површине. Мали пластици, како их називамо, стигли су у Србију из Дубне, 1994. године, ентузијазмом професора Аничина и Миодрага Крмара. Детектори су комплетирани у нашој Лабораторији, спајањем сцинтилатора са светловодом и по једним фотомултипликатором. И данас су у функцији са још увек беспрекорном дискриминацијом мионског ΔE пика од нискоенергетског космичког и гама зрачења. Први резултати редом су представљани на светским, Јапан, 2003, Индија, 2005. и европским конференцијама о космичком зрачењу, Италија, 2004. и Португалија 2006. године [4]. На послетку, прецизно одређен флуks космичких миона, први пут на нашим географским ширинама и дужинама, публикован је у [5]. Крајем 2005. године, сналажљивошћу колеге Драгића, у склопу набавке германијумског детектора, успели смо значајно да подигнемо квалитет мерења космичког зрачења, набавком два идентична, 8 пута по површини већа сцинтилатора. Боља статистика мерења значила је и упуштање у временску спектоскопију космичког зрачења, посебно након набавке првог дигиталног анализатора (CAEN), 2008. године, иако су и до тада анализиране временске серије и периодограми космичких података, [6].

Од прошле године у новој просторној конфигурацији расположивих пластичних сцинтилатора (названог ASYMUT, што је асиметрични мион телескоп), отвара се могућност енергетски диференцираног праћења процеса соларне модулације космичког зрачења, слика 1.

Много значајније за потенцијал Лабораторије од скромног опремања хардвером, јесте трансфер поново из Винче, овог пута колеге Димитрија Малетића, препоруком нашег професора Ивана. Његово велико знање стечено на CMS експерименту у CERN-у, на коме је и докторирао 2009. године, посебно софтверских алата, оснажило је способности групе да се применом ново развијених софтвера, на адекватан начин анализира све богатија база космичких података.

У Лабораторији је реализовано десетак дипломских радова, али се од млађих тек колега Никола Веселиновић, радећи најпре дипломски на теми плазма фокуса са

колегом Удовичићем, касније „усудио“ да анализира поменућу базу космичких података те тако управо ове године приводи рад на својој дисертацији. Његовим стопама је, најпре радећи дипломски рад о CAEN дигиталном анализатору, кренуо и колега Михаило Савић, па се ускоро може очекивати још једна дисертација из области космичког зрачења, [7].



Слика 1. ASYMUT конфигурација у подземној лабораторији, 1-мали пластици, 2-велики пластик, 3-Ge детектор у Pb заштити, и додатно 4-NaI детектор у Pb заштити, 5-радонометар

3. НИСКОФОНСКА ГАМА СПЕКТРОМЕТРИЈА

После 8 година од отварања, у Лабораторију је стигао германијумски детектор, у стандардној вертикалној геометрији криостата који је изабран да буде од нискофонских материјала. Релативне ефикасности од 35% и номиналне енергетске резолуције 1,72 keV, детектор је представљао изврстан инструмент за детаљно упознавање са свим компонентама фона гама зрачења у амбијенту подземне лабораторије. У почетку је пасивна заштита била недовољна, бст олова непознате историје (у смислу његовог порекла и старости). Неколико година касније после процене да је оптимална дебљина заштите 12 cm олова, опет уз помоћ колега из Новог Сада, изливени су дискови укупне масе око 900 килограма од довољно старог олова за које је процењен садржај Pb-210 око 25 Bqkg^{-1} . Већ је поменута тријажа грађевинских материјала у смислу избора оних са минималном концентрацијом урана, торијума и калујума 40, а за њом је следило зналачко пројектовање вентилационог система који је од највећег значаја за подземне лабораторије. Без њега, спонтана акумулација радона достиже два реда већу концентрацију па би у фонском спектру доминирале бројне пострадонске линије уз њихово интензивно варирање у времену. Непрестаним изменама целокупног ваздуха у подземној лабораторији (запремине око 130 m^3) скоро 4 пута на сат, и филтрацијом ваздуха на улазу у систем у два степена, прво филтером за праšину а потом и великим (око 50 kg) адсорберским филтером са активним угљем, концентрација радона је смање-

на на око 10 Bqm^{-3} . Временом је процењено да је и достигнутих 20 Bqm^{-3} довољно ниско, штедећи на честим заменама великог филтера. Поред филтрације, разликом у брзини упумпавања чистог и испумпавања радоном запрљаног ваздуха, пројектован је и надпритисак од преко 2 mbar -а, који спречава дифузију радона кроз евентуалне пукотине из алуминијумом пресвучених зидова и додатно доприноси релативној стабилности концентрације радона.

Још у пројектовању прве конфигурације са великим пластицима (1 m^2), реализована је вето-активна заштита Ge детектора, са растојањем оловног поклопаца до коаксијално постављеног великог пластика од око 60 cm . Управо је тежак оловни поклопац и начин приступа самом Ge детектору, захтевао релативно велико растојање што је због широке угаоне расподеле миона ($\cos^2\theta$) значајно умаљило учинак вето детектора. Континуирани мониторинг космичког зрачења и упоредо временска спектроскопија пружали су могућност да се у антикоинцидентном режиму смањи фон одбацујући део догађаја детектован у вету, док се у коинцидентном режиму управо анализирао део фонског спектра генерисан од стране космичког зрачења. Први резултати су представљени у [3]. Посебно је занимљива процена флукса неутрона генерисаних од миона у олову, који се детектују преко закаснелих коинциденција њиховом интеракцијом на изотопима германијума, [8]. Поменута ASYMUT конфигурација, слика 1, значајно је побољшала геометрију два детектора па се очекује и значајно нижи интегрални фон и интензитет анихилационе линије у вето режиму. Пре тога, карактеристике фона после дужег мерења представљене су у [9].

Током година континуираног мерења, било је од значаја анализирати утицај варијације радона и космичког зрачења на варијације фона, пошто су варијације фона у спрези са систематском грешком мерења малих активности. Мерења су сукцесивно обављана у обе лабораторије НЛ и ПЛ, и показана је очигледна предност остварених нискофонских услова у подземној лабораторији, [10]. Ово је била и тема дисертације колеге Радомира Бањанца, одбрањене 2011. године.

Нискоенергетски део спектра фона германијумских детектора истраживан је и са аспекта утицаја „skyshine“ радијације у односу на конкурентски допринос космичког зрачења. Миони космичког порекла производе континуирани спектар губитака енергије који има максимум интензитета на високим енергијама, реда неколико десетина MeV , која је најчешће изван области интересовања, али дају допринос и у нискоенергетској области. Свеукупни инструментални фонски спектри одликују се изразитим максимумом, који је у зависности од величине детектора у близини 100 keV . Интензитет, природа и порекло фона у овој енергетској области испитивано је апсорпционим мерењима и закључено је да је зрачење континуираног спектра двојаког порекла. Једним делом оно представља расејано и деградирано зрачење електромагнетне компоненте космичког зрачења, док другим делом представља од целокупне околине расејано зрачење терестријалног порекла, често познатог под називом „skyshine radiation“, [11].

Важно је поменути, као што је случај и код проблематике космичког зрачења, да се у анализама фона неизоставно користе симулациони пакети, најчешће церновски GEANT4, [12], и у области космичког зрачења, CORSICA.

4. ДЕТЕКЦИЈА РАДОНА

Радон је свуда присутан јер је по природи гас па дифундује и кроз зидове лабораторија, при томе је и инертан па га је тешко филтрирати и хемијски изоловати. У нискофонској гама спектрометрији увек својим релативно кратким животом, генерише значајну активност потомака који потом својим распадањем продукују мноштво пострадонских гама линија, посебно Рb-214 и Bi-214. Један од начина детекције радона је управо анализом интензитета пострадонских линија након што је сам радон адсорбован у канистрима са активним угљем. Време акумулације је обично 2 дана, а још једна, тзв. пасивна метода је пребројавање трагова од радонових алфа честица у чврстим детекторима (CR-39 и LR-115) после времена експонирања од најмање 3 месеца. Већ је поменуто да радон као сметња у нискофонским мерењима осим што генерише непријатан фон у виду мноштва гама линија и припадајућег Комптоновског континуума, додатно утиче у варијацији, најчешће дневној, истих линија. Начин да се поузданије процени утицај овог варирања јесте активна метода детекције радона која у реалном времену сакупља податке, концентрације радона као и релевантних метеоролошких параметара, температуре и релативне влажности ваздуха. Од 2008. године Лабораторија располаже једним таквим бројачем, радонометром, који је далеко јефтинији од активних спектрометара (Rad7 и AlphaGuard), али подједнако прецизан. Дуготрајним мониторингом у амбијенту подземне лабораторије, радонометар је потврдио очекивано дневно варирање али показао и сезонску варијацију радона, [13].

Активни уређај пружио је и могућност примене напредних мултиваријантних техника анализе, које се успешно тренирају на актуелно измереној бази података радона и метео параметара, и потом успешно врше предикцију динамике радона у контролисаним условима подземне лабораторије, [14].

Већ неколико година активан је сајт, <http://cosmic.ipb.ac.rs/index.html>, наше Лабораторије са линковима на ажуриране податке мерења космичког зрачења, <http://147.91.87.156/cgi-bin/bcrs> и евалуационе концентрације радона у ПЛ, http://147.91.87.156/nf-cosmic/rad3/Radon_alarm/.

Знањем стеченим применом разноликих техника детекције радона, не само унутар ПЛ/НЛ простора већ систематски и у реалном амбијенту ван лабораторија, [15], уз подршку Агенције за јонизујућа зрачења и нуклеарну сигурност Републике Србије, и реализовану преко ИАЕА фондова, нови руководиоца Лабораторије др Владимир Удовичић успешно је координирао великом кампањом мапирања радона и добијањем прве радонске мапе Србије 2016. године, [16].

5. УМЕСТО ЗАКЉУЧКА

Надајући се да ће се кроз 10 или 20 година поново пружити прилика писању рада сличног садржаја, очекујући напослетку боље опремање Лабораторије хардвером и уз задржавање високог нивоа ентузијазма сарадника, сматрамо досадашње ангажовање успешним, а постојање наше Лабораторије оправданим.

Ово је прилика да се присетимо непосредније сарадње током ових двадесет година и са колегама из Винче, Милојком Ковачевићем, Зором Жунић, Иваном Вуканац, Драганом Тодоровић, Јеленом Крнета Николић, Предрагом Ујићем, и колегама из Новог Сада Миодрагом Крмаром, Софијом Форкапић и Николом Јованчевићем. Управо је наш најмлађи сарадник, Давид Кнежевић, долазећи из јаке новосадске школе нуклеарне физике додатна нада у покретање нових тема.

Наравно, ту је и велики број наших колега из самог Института за физику, заинтересованих за наш рад од којих се од самог формирања Лабораторије у сваком афирмативном смислу истиче др Александар Белић.

Може се ипак закључити да су почетна мерења концентрације радона, интензитета космичког зрачења и фона гама зрачења временом, методолошким приступом, прерасла у континуирани мониторинг. Статистички значајни резултати добијени након дуготрајних мерења, допуњени поузданим симулацијама и анализирани напредним мултиваријантним техникама јасно идентификују Нискофонску лабораторију у свим њеним областима истраживања.

На крају, као и сваком приликом, радо се сећамо нашег драгог професора Ивана Аничина који је у најтеже време, када је опстанак Лабораторије био угрожен, али и након одласка у пензију, својом харизмом, неограниченим знањем и свеprisутном љубављу међу нама надахњивао истраживачки дух и одржавао јединство свих сарадника Лабораторије.

6. ЛИТЕРАТУРА

- [1] R. Antanasijević, I. Aničin, I. Bikit, R. Banjanac, A. Dragić, D. Joksimović, Đ. Krmpotić, V. Udovičić, J.B. Vuković Radon measurements during the building of a low-level laboratory Radiation Measurements 31, (1999) 371
- [2] I. Aničin, R. Banjanac, A. Dragić, D. Joković, V. Udovičić, Investigation of the Uranium Solubility and Absorption Physica Scripta T118 (2005) 39-40
- [3] Aleksandar Dragić, Vladimir Udovičić, Radomir Banjanac, Dejan Joković, Dimitrije Maletić, Nikola Veselinović, Mihailo Savić, Jovan Puzović, Ivan V. Aničin. The new set-up in the Belgrade low-level and Cosmic-ray laboratory. *Nuclear Technology and Radiation Protection Vol. XXVI, No. 3, 181-192 (2011)*
- [4] (a) J. Puzović, A. Dragić, V. Udovičić, D. Joković, R. Banjanac, I. Aničin, Analysis of continuous cosmic ray measurements in Belgrade *Proceedings of 28th International Cosmic Ray Conference 1199-1202, Japan, (2003)*
(б) A. Dragić, R. Banjanac, V. Udovičić, D. Joković, J. Puzović, I. Aničin, Variations of CR-Muon Intensity in the Declining Phase of the 23rd Solar Cycle in Ground and Shallow Underground Data *Proceedings of 29th International Cosmic Ray Conference 101-104, Pune, India, (2005)*
(в) A. Dragić, R. Banjanac, V. Udovičić, D. Joković, I. Aničin, J. Puzović, Comparative Study of Power Spectra of Ground and Shallow Underground Muon Data *Proceedings of 19th European Cosmic Ray Symposium (Published in International Journal of Modern Physics A 29 (2005) 6953-6955), Florence, Italy, (2004)*
(г) A. Dragić, R. Banjanac, V. Udovičić, D. Joković, I. Aničin, J. Puzović, Diurnal and seasonal variations of CR-muon intensity in the declining phase of the 23rd solar cycle in ground and 25 m.w.e. underground data at 45oN *Proceedings of 20th European Cosmic Ray Symposium, Lisbon, Portugal, (2006), <http://www.lip.pt/events/2006/ecrs/proc/ecrs06-s2-76.pdf>*
- [5] A. Dragić, D. Joković, R. Banjanac, V. Udovičić, B. Panić, J. Puzović, I. Aničin. Measurement of cosmic ray muon flux in the Belgrade ground level and

- underground laboratories *Nuclear Instruments and Methods in Physics Research A* 591 (2008) 470-475
- [6] A. Dragić, R. Banjanac, V. Udovičić, D. Joković, J. Puzović, I. Aničin Periodic Variations of CR Muon Intensity in the Period 2002-2004. *Proceedings of the 21st European Cosmic Ray Symposium, Košice, Slovakia (2008)* 368-373.
- [7] (a) N. Veselinović A. Dragić, M. Savić, D. Maletić, D. Joković, R. Banjanac, V. Udovičić. Utilization of a shallow underground laboratory for studies of the energy dependent CR solar modulation. *XXV European Cosmic Ray Symposium, Torino, Sept. 4-9 (2016)*
 (б) M. Savić, A. Dragić, N. Veselinović, V. Udovičić, R. Banjanac, D. Joković, D. Maletić. Effect of pressure and temperature corrections on muon flux variability at ground level and underground. *XXV European Cosmic Ray Symposium, Torino, Sept. 4-9 (2016)*
- [8] (a) A Dragić, I Aničin, R Banjanac, V Udovičić, D Joković, D Maletić, M Savić, N Veselinović and J Puzović. Neutrons produced by muons at 25 mwe. *Proceedings of the 23rd European Cosmic Ray Symposium (and 32nd Russian Cosmic Ray Conference), Moscow, Russia, July 3 - 7, (2012), J. Phys.: Conf. Ser. 409 012054* doi:10.1088/1742-6596/409/1/012054.
 (б) N. Veselinović, D. Maletić, D. Joković, R. Banjanac, V. Udovičić, M. Savić, J. Puzović, I.V. Aničin, A. Dragić. Some peculiarities of digital gamma-ray spectroscopy with germanium detectors. performed in presence of neutrons. *GAMMA-2 Scientific Workshop on Nuclear Fission Dynamics and the Emission of Prompt Neutrons and Gamma Rays, 24 – 26 September 2013, Sremski Karlovci, Serbia. Physics Procedia, 59, pp. 63-70 (2014)*
- [9] Radomir Banjanac, Vladimir Udovičić, Dejan Joković, Dimitrije Maletić, Nikola Veselinović, Mihailo Savić, Aleksandar Dragić, Ivan Aničin. Background spectrum characteristics of tfe HPGe detector long-term measurements in the Belgrade low-background laborator.y *Proceedings of Third International Conference on Radiation and Dosimetry in various fields of Research, RAD2015, JUNE 8 – 12, 151-153 (2015)*
- [10] R. Banjanac, A. Dragić, V. Udovičić, D. Joković, D. Maletić, N. Veselinović, M. Savić. Variations of Gamma-Ray Background in the Belgrade Shallow Underground Low-Level Laboratory. *Applied Radiation and Isotopes, 87 (2014)* 70-72 <http://dx.doi.org/10.1016/j.apradiso.2013.11.091>
- [11] R. Banjanac, D. Maletić, D. Joković, N. Veselinović, A. Dragić, V. Udovičić, I. Aničin. On The Omnipresent Background Gamma Radiation Of The Continuous Spectrum. *Nuclear Instruments and Methods in Physics Research A 745 (2014) pp. 7-11* <http://dx.doi.org/10.1016/j.nima.2014.01.065>
- [12] D. R. Joković, A. Dragić, V. Udovičić, R. Banjanac, J. Puzović, I. Aničin. Monte Carlo simulations of the response of a plastic scintillator and an HPGe spectrometer in coincidence. *Applied Radiation and Isotopes 67 (2009) 719-722*
- [13] (a) V. Udovičić, B. Grabež, A. Dragić, R. Banjanac, D. Joković, B. Panić, D. Joksimović, J. Puzović, I. Aničin. Radon problem in an underground low-level laboratory. *Radiation Measurements 44 (2009) 1009-1012*
 (б) Udovičić V., Aničin I., Joković D., Dragić A., Banjanac R., Grabež B., Veselinović N. Radon Time-series Analysis in the Underground Low-level Laboratory in Belgrade, Serbia. *Radiation Protection Dosimetry 145 (2-3) (2011):155-158*

- (b) V. Udovičić, J. Filipović, A. Dragić, R. Banjanac, D. Joković, D. Maletić, B. Grabež and N. Veselinović. Daily and Seasonal radon variability in the underground low-background laboratory in Belgrade, Serbia. *Radiation Protection Dosimetry* 160 (1-3): pp. 62-64 (2014)
- [14] (a) Dimitrije M. MALETIĆ, Vladimir I. UDOVIČIĆ, Radomir M. BANJANAC, Dejan R. JOKOVIĆ, Aleksandar L. DRAGIĆ, Nikola B. VESELINOVIĆ, and Jelena Z. FILIPOVIĆ. Comparison of multivariate classification and regression methods for the indoor radon measurements. *Nuclear Technology and Radiation Protection Vol. XXIX, No. 1, 17-23 (2014)*
- (b) D. M. Maletić, V. I. Udovičić, R. M. Banjanac, D. R. Joković, A. L. Dragić, N. B. Veselinović, J. Filipović. Correlative and Multivariate analysis of increased radon concentration in underground laboratory. *Radiation Protection Dosimetry*, 162 (1-2): pp. 148-151 (2014) doi:10.1093/rpd/ncu248
- [15] Vladimir Udovicic, Dimitrije Maletic, Jelena Zivanovic, Aleksandar Dragic, Radomir Banjanac, Dejan Jokovic, Sofija Forkapic. Long-term indoor radon measurements in a family house – a case study in Serbia. In: *Book of Abstracts of 8th Conference of Protection against Radon at Home and at Work, 12 - 14 of September 2016, Prague, Czech Republic, Book of Abstracts, pp. 79*
- [16] Udovičić V, Maletić D, Eremić Savković M, Pantelić G, Ujić P, Čeliković I, Forkapić S, Nikezić D, Marković V, Arsić V, Ilić J, Nilsson P. Preliminary results of the first national indoor radon survey in Serbia. In: *Book of Abstracts of 8th Conference of Protection against Radon at Home and at Work, September 12-14, 2016; Prague, Czech Republic.*

LOW-BACKGROUND LABORATORY FOR NUCLEAR PHYSICS IN THE INSTITUTE OF PHYSICS -THE FIRST TWENTY YEARS OF EXISTENCE-

Vladimir UDOVIČIĆ, Aleksandar DRAGIĆ, Radomir BANJANAC, Dejan JOKOVIĆ, Dimitrije MALETIĆ, Nikola VESELINOVIĆ, Mihailo SAVIĆ, David KNEŽEVIĆ

Institute of Physics, Belgrade, Serbia, banjanac@ipb.ac.rs

ABSTRACT

The most important scientific activities in the Low-background laboratory are described for the entire period of its existence. Over the period of twenty years, initial measurements of radon concentration, cosmic-rays intensity as well as gamma radiation background through metodological approach evolved into consistent continual monitoring. Statistically significant results obtained by long-term measurements, enriched by reliable simulation and analyzed using advanced analysis tools clearly identify our Lab.

MONTE KARLO SIMULACIJA FONA HPGe DETEKTORA OD RADIONUKLIDA, KOSMIČKOG I SKYSHINE ZRAČENJA

Dimitrije MALETIĆ, Vladimir UDOVIČIĆ, Dejan JOKOVIĆ, Radomir BANJANAC, Aleksandar DRAGIĆ, Mihailo SAVIĆ, Nikola VESELINOVIĆ

Institut za fiziku, Univerzitet u Beogradu

SADRŽAJ

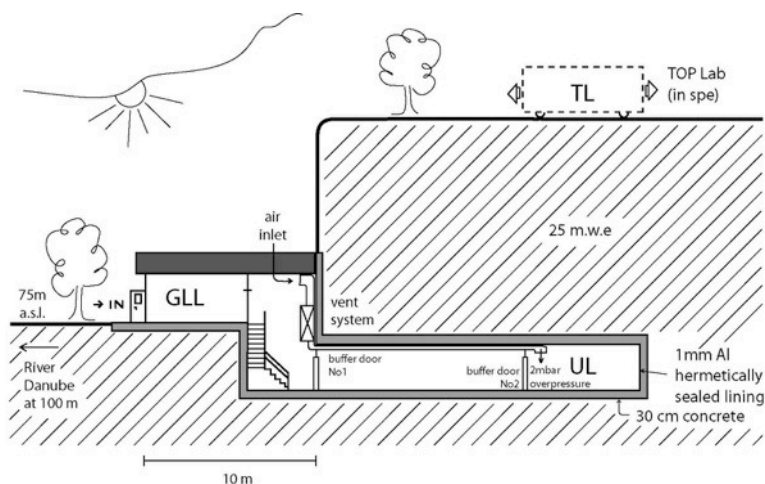
U Niskofonskoj laboratoriji za Nuklearnu fiziku, više godina se izučavaju osobine fona HPGe detektora. Izučavanje fona važno je za eksperimente sa malim brojem interesantnih događaja ili retkih procesa u podzemnim laboratorijama. Izučavanja fona u Niskofonskoj laboratoriji započeta su izučavanjem fona zračenja od radionuklida, kao i fona od kosmičkog zračenja, koincidentnim tehnikama. Nedavno je izučavan i fon od skyshine zračenja. U ovom radu je predstavljena Monte Karlo simulacija fona HPGe detektora koji dolazi od pomenuta tri izvora zračenja. Rezultati simulacija kosmičkog zračenja odlično se slažu sa eksperimentalnim rezultatima, dok se za druge komponente mogu poboljšati. Postoji prednost simulacija koje daju razloženi fon na tri komponente, koja omogućava da se rezultati simulacija tri komponente fona za jednu laboratoriju mogu simulirati za druge podzemne ili nadzemne laboratorije menjanjem parametara u simulacionim programima. Fon se može simulirati za laboratorije koje mogu biti na različitoj geografskoj širini, nadmorskoj visini, sa različitim sastavom radionuklida u zemljištu i geometrijom laboratorije u kojoj se vrše merenja. Predstavljani su nedostaci simulacija i da se rezultati mogu poboljšati radeći na detaljima u nekoliko faza simulacije.

1. UVOD

U Niskofonskoj laboratoriji za Nuklearnu fiziku u Institutu za fiziku Beograd, vrše se merenja komponentata zračenja prirodnog fona [1]. Prvenstveno se vrše merenja gama zračenja HPGe detektorom sa i bez olovne zaštite, takodje se vrši kontinualno merenje mionske komponente kosmičkog zračenja korišćenjem plastičnih scintilatora površine od po jednog kvadratnog metra, i to i u nadzemnoj i podzemnoj laboratoriji, kao i merenje radona aktivnim i pasivnim metodama, prvenstveno u podzemnoj laboratoriji. Podzemna laboratorija se nalazi 12 metara pod zemljom, što se predstavlja kao da se merenja vrše ispod vodenog absorbera visine od 25 metara, slika 1. Ekvivalencija je dobijena poznavajući sastav zemljišta, odnosno lesa koji je karakterističan za područje Zemuna. Pored merenja, u ovom radu se koriste i Monte Karlo simulacije, koje služe za poredjenje simulacija sa eksperimentalnim rezultatima, ili služe za izučavanje pojedinih komponentata fona. Monte Karlo simulacioni program koji se koristi je programski paket Geant4 [2], razvijen za potrebe simulacije prolaska čestica kroz materiju, odnosno za simulaciju deponovane energije i odziva detektora. Geant4 programski paket je najrašireniji programski paket za Monte Karlo simulacije i razvija se u CERN-u, prvenstveno za potrebe eksperimenata iz Fizike elementarnih čestica. Za simulacije kosmičkog zračenja koristi se programski paket CORSIKA [3] razvijen za potrebe eksperimenata koji izučavaju mionsku i elektromagnetnu komponentu visokoenergetskih kaskada koje se dobijaju upadom visokoenergetskih čestica primarnog kosmičkog zračenja koje interaguje sa atmosferom Zemlje. Ovaj programski paket razvijen je za potrebe Kaskade

eksperimenta u Tehnološkom institutu Karlsruhe, u Nemačkoj. Za potrebe korišćenja oba ova programa za namenu simulacija odgovora plastičnih scintilatora i HPGe detektora, u Niskofonskoj laboratoriji je razvijen poseban interfejs program koji omogućuje da se rezultati CORSIKA simulacija koriste u Geant4 simulacijama detektora u Niskofonskoj laboratoriji. Detaljno izučavanje prirodnog fona upotpunjeno je i simulacijama skyshine zračenja. Skyshine gama zračenje do HPGe detektora dolazi ne direktnom linijom od radionuklida iz zemljišta i građevinskog materijala, već odbijanjem i rasejanjem gama zračenja od atome okolnog vazduha, tj. atmosfere. U Niskofonskoj laboratoriji je izučavana meka komponenta gama spektra kojeg dobijamo merenjima HPGe detektorom, i zaključeno je da ona dolazi dominantno od skyshine zračenja, a manji deo od kosmičkog zračenja [4]. Simulacije skyshine zračenja su veoma zahtevne u pogledu kompjuterskog vremena za simulacije, pa je poželjno simulacije raditi na kompjuterskim klasterima.

Cilj ovog rada je predstavljanje eksperimentalnih rezultata fona HPGe detektora koji dolazi od radionuklida, kosmičkog zračenja i skyshine zračenja, poredjenje sa Monte Karlo simulacijama, i predstavljanje načina kombinovanja ove tri komponente fona za različita merena mesta.



Slika 1. Grafički prikaz preseka Niskofonske laboratorije za Nuklearnu fiziku

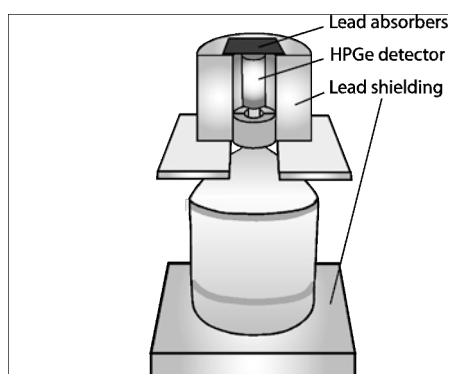
2. EKSPERIMENTALNA POSTAVKA

Eksperimentalna postavka u podzemnoj i nadzemnoj laboratoriji je identična i sastoji se od HPGe detektora u olovnoj zaštiti, koja je otvorena na gore, ili se kao „krov“ stavljaju tanki apsorberi, slika 2. Iznad HPGe detektora nalazi se plastični scintilator, koji koristi kao veto zaštita ako je postavljen u anti-koincidentnom modu, ili izdvaja komponentu u HPGe detektoru koju dobijamo od kosmičkog zračenja, ako je scintilator postavljen u koincidentnom modu, što je slučaj u ovom radu. Prikupljanje podataka se vrši analogno-digitalnom konverter karticom, koji zapise signala oba detektora šalje na računar. Potom se (off-line) vrši koincidiranje signala i obraduju rezultati.

3. MONTE KARLO SIMULACIJE

Simulacije počinju programskim paketom CORSIKA, zadavanjem komponenata primarnog kosmičkog zračenja koje upada na atmosferu Zemlje od 90% protona i 10%

alfa čestica. Ovo primarno kosmičko zračenje sudara se sa jezgrima atoma vazduha u atmosferi i produkuje sekundarno kosmičko zračenje, koje ima mionsku, elektromagnetnu i hadronsku komponentu koja se sastoji od protona, neutrona i rezultujućih jezgara koji brzo gube energiju u vazduhu. Kao parametri simulacija zadaje se nadmorska visina na kojoj se nalaze detektori u Niskofonskoj laboratoriji, kao i geografska dužina i širina laboratorije. Na ovaj način se za svako merno mesto zadaju različiti parametri i simulacija ima različite spektre za različita merna mesta (laboratorije). Potom se vrši ili simulacija Geant4 programskim paketom i to plastičnog scintilatora i HPGe detektora u olovnoj zaštiti ili simulira prolaz kosmičkog zračenja kroz 12 metara zemlje, pa onda simulira odgovor plastičnog scintilatora i HPGe detektora u podzemnoj laboratoriji.



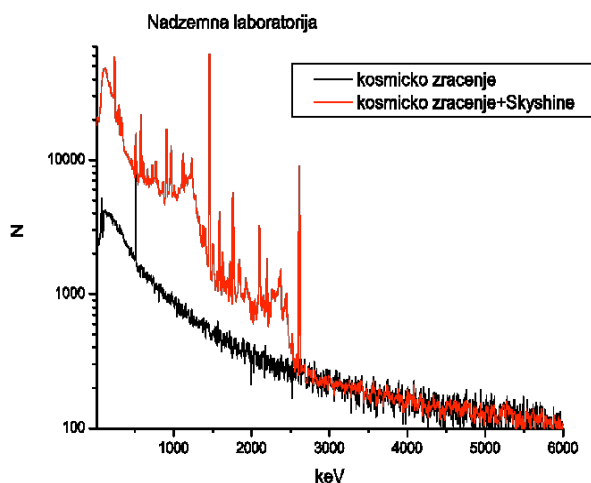
Slika 2. Prikaz postavke HPGe detektora i olovne zaštite otvorene na gore, sa tankim apsorberom na vrhu

Skyshine simulacije se vrše programskim paketom Geant4. Kao ulaz u simulaciju, koristi se pripremljeni set čestica sa pripadajućom energijom koji dolazi iz zemlje i okolnog materijala. Set čestica se priprema tako što se prvo iz snimljenog eksperimentalnog spektra HPGe detektora, uz poznavanje njegove krive efikasnosti, određuje odnos intenziteta linija radionuklida iz okoline. Potom ovi podaci služe za određivanje frekvencije pojavljivanja čestica zračenja od pojedinih radionuklida, što predstavlja ulaz u Geant4 simulaciju (generator primarnih čestica). Za nastavak simulacije, potrebno je definisati dimenzije i položaj zidova mernog mesta (laboratorije), kako bi se definisala zapremina vazduha i položaj zidova od kojih se zračenje radionuklida rasejava - što je i definicija skyshine zračenja. Simulirani spektar HPGe detektora od radionuklida sa uključenim skyshine zračenjem prikazan je na slici 3.

3. REZULTATI I DISKUSIJA

Monte Karlo simulacioni spektar HPGe detektora u koincidenciji sa scintilacionim veto detektorom u nadzemnoj laboratoriji, koji je predstavljen u ovom radu, dobijen je u dva koraka. Prvi korak se sastoji u simulaciji primarnog kosmičkog zračenja programskim paketom CORSIKA do nadmorske visine laboratorije (sekundarno kosmičko zračenje). Drugi korak je simulacija interakcije sekundarnog kosmičkog zračenja sa HPGe detektorom, a koje ujedno prolazi i kroz veto detektor (koincidentni signal). Drugi korak se simulira korišćenjem Geant4 programskog paketa. Simulacioni spektar HPGe detektora u koincidenciji sa scintilacionim veto detektorom u nadzemnoj laboratoriji prikazan je na slici 3, (crna boja, spektar sa nižim odbrojem), a odlično se slaže sa eksperimental-

nim koincidentnim spektrom. Simulacioni spektar HPGe detektora koji sadrži doprinos od simulacije kosmičkog zračenja i simulacije skyshine zračenja prikazan je na slici 3 (crvena boja, spektar sa višim odbrojem).



Slika 3. Simulacioni spektar HPGe detektora sa doprinosom kosmičkog zračenja i skyshine i samo doprinosom kosmičkog zračenja – nadzemna laboratorija

Sličnost simulacionog i eksperimentalnog spektra u prikazanim prvim rezultatima nije zanemarljiva. Iako simulacioni spektar u značajnoj meri ne odgovara eksperimentalnom, treba istaći da postoji dosta mesta za unapređenje i popravku simulacije. Prvi rezultati ohrabruju, i treba nastaviti sa detaljnijim simulacijama da bi se poboljšalo slaganje eksperimenta i simulacije.

Nedostaci prvih rezultata simulacija odgovora HPGe detektora na skyshine simulacije u velikoj meri dolaze od toga što je odnos intenziteta linija određen samo po maksimumu linija a ne integralu linija, potom nedostaci dolaze od toga što je kriva efikasnosti HPGe detektora dobijena simulacijama tačkastih izvora, zanemarujući da zračenje dolazi iz cele polu-sfere iznad detektora, slika 2. Potom nedostaci dolaze od toga što je geometrija laboratorijskih zidova i materijala bila veoma aproksimativna i pojednostavljena, kao i da su u cilju ubrzavanja simulacija, kako bi se dobio prvi rezultat, odabrani pojednostavljeni modeli niskoenergetskih interakcija u Geant4 programskom paketu.

4. ZAKLJUČAK

U ovom radu su prikazani prvi rezultati Monte Karlo simulacija odgovora HPGe detektora na upadno kosmičko zračenje, doprinos od radionuklida iz okoline i doprinos od skyshine zračenja. Rezultati simulacija kosmičkog zračenja dobro se slažu sa eksperimentalnim rezultatima. Prednost simulacija koje daju razloženi fon na tri komponente, omogućavaju da se rezultati simulacija neke od tri komponente fona za jednu laboratoriju mogu koristiti za druge podzemne ili nadzemne laboratorije. Na primer, ako je HPGe detektor sličan i nalazi se u sličnoj zaštiti ali drugoj laboratoriji može da se koriste postojeći rezultati simulacija na doprinos od radionuklida i skyshine zračenja, potom ako su laboratorije na sličnoj geografskoj širini i dužini i nadmorskoj visini može se koristiti ista simulacija doprinosa od kosmičkog zračenja. Delovi simulacija koji ne mogu da se koriste ponovo, simuliraju se koristeći iste simulacione

programime samo sa modifikovanim parametrima (nadmorska visina, geometrija laboratorije i dr.). Tako se fon koji dolazi od kosmičkog zračenja može simulirati za laboratorije koje mogu biti na različitoj geografskoj dužini i širini i nadmorskoj visini menjanjem parametara u simulaciji CORSIKA programskim paketom). Ako laboratorije imaju različit sastav radionuklida u zemljištu i različitu geometriju laboratorije u kojoj se vrše merenja, simulira se modifikovanjem postavki Geant4 programa za simulaciju HPGe detektora. U radu su predstavljeni nedostaci simulacija i načinkako se rezultati mogu poboljšati radeći na detaljima u nekoliko faza simulacije.

5. ZAHVALNICA

Ovaj rad je urađen uz pomoć Ministarstva prosvete, nauke i tehnološkog razvoja Republike Srbije unutar projekta osnovnog istraživanja pod oznakom OI171002.

6. LITERATURA

- [1] Dragic Aleksandar, Udovicic Vladimir, Banjanac Radomir, Jokovic Dejan, Maletic Dimitrije, Veselinovic Nikola, Savic Mihailo, Puzovic Jovan, Anicin Ivan V. The New Set-Up in the Belgrade Low-Level and Cosmic-Ray Laboratory. *NTRP*, vol. 26, br. 3, 2011, 181-192.
- [2] S. Agostinelli et al. Geant4 - a simulation toolkit. *NIMA*. 506, 2003, 250-303.
- [3] D. Heck, J. Knapp, J.N. Capdevielle, G. Schatz, T. Thouw. CORSIKA: A Monte Carlo Code to Simulate Extensive Air Showers, *Forschungszentrum Karlsruhe Report, 6019*, 1998.
- [4] Banjanac Radomir, Maletic Dimitrije, Jokovic Dejan, Veselinovic Nikola, Dragic Aleksandar, Udovicic Vladimir, Anicin Ivan. On the omnipresent background gamma radiation of the continuous spectrum, *NIMA*. 745, 2014, 7-11.

MONTE KARLO SIMULATION OF HPGe DETECTOR BACKGROUND COMING FROM RADIONUCLIDS, COSMIC AND SKYSKINE RADIATION

**Dimitrije MALETIĆ, Vladimir UDOVIČIĆ, Dejan JOKOVIĆ, Radomir
BANJANAC, Aleksandar DRAGIĆ, Mihailo SAVIĆ, Nikola VESELINOVIĆ**

Institute of Physics, University of Belgrade

ABSTRACT

In the Low Background Laboratory for Nuclear Physics background radiation of the HPGe detector was researched. This research is important for experiments with small number of interesting events or rare processes studied in underground laboratories. The background radiation research started with research of background from radionuclides and Cosmic rays using coincidence techniques. Recently, the skyshine radiation was researched. In this paper the Monte Carlo simulation of HPGe background is presented. Results for cosmic ray simulations agree very good with the experimental results, and for others can be improved. The simulation for other ground and underground laboratories can be done, by changing longitude, latitude and elevation, composition of radionuclides in soil. The possible improvements of the simulations are discussed.



ЗБОРНИК РАДОВА



XXX СИМПОЗИЈУМ ДРУШТВА ЗА ЗАШТИТУ ОД ЗРАЧЕЊА СРБИЈЕ И ЦРНЕ ГОРЕ

2. - 4. октобар 2019. године
Хотел “Дивчибаре”, Дивчибаре, Србија

**XXX СИМПОЗИЈУМ ДРУШТВА
ЗА ЗАШТИТУ ОД ЗРАЧЕЊА
СРБИЈЕ И ЦРНЕ ГОРЕ**
Дивчибаре, од 2.10. до 4.10.2019. године

Организатори:

ДРУШТВО ЗА ЗАШТИТУ ОД ЗРАЧЕЊА СРБИЈЕ И ЦРНЕ ГОРЕ

ИНСТИТУТ ЗА НУКЛЕАРНЕ НАУКЕ „ВИНЧА“

Лабораторија за заштиту од зрачења и заштиту животне средине „Заштита“

Организациони одбор:

Председник: Гордана Пантелић

Чланови:

Михајло Јовић, Институт за нуклеарне науке „Винча“, Београд
Маја Еремић Савковић, Директорат, Београд
Никола Свркота, ЦЕТИ, Подгорица, Црна Гора
Иван Кнежевић, Нуклеарни објекти Србије, Београд
Јелена Пајић, Институт за медицину рада Србије „Др Драгомир Карајовић“,
Београд
Кристина Бикит, Природно математички факултет, Нови Сад
Андреа Којић, Институт за нуклеарне науке „Винча“, Београд
Милица Рајачић, Институт за нуклеарне науке „Винча“, Београд
Наташа Сарап, Институт за нуклеарне науке „Винча“, Београд
Никола Кржановић, Институт за нуклеарне науке „Винча“, Београд
Предраг Божовић, Институт за нуклеарне науке „Винча“, Београд
Марко Крајиновић, Институт за нуклеарне науке „Винча“, Београд

Редакциони одбор:

др Невенка Антовић, Природно математички факултет, Подгорица
др Душан Мрђа, Природно математички факултет, Нови Сад
др Софија Форкапић, Природно математички факултет, Нови Сад
др Биљана Миленковић, Природно математички факултет, Крагујевац
др Јелена Стајић, Природно математички факултет, Крагујевац
др Ненад Стевановић, Природно математички факултет, Крагујевац
др Јелена Ајтић, Факултет ветеринарске медицине, Београд
др Владимир Удовичић, Институт за физику, Земун, Београд
др Наташа Лазаревић, Нуклеарни објекти Србије, Београд
др Драгана Тодоровић, Институт за нуклеарне науке „Винча“, Београд
др Гордана Пантелић, Институт за нуклеарне науке „Винча“, Београд
др Ивана Вуканац, Институт за нуклеарне науке „Винча“, Београд
др Ивана Смичиклас, Институт за нуклеарне науке „Винча“, Београд
др Јелена Крнета Николић, Институт за нуклеарне науке „Винча“, Београд
др Марија Јанковић, Институт за нуклеарне науке „Винча“, Београд
др Милош Живановић, Институт за нуклеарне науке „Винча“, Београд
др Оливера Цирај-Бјелац, Институт за нуклеарне науке „Винча“, Београд
др Игор Челиковић, Институт за нуклеарне науке „Винча“, Београд

PREGLED ISTRAŽIVANJA RADONA U PRETHODNIH 29 SIMPOZIJUMA DRUŠTVA ZA ZAŠTITU OD ZRAČENJA SRBIJE I CRNE GORE

Igor ČELIKOVIĆ¹, Vesna ARSIĆ², Sofija FORKAPIĆ³, Vladimir UDOVIČIĆ⁴ i Dragoslav NIKEZIĆ⁵

- 1) Univerzitet u Beogradu, Institut za nuklearne nauke „Vinča“, Beograd, Srbija, icelikovic@vin.bg.ac.rs
- 2) Institut za medicinu rada Srbije „Dr Dragomir Karajović“, Beograd, Srbija, s.vesna.a@gmail.com
- 3) Univerzitet u Novom Sadu, Prirodno-matematički fakultet, Departman za fiziku, Novi Sad, Srbija, sofija@df.uns.ac.rs
- 4) Univerzitet u Beogradu, Institut za fiziku u Beogradu, Institut od nacionalnog značaja za Republiku Srbiju, Beograd, Srbija, udovicic@ipb.ac.rs
- 5) Univerzitet u Kragujevcu, Prirodno-matematički fakultet, Kragujevac, Srbija, nikezic@kg.ac.rs

SADRŽAJ

Radon je prirodni radioaktivni gas, čije je prisustvo zbog svojih karakteristika nemoguće detektovati ljudskim čulima, već ga je neophodno meriti. Iako je otkriven na početku XX veka, kada su i izmerene visoke koncentracije radona u rudnicima srebra u Češkoj, tek je četiri decenije posle pretpostavljena veza između visoke koncentracije radona i kancera pluća, da bi se desetak godina kasnije ukazalo na radonove potomke kao moguće uzročnike kancera. Brojne epidemiološke studije su pokazale da radon sa svojim potomcima predstavlja drugi uzročnik kancera pluća posle pušenja. Važnost ispitivanja radona i njegovih potomaka je odmah uočena i u Srbiji, tako da je već na prvom skupu, tada Jugoslovenskog društva za radiološku zaštitu, održanom 1963 godine, bilo nekoliko radova posvećenih merenju koncentracije radona u rudnicima i banjama čime se dominantno bavio Institut za medicinu rada, iz Beograda.

U ovoj publikaciji data je kvalitativna analiza „radonskih“ radova sa prethodnih 29 simpozijuma Društva za zaštitu od zračenja. Diskutovana je aktuelnost problematike sa godinama, pregled tema koje su se širile s godinama, kao i pregled korišćenih mernih tehnika i njihov razvoj. Konačno, data je procena daljeg razvoja problematike radona.

1. Uvod

Radon je plemeniti gas čiji su svi izotopi radioaktivni. Radon je bez boje ukusa i mirisa, pa je njegovo prisustvo u nekoj sredini nemoguće registrovati čulima, već ga je potrebno meriti. Od 27 do sada identifikovanih izotopa radona, samo 3 su prirodnog porekla: ^{222}Rn , ^{220}Rn i ^{219}Rn koji su redom članovi u ^{238}U , ^{232}Th i ^{235}U nizu radioaktivnog raspada. Relativna važnost ovih izotopa raste sa povećanjem njihovog perioda poluraspada i njihove abundance. Pa se tako ^{219}Rn (kolokvijalno: aktinon) sa periodom poluraspada od 3,98 s, u odnosu na ^{222}Rn (kolokvijalno: radon) sa periodom

poluraspada od 3,82 dana redovno zanemaruje. S druge strane, ^{220}Rn (kolokvijalno: toron) sa periodom poluraspada od 55,8 s koji je znatno kraći od perioda poluraspada radona, se ne može uvek zanemariti, budući da ima regiona u kojima je koncentracija ^{232}Th znatno veća od koncentracije ^{238}U , pa se koncentracije torona ne mogu zanemariti. Više od 50% od ukupne godišnje efektivne doze usled izlaganju jonizujućem zračenju potiče od izlaganju radona i njegovim potomcima [1]. Na osnovu nedavnih epidemioloških studija je utvrđeno da je radon sa svojim potomcima drugi uzročnik kancera pluća, posle pušenja i da je odgovoran za između 3% - 14% svih kancera pluća [2]. Stoga je jasan značaj koji izučavanje radona ima u oblasti zaštite od zračenja, pa time ne iznenađuje činjenica da je problematika radona bila prisutna na svim simpozijumima Jugoslovenskog društva za zaštitu od zračenja, koji je potom promenio ime u Društvo za zaštitu od zračenja Srbije i Crne Gore.

U ovom radu je dat pregled istraživanja radona u prethodnih 29 Simpozijuma društva za zaštitu od zračenja (U daljem tekstu samo: Simpozijum). Nisu navođeni radovi, saradnika Društva koji su objavljivani u drugim zbornicima ili časopisima. S obzirom na pregledni karakter ovog rada, u sledećem poglavlju je dat istorijski pregled istraživanja radona u svetu, a potom slede poglavlja razvrstana po najznačajnijim temama vezana za ispitivanje radona i istorijskom pojavljivanju.

Istraživanje radona prikazano u zbornicima Simpozijuma se mogu podeliti u dve etape. U prvoj dominira ispitivanje radonu profesionalno izloženih lica, prvenstveno u uranskim i metalničnim rudnicima, dok je u drugoj etapi dominantno istraživanje izlaganja stanovništva u stambenim objektima kao i razvoj brojnih metoda merenja radona u vodi, vazduhu i zemlji, i modelovanje njegovog ponašanja. Prvo sledeće poglavlje je stoga radon u rudnicima, pa sledi izlaganje radona na ostalim radnim mestima. Potom sledi poglavlje: izlaganje stanovništva radonu i konačno metode merenja i simulacije radona i potomaka u životnoj sredini.

2. Istorijski pregled istraživanja radona

Problem radona datira još od XVI veka kad su Paracelsus i Agricola, pisali o velikoj stopi smrtnosti usled plućnih bolesti kod rudara u rudnicima srebra u Češkoj i Saksoniji [3]. Bolest je krajem XIX veka identifikovana kao kancer pluća, ali se i dalje nije znao njen uzrok. Godinu dana nakon što je Dorn 1900 godine otkrio radon, Elster i Geitel su detektovali visoku koncentraciju radona u rudnicima u Češkoj, mada i dalje radon nije dovođen u vezu sa kancerom pluća [4]. Tek je četiri decenije kasnije, Rajewski pretpostavio da postoji veza između visoke koncentracije radona i kancera pluća [5]. Konačno, 1951 godine, pola veka posle otkrića radona, Bale je ispravno pretpostavio da su radonovi kratkoživeći potomci glavni uzrok kancera pluća [6]. Usledila su brojne kohort studije sprovedene na rudarima u rudnicima urana u Americi i Čehoslovačkoj, na osnovu kojih je Međunarodna agencija za ispitivanje kancera 1988 godine identifikovala radon kao ljudski kancerogen.

S druge strane, ispitivanje radona u zatvorenim prostorijama je prvi put sprovedeno u Švedskoj, gde je od 225 ispitivanih kuća pronađena nekolicina sa veoma visokom koncentracijom [7]. U to vreme, radon u kućama još uvek nije bio shvaćen kao globalni problem, nego su tek posle dvadesetak godina započeta sistematska istraživanja radona u zatvorenim objektima kao i prvi nacionalni programi merenja radona [8]. Na osnovu objedinjenih epidemioloških studija, Svetska zdravstvena organizacija je identifikovala

radon kao drugi uzročnik kancera pluća, posle pušenja, pa ne čudi povećanje interesovanja za ispitivanje radona [2].

3. Radon u rudnicima

Kako u svetu, tako i u tadašnjoj Jugoslaviji, problem radona je na početku istraživanja bio vezan samo za rudnike, dok u stambenim objektima nije bio razmatran. Posle drugog svetskog rata, javila se ekspanzija izučavanja nuklearne energije i proizvodnje nuklearnih sirovina što je dovelo do povećanog broja radnika koji su bili izloženi visokim koncentracijama radona u procesima eksploatacije i obrade rude, i procesu proizvodnje nuklearne sirovine.

Različiti aspekti ispitivanja izloženosti rudara radonu i/ili njegovim potomcima su bili dominantno prisutni počev od I do XV Simpozijuma. Tek par tema (radova) nisu imali vezu sa izlaganjem radona u rudnicima. Saradnici Instituta za medicinu rada i radiološku zaštitu „Dr Dragomir Karajović“, Beograd (tj. Instituta za medicinu rada Srbije „Dr Dragomir Karajović“ – IMRS) predvođeni dr Danilom Hajdukovićem su se prvi bavili problematikom radona uopšte, i u prvih pet Simpozijuma jedini su saopštavali bilo kakve rezultate vezane za ispitivanje radona. Od petog Simpozijuma, grupa iz Instituta „Jožef Stefan“ iz Ljubljane predvođena dr Ivanom Kobalom se priključuje istraživanju radona, sa prvim radovima vezanim za izlaganje radonu u rudnicima. Od ukupno 61 rada sa problematikom radona saopštenih na prvih 15 Simpozijuma, čak 39 radova se na neki način tiče ispitivanja radona u rudnicima, od čega su 32 rada potpisali saradnici sa IMRS, a 7 saradnici sa Instituta IJS.

Kontrolna merenja koncentracije radona su vršena kako u uranskim rudnicima (Kalna, Žirovski Vrh i Zletoska Reka) tako i brojnim neuranskim metaličnim rudnicima olova, cinka, bakra, mangana i antimona.

Prva merenja su pokazala vrlo visoke koncentracije radona u rudnicima urana sa opsegom od par desetaka kBq/m³ do nekoliko stotina kBq/m³, što je bila posledica loših uslova rada i slabe ventilacije [9]. IJS je ispitivao uticaj ventilacije na nivo koncentracije radona u različitim tunelima i pokazano je da odgovarajuća ventilacija može da održava nivo radona u tunelu u dozvoljenim granicama [10]. Sa uvođenjem mehaničke ventilacije, pokazano je da su se koncentracije radona smanjile [11]. U istom radu je ispitivano i smanjenje koncentracije radonovih potomaka i faktora ravnoteže u zavisnosti od brzine ventilacije. Takođe, vršilo se i ispitivanje koncentracije radona za svaki od proizvodnih procesa, kao što su: miniranje, bušenje, utovar i transport rude.

U neuranskim rudnicima metaličnih ruda, koncentracije radona su, po pravilu, bile niže i kretale se od sedamdesetak Bq/m³ do par hiljada Bq/m³, mada je u jednom hodniku rudnika Sase, M. Kamenica, koncentracija radona dostigla 354 kBq/m³. Zaključeno je da na ovako visoke koncentracije radona utiču sadržaj ²²⁶Ra u stenama i veoma slaba ventilacija [12].

Pored merenja koncentracije radona, od 1969, tj. od IV Simpozijuma se prezentuju i rezultati merenja kratkoživećih potomaka radona. Zanimljivo je da je do tada ispitivanje izloženosti radonu preko potomaka bilo isključivo razmatrano kroz merenje dugoživećeg ²¹⁰Po. Određivana je koncentracija ²¹⁰Po u urinu, krvi i kosi rudara, a potom i kod zečeva u cilju procene izloženosti radonu [13,14].

Sa razvojem tehnike merenja radona u vodi, kolege iz IJS su ispitivali koncentraciju radona u vodama u okolini rudnika urana Žirovski vrh. Povećane koncentracije su nađene u vodama u blizini Žirovskog vrha u koje su ve ulivale vode iz rudnika, dok su

vode izvan regiona rudnika sadržale veoma niske koncentracije radona [15].

U cilju što efikasnije optimizacije zaštite rudara vršeno je simultano ispitivanje izloženosti brojnim štetnim agensima: koncentraciji radona, radonovih potomaka, CO, CO₂, broju i tipu čestica prašine u zavisnosti od različitih uslova ventilacije [16]. Vrlo efikasnom zaštitom se pokazalo korišćenje posebno dizajniranih rudarskih šlemova sa ugrađenim ventilatorom i sistemom za ventilaciju. Faktor smanjenja koncentracije radonovih potomaka od spoljne sredine do vazduha pod šlemom koji se udiše je bio od par desetina do par stotina puta [17].

Zbog značaja koji radon ima na razvoj respiratornih bolesti, saradnici instituta IMRS su već od prvog Simpozijuma prezentovali svoja istraživanja na temu zdravstvenog uticaja radona: praćeno je medicinsko stanje ruda urana u Kalni, sa posebnim naglaskom na respiratorne bolesti, ispitivan je uticaj dugoročne inhalacije radonu i potomcima i kvarcne prašine na respiratorni sistem pacova, ispitivan je uticaj prašine i radioaktivnosti na povećanje aktivnosti pluća pri udisanju radona kako kod pacova, tako i ljudi, hromozomske aberacije usled izlaganja radonu i potomcima i drugo. Detalji ovih istraživanja se mogu naći u preglednom radu dr Hajdukovića i brojnim radovima prikazanim u prвих 15 Simpozijuma [12].

Konačno, sa stopiranjem nuklearnog programa u Srbiji i raspadom Socijalističke Federativne Republike Jugoslavije, u zbornicima Društva se više ne objavljuju radovi vezani za ispitivanje radona u rudnicima urana ili neuranskim metaličnim rudnicima.

4. Izlaganje radonu na ostalim radnim mestima

Ispitivanje profesionalnog izlaganja radonu, je bilo aktuelno od prvog Simpozijuma. Pored merenja izlaganja radona u rudnicima koji je opisan u prethodnom poglavlju, vršeno je i ispitivanje radona u banjama [18]. Radon je kontrolisan u inhalatorijumima banja: u Rimskim Toplicama, Banji Vrućici i Topuskom koncentracije nisu prelazile 1300 Bq/m³, nešto više koncentracije su izmerene u Soko Banji do 1800 Bq/m³, dok je u Niškoj Banji maksimalna koncentracija izmerena u inhalatorijumu bila oko 1 MBq/m³. Procedura je vremenom unapređena uvođenjem individualnih inhalatora [12].

Radon je meren i u radnim organizacijama koje su primenjivale ²²⁶Ra u terapeutske svrhe, merenjem u prostorijama za aplikacije i bunkerima u kojima su se čuvale radijumske igle [12]. U sklopu lekaskih pregleda radnika koji su radili na radioaktivnim bojama koji dominantno potiču od radijuma, spomenuto je izlaganje radonu kao jedan od potencijalnih problema nastalih pri inhalaciji radioaktivne prašine. Kontaminacija radijumom se određivala merenjem koncentracije izdahnutog radona.

Koncentracija radona i njegovih potomaka je merena i u nekim specifičnim radnim prostorijama gde se mogla očekivati povišena koncentracija, kao što su: kaptaža izvora za gradski vodovod, bolnička perionica, kuhinja studentskog doma i sl. Izmereno je da jedino u slučaju kaptaže izvora koncentracija radona prevazilazi preporučenu vrednost [19].

Na osnovu izloženog u prethodna dva poglavlja, može se uočiti da je tema procene štetnosti profesionalnom izlaganju radona vrlo kompleksna, značajna i datira do danas. Iako u regulativi u Srbiji postoje granice za profesionalno izlaganje (član 35, Pravilnika o granicama izlaganja jonizujućim zračenjima [20]) nije precizirano na koja radna mesta se to odnosi i na koji način se predviđa kontrola tih radnih mesta. Pravilnik će biti potrebno uskladiti, u što skorije vreme, sa direktivom Evropskog saveta

2013/59/EUROATOM vezanom za zaštitu od zračenja u okviru koje se član 45 odnosi na regulisanje radona na radnim mestima [21].

5. Izlaganje stanovništva radonu

Prva merenja radona su vršena 1964. godine u okolini rudnika urana Kalna u kućama u kojima žive rudari. Izmerene su koncentracije do 750 Bq/m^3 , međutim kako u to vreme nije bila regulisana maksimalna preporučena koncentracija radona u kućama, a maksimalna dozvoljena koncentracija u rudnicima je iznosila $11,1 \text{ kBq/m}^3$, dok su se sami rudari izlagali i znatno višim koncentracijama, ovom rezultatu nije pridodavan značaj [12]. Tek dve decenije kasnije se nastavlja merenje radona u zatvorenim prostorijama. U 14. zborniku Simpozijuma iz 1987. godine pojavljuju se 2 rada iz ove tematike. Kolege sa Pedagoškog fakulteta u Osijeku su korišćenjem LR-115 detektora ispitivali sezonsku varijaciju koncentracije radona u podrumu i na balkonu, dok su kolege iz IJS dizajnirali CR-39 detektor, a potom merili radon u rudniku urana, spoljašnjem vazduhu i odabranim kućama. Ovo ujedno predstavlja prvo pominjanje pasivnih, nuklearnih trag detektora. U sledeća dva Simpozijuma, problematikom izlaganja radona u zatvorenim prostorijama dominantno su se bavile kolege iz Slovenije i Hrvatske. Ispitivana je i koncentracija radona u kućama koje su građene od pepela skinutog sa elektrofiltra iz termoelektrane. Pored ispitivanja radona u kućama, od 1991 počinje da se prati koncentracija radona u vrtićima. Prve rezultate objavio je IJS na čelu sa dr Kobalom i saradnicima koji su razvili alfascintilacioni metod [22,23].

Sa prestankom objavljivanja radova koji razmatraju izlaganje radonu u rudnicima, intenzivira se izučavanje radona u zatvorenim prostorijama. Tako se od 1993. godine, u Zbornicima Simpozijuma pojavljuju radovi sa sve većim brojem institucija koje su u svoju problematiku istraživanja ubacili i ispitivanje uticaja radona na stanovništvo. Iste godine, pojavljuju se prve preporuke Međunarodne komisije za radiološku zaštitu (ICRP – International Commission on Radiological Protection) koje se tiču zaštite od radona u kućama i radnim mestima, a kao posledica istraživanja u okviru brojnih nacionalnih programa ispitivanja radona pokrenutih osamdesetih godina [24].

Sa pojavom pasivnih nuklearnih trag detektora i ugljenih kanistara, intenzivira se i merenje koncentracije radona u kućama [25, 26], a takođe i školama i vrtićima [27].

Desetak godina od kad se krenulo sa ispitivanjem radona u zatvorenim prostorijama, na XXI Simpozijumu, dr Žunić sa koautorima objavljuje prvi rad koji govori o naučnim osnovama za sprovođenje nacionalnog programa za radon [28]. Već na sledećem, XXII Simpozijumu se pojavljuje rad u kojem je data prva radonska mapa Vojvodine, sprovedene u svih 45 opština Vojvodine, korišćenjem CR-39 detektora [29]. Merenje koncentracije radona u školama, predškolskim ustanovama i stambenim objektima je nastavljeno i u narednih 5 Simpozijuma, u okviru kojih se objavljuju radovi sa Kosova i Metohije, Crne Gore, Slovenije, i po prvi put rezultati merenja radona u školama u Bosni i Hercegovini (o čemu svedoče brojni radovi saopšteni u Simpozijumima, počev od XXII).

Sa postavljanjem Laboratorije za elektrohemijско razvijanje u Vinči, objavljuje se rad u kojem je prvi put prikazano sistematsko merenje radona u ruralnim sredinama [30]. Radon je potom meren drugim detektorima i na Kosovu i Metohiji [31].

Na XXVII Simpozijumu, dr Udovičić priča o regulativi i strategiji nacionalnog programa za radon. U radu su dati okviri za održavanje jasnog i održivog radonskog nacionalnog plana [32]. Na sledećem, XXVIII Simpozijumu, prikazan je dizajn prve

nacionalne prospekcije radona u boravišnim prostorijama koju je sačinila radna grupa za radon [33]. Prateći predloženi dizajn, podeljeno je 6000 CR-39 detektora. Kampanja je uspešno realizovana, ali rezultati još nisu saopšteni na Simpozijumu. I pored uspešno realizovane kampanje, ostalo je još puno posla kako bi se izvršila implementacija radonskog akcionog plana i izvršilo usaglašavanje sa direktivama EU, što je donekle olakšano postojanjem aneksa XVIII koji kroz 14 elemenata predstavlja svojevrsni vodič za pripremu akcionog plana [21].

Prvu sanaciju objekta od visoke koncentracije radona je sproveo dr Jovanović u Sloveniji u kući u kojoj je maksimalna izmerena koncentracija radona iznosila 3000 Bq/m³. Sanacija je izvršena stavljanjem izolacije na pod podruma, čime je postignuta 25% niža koncentracija, a rezultat je prezentovan na Simpozijumu 1991. godine [34]. Iako sama sanacija nije postigla cilj i oborila koncentracije radona ispod preporučenih granica, rad je značajan kao prvi. Dva Simpozijuma posle, Departman za fiziku, Prirodno-matematičkog fakulteta, Univerziteta u Novom Sadu, prezentuje rad u kojem daje detaljan pregled građevinskih tehnika koje dovode do smanjenja koncentracije radona u zatvorenim prostorijama [35]. Na XXII Simpozijumu je prikazana prva uspešna redukcija nivoa radona u jednoj školi u Crnoj Gori. Tim istraživača predvođeni akademikom P. Vukotićem je uspešno identifikovala puteve ulaska radona u učionice korišćenjem aktivnog metoda detekcije radona, ponudila tehničko rešenje, koje je potom Građevinski fakultet iz Podgorice realizovao i smanjio nivo radona do 10 puta [36]. Kolege iz IMRS su takođe u jednom radu prezentovanom na XXVII Simpozijumu dali niz opštih postupaka kako smanjiti nivo radona u školskim i predškolskim ustanovama. I pored svega navedenog, u Srbiji do danas nije izvršena ni jedna sanacija objekta od visoke koncentracije radona, mada je skorije rađena pilot studija sa predlozima mere sanacije.

6. Metode merenja i simulacije radona i potomaka u životnoj sredini

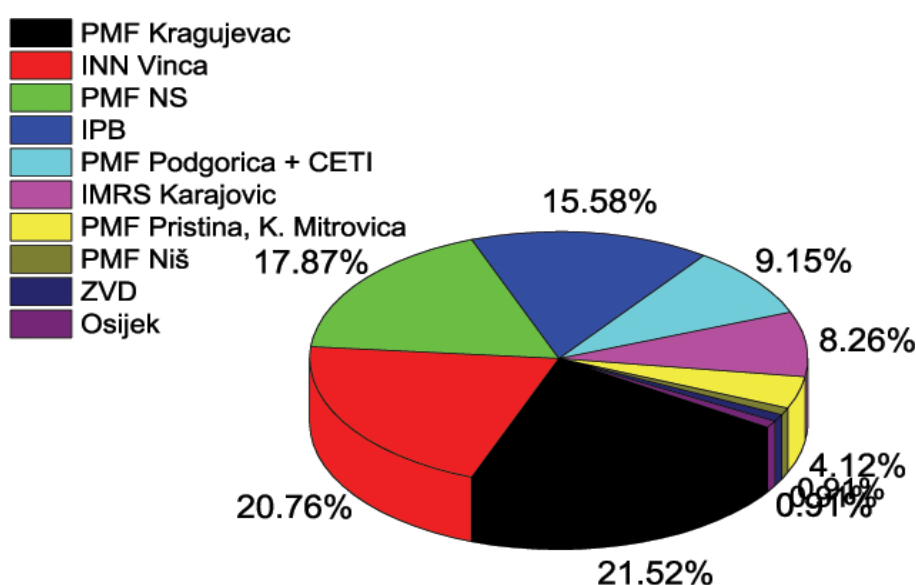
Prva etapa merenja radona se odnosi na ispitivanje profesionalnog izlaganja radona, prvenstveno rudara u uranskim i metalničnim rudnicima. S obzirom da su u pitanju merenja koja su sa početka istraživanja radona kao i da su se samo 2 institucije dominantno bavile ovom problematikom, to je i broj mernih tehnika bio manje raznovrstan nego u drugoj etapi kada je ispitivanje radona došlo u „zrelu fazu“ i kada se sve veći broj istraživača uključuje u ovu problematiku.

Tokom cele prve etape, IMRS je merenje radona vršio scintilacionom metodom korišćenjem staklenog balona zapremine 125 ml, koji je sa unutrašnje strane premazan sa ZnS(Ag). Od IV Simpozijuma IMRS uvodi dve metode merenja radonovih potomaka korišćenjem membranskih filtera. Alfa aktivnost na filtru se merila jonizacionom komorom i po jednoj metodi se određivala ukupna koncentracija radonovih potomaka, dok je po drugoj metodi bilo moguće meriti aktivnost stakog radonovog kratkoživećeg potomka ponaosob. IMRS je razvio i metod merenja niske koncentracije radona optimizovane da meri koncentraciju izdahnutog radona. Hajduković daje pregled postojećih metoda merenja radonovih potomaka kao i predlog optimalne tehnike za primenu u našim uslovima.

Institut IJS je radon takođe merio scintilacionom metodom, ali sa ćelijama zapremine oko 160 ml. Pored toga, uveli su 2 metode merenja niskih koncentracija radona u vodi bazirane na scintilacionim ćelijama pri čemu se kod jedne radon izdvaja prodivavanjem vode inertnim gasom, a kod druge kondenzacijom tekućim azotom. Uvedena je i

metoda merenje radonovih potomaka koristeći scintilacione pločice, uz pretpostavku ravnoteže između radona i potomaka. Na XI Simpozijumu, grupa iz IJS prva publikuje rad o razvoju uređaja za kontinualno merenje radona bazirano na jonizacionoj komori velike osjetljivosti.

Drugu etapu karakteriše ispitivanje izloženosti stanovništva radonu kao i brojnih pratećih faktora koji bi mogli doprineti boljem razumevanju njegovog ponašanja u životnoj sredini. Razvijaju se brojni detektori, razvijaju se različite tehnike merenja radona u vodi i zemnom gasu, usložnjava se analiza rezultata i sl. Na grafiku 1 je prikazan broj radova iz oblasti radona po instituciji u periodu od 1993 do 2017. Dominiraju radovi koji potiču sa Prirodno-matematičkog fakulteta, Univerziteta u Kragujevcu- 21,52%, iz Instituta za nuklearne nauke „Vinča“- 20,76%, Departmana za fiziku, Prirodno-matematičkog fakulteta, Univerziteta u Novom Sadu – 17,87% i Instituta za fiziku, Univerziteta u Beogradu (IPB) – 15,58%.



Slika 1. Pregled broja radova sa radonskom tematikom po institucijama u periodu od 1993 do 2017.

Od XIII Simpozijuma, pojavljuju se merenja bazirana na čvrstim nuklearnim trag detektorima. Prva takva merenja je objavio kolega sa Učiteljskog fakulteta u Osijeku, korišćenjem LR-115 stavljenim u otvorenoj i zatvorenoj sa filtrom plastičnoj čaši [37]. Na narednom simpozijumu saradnici IJS prikazuju rad na razvoju pasivnih detektora baziranih na CR-39 filmovima. Na XVI Simpozijumu, su saradnici takođe iz IJS-a, po prvi put prikazali merenja radona u zatvorenim objektima korišćenjem ugljenih kanistra, kao i alfa spektrometri koji su korišćeni za kontinualno merenje radonovih potomaka [38].

Period od XVI Simpozijuma do XXIX simpozijuma donosi razvoj različitih pasivnih metoda za merenje radona: detektori sa kombinacijom aktivnog uglja i polikarbonata, detektori sa različitim tipovima trag detektora: LR-115, CN-92, CR-39.

Od XVII Simpozijuma, grupa prof. Nikezića sa PMF u Kragujevcu u najvećoj meri doprinosi različitim aspektima istraživanja radona. Rađeno je na razvoju difuzione komore koja pored LR-115 ima i elektret u cilju povećanja efikasnosti detekcije radona, što su komparativna merenja i potvrdila [39]. Značajan pravac istraživanja predstavljaju razna modelovanja. Vršeno je dozimetrijsko modelovanje efekata inhalacije radona i njegovih potomaka u plućima. Razvijen je model za računarsko određivanje kalibracionog koeficijenta za merenje radona pomoću CR-39 detektora, što je ujedno i prva primena Monte Karlo metoda u problematici radona [40]. Jedan od problema u nauci o radonu je dugoročno merenje radonovih potomaka, pa je razvijana tehnika merenja radonovih potomaka i faktora ravnoteže trag detektorima, merenje ^{210}Po na staklu... Vršena je i simulacija veličine i raspodele tragova na CR-39 detektoru ozračenog radonom za različite faktore ravnoteže. Utvrđeno je da se mogu identifikovati tragovi koji potiču od ^{214}Po čime se dalje primenom Jacobi-Porstendorferovog modela mogu odrediti koncentracije ostalih potomaka [41].

Merenje radona ugljenim kanistrima po standardnoj EPA metodi predstavlja jedini pasivni metod po kojem su čak tri Laboratorije u Srbiji akreditovane, a čije je međulaboratorijsko poređenje pokazalo dobro slaganje dobijenih rezultata [42].

U Srbiju je merenje radona ugljenim kanistrima uveo IMRS 1991 godine, a 1997. godine objavljuje rezultate koncentracija radona merenih u 555 slučajno izabranih stanova u gradovima širom Srbije [26]. Dve godine kasnije i Departman za fiziku, PMF Novi Sad, objavljuje koncentracije radona u vrtićima i školama dobijenih ugljenim kanistrima [27]. Pored samih merenja, vršena su teoretska i eksperimentalna razmatranja parametara koji utiču na sam metod, Vršena je simulacija adsorpcije na aktivnom uglju metodom konačnih elemenata u zavisnosti od temperature i varijacije koncentracije radona. Dobro slaganje sa eksperimentalnim rezultatima ukazuje da bi se ovakvim pristupom mogla olakšati ekstenzivna procedura kalibracije i predvideti odzivi pri varijaciji različitih parametara [43]. Metodom konačnih elemenata je vršena i simulacija skim-off metode u cilju smanjenja efekata ekstremnih varijacija u koncentraciji radona merenoj aktivnim ugljem [44]. Takođe je ispitivan i uticaj kalibracionog faktora na rezultat koncentracije radona kao i opravdanost korišćenja EPA krivih za korekciju na relativnu vlažnost za ugljene kanistre [45,46].

Vremenom su se aktivni uređaji na svetskom tržištu znatno unapredili, postali su veće osetljivosti, sa više opcija i finansijski dostupniji, pa su ih radonski eksperti Društva uveli u upotrebu u svojim laboratorijama. To je dovelo do uvođenja novih i/ili ekspanzije postojećih metoda merenja koje je prethodno bilo teže izvoditi.

Razvijaju se modeli merenja brzine ekshalacije iz građevinskog materijala [47,48], kao i merenje koeficijenata difuzije [49]. Razvijen je i gama spektrometrijski metod kojim se omogućava istovremeno određivanje brzine ekshalacije, difuzione dužine i koeficijenta emanacije [48].

Uspostavljaju se metode merenja radona u vodi i ujedno se ispituje koncentracija radona u pijaćoj vodi, fontanama i izvorskoj vodi. Uvedene su 4 metode merenja radona u vodi, dve bazirane na tačnom scintilacionom brojaču, jedna na alfa spektrometru, dok je četvrta metoda gama-spektrometrijska [50].

Merene su i koncentracije radona i torona u zemljištu. Međutim, kako koncentracija radona u zemnom gasu varira od sadržaja vlage u zemljištu, u svetu je uvedena veličina geogeni radon potencijal (GRP) koji pored koncentracije radona u zemljištu uzima u obzir i permeabilnost zemljišta. Prvi rad na ovu temu u Zborniku je vezan za mapiranje GRP na osnovu 400 merenja širom Hrvatske [51]. Saradnici iz Novog Sada i IPB su na

osnovu rezultata koncentracije radona u zatvorenim prostorijama i brojnih raspoloživih geohemijskih podataka o zemljištu pokušali korišćenjem multivarijantne analize proceniti GRP. Izdvojene su dve metode bazirane na veštačkoj neuralnoj mreži, a dobijeni rezultati daju uvid u zavisnost i značaj svakog parametra u predviđanju koncentracije radona [52].

U niskofonskoj podzemnoj laboratoriji, sa uvođenjem kontinualnog merenja radona, brojni radovi se posvećuju ispitivanju varijacije koncentracije radona, korelacijom sa fonom gama zračenja kao i meteorološkim parametrima, kao i analizom vremenskih serija koncentracije primenom različitih metoda [53,54]. Ispitana je i mogućnost da se kontinualno merenje radona, koje je vršeno u Niskofonskoj laboratoriji, iskoristi za predviđanje zemljotresa. Uočena je nagla promena koncentracije radona pre zemljotresa, tako da postoji osnov za dalja istraživanja na tu temu. U gama spektrometriji, radon se javlja kao problem jer povećava fon. O toj problematici je već pisano na II Simpozijumu gde se spominju radon i toron kao gasovi čiju je koncentraciju potrebno smanjiti u sobi gde se nalazi uređaj za merenje radioaktivnosti celog tela. Posebna pažnja smanjenju koncentracije radona zbog kvaliteta gamaspektrometrijskih rezultata je obraćana pri konstrukciji Niskofonske podzemne laboratorije u Institutu za fiziku, Beograd. Zidovi niskoaktivnog betona su hermetički zatvarani aluminijumskim limom debljine 1mm, uveden je nadpritisak od 1,5-2 mbara, instalirana je ventilacija sa dvostepenim sistemom dva filtra: te se postiglo smanjenje koncentracije radona od 1200 Bq / m³ do 10,4 Bq / m³ [55].

I sam pristup obradi rezultata merenja se menjao od prvog do poslednjeg Simpozijuma. U prvim radovima, praktično nije bilo analize već su samo prikazivani rezultati merenja. Događalo se čak da su rezultati prikazivani bez standardne devijacije. Vremenom analiza rezultata se usložila, pa je minimum statističke analize uključivala deskriptivnu statistiku. Budući da raspodela koncentracije radona na određenom prostoru prati log-normalnu raspodelu, jedan od standardnih testiranja je i test na log-normalnu raspodelu. Postavljanje radonskih detektora u zatvorenim prostorijama je često praćeno popunjavanjem upitnika o samom objektu, geološkoj podlozi samog objekta i slično. Stepem korelacije između izmerene koncentracije radona i brojnih parametara se određivao multi-regresionom analizom. Konačno, kolege iz IPB su koristeći svoje iskustvo iz analize podataka u fizici visokih energija, uvele multivarijantni metod klasifikacije. Stepem složenosti analize rezultata koja je prikazivana na poslednjim Simpozijumima može da parira postojećim modelima i analizama koji se koristi u svetu.

7. Zaključak

O važnosti ispitivanja radona i njegovih potomaka zbog njihovog uticaja na razvoj kancera pluća se znalo 50-tih godina, pa ne iznenađuje da se već od prvog Simpozijuma održanog 1963 pojavljuju radovi posvećeni merenju radona. Istraživanje radona unutar Društva se može podeliti na dve etape. U prvoj etapi ispitivano je profesionalno izlaganje radonu, prvenstveno u rudnicima urana, čime su se dominantno bavile 2 institucije: IMRS i IJS. Sa pokretanjem nacionalnih radonskih programa u svetu i donošenjem ICRP preporuka o nivoima koncentracije radona u kućama, kao i odumiranja nuklearnog programa kod nas, počinje druga etapa u kojoj se sve više institucija bavi istraživanjem radona, prvenstveno izlaganjem stanovništva. Najvažniji pravci istraživanja u drugoj etapi su merenje radona u kućama i školskim i predškolskim ustanovama, razvoj metoda merenja radona u vazduhu, vodi i zemljištu, modelovanje

doza koje stanovništvo primi usled izlaganja radonu... Analize rezultata merenja su prešle „dalek put“ od vrlo trivijalnih, dajući samo izmerene vrednosti, preko deskriptivne statistike, do primene veoma naprednih alata za analizu u čemu pratimo korak sa svetom.

Jedna od stvari koja ostaje za neposrednu budućnost je usklađivanje zakona o jonizujućem zračenju sa evropskim, implementacija radonskog akcionog plana kao i sprovođenje mera za sanaciju objekata od visoke koncentracije radona. Sa identifikacijom radonski prioriternih oblasti očekuje se intenziviranje merenja radona na radnim mestima...

8. Zahvalnica

Ovaj rad je podržan od strane Ministarstva prosvete, nauke i tehnološkog razvoja, kroz projekte: OI 171018, OI 171021 i III 171002.

9. Literatura

- [1] UNSCEAR (United Nation Scientific Committee on the Effects of Atomic Radiation Report), Sources and Effects of Ionizing Radiation, Report to the General Assembly. United Nations, New York. 2008.
- [2] World Health Organisation, WHO Handbook on Indoor Radon. WHO, Geneva, (2009).
- [3] Paracelsus, 1567. Von der Bergsucht und anderen Bergkrankheiten; s., Schriften aus dem Gesamtgebiet der Gewerbehygiene, Neue Folge. J Springer, Berlin 1925.
- [4] J. Elster, H. Geitel. Über eine fernere Analogie in dem elektrischen Verhalten der natürlichen und der durch Becquerelstrahlen abnorm leiteten gemachten Luft. *Phys. Z.* 2, 1901, 590–593.
- [5] B. Rajewsky, Bericht über die Schneeberger Untersuchungen. *Z. Krebsforsch* 49, 1940, 315–340.
- [6] W.F. Bale, W.F., 1951. Hazards Associated with Radon and Thoron. Unpubl. Memo. to U.S. At. Energy Comm. (reprinted *Heal. Phys.* 38, 1061).
- [7] B. Hultqvist, B., Studies on naturally occurring ionising radiation, with special reference to radiation doses in Swedish houses of various types. *K. Sven. Vetenskap. Handl.* 4, 1956, 6.
- [8] UNSCEAR (United Nation Scientific Committee on the Effects of Atomic Radiation Report), Annex B: Exposure due to Natural Radiation Sources. Vol. 1, United Nation, New York, 2000.
- [9] M. Međedović, D. Panov, M. Vukotić, P. Raičević, D. Hajduković, Kontaminacija Ra226 i potomcima u rudniku urana. *Zbornik radova II jugoslovenskog simpozijuma o radiološkoj zaštiti*, Mostar 1-4 novembra 1965, 275-284.
- [10] J. Kristan, I. Kobal, M. Ančik, T. Sedovšek, Kontrola kontaminacije ^{222}Rn i njegovih kratkoživećih potomaka u rudniku urana u Žirovskom Vrhu, *Zbornik radova VI simpozijuma Jugoslovenskog društva za zaštitu od zračenja*, Ohrid 25-28. April, 1972, 253-260.

- [11] D. Hajduković, M. Vukotić, I. Prijatelj, Kontrola merenja radona i potomaka u rudniku urana Žirovski vrh, D. Hajduković, *Zbornik radova XIII simpozijuma Jugoslovenskog društva za zaštitu od zračenja* (1961 – 1984), Pula, 10.-13. 06, 1985, 533-536
- [12] D. Hajduković Trideset godina merenja radona-222 u radnoj i životnoj sredini (1960 – 1990), *Zbornik radova XVI simpozijuma Jugoslovenskog društva za zaštitu od zračenja*, Neum, 28-31. Maj 1991, 39-44.
- [13] D. Đurić, D. Panov, M. Kilibarda, Lj. Novak, M. Vukotić, Polonijum u urinu rudara kao merilo ekspozicije radonu, *Zbornik radova I jugoslovenskog simpozijum o radiološkoj zaštiti*, Portorož, 8-12 oktobra, 1963, 11-12.
- [14] D. Panov, D. Petrović, M. Ranković, Ekskrecija polonijuma-210 posle ekspozicije zečeva radonu, D. Panov, *Zbornik radova VI simpozijuma Jugoslovenskog društva za zaštitu od zračenja*, Ohrid, 25.-28. April, 1972, 431-438.
- [15] D. Novak, I. Kobal, Kratak pregled naravnega ojadja radioaktivnosti voda v Žirovskem vrhu, *Zbornik radova VIII simpozijuma Jugoslovenskog društva za zaštitu od zračenja*, Herceg Novi, 20-23. Maj 1975, 327-338.
- [16] D. Hajduković, I. Prijatelj, Simultana kontrola izloženosti štetnim agensima radnika u uranskom rudniku kod menjanja uslova ventilacije, *Zbornik radova XIII Jugoslovenskog društva za zaštitu od zračenja*, Pula 10-13. Juna 1985, 529-532.
- [17] D. Hajduković, I. Prijatelj, J. Rojc, V. Štruc, Ispitivanje efikasnosti zaštitnih šlemova u kontaminiranom delu jame rudnika urana RUŽV, *Zbornik radova XV simpozijuma Jugoslovenskog društva za zaštitu od zračenja*, Priština, 06-09. Juna 1989, 99-100.
- [18] R. Dajlević, M. Vukotić-Conić, Rezultati merenja koncentracije radona u rudniku urana i banjanskim mestima, *Zbornik radova I jugoslovenskog simpozijuma o radiološkoj zaštiti*, Portorož 8-12. oktobra 1963, 8-9.
- [19] D. Radusinović, T. Anđelić, P. Vukotić, Radon u nekim specifičnim radnim prostorijama, *Zbornik radova XX simpozijuma Jugoslovenskog društva za zaštitu od zračenja*, Tara, 3-5. Novembra, 1999, 145-148.
- [20] Pravilnik o granicama izlaganja jonizujućim zračenjima i merenjima radi procene nivoa izlaganja jonizujućim zračenjima (Sl. gl. RS 86/11 i Sl. gl. RS 50/18)
- [21] European Council (EC). Council Directive 2013/59/Euratom laying down basic safety standards for protection against the dangers arising from exposure to ionising radiation. *Off. J. Eur. Union L13*; 57, 2014.
- [22] G. Đurić, D. Popović, J. Vaupotič, I. Kobal, P. Stegnar, Koncentracije radona u dečijim vrtićima u Beogradu i okolini, *Zbornik radova XVI simpozijuma Jugoslovenskog društva za zaštitu od zračenja*, Neum, 28-31. maj, 1991, 31-34.
- [23] M. Peternel, B. Čanč, J. Vaupotič, M. Škofljanec, I. Kobal, P. Stegnar, Koncentracije radona v vrtcih iz Maribora in okolice, *Zbornik radova XVI simpozijuma Jugoslovenskog društva za zaštitu od zračenja*, Neum, 28-31. maj, 1991, 111-114.
- [24] ICRP, Protection Against Radon-222 at Home and at Work. ICRP Publication 65, Ann. ICRP 23(2). 1993.

- [25] O. Čuknić, S. Đurov, D. Nikezić, P. Marinković, Merenje koncentracije radona u zatvorenim prostorijama Požarevca i Svilajнца, *Zbornik radova XVII jugoslovenskog simpozijuma za zaštitu od zračenja*, Beograd-Vinča, 25-28. Mart, 1993, 99-102.
- [26] I. Petrović, G. Pantelić, R. Maksić, Ispitivanje koncentracije radona u stanovima u Republici Srbiji, *Zbornik radova XIX jugoslovenskog simpozijuma zaštite od zračenja*, Golubac, 18-20. Jun, 1997, 207-209.
- [27] N. Žikić, Lj. Čonkić, I. Bikit, M. Krmar, Ž. Đurčić, M. Vesković, J. Slivka, Određivanje koncentracije ^{222}Rn u zatvorenim prostorinama, *Zbornik radova XX simpozijuma Jugoslovenskog društva za zaštitu od zračenja*, Tara, 3-5. Novembar, 1999, 83-86.
- [28] Z.S. Žunić, M. Kovačević, D. Alavantić, M.B. Spasić, Značaj istraživanja izloženosti stanovništva radonu, *Zbornik radova XXI simpozijuma Jugoslovenskog društva za zaštitu od zračenja*, Kladovo, 10-12. Oktobar, 2001, 119-124.
- [29] S. Ćurčić, I. Bikit, Lj. Čonkić, M. Vesković, J. Slivka, E. Varga N. Žikić-Todorović, D. Mrđa, Prva Radonska Mapa Vojvodine, *Zbornik radova XXI simpozijuma Jugoslovenskog društva za zaštitu od zračenja*, Petrovac n/m 29. Septembar - 1. Oktobar, 2003, 195-198.
- [30] Z.S. Žunić, I. Čeliković, P. Ujić, K. Fujimoto, A. Birovljev, I. V. Yarmoshenko, Istraživanje izloženosti radonu i toronu u ruralnim zajednicama, *Zbornik radova XXI simpozijuma Jugoslovenskog društva za zaštitu od zračenja*, Petrovac n/m 29. Septembar - 1. Oktobar, 2003, 207-210.
- [31] G. Milić, B. Vučković, Lj. Gulan, I. Čeliković, Z.S. Žunić, Raspodela koncentracije aktivnosti radona i torona u kućama na Kosovu i Metohiji, *Zbornik radova XXVI simpozijuma Društva za zaštitu od zračenja Srbije i Crne Gore*, Tara, 12-14. Oktobar, 2011, 150-154.
- [32] V. Udovičić, Nacionalni program za radon, regulativa i strategija. *Zbornik radova XXVII simpozijuma Društva za zaštitu od zračenja Srbije i Crne Gore*. Vrnjačka Banja 2-4. Oktobra, 2013, 134-138.
- [33] V. Udovičić, D. Maletić, M. Eremić Savković, G. Pantelić, P. Ujić, I. Čeliković, S. Forkapić, D. Nikezić, V. Marković, V. Arsić, J. Ilić, *Zbornik radova XXVIII simpozijuma Društva za zaštitu od zračenja Srbije i Crne Gore*, Vršac, 30. Septembar – 2. Oktobar, 2015, 173-180.
- [34] P. Jovanović, Sanacija bivalnoga objekta z visokimi koncentracijama radona in radonovih potomcev, *Zbornik radova XVI simpozijuma Jugoslovenskog društva za zaštitu od zračenja*, Neum, 28-31. maj, 1991, 45- 50.
- [35] B. Pavlić, I. Bikit, J. Slivka, Lj. Čonkić, M. Krmar, Građevinski postupci za smanjenje koncentracije radona u zgradama, *Zbornik radova XVIII Simpozijuma Jugoslovenskog društva za zaštitu od zračenja*, Bečići, 24-26. maj 1995, 257-260.
- [36] R. Zekić, P. Vukotić, T. Anđelić, J. Kalezić, D. Vuksanović, R. Žižić, N. Svrkota, Redukcija nivoa radona u osnovnoj školi „Štampar Makarije“ u Podgorici, *Zbornik radova XXII Simpozijuma Jugoslovenskog društva za zaštitu od zračenja*, Petrovac n/m, 29 septembar – 1. oktobar 2003, 203-206.

- [37] J. Planinić, Mjerenje koncentracije radona u zraku, *Zbornik radona XIII Jugoslovenskog simpozijuma zaštite od zračenja*, Pula 10-13. Lipnja 1985, 169.
- [38] M. Križman, Značilni primeri visokih koncentracij radona-222 v zaprtih prostorih Sloveniji in ukrepi za njihovo zmanjševanje, *Zbornik radona XVI Jugoslovenskog simpozijuma za zaštitu od zračenja*, Neum, 28-31. Maj 1991, 59-63.
- [39] D. Krstić, D. Nikezić, P. Marković, Difuziona komora za merenje radona sa elektretom i trag detektorom LR-115-2, *Zbornik radova XVII Jugoslovenskog simpozijuma za zaštitu od zračenja*, Beograd-Vinča, 25-28. Mart, 1993, 85-88.
- [40] B. Jovanović, D. Nikezić, Računanje kalibracionog koeficijenta za merenje radona trag detektorom CR-39. *Zbornik radova XVII Jugoslovenskog simpozijuma za zaštitu od zračenja*, Beograd-Vinča, 25-28. Mart, 1993, 89-92.
- [41] D. Kostić, D. Nikezić, D. Krstić, Raspodela tragova na detektoru CR-39 ozračenog radonom za različite faktore ravnoteže, *Zbornik radova XX simpozijuma Jugoslovenskog društva za zaštitu od zračenja*, Tara, 3-5. Novembra, 1999, 159-163.
- [42] S. Forkapić, K. Bikit, V. Arsić, J. Ilić, G. Pantelić, M. Živanović, Rezultati nacionalnog međulaboratoriskog poređenja u merenju koncentracije radona u vazduhu zatvorenih prostorija Beograd-Noví Sad 2015, godine. *Zbornik radova XXVIII Simpozijuma DZZSCG*, Vršac, 30. Septembar – 2. Oktobar, 2015, 212-221.
- [43] V. Urošević, D. Nikezić, Simulacija adsorpcije radona metodom konačnih elemenata i eksperimentalna verifikacija, *Zbornik radova XIX Jugoslovenskog simpozijuma zaštite od zračenja*, Golubac, 18-20. Jun, 1997, 229-233.
- [44] V. Urošević, D. Nikezić, Simulacija skim-off metode za merenje koncentracije radona aktivnim ugljem, *Zbornik radova XX Jugoslovenskog simpozijuma zaštite od zračenja*, Tara, 3-5. Novembar, 149-153.
- [45] G. Pantelić, M. Živanović, M. Rajačić, J. Nikolić, D. Todorović, Uticaj kalibracionog faktora na rezultat koncentracije radona, *Zbornik radova XXVII simpozijuma DZZSCG*, Vrnjačka Banja 2-4. Oktobra, 2013, 147-151.
- [46] M. Živanović, G. Pantelić, M. Rajačić, J. Nikolić, D. Todorović, Opravdanost korišćenja EPA krivih za korekciju na relativnu vlažnost vazduha kod merenja radona pomoću ugljenih filtera, *Zbornik radova XXVIII simpozijuma DZZSCG*, Vršac, 30. Septembar – 2. Oktobar, 2015, 234-240.
- [47] P. Ujić, I. Čeliković, A. Kandić, I. Vukanac, M- Đurašević, A. Demajo, Z. Žunić, Merenje brzine ekshalacije radona iz građevinskih materijala metodom zatvorene komore, *Zbornik radova XXIV simpozijuma DZZSCG*, Zlatibor, 3-5. Oktobar, 2007, 99-103.
- [48] P. Ujić, I. Čeliković, A. Awhida, B. Lončar, G. Pantelić, I. Vukanac, P. Kolarž, A. Kandić, M. Đurašević, M. Živanović, Merenje ekshalacije radona iz građevinskih materijala. *Zbornik radova XXIX simpozijuma DZZSCG*, Srebrno jezero, 27-29. Septembar, 2017, 219-224.
- [49] S. Grujić, A. Radukun-Kosanović, I. Bikit, D. Mrđa, S. Forkapić, Analiza difuzije radona kroz građevinske materijale. *Zbornik radova XXV simpozijuma DZZSCG*. Kopaonik, 30.9-2.10. 2009, 89-93.

- [50] J. Nikolić, N. Todorović, I. Stojković, B. Tenjović, A. Vranićar, J. Knežević, S. Vuković, metode merenja ^{222}Rn u vodi. *Zbornik radova XXIX simpozijuma DZZSCG*, Srebrno jezero, 27-29. Septembar, 2017, 500-506.
- [51] V. Radolić, M. Poje Sovilj, D. Stanić, I. Miklavčić. Radon in soil gas and constructed geogenic radon potential in Croatia. *Zbornik radova XXIX simpozijuma DZZSCG*, Srebrno jezero, 27-29. Septembar, 2017, 192-199.
- [52] S. Forkapić, D. Maletić, J. Vasin, K. Bikit, D. Mrđa, I. Bikit, V. Udovičić, R. Banjanac. Korišćenje multivarijantne analize za predviđanje geogenog radonskog potencijala. *Zbornik radova XXIX simpozijuma DZZSCG*, Srebrno jezero, 27-29. Septembar, 2017, 210-218.
- [53] V. Udovičić, S. Forkapić, B. Grabež, A. Dragić, R. Banjanac, D. Joković, B. Panić. Varijacija koncentracije aktivnosti radona u Niskofonskoj podzemnoj laboratoriji u Beogradu. *Zbornik radova XXIV simpozijum DZZSCG*, Zlatibor, 2007, 77-81.
- [54] V. Udovičić, D. Maletić, A. Dragić, R. Banjanac, D. Joković, N. Veselinović, J. Filipović. Primena različitih metoda u analizi vremenskih serija koncentracije radona. *Zbornik radova XXVII simpozijum DZZSCG*, Vrnjačka Banja, 2013, 167-170.
- [55] R. Banjanac, V. Udovičić, A. Dragić, D. Joković, J. Puzović, I. Aničin. Karakteristike niskofonske podzemne laboratorije Instituta za fiziku u Zemunu. *Zbornik radova XXI simpozijuma Jugoslovenskog društva za zaštitu od zračenja*. Petrovac n/m 29. Septembar - 1. Oktobar, 2003, 91-94.

OVERVIEW OF RADON RESEARCH PUBLISHED IN THE FIRST 29 SYMPOSIUMS OF RADIATION PROTECTION SOCIETY OF SERBIA AND MONTENEGRO

**Igor ČELIKOVIĆ¹, Vesna ARSIĆ², Sofija FORKAPIĆ³, Vladimir UDOVIČIĆ⁴
and Dragoslav NIKEZIĆ⁵**

- 1) *University of Belgrade, Institute of Nuclear Sciences „Vinča“, Belgrade, Serbia, icelikovic@vin.bg.ac.rs*
- 2) *Serbian Institute of Occupational Health „Dr Dragomir Karajović“, Belgrade, Serbia, s.vesna.a@gmail.com*
- 3) *University of Novi Sad, Department of Physics, Faculty of Sciences, Novi Sad, Serbia, sofija@df.uns.ac.rs*
- 4) *University of Belgrade, Institute of Physics, Belgrade, Serbia, udovicic@ipb.ac.rs*
- 5) *University of Kragujevac, Faculty of Science, Kragujevac, Serbia, nikezic@kg.ac.rs*

ABSTRACT

Radon is natural radioactive gas. It is colourless, tasteless, odourless and therefore it cannot be detected by human senses, but should be measured. It was discovered at the beginning of XX century. At that time, high radon concentrations were measured in the Bohemian silver mines. However it took four decades before a connection between high radon concentration and lung cancer was assumed and one decade more to link radon progeny as a possible cause of lung cancer. Numerous epidemiological studies have shown that radon with its progeny represents second cause of lung cancer after smoking. The importance of investigation of radon and its progeny was acknowledged at the very beginning of Symposiums of Yugoslav society of radiation protection. Thus, already at the first Symposium, held in 1963, there were already several papers published regarding radon concentration measurements in mines and spas. In the first few proceeding of the Symposium the main contribution was from Serbian Institute of Occupational Health.

In this publication, an overview of research on radon, published in previous 29 Proceedings of symposiums of Radiation Protection Society, was given. Evolution of actuality of different radon topics was discussed and overview of used measurement techniques was given. Finally, it was estimated in which directions development of radon topics might go.

DISTRIBUCIJA KONCENTRACIJE RADONA PO SPRATNOSTI STAMBENIH ZGRADA

**Vladimir UDOVIĆIĆ¹, Dimitrije MALETIĆ¹, Aleksandar DRAGIĆ¹,
Radomir BANJANAC¹, Dejan JOKOVIĆ¹, Nikola VESELINOVIĆ¹,
Mihailo SAVIĆ¹, David KNEŢEVIĆ¹ i Maja EREMIĆ-SAVKOVIĆ²**

- 1) *Institut za fiziku u Beogradu, Institut od nacionalnog znaĉaja za Republiku Srbiju, Beograd, Srbija, udovic@ipb.ac.rs, maletic@ipb.ac.rs, dragic@ipb.ac.rs, banjanac@ipb.ac.rs, yokovic@ipb.ac.rs, veselinovic@ipb.ac.rs, msavic@ipb.ac.rs, davidk@ipb.ac.rs*
- 2) *Direktorat za radijacionu i nuklearnu sigurnost i bezbednost Srbije, Beograd, Srbija, eremic.savkovic@srbatom.gov.rs*

SADRŢAJ

Dobro je poznato da je jedan od faktora koji utiĉe na varijabilnost radona u zatvorenom prostoru spratnost stambenih zgrada. Imajući u vidu ĉinjenicu da glavni izvor radona u zatvorenim prostorijama potiče iz zemljišta, oĉekuje se smanjenje koncentracije radona na višim spratovima. Na višim spratovima dominantan izvor radona potiče od graĉevinskog materijala, a u nekim sluĉajevima moŹe doći do odstupanja od ove opšte utvrĉene pravilnosti. S druge strane, varijabilnost radona zbog spratnosti, posebno u velikim gradovima, sa mnogo većim brojem visokih zgrada i gustinom naseljenosti u poreĉenju sa ruralnim sredinama, moŹe uticati na procenu kolektivne doze koja potiče od radona. U tom smislu, a u svrhu naših istraŹivanja, izabrali smo jednu tipičnu porodiĉnu kuću sa potkrovljem i jedan šesnaestospratni soliter. Merenje koncentracije radona u odabranim stambenim objektima izvršeno je sa dva aktivna ureĉaja. Jedan je bio fiksiran u dnevnoj sobi u prizemlju, a drugi je menjao poziciju po spratovima u stambenim zgradama. Svaki merni ciklus na datom spratu trajao je sedam dana uz vreme uzorkovanja od dva sata. U ovom radu detaljno je uraĉena analiza dobijenih rezultata.

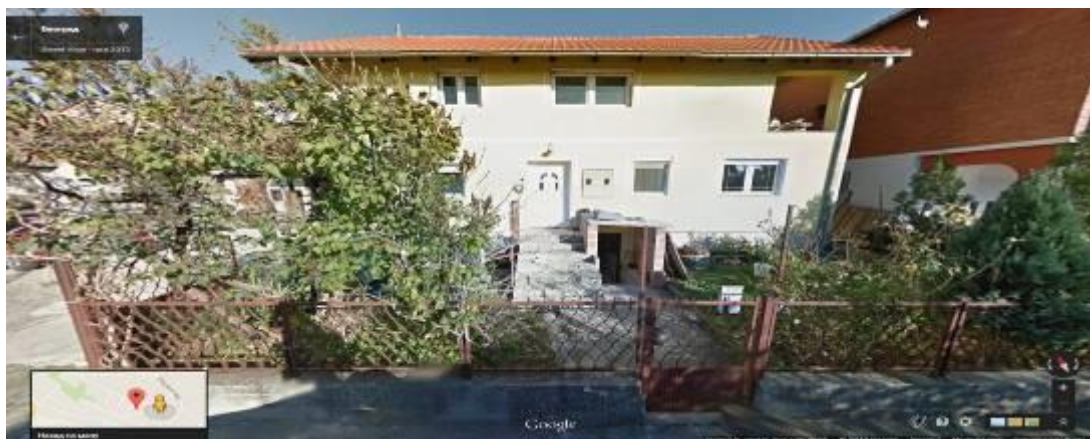
1. Uvod

Izvori radona u stambenim i poslovnim zgradama su, pre svega iz zemljišta, graĉevinskog materijala i vode. S obzirom na prirodu nastanka i svih pomenutih izvora, koncentracija radona je veša u prizemnim prostorijama u odnosu na stanove na višim spratovima stambenih objekata. U literaturi se moŹe pronaći dosta radova koji se bave uticajem raznih faktora na nivo i varijabilnost radona u zatvorenim prostorijama, pa izmeĹu ostalih i uticajem spratnosti [1-4]. U sluĉaju velikih stambenih objekata sa većim brojem spratova, moŹe se uoŹiti odstupanje od opšte pravilnosti, jer je na višim spratovima dominantan izvor radona graĉevinski materijal, te se mogu uoŹiti povešane koncentracije radona u odnosu na situaciju na niŹim spratovima. U tom smislu, uraĉena su merenja radona u dva tipična stambena objekta. Izbor zgrada je baziran na rezultatima iz monografije „Nacionalna tipologija stambenih zgrada Srbije—grupe autora sa Arhitektonskog fakulteta [5]. S obzirom na specifiĉnosti gradnje u Srbiji, broj

tipova zgrada je tako sveden na šest kategorija, dve za porodično stanovanje i četiri kategorije za kolektivno stanovanje; porodično stanovanje: 1. slobodnostoješa kuša, 2. kuša u nizu i kolektivno stanovanje: 3. slobodnostoješa zgrada, 4. zgrada u nizu, 5. zgrada u nizu tipa lamele (ponavlja se više zgrada rađanih po istom projektu, zgrada sa više ulaza...) i 6. soliter (slobodnostoješa zgrada velike spratnosti). Pokazuje se da više od 97% svih stambenih zgrada čine samostoješe porodične kuše. Takođe, za sve definisane tipove zgrada broj spratova se kreše od jednog do osam, pri čemu su samostoješe porodične kuše uglavnom prizemne (37%) ili prizemne sa potkrovljem (26%), dok je veoma niska zastupljenost kuša koje imaju više od dva sprata (5%), sa prosečnom visinom porodičnih zgrada od 1,4 [5].

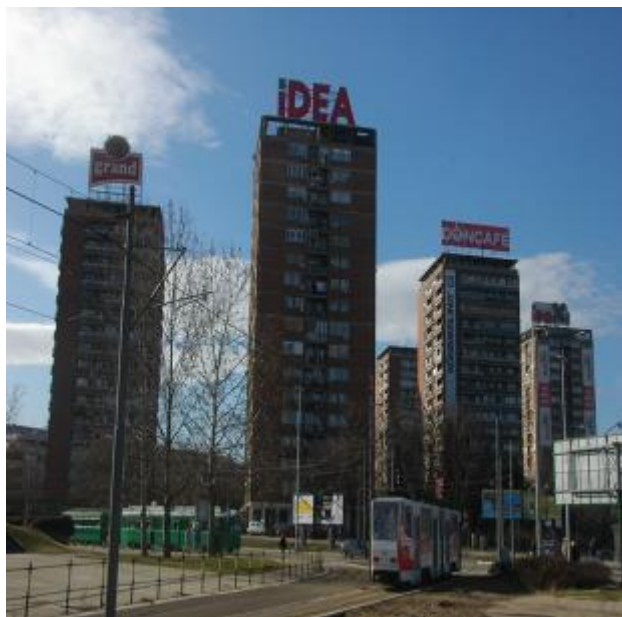
2. Eksperimentalna postavka

Izabrana su dva stambena objekta, jedan iz grupe za porodično stanovanje i jedan soliter iz grupe za kolektivno stanovanje. Porodična kuša (slika 1) ima karakterističan stil gradnje u kome se kuša gradi više godina uz konstantno dograđivanje i nadogradnju, što potencijalno može biti izvor ulaska radona u takve kuše. Kuša ima podrum i izgrađena je od standardnih materijala (cigla-blok, beton, malter). Na kraju je urađena i izolacija korišćenjem stiropora debljine 5 cm. U kući su već vršena višegodišnja merenja koncentracije radona različitim metodama, o čemu je do sada publikovano nekoliko naučnih radova [6-8].



Slika 1. Tipična porodična kuša u Beogradu.

Iz grupe stambenih zgrada za kolektivno stanovanje izabran je soliter na Novom Beogradu (slika 2). Izgrađen je šezdesetih godina prošlog veka, blokovskog tipa. Soliter ima podrum, dok se u prizemlju nalaze lokali i poslovne prostorije. Stanovi se nalaze od prvog sprata pa naviše. Soliter ima 16. spratova.



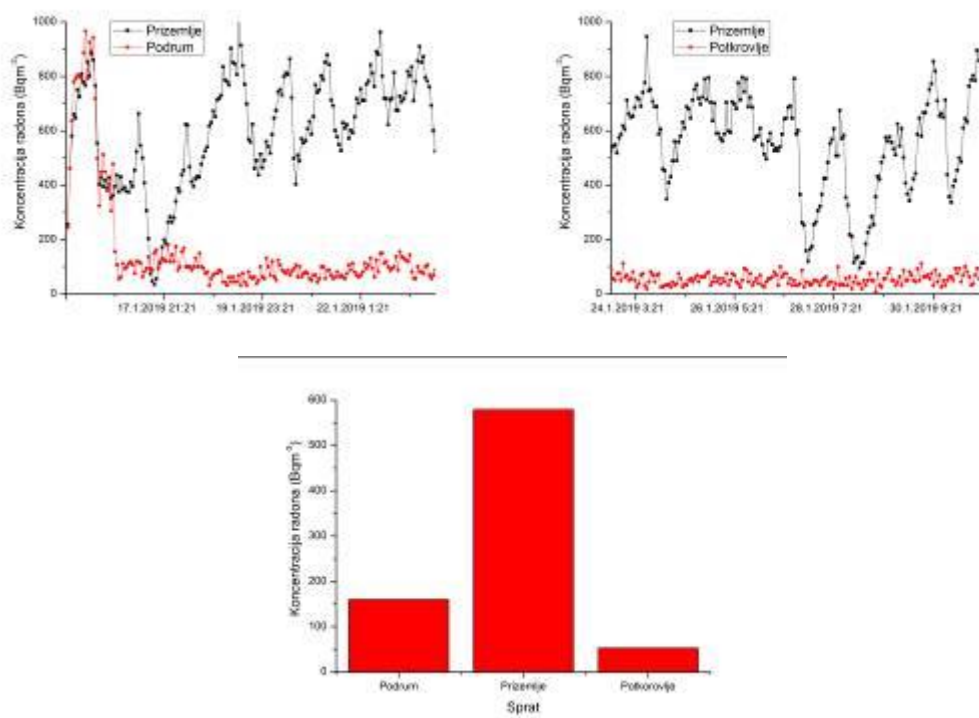
Slika 2. Soliter na Novom Beogradu.

Vremenske serije merenih koncentracija radona u ispitivanim stambenim objektima dobijene su pomoću dva aktivna uređaja SN1029 i SN1030 (proizvođača Sun Nuclear Corporation). To su merni uređaji jednostavne konstrukcije i primene u praksi. U suštini, radi se o brojaču sa dodatkom senzora za merenje meteoroloških parametara. Nedostatak uređaja je nemogućnost merenja koncentracije radona u zemljištu i vodi. Operater može podešiti vremenske sekvence od 0,5 do 24 sati. Jedan ciklus merenja može trajati 1000 sati ili ukupno 720 vremenskih sekvenci (broj sukcesivnih merenja, odnosno tačaka u vremenskoj seriji). Uređaji su bili podešeni da rade u vremenskoj sekvenci od 2 sata. Jedan je bio fiksiran u dnevnoj sobi u prizemlju, a drugi je menjao poziciju po spratovima u stambenim zgradama. Svaki merni ciklus na datom spratu trajao je sedam dana.

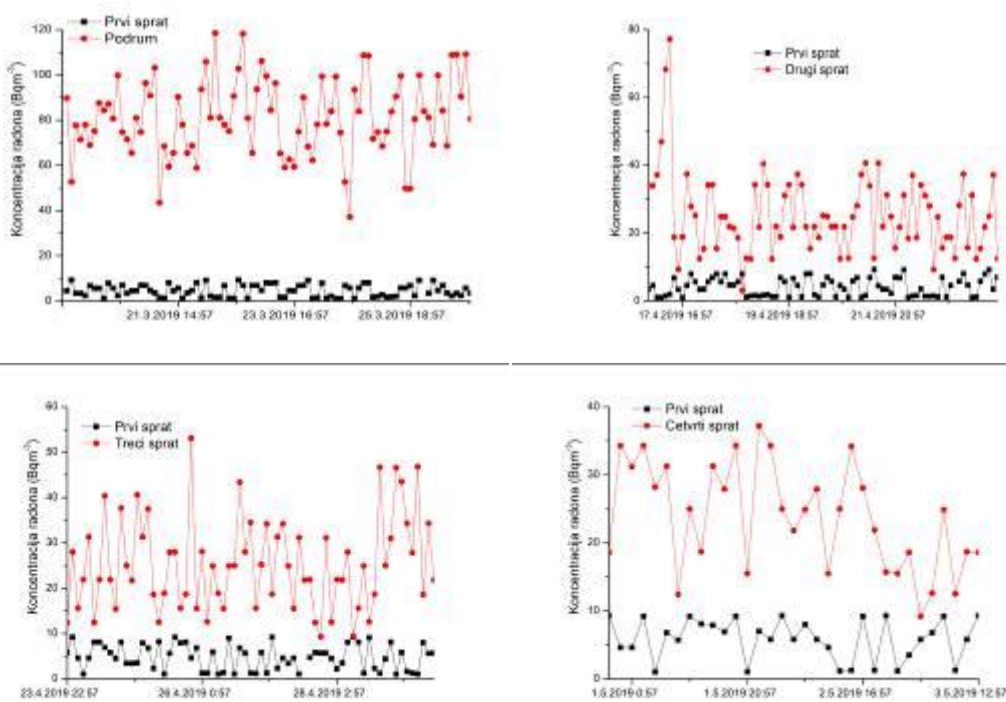
3. Rezultati i diskusija

Na slikama 3 i 4 su prikazani dobijeni rezultati merenja, kako vremenske serije tako i usrednjene koncentracije radona u ispitivanim stambenim objektima za zadati ciklus merenja od sedam dana.

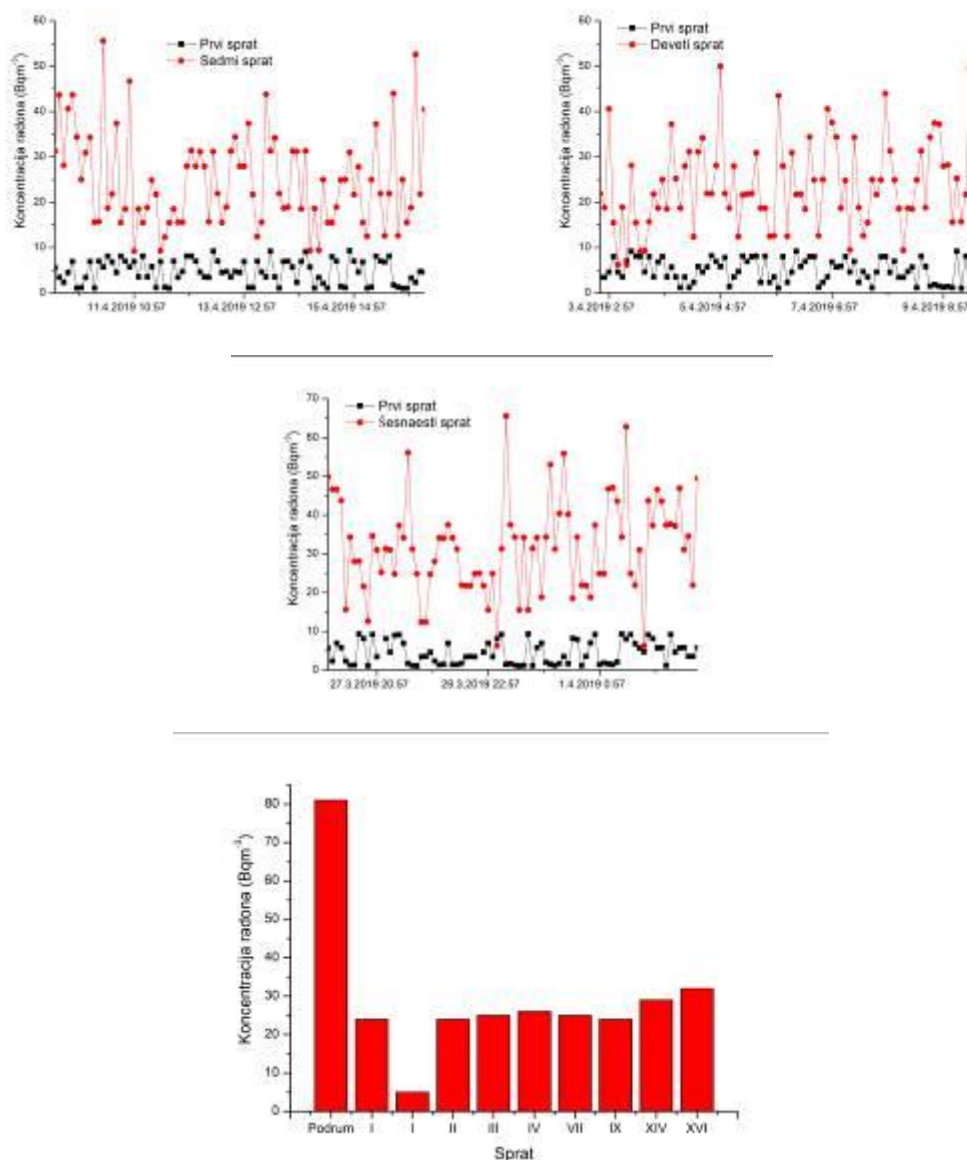
S obzirom da je detektor koji je sve vreme stajao u prizemlju solitera pokazao neobično niske vrednosti za koncentraciju radona, uradili smo uporedno merenje sa drugim detektorom u susednom, kao i u stanu u kome se nalazio fiksirani detektor. Dobijeni rezultati pokazuju izvesnu razliku, ali s obzirom da se radi o domenu izrazito niskih nivoa radona, pretpostavka je da su i merne nesigurnosti velike.



Slika 3. Vremenske serije i srednja koncentracija radona po spratovima u porodičnoj kući.



Slika 4. Vremenske serije i srednja koncentracija radona po spratovima u soliteru.



Slika 4. Nastavak.

4. Zaključak

Dobijeni rezultati pokazuju da je ponašanje radona u dva različita stambena objekta dijametralno suprotno. U porodičnoj kuši je moguše uoiti izrazite varijacije koncentracije radona uz jednodnevnu periodiku. Takođe, interesantan je odnos koncentracije radona u prizemlju, u odnosu na podrum kuše, koji je suprotan od uobičajene situacije kod kuša sa podrumom. Ovo inverzno ponašanje moe se protumaiti injenicom da podrum ne prekriva celo prizemlje veš njegov manji deo. Ostali deo prizemlja je pokriven betonskom ploom kao podlogom, ali sa pukotinama i lošim spojem sa zidovima predstavlja potencijalni izvor povišenog radona. Kod solitera je situacija suprotna i moe se smatrati da veš od prvog sprata dominantan izvor radona je graevinski materijal. Tak se moe uoiti blagi rast srednje koncentracije radona na

višim spratovima. No, dobijeni rezultati u soliteru se mogu predvideti, a na osnovu rada grupe autora koji su odredili interno izlaganje iz građevinskog materijala, koji se koristi u Srbiji, a koje potiče od eshalacije radona i torona [9].

5. Zahvalnica

Ovaj rad je realizovan uz podršku Ministarstva prosvete, nauke i tehnološkog razvoja Republike Srbije u okviru projekta pod brojem III43002.

6. Literatura

- [1] F. Bochicchio, G. Campos-Venuti, S. Piermattei, C. Nuccetelli, S. Risica, L. Tommasino, G. Torri, M. Magnoni, G. Agnesod, G. Sgorbati, M. Bonomi, L. Minach, F. Trotti, M.R. Malisan, S. Maggiolo, L. Gaidolfi, C. Giannardi, A. Rongoni, M. Lombardi, G. Cherubini, S. D'Ostilio, C. Cristofaro, M. Pugliese, V. Martucci, A. Crispino, P. Cuzzocrea, A. Sansone Santamaria, M. Cappai. Annual average and seasonal variations of residential radon concentration for all the Italian Regions. *Radiat. Meas.* 40, 2005, 686-694.
- [2] H. Friedmann. Final Results of the Austrian Radon Project. *Health Phys.* 89(4), 2005, 339-348.
- [3] R. Borgoni, D. De Francesco, D. De Bartolo, N. Tzavidis. Hierarchical modeling of indoor radon concentration: how much do geology and building factors matter? *J. Environ. Radioact.* 138, 2014, 227-237.
- [4] M. Lorenzo-González, A. Ruano-Ravina, J. Peón, M. Piñeiro, J. Miguel Barros-Dios. Residential radon in Galicia: a cross-sectional study in a radon-prone area. *J. Radiol. Prot.* 37(3), 2017, 728-741.
- [5] M. Jovanović Popović, D. Ignjatović, A. Radivojević, A. Rajtić, N. Šuković Ignjatović, Lj. Đukanović, M. Nedić. National Typology of Residential Buildings in Serbia, Faculty of Architecture University of Belgrade, Belgrade, 2013, ISBN 978-86-7924-102-3.
- [6] V. Udovičić, D. Maletić, R. Banjanac, D. Joković, A. Dragić, N. Veselinović, J. Tivanović, M. Savić, S. Forkapić. Multiyear Indoor Radon Variability in a Family House – a Case Study in Serbia. *Nucl. Tech. Radiat. Protect.* XXXIII (2), 2018, 174-179.
- [7] D. Maletić, V. Udovičić, R. Banjanac, D. Joković, A. Dragić, N. Veselinović, J. Filipović. Comparison of multivariate classification and regression methods for indoor radon measurements. *Nucl. Tech. Radiat. Protect.* 29, 2014, 17-23.
- [8] J. Filipović, D. Maletić, V. Udovičić, R. Banjanac, D. Joković, M. Savić, N. Veselinović. The use of multivariate analysis of the radon variability in the underground laboratory and indoor environment. *Nukleonika* 61(3), 2016, 357-360.
- [9] P. Ujić, I. Telić, A. Kandić, I. Vukanac, M. Đurašević, D. Dragosavac, Z. S. Tunić. Internal exposure from building materials exhaling ^{222}Rn and ^{220}Rn as compared to external exposure due to their natural radioactivity content. *Appl. Radiat. Isot.* 68, 2010, 201–206.

INDOOR RADON DISTRIBUTION DUE TO FLOOR LEVEL IN THE RESIDENTIAL BUILDINGS

**Vladimir UDOVICIC¹, Nikola VESELINOVIC¹, Dimitrije MALETIC¹,
Radomir BANJANAC¹, Aleksandar DRAGIC¹, Dejan JOKOVIC¹,
Mihailo SAVIC¹, David KNEZEVIC¹ and Maja EREMIC-SAVKOVIC²**

*1) Institute of Physics Belgrade, University of Belgrade, Belgrade, Serbia,
udovicic@ipb.ac.rs, maletic@ipb.ac.rs, dragic@ipb.ac.rs, banjanac@ipb.ac.rs,
yokovic@ipb.ac.rs, veselinovic@ipb.ac.rs, msavic@ipb.ac.rs, davidk@ipb.ac.rs*

*2) Serbian Radiation and Nuclear Safety and Security Directorate, Belgrade,
Serbia, eremic.savkovic@srbatom.gov.rs*

ABSTRACT

It is well known that one of the factors influencing indoor radon variability is the floor level of residential buildings. Bearing in mind the fact that the main source of indoor radon is from radon in soil gas, a radon concentration on upper floors is expected to decrease. On the upper floors, the dominant source of radon originates from building materials, and in some cases there may be deviations from this generally established regularity. On the other hand, radon variability due to floor level, especially in large cities, with a much larger number of high buildings and density of population compared to rural areas, can affect the estimation of the collective dose derived from radon. In this sense, and for the purpose of our research, we chose a typical family house with a loft and sixteen high-rise building. Indoor radon measurements in selected residential buildings were done with two active devices. One was fixed in the living room on the ground floor, while the other was changing the position on the floors in residential buildings. Each measuring cycle on the floor lasted for seven days with a sampling time of two hours. In this paper, an analysis of the obtained results has been done in detail.

PROCENA TEMPERATURSKOG PROFILA ATMOSFERE NA OSNOVU DETEKTOVANOG FLUKSA KOSMIČKIH MIONA

Mihailo SAVIĆ, Vladimir UDOVIČIĆ, Dimitrije MALETIĆ,
Aleksandar DRAGIĆ, Radomir BANJANAC, Dejan JOKOVIĆ,
Nikola VESELINOVIĆ i David KNEŽEVIĆ

Institut za fiziku u Beogradu, Institut od nacionalnog značaja za Republiku Srbiju,
Beograd, Srbija, msavic@ipb.ac.rs, udovicic@ipb.ac.rs, maletic@ipb.ac.rs,
dragic@ipb.ac.rs, banjanac@ipb.ac.rs, yokovic@ipb.ac.rs, veselinovic@ipb.ac.rs,
davidk@ipb.ac.rs

SADRŽAJ

Uticaj atmosferskih parametara na intenzitet mionske komponente sekundarnog kosmičkog zračenja dobro je poznat. Dominantan doprinos varijaciji fluksa kosmičkih miona usled atmosferskih parametara daju dva meteorološka efekta - barometarski (usled varijacije atmosferskog pritiska) i temperaturski (usled varijacije temperature atmosfere). Postoji više teorijskih i empirijskih modela koji dobro opisuju ove zavisnosti. Obično se na osnovu ovih modela vrši korekcija kako bi se eliminisala varijacija fluksa kosmičkih miona atmosferskog porekla.

Obrnuto, osetljivost mionskih detektora na varijacije atmosferskih parametara može se iskoristiti da se na osnovu poznatih parametara modela i poznatog odbroja kosmičkih miona odredi temperatura različitih nivoa atmosfere. U ovom radu ćemo demonstrirati ovaj pristup na osnovu podataka merenih mionskim monitorima Niskofonske laboratorije za nuklearnu fiziku Instituta za fiziku u Beogradu i primenom empirijskog modela meteoroloških efekata, zasnovanog na tehnici dekompozicije na osnovne komponente.

1. Uvod

Intenzitet pljusкова sekundarnog kosmičkog zračenja zavisi od atmosferskih meteoroloških parametara. To se naročito odnosi na mionsku komponentu sekundarnog kosmičkog zračenja. Dva efekta dominantno utiču na fluks sekundarnih miona: barometarski koji opisuje antikorelaciju fluksa kosmičkih miona sa atmosferskim pritiskom [1] i temperaturski koji se odnosi na uticaj varijacije atmosferske temperature na detektovani intenzitet miona [2].

Osim fundamentalnog, detaljno poznavanje meteoroloških efekata ima značaj u proceduri korekcije na date efekte, time se povećava osetljivost zemaljskih detektora kosmičkog zračenja na varijacije neatmosferskog porekla. Alternativno, dobar model meteoroloških efekata bi u principu omogućio predviđanje atmosferskih parametara na osnovu merenja fluksa miona. Ovo je potencijalno značajno za određivanje temperatura pojedinih slojeva atmosfere u slučaju da su druge metode nedostupne.

Postoji više predloženih metoda za predikciju atmosferskih meteoroloških parametara na osnovu merenja intenziteta kosmičkog zračenja zemaljskim detektorima. Mogu se

bazirati na merenju različitih komponenti fluksa kosmičkih miona [3, 4], simultanom merenju neutronske i mionske komponente [5] ili upotrebi mionskog teleskopa sposobnim da meri ugaonu distribuciju intenziteta [6]. Sve pomenute metode karakteriše relativna kompleksnost eksperimentalne postavke i analize. Takođe, zajedničko svim pomenutim metodama je da se u proceduri određivanja atmosferskih temperatura oslanjaju na teorijski izračunate koeficijente za opisivanje zavisnosti intenziteta miona od temperaturskog profila atmosfere. Ovaj pristup ima određeni ograničenja usled nužno aproksimativnog karaktera i neprilagođenosti konkretnom detektorskom sistemu.

U ovom radu, mi ćemo demonstrirati upotrebljivost jednostavnije eksperimentalne postavke i primenu empirijskog modela meteoroloških efekata na određivanje temperaturskog profila atmosfere.

2. Eksperimentalni podaci i obrada

U Niskofonskoj laboratoriji za nuklearnu fiziku Instituta za fiziku u Beogradu mionski fluks se meri kontinualno od 2009. godine, na nivou zemlje i na dubini od 25 m.w.e. Eksperimentalna postavka se sastoji od scintilacionog detektora i sistema za akviziciju. Detektor je plastični scintilator dimenzija 100cm×100cm×5cm sa četiri fotomultiplikatora postavljena na šoškove. U srcu sistema za akviziciju nalazi se brzi analogno-digitalni konverter sposoban da u realnom vremenu precizno određuje vreme detekcije i amplitudu signala [7]. U ovoj analizi korišćeni su podaci snimljeni detektorom na nivou zemlje u periodu od 01.06.2010. do 31.05.2011. godine.

Za opisivanje meteoroloških efekata na kosmičke mione, u okviru Niskofonske laboratorije razvijen je empirijski model baziran na tehnici dekompozicije na osnovne komponente (Principal Component Analysis - PCA) [8]. Metod se zasniva na ideji da se u analizi meteoroloških efekata sa skupa visoko korelisanih meteoroloških parametara pređe na skup linearno nezavisnih promenljivih, kao i potencijalno smanji dimenzionalnost problema zadržavanjem samo statistički značajnih osnovnih komponenti u analizi. Koeficijenti zavisnosti detektovanog odbroja miona od tako određenih osnovnih komponenti su pouzdaniji, jer su manje podložni statističkim fluktuacijama. Ovde ćemo primeniti ovaj model kako bismo na osnovu odbroja miona merenog u nadzemnoj laboratoriji odredili temperature različitih nivoa atmosfere.

Neka je C_X matrica tipa $n \times m$ koja predstavlja m merenja n različitih meteoroloških parametara. Dekompozicijom na osnovne komponente se sa skupa n meteoroloških varijabli prelazi na skup n osnovnih komponenti, čije vrednosti su reprezentovane matricom C_Y , takođe tipa $n \times m$. Ova relacije se mogu predstaviti jednačinom:

$$C_Y = PC_X, \quad (1)$$

gde je P matrica transformacije čiji redovi predstavljaju kompoziciju osnovnih komponenti.

Na slici 1 prikazana je kompozicija prvih 9 osnovnih komponenti. Na x-osi su meteorološke promenljive: pritisak, temperature 24 izobarna nivoa (10, 20, 30, 50, 70, 100, 150, 200, 250, 300, 350, 400, 450, 500, 550, 600, 650, 700, 750, 800, 850, 900, 925 i 975 mb) i temperatura na nivou tla. Na y-osi su prikazane vrednosti kosinusa uglova rotacije pri prelasku sa skupa meteoroloških varijabli na skup osnovnih komponenti.

Na osnovu statističke i korelacione analize zaključeno je da su za meteorološke efekte od značaja samo pet osnovnih komponenti, i to komponente 1, 3, 4, 5 i 6 [8]. Zavisnost varijacije detektovanog odbroja miona od ovih komponenti, usled meteoroloških efekata, data je jednačinom:

$$\delta N_{PC} = \sum_i k_i PC_i, \quad i = 1, 3, 4, 5, 6 \quad (2)$$

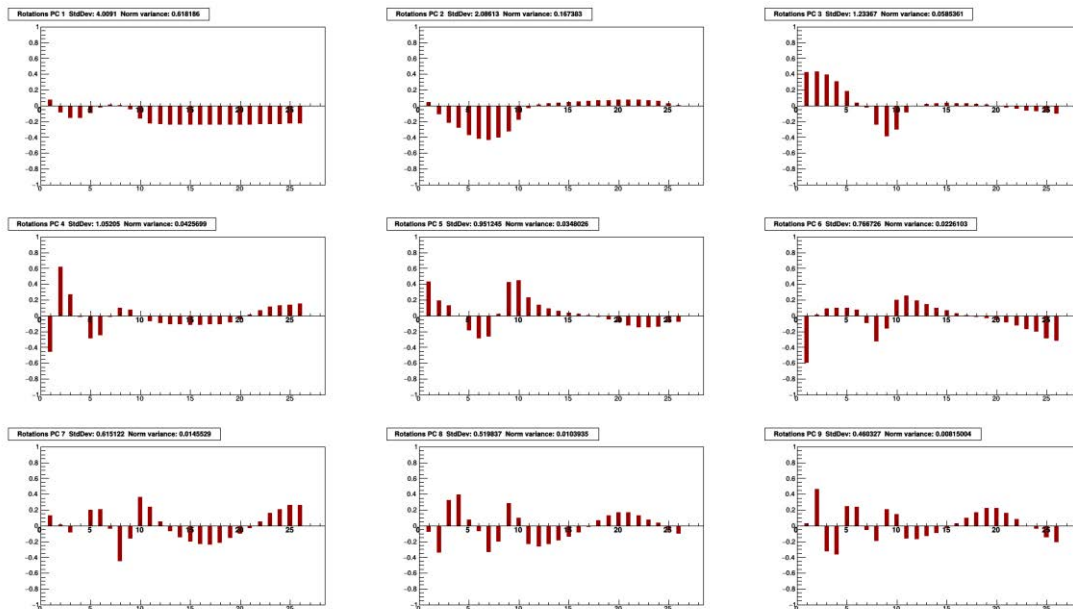
gde su PC_i osnovne komponente a k_i odgovarajući koeficijenti.

Pomoću ove relacije u principu je moguće proceniti vrednosti osnovnih komponenti na osnovu poznatog odbroja.

Dalje, transformišući jednačinu 1 kao:

$$C_X = P^{-1} C_Y = P^T C_Y \quad (3)$$

na osnovu procenjenih vrednosti osnovnih komponenti sada je moguće odrediti procenjene vrednosti meteoroloških parametara.



Slika 1. Kompozicija prvih devet osnovnih komponenti. Na x-osi su meteorološke promenljive: pritisak, temperatura 24 izobarna nivoa (10, 20, 30, 50, 70, 100, 150, 200, 250, 300, 350, 400, 450, 500, 550, 600, 650, 700, 750, 800, 850, 900, 925 i 975 mb) i temperatura na nivou tla. Na y-osi su prikazane vrednosti uglova rotacije.

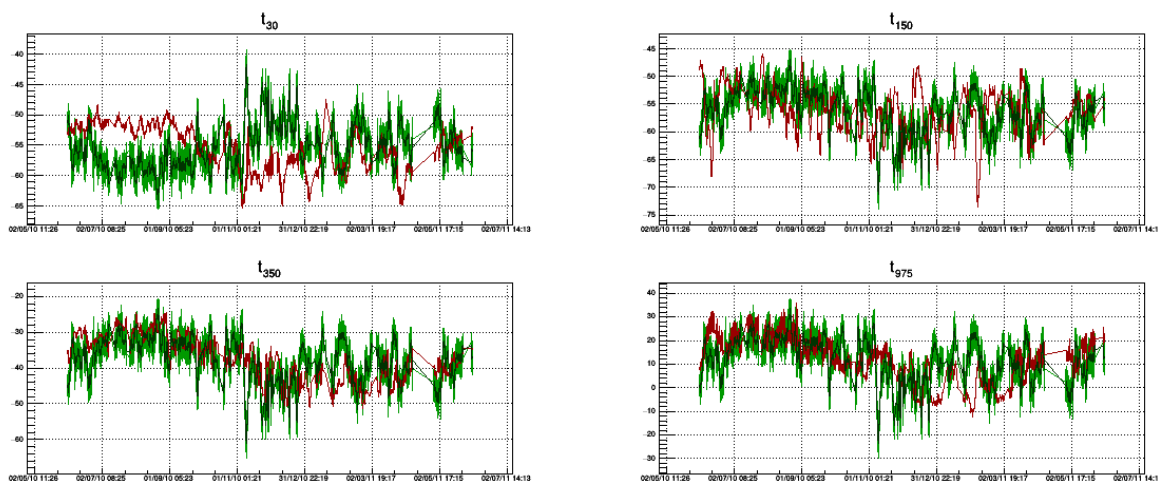
3. Rezultati i diskusija

Za pomenuti referentni period određeni su koeficijenti u jednačini 2, uzimajući u obzir samo geomagnetno mirne dane [8]. Pomoću ovako određenih koeficijenata i merenog odbroja određene su procenjene vrednosti za pet signifikantnih osnovnih komponenti za ceo referentni period. Zatim su na osnovu jednačine 3 određene procenjene vrednosti meteoroloških parametara. Na slici 2 prikazane su vremenske serije merenih i procenjenih vrednosti meteoroloških parametara za izabrane izobarne nivoe.

Zbog preglednosti, prikazani su grafici za četiri različita nivoa. Kao referentni izabrani su nivoi od 30 mb (stratosfera), 150 mb (tropopauza/gornja troposfera), 350 mb (troposfera) i 975 mb (u blizini zemlje). Na plotovima crvenom linijom prikazane su merene vrednosti a svetlo zelenom vrednosti procenjene na osnovu merenog odbroja miona. Takođe, kako bi se dala jasnija slika i smanjio efekat fluktuacija merenog odbroja, vremenska serija predviđenih vrednosti je smutovana (*smoothing*) i prikazana na graficima tamno zelenom bojom.

Na slici 3 prikazana je raspodela razlika merenih i procenjenih vrednosti meteoroloških parametara.

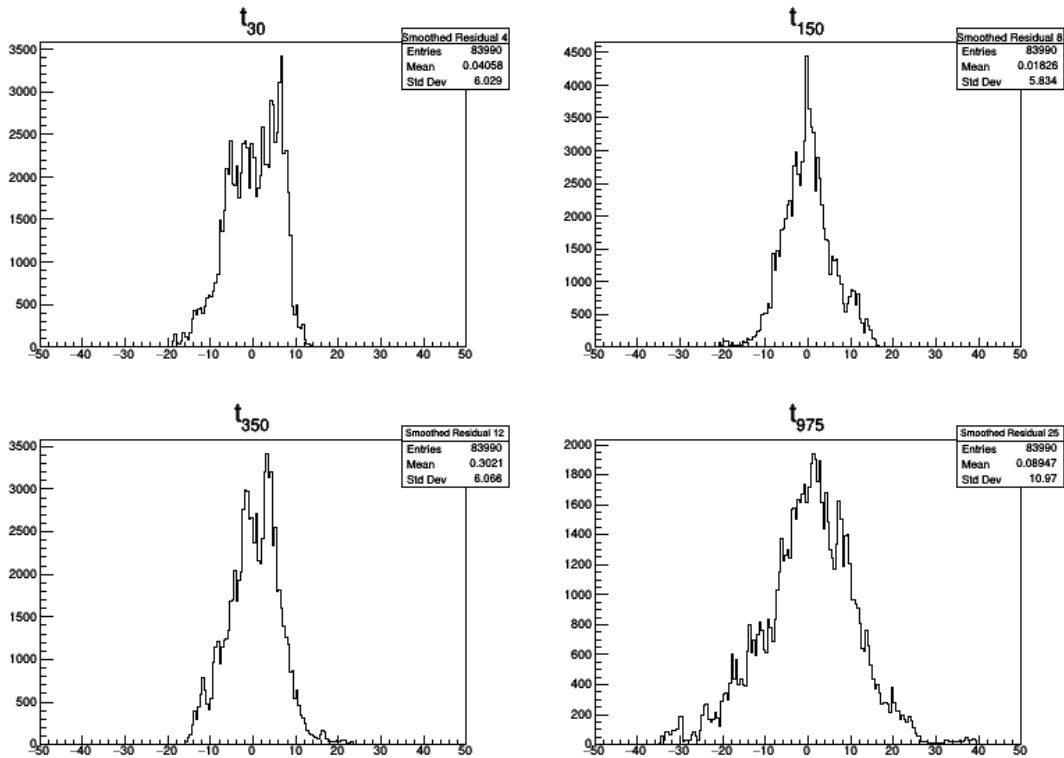
Osim analize vremenskih serija, još jedan kriterijum za određivanje efikasnosti predviđanja temperature pojedinih nivoa mogao bi biti na osnovu širine prikazanih raspodela. Međutim, varijacija temperatura različitih nivoa nije ista tako da ovo može dati nepotpunu sliku. Stoga su u tabeli 1 prikazane vrednosti standardnih devijacija ovih raspodela, standardnih devijacija merenih vrednosti, kao i relativan odnos ove dve veličine koji daje bolji uvid u efikasnost predikcije temperatura pojedinih nivoa atmosfere.



Slika 2. Vremenske serije merenih i procenjenih vrednosti meteoroloških parametara za izabrane nivoa od 30, 150, 350 i 975 mb. Merene vrednosti - crvena linija, procenjene - svetlo zelena linija i smutovane procenjene - tamno zelena linija.

Na osnovu predstavljenih grafika i tabela možemo videti da se najbolje slaganje dobija za sloj atmosfere od 300 do 600 mb. Nešto slabije slaganje dobija se za nivoa u blizini tla, što je u skladu sa kompleksnijom dinamikom temperatura u ovih slojevima, kao i za slojeve od 100 do 200 mb, u kojima dominantno dolazi do produkcije miona. Ovaj drugi podatak je moguća posledica činjenice da je za mione detektovane na površini zemlje značajniji negativni temperaturski efekat, asociran sa jonizacionim gubicima i verovatnošom raspada miona u nižim slojevima atmosfere, dok pozitivni temperaturski efekat u vezi sa verovatnošom nastanka miona u sloju između 100 i 200 mb ima manji doprinos. Najslabije slaganje dobija se za neke od nivoa u stratosferi i tropopauzi, što se može videti na primeru temperature nivoa od 30 mb koji je u značajnom delu godine antikorelisan sa procenjenom temperaturom. Ovo je možda uslovljeno manjim varijacijama temperature na ovim nivoima kao i činjenicom da postoji značajna

varijacija temperature ovih nivoa koja nije korelisana sa intenzitetom kosmičkih miona, sadržana u osnovnoj komponenti 2 (slika 1).



Slika 3. Raspodela razlika merenih i procenjenih vrednosti meteoroloških parametara za izobarne nivoe od 30, 150, 350 i 975 mb.

Tabela 1. Standardna devijacija raspodela razlika merenih i procenjenih vrednosti (σ_r), raspodele vrednosti merenih temperatura (σ_t) i relativan odnos ove dve vrednosti (σ_r/σ_t).

	t ₁₀	t ₂₀	t ₃₀	t ₅₀	t ₇₀	t ₁₀₀	t ₁₅₀	t ₂₀₀	t ₂₅₀	t ₃₀₀	t ₃₅₀	t ₄₀₀
σ_r	9,314	5,246	6,029	3,645	3,940	4,032	5,834	7,455	5,761	5,679	6,066	6,297
σ_t	7,154	4,844	3,669	3,320	2,862	3,055	4,012	5,754	5,111	5,658	6,237	6,460
σ_r/σ_t	1,302	1,083	1,643	1,098	1,377	1,320	1,454	1,296	1,127	1,004	0,973	0,975

t ₄₅₀	t ₅₀₀	t ₅₅₀	t ₆₀₀	t ₆₅₀	t ₇₀₀	t ₇₅₀	t ₈₀₀	t ₈₅₀	t ₉₀₀	t ₉₂₅	t ₉₇₅	t _{ground}
6,386	6,415	6,389	6,387	6,504	6,863	7,340	8,085	8,985	9,956	10,40	10,97	11,20
6,518	6,510	6,466	6,415	6,428	6,616	6,841	7,253	7,793	8,456	8,810	9,444	9,523
0,980	0,985	0,988	0,996	1,012	1,037	1,073	1,115	1,153	1,177	1,181	1,161	1,176

4. Zaključak

Preliminarna analiza je pokazala da postoji dosta dobro slaganje merenih i procenjenih atmosferskih temperatura za veši broj nivoa. Procenjene temperature imaju uglavnom konzistentne vremenske serije i dobro opisuju godišnju varijaciju. Najbolje slaganje sa merenim vrednostima dobija se u višim slojevima troposfere. Stoga, prikazani rezultati predstavljaju dobru polaznu osnovu za dalju analizu.

5. Zahvalnica

Ovaj rad je realizovan uz podršku Ministarstva prosvete, nauke i tehnološkog razvoja Republike Srbije u okviru projekta pod brojem OI 171002.

6. Literatura

- [1] L. Myssowsky, L. Tuwim. Unregelmäßige Intensitätsschwankungen der Höhenstrahlung in geringer Seehöhe. *Zeitschrift für Physik* 39, 1926, 2-3.
- [2] A Duperier. The Temperature Effect on Cosmic-Ray Intensity and the Height of Meson Formation. *Proc. Phys. Soc.* 61, 1948, 34-40.
- [3] Y. Miyazaki, M. Wada. Simulation of cosmic ray variation due to temperature effect. *Acta phys. Acad. Sci. hung.* 29, 1970, 591-595.
- [4] T. Kohno, K. Imai, A. Inue, M. Kodama, M. Wada. Estimation of the Vertical Profile of Atmospheric Temperature from Cosmic-Ray Components. *Proceedings of the 17th International Cosmic Ray Conference, held in Paris, France.* Volume 10., p.289.
- [5] L.I. Dorman. *Cosmic Rays in the Earth's Atmosphere and Underground*, Springer 2004.
- [6] V.V. Borog, O.V. Belonosova, A.S. Davydov, G.M. Kruchenitskii, S.P. Perov, V.G. Yanke. Study of Atmospheric Temperature at Different Altitudes using Muon Angular Distribution at Sea Level. *29th International Cosmic Ray Conference Pune, 2005*, 381-384.
- [7] A. Dragic, V. Udovicic, R. Banjanac, D. Jokovic, D. Maletic, N. Veselinovic, M. Savic, J. Puzovic. The New Setup in the Belgrade Low-Level and Cosmic-Ray Laboratory. *Nucl. Tech. Radiat. Protect.* 26, 2011, 181-192.
- [8] M. Saviš, A. Dragiš, D. Maletiš, N. Veselinoviš, R. Banjanac, D. Jokoviš, V. Udovič iš. A novel method for atmospheric correction of cosmic-ray data based on principal component analysis. *Astropart. Phys.* 109, 2019, 1-11.

**ATMOSPHERIC TEMPERATURE PROFILE ESTIMATION
BASED ON MEASURED COSMIC RAY MUON FLUX**

**Mihailo SAVIĆ, Vladimir UDOVIČIĆ, Dimitrije MALETIĆ,
Aleksandar DRAGIĆ, Radomir BANJANAC, Dejan JOKOVIĆ,
Nikola VESELINOVIĆ and David KNEŽEVIĆ**

*Institute of Physics Belgrade, University of Belgrade, Belgrade, Serbia,
msavic@ipb.ac.rs, udovicic@ipb.ac.rs, maletic@ipb.ac.rs, dragic@ipb.ac.rs,
banjanac@ipb.ac.rs, yokovic@ipb.ac.rs, veselinovic@ipb.ac.rs,
davidk@ipb.ac.rs*

ABSTRACT

The effect of atmospheric parameters in secondary cosmic ray muon component is well known. This is mainly through two dominant meteorological effects - barometric (due to atmospheric pressure variation) and temperature (due to atmospheric temperature variation). There are several theoretical and empirical models that describe these effects well. Usually this knowledge is used to correct for secondary cosmic ray variations due to atmospheric effects.

Alternatively, once model parameters are established, sensitivity of cosmic ray muon detectors to variations of atmospheric origin can be used to estimate temperatures for different layers of the atmosphere. In this work we will demonstrate this procedure using cosmic ray data measured in Low Background Laboratory for Nuclear Physics at Institute of Physics Belgrade, combined with parameters of empirical model for meteorological effects based on principal component analysis.

ЗБОРНИК РАДОВА



XXXI Симпозијум Друштва за заштиту од зрачења Србије и Црне Горе



**06-08. октобар 2021.
Београд, Србија**

**XXXI СИМПОЗИЈУМ ДРУШТВА
ЗА ЗАШТИТУ ОД ЗРАЧЕЊА
СРБИЈЕ И ЦРНЕ ГОРЕ**

Београд, 06-08.10.2021.

Организатори:

ДРУШТВО ЗА ЗАШТИТУ ОД ЗРАЧЕЊА СРБИЈЕ И ЦРНЕ ГОРЕ

ИНСТИТУТ ЗА НУКЛЕАРНЕ НАУКЕ „ВИНЧА“

Лабораторија за заштиту од зрачења и заштиту животне средине „Заштита“

Организациони одбор:

Председник: Ивана Вуканац

Чланови:

Гордана Пантелић, Институт за нуклеарне науке „Винча“, Београд
Софија Форкапић, Природно математички факултет, Нови Сад
Маја Еремић Савковић, Директорат за радијациону и нуклеарну сигурност и безбедност Србије, Београд
Милица Рајачић, Институт за нуклеарне науке „Винча“, Београд
Милош Ђалетић, Институт за нуклеарне науке „Винча“, Београд
Наташа Сарап, Институт за нуклеарне науке „Винча“, Београд
Андреа Којић, Институт за нуклеарне науке „Винча“, Београд
Јелена Станковић Петровић, Институт за нуклеарне науке „Винча“, Београд
Војислав Станић, Институт за нуклеарне науке „Винча“, Београд
Предраг Божовић, Институт за нуклеарне науке „Винча“, Београд
Велибор Андрић, Институт за нуклеарне науке „Винча“, Београд
Кристина Бикит, Природно математички факултет, Нови Сад
Ивана Максимовић, Нуклеарни објекти Србије, Београд

Научни одбор:

др Драгана Тодоровић, Институт за нуклеарне науке „Винча“, Београд
др Душан Мрђа, Природно математички факултет, Нови Сад
др Никола Свркота, ЦЕТИ, Подгорица, Црна Гора
др Драгана Крстић, Природно математички факултет, Институт за физику, Крагујевац
др Биљана Миленковић, Институт за информационе технологије, Крагујевац
др Јелена Стајић, Институт за информационе технологије, Крагујевац
др Јелена Ајтић, Факултет ветеринарске медицине, Београд
др Владимир Удовичић, Институт за физику, Земун, Београд
др Наташа Лазаревић, Нуклеарни објекти Србије, Београд
др Ивана Смичиклас, Институт за нуклеарне науке „Винча“, Београд
др Јелена Крнета Николић, Институт за нуклеарне науке „Винча“, Београд
др Марија Јанковић, Институт за нуклеарне науке „Винча“, Београд
др Игор Челиковић, Институт за нуклеарне науке „Винча“, Београд
др Александар Кандић, Институт за нуклеарне науке „Винча“, Београд
др Србољуб Станковић, Институт за нуклеарне науке „Винча“, Београд
др Милош Живановић, Институт за нуклеарне науке „Винча“, Београд

НАЦИОНАЛНИ АКЦИОНИ ПЛАН ЗА РАДОН У РЕГУЛАТИВНОМ ОКВИРУ РЕПУБЛИКЕ СРБИЈЕ

Маја ЕРЕМИЋ САВКОВИЋ¹ и Владимир УДОВИЧИЋ²

- 1) Директорат за радијациону и нуклеарну сигурност и безбедност Србије, Београд, Србија, eremic.savkovic@srbatom.gov.rs
- 2) Институт за физику у Београду, Институт од националног значаја за Републику Србију, Београд, Србија, udovicic@ipb.ac.rs

САДРЖАЈ

Доношењем Закона о радијационој и нуклеарној сигурности и безбедности 2019. године, а у складу са захтевима Директиве Савета Европске уније 2013/59/Euroatom од 5. децембра 2013. којом се утврђују основни сигурносни стандарди за заштиту од опасности које потичу од излагања јонизујућем зрачењу, стекли су се услови да се проблематици радона приђе на један систематски и свеобухватан начин. Ради обезбеђења услова за спровођење политике у области радијационе сигурности у Републици Србији, законом је предвиђено доношење Стратегије управљања ситуацијама постојећег излагања у којој ће акциони план за радон бити њен саставни део. Израда акционог плана за радон такође била је једна од активности националног пројекта под називом SRB/9/006 - *Upgrading National Capabilities and Infrastructure for a Systematic Approach to Control Public Exposure to Radon*“ који је Директорат за радијациону и нуклеарну сигурност и безбедност Србије реализовао кроз техничку сарадњу са Међународном агенцијом за атомску енергију. У овом раду биће представљени елементи нацрта овог акционог плана који се односе на контролу и смањење концентрације радона у Републици Србији првенствено у објектима за потребе овог пројекта.

1. Увод

1.1. Основ за доношење акционог плана

Директорат за радијациону и нуклеарну сигурност и безбедност Србије (у даљем тексту: Директорат) је кроз техничку сарадњу са Међународном агенцијом за атомску енергију (у даљем тексту: МААЕ), у периоду 2018.-2019. година реализовао национални пројекат под називом „Унапређење националних капацитета и инфраструктуре у систематском приступу контроли изложености радону“ (*Upgrading National Capabilities and Infrastructure for the Systematic Approach to the Control of Public Exposure to Radon*“). Највећи број планираних активности у оквиру овог пројекта односио се на спровођење мерења концентрације радона у јавним објектима, првенствено школама и предшколским установама у Републици Србији. Једна од пројектних активности била је и израда акционог плана за контролу радона у затвореном простору у становима, јавним објектима и радним местима у циљу успостављања система заштите становништва и радника од штетног дејства овог радиоактивног гаса.

Доношењем Закона о радијационој и нуклеарној сигурности и безбедности 2019. године, дата је основа за доношење стратешких докумената који дугорочно одређују и усмеравају правце деловања у области радијационе и нуклеарне сигурности и безбедности у складу са међународним стандардима и принципима у овој области као и преузетим међународним обавезама. Садржај стратегија

прописан је чланом 6. закона и садржи: 1) жељено стање чијем достизању доприноси постизање општих и посебних циљева стратегије; 2) анализу и оцену постојећег стања; 3) опште и посебне циљеве и јасне временске оквире за њихово остваривање; 4) мере за постизање општих и посебних циљева; 5) кључне показатеље учинка; 6) институционални оквир, план за праћење спровођења и институције одговорне за праћење спровођења стратегије; 7) акционе планове за спровођење стратегија. Стратегија се доноси за период од седам година. Саставни део стратегије је акциони план за њихово спровођење. Акциони план садржи мере за постизање општих и посебних циљева које дефинише стратегија. Законом о радијационој и нуклеарној сигурности и безбедности предвиђена је израда четири стратешка документа у области радијационе и нуклеарне сигурности и безбедности. У оквиру Стратегије управљања ситуацијама постојећег излагања, једна од препознатих ситуација постојећег излагања односи се на радон у затвореном простору, становима и радним местима.

Израда нацрта акционог плана за радон заснована је на свим елементима прописаним како домаћим законодавним оквиром тако и међународним стандардима и принципима у области која регулише проблеме везане за радон. Израда нацрта суштински је била заснована на анализи и сазнањима везаним за спроведена мерења концентрације радона у нашој земљи у предходном периоду и постојећим капацитетима укљученим у систем смањења штетног утицаја овог радиоактивног гаса на становништво и раднике, а у складу са захтевима стандарда у овој области.

1.2. Анализа и евалуација резултата изложености радону у Републици Србији

Концентрација радона у становима и јавним објектима (школама и предшколским установама) мери се у оквиру систематског испитивања радиоактивности у животној средини на територији наше земље, а у складу са Правилником о утврђивању програма систематског испитивања радиоактивности у животној средини (Сл. гл. РС 100/10 од 28.12. 2010) од 2010. године. Мерења концентрације радона врше се једном годишње у 45 станова и 24 јавних објеката (школа и прешколских установа) на 7 локација у Републици Србији (Београд, Нови Сад, Суботица, Ниш, Зајечар, Ужице и Врање). Резултати ових мерења део су годишњег извештаја о спроведеном систематском испитивању радиоактивности у животној средини на територији наше земље и доступни су на сајту Директората <http://www.srbatom.gov.rs/srbatommm/monitoring-radioaktivnosti/>.

У периоду 2015.-2016. година кроз национални пројекат (SRB/9/003) у оквиру техничке сарадње са МААЕ, спроведена су мерења концентрације радона у око 5000 кућа и станова на територији наше земље. Мерења су спроведена у сврху мапирања односно формирања радонске мапе и потенцијалног проналажање области са повишеним концентрацијама радона. Анализом измерених концентрација радона, а у складу са постојећим регулаторним оквиром [2], 97 % измерених вредности било је испод 400 Bq/m^3 што предствља интервентни ниво за хронично излагање радону у становима за постојеће објекте. Просечна вредност концентрације радона на основу ових мерења износи 105 Bq/m^3 . Измерена концентрација радона преко 400 Bq/m^3 је у 3 % измерених вредности, док је у 14 објеката односно 0.3 % измерених вредности концентрација радона у затвореном простору била изнад 1000 Bq/m^3 [4].

У периоду 2018-2019. година кроз национални пројекат SRB/9/006 - Upgrading National Capabilities and Infrastructure for a Systematic Approach to Control Public

Exposure to Radon“ Директората и МААЕ, спроведена су мерења концентрације радона у јавним објектима, школама и предшколским установама. Раподела измерених концентрација радона анализирана је у складу са важећом регулативом [2] и износила је:

- 96 % измерених вредности било је испод 400 Bq/m^3
- 3,8 % измерених вредности прелазила је вредност од 400 Bq/m^3
- 0,2 % измерених вредности прелазила је вредност 1000 Bq/m^3 .

Директорат је током 2016. и 2017. године спровео две јавне набавке које су се односиле на мерење концентрације радона у води за пиће. Мерења су вршена на 40 локација у 24 града на територији Републике Србије. Узорковање је вршено са јавних чесми. У табели 1 представљени су резултати мерења и процена ефективне дозе за становништво.

Табела 1. Мерење концентрације радона у води за пиће на територији Републике Србије.

Локација	Концентрација радона (Bq/l)	Просечна ефективна доза (ингестија) mSv/year
Београд 4	$25,8 \pm 2,6$	$0,19 \pm 0,02$
Враће 2	21 ± 4	$0,15 \pm 0,03$
Зајечар	$25,2 \pm 2,2$	$0,18 \pm 0,02$
Јагодина	$15,2 \pm 2,7$	$0,11 \pm 0,02$
Крушевац 1	70 ± 7	$0,51 \pm 0,05$
Крушевац 2	$15,4 \pm 1,9$	$0,11 \pm 0,02$
Лесковац 2	11 ± 5	$0,08 \pm 0,02$
Ниш 2	$12,0 \pm 2,2$	$0,09 \pm 0,02$
Нови Сад 1	$22,2 \pm 1,8$	$0,16 \pm 0,02$
Нови Сад 2	$27,0 \pm 1,0$	$0,20 \pm 0,01$
Нишка Бања 1	622 ± 12	$4,54 \pm 0,09$

На основу приказаних мерења у табели 1. може се закључити да на свим локацијама осим локације Нишка Бања, радон не представља опасност по становништво са аспекта заштите од јонизујућег зрачења. Према Правилнику о границама садржаја радионуклида у води за пиће, животним намирницама, сточној храни, лековима, предметима опште употребе, грађевинском материјалу и другој роби која се ставља у промет (Сл. гл. РС 36/18 од 10.05.2018) параметарска вредност за радон у води износи 100 Bq/l . Конзумирањем воде на локацији Нишка Бања просечна одрасла особа могла би да прими дозу од $4,5 \text{ mSv}$ што прелази препоруку о годишњем излагању становништва од 1 mSv .

У оквиру процене излагања радника у индустријским објектима у којима се ради са НОРМ материјалима, између осталог, вршена су и мерења концентрације радона у Институту за лечење и рехабилитацију „Нишка Бања“, установи која располаже са шест објеката. Подручје на коме је изграђен комплекс је стеновито. У његовом саставу доминира бигар-седиментна шупљикава стена. Ова стена садржи Ra-226 у високим концентрацијама, стога је радон присутан у овом подручју, како у земљишту тако и у води. Мерења су вршена два пута. Прва

мерења обављена су са канистрима са активним угљем, поновљена мерења вршена су са пасивним детекторима за мерење радона CR-39. Резултати мерења концентрације радона на појединим радним местима указују да би раднике на појединим радним местима у институту требало пратити у складу са захтевима који се односе на изложене раднике [2].

2. Акциони план за радон

Нацрт акционог плана за радон садржи неколико тематских целина. Свака дефинише циљеве као и активности које прате реализацију истих. То су: управљање акционим планом, израда и имплементација комуникацијског плана, јачање регулаторног оквира, успостављање националног програма мерења радона, изградња система за смањење радијационог ризика од излагања становништва и радника радону и истраживање и развој. Сви ти циљеви и активности треба да допринесу основном стратешком дугорочном циљу, а то је: смањење ефективне дозе, односно мере радиолошке оптерећености становништва Републике Србије која је последица удисања радона, уношења истог ингестијом преко воде за пиће која је оптерећена радоном, применом одговарајућих превентивних и ремедијационих мера. У наставку рада биће детаљније описана свака тематска целина.

2.1. Управљање Акционим планом за радон

Као у случају било ког акционог плана, потребно је реализовати низ активности које захтевају одговорност и координацију различитих тела, државних и јавних, те других учесника које се утврђују овим акционим планом. У том смислу, према процени и потребама извршења појединих активности, носиоци и учесници могу укључити и друге чиниоце у сврху реализације активности дефинисаних овим акционим планом. Процена степена имплементације акционог плана прати се кроз мониторинг, евалуацију и извештавање о његовом спровођењу. У циљу неопходне координације радом одговорних и заинтересованих институција и надлежних државних органа, органа управе, јединица локалне самоуправе и невладиних организација, акционим планом планирано је формирање радне групе, коју ће чинити представници наведених институција. У циљу ефикаснијег рада, предвиђено је да Директорат има улогу координатора у раду радне групе. Радна група свој рад вршиће у складу са пословником о раду, којим би се дефинисале следеће надлежности:

- а) координација у раду на имплементацији акционог плана;
- б) вршење редовног мониторинга и евалуације реализованих планираних активности и мера;
- ц) извештавање Директората о напретку у реализацији акционог плана;
- е) на крају периода за који је донесен акциони план давање препоруке за даље активности на плану заштите од радона;
- ф) остале релевантне активности.

2.2. Израда и имплементација комуникацијског плана

С обзиром на недовољну видљивост проблематике радона у медијима и јавности, посебну пажњу треба посветити подизању свести код становништва о штетном утицају радона на здравље људи. Неки од елемената комуникацијског плана су: успостављање централне веб странице, као и друштвених мрежа које садрже информације о радону, водиче за мерење радона за становништво и послодавце као и спискове овлашћених правних лица одговорних за мерење и санацију

објеката са повишеним концентрацијама радона, обележавање Европског дана радона, организација радионица са представницима заинтересованих страна.

2.3. Јачање регулаторног оквира

Сваки од дефинисаних елемената акционог плана, садржи елементе чија имплементација зависи од регулаторног оквира. Акционим планом планира се доношење референтног нивоа концентрације радона у затвореним боравишним и радним срединама као и дефинисање критеријума за утврђивање радонских приоритетних области, спецификација радних места која захтевају мерења концентрације радона ради процене нивоа изложености јонизујућем зрачењу у складу са законом, препорука које се односе на ремедијацију, као и превенцију а у складу са правилима изградње („Building codes“).

2.4. Успостављање националног програма мерења радона

У периоду реализације акционог плана, нацртом се планира и развој националног програм мерења концентрације радона у Републици Србији. Програм би подразумевао:

- Припрему протокола и методологије за мерење концентрације радона у боравишном простору кућама и становима и на радним местима препознатим да су простори у којима може доћи до излагања радника радону;
- Припрема протокола и методологије за мерење радона у земљишту и дефинисање радон потенцијалних области;
- Припрема протокола за мерење радона у води која се користи за људску потрошњу и
- Успостављање националне радон базе.

Важан сегмент ових програма обухватио би и успостављање система контроле квалитета мерења, а све са сврхом верификације свих резултата мерења који би били садржани у националној радон бази. Национална радон база, како нацрт планира била би у надлежности Директората.

2.5. Изградња система за смањење радијационог ризика од излагања становништва и радника радону

Значајан део акционог плана представља развој и примена корективних и превентивних мера као техничких решења која служе за смањење концентрације радона у затвореном простору. За успешну реализацију овог циља неопходно је у акциони план пре свега укључити надлежно министарство, експерте и остала професионална удружења у области грађевине. Акциони план предвиђа организацију обука за професионалце у грађевинском сектору као и израду упутстава и водича за примену техничких решења која служе за смањење концентрације радона у затвореном простору. У даљем развоју овог програма, неопходно је успоставити систем контроле квалитета обављених послова кроз процес овлашћења и давања лиценци фирмама које би радиле на овом програму санације. Важан сегмент представља и успостављање механизма за субвенционисање санације постојећих зграда и стамбених објеката, као и финансијских средстава за санацију школа, вртића и јавних зграда са повишеним нивоом радона. С обзиром на мултидисциплинарност ове области потребно је развијати сарадњу и ове активности повезати са националним програмима о енергетској ефикасности, побољшању квалитета ваздуха, заштити од изложености дуванском диму.

2.6. Истраживање и развој

Циљаним истраживањима потребно је повећавати домаћа специфична знања и вештине. За постизање овог циља потребно је развити мерне технике које би омогућиле да се кратким мерењем радона, у трајању до месец дана, а узимајући у обзир сезонске варијације и друге факторе које утичу на ниво радона, довољно поуздано процени средња годишња концентрација радона у затвореном простору. У циљу боље процене ризика од радона неопходно је проучавати варијације концентрација радона од године до године, зависно од климатских промена (метеоролошких параметара), у различитим типовима зграда и у различитим климатским подручјима у Србији. Осим тога потребно је:

- утврдити повезаност геолошке подлоге, порозности површинског слоја терена са измереним концентрацијама радона;
- утврдити утицај грађевинског материјала (мерењем есхалације радона из грађевинских материјала који се најчешће користе у грађевинској индустрији у Србији) на ниво радона у згради;
- анализирати методе за брзу дијагностику повишених нивоа радона у затвореним просторима и спровести процедуре неопходне за контролу квалитета добијених резултата;
- испитати расподелу концентрације активности радона унутар зграда по спратности, посебно у условима постојања централног вентилационог система и карактеристике зграда које се могу повезати са високим нивоом радона у њима.

3. Закључак

Нацрт акционог плана за радон, настао као део пројектне активности Директората са МААЕ, представља добру основу за даљи рад на важном стратешком документу Стратегији управљања ситуацијама постојећег излагања у којој ће акциони план за радон бити њен саставни део. Осим испланираних активности, важан део акционог плана чине временски оквири за реализацију планираних активности, као и јасно дефинисане институције, заинтересоване стране укључене у спровођење свих елемената акционог плана.

Нацрт акционог плана за радон у складу је са захтевима европског законодавства и стандардима МААЕ и представља низ корака ка унапређењу система контроле радона, процене његовог штетног утицаја на здравље становништва, процене могуће изложености радника, мерама за његово смањење и елементима превенције његовог утицаја у новоизграђеним објектима. Спровођењем акционог плана у целини циљ је да се успостави систем у Републици Србији који би повезао све сегменте утицаја овог радиоактивног гаса на раднике и становништво у целини са аспекта заштите од јонизујућег зрачења.

4. Литература

- [1] Правилник о границама излагања јонизујућим зрачењима и мерењима ради процене нивоа излагања јонизујућим зрачењима („Службени гласник РС“ бр. 86/11 и 50/18).
- [2] Извештај о процени излагања радника у индустријским објектима у којима се ради са НОРМ материјалима у следећа три објекта-институције: Рудник мрког угља „СОКО“, Нишка бања и Железара Смедерево
- [3] Игор Челиковић, Весна Арсић, Софија Форкапић, Владимир Удовичић, Драгослав Никезић. Преглед истраживања радона у претходних 29

Симпозијума Друштва за заштиту од зрачења Србије и Црне Горе. *Зборник радова XXX Симпозијум ДЗЗСЦГ*, Дивчибаре 2- 4. октобар 2019, 177-191.

- [4] Maja Eremić Savković, Vladimir Udovičić, Dimitrije Maletić, Gordana Pantelić, Predrag Ujić, Igor Čeliković, Sofija Forkapić, Vladimir Marković, Vesna Arsić, Jovana Ilić, Branko Markoski. Results of the first national indoor radon survey performed in Serbia. *J. Radiol. Prot.* 40, 2020, N22.

**NATIONAL RADON ACTION PLAN IN THE REGULATORY FRAMEWORK
OF THE REPUBLIC OF SERBIA**

Maja EREMIĆ SAVKOVIĆ¹ and Vladimir UDOVIĆIĆ²

- 1) *Serbian Radiation and Nuclear Safety and Security Directorate, Belgrade, Serbia,*
eremic.savkovic@srbatom.gov.rs
- 2) *Institute of Physics Belgrade, University of Belgrade, Belgrade, Serbia,*
udovicic@ipb.ac.rs

ABSTRACT

The adoption of the new Law on Radiation and Nuclear Safety and Security in 2019, which is harmonized with the European Union Council Directive 2013/59/ Euratom of 5 December 2013, which prescribes safety standards for protection against the harmful effects of ionizing radiation exposure, necessary and sufficient conditions to approach the radon issues in a systematic and comprehensive way. In order to provide conditions for the implementation of the policy in the field of radiation safety and security in the Republic of Serbia, the adoption of the Strategy for managing the situations of the existing exposure is envisaged, in which the National Action Plan for Radon will be an integral part. Within the national project of the Directorate at the International Atomic Energy Agency SRB/9/006 - Upgrading National Capabilities and Infrastructure for a Systematic Approach to Control Public Exposure to Radon, a draft national strategy and action plan for control and reduction of radon concentration in facilities was prepared for the purposes of this project. This paper will present this draft in more detail.

SIMULACIJA PRODUKCIJE NEUTRONA MIONIMA IZ KOSMIČKOG ZRAČENJA U OLOVNOJ ZAŠTITI GERMANIJUMSKOG DETEKTORA

**Dejan JOKOVIĆ, Dimitrije MALETIĆ, Vladimir UDOVIČIĆ,
Radomir BANJANAC, Aleksandar DRAGIĆ, Mihailo SAVIĆ,
Nikola VESELINOVIĆ i David KNEŽEVIĆ**

*Institut za fiziku u Beogradu, Univerzitet u Beogradu, Beograd, Srbija,
yokovic@ipb.ac.rs, maletic@ipb.ac.rs, udovicic@ipb.ac.rs, banjanac@ipb.ac.rs,
dragic@ipb.ac.rs, msavic@ipb.ac.rs, veselinovic@ipb.ac.rs, davidk@ipb.ac.rs*

SADRŽAJ

Zbog svojih osobina, olovo se uobičajeno koristi kao materijal za zaštitu germanijumskih detektora. Mioni iz kosmičkog zračenja u interakcijama sa olovom proizvode sekundarno zračenje, koje doprinosi ukupnom fonu detektora. Značajan deo ove komponente fona čine neutroni proizvedeni u interakcijama miona u olovnoj zaštiti. Neutroni mogu biti poseban problem u eksperimentima u dubokim podzemnim laboratorijama. U podzemnoj laboratoriji u Institutu za fiziku u Beogradu, germanijumski detektor, koji se nalazi u olovnoj zaštiti, može raditi u koincidenciji sa mionskim detektorom. U ovom režimu rada mogu se proučavati različiti efekti u germanijumskom detektoru izazvani mionima, posebno efekti koji potiču od neutrona proizvedenih mionima. Ovde su predstavljeni rezultati Geant4 simulacija produkcije neutrona u olovu mionima iz kosmičkog zračenja. Rezultat ovih simulacija je procena prinosa neutrona – broja proizvedenih neutrona u olovu po jedinici dužine puta – u interakcijama miona. Pored toga, određena je raspodela multipliciteta neutrona, kao broja proizvedenih neutrona u jednoj interakciji.

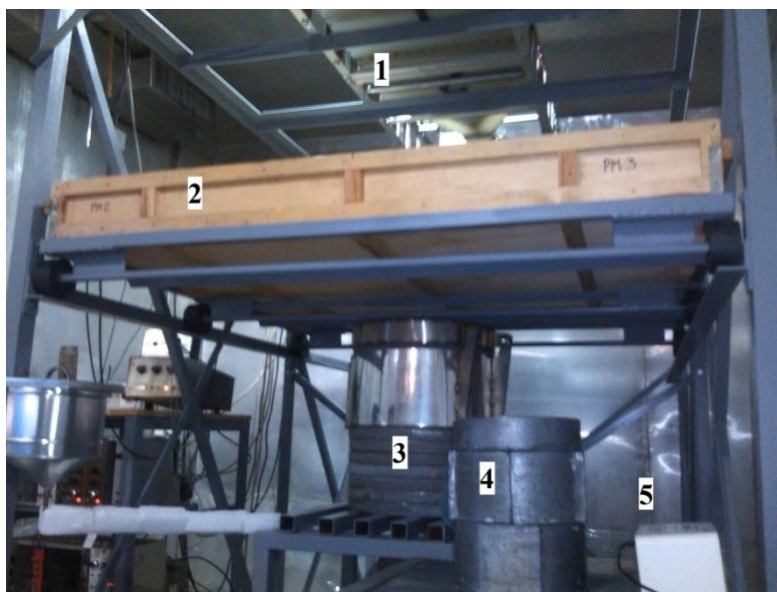
1. Uvod

U eksperimentima u kojima se traže retki događaji glavni problem je redukcija fonskog zračenja. Zato se ovi eksperimenti vrše u podzemnim laboratorijama, gde je fon u odnosu na površinu Zemlje znatno niži. Međutim, mioni iz kosmičkog zračenja su veoma prodorne čestice, prisutne i u dubokim podzemnim laboratorijama, i zato čine važan izvor fonskog zračenja u ovakvim osetljivim eksperimentima. Poseban problem je mionima indukovano sekundarno zračenje u detektorima i njihovoj okolini (detektorskoj zaštiti, zidovima, itd). Značajan doprinos fonu potiče od neutrona proizvedenih u interakcijama miona sa materijalom u okolini detektora [1].

U Niskofonskoj laboratoriji Instituta za fiziku u Beogradu intenzitet kosmičkog zračenja kontinuirano se meri od 2002. godine [2,3]. Geografski položaj laboratorije je takav da se kosmičko zračenje koje se detektuje u osnovi sastoji od mionske tvrde komponente, uz izvestan procenat meke elektromagnetne komponente. Laboratorija se sastoji od nadzemnog i plitko ukopanog podzemnog dela na dubini od 12 m ispod površine. Zemljište (les) iznad podzemne laboratorije ima gustinu približno $2,0 \text{ g/cm}^3$ – efektivni apsorpcioni sloj iznosi približno 25 hg/cm^3 (25 m.w.e.). Na toj dubini prisutna je praktično samo mionska komponenta kosmičkog zračenja. Zbog svojih niskofonskih karakteristika, laboratorija je osposobljena za izučavanja različitih pojava generisanih kosmičkim zračenjem, pre svega događaja indukovanih mionima iz kosmičkog zračenja u germanijumskim detektorima, kao i u pasivnoj zaštiti detektora.

U podzemnoj laboratoriji nalazi se HPGe detektor deklarisanе aktivne zapremine 149 cm^3 i relativne efikasnosti 35 %. Podzemna pozicija detektora, zajedno sa olovnom

zaštitom debljine 12 cm, daje značajno smanjenje fonskog zračenja. Pored pasivne zaštite, za aktivnu veto zaštitu germanijumskog detektora mogu se koristiti postojeći scintilacioni detektori kosmičkog zračenja. Plastični scintilacioni detektor nalazi se neposredno iznad olovne zaštite; dimenzije detektora su 100 cm × 100 cm × 5 cm. Oba detektora – HPGe i scintilacioni – vezani su za analogno-digitalni konvertor, koji omogućava snimanje i čuvanje svih detektovanih događaja. Svi događaji analiziraju se *off-line*. Uz odgovarajuće selekzione kriterijume mogu se izdvojiti svi koincidentni i/ili antikoincidentni događaji u scintilacionom i HPGe detektoru [4,5].



Slika 1. Ekperimentalna konfiguracija u podzemnoj laboratoriji: scintilacioni detektori (1,2) i germanijumski detektor u olovnoj zaštiti (3).

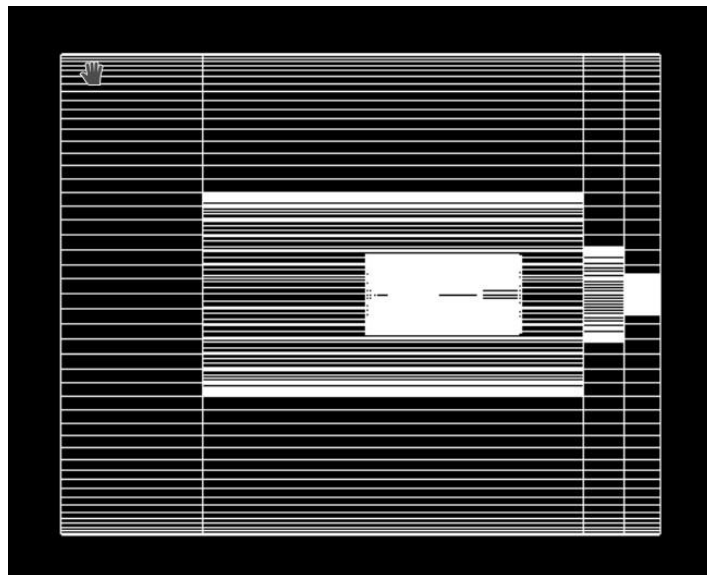
Prvi rezultati merenja produkcije neutrona mionima iz kosmičkog zračenja u olovnoj zaštiti HPGe detektora objavljeni su 2013. godine. Podaci su snimani tokom više od 400 dana merenja, u koincidentnom režimu rada scintilator-HPGe detektor. Analizom ovih podataka dobijen je rezultat za fluks neutrona proizvedenih mionima, na dubini naše podzemne laboratorije [6]. Merenja su kontinuirano nastavljena, sa većom statistikom snimljenih događaja; analiza ovih podataka je u toku. Pored eksperimentalnih merenja, uporedo su urađene Monte Carlo simulacije produkcije neutrona u olovnoj zaštiti, bazirane na Geant4 *framework*-u. Ovde su predstavljeni prvi rezultati simulacija: procena prinosa neutrona (broj neutrona po jedinici dužine) u interakcijama miona, kao i raspodela multipliciteta proizvedenih neutrona.

2. Metod

Geant4 je softverski paket za Monte Carlo simulacije transporta i interakcija čestica sa materijom [7]. On sadrži kompletan alat za modelovanje geometrije detektora, fizičkih procesa, primarnih i sekundarnih događaja, kao i odziva detektora. Na osnovi Geant4 platforme razvijena je posebna aplikacija za simulacije odziva germanijumskog i scintilacionih detektora u laboratoriji. Aplikacija je fleksibilna i omogućuje simulacije pojedinačnih i koincidentnih režima rada detektora. Prethodno je korišćena u različitim

slučajevima koji su zahtevali precizne simulacije scintilacionih i germanijumskih detektora [2,4,8,9].

Olovna zaštita je geometrije šupljeg cilindra, unutar kojeg se nalazi germanijumski detektor. Visina cilindra je 51 cm, prečnik osnove 41 cm, a debljina olovnog zida je 12 cm. Detektor je konstruisan prema specifikaciji proizvođača. Skica detektora i olovnog cilindra prikazana je na slici 2.



Slika 2. Skica olovne zaštite germanijumskog detektora.

Primarni događaji generisani su definisanjem incidentne čestice, njene pozicije, pravca kretanja i energije. Incidentne čestice su pozitivni i negativni mioni; odnos broja pozitivnih i broja negativnih miona je 1,3. Početne pozicije miona na površini olovnog cilindra određene su na sledeći način: prvo se odabere gornja horizontalna strana ili vertikalna strana cilindra, prema verovatnoći da kosmički mion pogodi horizontalnu ili vertikalnu stranu, a zatim se odabere pozicija na datoj površini iz uniformne raspodele. Pravac kretanja miona simpliran je iz raspodele miona po pravcima, u funkciji od zenitnog ugla θ , koja je proporcionalna $\cos^{1.55}\theta$. Energija miona određena je iz energijske raspodele miona na površini Zemlje, pri čemu se uzimaju oni mioni koji uspeju da prođu kroz 12 m zemljišta. Detaljnija procedura generisanja primarnih događaja i izvođenje raspodele miona po pravcima i energijama može se videti u [4].

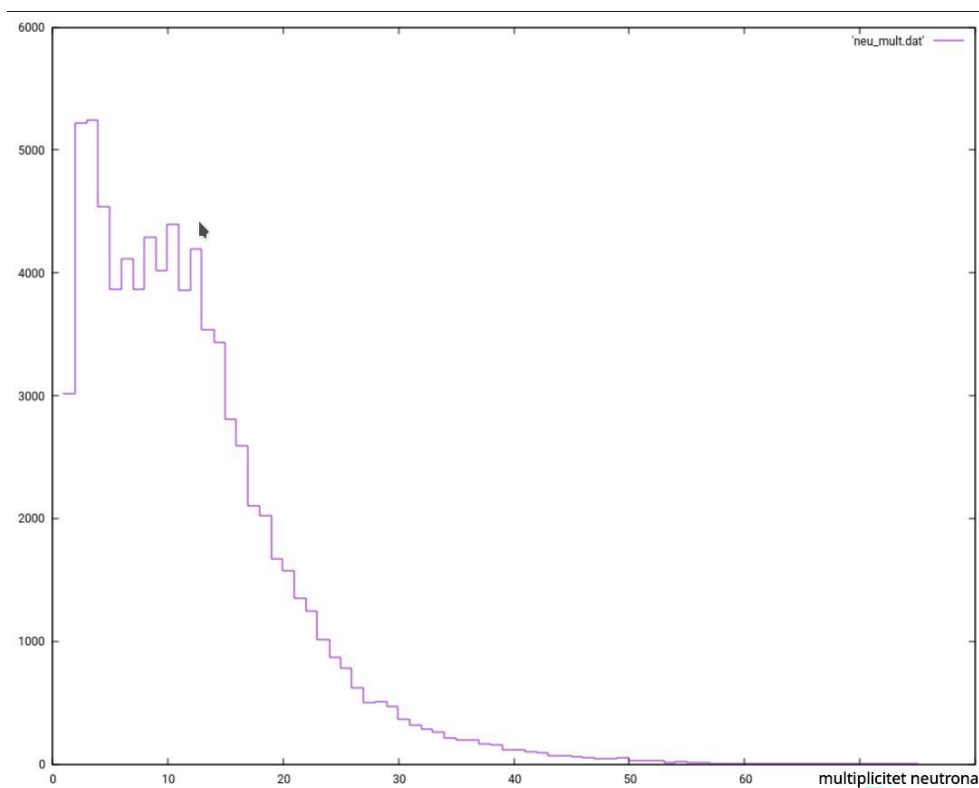
Fizički procesi u kojima učestvuju mioni – elektromagnetni i nuklearni – uključeni su u simulaciju kroz predefinisane Geant4 klase QGSP_BERT_HP; ova klasa omogućava simulacije interakcija čestica sa velikom preciznošću.

3. Rezultati i diskusija

Prvi cilj simulacije bio je da se odredi broj proizvedenih neutrona u interakcijama miona sa jezgrom olova, po jedinici dužine puta, pri njihovom prolasku kroz olovnu zaštitu germanijumskog detektora. Generisanih primarnih događaja bilo je 10^8 ; ovaj broj može biti povezan sa vremenom eksperimentalnih merenja, uzimajući u obzir fluks miona u podzemnoj laboratoriji.

Ukupan broj proizvedenih neutrona bio je 934 000. Odavde je određen prinos neutrona, kao odnos broja neutrona i proizvoda gustine olova i srednje dužine puta miona kroz

olovo. Srednja dužina puta miona je 26,6 cm, a proizvod gustine olova i srednje dužine puta iznosi 302 g/cm^3 . Dobijena vrednost za prinos neutrona je $3,1 \times 10^{-5} \text{ neut.}/(\text{gcm}^{-2})$. Pored prinosa neutrona, određena je raspodela multipliciteta neutrona – broja neutrona proizvedenih u interakciji jednog miona sa olovom. Mion može proizvesti više od jednog neutrona na svom putu kroz olovo, što za rezultat ima više neutronske fonske događaja u detektoru koji potiču od jednog miona. Događaji su vremenski razdvojeni, odnosno detektuju se sa vremenskim razmakom, u zavisnosti od trenutka i mesta produkcije neutrona. Ovi događaji registruju se u detektoru kao signali sa vremenskim kašnjenjem, unutar definisanog vremenskog prozora mionskog događaja. To može poslužiti za selekciju fonskih događaja koji potiču od neutrona indukovanih mionima. Raspodela multipliciteta neutrona prikazana je na slici 3. Najveći broj miona proizvede manje od 10 neutrona u kaskadi, dok srednji multiplicitet neutrona iznosi 11,5. Dobijena raspodela slaže se sa rezultatima ranijih sličnih simulacija [10].



Slika 3. Raspodela multipliciteta neutrona proizvedenih mionima iz kosmičkog zračenja u olovnoj zaštiti HPGE detektora.

Rezultati simulacije pokazali su da ovaj metod može biti koristan za procenu produkcije neutrona mionima iz kosmičkog zračenja. On može dati detaljniji uvid u mehanizam produkcije neutrona. Osim toga, rezultati simulacije mogu pomoći u analizi podataka eksperimentalnih merenja, njihovom boljem razumevanju i evaluaciji.

4. Zahvalnica

Ovaj rad finansiran je od Instituta za fiziku u Beogradu kroz projekat Ministarstva prosvete, nauke i tehnološkog razvoja Republike Srbije.

5. Literatura

- [1] D. Mei, A. Hime. Muon-induced background study for underground laboratories. *Phys. Rev. D* 73, 2006, 053004.
- [2] A. Dragić, D. Joković, R. Banjanac, V. Udovičić, B. Panić, J. Puzović, I. Aničin. Measurement of cosmic ray muon flux in the Belgrade ground level and underground laboratories. *Nucl. Instr. Meth. A* 591, 2008, 470-475.
- [3] M. Savić, A. Dragić, D. Maletić, N. Veselinović, R. Banjanac, D. Joković, V. Udovičić. A novel method for atmospheric correction of cosmic-ray data based on principal component analysis. *Astropart. Phys.* 109, 2019, 1-11.
- [4] D. Joković, A. Dragić, V. Udovičić, R. Banjanac, J. Puzović, I. Aničin. Monte Carlo simulations of the response of a plastic scintillator and an HPGe spectrometer in coincidence. *Appl. Radiat. Isot.* 67, 2009, 719-722.
- [5] A. Dragić, V. Udovičić, R. Banjanac, D. Joković, D. Maletić, N. Veselinović, M. Savić, J. Puzović, I. Aničin. The new set-up in the Belgrade low-level and cosmic-ray laboratory. *Nucl. Techn. Radiat. Prot.* 26, 2011, 181-192.
- [6] A. Dragić, I. Aničin, R. Banjanac, V. Udovičić, D. Joković, D. Maletić, M. Savić, N. Veselinović, J. Puzović. Neutrons produced by muons at 25 mwe. *J. Phys.: Conf. Ser.* 409, 2013 012054.
- [7] S. Agostinelli et al. Geant4 – a simulation toolkit. *Nucl. Instr. Meth. A* 506, 2003, 250-303.
- [8] M. Krmar, J. Hansman, N. Jovančević, N. Lalović, J. Slivka, D. Joković, D. Maletić. A method to estimate a contribution of Ge(n,n') reaction to the low-energy part of gamma spectra of HPGe detectors. *Nucl. Instr. Meth. A* 709, 2013, 8-11.
- [9] J. Nikolić, T. Vidmar, D. Joković, M. Rajačić, D. Todorović. Calculation of HPGe efficiency for environmental samples: comparison of EFFTRAN and GEANT4. *Nucl. Instr. Meth. A* 763, 2014, 347-353.
- [10] L. Reichhart et al. Measurement and simulation of the muon-induced neutron yield in lead. *Astropart. Phys.* 47, 2017, 67-76.

MONTE CARLO SIMULATION OF THE COSMIC RAY MUON INDUCED NEUTRON PRODUCTION IN THE LEAD SHIELD OF THE GERMANIUM DETECTOR

**Dejan JOKOVIĆ, Dimitrije MALETIĆ, Vladimir UDOVIČIĆ,
Radomir BANJANAC, Aleksandar DRAGIĆ, Mihailo SAVIĆ,
Nikola VESELINOVIĆ and David KNEŽEVIĆ**

*Institute of Physics Belgrade, University of Belgrade, Belgrade, Serbia,
yokovic@ipb.ac.rs, maletic@ipb.ac.rs, udovicic@ipb.ac.rs, banjanac@ipb.ac.rs,
dragic@ipb.ac.rs, msavic@ipb.ac.rs, veselinovic@ipb.ac.rs, davidk@ipb.ac.rs*

ABSTRACT

Lead is usually used as a common shielding material for germanium detectors. Cosmic ray muons produce secondary particles in their interactions with lead nuclei, which contribute to overall background radiation detected by germanium detectors. Neutrons produced in muon interactions in lead shield make a significant part of this background component. Cosmic ray induced neutrons are a particular problem in experiments carried out in deep underground laboratories.

In the low-level underground laboratory at Institute of Physics Belgrade, a germanium detector and a muon detector operate in coincidence. This provides studying of different effects in the germanium detector induced by cosmic rays, especially effects originated from the cosmic ray induced neutrons.

Here, the results of Geant4 simulations of the cosmic ray muon induced neutron production in the lead shield of the germanium detector are presented. Estimate of the neutron yield – number of neutrons produced per unit path length – in muon interactions is obtained. The result is 3.1×10^{-5} neutrons/(gcm⁻²). Also, the neutron multiplicity distribution is determined, as a distribution of number of neutrons produced per muon interaction. The average multiplicity is 11.5.



European
Commission

EUROPEAN ATLAS OF NATURAL RADIATION



EUROPEAN ATLAS OF NATURAL RADIATION

Publication details

To refer to this 1st edition of the European Atlas of Natural Radiation please cite as follows:

Cinelli, G., De Cort, M. & Tollefsen, T. (Eds.), *European Atlas of Natural Radiation*, Publication Office of the European Union, Luxembourg, 2019.

The full version of this atlas will be available online at: <https://remon.jrc.ec.europa.eu/About/Atlas-of-Natural-Radiation>

This URL gives access to the index and leads to an interactive map interface where map layers compiled using the convergence of evidence concept can be interrogated.

Individual pages in this atlas contain QR codes which, when scanned, bring the reader to the exact online location to access the related page content.

Luxembourg: Publications Office of the European Union, 2019.

© European Union, 2019.

Copyright notice and disclaimer

© European Union, 2019

The information and views set out in this book are those of the authors and do not necessarily reflect the official opinion of the European Union. Neither the European Union institutions and bodies nor any person acting on their behalf may be held responsible for the use which may be made of the information contained therein.

The reuse policy of the European Commission is implemented by Commission Decision 2011/833/EU of 12 December 2011 on the reuse of Commission documents (OJ L 330, 14.12.2011, p. 39).

Reuse is authorised, provided the source of the document is acknowledged and its original meaning or message is not distorted. The Commission is not liable for any consequence stemming from the reuse of this publication.

Reuse of photos/figures/diagrams/data with source: EANR, EC-JRC, 2019 is authorised.

For reuse of photos/figures/diagrams/data of a third-party source (i.e. any other than EANR, EC-JRC, 2019), permissions must be sought directly from the source.

Sources are indicated throughout the Atlas by: Source: [identification of the source].

Published by the Publications Office of the European Union, L-2995 Luxembourg, Luxembourg.

European Atlas of Natural Radiation

Printed version

ISBN 978-92-76-08259-0

doi:10.2760/520053

Catalogue number KJ-02-19-425-EN-C

Online version

ISBN 978-92-76-08258-3

doi:10.2760/46388

Catalogue number KJ-02-19-425-EN-N

2019 – 190 pp. – 30.1 × 42.4 cm

Printed by Bietlot in Belgium

Printed on elemental chlorine-free bleached paper (ECF).

Cartographic Representations

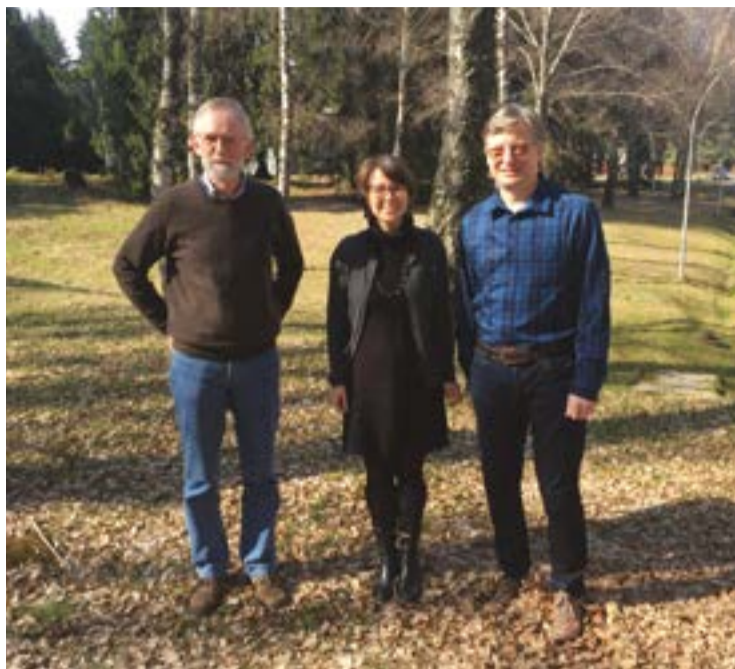
Underlying cartographic features depicted on the maps in this atlas are derived from the Digital Chart of the World and Lovell Johns Cartographic Base. These data do not have any explicit legal status; hence, no legal aspects should be derived from the information depicted on any of the maps in this publication.

http://en.wikipedia.org/wiki/Digital_Chart_of_the_World

www.lovelljohns.com

Due to the resolution of the underlying data which is often still too large to represent small islands, the maps represented in this atlas might not or not always represent a number of small Pacific islands. These are included in the interactive online version when provided in the datasets.

All the maps are represented according to the Robinson projection.



The Editorial Board (Marc, Giorgia and Tore) pictured at JRC, Ispra.
Source: EANR, EC-JRC, 2019.

Disclaimer of Liability

This is a publication of the Joint Research Centre (JRC), the European Commission's science and knowledge service. It aims to provide evidence-based scientific support to the European policymaking process. The scientific output expressed does not imply a policy position of the European Commission. Neither the European Commission nor any person acting on behalf of the Commission is responsible for the use that might be made of this publication. For information on the methodology and quality underlying the data used in this publication for which the source is neither Eurostat nor other Commission services, users should contact the referenced source. The designations employed and the presentation of material on the maps do not imply the expression of any opinion whatsoever on the part of the European Union concerning the legal status of any country, territory, city or area or of its authorities, or concerning the delimitation of its frontiers or boundaries.

Design and graphic support

Final design and graphic support by Lovell Johns Limited, 10 Hanborough Business Park, Long Hanborough, Witney, Oxfordshire, OX29 8RU, United Kingdom.

<http://www.lovelljohns.com>



GETTING IN TOUCH WITH EU

In person

All over the European Union there are hundreds of Europe Direct information centres. You can find the address of the centre nearest you at: https://europa.eu/european-union/contact_en

On the phone or by email

Europe Direct is a service that answers your questions about the European Union. You can contact this service:

- by freephone: 00 800 6 7 8 9 10 11 (certain operators may charge for these calls),
- at the following standard number: +32 22999696, or
- by electronic mail via: https://europa.eu/european-union/contact_en

FINDING INFORMATION ABOUT THE EU

Online

Information about the European Union in all the official languages of the EU is available on the Europa website at: https://europa.eu/european-union/index_en

EU publications

You can download or order free and priced EU publications from EU Bookshop at: <https://publications.europa.eu/en/publications>. Multiple copies of free publications may be obtained by contacting Europe Direct or your local information centre (see https://europa.eu/european-union/contact_en).

Acknowledgements

The European Atlas of Natural Radiation (EANR) is the result of fruitful collaborations between more than 100 experts from national and international institutions, universities and research centres around Europe. We acknowledge all of the contributing Authors and Reviewers: without their contributions, support and encouragement this publication would not have been possible.

We would like to thank the Advisory Committee, Valeria Gruber and Peter Bossew, for having worked from the begin of the project with constant passion and dedication as well as Gregoire Dubois, who, as one of the founders of the Atlas project, did invaluable work to explore and develop the concept and establishing a European network of institutions and experts.

Two head of units, Franck Wastin and Willem Janssens are acknowledged for their managerial support to the project.

We also would like to express our great thanks to the JRC Radioactivity Environmental Monitoring group (JRC, Ispra), in particular Luca De Felice, Konstantins Bogučarskis, Stefano Vanzo, Pier Valerio Tognoli and Daniel Jianu for their constant assistance in technical issues and in developing the EANR website. Also, for providing support, we acknowledge Elena Moneta, Fanny May and Gabriele Tamborini.

Our special thanks go to Ian Dewsbury from Lovell Johns Ltd. (UK) for his professional guidance in graphic design and cartography, for keeping our scientific, sometimes over-enthusiastic, ideas within publication limits and for turning these into an attractive and modern-looking atlas. William Adnams gave his expertise in GIS/cartographic matters, Clare Varney provided graphical assistance and Symon Porteous for smoothing out the contractual details.

The EU Publications Office and the JRC Central IP Service are acknowledged for their assistance and guidance.

The topic of natural radiation is of great significance to the scientific community, population and national authorities; the latter are thanked for their support and for their agreement on the final version of the maps. We apologise for any unintentional omissions, it is impossible to credit all people who give their direct or indirect contribution.

This QR code points to the full online version of the Atlas, where the most updated content may be freely accessed



Contributors

Editorial Board

Cinelli, Giorgia	European Commission, Joint Research Centre, Ispra, Italy
De Cort, Marc	European Commission, Joint Research Centre, Ispra, Italy
Tollefsen, Tore	European Commission, Joint Research Centre, Ispra, Italy

Contributing Authors

Achatz, Michaela	German Federal Office for Radiation Protection, Berlin, Germany
Ajtić, Jelena	Faculty of Veterinary Medicine, University of Belgrade, Belgrade, Serbia
Ballabio, Cristiano	European Commission, Joint Research Centre, Ispra, Italy
Barnet, Ivan	Czech Geological Survey, Prague, Czech Republic
Borelli, Pasquale	Environmental Geosciences, University of Basel, Basel, Switzerland
Bossew, Peter	German Federal Office for Radiation Protection, Berlin, Germany
Brattich, Erika	Department of Physics and Astronomy, Alma Mater Studiorum University of Bologna, Bologna, Italy
Briganti, Alessandra	Department of Science, Roma Tre University, Rome, Italy
Castelluccio, Mauro	Department of Science, Roma Tre University, Rome, Italy
Chiaberto, Enrico	Regional Agency for the Protection of the Environment, Piemonte, Italy
Cinelli, Giorgia	European Commission, Joint Research Centre, Ispra, Italy
Ciotoli, Giancarlo	National Research Council, Rome, Italy
Coletti, Chiara	Department of Geosciences, University of Padova, Padova, Italy
Cucchi, Anselmo	Regional Agency for the Protection of the Environment, Piemonte, , Italy
Daraktchieva, Zornitza	Centre for Radiation, Chemical and Environmental Hazards, Public Health England, Chilton, UK
De Cort, Marc	European Commission, Joint Research Centre, Ispra, Italy
Domingos, Filipa	Department of Earth Sciences, University of Coimbra, Coimbra, Portugal
Dudar, Tamara	Department of Environmental Studies, National Aviation University, Kiev, Ukraine
Elío, Javier	Trinity College Dublin, Dublin, Ireland
Falletti, Paolo	Regional Agency for the Protection of the Environment, Piemonte, Italy
Ferreira, Antonio	British Geological Survey, Keyworth, UK
Finne, Ingvild Engen	Norwegian Radiation and Nuclear Safety Authority, Østerås, Norway
Fuente Merino, Ismael	University of Cantabria, Santander, Spain
Galli, Gianfranco	Istituto Nazionale di Geofisica e Vulcanologia, Rome, Italy
García-Talavera, Marta	Consejo de Seguridad Nuclear, Madrid, Spain
Gruber, Valeria	Department for Radon and Radioecology, Austrian Agency for Health and Food Safety, Linz, Austria
Gutiérrez Villanueva, José-Luis	Radonova Laboratories, Uppsala, Sweden
Hernandez Ceballos, Miguel Angel	European Commission, Joint Research Centre, Ispra, Italy
Hoffmann, Marcus	Radon Competence Centre, University of Applied Sciences and Arts of Southern Switzerland, Canobbio, Switzerland
Iurlaro, Giorgia	Italian National Agency for New Technologies, Energy and Sustainable Economic Development, Ispra, Italy
Ivanova, Kremena	National Centre of Radiobiology and Radiation Protection, Sofia, Bulgaria
Jones, Arwyn	European Commission, Joint Research Centre, Ispra, Italy
Kovalenko, Grygoriy	Ukrainian Scientific Research Institute of Ecological Problems, Kharkiv, Ukraine
Kozak, Krzysztof	Institute of Nuclear Physics IFJ-PAN, Krakow, Poland
Lawley, Russell	British Geological Survey, Keyworth, UK
Lehné, Rouwen	Hessian Agency for Nature Conservation, Environment and Geology, Darmstadt, Germany
Lister, Bob	British Geological Survey, Keyworth, UK
Long, Stephanie	Environmental Protection Agency, Dublin, Ireland
Lucchetti, Carlo	Department of Science, Roma Tre University, Rome, Italy
Magnoni, Mauro	Regional Agency for the Protection of the Environment, Piemonte, Italy

Reviewers

Bochicchio, Francesco	National Center for Radiation Protection and Computational Physics – Italian National Institute of Health, Rome, Italy
Braga, Roberto	Uiversita' of Bologna, Dipartimento di Scienze Biologiche, Geologiche e Ambientali Bologna, Italy
Carpentieri, Carmela	National Center for Radiation Protection and Computational Physics – Italian National Institute of Health, Rome, Italy
Castellani, Carlo Maria	Italian National Agency for New Technologies, Energy and Sustainable Economic Development, Bologna, Italy
Christian, Di Carlo	National Center for Radiation Protection and Computational Physics – Italian National Institute of Health, Rome, Italy
De France, Jennifer	World Health Organization, Department of Public Health, Environmental and Social Determinants of Health, Geneva, Switzerland
Dehandschutter, Boris	Federal Agency for Nuclear Control, Bruxelles, Belgium
Elío, Javier	Geology, School of Natural Sciences, Trinity College, Dublin, Ireland
Fontana, Claudia	Centro di ricerca Agricoltura e Ambiente, Rome, Italy
German, Olga	International Atomic Energy Agency, Radiation Safety and Monitoring Section, Vienna, Austria
Grossi, Claudia	Universitat Politècnica de Catalunya, Barcelona, Spain
Gruber, Valeria	Austrian Agency for Health and Food Safety Department for Radon and Radioecology, Linz, Austria

The European Radon Association (ERA) (<http://radoneurope.org/>) contributed by writing the summary for each chapter. The following ERA-members are acknowledged:

Dehandschutter, Boris	Federal Agency for Nuclear Control, Bruxelles, Belgium
Gutierrez, Villanueva Jose Luis	Radonova Laboratories, Uppsala, Sweden
Hansen, Maria	GM Scientific, Bristol, UK
Hurst, Stephanie	Saxon state ministry of the environment and agriculture Radiation Protection, Genetic Engineering, Chemicals, Dresden Germany
Kozak, Krzysztof	Institute of Nuclear Physics IFJ-PAN, Krakow, Poland
Mazur, Jadwiga	Institute of Nuclear Physics IFJ-PAN, Krakow, Poland

Advisory Committee

Bossew, Peter	German Federal Office for Radiation Protection, Berlin, Germany
Gruber, Valeria	Austrian Agency for Health and Food Safety, Department for Radon and Radioecology, Linz, Austria
Matolin, Milan	Faculty of Science, Charles University, Prague, Czech Republic
Mazur, Jadwiga	Institute of Nuclear Physics IFJ-PAN, Krakow, Poland
Mazzoli, Claudio	Department of Geosciences, University of Padova, Padova, Italy
Mollo, Mara	Mara Mollo Total Consulting, Vercelli, Italy
Mostacci, Domiziano	Department of Industrial Engineering, Alma Mater Studiorum University of Bologna, Bologna, Italy
Mundigl, Stefan	Radiation Protection and Nuclear Safety Unit, European Commission, Directorate-General Energy, Luxembourg, Luxembourg
Nesbor, Dieter	Hessian Agency for Nature Conservation, Environment and Geology, Darmstadt, Germany
Neves, Luis	Department of Earth Sciences, University of Coimbra, Coimbra, Portugal
Nikolov, Jovana	Faculty of Sciences, Department of Physics, University of Novi Sad, Novi Sad, Serbia
Nogarotto, Alessio	University of Bologna, Bologna, Italy
Onischenko, Aleksandra	Institute of Industrial Ecology, Russian Academy of Sciences, Ekaterinburg, Russia
Orgiazzi, Alberto	European Commission, Joint Research Centre, Ispra, Italy
Pacherová, Petra	Czech Geological Survey, Prague, Czech Republic
Panagos, Panos	European Commission, Joint Research Centre, Ispra, Italy
Pereira, Alcides	Department of Earth Sciences, University of Coimbra, Coimbra, Portugal
Pokalyuk, Vladimir	Institute of Environmental Geochemistry, National Academy of Sciences of Ukraine, Kiev, Ukraine
Quindós Poncela, Luis Santiago	University of Cantabria, Santander, Spain
Sassi, Raffaele	Department of Geosciences, University of Padova, Padova, Italy
Smedley, Pauline	British Geological Survey, Keyworth, UK
Soligo, Michele	Department of Sciences, Roma Tre University, Rome, Italy
Stoulos, Stylianos	Nuclear Physics Laboratory, Aristotle University Thessaloniki, Thessaloniki, Greece
Szabó, Katalin	Nuclear Security Department, Hungarian Academy of Sciences, Centre for Energy Research, Budapest, Hungary
Täht-Kok, Krista	Geological Survey of Estonia, Tallinn, Estonia
Todorović, Nataša	Faculty of Sciences, Department of Physics, University of Novi Sad, Novi Sad, Serbia
Tollefsen, Tore	European Commission, Joint Research Centre, Ispra, Italy
Tuccimei, Paola	Department of Sciences, Roma Tre University, Rome, Italy
Turtiainen, Tuukka	Radiation and Nuclear Safety Authority, Helsinki, Finland
Tye, Andrew	British Geological Survey, Keyworth, UK
Udovičić, Vladimir	Institute of Physics, Belgrade, Serbia
Vasilyev, Aleksey	Institute of Industrial Ecology, Russian Academy of Sciences, Ekaterinburg, Russia
Verdelocco, Stefania	Conseil et Etude en Radioprotection, Ispra, Italy
Verkhovtsev, Valentin	Institute of Environmental Geochemistry, National Academy of Sciences of Ukraine, Kiev, Ukraine
Voltaggio, Mario	Istituto di Geologia Ambientale e Geingegneria, National Research Council, Rome, Italy
Zhukova, Olga	Republican Centre for Hydrometeorology, Control of Radioactive Contamination, and Environmental Monitoring, Minsk, Belarus
Zhukovsky, Michael	Institute of Industrial Ecology, Russian Academy of Sciences, Ekaterinburg, Russia

Hernandez-Ceballos, Miguel Angel	European Commission, Joint Research Centre, Ispra, Italy
Iurlaro, Giorgia	Italian National Agency for New Technologies, Energy and Sustainable Economic Development, Ispra, Italy
Jobbagy, Viktor	European Commission, Joint Research Centre, Geel, Belgium
Matolin, Milan	Charles University, Faculty of Science, Institute of Hydrogeology, Engineering Geology and Applied Geophysics , Prague, Czech Republic
McLaughlin, James	School of Physics, University College Dublin, Dublin, Ireland
Mundigl, Stefan	European Commission, Directorate-General Energy, Radiation Protection and Nuclear Safety Unit, Luxembourg, Luxembourg
Nezmal, Matej	RADON v.o.s., Prague, Czech Republic
Perez, Maria Del Rosario	World Health Organization, Department of Public Health, Environmental and Social Determinants of Health, Geneva, Switzerland
Rossi, Francois	European Commission, Joint Research Centre, Petten, Netherlands
Sangiorgi, Marco	European Commission, Joint Research Centre, Ispra, Italy
Simic, Zdenko	European Commission, Joint Research Centre, Petten, Netherlands
Socciarelli, Silvia	Centro di ricerca Agricoltura e Ambiente, Rome, Italy
Tolton, Richelle	International Atomic Energy Agency, Radiation Safety and Monitoring Section, Vienna, Austria
Venoso, Gennaro	National Center for Radiation Protection and Computational Physics – Italian National Institute of Health, Rome, Italy

McLaughlin, James	University College Dublin School of Physics Dublin, Dublin, Ireland
Nilsson, Per	Driftwood consulting, Visby, Sweden
Pressyanov, Dobromir	University of Sofia, Sofia, Bulgaria
Ringer, Wolfgang	Austrian Agency for Health and Food Safety Department for Radon and Radioecology, Linz, Austria
Udovicic, Vladimir	Institute of Physics, Belgrade, Serbia

23.2.2015.

Poštovani,

Sa zadovoljstvom Vas obaveštavam da je *Naučni odbor V Međunarodnog kongresa BIOMEDICINA I GEONAUKE - UTICAJ ŽIVOTNE SREDINE NA LJUDSKO ZDRAVLJE* (Beograd, 3-4. mart 2015. godine) prihvatio rad: **NACIONALNI PROGRAM KONTROLE IZLOŽENOSTI STANOVNIŠTVA RADONU U SRBIJI**, autora: *V. Udovičić, D. Maletić, M. Eremić Savković, G. Pantelić, P. Ujić, I. Čeliković, S. Forkapić, D. Nikezić, V. M. Marković, V. Arsić.*

Molim Vas da imate u vidu da ćete rad izložiti kao **predavač po pozivu** (u trajanju 15-20 minuta) u okviru *Plenarne sesije* Kongresa, 3.3.2015. godine.

Podsećam Vas da je kotizaciju potrebno uplatiti na račun *Asocijacije geofizičara i ekologa Srbije AGES: Komercijalna banka*, No.: 205-129603-55 (svrha uplate: *kotizacija*) ili prilikom registracije na samom Kongresu. Kotizacija iznosi 7 000,00 din (za strane učesnike: 60 Eura) i plaćaju je svi učesnici Kongresa, a ona obuhvata: štampanje rad(ov)a u Zborniku radova na CD-u, koktel dobrodošlice, torbu sa kongresnim materijalima, program Kongresa i kafe pauze.

Do skorog viđenja u Beogradu, srdačno Vas pozdravljam!

S poštovanjem,



Prof. dr Snežana Komatina,
predsednik AGES





UNIVERSITY OF PANNONIA
Institute of Radiochemistry and Radioecology
H-8201 HUNGARY, Veszprém, Egyetem u. 10., P.O.B. 158.
Tel: (+36)-(88)- 624 178



3rd May 2013

Vladimir Udovicic
Institute of Physics, University of
Belgrade
SERBIA

LETTER of INVITATION

Dear Vladimir Udovicic,

We are pleased to let You know that the organizing board of the conference on environment protection titled 'VIIth Hungarian Radon Forum and Radon in Environment Workshop, 16-17th May 2013 Veszprém HUNGARY' would like to ask You to give a lecture as invited lecturer. Your participation at the conference is free of registration fee.

Best Regards,

A handwritten signature in blue ink, appearing to be 'T. Kovacs'.

Dr Tibor Kovacs
secretary of conference



About

[Overview](#)

[Executive Committee](#)

[General Assembly](#)

[History](#)

ERA Executive Committee (2018-2019)

President

Per Nilsson (Driftwood Consulting AB- Sweden)

Experienced radon expert with a demonstrated history of working in the environmental services industry. Skilled in Radiation Safety, Medical Devices, Sales, Customer Relationship Management (CRM), and Dosimetry. Strong business development skills.

Vice-President

Carmela Carpentieri (ISS – Italy)

Carmela Carpentieri graduated in physics at “Federico II” University in Naples in 2000, studied for her PHD in high energy physics at “Albert Ludwig” University in Freiburg and post-graduated in medical physics at Pisa University. Since 2009, she has been working as a researcher of the National Center for Radiation Protection and Computational Physics, within the Italian National Institute of Health (Istituto Superiore di Sanità – ISS). Her research activities cover radioactivity, both from natural and artificial sources, from a radioprotection point of view, with a strong focus on radon isotopes. The areas of interest include measurement protocols and techniques, dosimetry, epidemiology, risk assessment, remediation and prevention, policies and regulation. She is involved in several projects national and international and also in activities within the current Italian National Radon Action Plan, as well as in developing the new NRAP according to the requirements of the 2013/59/Euratom directive.

Treasurer

Boris Dehandschutter (FANC – Belgium)

Boris Dehandschutter is active in the field of radiation protection. The research topic of his PhD (in Geology, 2001) has been the structural evolution of sedimentary basins, using among others environmental radioactivity measurements and mapping. After post-doctoral research on the geological aspects of radioactive waste disposal (fracture development and fracture permeability of argillaceous sediments), he coordinated several international projects related to natural radioactivity and its environmental impact. Since 2007 he works at the Belgian radiation protection authority (FANC) on the topics of natural radioactivity (NORM and radon). He is responsible for the national radon programme of Belgium, including radon risk mapping, radon measurement campaigns in dwellings and workplaces, radon awareness activities, training and development of regulations regarding radon.

Secretary

José - Luis Gutiérrez (Radonova laboratories AB – Sweden)

José - Luis Gutiérrez Villanueva is specialist radon measurement advisor at Radonova Laboratories AB (Sweden). He is a PhD. on Physics with the Thesis entitled “Radon concentrations in air, soil and water in a granitic area: instrumental development and measurements”. His research involves radon gas and natural radioactivity as well as monitoring of

[View our](#)

[Code of Ethics](#)

(<https://radoneurope.org/code-of-ethics/>)

[View our](#)

[Statutes](#)

(<https://radoneurope.org/statutes/>)

[View our](#)

[Election EC of ERA](#)

(<https://radoneurope.org/election-of-the-ec-of-era/>)

radioactivity at steel factories. He has expertise on metrology techniques for natural and artificial radioactivity such as gamma spectrometry, liquid scintillation counting and measurement of radon gas both passive and active methods (air, soil and water).

Bernard Collignan (CSTB – France)

Bernard Collignan is a Senior Research Engineer, Ph-D in the field of Fluid Mechanics and Energy. He works at the Centre Scientifique et Technique du Bâtiment (CSTB) since 1996, initially in thermal and ventilation of buildings and now in the field of Indoor Air Quality. He is involved for several years in the field of management of the impact of soil gaseous pollutants on Indoor Air Quality: industrial pollution (VOCs) or natural (radon). His work includes the development of models to study the transfer of soil gaseous pollutants to indoor environments for the characterization of indoor exposures, the development and the design of solutions to protect buildings from these pollutants, and in a more general way, as scientific and technical support for public authorities in the management of these issues and the dissemination of information to building professionals and users.

Maria Hansen (GM Scientific- UK)

Maria Hansen is the Director of GM Scientific. Maria has a PhD in particle physics, she ventured into the commercial side of passive track etch measurements. She worked for a spin-off company from Bristol university until last year, manufacturing CR-39, selling automated analysis equipment and setting up and running a radon measurement service. She has since been continuing the work with measurement laboratories, training staff, installing and maintaining equipment and provided equipment and materials when required. She has an interest in improving the materials used in the passive track etch technology to ultimately improve the measurement capability of these types of detectors to ensure the data used in research is as good as possible and the uncertainties minimised. Maria has been involved with the two radon bodies in the UK over the years; the UK Radon Association and The Radon Council before joining the ERA executive committee in 2017.

James Mc Laughlin(University College Dublin – Ireland)

James Mc Laughlin is an Emeritus Academic Member of the School of Physics, University College Dublin where, inter alia, he was leader of the Radon Research Group. He is the author of circa 140 scientific publications mostly in the radon field. He is a Fellow of the Institute of Physics (London) and has also been Visiting Professor at the Faculty of Medicine, University of Belgrade. In the mid 1980s he designed and carried out the first national Irish survey of indoor radon which identified for the first time high radon areas in Ireland. He has been a participant in a number of European Commission and World Health Organisation activities in the field of Indoor Air Quality. Over the years he has participated in several research projects funded by the European Commission most recently as leader of the Radon Risk Communication Work Package in the RADPAR (Radon Prevention and Remediation) Project (2005-2009). He was also Leader of the Radon Risk Communication Working Group of the World Health Organisation International Radon Project (2005-2009) and on a number of occasions has served as a consultant/technical expert to the IAEA (International Atomic Energy Agency) on radon topics. Recently (2011-2014) he has been a member of the ICRU (International Commission on Radiation Units) Report Committee on Measurement and Reporting of Radon Exposures. He is a Member of the Environmental Radioactivity Advisory Committee to the Radiological Protection Institute of Ireland and was a member of the Irish Government Advisory Expert Committee on the introduction of the Workplace Smoking Ban Legislation in 2004. His current interest is in the area of risk communication in the context of strategies to reduce the public health impact of radon exposure in Europe.

Paulo Pinto (Radosys Atlantic – Portugal)

Paulo Norte Pinto is the Managing Partner, Radosys Atlantic Lda based in Portugal. Paulo has worked for several years in the Natural Radioactivity Laboratory of the University of Coimbra, in Portugal, using different technologies and techniques, and co-designing the first radon

mitigation projects in the country. In 2013 he co- founded the Radosys Atlantic, a spin-off company from the LRN and the Radosys. With activities in the Portuguese & Spanish speaking countries, and Africa, he has been responsible for the installation of several passive radon dosimetry laboratories, with local staff training.

Dobromir Pressyanov (U. Sofia – Bulgaria)

Dobromir Pressyanov graduated nuclear physics in 1985 and worked as a health physicist in uranium industry and its health inspection till 1994. He acquired PhD in 1993 and DSc in 2013. Since 1994 Dr. Pressyanov works at Sofia University “St. Kliment Ohridski” where currently he is professor of physics (dosimetry and radiation protection). Most of his research (more than 120 publications and 4 patents) is related to radon and thoron. Particular topics that are worth to mention include retrospective measurements of radon and thoron (by CD/DVDs), organizing radon surveys in radon priority areas in Bulgaria, consultancy on mitigation of buildings. So far Dobromir Pressyanov has provided technical consultancy for mitigation of 24 buildings (most of them kindergartens and schools) in Bulgaria and have designed two radon prevention systems in new buildings (kindergartens). He was engaged as an expert in the International Radon Project of the World Health Organisation (2005-2008). In 2017 he served as Guest editor of special issues of Journal of Environmental Radioactivity and Radiation Protection Dosimetry, dedicated to radon. He has been head/member of organizing or scientific committees of international conferences and invited lecturer at conferences and institutions in different countries in Europe and North America. He is involved in national and international radon related projects and frequently invited to speak on radon on TV and radio programs in Bulgaria.

Vladimir Udovicic (Institute of Physics Belgrade – Serbia)

Vladimir Udovicic has Ph.D. in nuclear physics on the research focussed on light-ion induced nuclear reactions obtained by electrical discharges. After he completed Ph.D. in 2006, he started research work on radon topics: radon monitoring using active and passive devices, study connections of meteorological variables and radon concentrations variability using multivariate classification and regression methods, modelling of the indoor radon behaviour and radon policy, action plan and mapping. From 1996 he is permanently employed in the Institute of Physics Belgrade, currently at the position of Senior Research Associate and Head of Low-Background Laboratory for Nuclear Physics. From the beginning of the career, he worked on the national research projects of the Ministry of Science of the Republic of Serbia and international regional projects funded by IAEA as a counterpart for Serbia. From 2013, he is the chairman of the board of Serbian Radiation Protection and Nuclear Safety Agency, Serbian regulatory body in the field of radiation protection. From 2011, he is the member of the Executive Board of Society for Radiation Protection of Serbia and Montenegro.

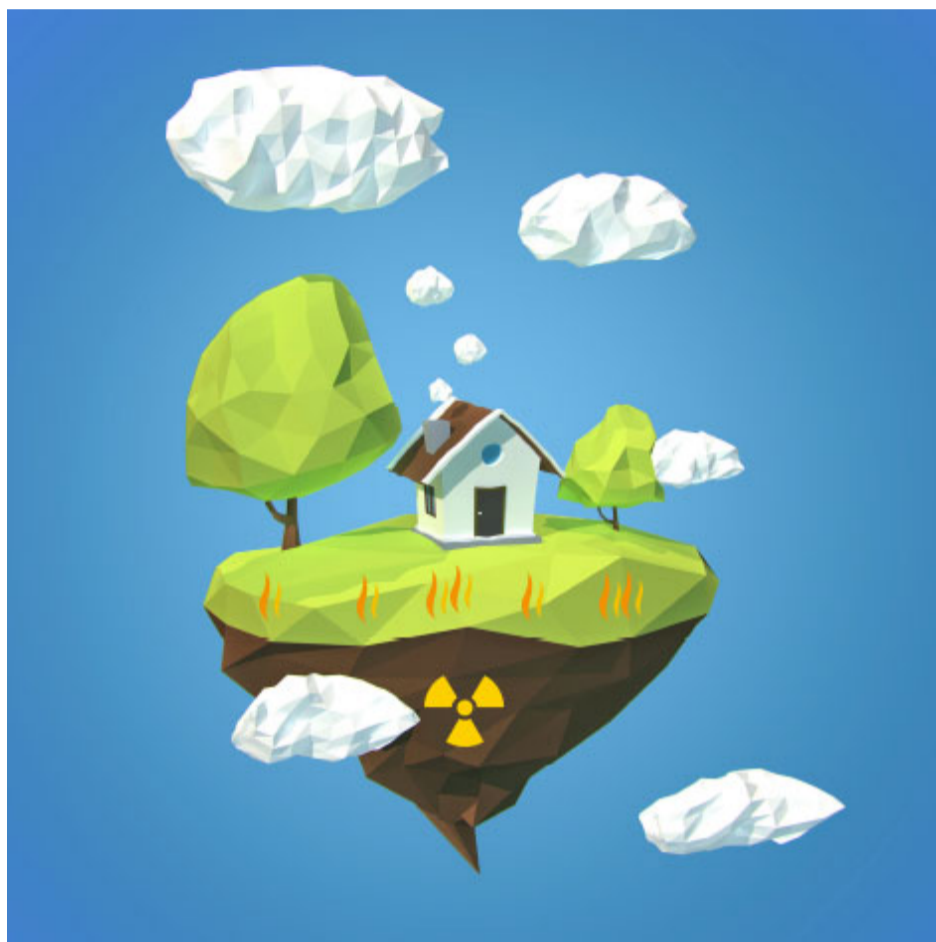
Bety-Denissa Burghel (Babeş-Bolyai University, Romania)

Valeria Gruber (AGES, Austria)

Gary Moss (TASL, UK)

Monika Nordqvist (Eurofins Radon Laboratory, Sweden)

Our Mission



The Association objectives are:

- To promote and to participate in activities to reduce radon risk within the population, recognizing radon as the second cause for lung cancer
- To promote public awareness of radon risk, radon measurement, radon mitigation and radon preventative techniques.
- To ensure/develop/adopt quality standards in radon measurement, radon mitigation and radon prevention in new constructions.
- To provide an effective partnership between radon professionals in the field and other interested public and private stakeholders.
- To serve as a consultative body with regards to laws and regulations concerning radon. To organize an annual Radon conference or workshop combining scientific presentations and technical exhibitions from companies working with radon.
- Strive for the highest standard of fairness and integrity

The Association is unselfish in its activity. In their use for the public benefit, its funds may only be utilised for purposes in accordance with the statutes. It may not favour any person by means of expenditures which are foreign to the objectives of the Association.

ERA Publicity Leaflet

An information leaflet with basic details about ERA has been produced in several different languages. This leaflet can be distributed at meetings and events to give a general introduction to ERA's aims and objectives. Below you can find the leaflet in different languages:

English



[Download\(\)](#)

ERA welcomes membership applications from those who have an active interest in the field of radon

[Join now
\(https://radoneurope.org/become-a-member/\)](https://radoneurope.org/become-a-member/)



Ispra, 27th September 2017
FW/MDC/em

Mr UDOVICIC Vladimir
Institute of Physics Belgrade
Belgrade (Serbia)
e-mail: udovicic@ipb.ac.rs

Invitation to the 2nd International Workshop on the European Atlas of Natural Radiation (IWEANR 2017)

Dear Mr Udovicic,

I am pleased to invite you as an expert to the meeting "**2nd International Workshop on the European Atlas of Natural Radiation (IWEANR 2017)**" which will take place in Verbania, Italy, **from 6th to 9th November 2017.**

- We confirm that the JRC, Dir. G - Knowledge for Nuclear Safety, Security and Safeguards Unit will cover the costs of accommodation (max 5 nights) and will reimburse you for the travel costs (in economy class) and for daily allowance (max 3.5 days).
- Further details on the conditions of reimbursement of your expenses can be found in the attached "JRC's Quick Glance at the Rules". If you wish to claim such reimbursement, please proceed according to the following steps:
- Upon receipt of this letter, I kindly ask you to reserve as soon as possible your flight tickets and book your hotel room, in order to avoid high prices or non-availability.
- Prior to the workshop you must complete the "Financial Identification Form" and the "Legal Entity Form" which you will find attached (please choose the type of legal entity as appropriate). These documents can also be downloaded in other languages from:
http://ec.europa.eu/budget/contracts_grants/info_contracts/financial_id/financial_id_en.cfm
and http://ec.europa.eu/budget/contracts_grants/info_contracts/legal_entities/legal_entities_en.cfm

Both forms, together with the annexes requested therein, should be sent back to our meeting secretary Mrs Elena Moneta (JRC-IWEANR2017@ec.europa.eu) before the start of the meeting.

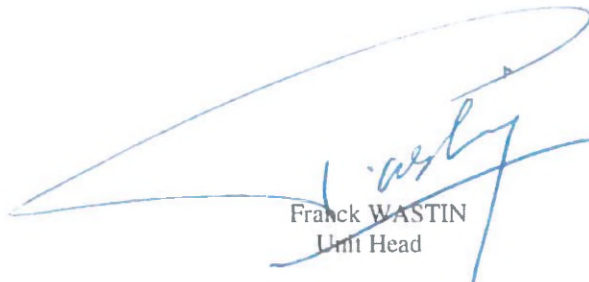
If you have previously received reimbursement from the European Commission and your personal details have not changed, re-submission of the documents is not required.

- At the start of the workshop you will be requested to complete and to hand in the "Application for Reimbursement of Expenses" form (see attached), duly dated and signed, including its supporting documents.
- Please note that all documents necessary for reimbursement must reach the European Commission at the latest 30 days after the final day of the meeting. Beyond this deadline, the Commission is absolved from any obligations to reimburse travel expenses or pay any allowances.
- Please note that this invitation covers travel directly between your residence or place of work and the meeting venue (Malpensa or Linate Airport), as close as possible to the meeting dates and times. If you wish to make any other journey, or to extend your trip, this must be agreed in advance with us, upon submission of a comparison quote of a regular round trip "place of origin-meeting place".

Regarding the processing of your personal data in line with this event, we inform you that when confirming your attendance, we consider you agree to the privacy statement published on this website link: <http://ec.europa.eu/dpo-register/download?metaId=1419871>

For any further questions, please do not hesitate to contact our meeting secretary Mrs Elena Moneta (JRC-IWEANR2017@ec.europa.eu).

Yours sincerely,



Franck WASTIN
Unit Head

CC: Mrs G. SCARLAT, Mr A. BALIYANGA (JRC.R.8)
Mr M. DE CORT, Mr T. TOLLEFSEN, Mrs G. CINELLI (JRC.G.10)

Enclosure: Who?-What?-How? – JRC's Quick Glance at the Rules" – Information Sheet
Application for Reimbursement Form
Financial Identification Form
Legal Entity Form

Joint Research Centre

Westerduinweg 3, PO Box 2, 1755 ZG Petten, The Netherlands
Email: franck.wastin@ec.europa.eu; Direct +31.224.56.5066 - fax +31.224.56.5637
Internet: <http://ec.europa.eu/jrc/>



journal of the
European Radon Association

[ABOUT JERA](#)[TABLE OF CONTENTS](#)[AUTHOR GUIDELINES](#)[JOURNAL POLICIES](#)

[HOME](#) / [Editorial Team](#)

Editorial Team

Editor-in-Chief

José – Luis Gutiérrez-Villanueva (Radonova Laboratories AB, Sweden)

Editorial Board

Wolfgang Ringer (AGES, Austria)

Per Nilsson (ÅF, Sweden)

Boris Dehandschutter (FANC, Belgium)

Rebecca Coates (PropertECO – UK)

Bernard Collignan (CSTB – France)

Erik Hulber (Radosys - Hungary)

Maria Hansen (TASL - UK)

Stephanie Hurst (Saxony Ministry of Environment & Agriculture– Germany)

Geraldine Ielsch (IRSN – France)

Krzysztof Kozak (Institute of Nuclear Physics PAN – Poland)

James Mc Laughlin (University College Dublin – Ireland)

Matej Neznal (Radon v.o.s – Czech Republic)

Dobromir Pressyanov (U. Sofia - Bulgaria)

Vladimir Udovicic (Institute of Physics Belgrade – Serbia)

About the journal

JERA is a non-profit, peer-reviewed and open access journal of the **European Radon Association** that focuses on radon research and practices.

The purpose of JERA is to publish original research, review articles and/or technical papers relating to radon, thoron and decay products.

Learn more about the journal's **Aims & Scope**.

submit manuscript



Published by the European Radon Association

Tweets by @RadonEurope

 **European Radon Assoc**
@RadonEurope

Save the date and register for ROOMS 2022 and ERA Workshop plus General Assembly: radoneurope.org/rooms-2022-and...

When? 27-29 Sep 2022

Where? Bergen, Norway [#workingtogether](#) [#radon](#) [#radonmitigation](#) [#visitNorway](#)

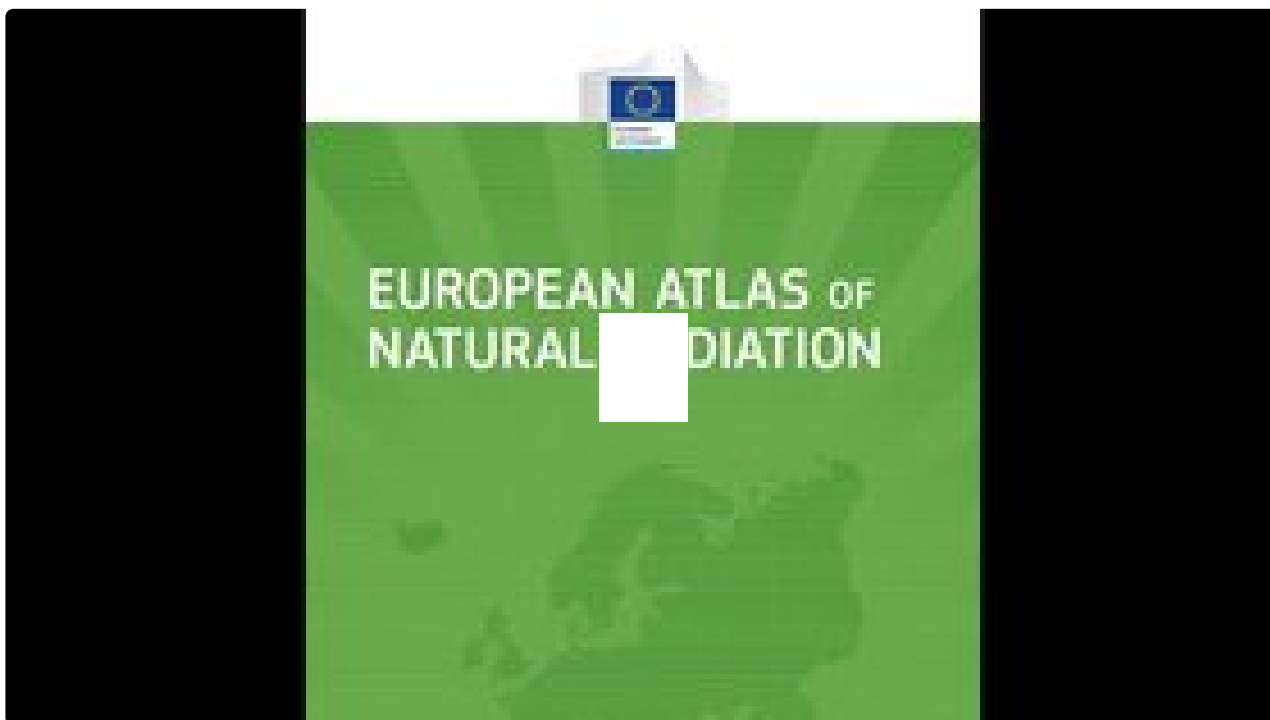
Jul 27, 2022

 **European Radon Assoc**
@RadonEurope

Watch the ERA webinar about the European Atlas of Natural Radiation: youtu.be/89UruVKWHUI

Speakers: Giorgia Cinelli and Marc De Cort [#onlinewebinar](#) [#naturalradiation](#) [#radon](#)

 **YouTube** @YouTube



Jul 19, 2022

 **European Radon Assoc**
@RadonEurope

Save the date and register for ROOMS 2022 and ERA Workshop plus General Assembly: radoneurope.org/rooms-2022-and...

When? 27-29 Sep 2022

Where? Bergen, Norway [#workingtogether](#) [#radon](#) [#radonmitigation](#) [#visitNorway](#)

Jul 13, 2022

[Embed](#)

[View on Twitter](#)

MOST READ THIS MONTH

Metrology aspects (sampling, storage, transportation, and measurement) of radon in water

👁 81

The European Cancer Information System: exploring linkages between indoor radon concentrations and data on cancer burden

👁 48

On harmonization of radon maps

👁 17

Similarities and differences between radon surveys across Europe: results from MetroRADON questionnaire

👁 15

Radon risk assessment and mitigation deadlines

👁 15

INFORMATION

For Readers

For Authors

For Librarians



OPEN ACADEMIA
PUBLISHING SERVICES

Published in cooperation with Open Academia

Journal of the European Radon Association | ISSN: 2736-2272 | Editor-in-Chief:

Jose Luis Gutierrez Villanueva

Published open access under the terms of the Creative Commons CC-BY 4.0 license.

[Contact](#) | [Privacy Policy](#) | [Copyright & Licensing](#)

Platform &
workflow by
OJS / PKP



GREEN BUILDING EXPO
INTERNATIONAL EXHIBITION & CONFERENCE
2-4 NOVEMBER - BELGRADE SERBIA

19.10. 2016.

Vladimir Udovičić
Institute of Physics,
University of Belgrade
SERBIA

LETTER of INVITATION

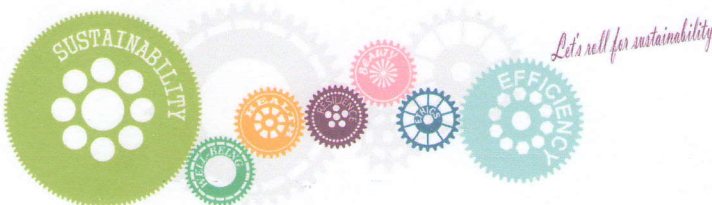
Dear dr Vladimir Udovičić,

We are pleased to let You know that the organizing board of the Green Building Expo & Conference that will be held from 02 -04. November 2016. in Belgrade would like to ask You to give a lecture as invited lecturer about Radon mapping of Serbia.

Best Regards,

Marija Golubović

Marija Golubović
Conference organizer



The Green Building Expo and Conference is organized by ENERGO
Kneza Miloša 53, 11000 Beograd - Srbija
Tel. +381 11 4088393, info@greenbuildingexpo.rs,
www.greenbuildingexpo.rs

IWEANR 2017

Verbania, Italy, 6 – 9 November 2017



2nd International Workshop on the European Atlas of Natural Radiation

First announcement

Dear Colleagues,

We are happy to invite you to attend the 2nd International Workshop on the European Atlas of Natural Radiation (IWEANR 2017), which will take place from Monday 6 (at 14:00) to Thursday 9 (at 12:30) November 2017 in Verbania at Lake Maggiore, Italy.

This workshop aims to address the following topics (indicative list, subject to modifications) in the framework of the European Atlas of Natural Radiation:

- Radon policies
- Indoor radon
- Sources of natural radiation
- Relationship between radon-related quantities
- Radon-priority areas
- Round-table discussions: preparation of Atlas publication, further maps, total dose estimation

Call for abstracts

All participants are invited to submit an abstract in English (max. 1 page, A4 format, single-spaced), linked to the topics proposed below, by **16 June 2017**. The abstract should be submitted as e-mail attachments and sent to: **JRC-IWEANR2017@ec.europa.eu**. Please indicate the topic under which you are submitting your abstract.

Based on the scientific quality of the abstracts, the scientific committee will select those to be developed into oral presentations. The outcome of this selection will be communicated by 30 June 2017.

The oral presentations should be aimed to match the next, necessary steps of the Atlas. While the scientific committee will design a main part of the workshop programme by inviting speakers, it will also leave room for these selected presentations.

Proposed Topics

- *Radon policies*: European Basic Safety Standards, international organizations' positions, other international projects
- *Indoor radon*: new participants to the European map, new datasets
- *Sources of natural radiation and their mapping*: cosmic, geochemical, terrestrial gamma, radon, water, building materials etc.
- *Relationship between radon-related quantities*: multivariate analysis, dimensionality reduction, radon hazard index
- *Radon-priority areas*: concepts, predictors, classification, risk, mapping issues (geological, gridded, administrative units)

Scientific Committee

Peter Bossew – German Federal Office for Radiation Protection, Berlin, Germany

Giorgia Cinelli – European Commission, JRC, Ispra, Italy

Marc De Cort – European Commission, JRC, Ispra, Italy

Boris Dehandschutter – Federal Agency for Nuclear Control, Brussels, Belgium

Marta García-Talavera – Nuclear Safety Council, Madrid, Spain

Valeria Gruber – Austrian Agency for Health and Food Safety, Linz, Austria

Stefan Mundigl – European Commission, Directorate-General for Energy, Luxembourg

Petra Pacheroová – Czech Geological Survey, Prague, Czech Republic

Tore Tollefsen – European Commission, JRC, Ispra, Italy

Vladimir Udovičić – University of Belgrade, Serbia

Local Committee

Giorgia Cinelli – European Commission, JRC, Ispra, Italy

Marc De Cort – European Commission, JRC, Ispra, Italy

Tore Tollefsen – European Commission, JRC, Ispra, Italy



DRUŠTVO ZA ZAŠTITU OD ZRAČENJA SRBIJE I CRNE GORE
ДРУШТВО ЗА ЗАШТИТУ ОД ЗРАЧЕЊА СРБИЈЕ И ЦРНЕ ГОРЕ
RADIATION PROTECTION ASSOCIATION OF SERBIA AND MONTENEGRO

=====

M. P. Alasa 12-14, P.O.Box 522, 11000 Belgrade, Serbia
tel/fax: +381 11 630 84 38, tel: +381 11 6453 867, emial: ociraj@vinca.rs; office@dzz.org.rs
www.dzz.org.rs

=====

Broj: 20/13 od 10.6.2013.

Dr Vladimir Udovičić
Institut za fiziku
Pregrevica 118, Zemun

Poštovani dr Udovičić,

Društvo za zaštitu od zračenja Srbije i Crne Gore se organizovano bavi unapređenjem naučnog rada u oblasti zaštite od zračenja a takođe i praktičnim aspektima zaštite životne sredine, zaštitom zdravlja ljudi i životinja kao i materijalnih dobara od štetnog delovanja jonizujućih zračenja.

XXVII Simpozijum Društva za zaštitu od zračenja biće održan u Vrnjačkoj Banji od 2. do 4. oktobra 2013. godine. Skupu ce prisustvovati naučnici i stručnjaci iz velikog broja naučno-istraživačkih organizacija i fakulteta u zemlji, kao i gosti iz inostranstva.

Ovogodišnji Simpozijum je posebno značajan usled činjenice da Društvo obeležava izuzetan jubilej - 50 godina organizovane zaštite od zračenja na ovim prostorima. Jugoslovensko društvo za zaštitu od zračenja osnovano je 1963. godine i ovom jubileju će na Simpozijumu biti posvećena posebna sesija.

Vaše prisustvo bi nam učinilo veliku čast i dalo značajnu podršku našem daljem radu, te Vas pozivamo da prisustvujete XXVII Simpozijumu, i održite uvodno predavanje iz oblasti kojoj ste svojim dosadašnjim aktivnostima dali poseban doprinos, sa posebnim osvrtom na izazove u oblasti zaštite od zračenja vezane za problematiku radona.

Simpozijum će biti održan u hotelu "Breza" a otvaranje je predviđeno za sredu, 2.10. 2013. godine.

U nadi da ćete naći vremena da prisustvujete Simpozijumu srdačno Vas pozdravljamo.

Vinča, 10.6.2013.

S poštovanjem,


Dr Olivera Ciraj-Bjelac, dipl. fizičar
Predsednik Društva za zaštitu od zračenja SCG





EUROPEAN COMMISSION
JOINT RESEARCH CENTRE

Institute for Transuranium Elements
Head of Unit - Nuclear Security

Ispra, 18/09/2015
JRC E08/WJ/sf Ares(2015)

Dr Vladimir UDOVICIC
University of Belgrade

Belgrade
Serbia

**Invitation to the "International Workshop on the European Atlas of Natural Radiation"-
P2015022222**

Dear Dr Udovicic,

I am pleased to invite you as an expert to the "**International Workshop on the European Atlas of Natural Radiation**" which will take place in **Verbania, Italy from the 09th to the 13th November 2015**.

We confirm that the JRC - ITU covers the costs of accommodation (max 6 nights) and will reimburse you for the travel costs (in economy class) and for daily allowance (max 4,5 days).

If you wish to claim such reimbursement, please proceed according to the following steps:

- Upon receipt of this letter, I kindly ask you to reserve as soon as possible your flight tickets, in order to avoid high prices or non-availability.
- Prior to the workshop you must complete the "Financial Identification Form" and the "Legal Entity Form" which you will find attached (please choose the type of legal entity as appropriate). These documents can also be downloaded in other languages from:
http://ec.europa.eu/budget/contracts_grants/info_contracts/financial_id/financial_id_en.cfm and
http://ec.europa.eu/budget/contracts_grants/info_contracts/legal_entities/legal_entities_en.cfm
- Both forms, together with the annexes requested therein, should be sent back to our meeting secretaries Silvia Fasani and/or Barbara Bassi (JRC-NUSAF-SECRETARIAT@ec.europa.eu) before the start of the workshop. If you have previously received reimbursement from the European Commission and your personal details have not changed, re-submission of the documents is not required. Just complete the part of the Financial Identification Form (name and bank details); neither the bank stamp and signature, nor the Legal Entity Form are necessary.

- At the start of the workshop you will be requested to complete and to hand in the "Application for Reimbursement of Expenses" form (see attached), duly dated and signed, including its supporting documents.
- Please note that all documents necessary for reimbursement must reach the European Commission at the latest 30 days after the final day of the meeting. Beyond this deadline, the Commission is absolved from any obligations to reimburse travel expenses or pay any allowances.
- Please note that this invitation covers travel directly between your residence or place of work and the meeting venue (Malpensa or Linate airport), as close as possible to the meeting dates and times. If you wish to make any other journey, or to extend your trip, this must be agreed in advanced with us, upon submission of a comparison quote of a regular round trip "Place of origin-meeting place".

Regarding the processing of your personal data in line with this event, we inform you that when confirming your attendance, we consider you agree to the privacy statement published on this website link: <http://www.jrc.ec.europa.eu/privacy/experts>

For any further questions, please do not hesitate to contact our meeting secretaries Silvia Fasani and/or Barbara Bassi (JRC-NUSAF-SECRETARIAT@ec.europa.eu).

Yours sincerely,



Willem Janssens
Head of Unit

CC: M. Betti, J.Ribeiro, T.Tollefsen, L.Ciafrè

Enclosure: Application for Reimbursement Form
Financial Identification Form
Legal Entity Form



Овим документом потврђујем да је др Владимир Удовичић, виши научни сарадник Института за физику у Београду, Института од националног значаја за Републику Србију, био руководилац регионалних пројеката Међународне агенције за атомску енергију за Републику Србију у три пројектна циклуса и то:

- **RER/9/127** – „Establishing Enhanced Approaches to the Control of Public Exposure to Radon“ за период 2014-2015.
- **RER/9/136** - „Reducing Public Exposure to Radon by Supporting the Implementation and Further Development of National Strategies“ за период 2016-2017.
- **RER/9/153** - „Enhancing the Regional Capacity to Control Long Term Risks to the Public due to Radon in Dwellings and Workplaces“ за период 2018-2021.

У оквиру руковођења тим пројектима, урађено је више потпројеката од националног значаја везаних за област заштите од зрачења, од којих се издвајају: израда прве националне мапе радонског ризика у кућама и становима у Републици Србији, израда прве националне радонске мапе за вртиће, основне и средње школе у Републици Србији, као и писање првог националног акционог плана за радон у Србији, који ће постати саставни део будуће националне стратегије управљања ситуацијама постојећег излагања.

Документ се издаје у сврху избора др Владимира Удовичића у научно звање научни саветник.



Др Александар Богојевић

Директор Института за физику у Београду,
Института од националног значаја за Републику Србију

У Београду, 12.08.2022.